

# UNCLASSIFIED

AD NUMBER
AD865354
NEW LIMITATION CHANGE
TO Approved for public release, distribution unlimited
FROM Distribution authorized to U.S. Gov't. agencies and their contractors; Critical Technology; FEB 1970. Other requests shall be referred to Office of Naval Research, Arlington, VA 22203.
AUTHORITY
ONR ltr, 2 Mar 1979

THIS PAGE IS UNCLASSIFIED

THIS REPORT HAS BEEN DELIMITED  
AND CLEARED FOR PUBLIC RELEASE  
UNDER DOD DIRECTIVE 5200.20 AND  
NO RESTRICTIONS ARE IMPOSED UPON  
ITS USE AND DISCLOSURE.

DISTRIBUTION STATEMENT A

APPROVED FOR PUBLIC RELEASE;  
DISTRIBUTION UNLIMITED.

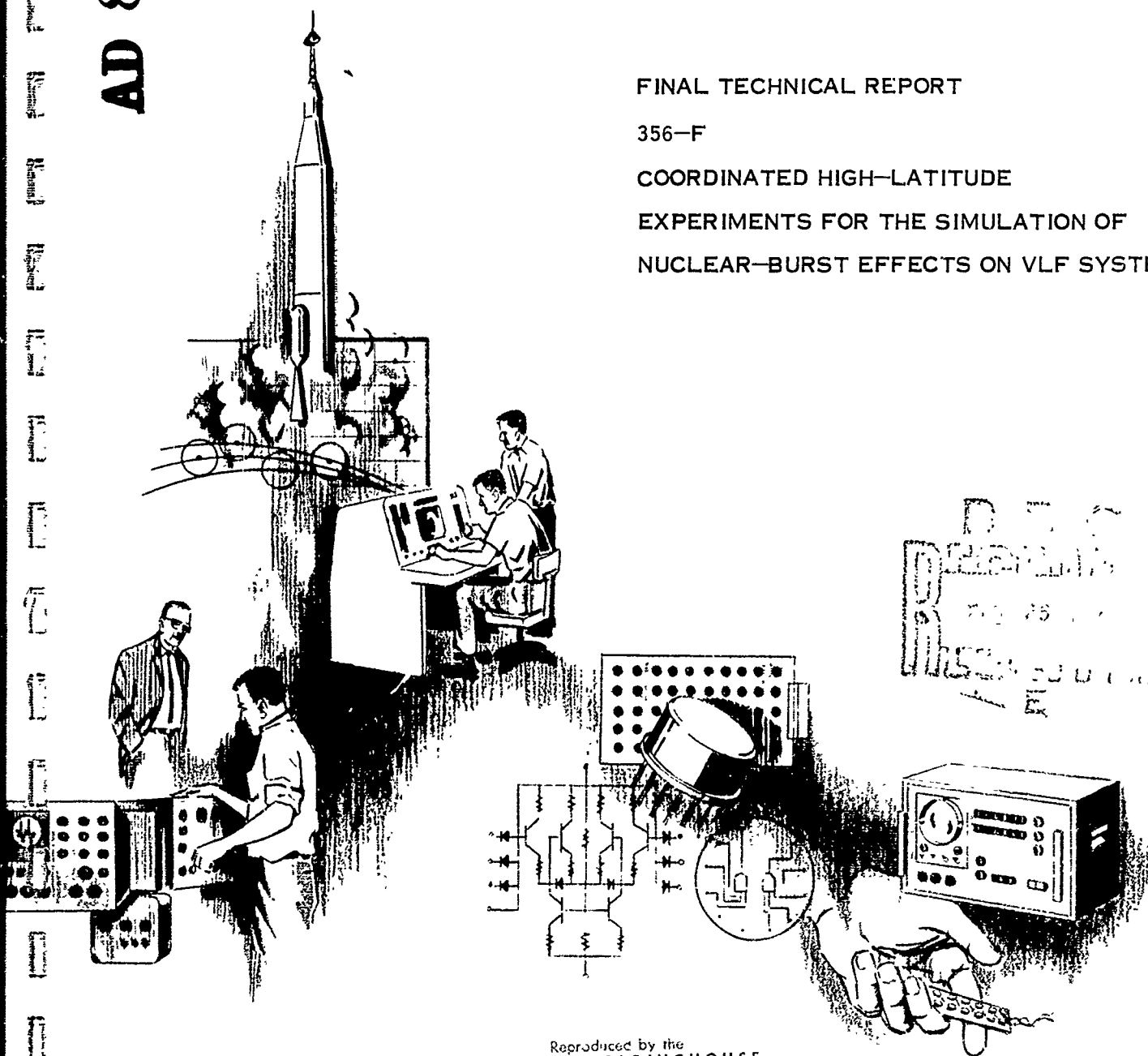
AD 865354

# HRB-SINGER, INC.

FINAL TECHNICAL REPORT

356-F

COORDINATED HIGH-LATITUDE  
EXPERIMENTS FOR THE SIMULATION OF  
NUCLEAR-BURST EFFECTS ON VLF SYSTEMS



Reproduced by the  
CLEARINGHOUSE  
for Federal Scientific & Technical  
Information Springfield Va 22151

## WARNING

"This document is subject to special export controls and each transmittal to foreign governments or foreign nationals may be made only with prior approval of the Office of Naval Research, Field Projects Branch, Washington, D.C. 20360"

**SINGER**  
INFORMATION SCIENCES

305

**HRB-SINGER, INC.**

SCIENCE PARK, BOX 60 • STATE COLLEGE, PA 16801  
A SUBSIDIARY OF THE SINGER COMPANY

**FINAL TECHNICAL REPORT**

**356-F**

**COORDINATED HIGH-LATITUDE**

**EXPERIMENTS FOR THE SIMULATION OF**

**NUCLEAR-BURST EFFECTS ON VLF SYSTEMS**

**PREPARED BY**

**E. J. OELBERMANN, G. W. IMHOF  
M. BRIGGS**

**CONTRIBUTIONS BY J. RIEKER**

**PROJECT DIRECTOR E. J. OELBERMANN**

**APPROVED BY**

**T. R. ORY**

**ANNUAL TECHNICAL REPORT NO. 5  
UNDER CONTRACT NONR-3851 (00)**

**FEBRUARY 1970**

**COPY NO. 87 OF 145 COPIES**

**WARNING**

*"This document is subject to special export controls and each transmittal to foreign governments or foreign nationals may be made only with prior approval of the Office of Naval Research, Field Projects Branch, Washington, D.C. 20360"*

*"This research was sponsored by the Defense Atomic Support Agency and was conducted under Office of Naval Research Contract No. NONR-3851(00), Task NR 087-146."*

**-i-  
Reverse (Page ii) Blank**

**SINGER**  
INFORMATION SCIENCES



## ABSTRACT

This report is the fifth and final report on coordinated high-altitude experiments which have been conducted by HRE-Singer, Inc. for simulating nuclear-burst effect on long-range VLF propagation.

Since this is a final report it summarizes and draws together, in as concise a way as possible, the results of five years of experiments which have included:

1. Collection and study of VLF phase and amplitude data over six long-range, high-altitude VLF propagation paths and 2-middle-latitude control paths.
2. Collection and study of ionospheric data (cosmic noise absorption data) near Reykjavik, Iceland, and Thule, Greenland.
3. Collection and study of other VLF data and ionospheric data from external sources (including satellite data).
4. Study and comparison of items 1 through 3 with nuclear test VLF data.
5. Collection and study of rapid phase VLF data at Thule, Greenland.

## TABLE OF CONTENTS

	<u>Page</u>
ABSTRACT	iii
LIST OF ILLUSTRATIONS	vii
LIST OF TABLES	ix
I. INTRODUCTION	1
II. MAJOR RESULTS AND CONCLUSIONS	5
III. PCA STATISTICS FOR THE MAJOR PCA'S OBSERVED ON THIS PROGRAM	11
IV. A DISCUSSION OF SOME RAPID PHASE VLF MEASUREMENTS AT THULE	25
A. PURPOSE OF THE RAPID PHASE VLF MEASUREMENTS	25
B. RAPID PHASE RECORDING AND PROCESSING SYSTEM	27
C. RAPID PHASE RECORDING	29
D. DATA REDUCTION	29
1. Method 1	31
2. Method 2	35
E. RAPID PHASE RESULTS	38
REFERENCES	49
APPENDIX A -- VLF DATA COLLECTED DURING RECENT POLAR CAP EVENTS	A-1
APPENDIX B -- COMPUTER PLOTS OF RIOMETER ABSORPTION DURING RECENT POLAR CAP EVENTS	B-1
APPENDIX C -- DISTRIBUTION LIST	C-1

# LIST OF ILLUSTRATIONS

<u>Figure</u>		<u>Page</u>
1	Transpolar and Transauroral Zone VLF Experiment	2
2	Summary of VLF PCA Periods, NPG-Switzerland, 1965 to 1969	9
3	Frequency Curve, Duration of VLF-PCA Effects for Path NPG-Switzerland	10
4	VLF Attenuation During First 24 Hours of Selected PCA's July 7, 1966 Through November 2, 1967	15
5	VLF Attenuation During First 24 Hours of Selected PCA's December 3, 1967 Through January 24, 1969	17
6	VLF Attenuation During First 24 Hours of Selected PCA's February 25, 1969 Through April 12, 1969	19
7	Block Diagram, Rapid Phase Recording and Processing System	28
8	Block Diagram, One Channel of HRB-Singer, Inc., Rapid Phase Recording System at Thule, Greenland	30
9	Block Diagram, HRB-Singer, Inc., Rapid Phase VLF Data Reduction System Method 1	31
10	Examples of 180° Phase Errors	33
11	Rapid Phase Playback	34
12	Block Diagram, Rapid Phase Data Reduction System, Method 2	35
13	Rapid Phase Presentation NPM-Thule Signal -- November 18, 1968, Time 1618 UT	37
14	Normal and Rapid Phase Perturbations NPM-Thule, July 2, 1968, July 5, 1968, February 28, 1969	39
15	Polar and Transpolar VLF-PCA Effect November 18, 1968	43
16	Sudden Proton Flare Effect -- NPM-Thule, November 18, 1968	44
17	Rapid Phase Sample System -- NPM-Thule, November 18, 1968, 1618 UT	46
18	Analysis of NPM-Thule Rapid Phase Data -- November 18, 1968, 1618 UT	47

## LIST OF TABLES

<u>Table</u>		<u>Page</u>
1	Table of VLF -- Effect PCA's -- March 1, 1965 to September 30, 1969	6
2	Statistics on Polar Path VLF Attenuation	12
3	Standard Deviations (dB), NPG and NPM to Payerne Signal Strength During Five-Day Quiet Periods and During PCA's	22
4	Standard Deviations in (dB) of Hour to Hour NPG-Payerne Field Strength During Quiet Days and PCA Days	23
5	Standard Deviations of Nighttime and Daytime NPG-Payerne Field Strength Through November 18, 1968 PCA	24

## I INTRODUCTION

Very low frequency, VLF, radio propagation can be theoretically interpreted as a sum of modes in a wave guide formed by the earth's surface and the lower ionosphere or D region. Therefore, geophysical phenomena that influence the structure of the lower ionosphere or the conductivity of the ground will affect VLF propagation.

Nuclear detonations and solar proton events both produce drastic changes in the structure of the D-region, a general lowering of the height of reflection and increased radio wave absorption due to the production of free electrons and heavier ions at low levels.

Although the mechanisms and the time scales of nuclear and PCA perturbations are vastly different, the long term nuclear and PCA effects on VLF are very similar. These are mainly particle effects due to the bombardment of the ionosphere by high energy particles in the 1 to 100 Mev range.

It has been pointed out in previous reports on this project that a PCA is probably the event which most closely resembles the bombardment of the ionosphere during high altitude nuclear explosions.

The region irradiated by the beta particles from the debris cloud produced by a lower altitude nuclear burst is also similar in many respects to the lower ionosphere during a PCA. The principle differences are: a higher level of ionization in the beta patch than in the D-layer during a PCA; different ionizing agents (beta particles versus protons) and differences in the size of the geographical region affected by each of these phenomena -- although recent evidence on this project indicates that some PCA's affect relatively small areas in the polar cap.

A simple outline of the experiments is shown in Figure 1. The VLF experiments are designed to provide two types of nuclear effects simulation data: data on signals which have passed entirely through the disturbed area, (i.e., NPM and NPG to Payerne and Slough); and data on signals which are received in the approximate center of the disturbed region (NPM and NPG to Thule).

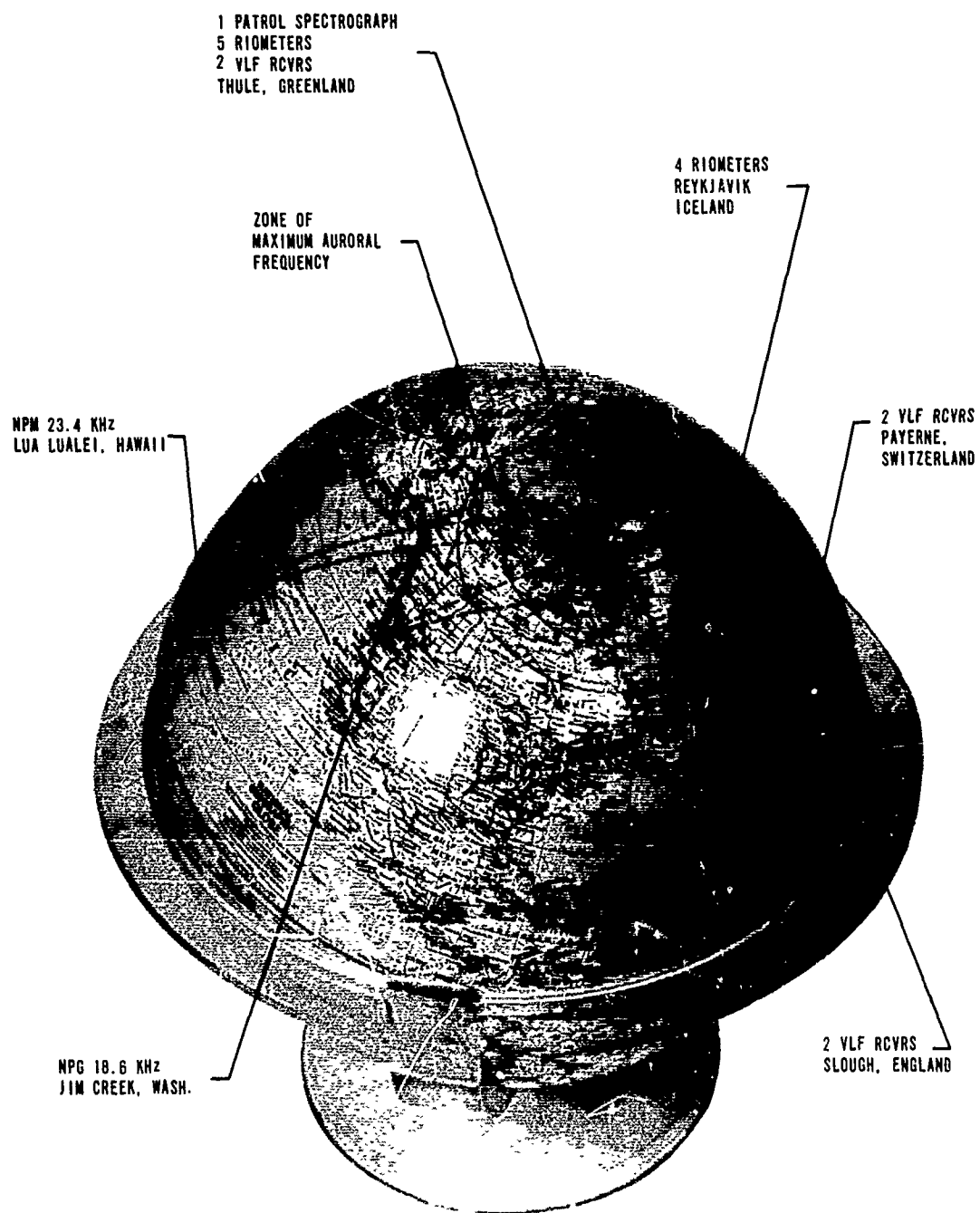


FIG. 1 TRANSPOLAR AND TRANSAURORAL ZONE VLF EXPERIMENT

The Polar Cap, for the purpose of this study, is defined as the region inside the inner circle on Figure 1. This is a circle centered on the Geomagnetic Pole (Thule, Greenland) which incloses the area of North of 75 degrees Geomagnetic latitude. This boundary represents an average upper limit to electron precipitation  $E \geq 40$  Kev described by Frank, Van Allen and Craven (1964). The outer circle in Figure 1, 70 degrees Geomagnetic North, is an approximate lower limit for the nighttime electron precipitation zone for  $E \geq 40$  Kev.

Solar proton events inside the polar cap are relatively uncontaminated by auroral electron precipitation. The ring between the two circles defines a zone of maximum auroral precipitation where rapid fluctuations in riometer absorption are observed.

On examining VLF attenuation statistics on 20 of the major PCA events which have occurred during the past five years it is observed that, on the average, the long trans polar paths are attenuated three times as much as the paths which terminate at Thule.

Reder and Westerlund (1967) have attributed this to the presence of the Greenland ice pack which must be crossed on the transpolar paths but not on the paths to Thule. This explanation seems valid except for two contradictory cases, both summertime PCA's, where little or no disturbance was observed on some ice paths but large effects were observed at Thule. The "Ice-Pack Effect" should produce more attenuation along the NPM to Europe paths (approximately 1200 kilometers of ice) than it does along the NPG to Europe paths (approximately 660 kilometers of ice). The opposite effect occurs, however, indicating that in 85% of the cases the shorter ice path through southern Greenland is more heavily attenuated.

Although much more evidence needs to be collected on this subject it appears that in addition to the Ice-Pack effect there tends to be selective VLF absorption in the southern part of the polar cap where the auroral zone dips below the arctic circle. This zone is sometimes very sharply defined so that paths just outside the region are not affected whereas paths through any part of the region are heavily attenuated. It is not known whether the sharply defined region is a region of selective precipitation such as a dumping region or whether summertime illumination and the geometry (relative angle) between the sunrise-sunset terminator and the radio path results in excess absorption along this path. It is recommended that

future studies of polar VLF propagation attempt to map PCA's in an effort to answer some of these questions.

Many questions have been answered by these experiments. These will be discussed in the following sections of this report which include Section II, Major Results and Conclusions; Section III, PCA Statistics for the major PCA's observed on this program; and Section IV, a discussion of some Rapid Phase VLF Measurements at Thule. Appendix A will be devoted to a presentation of raw VLF data and Appendix B will consist of computer plots of riometer absorption during recent PCA events.



## II. MAJOR RESULTS AND CONCLUSIONS

During the past four and one-half years the coordinated, high latitude experiments have continued to provide valuable information and data on polar cap events.

In this period, (March, 1965 to September 30, 1969) at least 33 solar proton associated events have been detected in the VLF data.

A review of these data indicates that PCA's were definitely observed on the dates listed in Table 1. Outstanding events with respect to intensity, duration or other special features of interest are underlined. Special features are listed in column two. Number of events per year is tabulated under column three.

The first major event encountered on this program was the July 7, 1966 event which was treated rather thoroughly in HRB-Singer report 356-R-8, (1966). The July 7, 1966 event was characterized by (Hakura, 1967) as a two-stepped onset PCA corresponding to the differential arrival of solar electrons and protons at the earth detected by the satellite IMP-3. The two-stepped onset pattern in the VLF-PCA is the first evidence that long path VLF can be used to study PCA phases. This is also the first evidence of VLF detection of a polar electron event.

The September 2, 1966 polar cap disturbance was the first intense PCA encountered in this program. The maximum perturbation of the electron density profile at the peak of this event approached the STARFISH profile measured during the U.S. nuclear tests. This PCA was preceded by a very intense proton flare on August 28, 1966 and a type IV noise burst which saturated both the 30 MHz and 40 MHz riometers at the Iceland riometer station. During the four day period preceding the September 2, 1966 PCA smaller PCA effects were observed on both the riometers and the VLF systems indicating the arrival of smaller or less dense clouds of solar particles. VLF absorption effects persisted for seven days following the September 2, 1966 event.

The January 28, 1967 solar proton event was a rare event from several aspects. No type IV noise burst and no solar flare were observed immediately preceding this event. Though no optical flare was reported the NPM-Payerne initial phase effects resembled a solar flare type Sudden Phase Anomaly (SPA).

TABLE 1. TABLE OF VLF-EFFECT PCA'S -- MARCH 1, 1965 TO SEPTEMBER 30, 1969		
DATE	SPECIAL FEATURES	NO OF EVENTS
DECEMBER 27, 1965		1 (1966)
MARCH 24, 1966 MAY 2, 1966 JULY 7, 1966 AUGUST 1, 1966 AUGUST 28, 1966 SEPTEMBER 2, 1966 SEPTEMBER 14, 1966	ELECTRON PHASE + BOUNDED VLF EFFECTS     VERY HARD EVENT	7 (1966)
JANUARY 12, 1967 JANUARY 28, 1967 FEBRUARY 26, 1967 MARCH 11, 1967 MAY 24, 1967 MAY 28, 1967 JUNE 6, 1967 NOVEMBER 2, 1967 NOVEMBER 12, 1967 DECEMBER 3, 1967 DECEMBER 16, 1967	GROUND LEVEL EVENTS GROUND LEVEL EVENT   EXTREMELY INTENSE EVENT EXTREMELY INTENSE EVENT	11 (1967)
FEBRUARY 11, 1968 JUNE 9, 1968 JULY 10, 1968 SEPTEMBER 29, 1968 OCTOBER 4, 1968 OCTOBER 31, 1968 NOVEMBER 18, 1968 DECEMBER 5, 1968	SHARPLY BOUNDED VLF EFFECTS     GROUND LEVEL EVENT, RAPID ONSET STRONG VLF ABSORPTION	8 (1968)
JANUARY 24, 1969 FEBRUARY 25, 1969 MARCH 22, 1969 MARCH 30, 1969 APRIL 12, 1969 SEPTEMBER 25, 1969	GROUND LEVEL EVENT	6 (1969)
TOTAL		33 EVENTS

It has been postulated that the January 28, 1967 proton event occurred on the back side of the sun (Innanen et al., 1967). Two enhancements of flux on January 28 produced a two stage PCA which was clearly observed in the VLF phase and amplitude data and on the IMP-3 satellite particle counters.

The January 28 event was a ground level event which resulted in the longest period of VLF absorption (19 days). The decay phase of the solar event lasted for approximately one solar rotation (27 days) with recurrent peaks at approximate two week intervals. (McDonald, 1968). HRB-Singer reported on coordinated VLF and riometer results on this event at the Spring URSI meeting in Washington, D. C., (Oelbermann et al., 1968).

The May 24 and May 28, 1967 solar proton events were the most intense PCA's detected on the HRB-Singer program. The first event, May 24, 1967 appears to have resulted from the occurrence of three large flares on May 23, 1967. The resulting SPA has a slow onset and the main phase of the PCA resulted in a gradual but continuous phase advance on the NPG-Payerne signal which lasted for 33 hours and reached 2-1/2 cycles. Before the phase recovered another 3B flare occurred which readvanced the phase to more than 2 cycles. Although these PCA's produced severe attenuation and complete loss of VLF signal for several hours on May 24, 25, and 28, 1966 the long term recovery of VLF signal strength lasted only 8 days as compared to 19 days for the January 28, 1966 event.

On June 9, 1968 a very unusual PCA was detected in which NPM to Thule and NPM to Payerne were hardly affected whereas the signals from NPG to Thule and NPG to Payerne were severely attenuated for a period of up to two days or longer (HRB-Singer 356-R-10, 1969).

The data on this event were compared with results from other investigators, (F. H. Reder, 1969). The combined results indicated that North Greenland paths (including ice-paths) were not very seriously affected whereas the South Greenland paths were attenuated during this event.

This result offered rather dramatic evidence that PCA effects are sometimes localized within small areas and do not always cover the entire polar cap.

The November 18, 1968 and December 5, 1968 PCA's both produced very severe VLF attenuation effects on the polar path signals. These events produced peak attenuations of NPG and NPM greater than 30 db and average attenuation for the first 24 hours of PCA on the order of 20 db.

The November 18, 1968 event was a rare, ground level event and thus had very high energy particle component,  $E > 800$  MEV.

The February 25, 1969 event, the last special PCA discussed in this report was also a ground level event. Though less than 30 of these events have ever been recorded, three of these have occurred during the HRB-Singer program. These were on January 28, 1967, November 18, 1969 and February 25, 1969.

Figure 2 is summary sheet which charts the 33 VLF-PCA's for the path NPG to Switzerland for the total period of this contract.

Each PCA is listed by date, month, year and duration in days of the VLF-PCA effects. The shaded regions in Figure 2 depict the duration in days on a 27 day solar rotation time base starting on December 1, 1965 (top left) and ending on October 3, 1969 (bottom right). PCA's are coded by the number on the left edge of each shaded block which represents the date that the PCA started. The shortest PCA's are two days long, the longest is 19 days long.

PCA's tend to group in succeeding solar rotations appearing in 2 or 3 cycles in a row then disappearing for several cycles. This is evident from the bar chart in the right hand side of Figure 2 which sums the number of PCA days for each solar rotation. Sometimes four or five solar rotations occur without any PCA effects. Since PCA effects occur in 25 out of 52 rotational periods the probability of PCA effects per solar rotation is about .48. If PCA effects have occurred or have not occurred in the previous solar rotational cycle the probabilities that the same thing will happen in the present cycle are .58 and .63 respectively.

Figure 3 is a frequency curve for the duration of VLF-PCA effects observed on the path NPG to Switzerland during this contract period. Note that the most probable duration of the VLF-PCA effects is three days. Ninety-six percent of the PCA's, all but the January 28, 1967 event, lasted eight days or less.

A discussion of PCA attenuation on individual, major events will be deferred to Part III of this report which discusses PCA statistics.

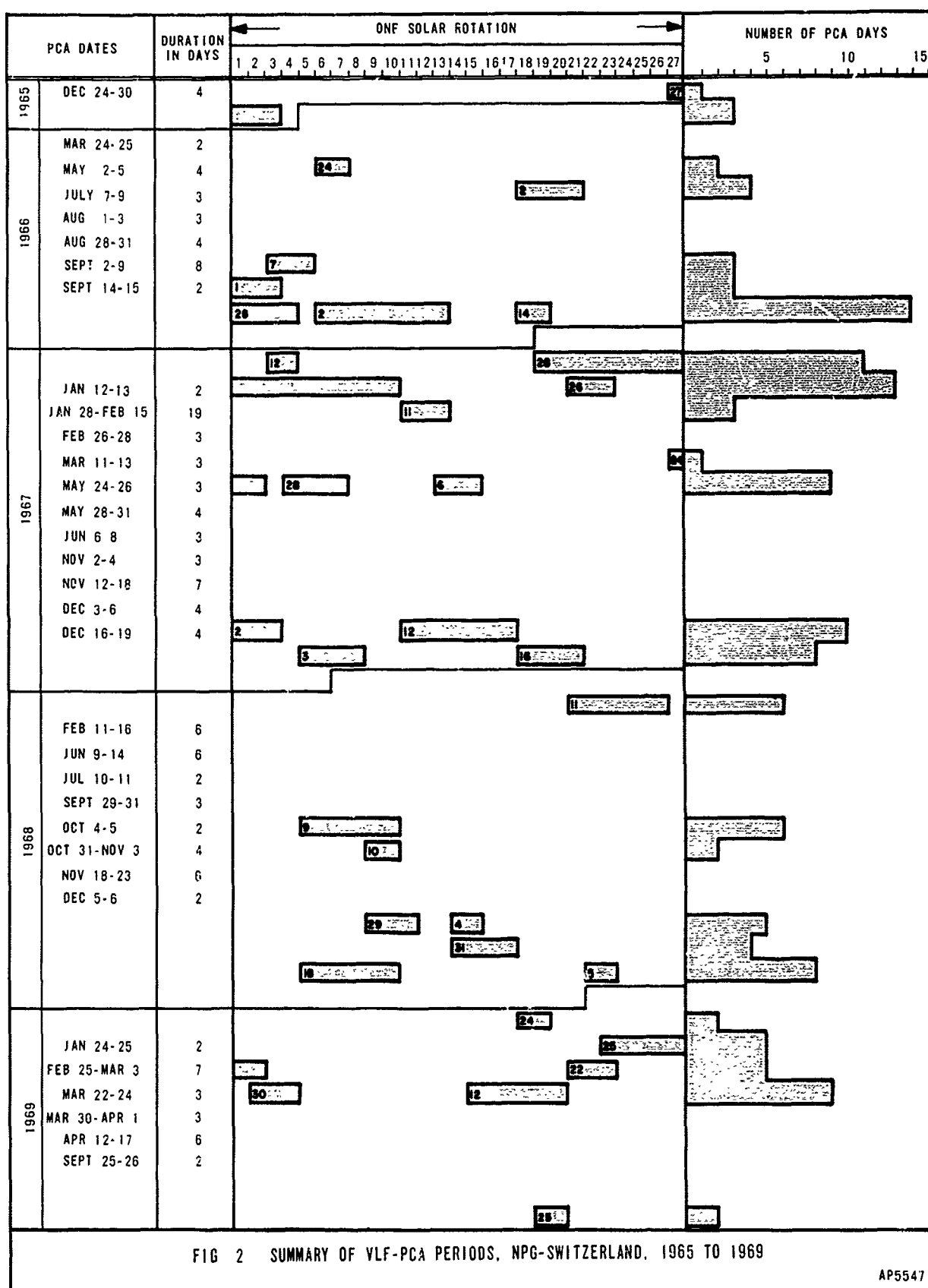


FIG 2 SUMMARY OF VLF-PCA PERIODS, NPG-SWITZERLAND, 1965 TO 1969

AP5547

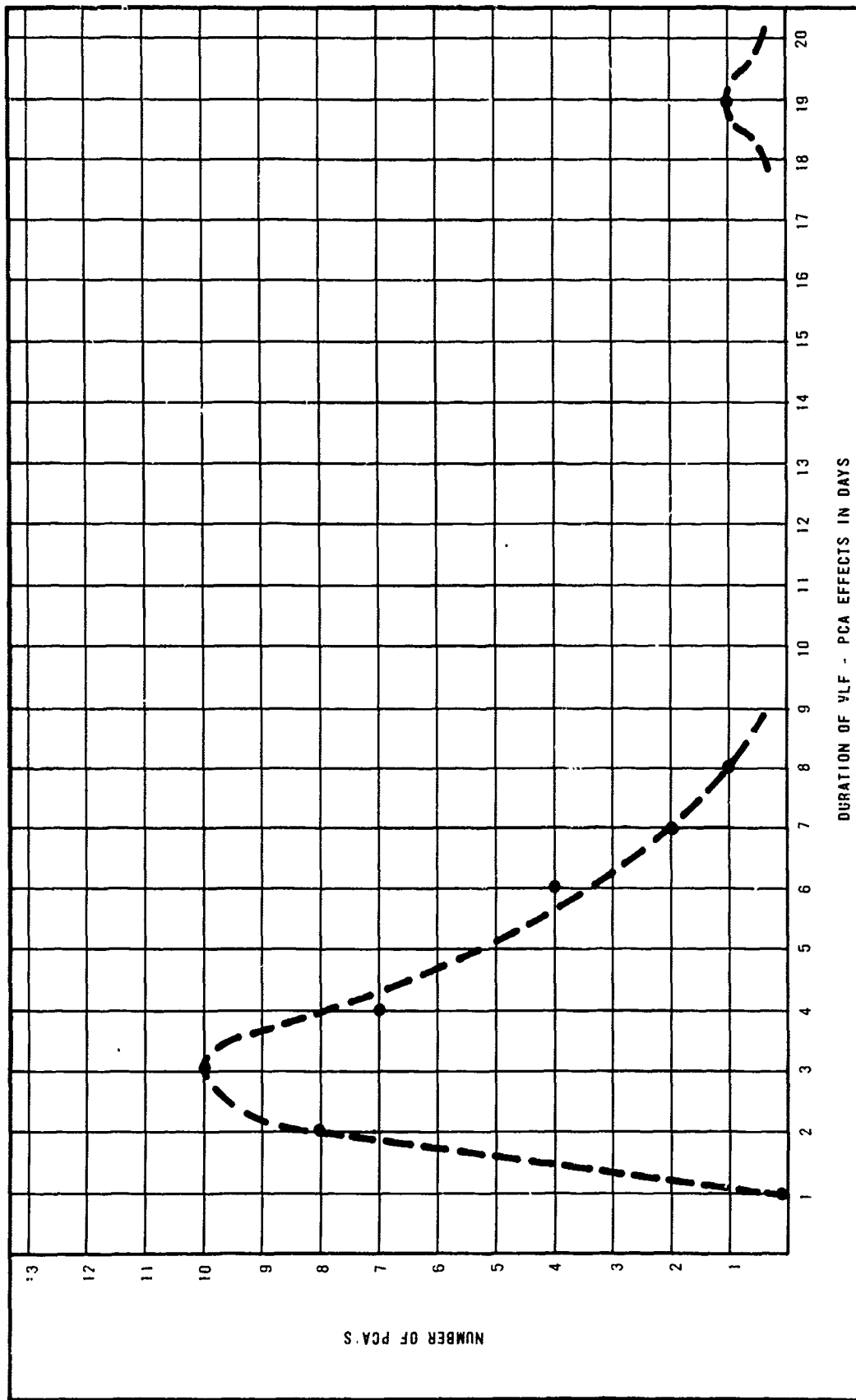


FIG 3 FREQUENCY CURVE, DURATION OF VLF PCA EFFECTS FOR PATH NPG SWITZERLAND

AP5540

### III. PCA STATISTICS FOR THE MAJOR PCA'S OBSERVED ON THIS PROGRAM

It was observed early on the polar-VLF project that PCA's are vastly different in time and spatial development. It is found that VLF attenuation fluctuates wildly during the first few hours of PCA, particularly on the transpolar VLF circuits.

The severity of PCA effects on VLF seems to depend to some extent on the time of day that the PCA begins, the season of the year, the radio path orientation, the frequency and the phase of the solar cycle.

In order to gain some statistical information on VLF attenuation, twenty (20) of the major PCA's between July 7, 1966 and April 12, 1969 were selected for statistical examination.

Average attenuation for each PCA was calculated by taking the average of the first 24 hours of Q-D for each PCA event where

D = Hourly VLF field strength during the first 24 hours of each PCA  
(24 D values).

Q = Hourly VLF field strength during a corresponding 24 hour quiet period  
(24 Q values).

$$\text{Average attenuation (db)} = \frac{\sum (Q-D)}{24}$$

If during certain hours of the selected quiet day the field strength is actually less than at that same hour during the PCA, Q-D becomes negative and the VLF effect is an enhancement.

Although enhancements occur at certain hours during some of the PCA's, in only one case was there an average enhancement over a 24 hour period. This was for the path NPM - Payerne on the PCA of March 21, 1969 when an average enhancement of 1.8 db was recorded.

Table 2 lists the dates of the twenty PCA's and the average attenuation which was calculated by the above method for the paths NPG and NPM to Payerne, and NPG and NPM to Thule. More Payerne data exists because the Thule operation did not begin until Fall of 1967.

TABLE 2 STATISTICS ON POLAR PATH VLF ATTENUATION				
PCA DATE	AVE. ATTENUATION ON PATH NPG-PAYERNE (DB)	AVE. ATTENUATION ON PATH NPM-PAYERNE (DB)	AVE. ATTENUATION ON PATH NPG-THULE (DB)	AVE. ATTENUATION ON PATH NPM-THULE (DB)
JULY 7, 1966	10 5	3.7		
AUG. 28, 1966	11 1	.8		
SEPT. 2, 1966	16.8	13.3		
JAN. 28, 1967	19.7	19.6		
MAR. 11, 1967	17.1	4.2		
MAY 24, 1967	10.2	3.3		
JUNE 7, 1967	13.6	1.9		
NOV. 2, 1967	12 5	6.3		
DEC. 3, 1967	17.0	16.3	2 6	3.3
JUNE 9, 1968	10 0	2.8	1.9	2.2
SEPT. 29, 1968	7 6	4 5	1.8	4
OCT. 4, 1968	9 5	5 2	3 6	2 7
OCT 31 1968	8 0	7.2	5.3	1 1
NOV. 18, 1968	18.1	21.1	4.4	1.7
DEC. 5, 1968	16 4	19.1	3.7	7.9
JAN. 24, 1969	9.6	10 1		
FEB. 25, 1969	16.1	6.6		
MAR. 21, 1969	8.8	-1.8 (SLIGHT ENHANCEMENT)		
MAR. 30, 1969	10 8	5.6	2.9	1 0
APR. 12 1969	13 0	1 4		
AVERAGE ATTENU- ATION ALL EVENTS	12 8	7.6	3 3	2.6
% OF EVENTS WITH GREATER EFFECTS ON NPG	85.0		62.5	
% OF EVENTS WITH GREATER EFFECTS ON NPM		15.0		37 5



It may be noted that the average PCA attenuation on the path NPG to Payerne for the 20 events is 12.8 db whereas the average NPM to Payerne attenuation is only 7.6 db. If the paths were identical this difference could be attributed to frequency sensitivity. NPG transmits at a lower frequency, 18.6 KHz, as compared to 23.4 KHz (and earlier 26.1 KHz) for NPM. This increased PCA sensitivity at lower frequencies would be in agreement with the PCA phase effect sensitivity reported on by Westerlund, Reder and Abom, (1968) who concluded that the magnitude of VLF phase anomalies increased with decreasing VLF frequency during 11 PCA events.

The paths NPG and NPM to Payerne are not identical, however. NPM-Payerne is almost 4000 km longer. It passes through the center of the polar cap across Northern Greenland. NPG-Payerne, on the other hand passes through a lower edge of the polar cap through central and southern Greenland.

The average attenuations on NPG and NPM to Thule are 3.3 and 2.6 db respectively. These paths are more similar in that they both run to the center of the Polar Cap. Neither of these latter paths cross the Greenland Ice. The small difference in average attenuation on these latter paths is believed to be attributable to the frequency difference.

The average attenuation at Thule for both NPG and NPM was only about 1/3 of the attenuation suffered along the paths to Payerne.

This is a little surprising unless one can impose some mechanism between Thule and Payerne to produce the remaining 2/3 rds of the attenuation.

An impact zone or an ice-pack zone in central or southern Greenland could explain this increased sensitivity.

The ice pack is there all the time, however, and should produce increased attenuation during quiet periods as well as during PCA's. Though this is generally the case, the ice-pack signal is sometimes very strong and unperturbed. There are also glaring exceptions during certain PCA's when the ice-pack signals are relatively unaffected and the non-ice pack signals are severely attenuated. Thus far, the ice-pack theory cannot explain these.

Individual events data in Table 2 show that 85 percent of the PCA's produced greater attenuation on NPG than on NPM for the Payerne signals. Similar Thule results show 62.5 percent of the events producing greater attenuation of NPG.

The largest average PCA attenuation was produced on the path NPM to Payerne on November 18, 1968 with the average attenuation of 21.1 db for the first 24 hours. The average attenuation on NPG-Payerne was also very high (18.1 db) during this period.

The second strongest event was the January 28, 1967 PCA event which produced average attenuations of 19.7 and 19.6 on NPG and NPM to Payerne.

Events number three and four for next strongest average VLF attenuation are the December 5, 1968 and September 2, 1966 events.

As mentioned at the beginning of this section, peak attenuation is very strong at certain hours during some of these PCA events. This is best shown by examining the diurnal plots of Q-D which were used to calculate the average PCA attenuation.

Figure 4 is a sample of the Q-D plots which were obtained by subtracting the disturbed value of the VLF field strength from the quiet day field strength. The Q-D values in db are calculated for the first 24 hours of the PCA.

The ordinate in Figure 4 represents the amount of absorption or attenuation of the VLF signal at each hour of the day during the first PCA day.

The Q-D plots in Figures 4, 5, and 6 are shown for each of the twenty PCA's listed in Table 3.

Note that the VLF attenuation fluctuates quite radically during the first day of the PCA. The NPM data is particularly subject to rapid fluctuations but is definitely less sensitive in the average attenuation to that of NPG.

Note that the January 28, 1967 event produces the greatest average attenuation with the Signal being lost during the period from 1200 to 2400.

The event of August 28, 1966 produced noticeable enhancement of the NPM-Payerne signal during the early hours of the day.

All of the selected PCA's hit peak attenuations of at least 25 db for short periods during the initial 24 hours.

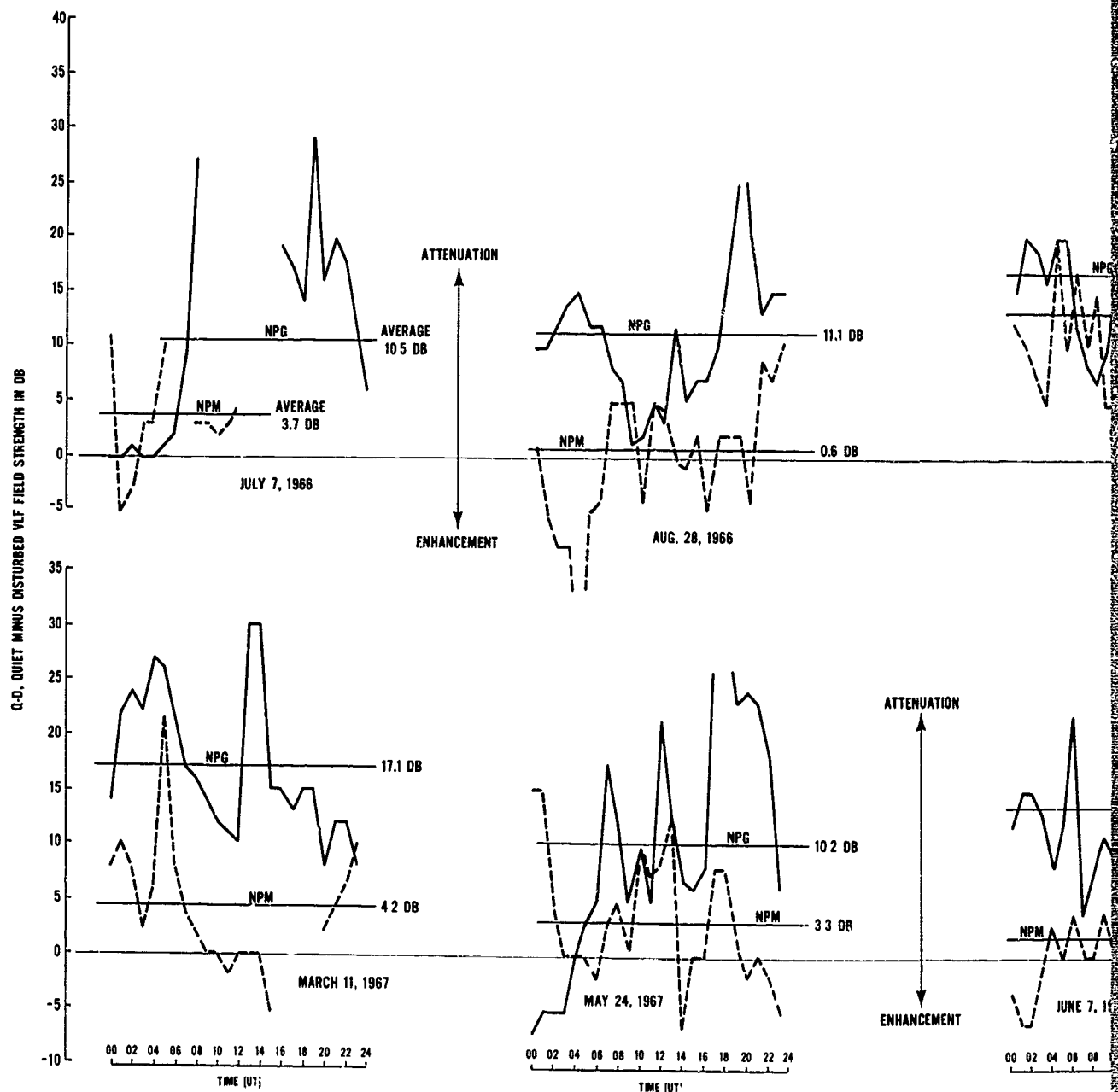


FIG. 4 VLF ATTENUATION DURING FIRST 24 HOURS OF SELECTED

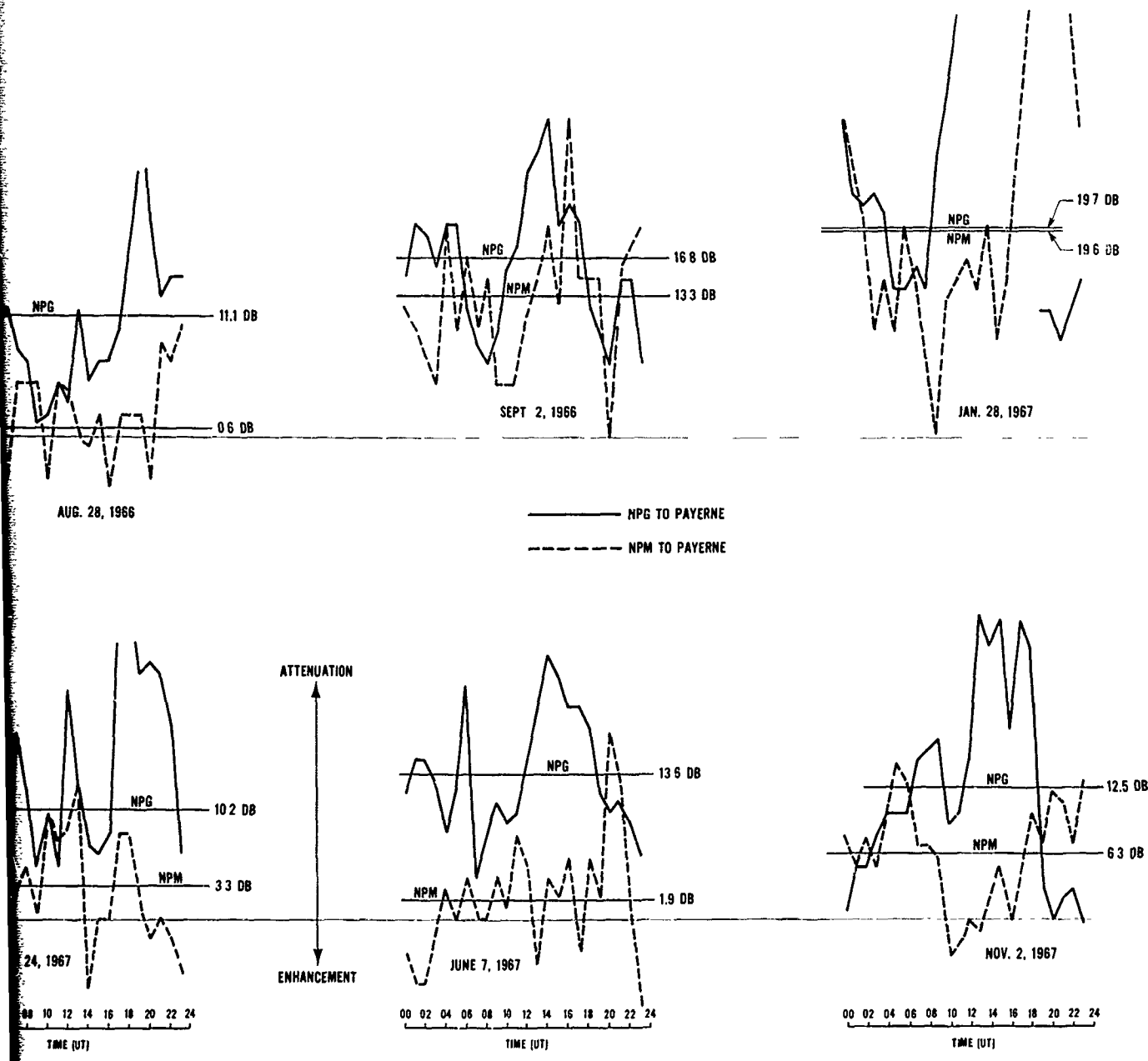


FIG. 4 VLF ATTENUATION DURING FIRST 24 HOURS OF SELECTED PCA'S

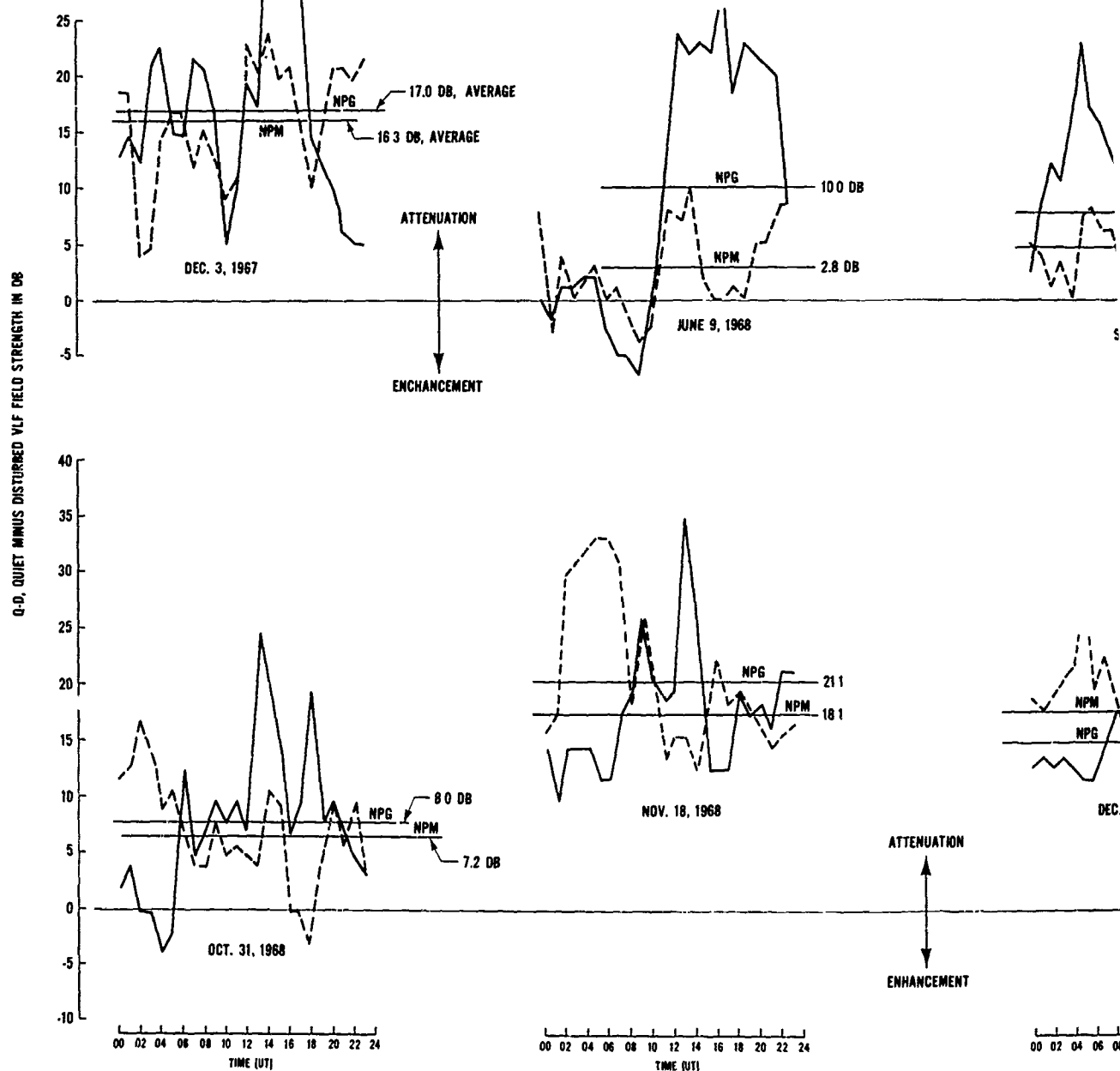


FIG. 5 VLF ATTENUATION DURING FIRST 24 HOURS OF SELECTED

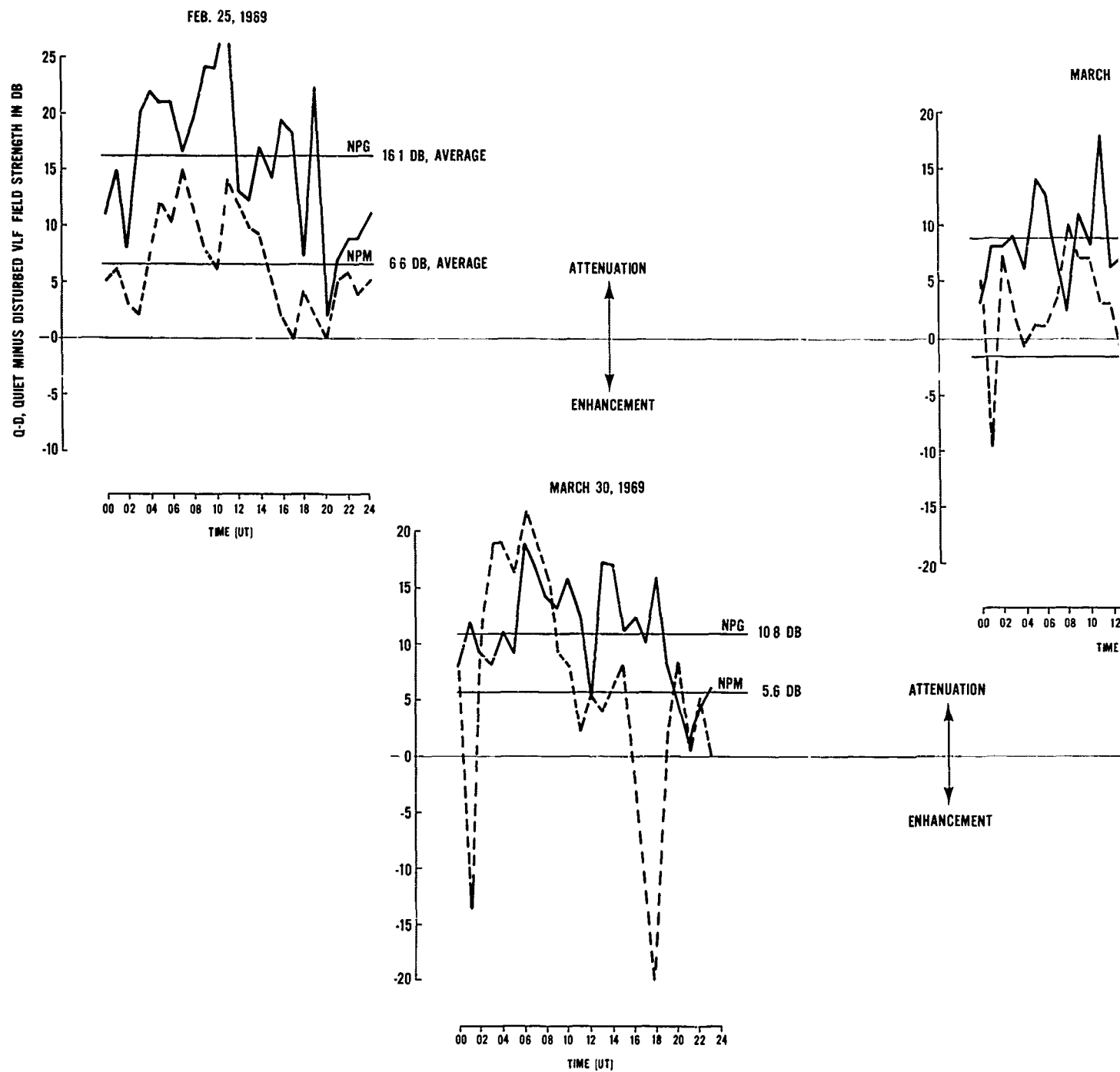
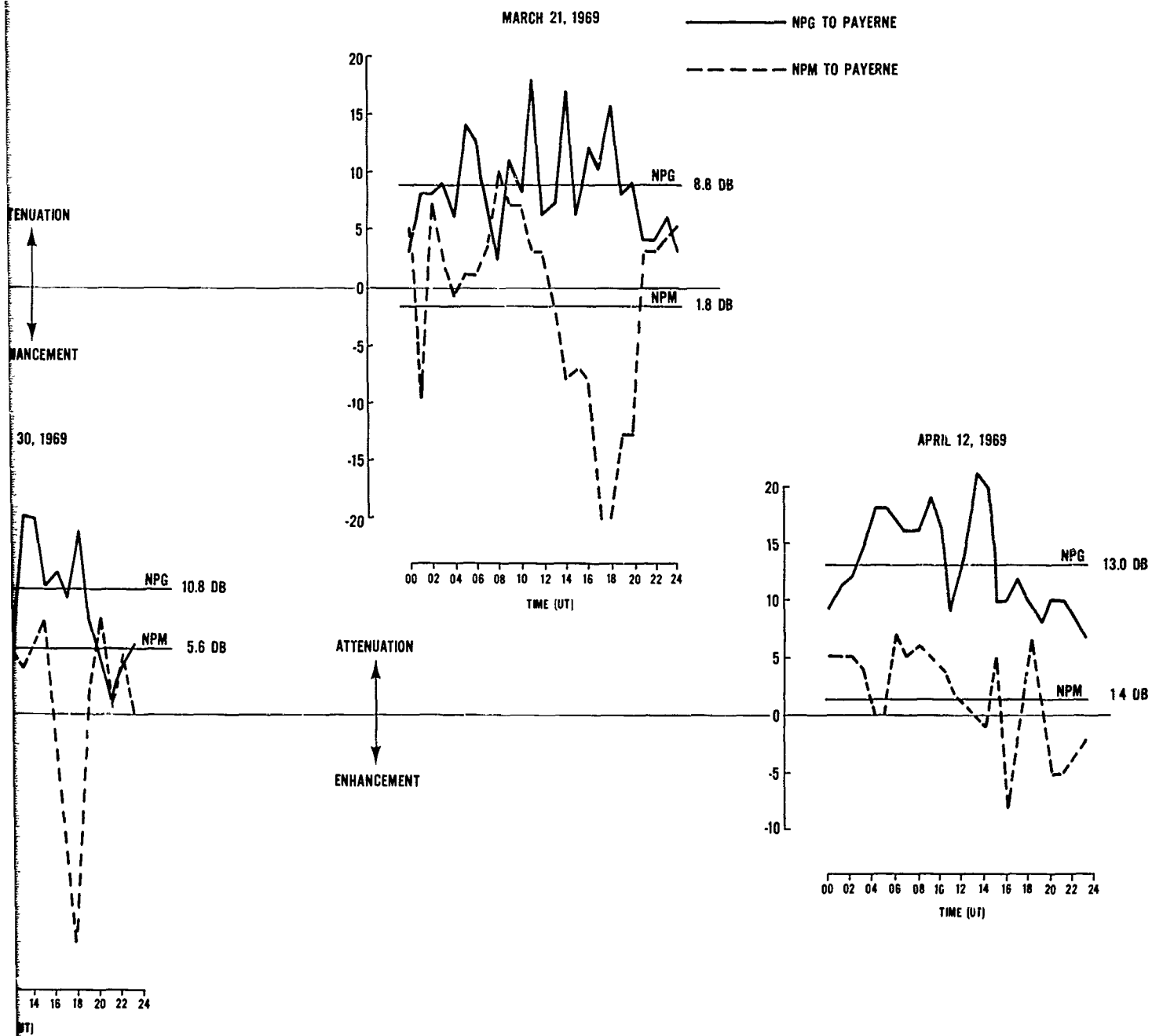


FIG. 6 VLF ATTENUATION DURING FIRST 24 HOURS OF SELECTED PCA'S



6 VLF ATTENUATION DURING FIRST 24 HOURS OF SELECTED PCA'S

The peak VLF attenuation on NPM-Payerne has a tendency to lag the peak VLF attenuation on NPG to Payerne on all events shown in Figure 4 except the July 7, 1966 event. An examination of the other 12 events (Figures 5 and 6) indicate an opposite effect -- that is -- a tendency for NPG to lag NPM.

The large ground level events of January 28, 1967 and November 18, 1968 both produced outstanding time lags in peak VLF attenuation on the NPG and NPM to Payerne paths.

The January 28 event peaked 6 hours later on NPM than it did for NPG as shown in the upper right hand portion of Figure 4.

The November 18 event peaked 7 hours earlier on NPM than it did for NPG as shown in Figure 5.

The fluctuations in VLF attenuation during PCA's might correlate closely with the actual proton flux which produces the PCA.

Although it has been shown by Oelbermann et al., (1967) that gross correlations exist, a statistical cross correlation study has never been done.

The hourly peaks in Q-D in Figure 4, 5, and 6 should be compared with particle data to determine these correlations.

Some calculations of the standard deviation of polar path VLF field strength have been made for a few PCA's and quiet periods.

In order to minimize sunrise-sunset effects the VLF field strength for NPG and NPM was measured at 0400 and 1600 UT. These are the hours when these paths are dark along the entire path or daylit along the entire path-i.e., there are no sunrise terminators on the path at this time.

The 0400 and 1600 readings were carefully selected from five quiet days around each equinox and each solstice for the years 1965 to 1968.

The quiet-day standard deviations in db for June 1965 to March 1968 are listed in the top section of Table 3.



TABLE 3. STANDARD DEVIATIONS (DB) NPG AND NPM TO PAYERNE SIGNAL STRENGTH DURING 5-DAY QUIET PERIOD AND DURING PCA'S.

DATE		NPG		NPM	
		NIGHT 0400	DAY 1600	NIGHT 0400	DAY 1600
QUIET DAYS	JUNE 1965	1.0	3.1		
	SEPT. 1965	2.4	0		
	DEC. 1965	4.4	4.6		
	MAR. 1966	6.8	4.7		
	JUNE 1968	0	0	0	1.3
	SEPT. 1968	4.5	2.4	4.7	6.0
	DEC. 1968	4.3	1.6	4.2	3.5
	MAR. 1968	2.8	2.5	2.8	8.7
PCA DAYS	SEPT. 2, 1966	6.8	8.5	8.0	14.0
	JAN. 28, 1967	8.9	13.5	6.0	6.0
	JUNE 9, 1968	1.0	10.5	6.7	2.0
	DEC. 5, 1968	5.5	4.1	9.1	5.7

No definite seasonal or daily trends seem obvious in the quiet day values which range from 1.0 db to 8.7 db. NPM standard deviations of VLF field are slightly higher than NPG's, particularly at night (1600).

In order to examine PCA effects on the standard deviation, VLF field strength of NPG and NPM to Payerne were also measured for a five-day period centered on the date of the PCA for four events. These are listed in the bottom section of Table 3.

Note that the standard deviations are definitely higher for the PCA data although there is still a wide range of s values from 1.0 to 14.0 db. The standard deviations of the disturbed samples are larger than those of the quiet samples because each 5-day PCA sample contains the change from quiet to disturbed conditions.

The greatest variability appears to be in the nighttime data and for the PCA's of September 2, 1966 and January 28, 1967.

These results are expected. The nighttime fluctuations of VLF field strength have always been greater than daytime fluctuations. The PCA's of September 2, 1966 and January 28, 1967 were very large events.

The five day method of calculating and comparing standard deviations will always yield an increase in S during the PCA sample.

It is also desirable to have a measure of hour to hour field strength variations within a PCA compared to field strength measurements during a quiet period.

Table 4 is a listing of the standard deviations of NPG to Payerne field strength in db for five hour periods within quiet days and within PCA's.

TABLE 4. STANDARD DEVIATIONS IN DB OF HOUR TO HOUR NPG-PAYERNE FIELD STRENGTH DURING QUIET DAYS AND PCA DAYS.			
		NIGHTTIME	DAYTIME
SEPT. 2 PCA 1966:	QUIET DAY	6.4	2.8
	PCA	1.6	5.8
DEC. 3, 1967:	QUIET DAY	1.7	3.7
	PCA	2.6	6.4
NOV. 18, 1967	QUIET DAY	.4	5.2
	PCA	1.7	8.0

In each case the five hourly samples were selected around 0400 and 1600 which represent nighttime and daytime respectively.

Within each PCA and within two out of three of the quiet days the daytime variability was higher than the nighttime variability in Table 4. This is a little surprising but might be accounted for by the fact that the polar path days were very short during November and December so that the 5 hour sample period might have included some sunset fades.

Except for one case, the nighttime September 2, 1966 PCA data, the data in Table 4 indicate a definite increase in S during a PCA. PCA S values are almost double the quiet-day S values for most cases.

Table 5 lists the standard deviation of NPG-Payerne field strength for five-hour nighttime and daytime periods during a series of days which include the November 18, 1968 PCA event.

TABLE 5. STANDARD DEVIATIONS OF NIGHTTIME AND DAYTIME NPG-PAYERNE FIELD STRENGTH THROUGH NOV. 18, 1968 PCA.							
	NOV. 16	17	18	19	20	21	22
NIGHT 0200-0600	.4	1.0	1.6	1.7	1.4	5.5	1.9
DAY 1400-1800	5.2	2.9	6.0	8.0	10.6	3.1	3.1

Note that the nighttime S value increases from .4 db on November 16 and 1.0 db on November 17 to 1.6 and 1.7 db on November 18 and 19.

The daytime S values which are larger than the nighttime values by several db also show a definite increase in data spread during the PCA.

The statistical data study should be extended to a study of the normal phase, rapid phase and rapid amplitude variations during quiet periods and during PCA periods.

Polar and transpolar statistics should be compared with low latitude statistics in any future work in this area.

#### IV. A DISCUSSION OF SOME RAPID PHASE VLF MEASUREMENTS AT THULE

Approximately two years ago, HRB-Singer started development on a technique and system for measuring rapid VLF phase perturbations which are beyond the tracking speed of normal VLF receivers.

This system has operated at Thule, Greenland for over a year now and has produced a supply of rapid-phase VLF tapes which can be analyzed to provide information on rapid, ionospheric phase shifts.

This section of the report will briefly describe the rapid phase recording and processing system and some sample results which have been obtained.

##### A. PURPOSE OF THE RAPID PHASE VLF MEASUREMENTS

The main purpose of these measurements is to determine the phase rate of VLF perturbations when the perturbations exceed the tracking capabilities of the normal VLF receiver (which employs an electronic servo).

We are concerned here with the possible vulnerability of an MSK VLF system if the phase shift during a solar flare or Cosmic event happens to exceed a rate which will cause loss of sync or loss of information.

With the advent of other systems besides CW Morse code such as FSK, coherent FSK, and MSK, the importance of synchronous detection has increased. Since many of these systems are used to transmit teletype signals, the detection of the bit becomes important rather than the detection of a letter. When using teletype, the redundancy is much less than that of Morse Code.

For a minimum shift keying system, MSK, operating at 50 baud, the length of a bit is 20 ms. In an MSK system, the detection technique is that of deciding which of four orthogonal phase values the carrier represents during any bit. Therefore, a bit error exists when the phase is in error by greater than  $45^{\circ}$ , caused by a rapid phase shift during the bit. A phase shift of  $45^{\circ}$  in 20 ms is the same as a phase rate of 8 ( $45^{\circ}$ ) in 8 (20 ms) or 1 cycle in 160 ms or 6 cycles in 1 sec. Therefore, for no error to be detected in such a system, any phase rate must be less than 6 cycles/sec. We, therefore, desire to detect phase rates greater than 5 cycles/sec. This refers to short-term phase variations only, those lasting for few seconds and then returning to the previous values.

## B. RAPID-PHASE RECORDING AND PROCESSING SYSTEM

The HRB-Singer rapid-phase recording and processing system consists basically of three assemblies which may be used together or separately in conjunction with communications and laboratory equipment to produce new information on rapid phase and amplitude variations.

The three blocks consists of:

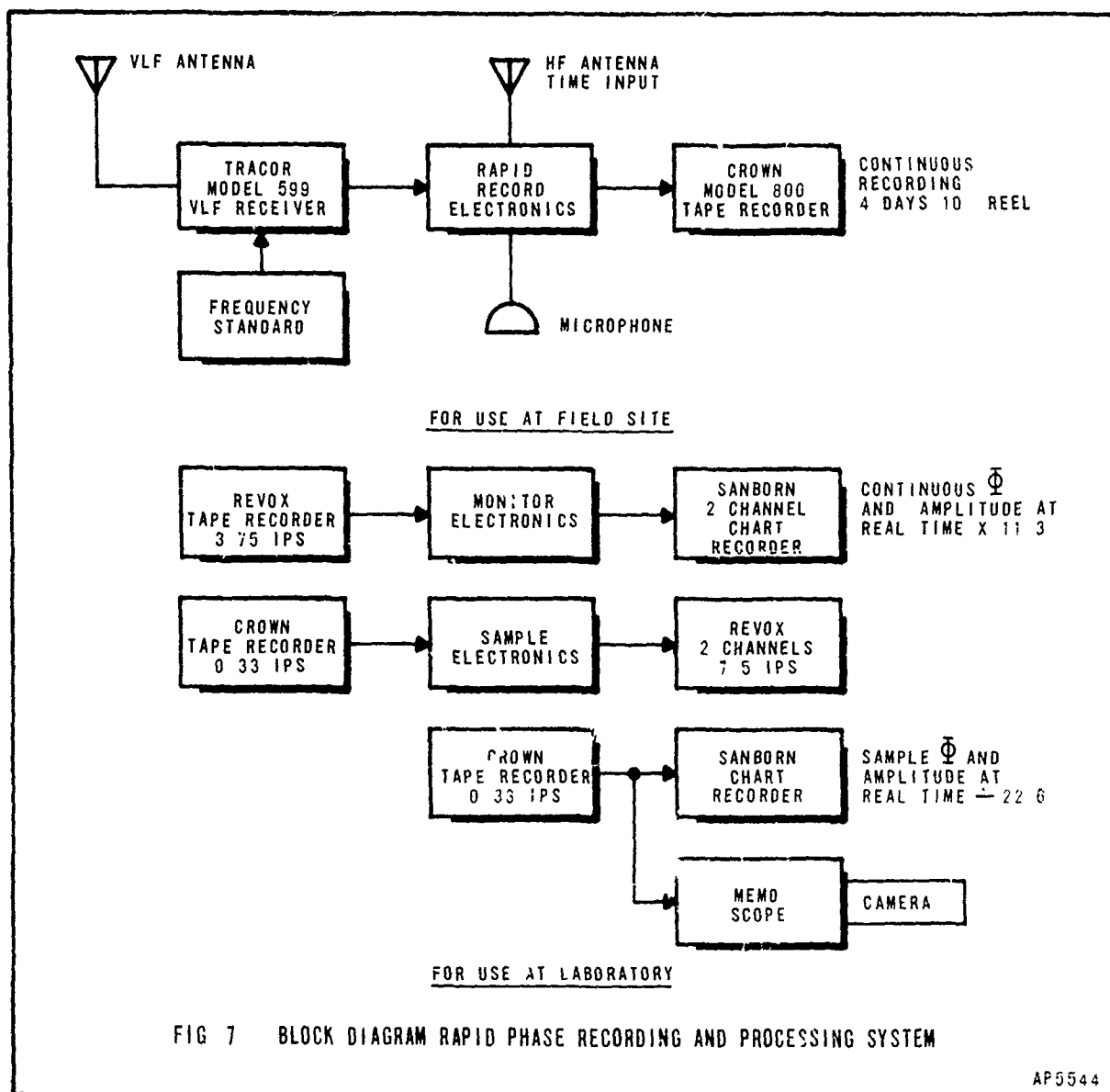
1. A record system
2. A monitor system
3. A sample system

Figure 7 is a block diagram which illustrates the deployment of the record, monitor and sample electronics along with a VLF receiver and various laboratory equipments. Data are collected at a field site using 10 inch reels of tape. The tapes are sent back to the laboratory and analyzed using continuous monitor and/or sample electronics.

In the monitor mode phase error between the 1 kHz IF signal and the restored 1 kHz phase shifted reference is monitored continuously on a 2-channel chart recorder.

In the sample mode the direct 1 kHz IF voltage and the 500 cps standard output are separated, converted to low audio frequencies and displayed on a Sanborn Model 322 dual channel chart recorder or a Tektronix Model 564 storage oscilloscope.

In the monitor mode, phase error rate is limited by the response time of the filters, phase detector amplifiers and chart recorder. This is a design parameter which can be altered to meet any particular situation. Maximum ionospheric VLF phase rates which have been observed on polar propagated signals are on the order of 600 degrees per second.



There is not much point in using the rapid-phase processor "on-line" for analysis of VLF phase data since large VLF phase anomalies are not very frequent--even over the polar paths. Impractical quantities of chart paper would be required for this operation. For this same reason, since large, fast phase anomalies do not occur frequently at VLF, a VLF fast-phase system should record continuously in order to avoid missing an important anomaly.

### C. RAPID PHASE RECORDING

Figure 8 is a block diagram of one channel of the HRB-Singer rapid phase recording system which has been operated at Thule, Greenland, for the past year.

The rapid phase recording system derives its input directly from a TRACOR model 599 VLF receiver which is being used to collect normal phase and amplitude data in chart form.

The rapid phase system utilizes two outputs from each VLF receiver, the phase-shifted 1 kHz reference voltage (standard square wave) and the 1 kHz keyed IF output. Both of these are available on the rear panel of the receiver.

Since two 1 kHz signals cannot be recorded on the same channel, the 1 kHz square wave is divided by two and the resulting 500 cps sine wave is added to the 1 kHz IF in an audio mixer. Spot voice announcements are added to identify the recording and to provide information on data and time. Hourly time marks are provided by a clock timer which interrupts the power supply voltage once per hour for a duration of approximately one minute.

The composite signals are recorded directly on one channel of a Crown Model 800 Tape Recorder operating at a speed of .33 inches per second. The bandwidth of the tape system is 300 cps to 3 kHz at the selected recording speed. The Crown System utilizes 10 inch tape reels which permit four (4) days of continuous data to be recorded on each reel.

### D. DATA REDUCTION

Two methods have recently been used at State College to reduce and analyze the rapid-phase VLF tapes from Thule, Greenland.

The first method uses a zero-crossing, synchronous phase detector to produce a continuous measure of the phase difference between the signal IF and the reference voltage.

When this method is employed, the raw Thule tapes are played back at more than ten times the recording speed to save analysis time. (Since the IF and reference are multiplexed onto the same tape channel, their phase relationship is preserved through all changes in recorder speed.)

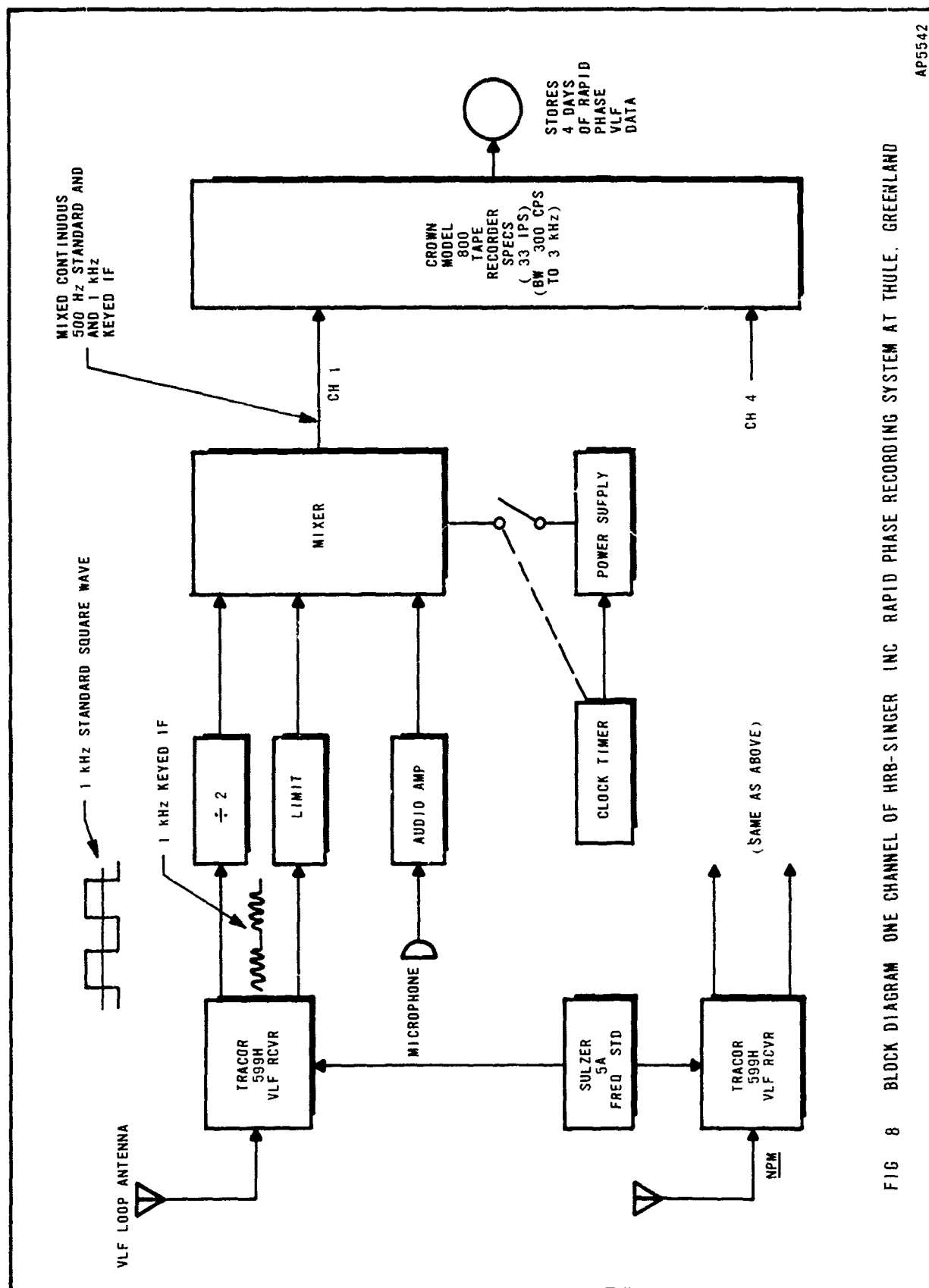


FIG 8 BLOCK DIAGRAM ONE CHANNEL OF HRB-SINGER INC RAPID PHASE RECORDING SYSTEM AT THULE, GREENLAND

AP5542

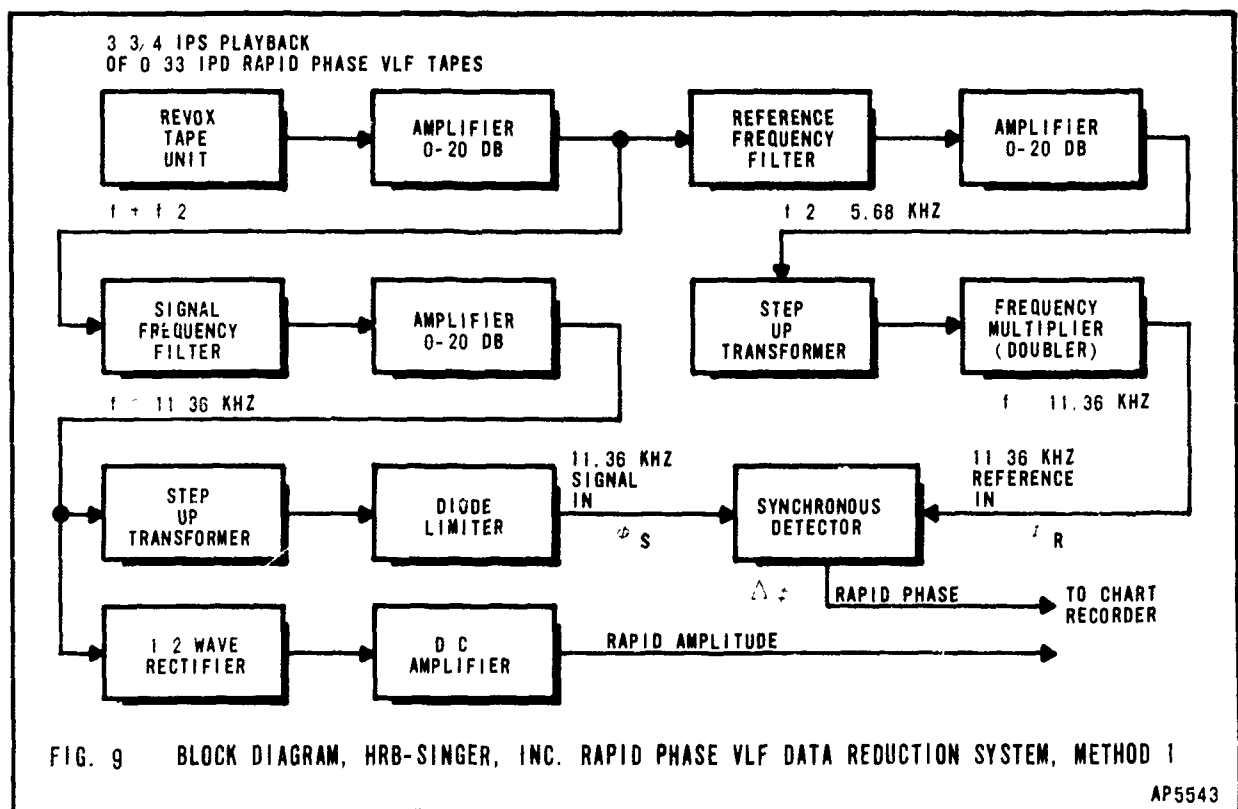


A second method which has been used for data reduction is simply a display technique which involves exactly the opposite of method 1, or downward frequency conversion which results from successively re-recording the data at higher speeds and playing it back at lower speeds until it can be studied on a chart recorder or memo-scope. Although this second method can be tedious, it permits one to study changes in phase within a single RF pulse (dot or dash) and on a pulse to pulse basis.

Duty cycle does not affect the determination of the phase in the latter system. Since pulse rise and decay phase shifts can also be avoided by selecting a group of carrier cycles within the constant phase center of each pulse, very accurate determination of ionospherically-induced phase variations can be made.

#### 1. Method 1

Figure 9 is a block diagram of the phase detector system used in Method 1. Thule VLF tapes which were initially recorded at .33 inches per second on a Crown Recorder are played back at 3-3/4 inches per second on a REVOX tape unit. Thus the multiplexed signal and reference frequencies are automatically



multiplied by 11.36, the ratio of playback to record speeds. The 11.36 kHz signal and the 5.68 kHz reference are separated by filters, amplified, limited and fed to a synchronous detector which yields a voltage proportional to the phase error between the signal and the reference:

$$E_o \sim \left[ \left| \cos \frac{1}{2} \cdot \left( \theta + \frac{\pi}{2} \right) \right| - \left| \sin \frac{1}{2} \cdot \left( \theta + \frac{\pi}{2} \right) \right| \right] \quad (1)$$

A linear shift of signal phase or reference phase will trace out this function.

A 180 degree phase shift can show up in a number of forms depending on the initial phase and the sense of the change. Sample 180° outputs are shown in Figure 10.

These outputs are essentially a measure of the phase error between the IF and the phase-shifted reference output of a TRACOR Model 599H VLF receiver with the phase servo time constant set on T = 50 seconds.

Because we are looking only at phase rates in excess of the tracking speed of the VLF receiver we do not see slow diurnal phase changes due to sunrise and sunset effects and the slow phase components of solar flares and PCA's.

Phase rates which exceed the tracking capability of the VLF receiver will however, appear as changes or discontinuities in the recording followed by slow recovery as the reference signal is corrected by the electronic phase shifter.

If the phase continues to shift steadily in one direction, the phase error curve will trace out a series of triangular waves which disclose the total amount and the rate of phase shift.

Figure 11 is an example phase record which shows the effects of sudden 180 degree phase reversals produced by switching the antenna terminals.

The slow recovery of phase following these reversals is due to the servo acting on the reference signal to correct its phase to the new value.

The triangular curves in Figure 11 are due to manual slewing of the receiver L. O. at a linear phase rate to simulate a steady phase shift of the VLF signal.

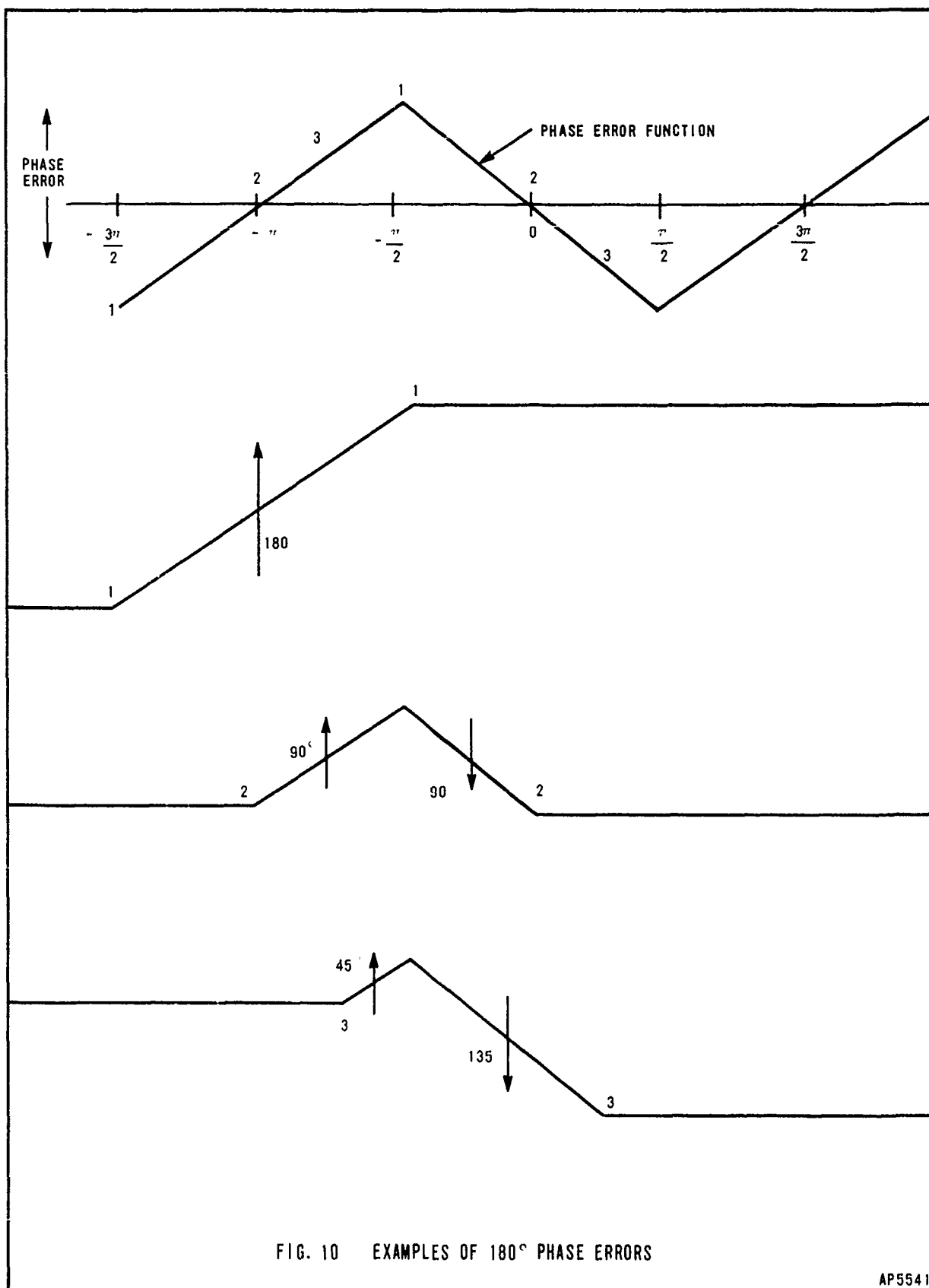


FIG. 10 EXAMPLES OF 180° PHASE ERRORS

AP5541

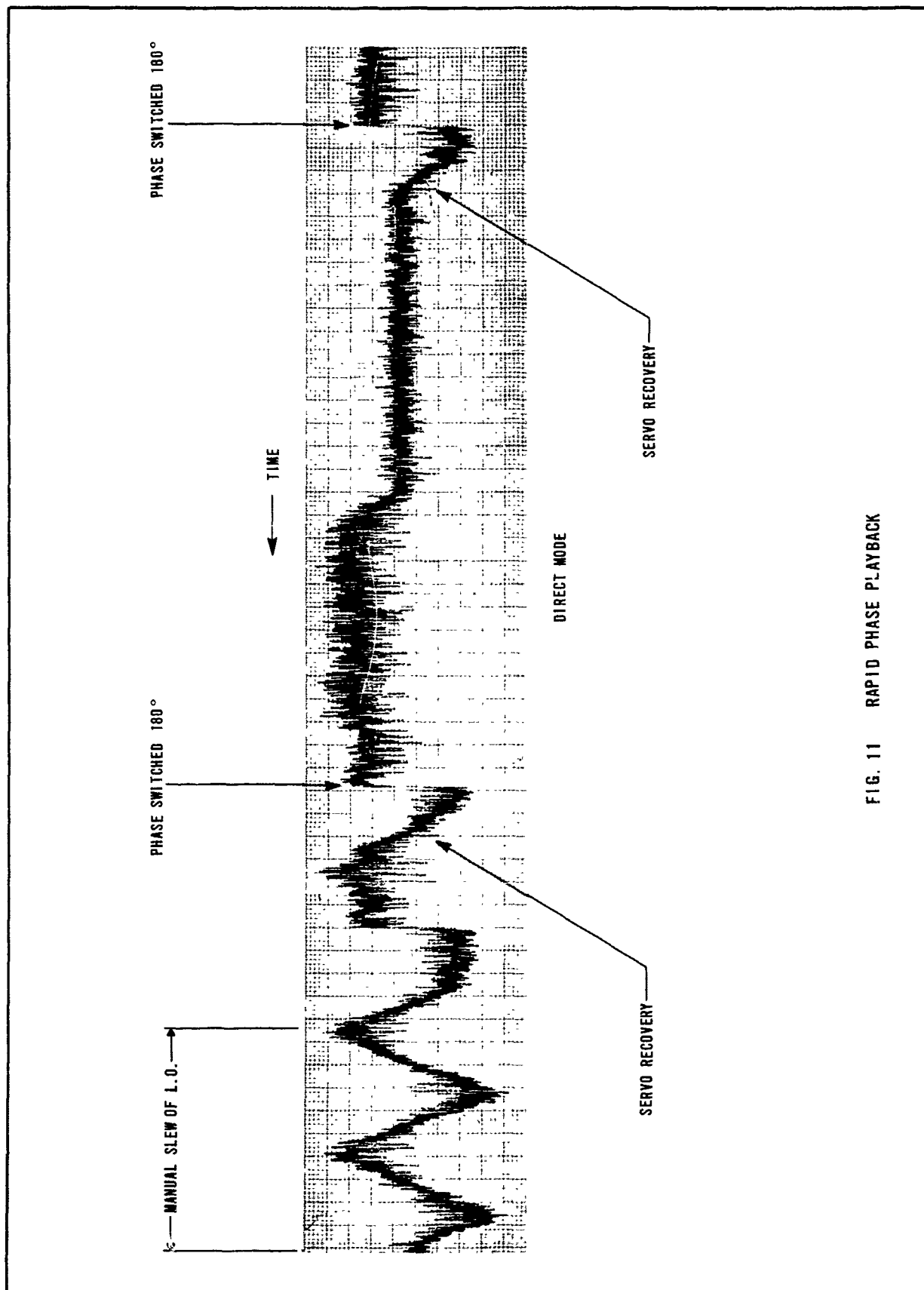


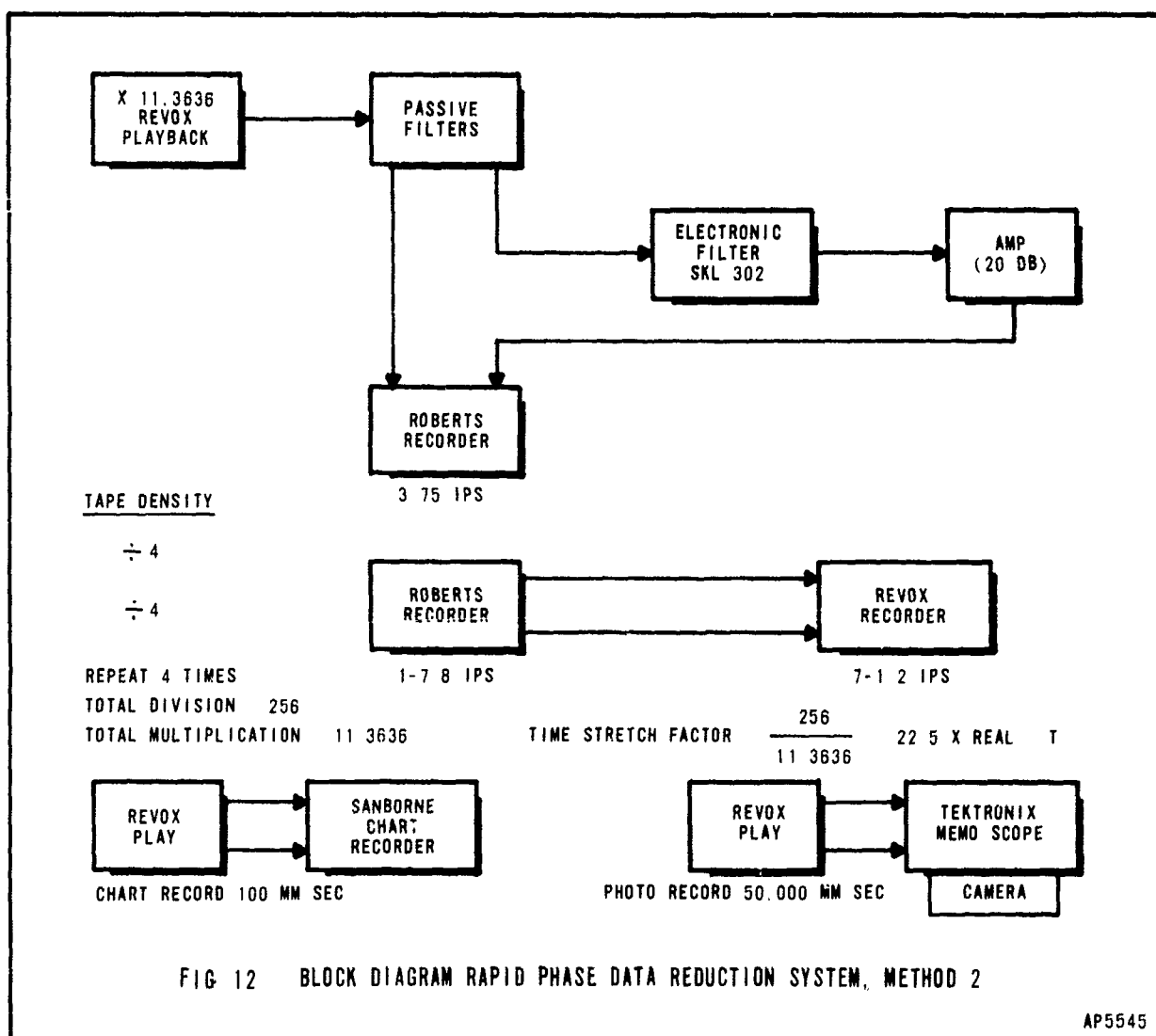
FIG. 11 RAPID PHASE PLAYBACK

## 2. Method 2

The block diagram in Figure 12 illustrates the second method of reducing and displaying the rapid phase VLF data for study of pulse-to-pulse changes.

Initially the raw tapes are played back at 3-3/4 IPS through the passive filters of the Method 1 system which separate the IF and standard. The separate outputs are recorded on two channels of a Roberts Tape Recorder which is operated at 7-1/2 IPS thereby dividing the tape density by two.

Stages 2, 3, and 4 in the reduction involve playback on the Roberts tape recorder at 1-7/8 IPS and recording on the REVOX system at 7-1/2 IPS. This results in a tape density division of  $4 \times 4 \times 4 = 64$ . A final division of 2 yields



a total division of 256 which combined with the initial multiplication of 11.36 results in a time stretch factor of approximately 22.5.

The Method 2 system could be accomplished in only one step if a Crown playback unit were available in State College. A signal playback at .33 IPS and recording at 7-1/2 IPS yields the same time stretch factor. The new system would, of course, require new filters to separate the 1 kHz IF signal and 500 cps reference.

Results of the Method 2 reduction can be displayed continuously on a chart recorder or sequentially on a memo-scope.

Figure 13 illustrates a sample of each of these. All time is real time. The interrupted dash was produced by shorting the input terminals to the Roberts Recorder at 1618 UT.

The selected data were obtained during an apparent modal phase step which occurred during the early part of the November 18, 1968 solar proton event. Further discussions of these data will follow in the results section.

The slow chart presentation in Part A of Figure 13 is useful for observing the instantaneous amplitude of the coded signal during disturbances. It yields visual evidence of sudden changes in duty cycle or manmade interference which might be confused with the natural propagation effects.

Fast chart playback, Part B of Figure 13 allows pulse-to-pulse comparison of the phase difference between the code and the reference signal.

Part C of Figure 13 is a photo-mosaic representation of the interrupted dash which is superimposed on the reference waveform using a memoscope.

In this representation it is possible to observe large, rapid phase shifts during the formation of the pulse.

During a 10 millisecond period, the IF in Figure 13 shifted approximately 40 degrees. This is  $4000^{\circ}$  per second or 11 Hz phase rate.

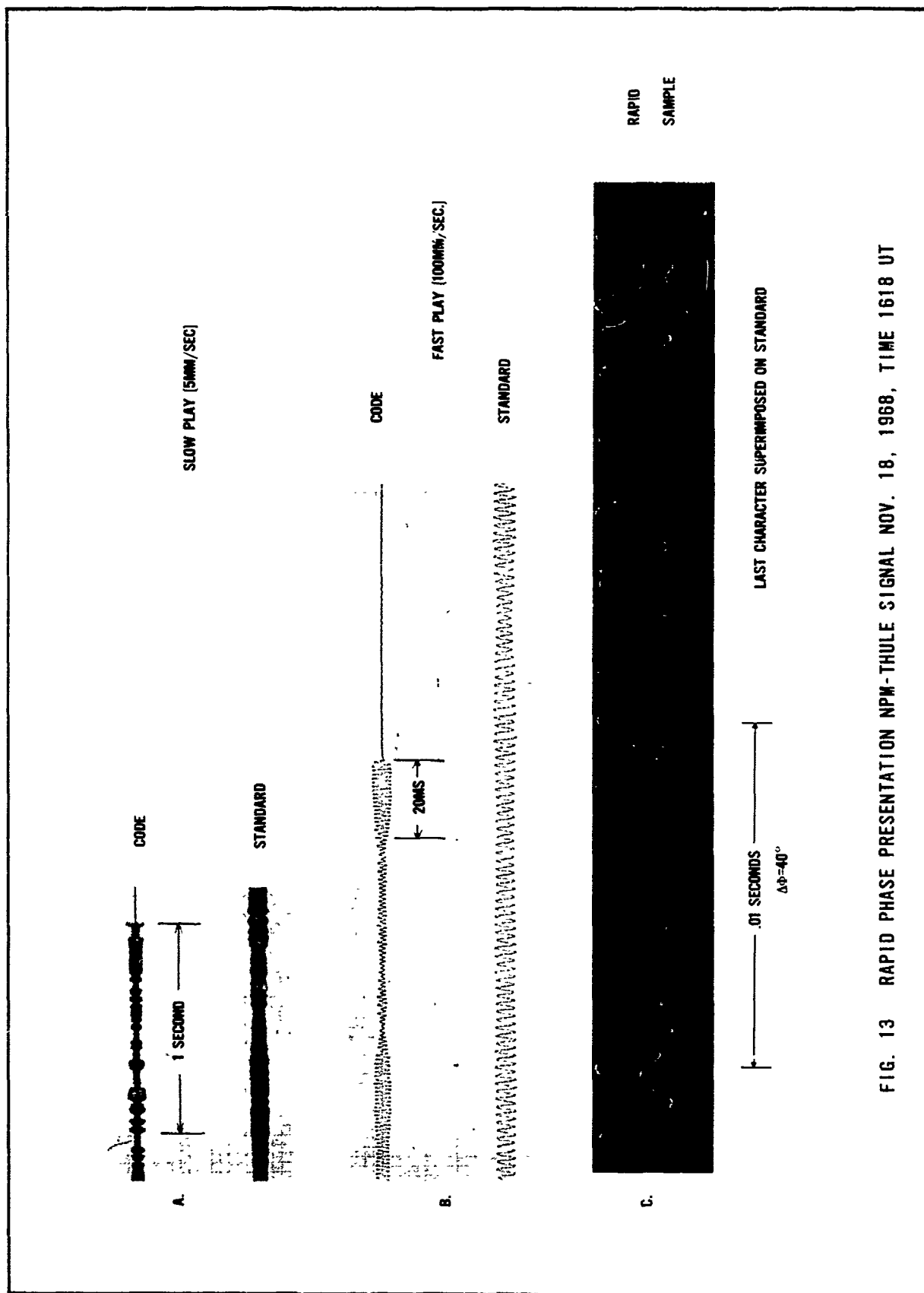


FIG. 13 RAPID PHASE PRESENTATION NPM-THULE SIGNAL NOV. 18, 1968, TIME 1618 UT

## E. RAPID PHASE RESULTS

The most rapid phase change encountered thus far in this study is the phase change which occurs during the formation of the rf pulse at the transmitter. An example of this has been shown in Figure 13.

This phase change of 40 degrees in .01 seconds is 4000 degrees per second or 11 kHz.

This rapid phase change is due mainly to the high Q of the VLF transmitting antenna. The Q is so high that the code elements become very rounded or "soft". The results is a shift in the phase of the code pulses during rise and fall times. This effect is simply averaged out in the normal operation of the VLF receiver but must be carefully considered in the rapid-phase system.

When one speaks of average phase it must be recognized that the average is taken over a great number of bauds or code elements. Theoretically, the only way succeeding pulses can stay in phase is for the sum of the pulse decay and formation phase shifts to equal 360 degrees or a multiple of 360 degrees.

The rapid-phase system has shown that the constant phase portions of succeeding pulses remain in phase depending only on the variation in the ionosphere.

Ionospherically induced VLF phase changes are normally much slower than the equipmental phase shifts described above. The most rapid ionospheric phase changes appear to be connected with the occurrence of modal phase steps and cycle slippage on the NPM to Thule path during sunrise-sunset transitions.

This effect which has been treated throughly by (Crombie, 1964) seems to be accentuated during PCA's causing complete and rapid dropout of the VLF signal at times.

Figure 14 is a composite chart which compares some normal and rapid phase VLF data for the path NPM to Thule during sunset and during a PCA of February 28, 1969 when cycle slippage occurred.

The data on the left are all normal phase and amplitude data with servo time constant  $T = 50$  seconds. The data on the right are rapid phase and amplitude at selected time constants. Note that time for the normal phase and amplitude records runs from left to right. Time runs in the opposite direction for the rapid-phase data.



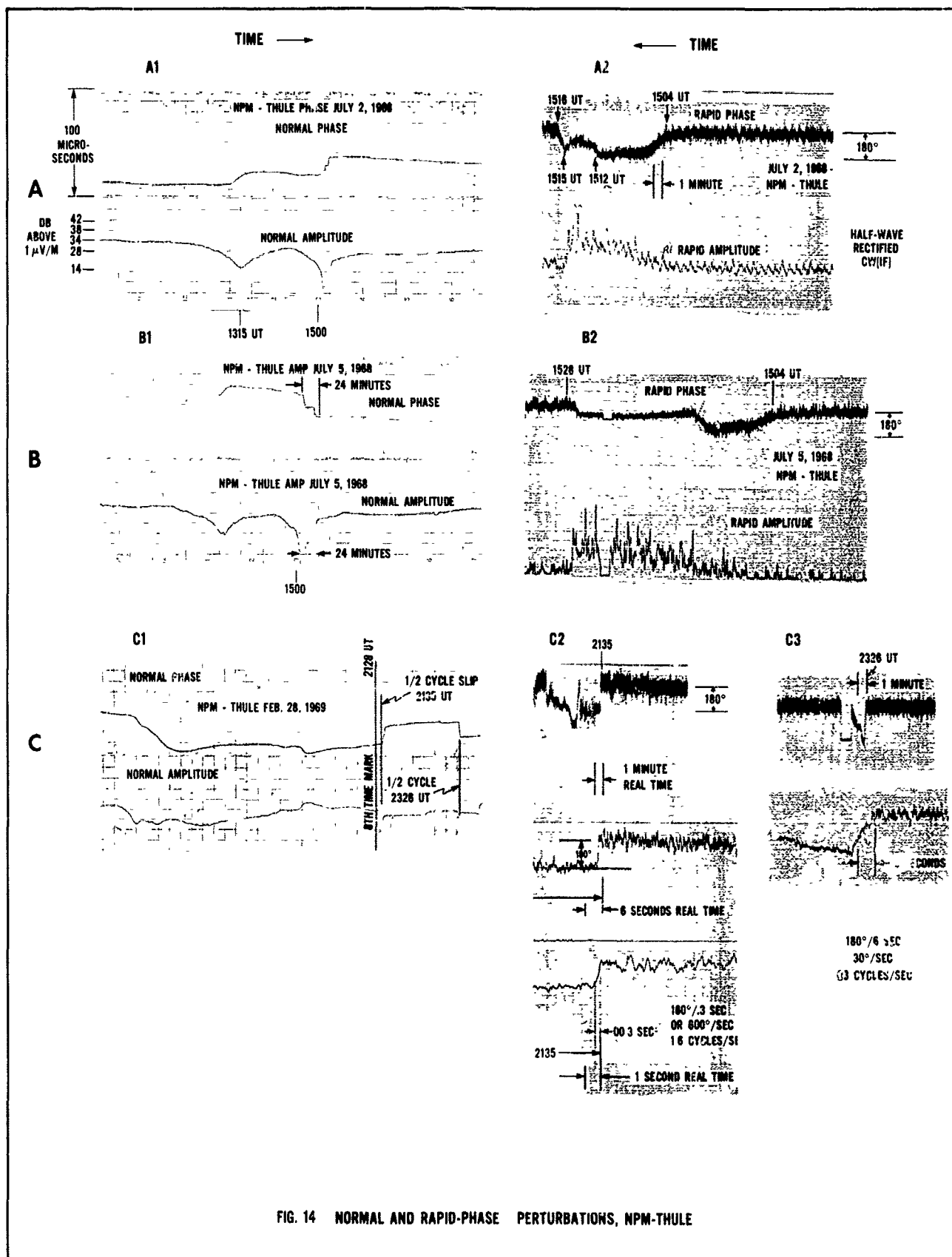


FIG. 14 NORMAL AND RAPID-PHASE PERTURBATIONS, NPM-THULE

Part A1 of Figure 14 is a classic example of SUNSET fades on the NPM to Thule path on July 2, 1968. Note the smooth phase step (advance) in the upper record the center of which coincides with a smooth fade at 1315 UT a second step at slightly after 1500 UT causes loss of synchronization indicated by the first plateau in the normal phase record. (When the servo in the TRACOR receiver unlocks, it leaves the phase shifter at the last setting producing a flat phase record until sync is regained.)

In this example, sync is regained momentarily but lost again, hence, the second plateau. On the second try, the servo regains lock after a total phase slip of approximately .21 microseconds (1/2 cycle).

The rapid-phase record in part A2 of Figure 14 (heavy trace) illustrates rather dramatically the phase rate errors during this 12 minute period. Reading the top record in part A2 from right to left one sees a phase error being at 1504 UT with a downward transition to a bottom plateau. The rapid-phase transition corresponds to the first phase step on the normal phase data during the period when the transition was too fast for the servo to follow it. Maximum tracking speed on the Tracor Servo is 51 degrees/min when  $T = 50$  seconds. The indicated phase rate between 1504 UT and 1505 UT is approximately 67 degrees/minute.

The plateau in the rapid phase data corresponds to a time interval of five or six minutes when the IF signal was lost, leaving the phase detector with a constant voltage on it. At 1512 UT and 1515 UT, the second and third phase errors appear. Respective phase rates are approximately 70 degrees and 90 degrees/minute. Part B1 in Figure 14 is the normal VLF phase and amplitude record during a sunset transition on the NPM to Thule path for July 5, 1968.

In this case, the phase steps shortly after 1500 UT, are in the opposite direction or direction of retardation.

Again the rapid phase data in part B2 indicate phase rates which are too rapid to be tracked by the Tracor receiver but much slower than the transmitter phase shifts. In each of the three transitions, the phase rate is approximately 60 to 70 degrees per minute. The sense of the phase error in A2 and B2 rapid phase presentations is the same even though one represents an advance and the other a retardation of phase.

The reason for this is that the phase detector has a tendency to remain at  $-\pi/2$ , a peak in the phase error function, due to fixed phase shifts in the system. Any phase change of the IF (an advance or a retardation) will produce a negative going phase error output.

The rapid amplitude records in A2 and B2 are simply i. f-wave rectified IF signals. The increase in amplitude during the phase anomalies is due to the AGC voltage going to zero during the rapid phase shifts. The AGC voltage in the Tracor receiver is derived from a quadrature detector.

Part C1 in Figure 14 is a normal phase representation of cycle slippage which occurred on the NPM-Thule signal during a PCA on February 28, 1969. The VLF phase underwent a rapid advance with slippage of  $1/2$  cycle at 2135 UT.

The rapid phase playback of this transition in C2 illustrates that the playback speed used when A2 and B2 is too slow to represent this phase change. The top record in C2 is charted at 1 mm/second (the same as A2 and B2). The second record in C2 is the initial transition at 2135 charted at 20 mm/second. This speed is also too slow to disclose the rate of the rapid phase change. The third record in C2, which is charted at 100 mm/second, indicates that the phase changed at a rate of 180 degrees in approximately 0.3 seconds during this transition, or at a rate of 1.6 cycles per second.

A second 180 degree phase step at 2326 UT, which returned the VLF phase to its normal value, produced the rapid phase record shown in C3. The phase rate for the second step is approximately 180 degrees in 6 seconds or .08 cycles/second. There is no need to play this back at speeds greater than 20 mm/second.

Parts A2, B2, C2 and C3 of Figure 14 are only four samples of the type of rapid phase shifts which are produced by the ionosphere during sunrise-sunset changes and during certain PCA's. It cannot definitely be ascertained that the rapid phase shifts in C2 and C3 are due to the PCA.

A power spectrum analysis or even a simple correlation study of phase rates during PCA periods and non-PCA periods might disclose whether these rapid shifts are a result of the PCA.

Rapid VLF phase shifts have occurred in other PCA's, notably during the November 18, 1968 event.

The normal phase and amplitude for this event are shown in Figure 15. Part A of Figure 15 is the VLF phase and amplitude record for NPM to Payerne, Switzerland. Part B is NPM to Thule, Greenland, Part C is NPG to Payerne and Part D is NPG to Thule.

In all four cases, the PCA, which begins about 1045 UT, produces phase advances, upward deflection of phase recorder, and attenuation of the polar or transpolar VLF signal to abnormally low levels.

Earlier about 1018 UT there is a sharp but small decrease in the amplitude of NPM to Payerne and NPM to Thule followed a few minutes later by a sharp advance of phase and a brief increase in amplitude prior to the onset of the main PCA effect. The sharp phase advance and brief increase in amplitude also show up on the NPG -- Payerne record in Part C but are not evident in NPG -- Thule, Part D.

The rapid phase NPM to Thule VLF data for the critical hour preceding the PCA (1000 UT to 1100 UT) shows one rapid-phase VLF effect at approximately 1018 UT.

This sudden fade effect is believed to be connected with the proton flare but its beginning and ending are so abrupt a momentary interference by some other source cannot be ruled out.

Figure 16 is a rapid phase playback of the "sudden proton flare effect" using the monitor system at three different speeds. The lower part of Figure 16 shows the actual IF pulses at the beginning of the sudden fade and at both beginning and end of the fade.

The bottom three pictures were taken using the rapid-phase sample mode.

If the rapid phase shift and fade in Figure 16 are due to proton flare effects in the ionosphere, these are indeed rapid. The onset of the phase perturbation exceeds the capability of the system;  $\Delta\phi = 25$  Hz.

The total phase shift is small, however, on the order of 90 degrees. The duration of the fade is approximately 13 seconds. The servo stays locked, hence, the normal NPM amplitude at Thule Figure 15, Part B does not drop out but suffers only a step decrease of 2 or 3 dB.

The main PCA phase shifts of Nov. 18, 1968 do not show up in the rapid phase data at 1045. (See steady, unperturbed rapid phase data and unperturbed

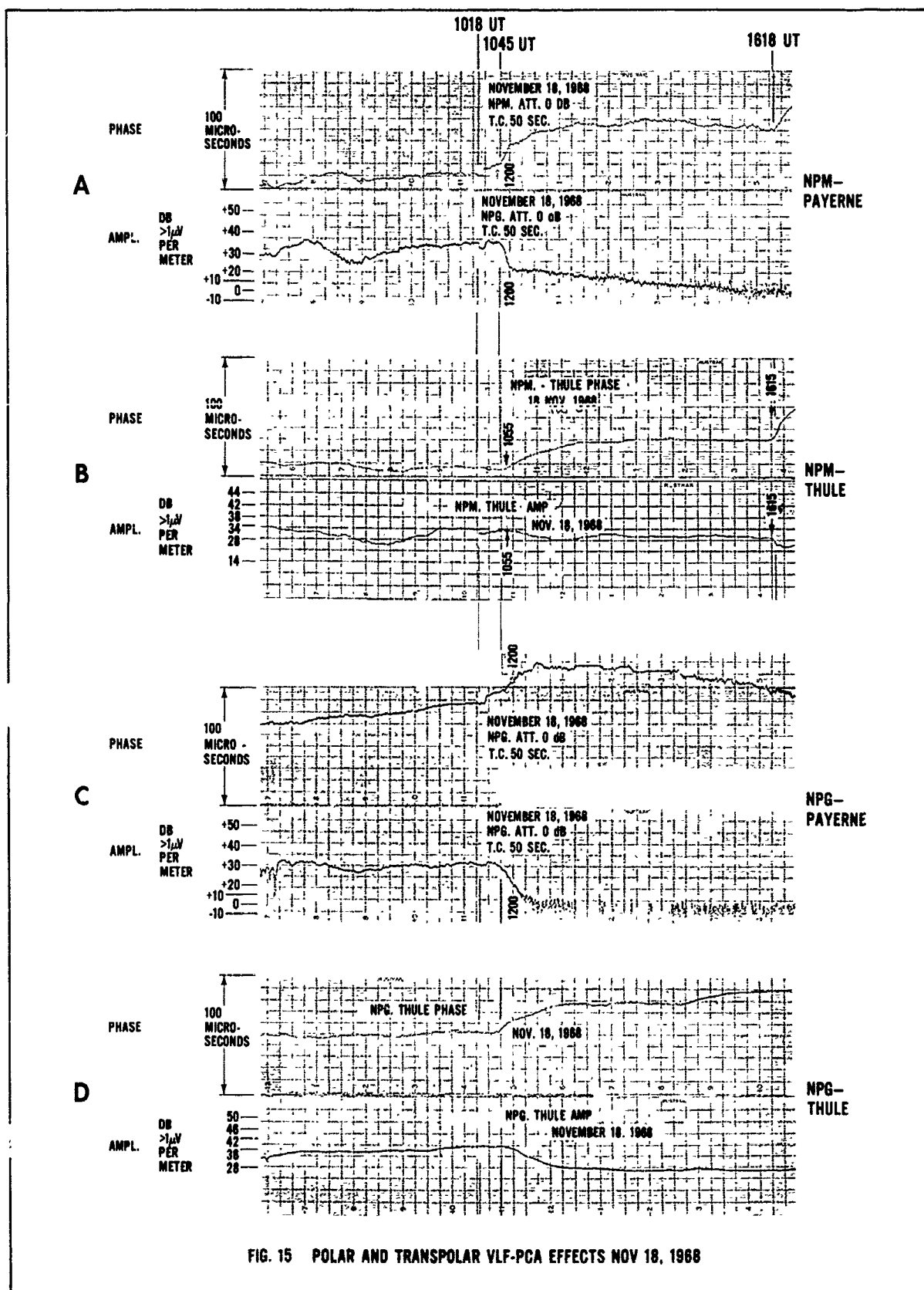


FIG. 15 POLAR AND TRANSPOLAR VLF-PCA EFFECTS NOV 18, 1968

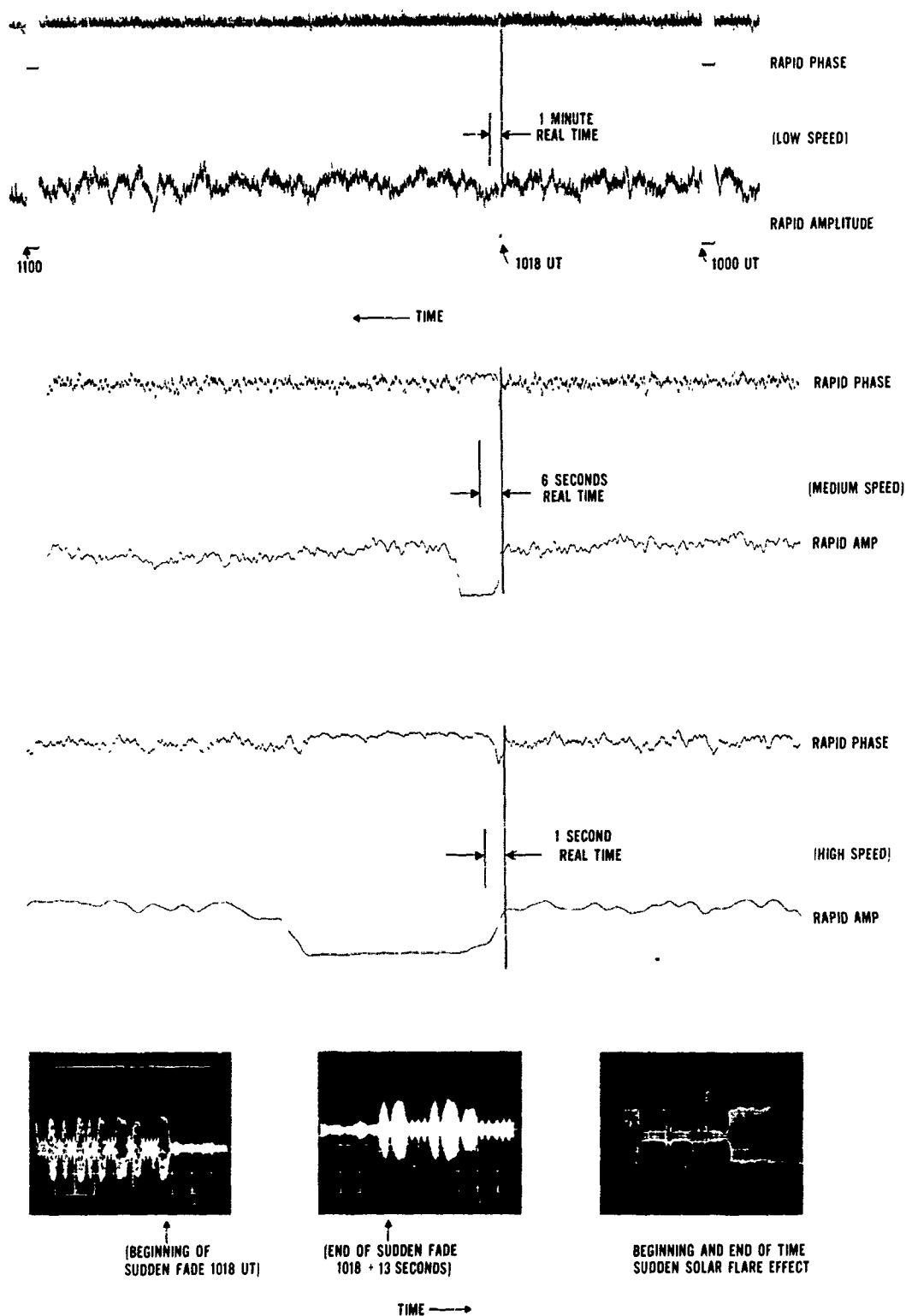


FIG. 16 SUDDEN PROTON FLARE EFFECT NPM-THULE NOV. 18, 1968

amplitude recording prior to 1100 UT in the top of Figure 16.) This indicates that phase lock was successfully maintained during the main PCA phase transition.

It may be noted from Figure 15, Part B, that the NPM -- Thule, phase shift during the onset of the main PCA (beginning at 1045 UT) is slower than a second PCA effect which begins at approximately 1618 UT.

Tracking errors during this second phase transition were studied using the rapid-phase sample method. Rapid phase samples were recorded once per second for a period of a few seconds then once per 0.2 seconds.

The rapid-phase samples in Figure 17 illustrate the variation in phase between the code and the standard at the 0.2 seconds frame rate.

The maximum phase rate on this figure is between  $\Delta\phi = 220$  degrees and  $\Delta\phi = 255$  degrees or 35 degrees in 0.2 seconds. This is 175 degrees per second or approximately 0.5 Hz.

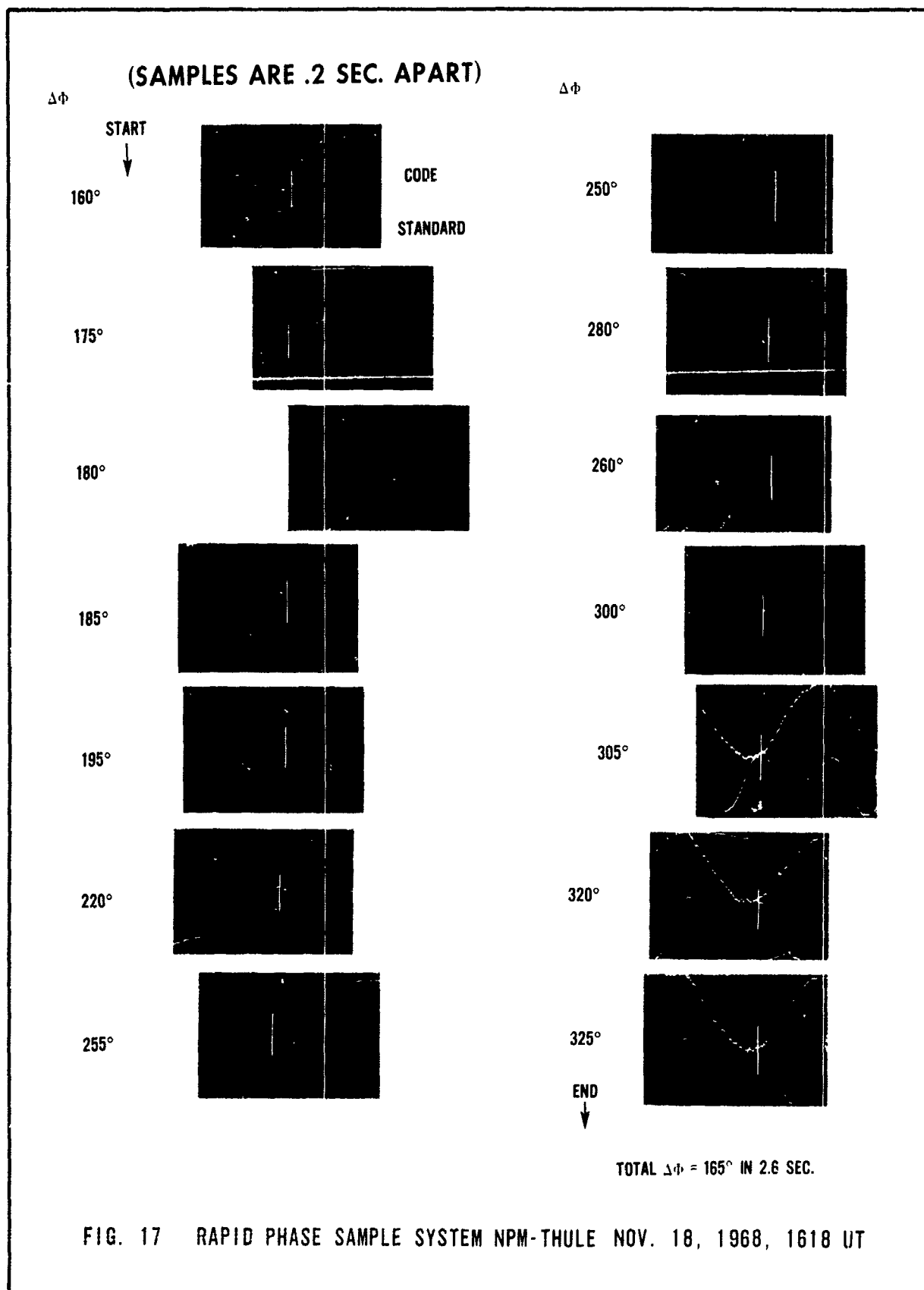
Figure 18 is a plot of the variations in rapid phase on the NPM -- Thule path during the November 18, 1968 PCA.

Note that the rapid phase transition are brief. Their average over a number of seconds approaches the per second average.

A statistical study of rapid phase rates during PCA's, sunrise-sunset transitions, and other events should be conducted. The phase rates during Solar Flares, PCA's and Magnetic Storms should be compared with quiet day rates and an analysis of variance should be conducted to determine variations between full daylight propagation, nighttime propagation, sunrise-sunset and during the various seasons.

Though such a study will be very fruitful and might produce new basic information on VLF propagation there is not enough funding or time left on the contract to do this.

This work will have to be left to a future project. It is recommended that this task be given high priority on any future efforts in this general work area.





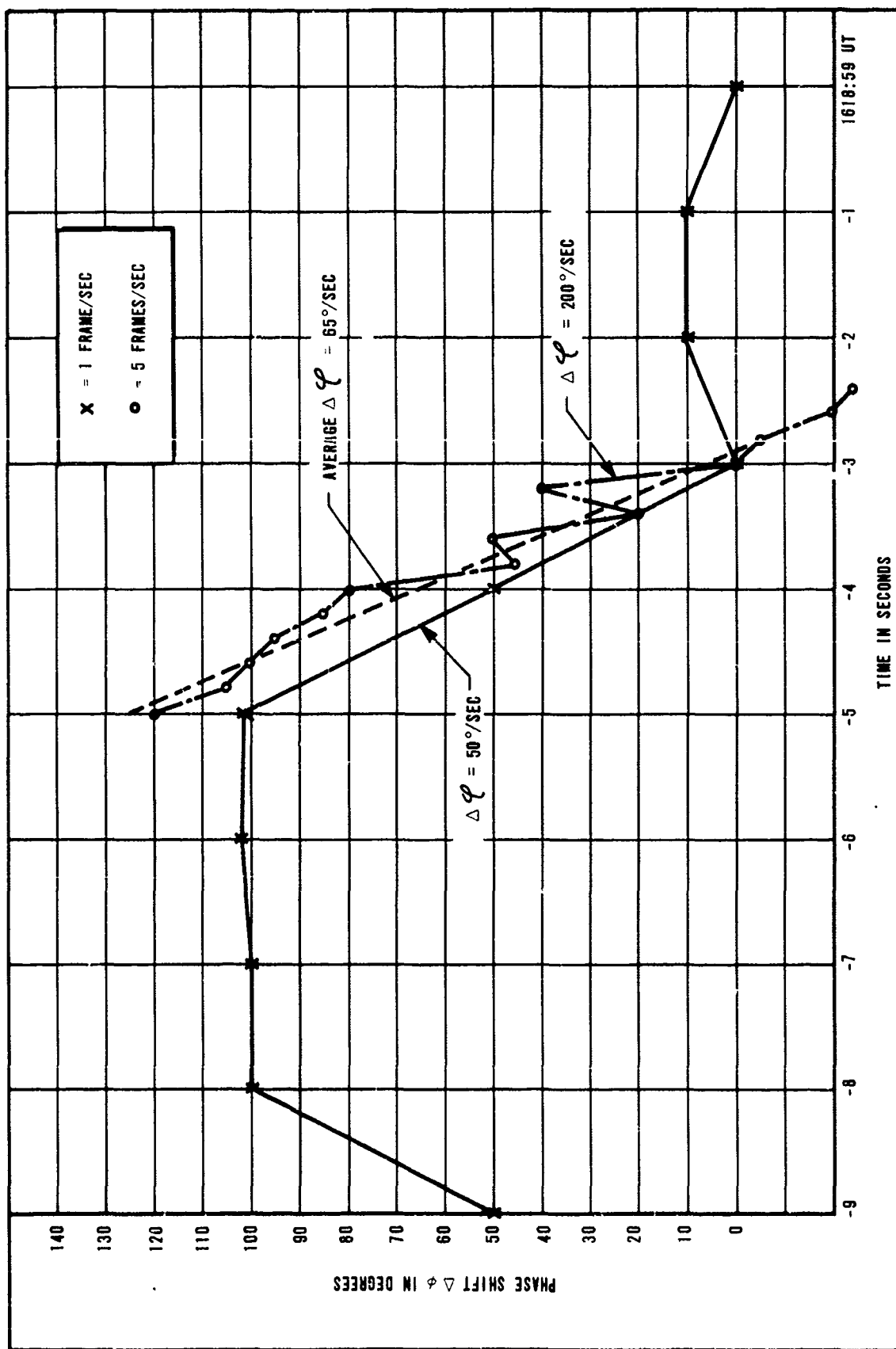


FIG. 18 ANALYSIS OF NPM-THULE RAPID PHASE DATA-NOV. 18, 1958 1618 UT

## REFERENCES

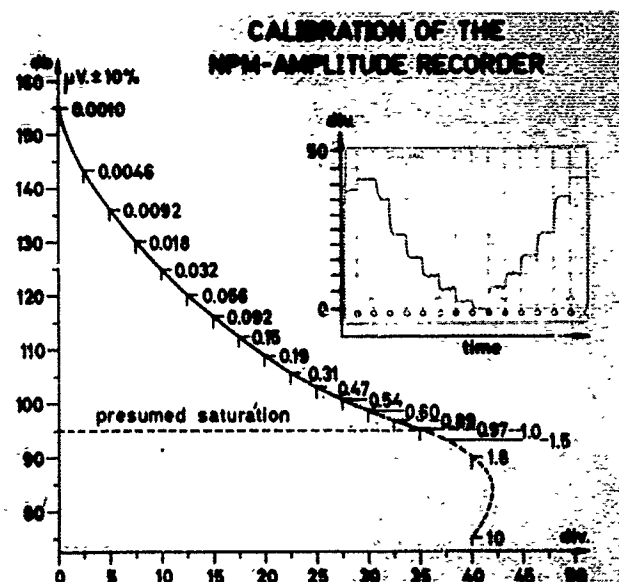
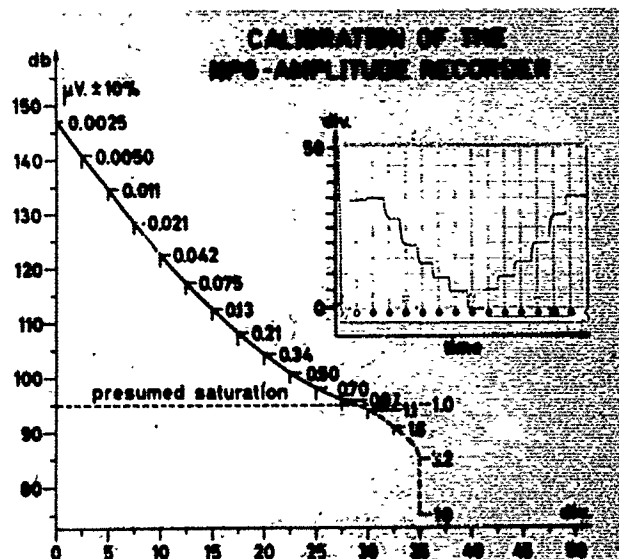
- Frank, L. A., VanAllen, J. A., Craven, J. D.; "Large Diurnal Variations of Geomagnetically Trapped and of Precipitated Electrons Observed at Low Altitudes" J. Geophys. Res. 69, No. 15, P. 3166, August, 1964.
- Reder, F. H. and Westerlund, S. "VLF Signal Phase Instabilities Produced by Propagation Medium -- Experimental Results" Proceedings AGARD-EWP Symposium ANKARA, Turkey, Oct. 9-12, 1967, p. 24.
- HRB-Singer, Inc., "Coordinated High Latitude Experiments" Report No. 356-R-8, October 1966.
- Hakura, Y., "The Polar Cap Absorption on July 7-10, 1966" NASA Report X-641-67-116, March 1967.
- Innanen, W. G., Krimigis, S. M., Armstrong, T. P.; "Solar Particle Observations from 24 January to 24 February, 1967" Paper presented at Midwest Cosmic Ray Conference, U. of Iowa, March 2, 1968.
- McDonald, F. B., "IMP Observations of Solar Cosmic Rays," Paper presented at Midwest Cosmic Ray Conference, U. of Iowa, March 2, 1968.
- HRB-Singer, Inc., "Coordinated High Latitude Experiments," Report No. 356-R-10, 1968.
- Reder, F. H., Institute for Exploratory Research Fort Monmouth, N. J., Private Communication, 1969.
- Crombie, D. D., Periodic Fading of VLF Signals Received Over Long Paths During Sunrise and Sunset, Radio Sci. J. Res. NBS 68D, No. 1, 27-34, 1964.
- Westerlund, S., Reder, F. H., and Abom, C.; "Effects of Polar Cap Absorption Events on VLF Transmissions," Planetary Space Science, Vol. 17, pp 1329-1374, 1969.
- Oelbermann, E. J., Musser, J. M., Imhof, G. W., Hass, R. W., "Analysis of Polar VLF, Riometer, and Cosmic Ray Perturbations During the January 28, 1967 Solar Cosmic Ray Event," paper presented at Spring URSI Meeting, Washington, D. C., April 1968.

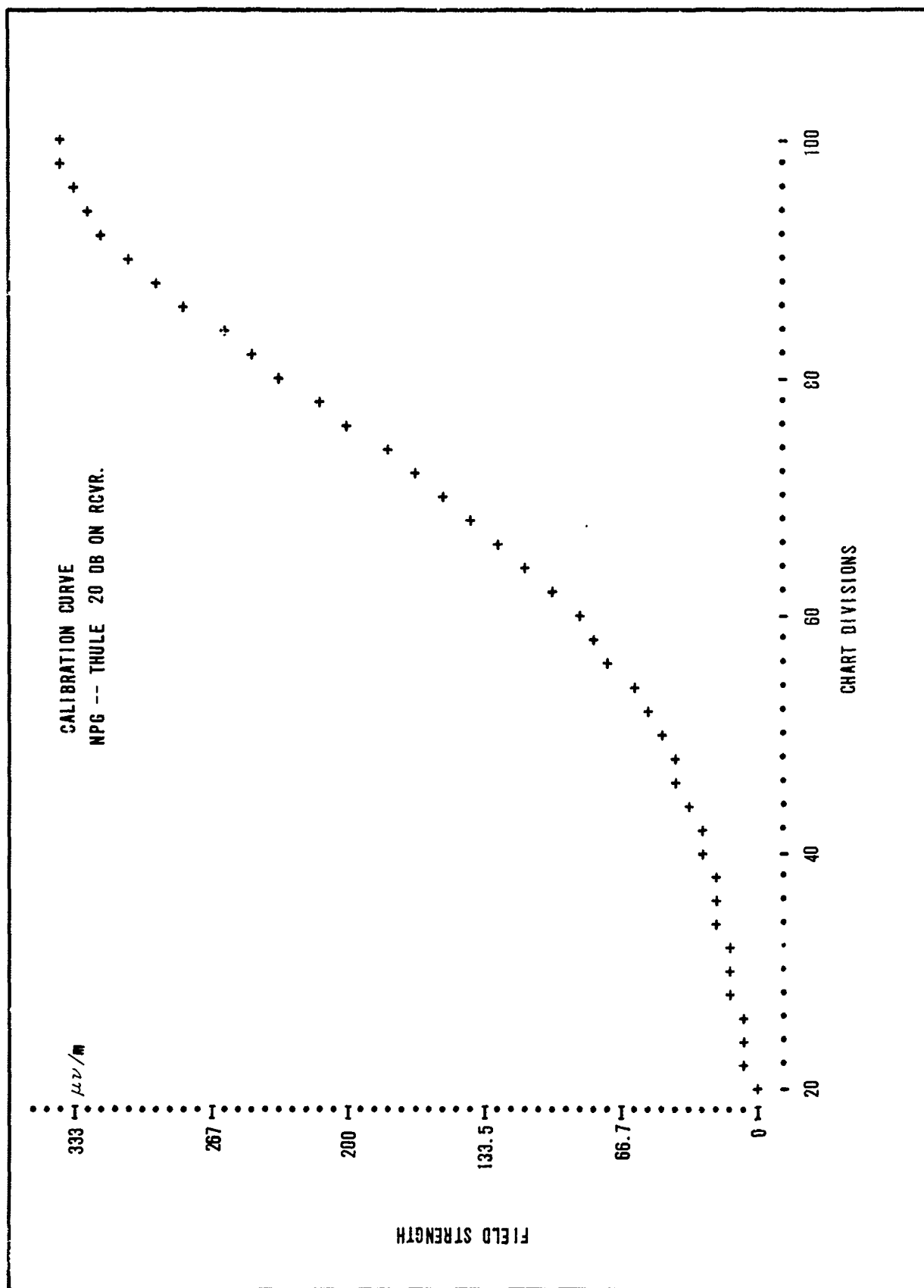
APPENDIX A  
VLF Data Collected During  
Recent Polar Cap Events

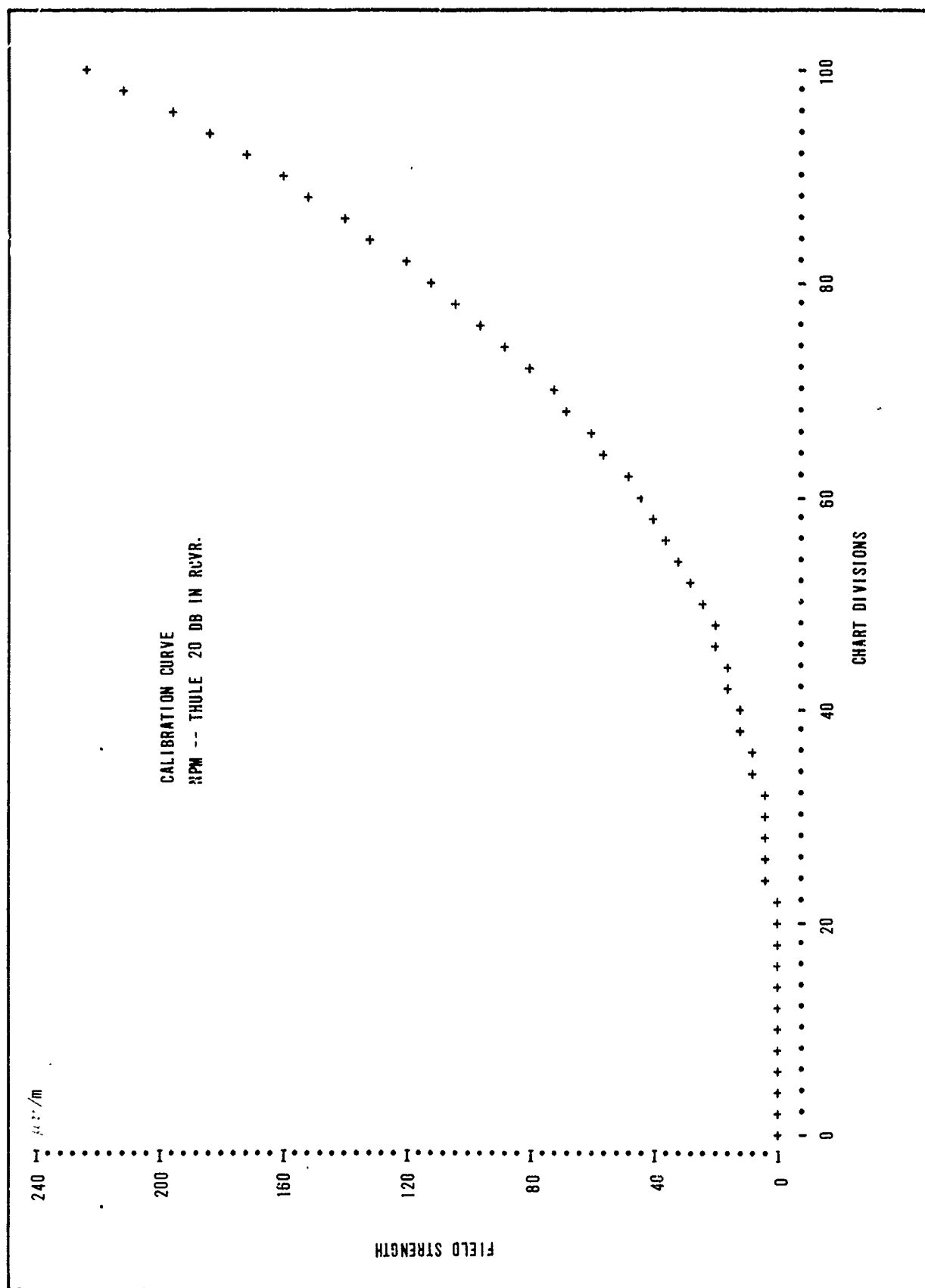
A-1  
Reverse (Page A-2) Blank

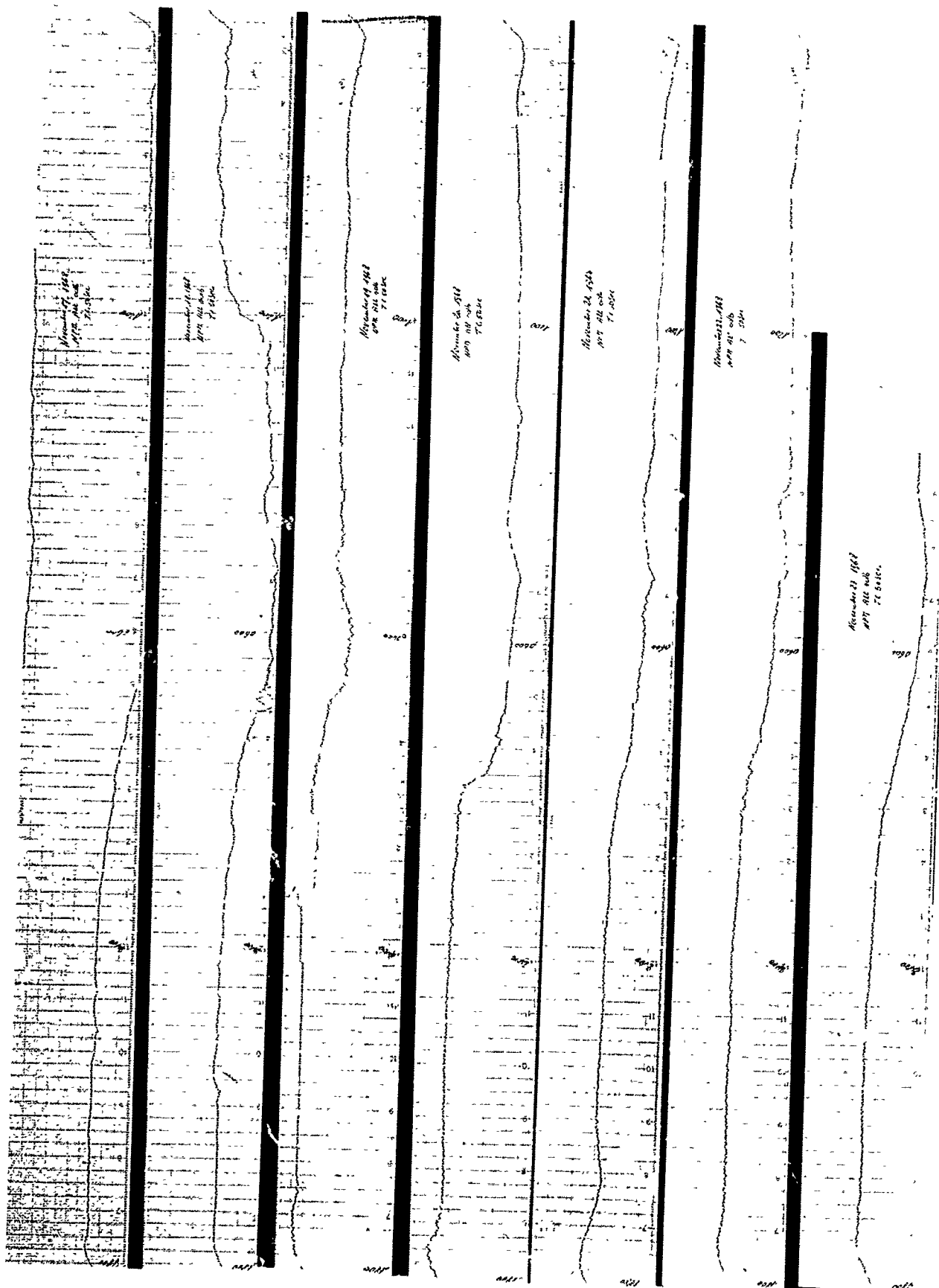
# RAW DATA ANNOTATIONS

<u>VLF RECORD</u>	<u>DATE</u>	<u>TIME</u>	<u>FAULT</u>
NPG-Payerne, Phase	Nov. 21, 1968	0745 CET	Adjust Freq Std. (1.)
NPM-Payerne, Phase	Feb. 22, 1969	0900 CET	(1.)
	Feb. 25, 1969	1315 CET	(1.)
	Feb. 26, 1969	0745 CET	(1.)
	Feb. 27, 1969	1630 CET	Time Adjustment
NPM-Slough, Ampl.	Feb. 28, 1969	1445 UT	Gain increased from 3/4 to F.S.
NPG-Payerne, Phase	Feb. 21, 1969	1800 CET	Chart not advancing (2.)
NPG-Payerne, Phase	Feb. 23, 1969	1630 CET	(2.)
NPG-Payerne, Phase	Feb. 23-24, 1969	1800-0800 CET	(2.)
NPG-Payerne, Phase	Feb. 25, 1969	0750 CET	(1.)
NPG-Payerne, Phase	Feb. 26, 1969	1630 CET	(2.)
NPG-Payerne, Phase	Feb. 27, 1969	1400 CET	Striker Broken, Change recorder (3.)
NPG-Payerne, Ampl.	Feb. 27, 1969	1400 CET	(3.)
NPG-Payerne, Phase	Feb. 28, 1969	0000-0800 CET	(1.)
NPG-Slough, Phase	Feb. 23, 1969	1345 UT	Loss of Signal
NPG-Slough, Ampl.	Feb. 28, 1969	1200 UT	RF Attenuation reduced, 20 dB to 10 dB
NPG-Payerne, Phase	Mar. 31, 1969	1115 CET	(1.)
NPM-Thule, Phase	Mar. 27, 1969	1215 UT	Power Failure (4.)
NPM-Thule, Ampl.	Mar. 27, 1969	1215 UT	(4.)
NPG-Thule, Phase	Mar. 27, 1969	1215 UT	(4.)
NPG-Thule, Ampl.	Mar. 27, 1969	1215 UT	(4.)



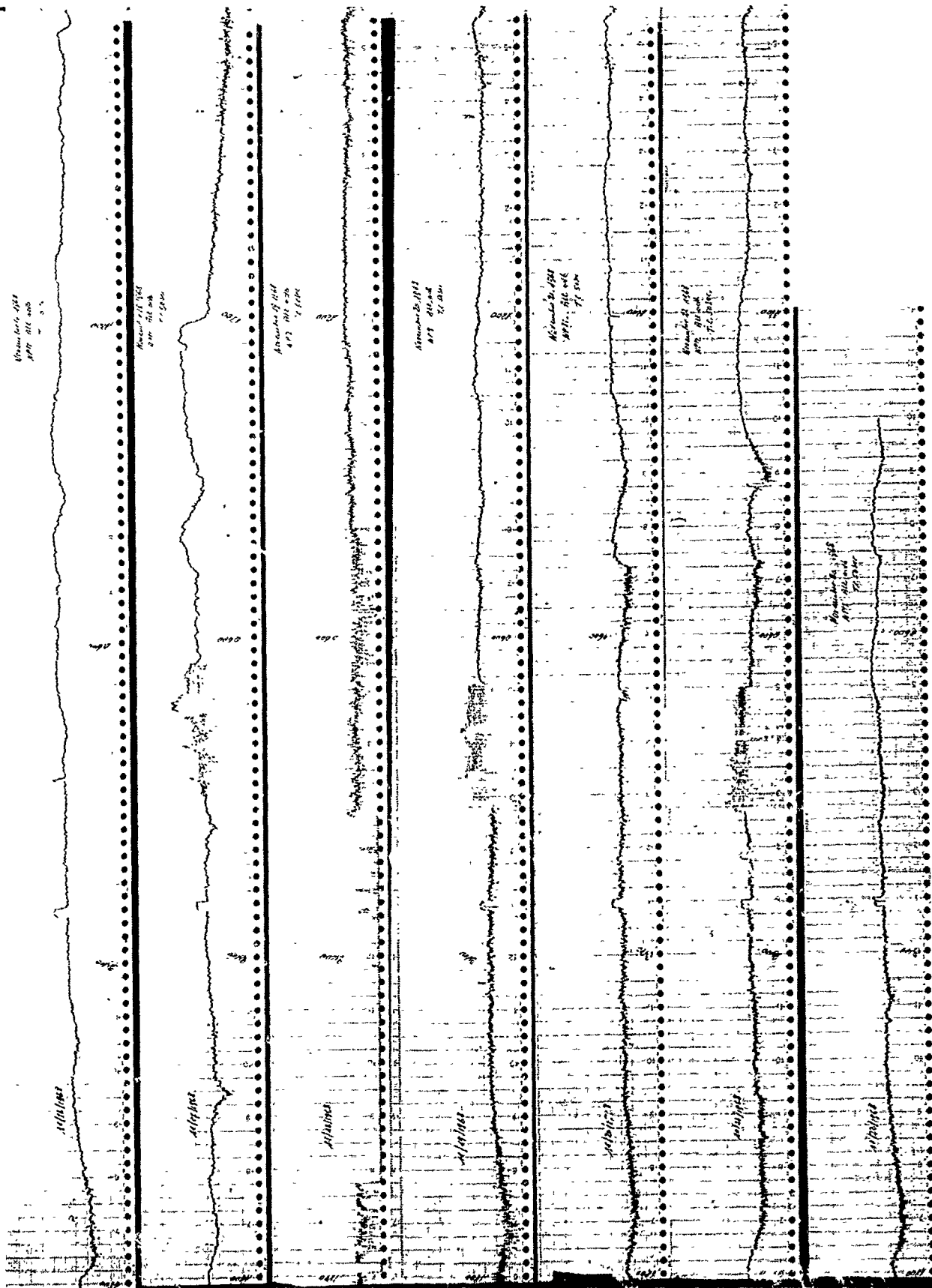


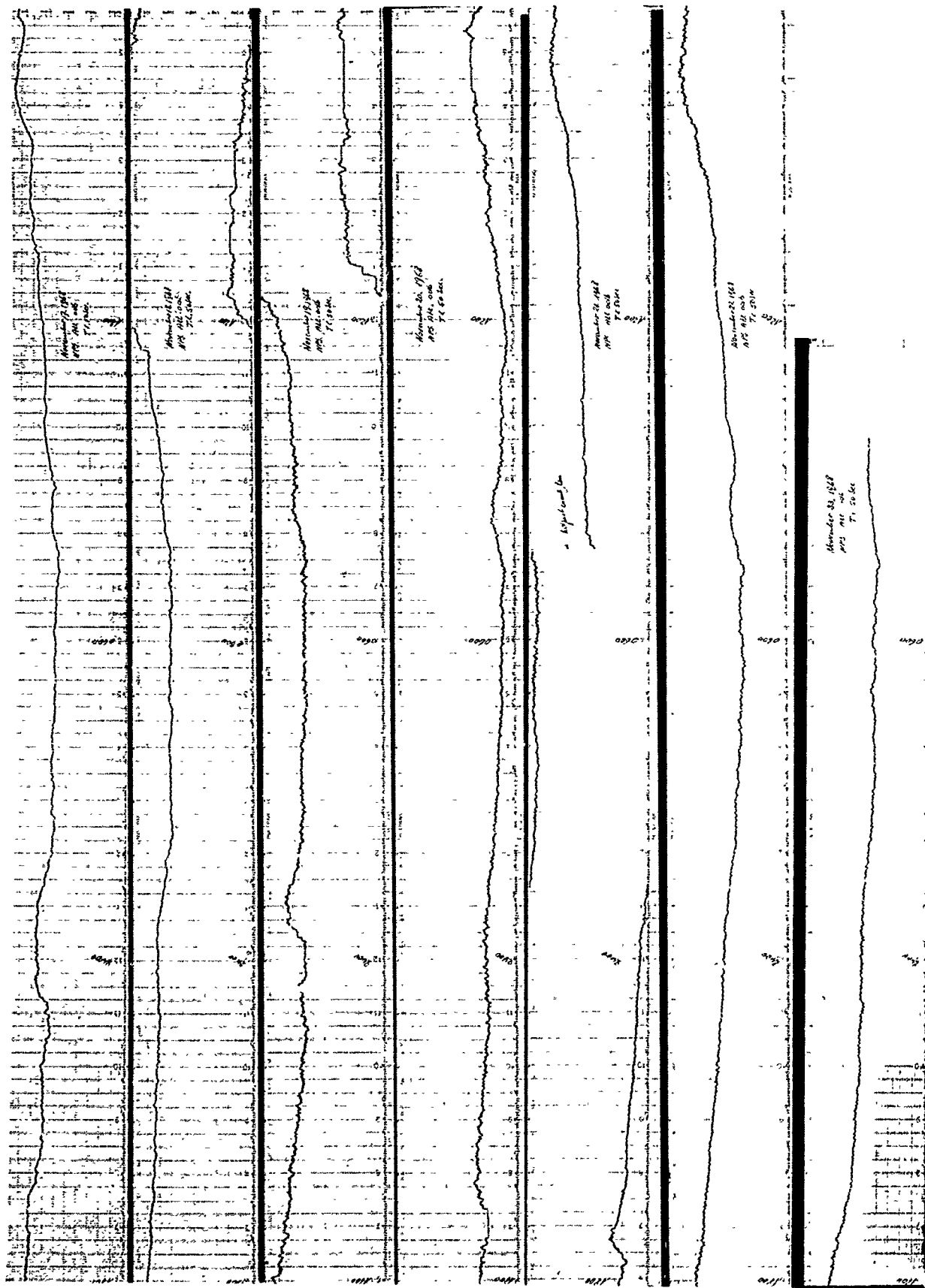


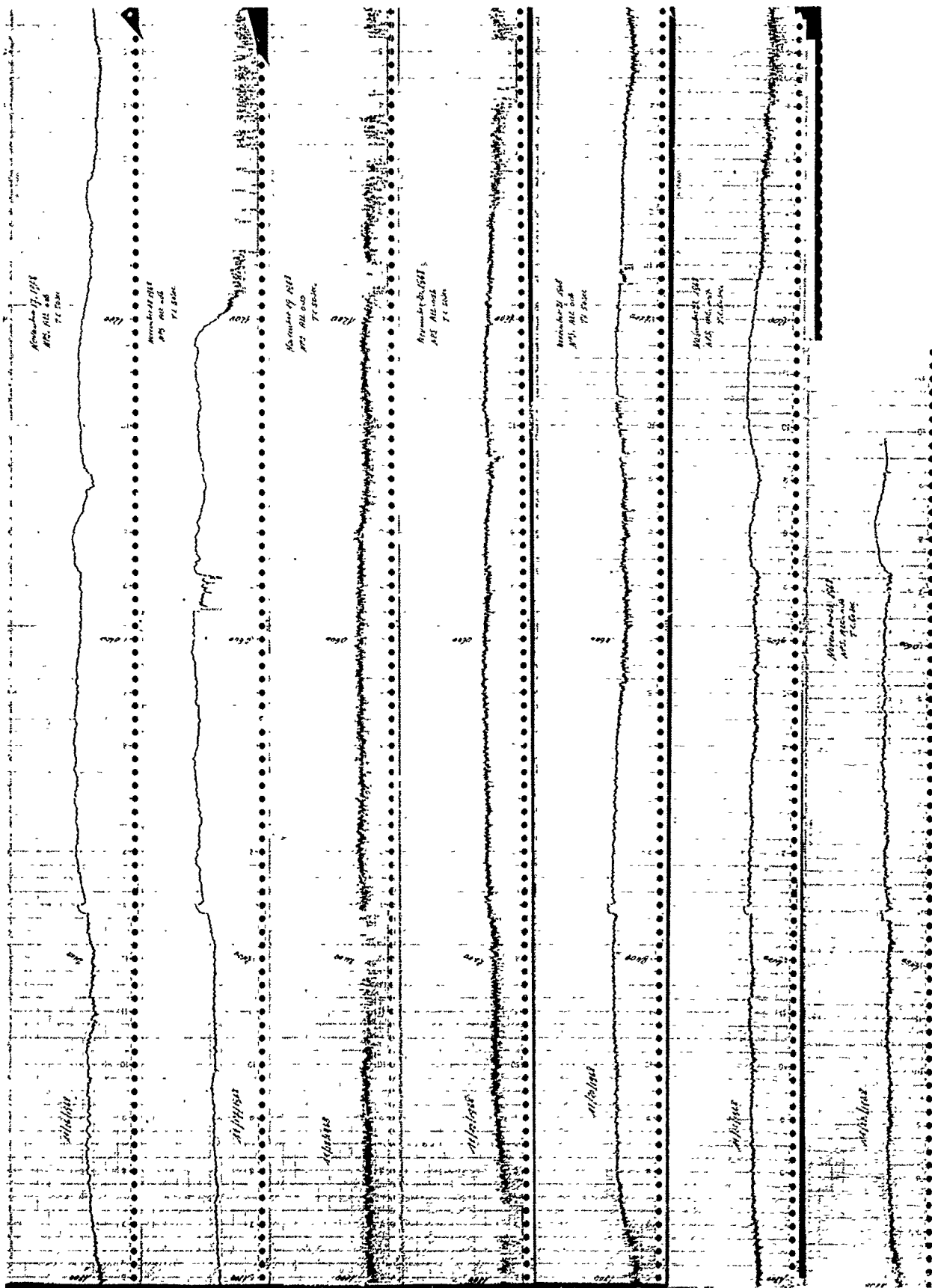


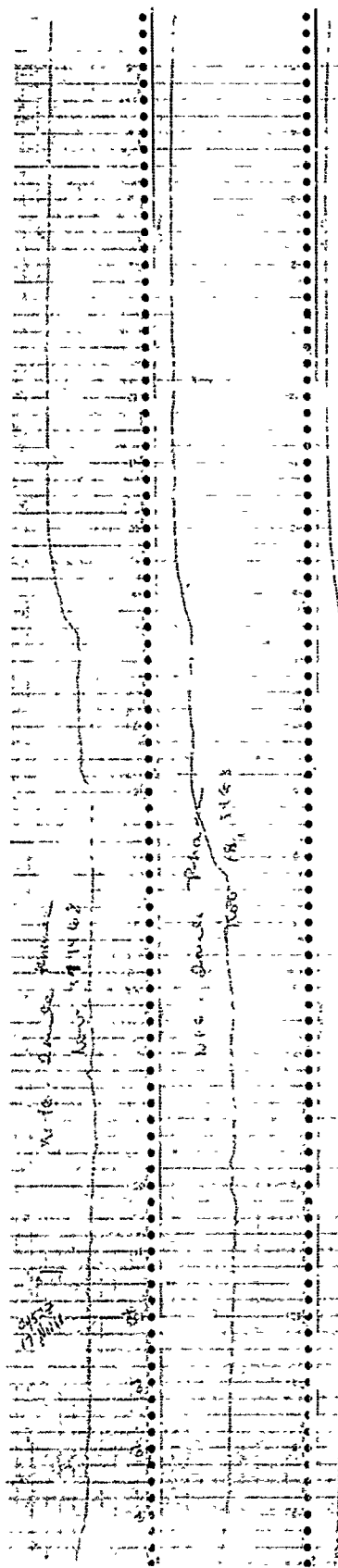


1. ☐ 2. ☐ 3. ☐ 4. ☐ 5. ☐ 6. ☐ 7. ☐ 8. ☐ 9. ☐ 10. ☐ 11. ☐ 12. ☐ 13. ☐ 14. ☐ 15. ☐ 16. ☐ 17. ☐ 18. ☐ 19. ☐ 20. ☐ 21. ☐ 22. ☐ 23. ☐ 24. ☐ 25. ☐ 26. ☐ 27. ☐ 28. ☐ 29. ☐ 30. ☐ 31. ☐ 32. ☐ 33. ☐ 34. ☐ 35. ☐ 36. ☐ 37. ☐ 38. ☐ 39. ☐ 40. ☐ 41. ☐ 42. ☐ 43. ☐ 44. ☐ 45. ☐ 46. ☐ 47. ☐ 48. ☐ 49. ☐ 50. ☐ 51. ☐ 52. ☐ 53. ☐ 54. ☐ 55. ☐ 56. ☐ 57. ☐ 58. ☐ 59. ☐ 60. ☐ 61. ☐ 62. ☐ 63. ☐ 64. ☐ 65. ☐ 66. ☐ 67. ☐ 68. ☐ 69. ☐ 70. ☐ 71. ☐ 72. ☐ 73. ☐ 74. ☐ 75. ☐ 76. ☐ 77. ☐ 78. ☐ 79. ☐ 80. ☐ 81. ☐ 82. ☐ 83. ☐ 84. ☐ 85. ☐ 86. ☐ 87. ☐ 88. ☐ 89. ☐ 90. ☐ 91. ☐ 92. ☐ 93. ☐ 94. ☐ 95. ☐ 96. ☐ 97. ☐ 98. ☐ 99. ☐ 100. ☐









NPG - Thule Phase  
Nov. 18, 1968

NPG - Thule Phase  
Nov. 20, 1968

NPG - Thule Phase  
Nov. 21, 1968

NPG - Thule Phase  
Nov. 22, 1968

NPG - Thule Phase  
Nov. 23, 1968

VLF PHASE, NPG-THULE NOV. 17, - NOV. 23, 1968 TIME - UT

NPG - 2nd Air Group  
Nov 17, 1963

NPG - 2nd Air Group  
Nov 3, 1968

NPG - 2nd Air Group  
Nov 19, 1968

NPG - 2nd Air Group  
Nov 20, 1968

NPG - Thule Air Base  
Nov 21, 1968

NPG - Thule Air Base  
Nov 22, 1968

NPG - Thule Air Base  
Nov 23, 1968

RENEW-CHA

RENEW-CHA

N CHART

RENEW-CHART

RENEW-CHART

RENEW-CHART

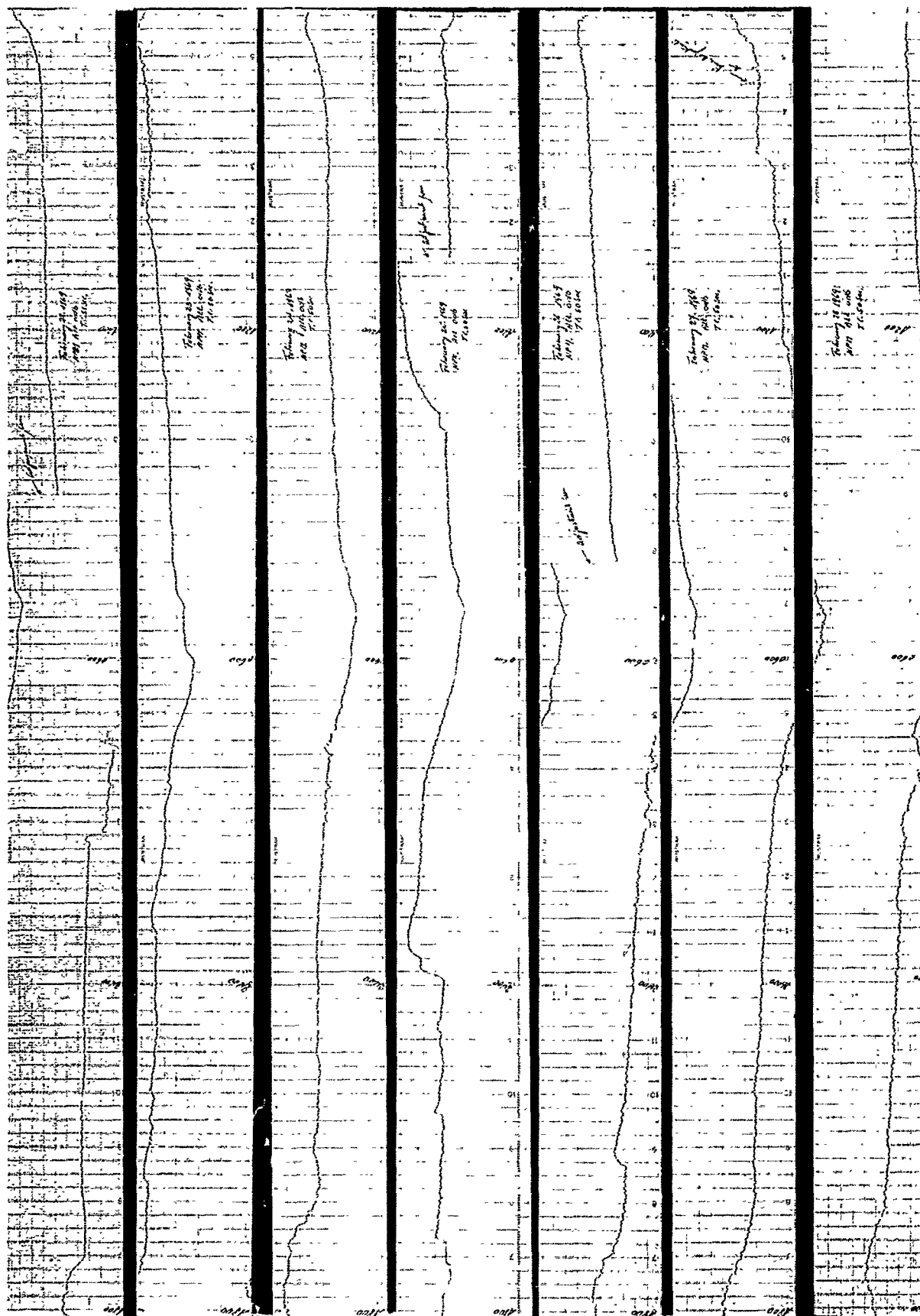
RENEW-CHART

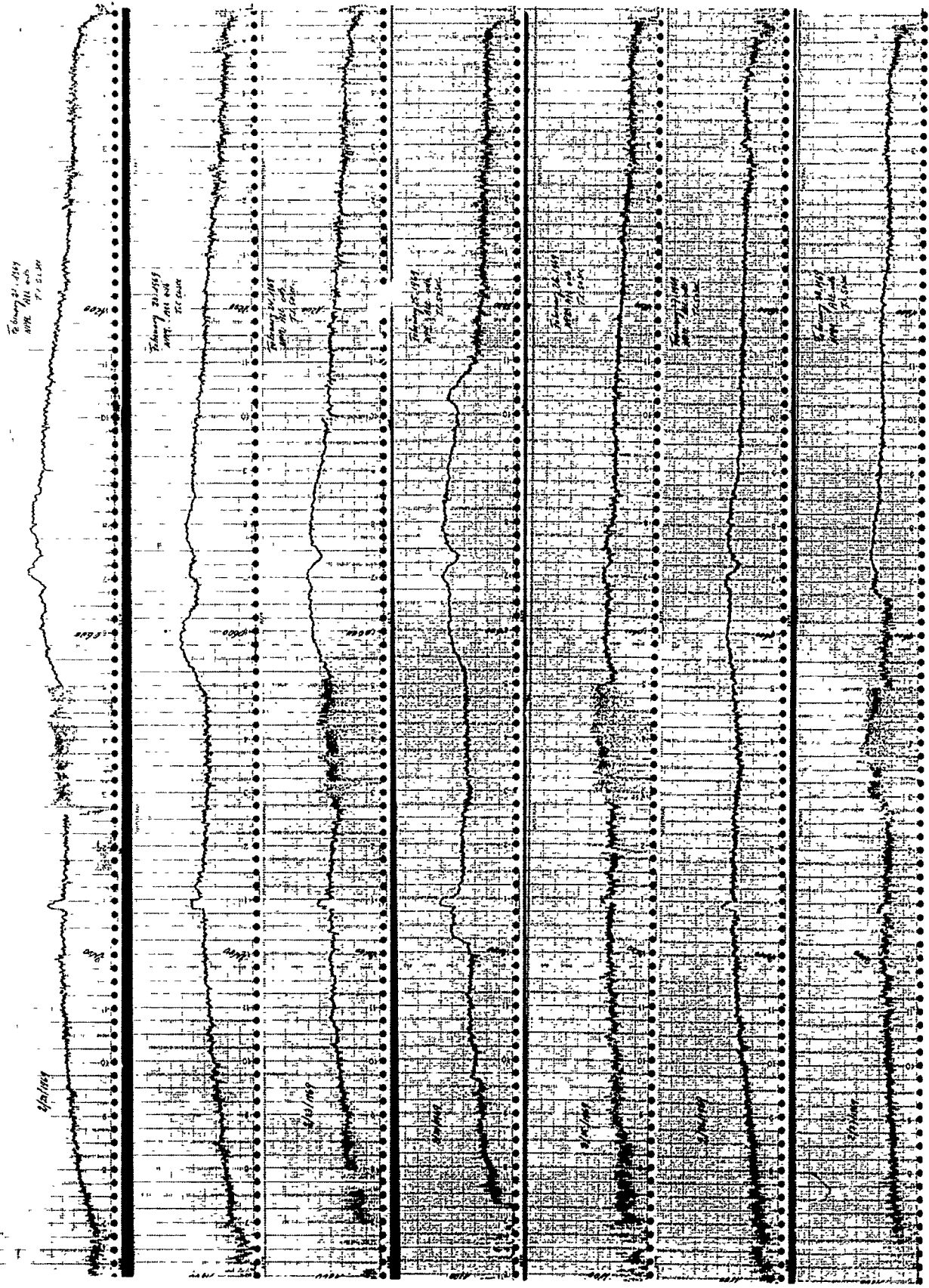
RENEW-CHART

RENEW-CHART

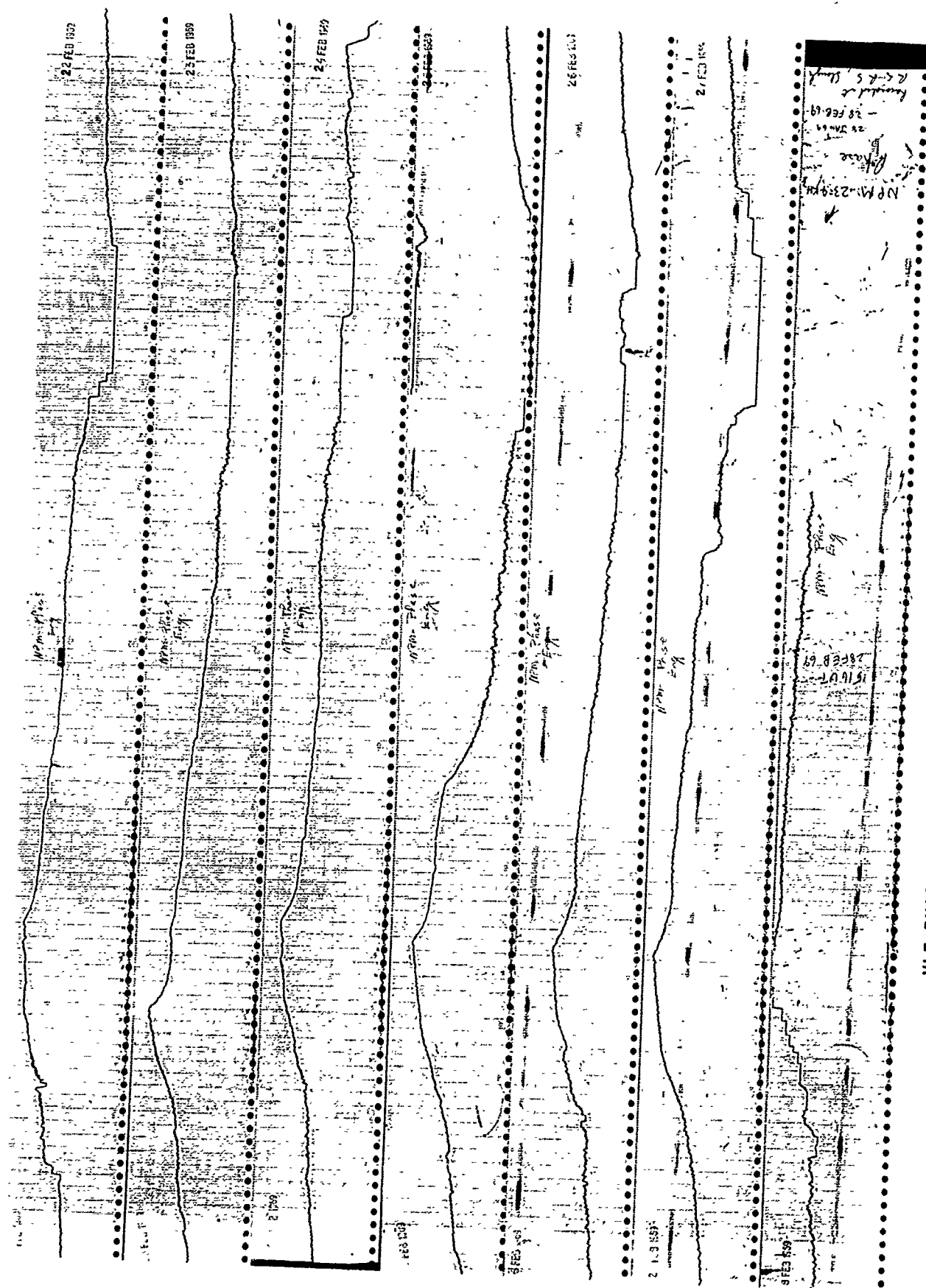
RENEW-CHART

REI



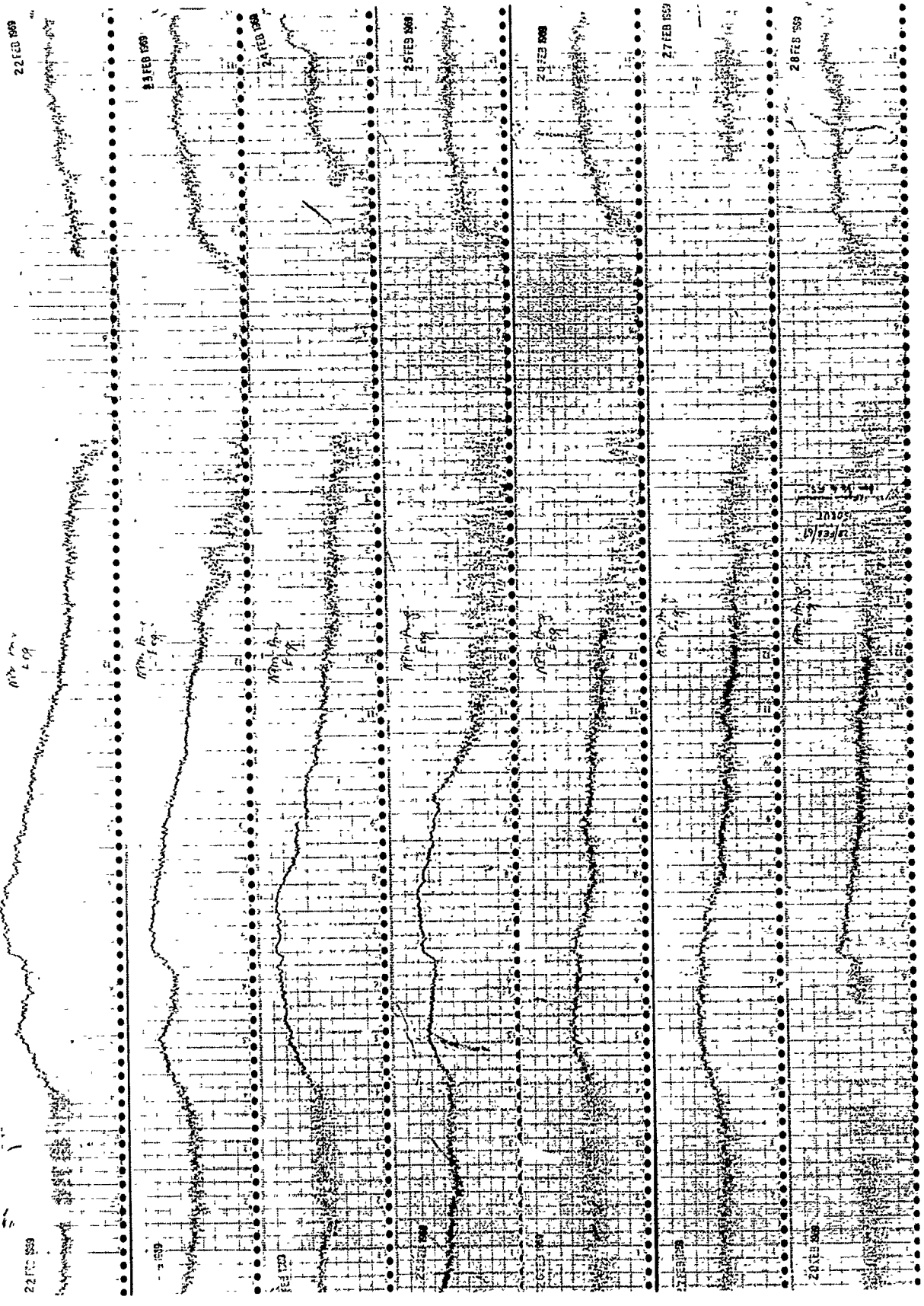


VLF AMPLITUDE, NPM-PAYERNE FEB. 22, - FEB. 28, 1969 TIME - UT + 1

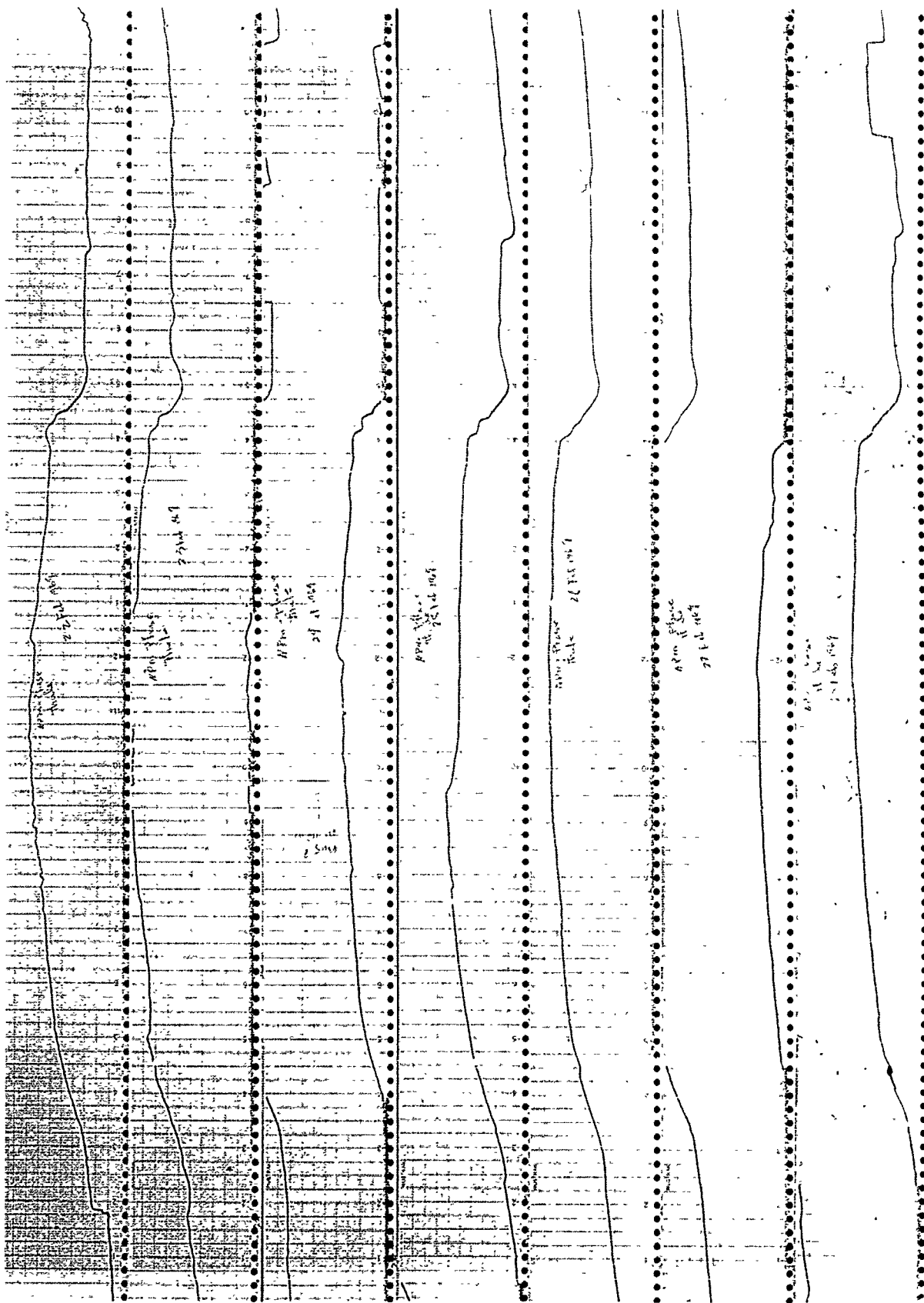


VLF PHASE, NPM-SLOUGH FEB. 22, - FEB. 27, 1969 TIME - UT

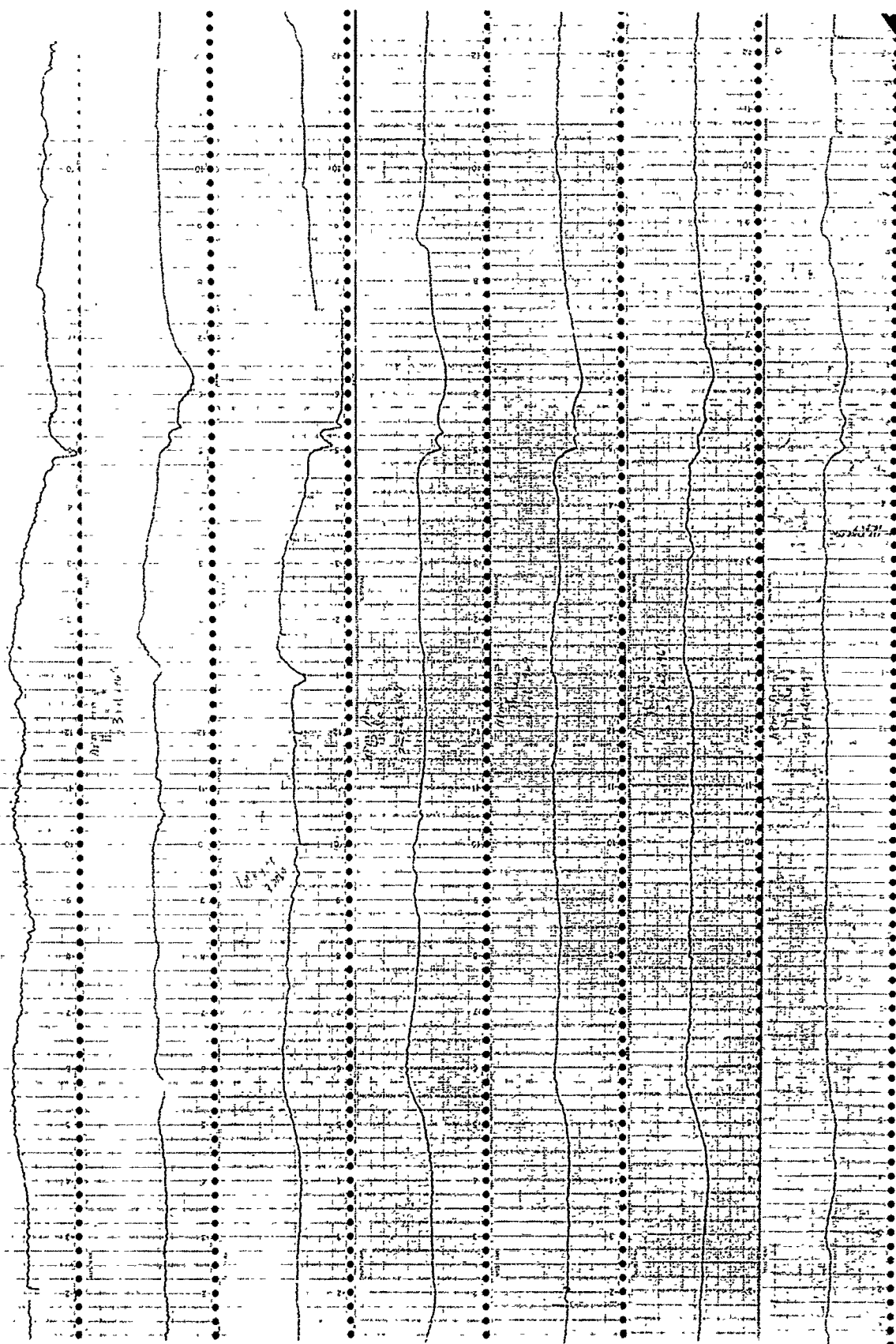




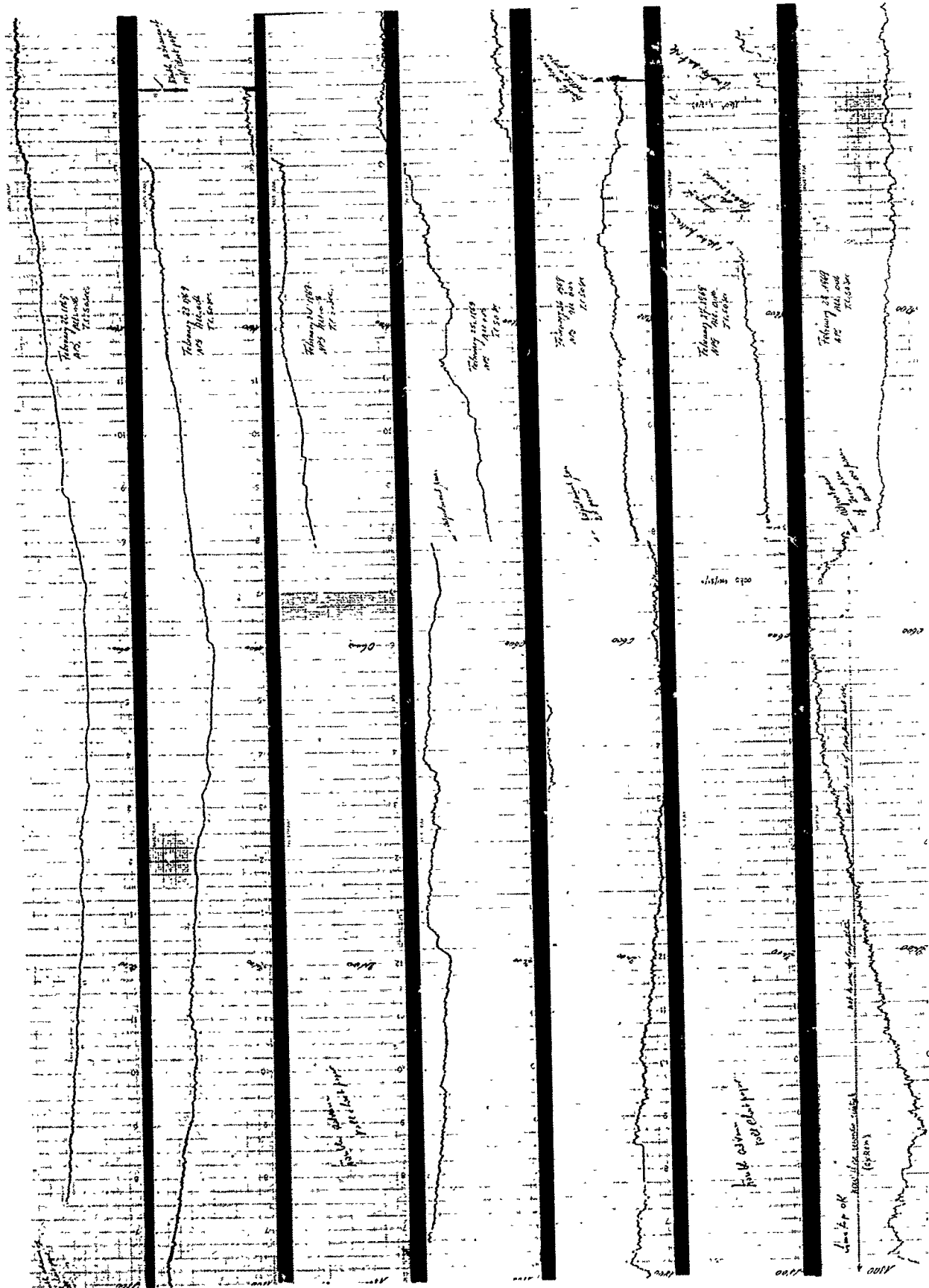
VLF AMPLITUDE, NPM-SLOUGH FEB. 22, - FEB. 28, 1969 TIME - UT



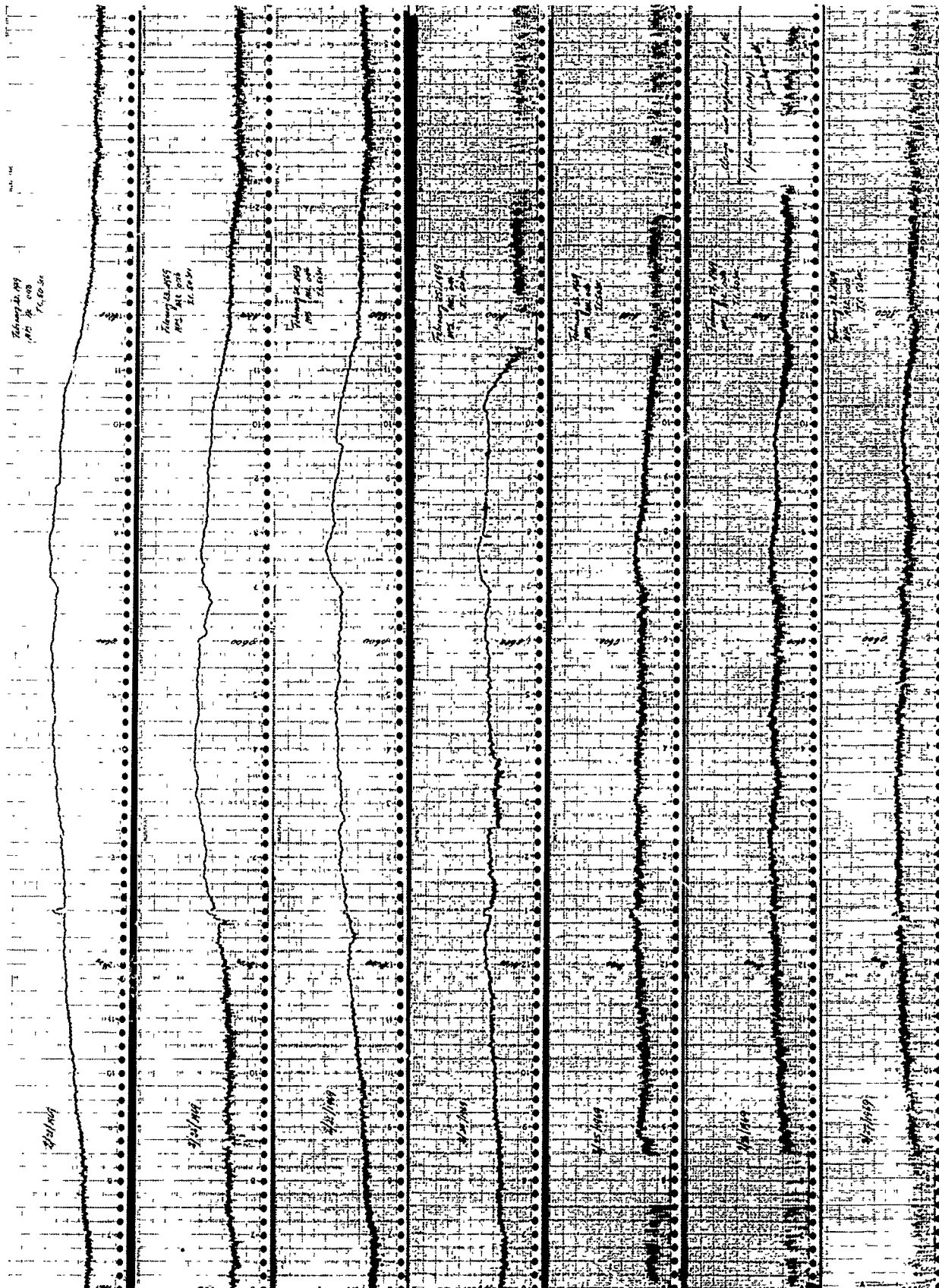
VLF PHASE, NPM-THULE FEB. 22, - FEB. 28, 1969 TIME - UT

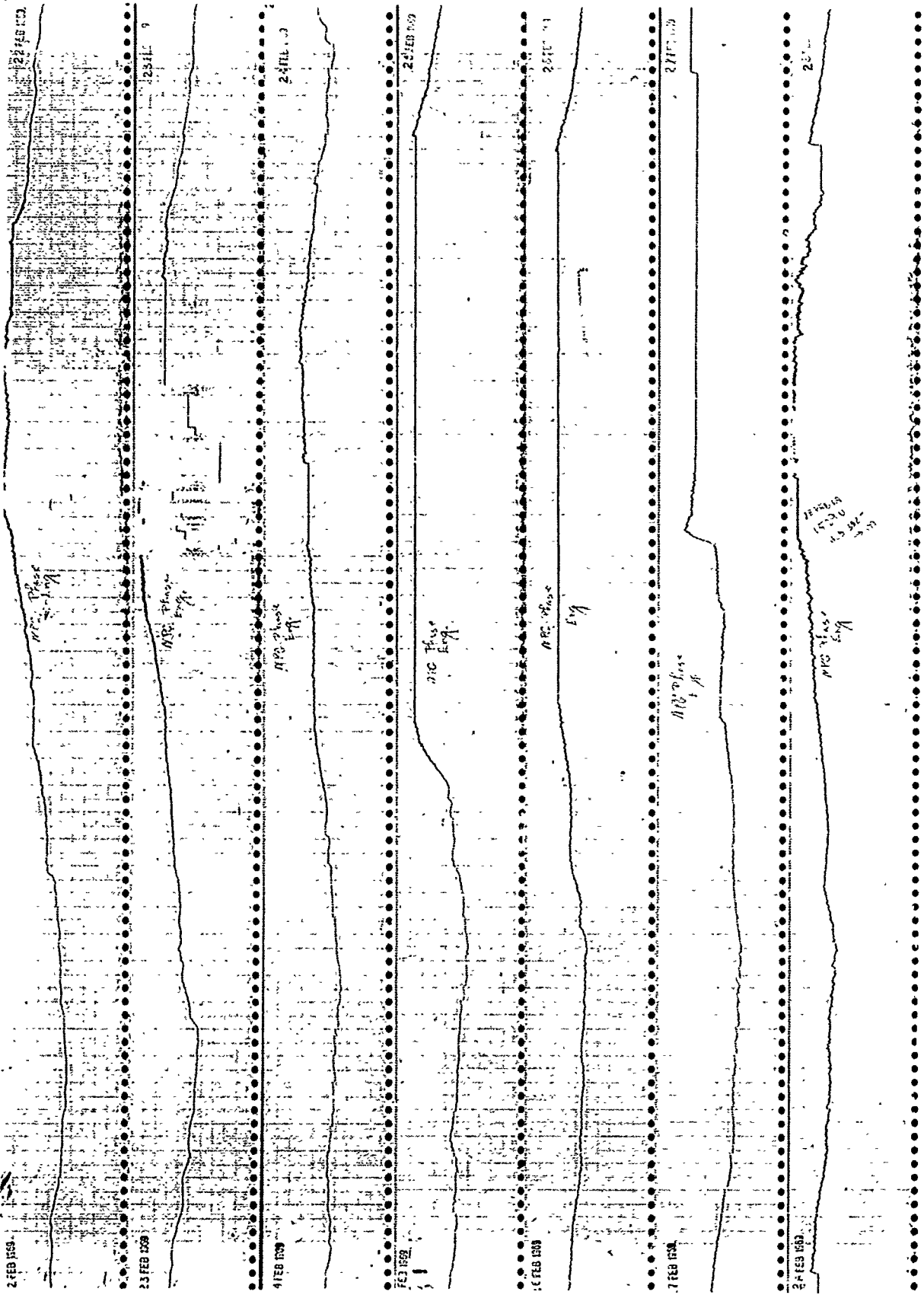


VLF AMPLITUDE, NPM-THULE FEB. 22, - FEB. 28, 1969 TIME - UT



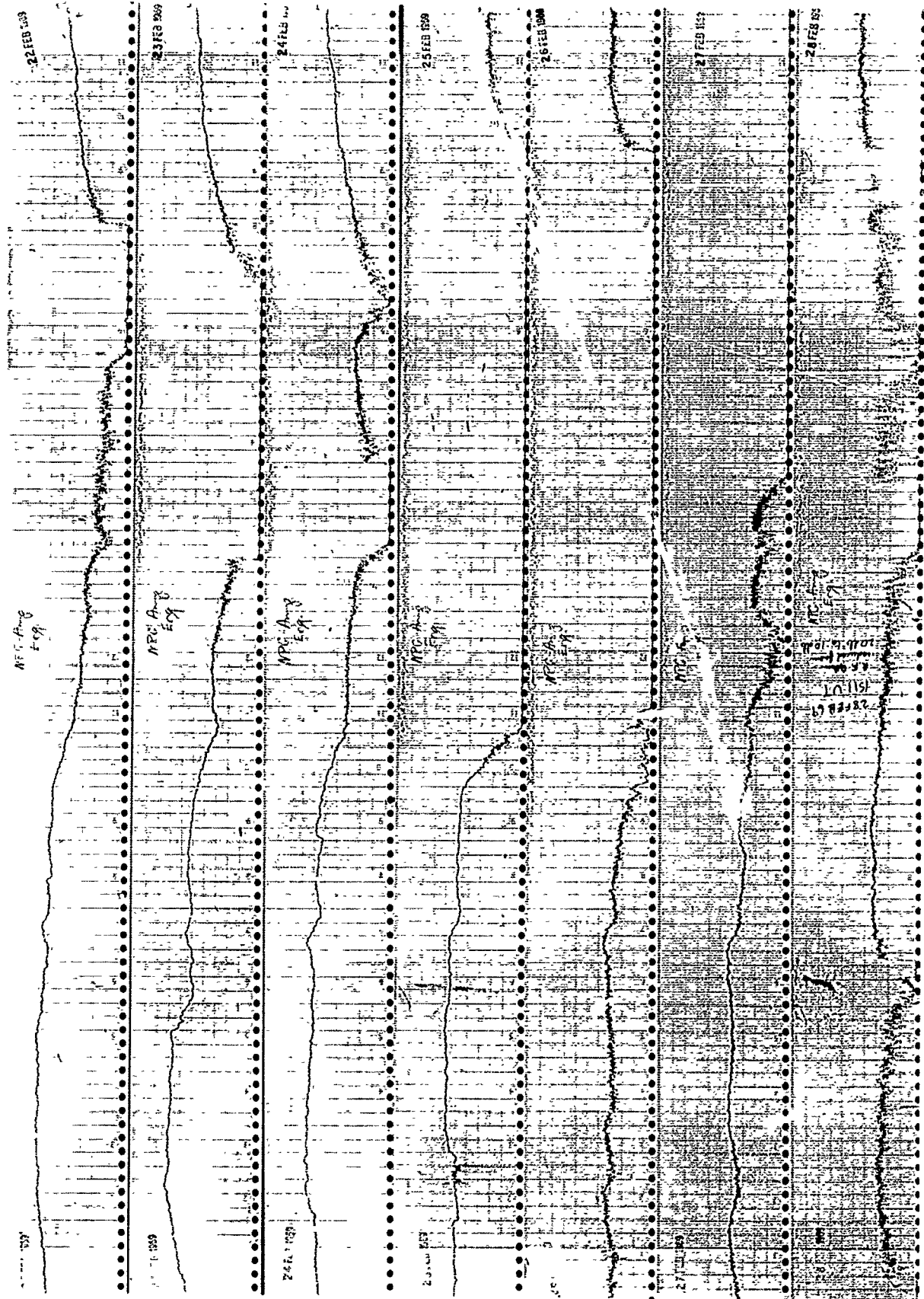
VLF PHASE, NPG-PAYERNE FEB. 22, - FEB. 28, 1969 TIME - UT + 1



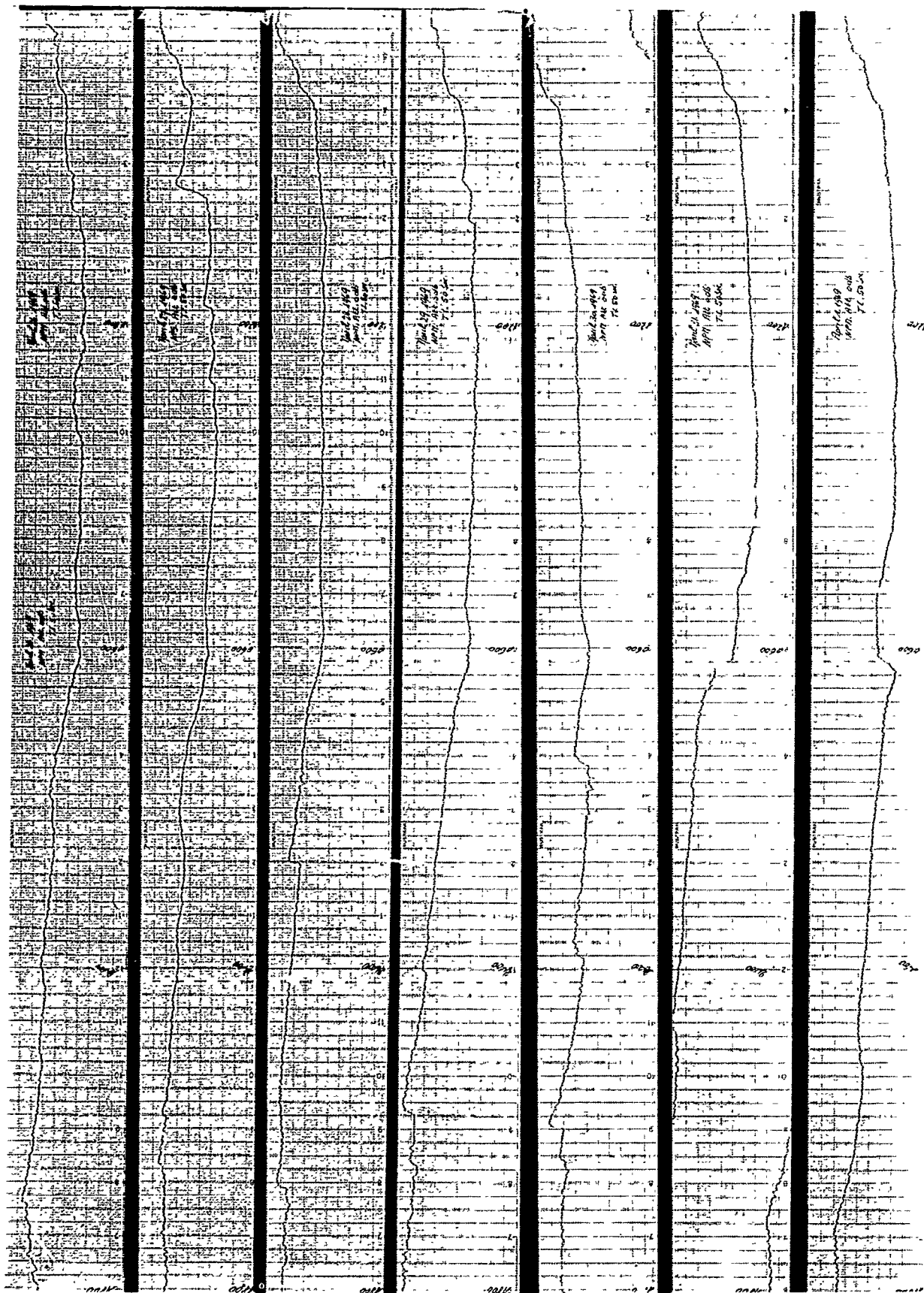


VLF PHASE, NPG-SLOUGH FEB. 22, - FEB. 28, 1969 TIME - UT



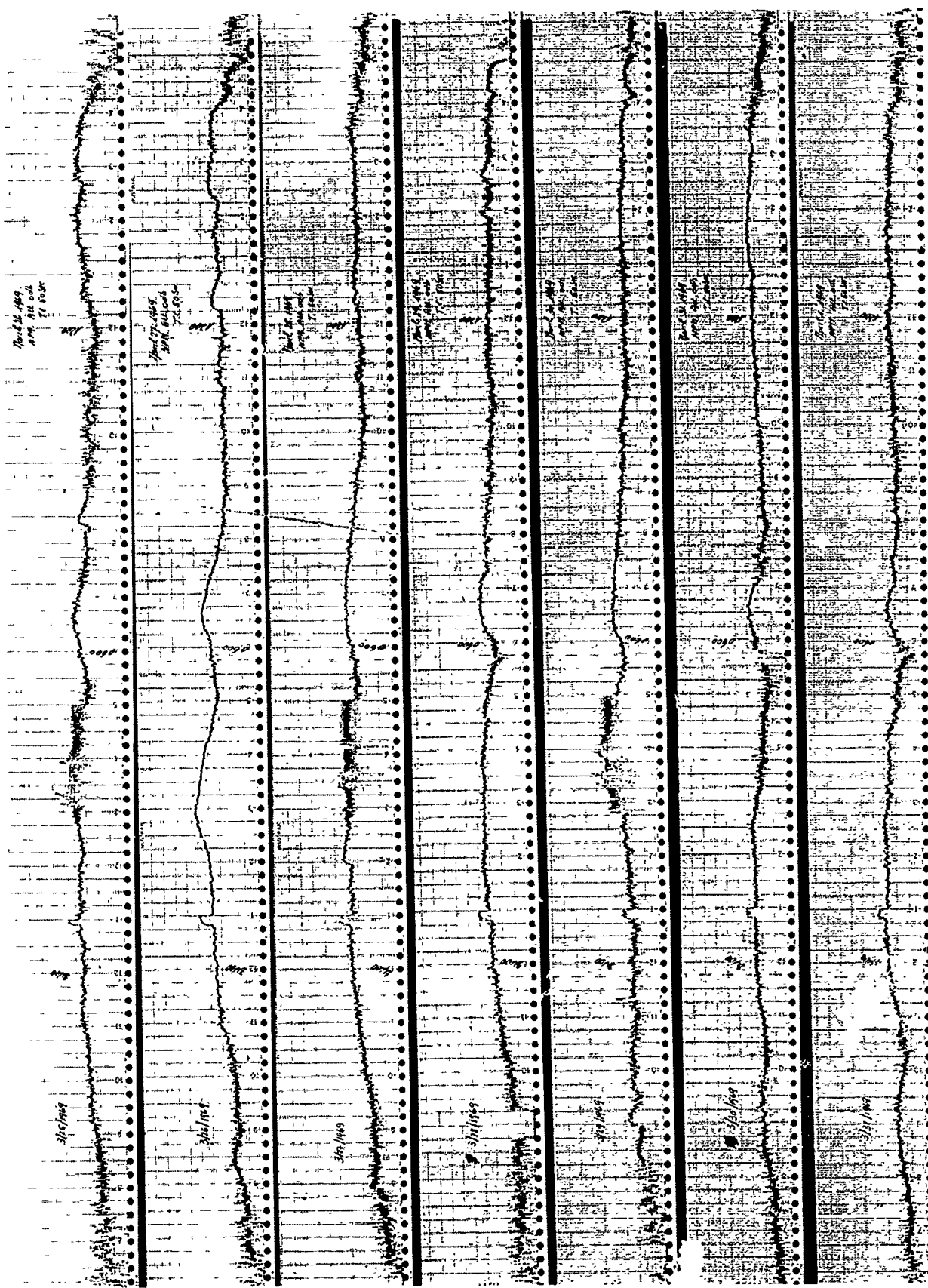


VLF AMPLITUDE, NPG-SLOUGH FEB. 22, - FEB. 28, 1969 TIME - UT

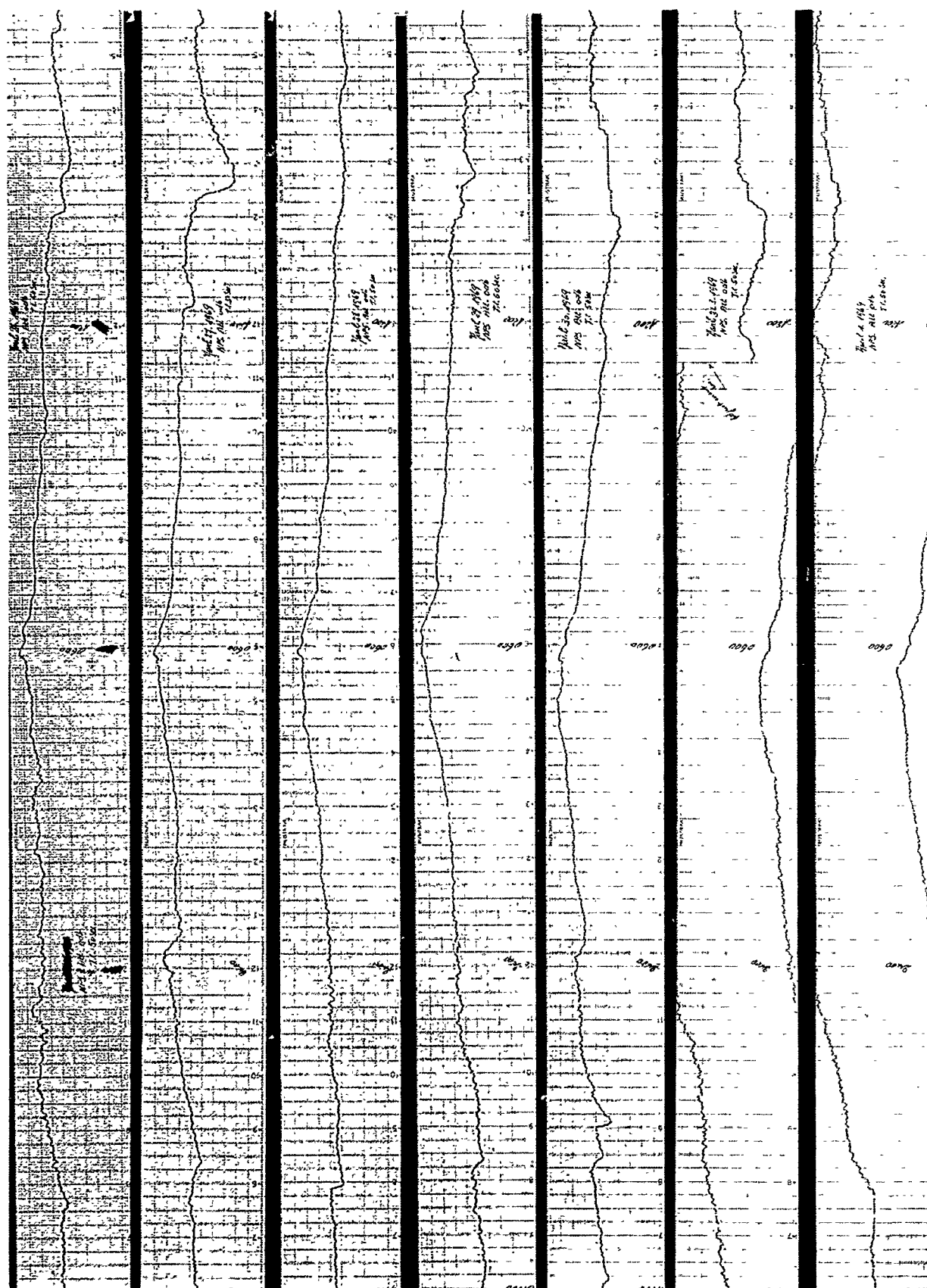


VLF PHASE. NPM-PAYERNE MARCH 26, - APRIL 1, 1969 TIME - UT

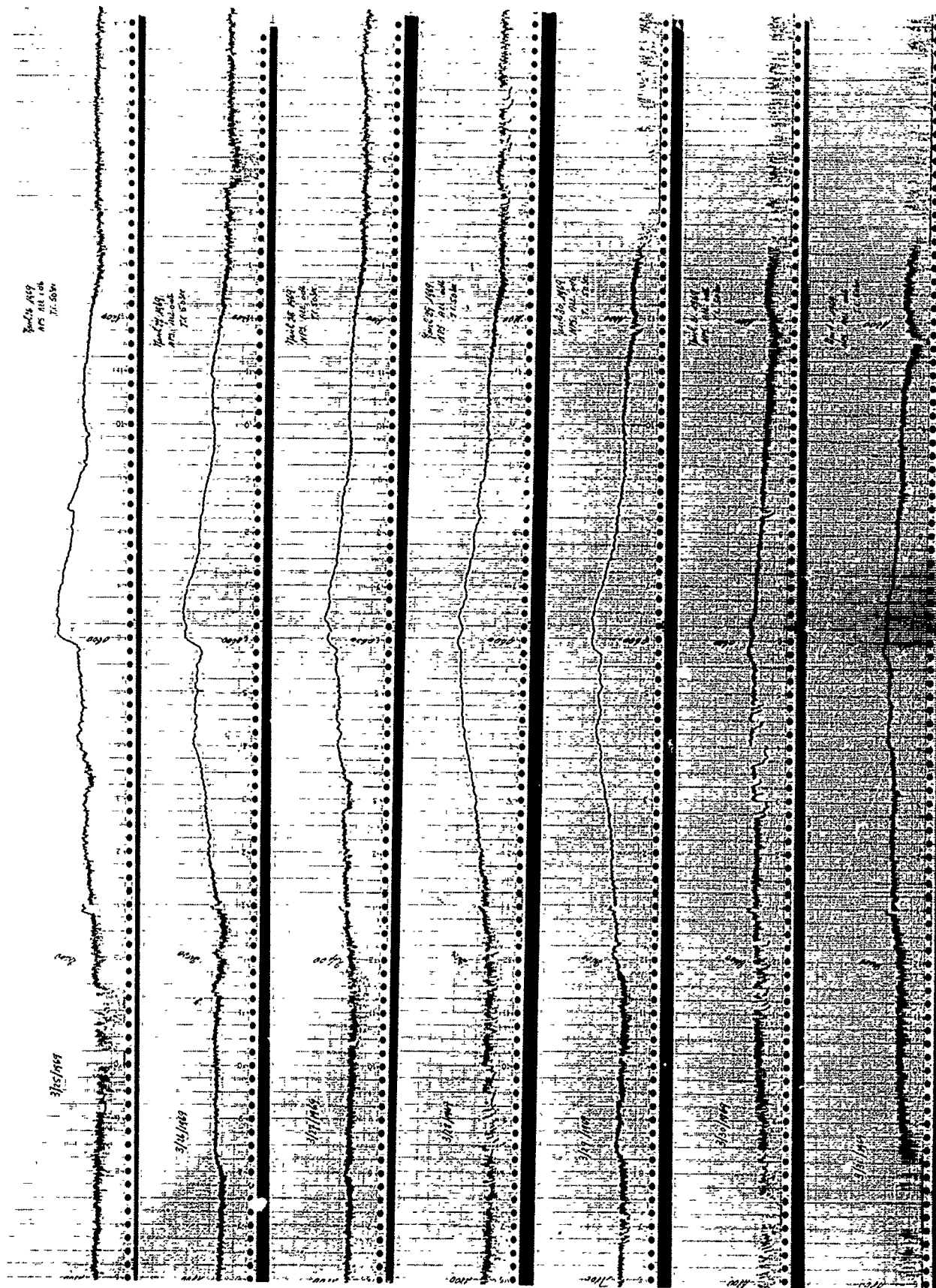


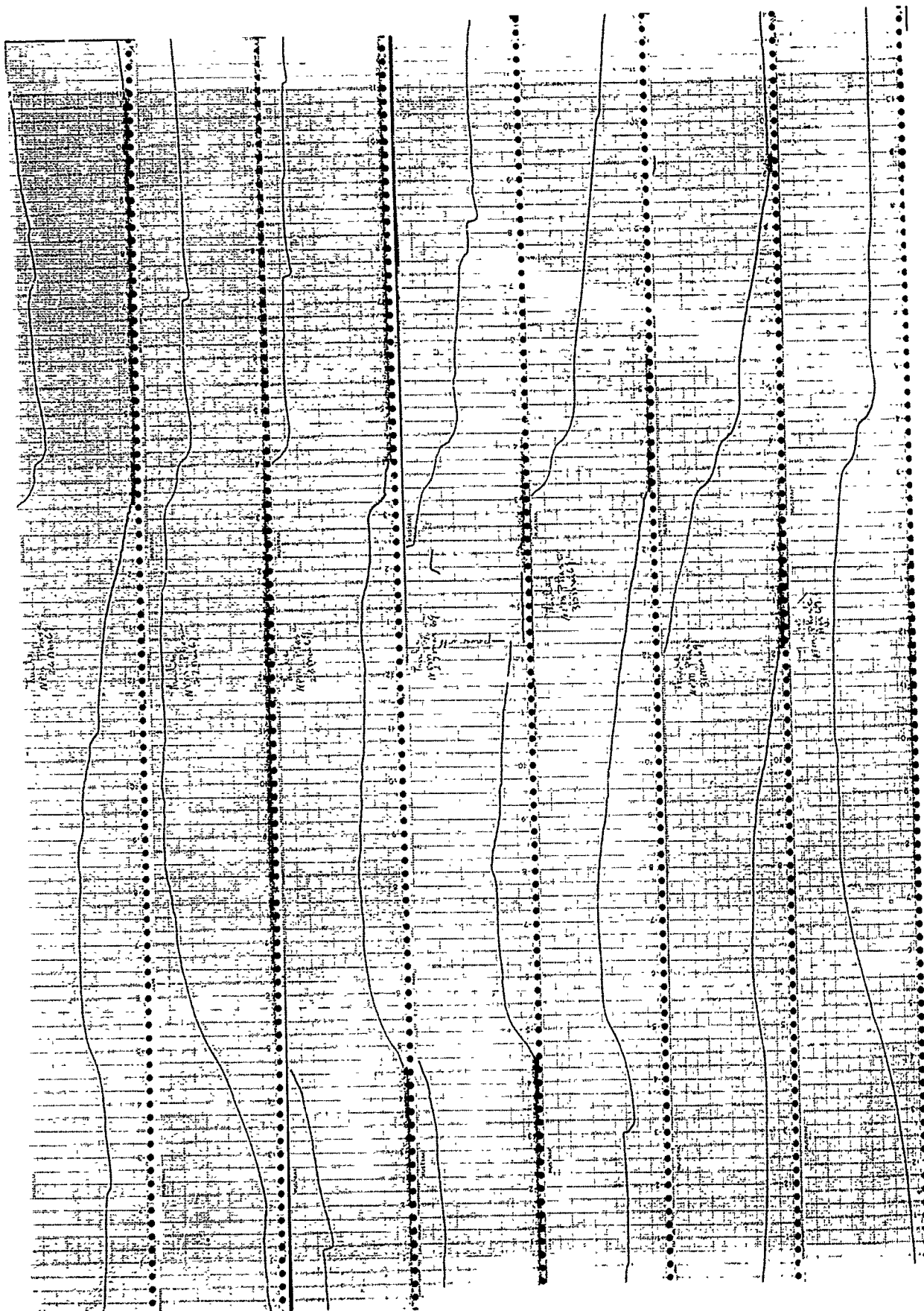


VLF AMPLITUDE, NPM-PAYERNE MARCH 26, - APRIL 1, 1969 TIME - UT + 1

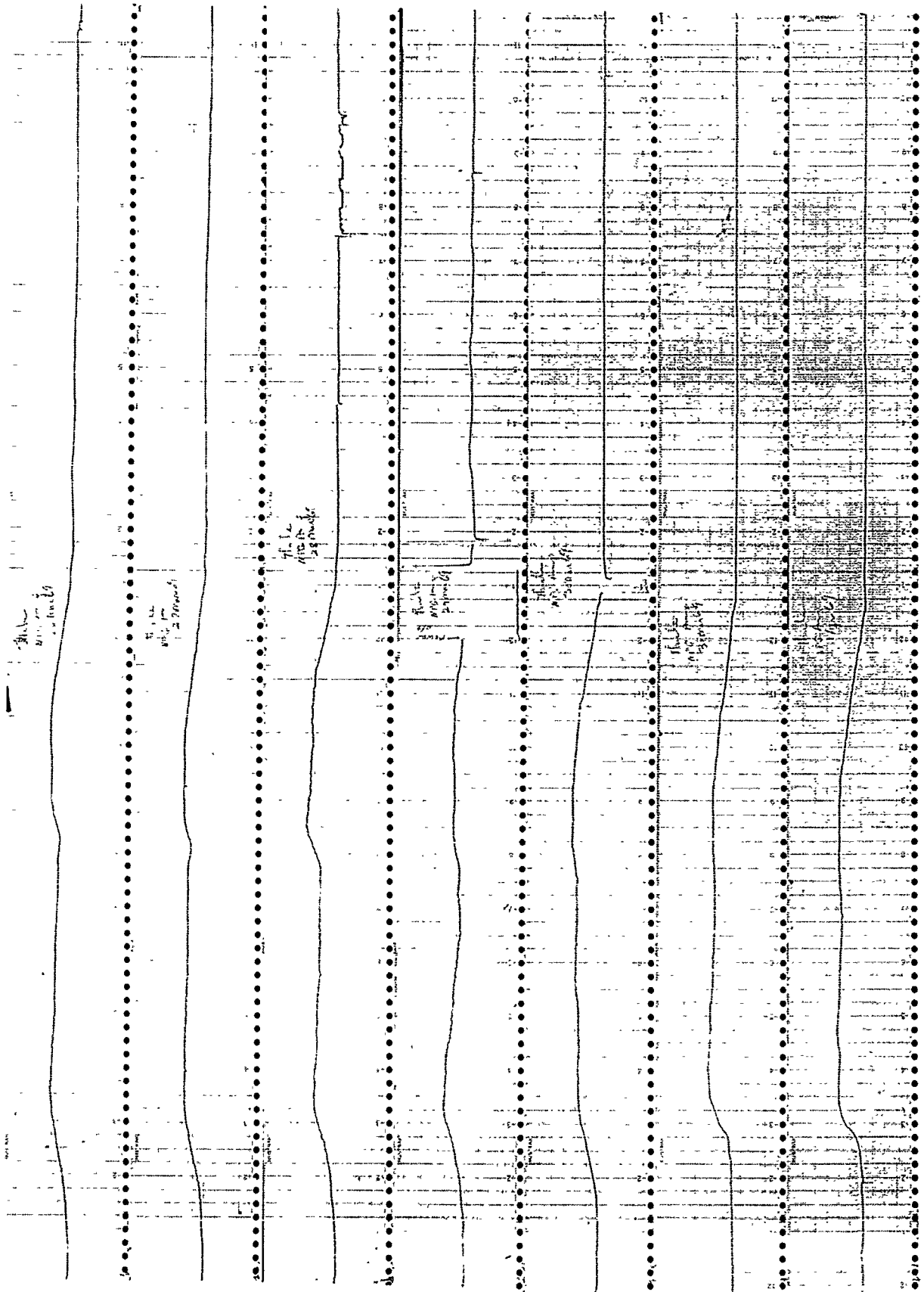


VLF PHASE, NPG-PAYERNE MARCH 26, - APRIL 1, 1969 TIME - UT + 1



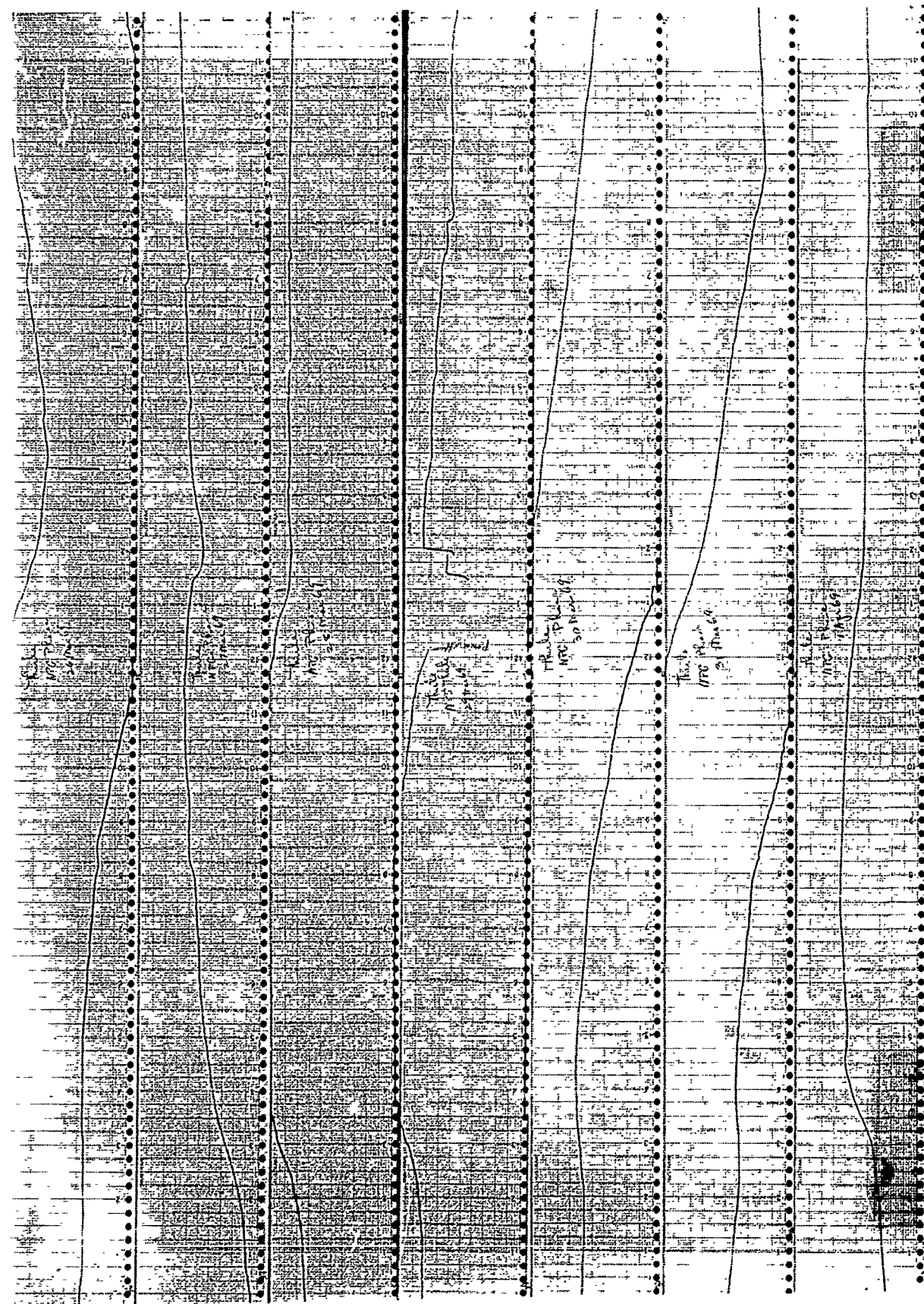


VLF PHASE, NPM-THULE MARCH 26, - APRIL 1, 1969 TIME - UT

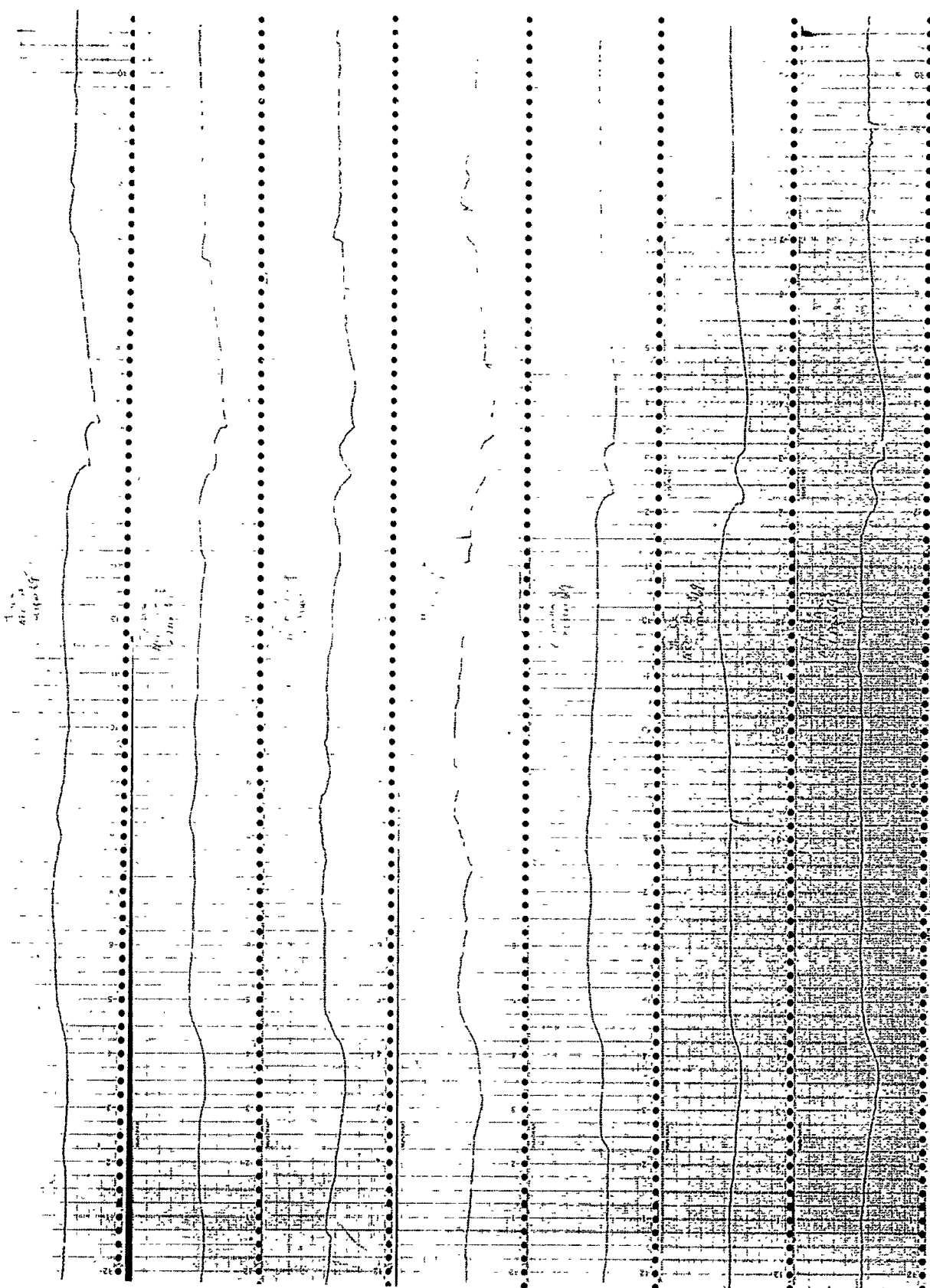


VLF AMPLITUDE, NPG-THULE MARCH 26, - APRIL 1, 1969 TIME - UT





VLF PHASE, NPG-THULE MARCH 26, - APRIL 1, 1969 TIME - UT



VLF AMPLITUDE, NPM-THULE MARCH 26, - APRIL 1, 1969 TIME - UT

APPENDIX B

COMPUTER PLOTS OF RIOMETER ABSORPTION  
DURING RECENT POLAR CAP EVENTS

B-1  
Reverse (Page B-2) Blank



The following section contains computer plots of the riometer broadband absorption obtained during PCA or suspected PCA events during the period from July 1968 through September 1969. Events prior to this period have been covered in previous reports.

The vertical axis is the broadband absorption and is plotted to the nearest tenth of a decibel. The upper limit of the plots is 12.0 dB. If the absorption exceeded 12.0 dB, an asterisk is plotted at the top of the page and the value of the absorption is typed on the page.

The horizontal axis is the time in Universal Time. The data shown was scaled and is plotted every hour on the hour. The plots contain two days per page.

Absorption is shown for the following periods:

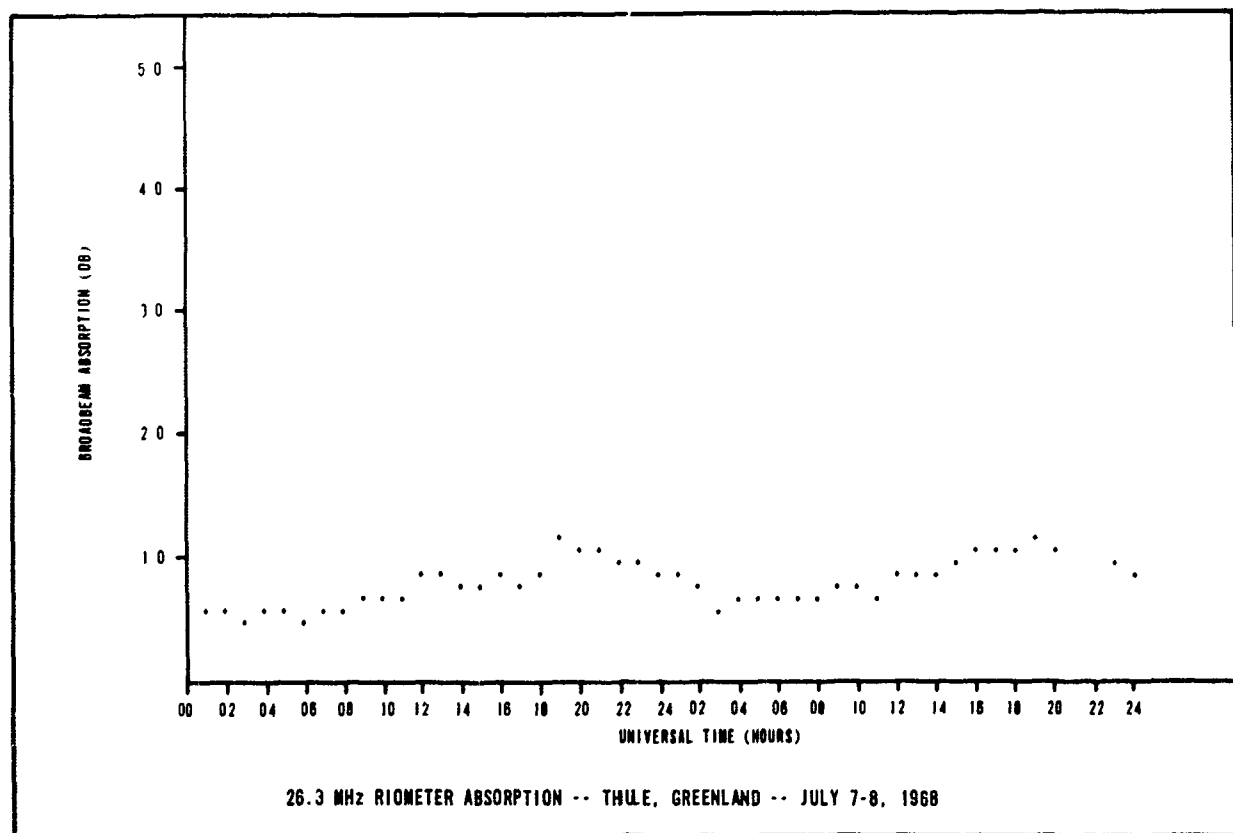
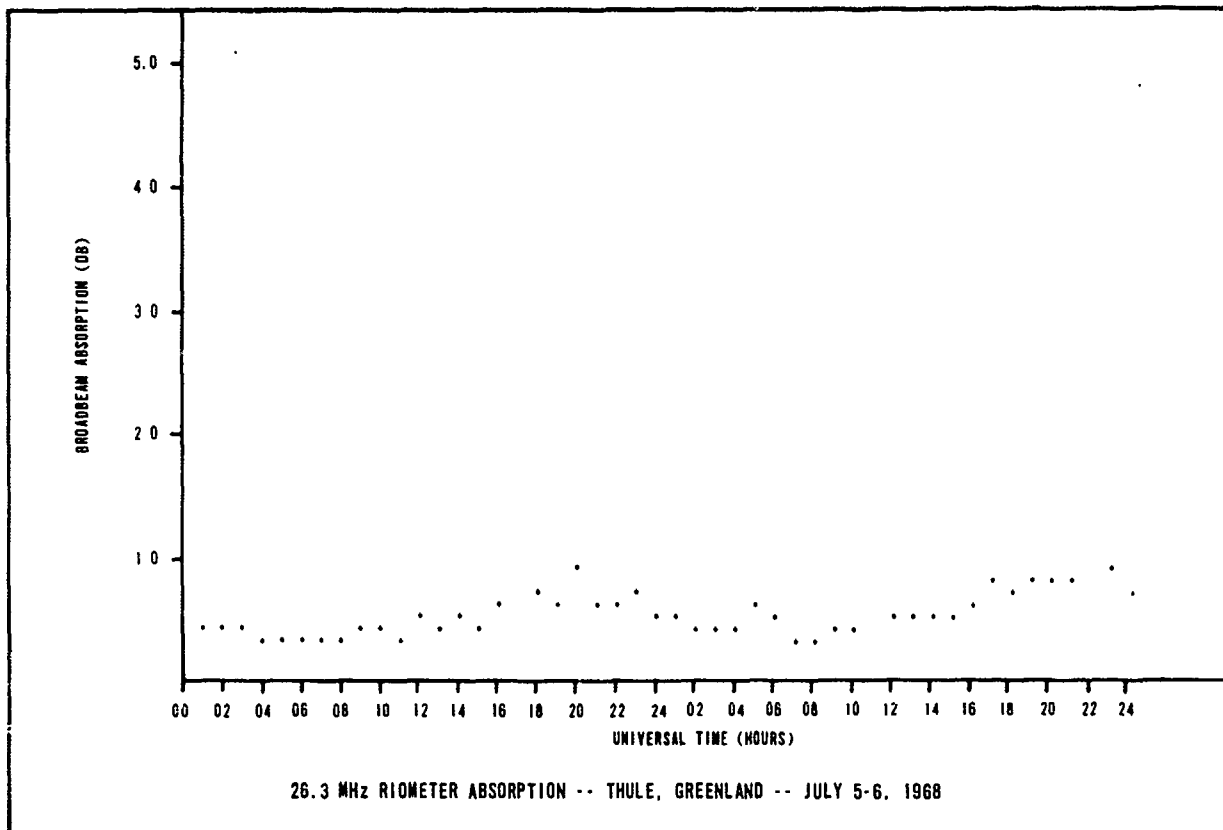
- July 5 - 16, 1968
- September 27 - October 2, 1968
- October 29 - November 5, 1968
- November 18 - 21, 1968
- December 1 - 10, 1968
- January 22 - 27, 1969
- February 23 - March 2, 1969
- March 19 - April 5, 1969
- April 9 - 24, 1969
- May 1 - 4, 1969
- May 14 - 17, 1969
- May 28 - 31, 1969
- June 7 - 12, 1969
- July 30 - 31, 1969
- September 24 - October 3, 1969 (Iceland only)

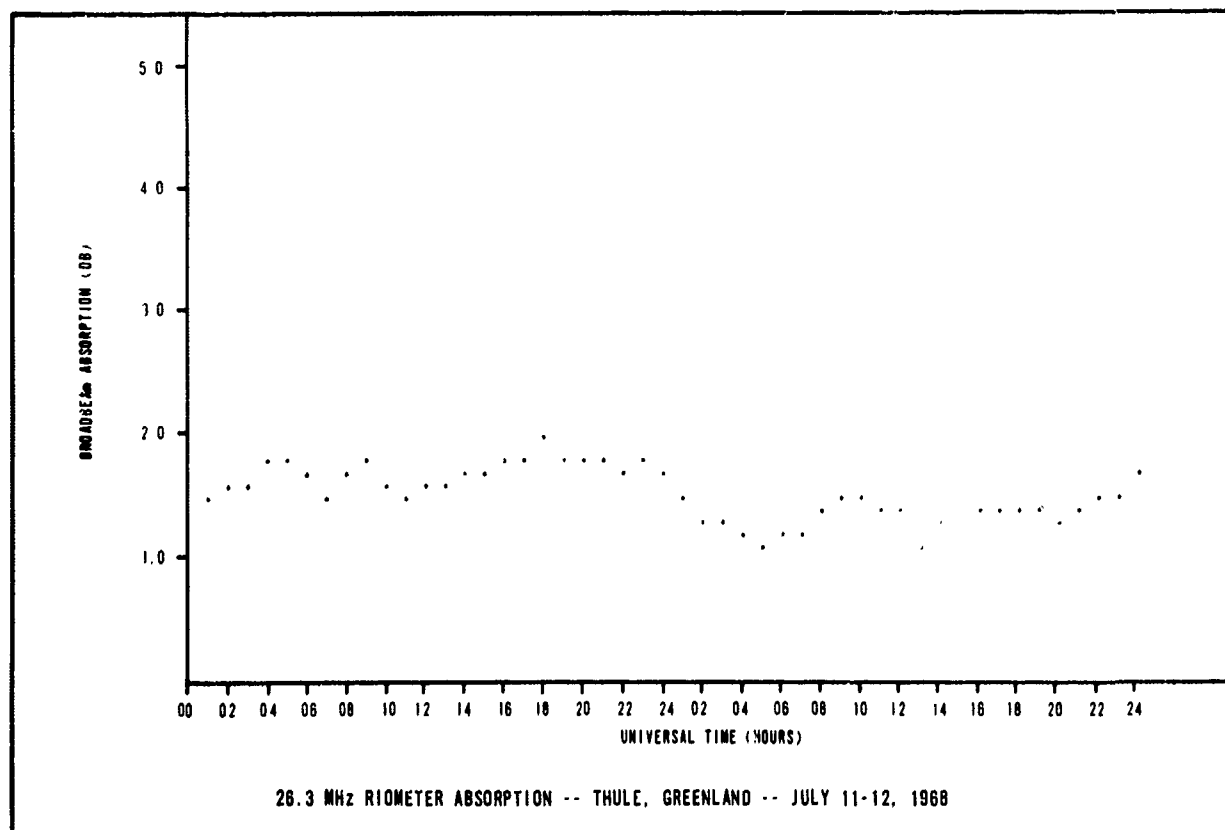
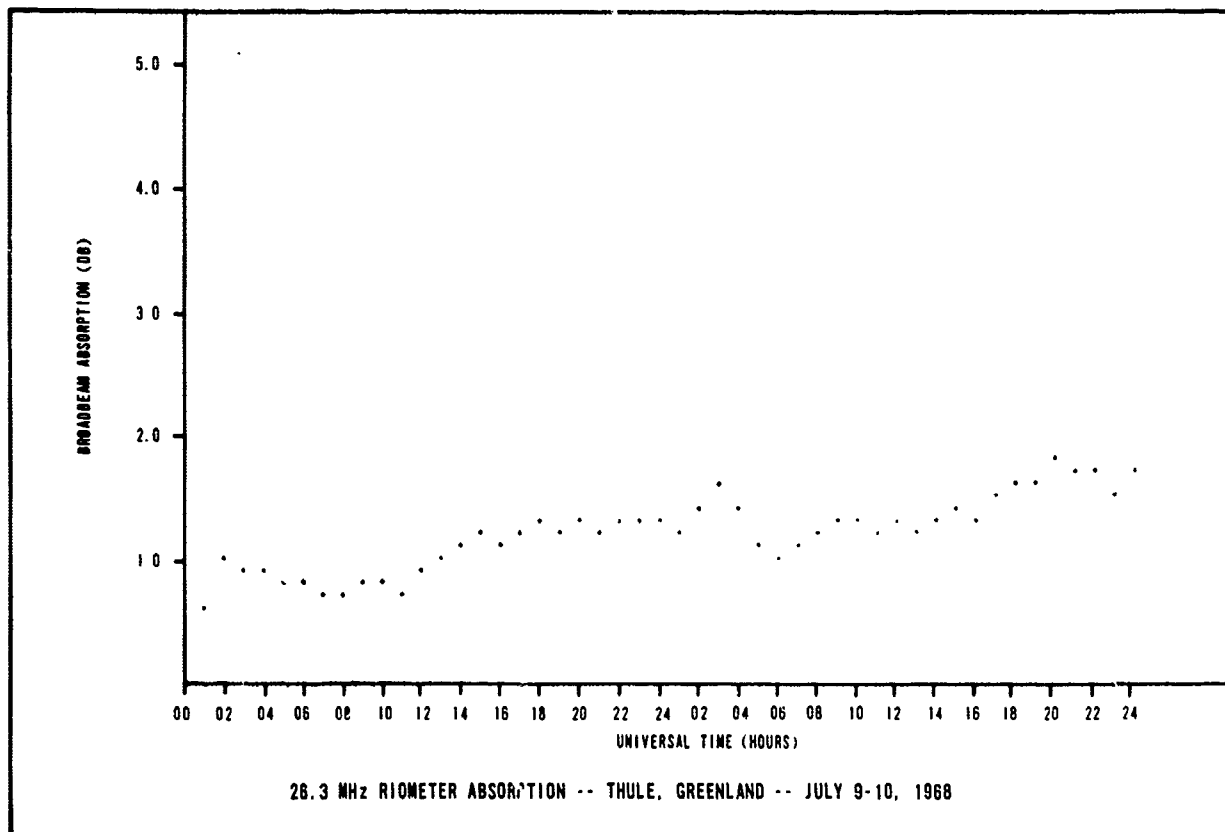
The antennas used in Iceland were parallel half-wave dipoles which were fed in phase. This yields a nearly symmetrical  $60^\circ$  half-power beamwidth. The correction factor for conversion from broadbeam to narrowbeam absorption of approximately 0.8.

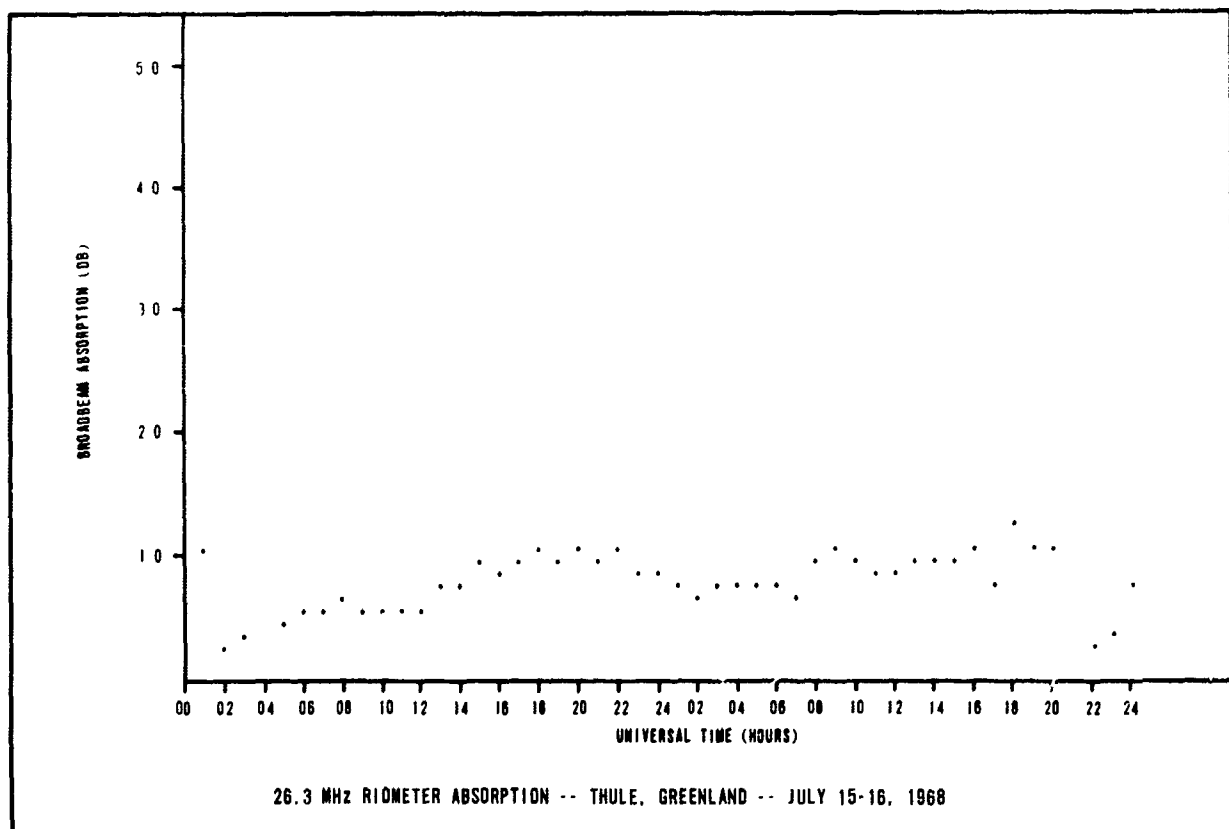
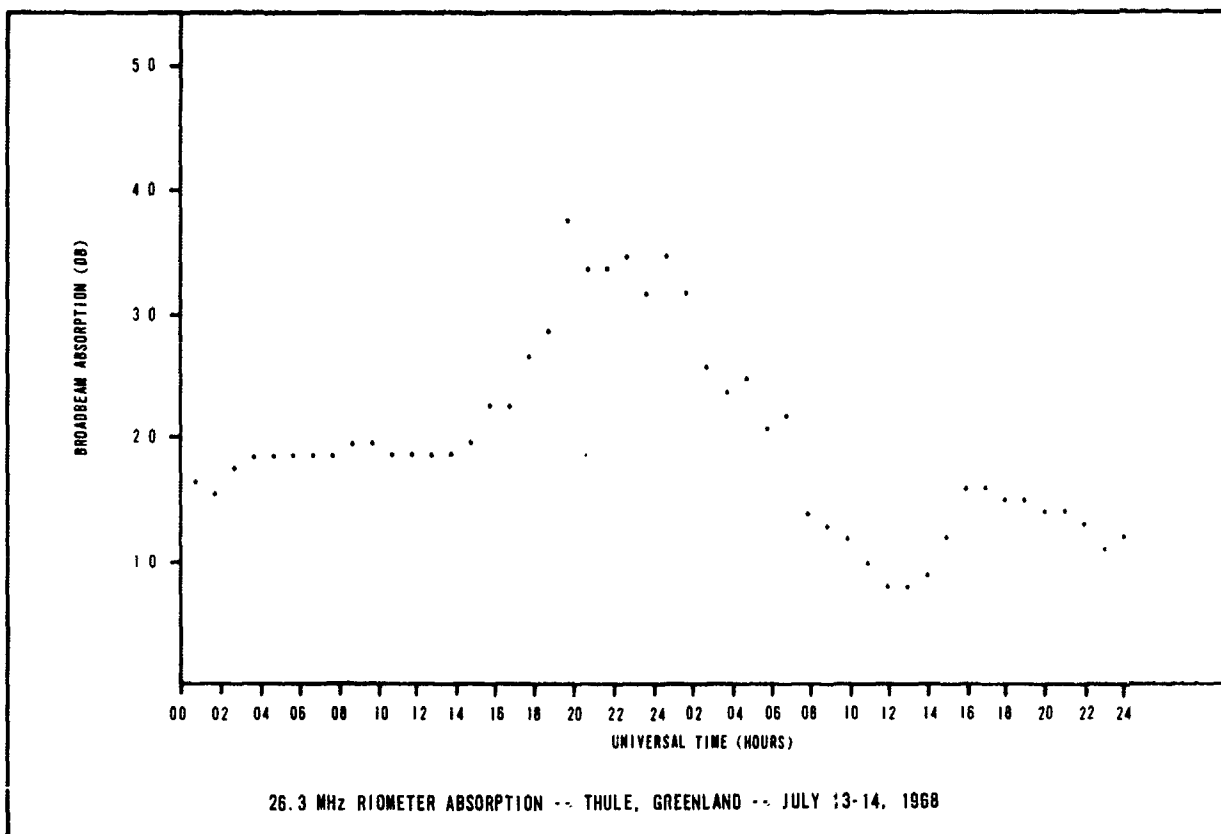
The antennas used at Thule were three element yagis with a  $60^\circ \times 100^\circ$  half-power beamwidth. This beamwidth was approximated by a  $90^\circ$  conical beam and a correction factor for narrowbeam absorption was found to be 0.85.

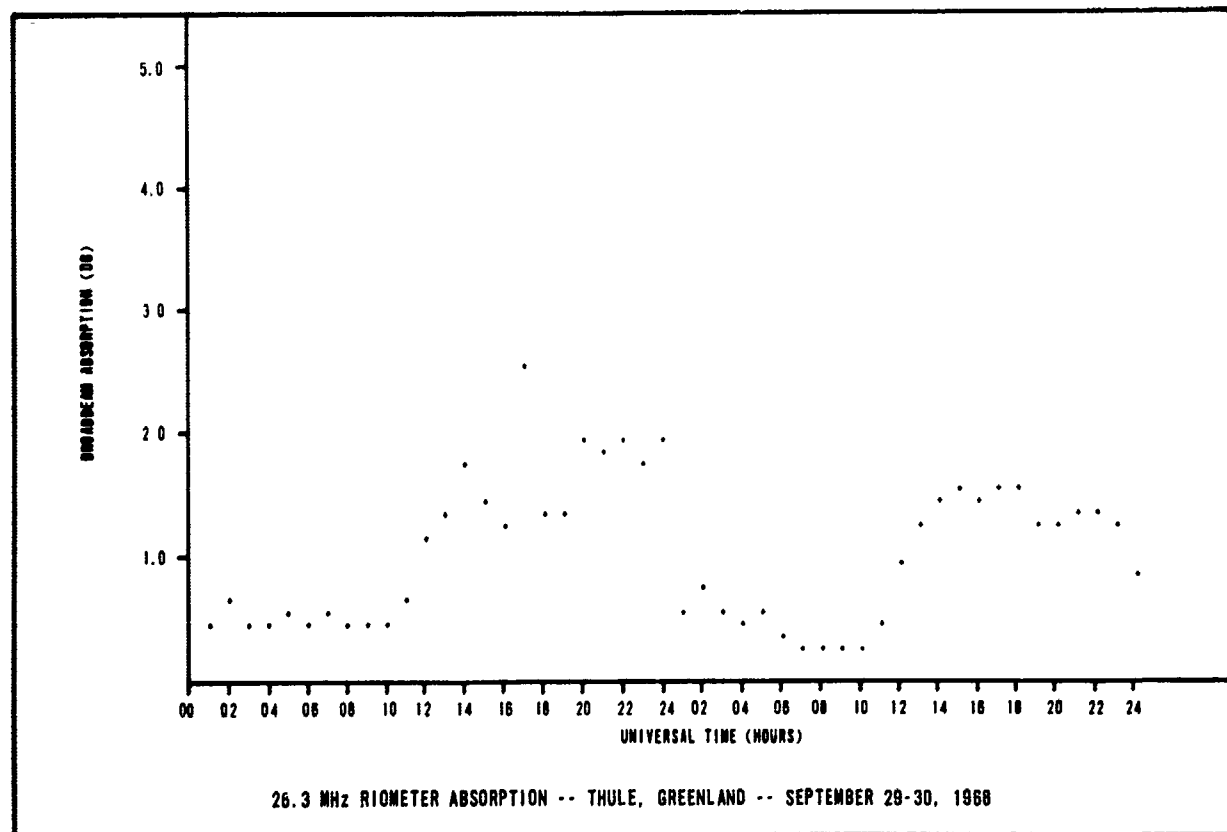
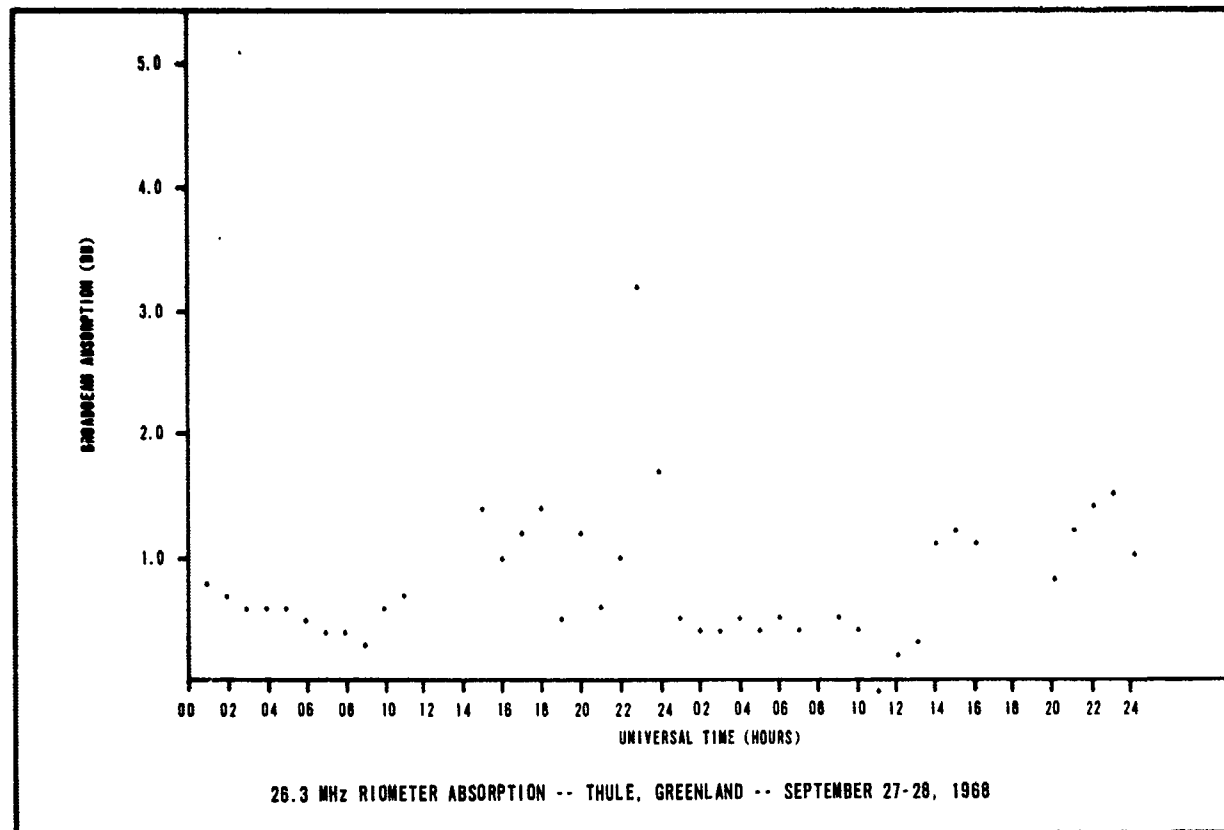
The 40 MHz riometer for Thule, Greenland was down for repair during the period from September 27 to October 2, 1968. The Greenland data for the September 24 to October 3, 1969 was not received in time for this report. The 20 MHz riometer at Reykjavik, Iceland did not produce any useful data after the end of April. It became so plagued with interference that it was impossible to reduce the data. The 30 MHz unit in Iceland was down for repairs during the entire month of December.

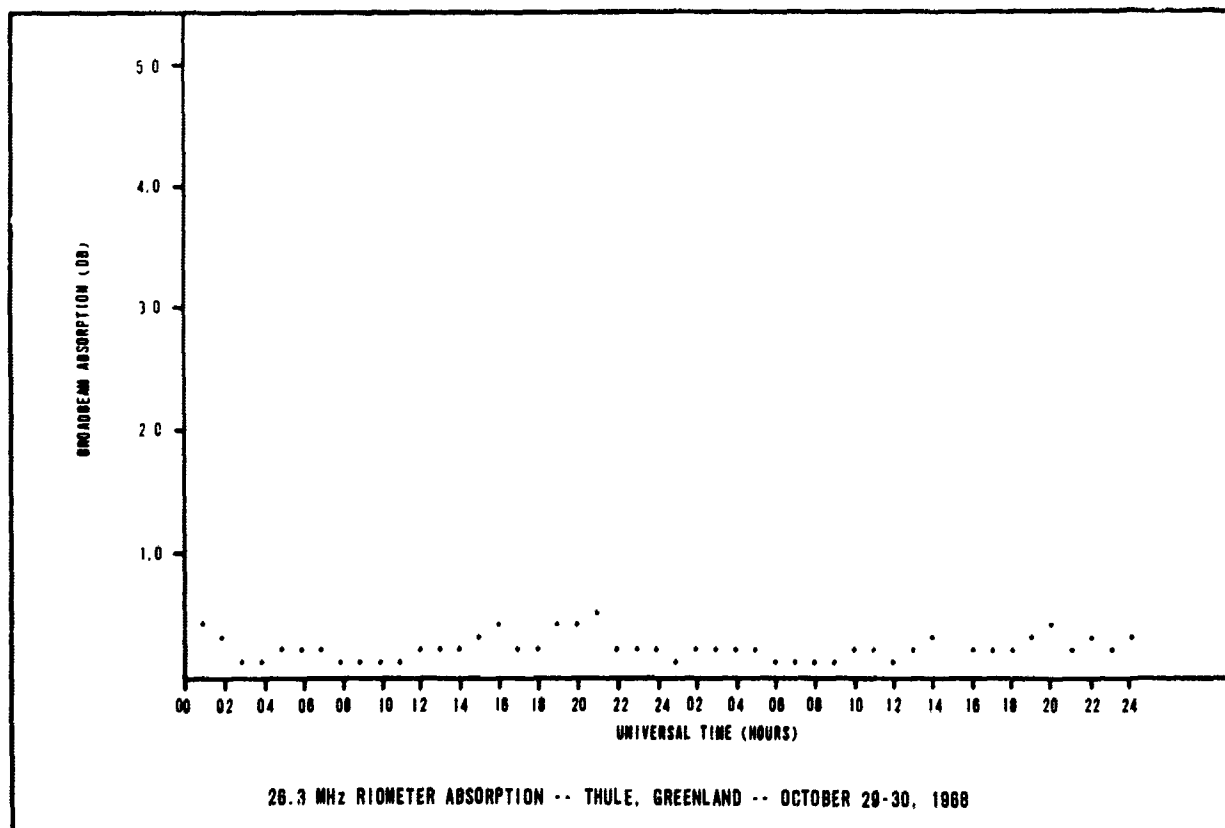
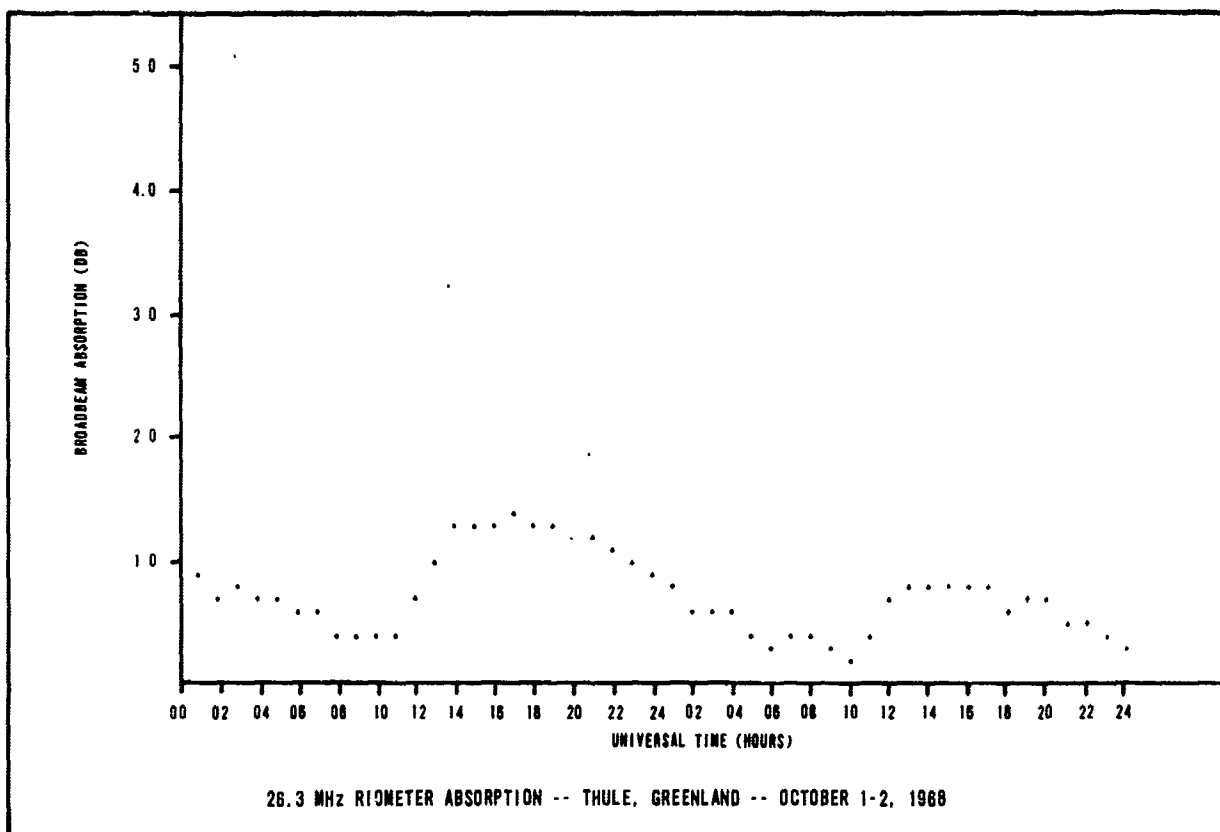
The quiet day reference curve used to determine the absorption in all cases was obtained during the winter months. In Greenland this is a period of total darkness. In Iceland there is a short period of daylight even at this time of the year. The values of absorption then include the contribution of the sun as well as the PCA for those cases when there was daylight conditions.

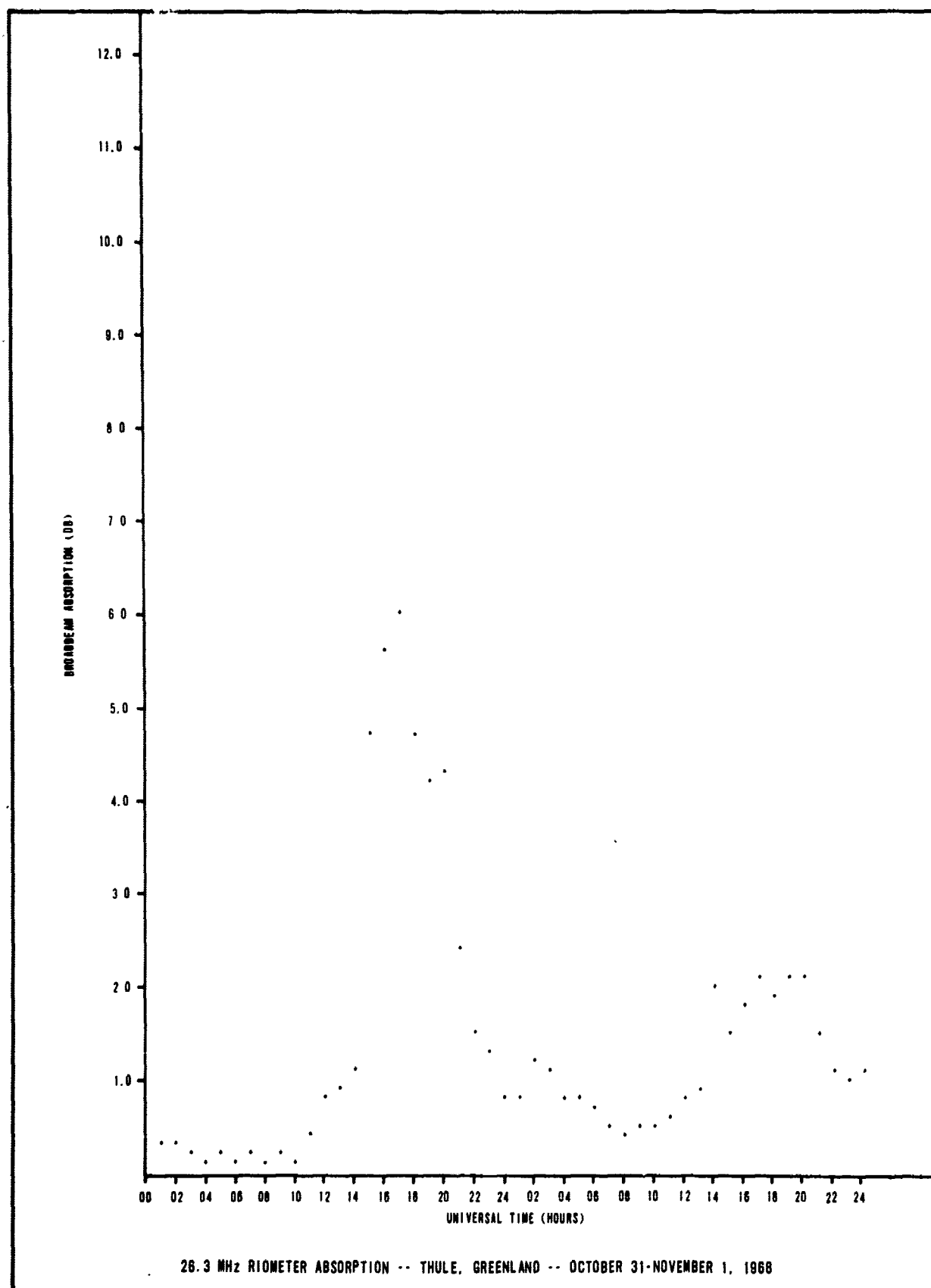




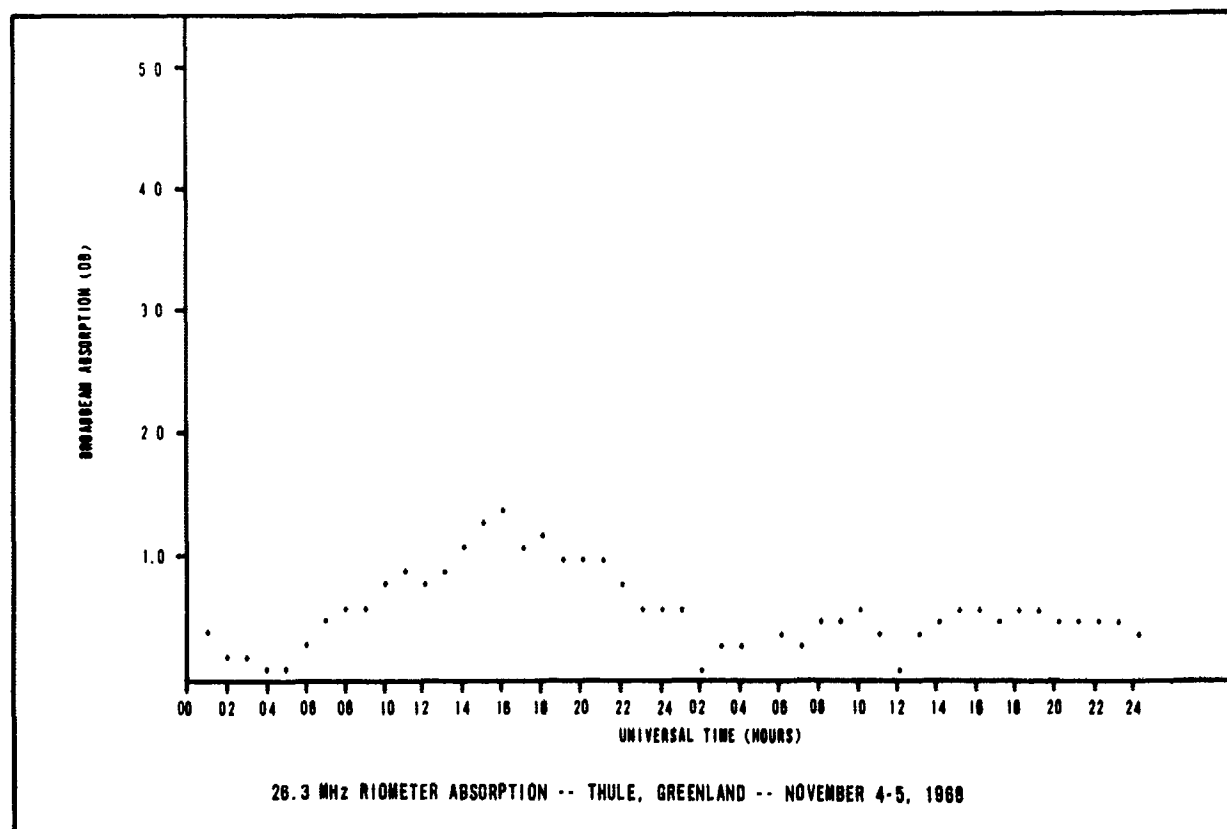
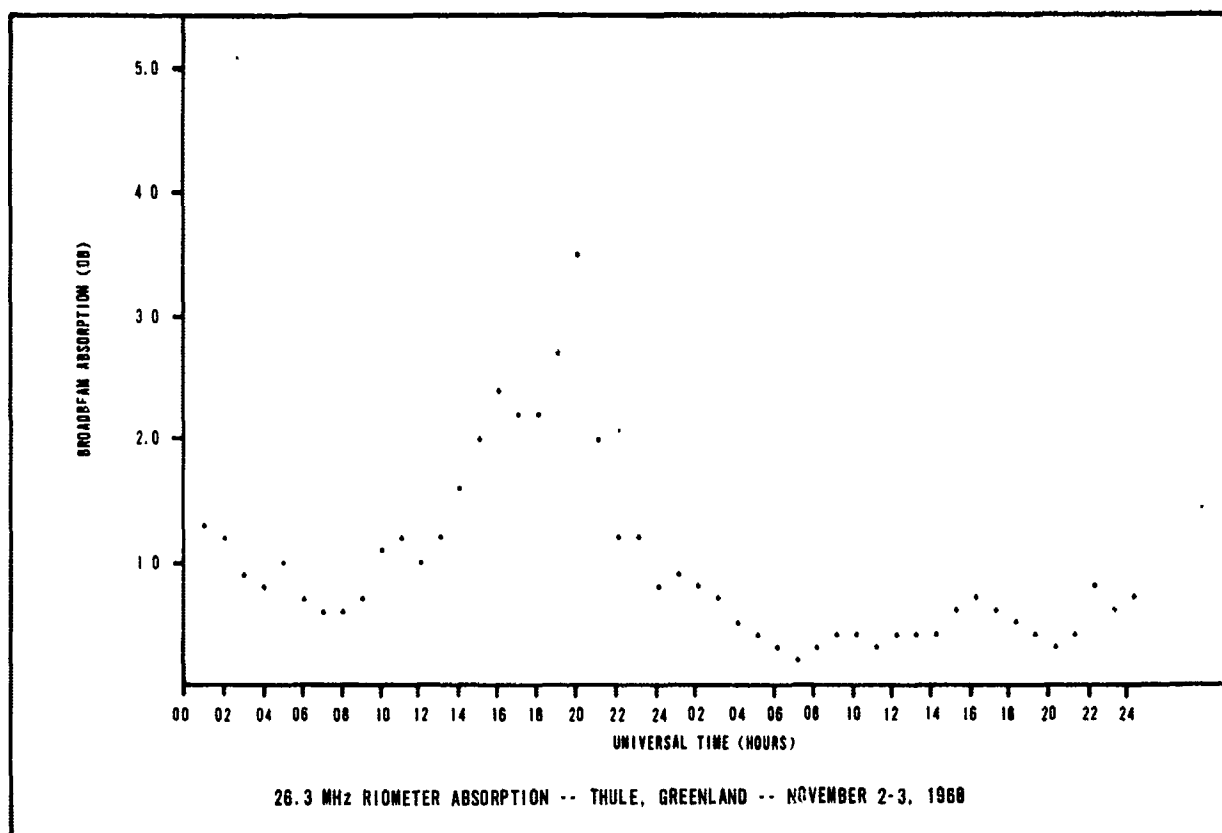


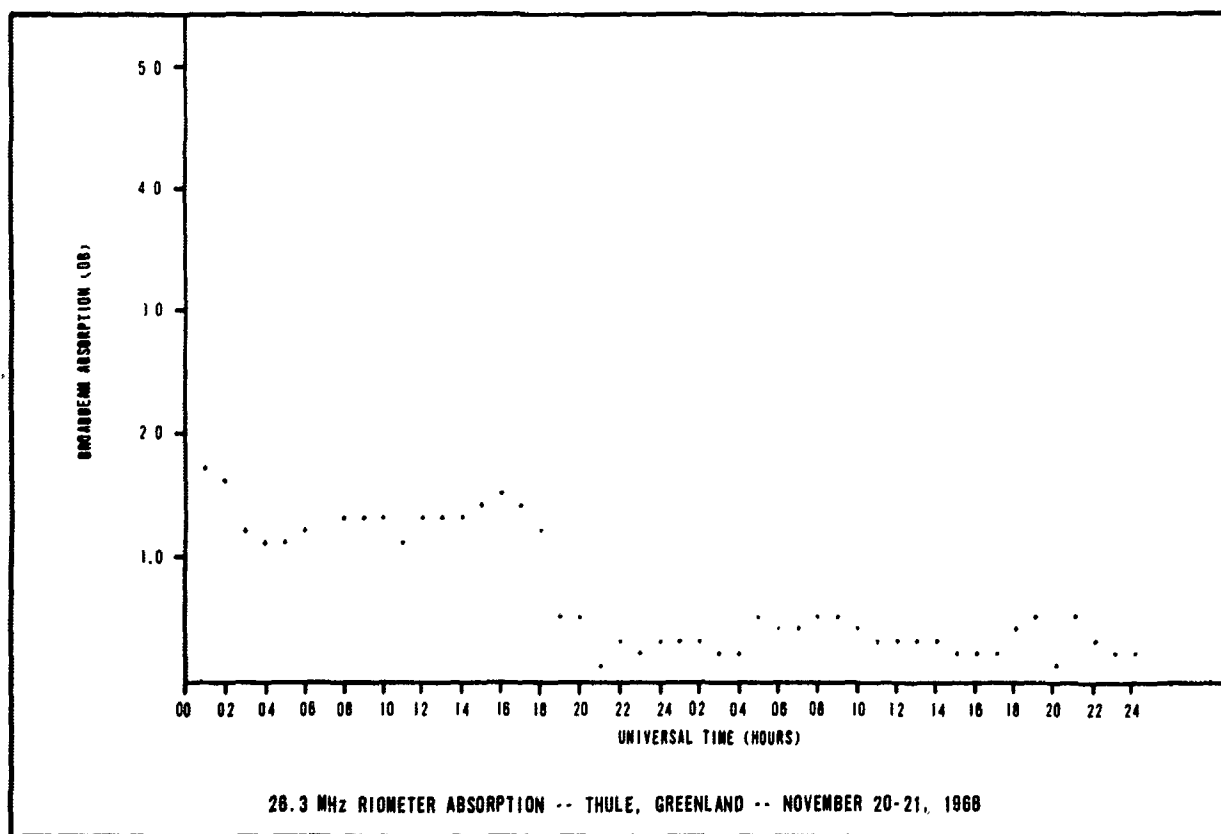
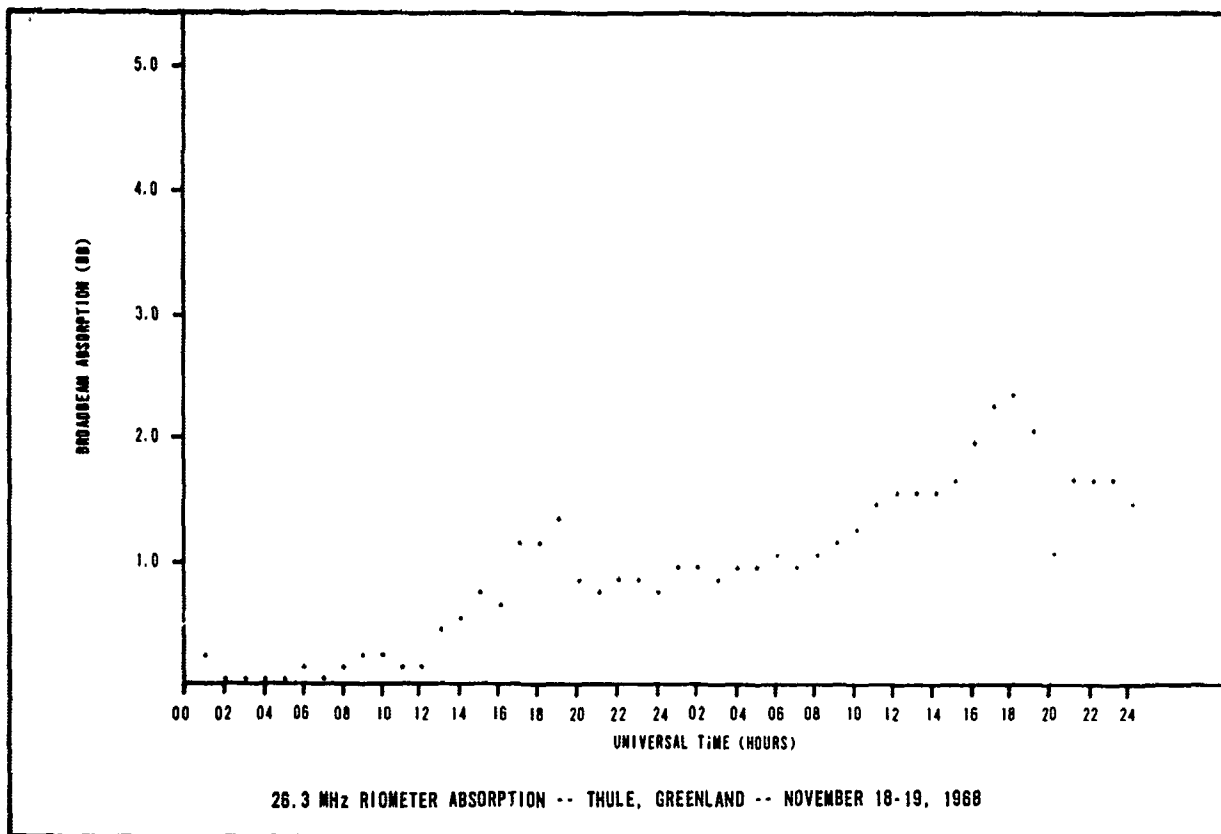


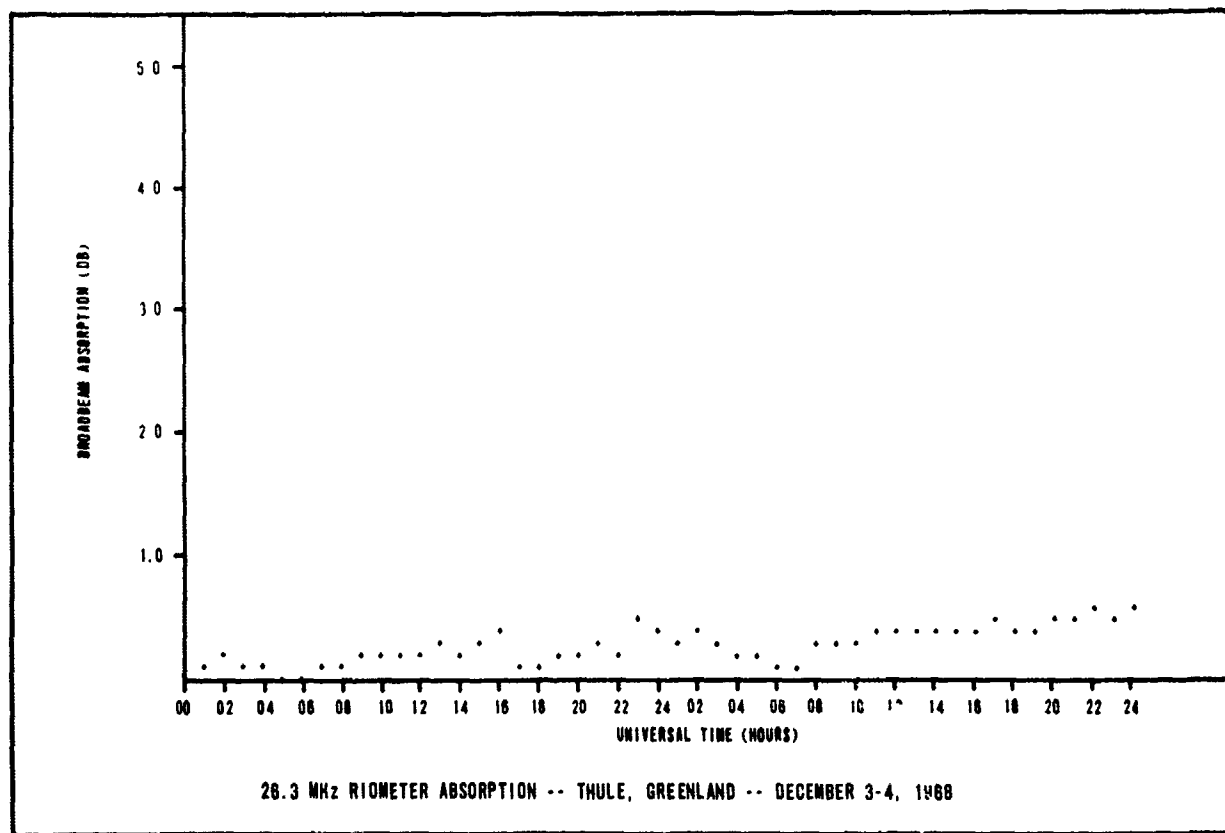
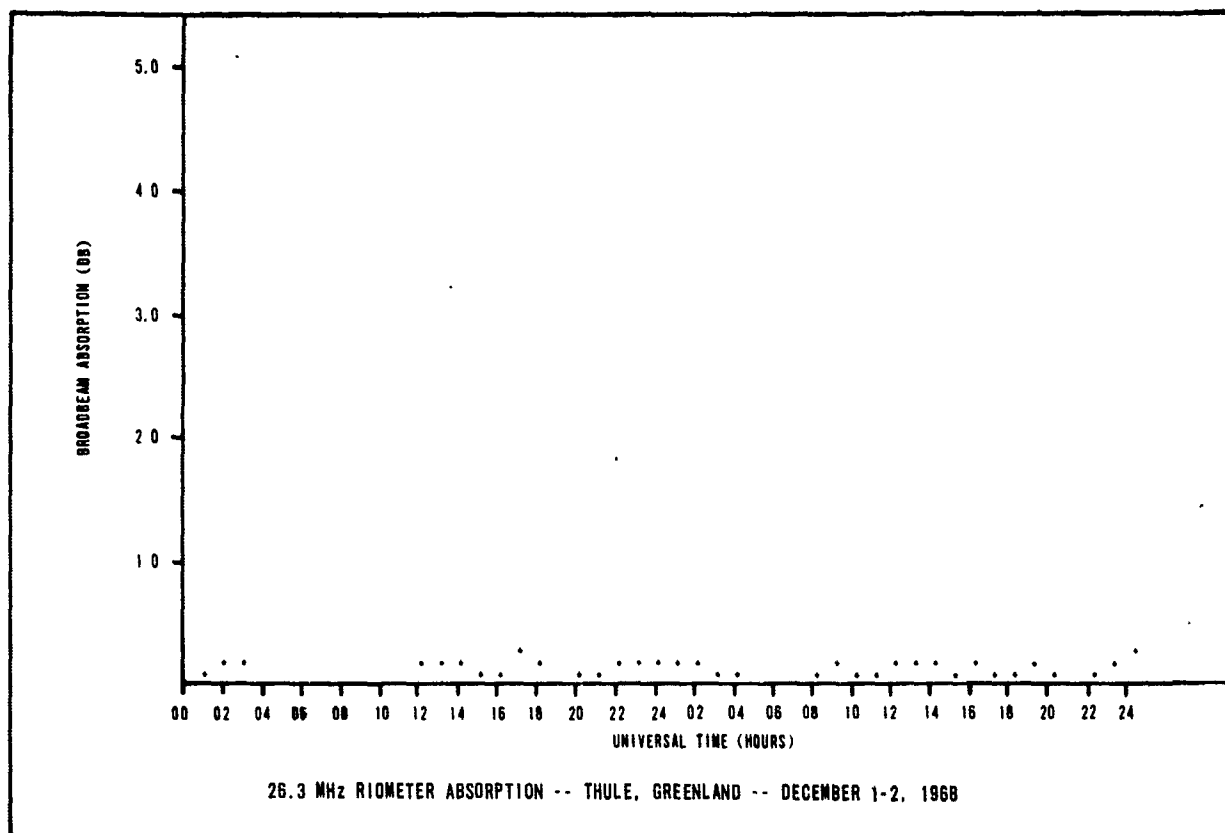


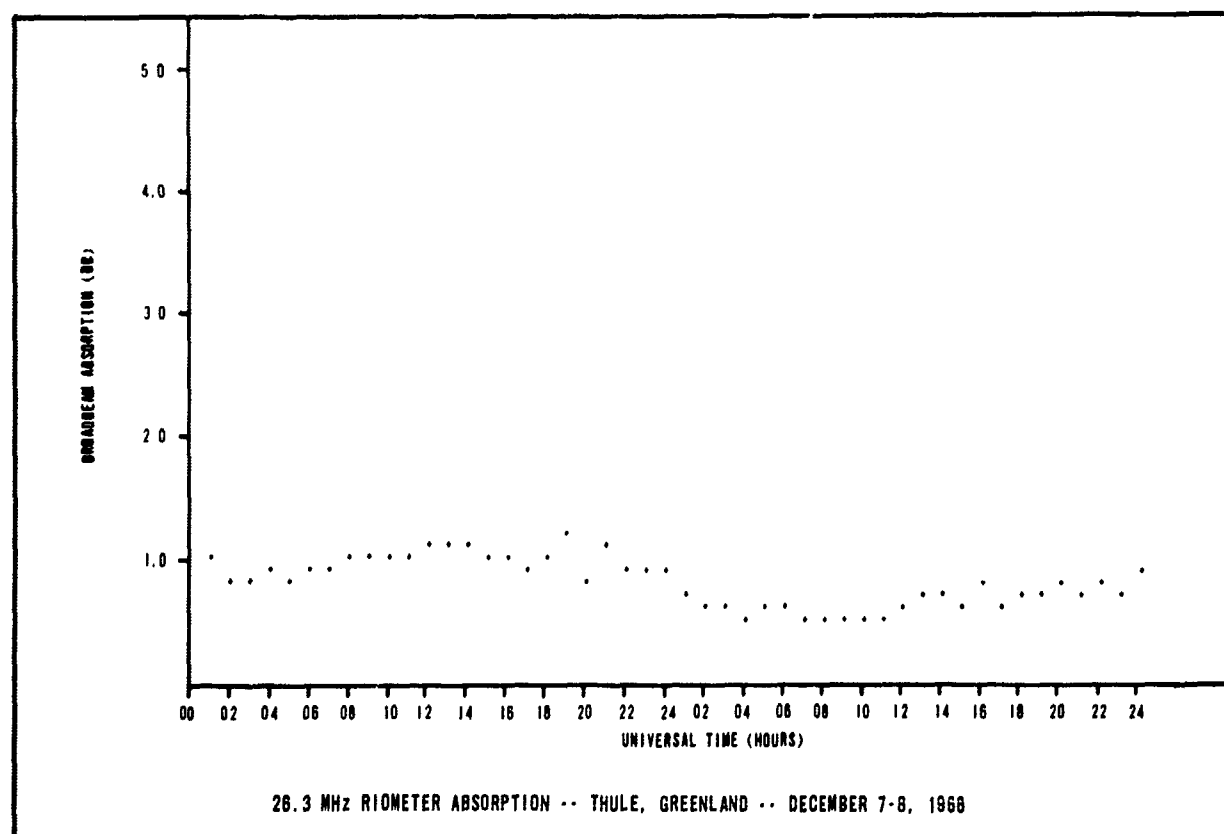
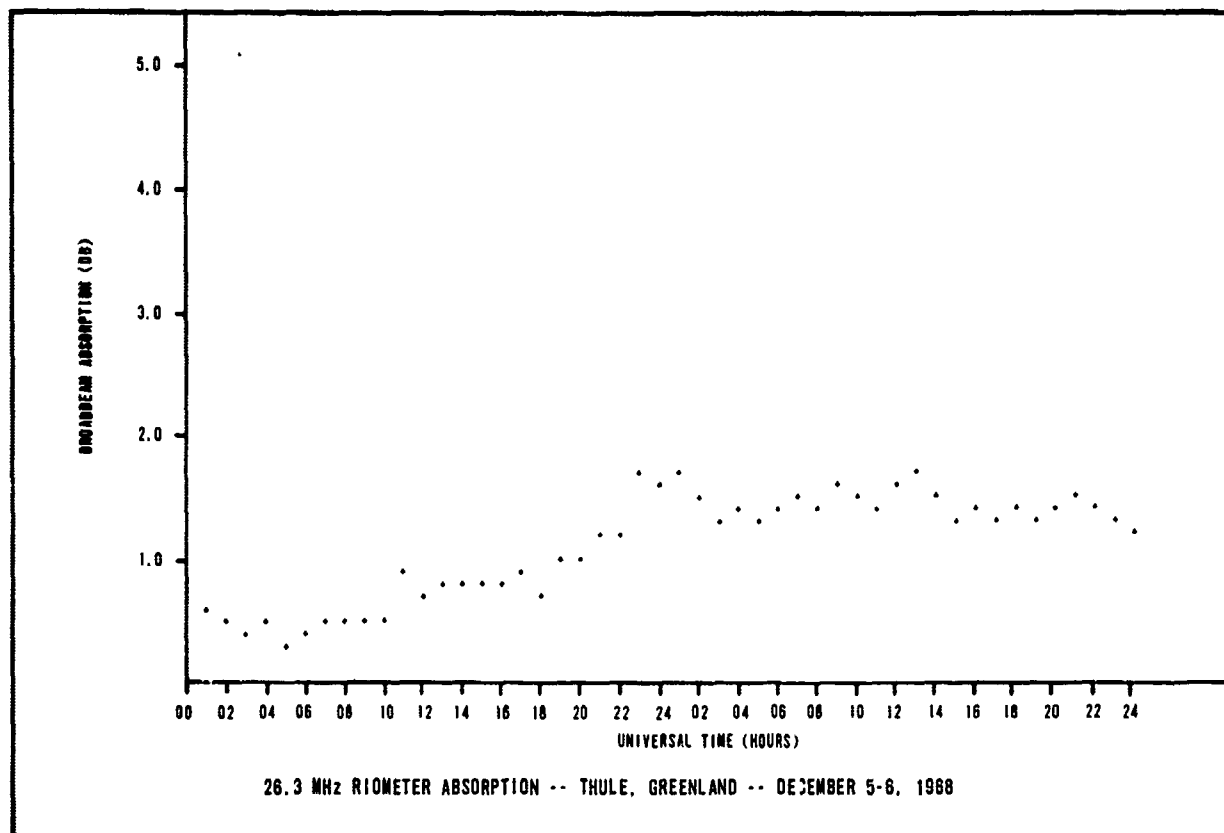


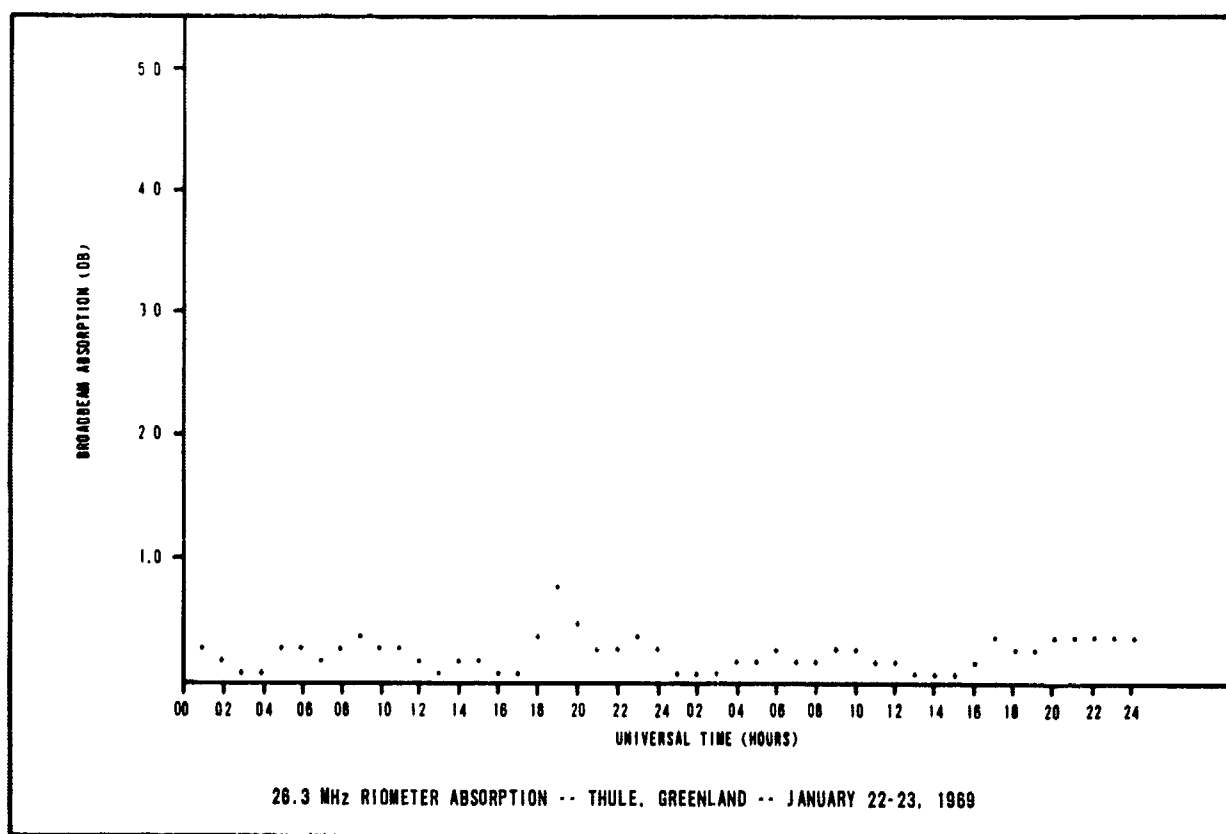
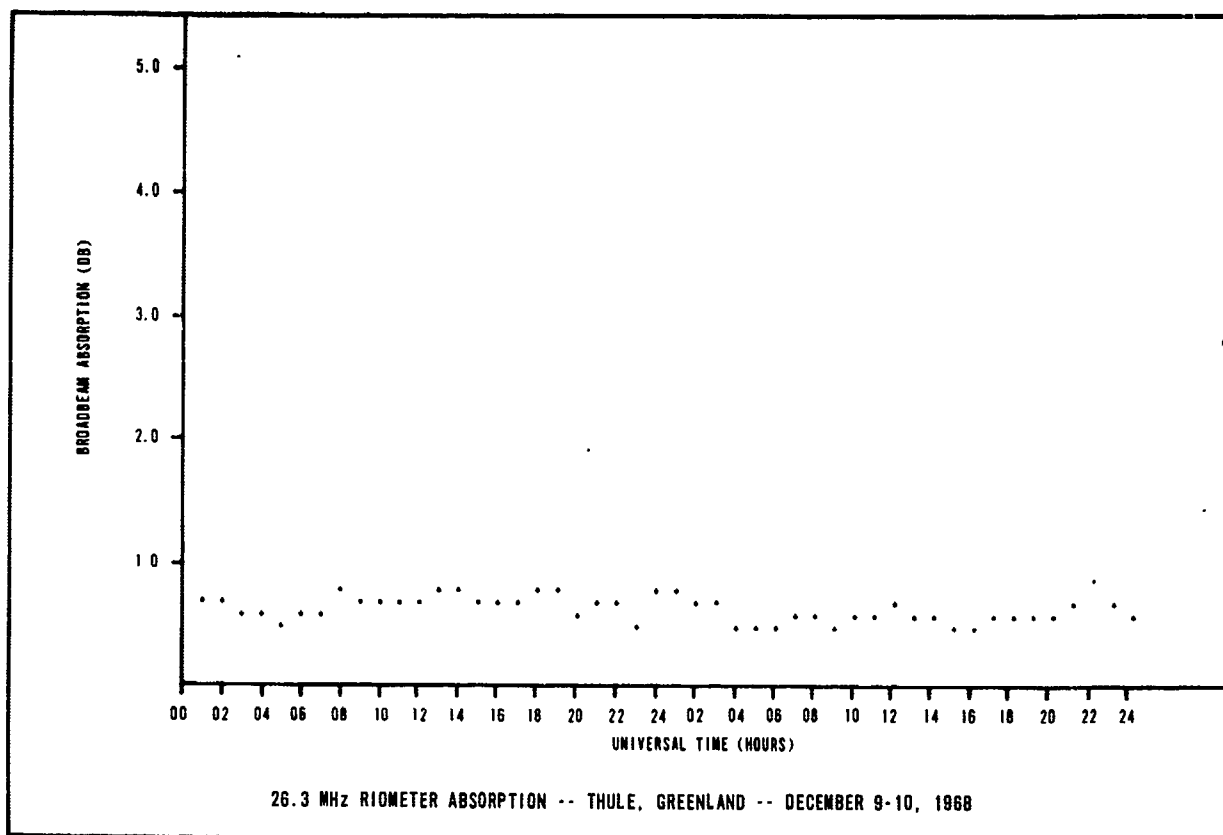


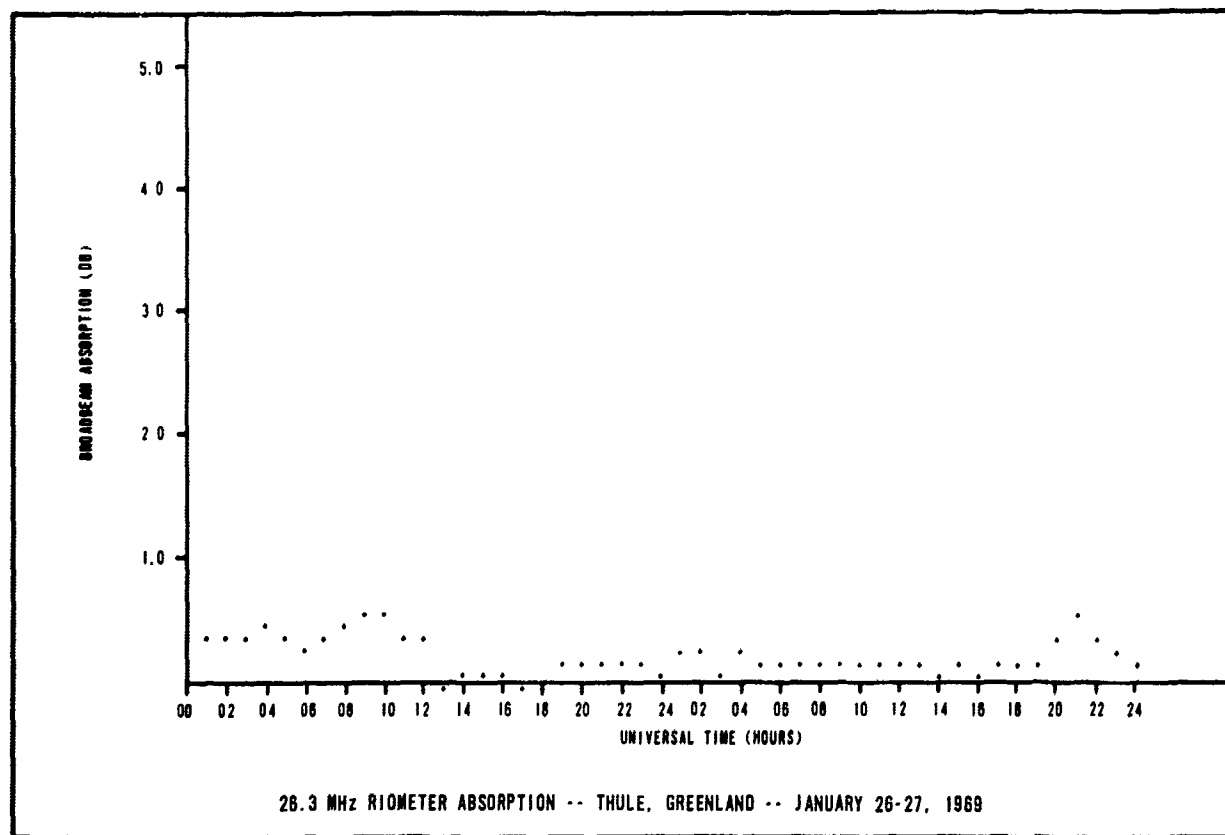
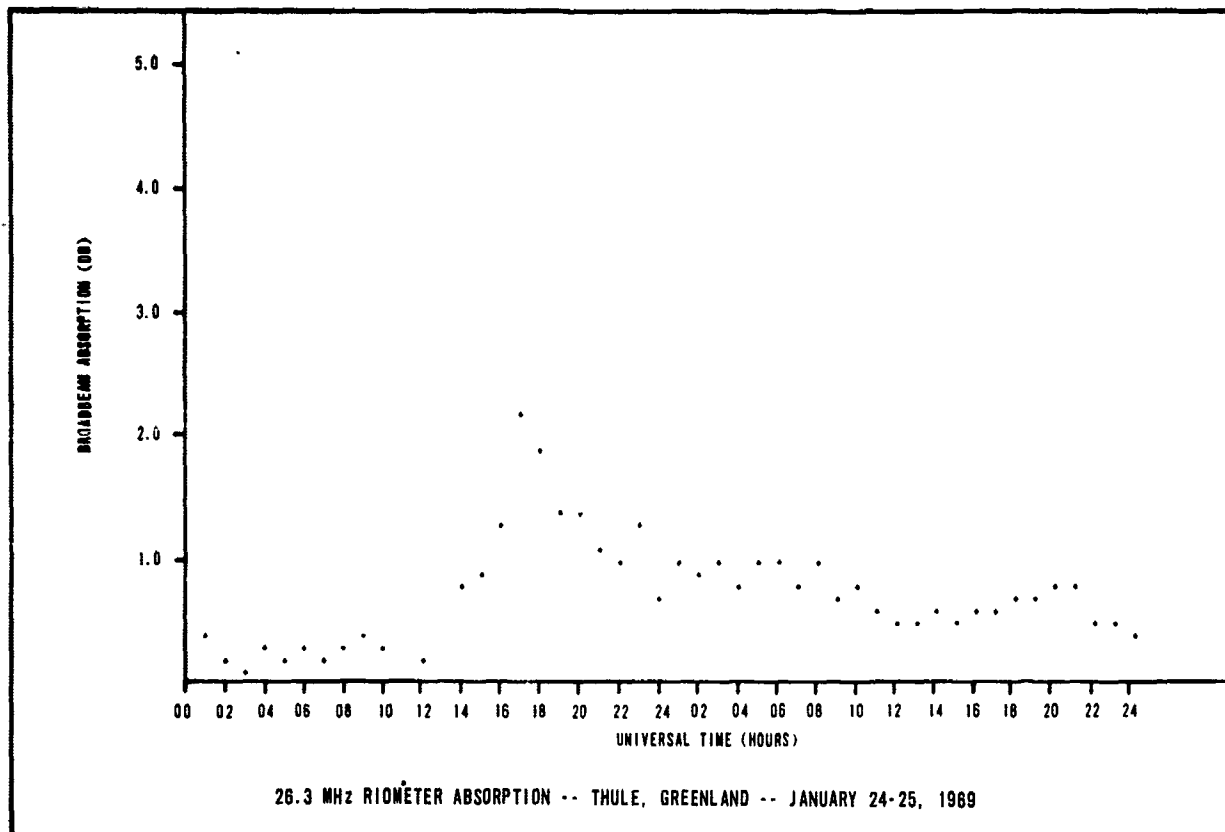


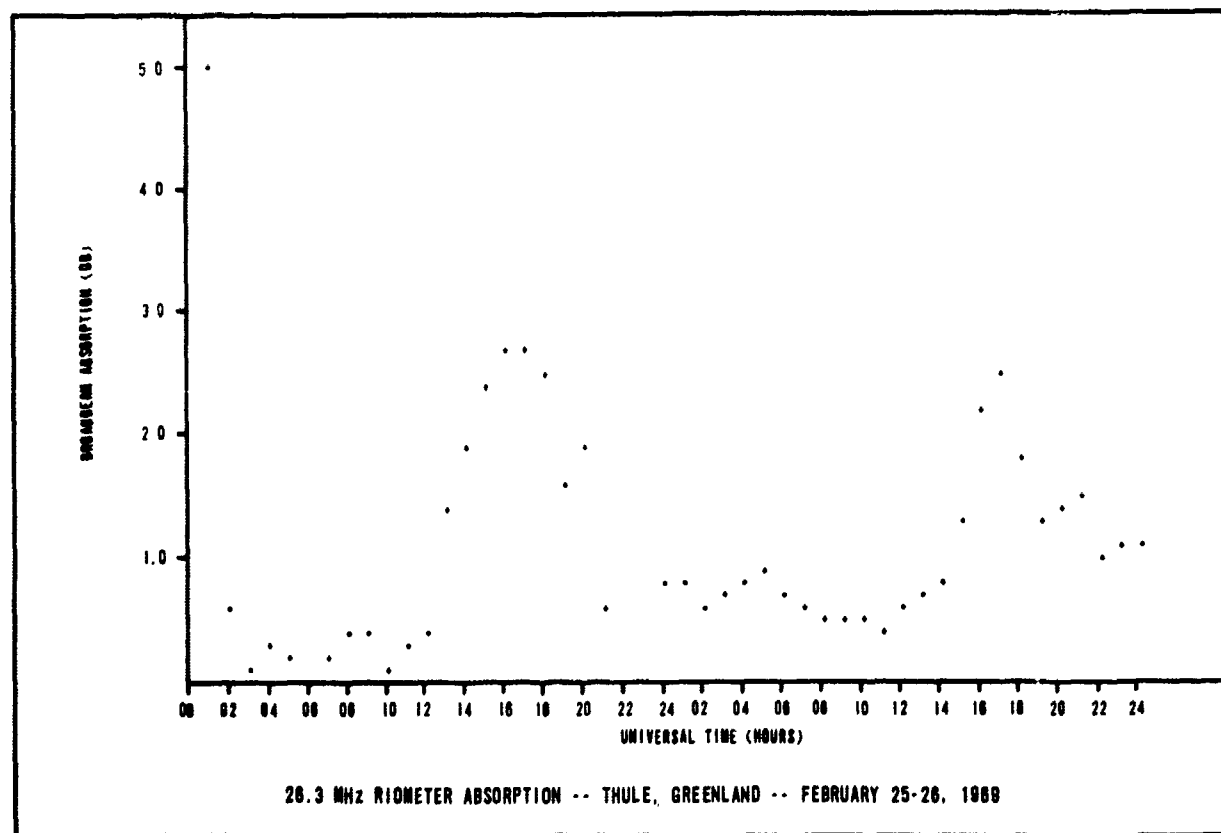
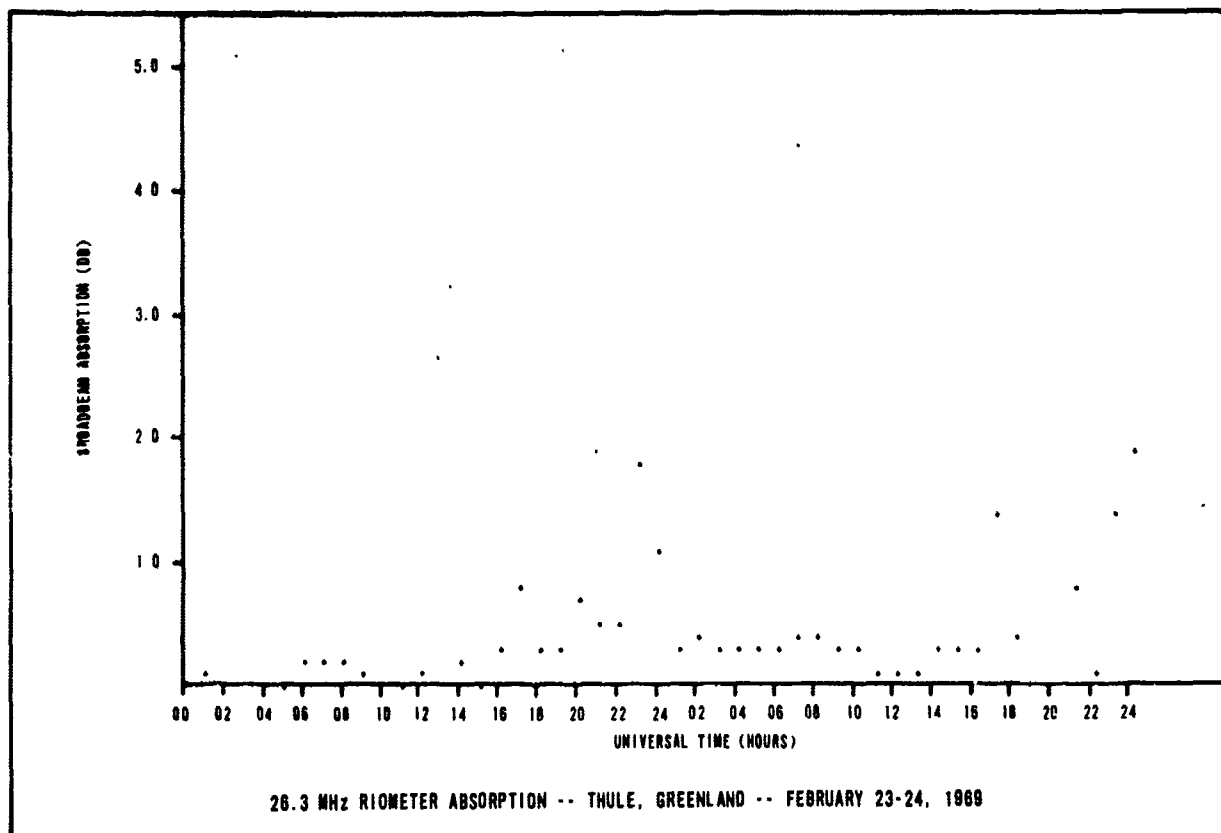


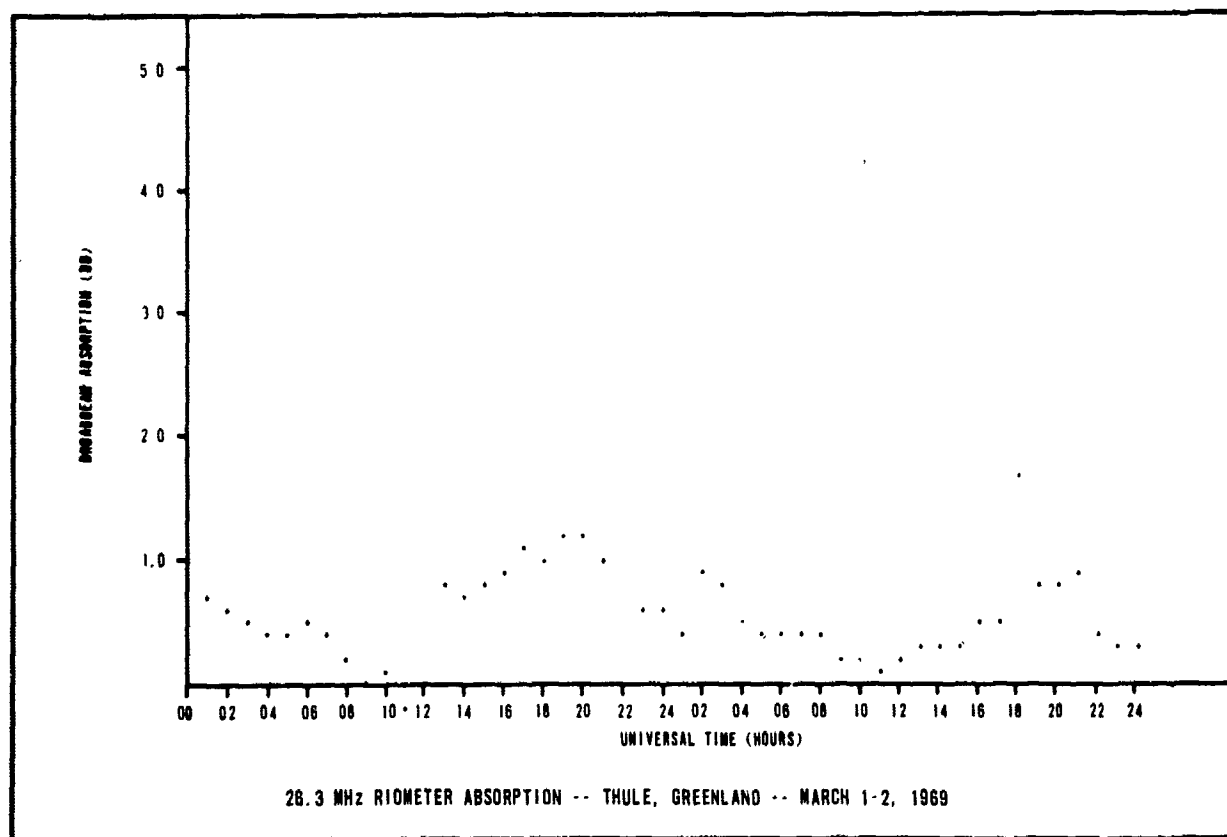
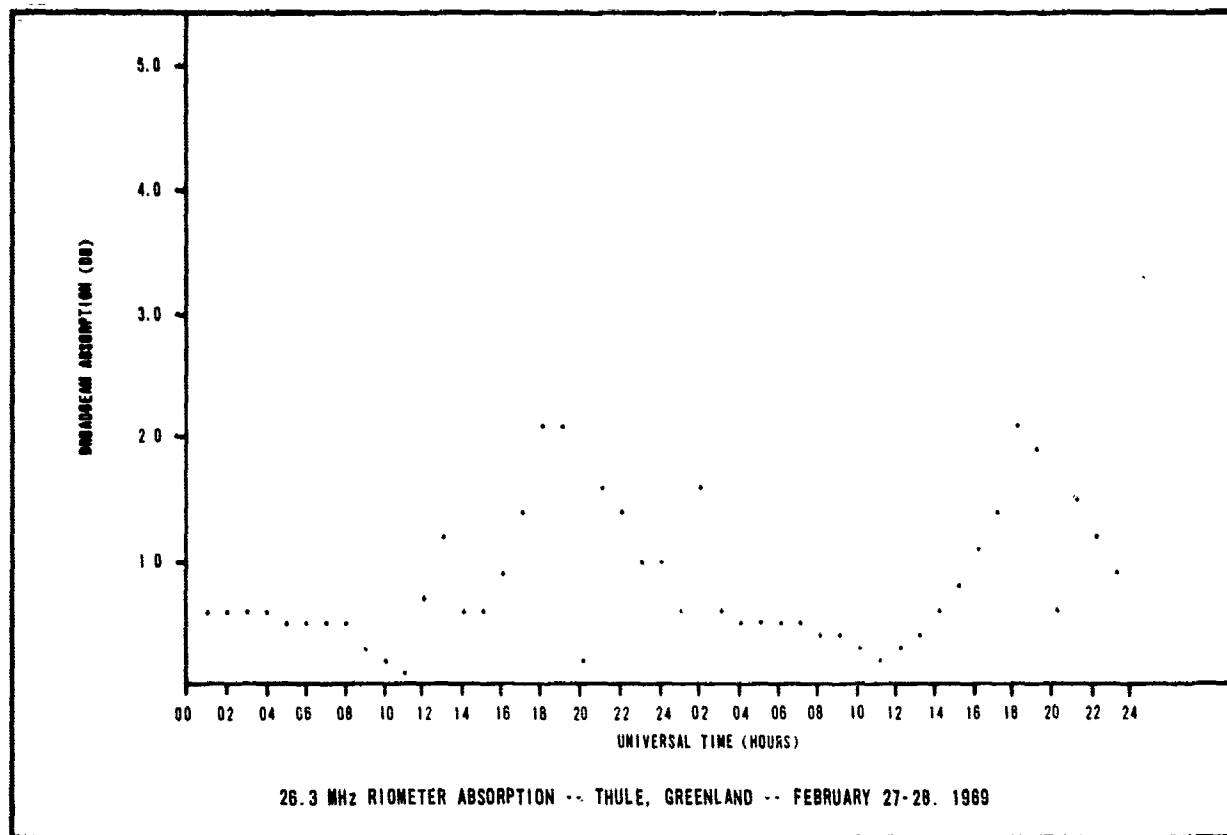




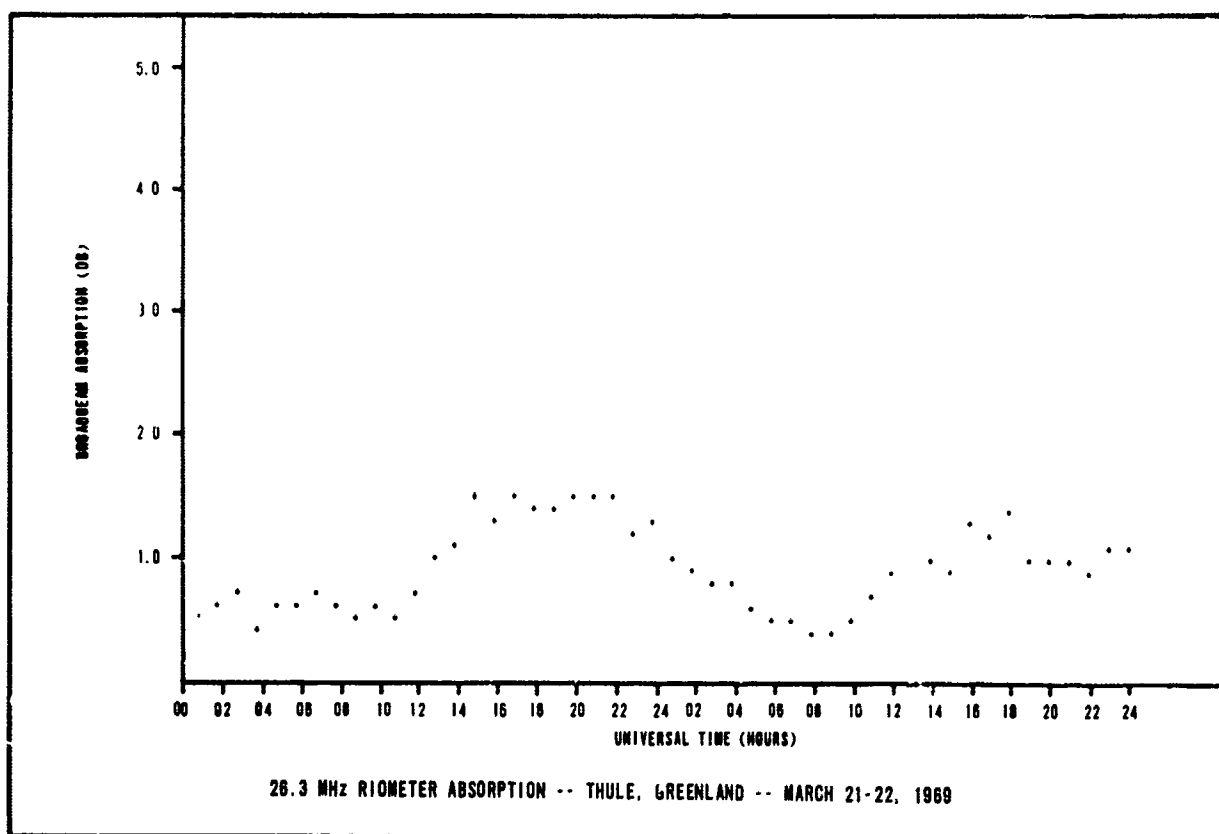
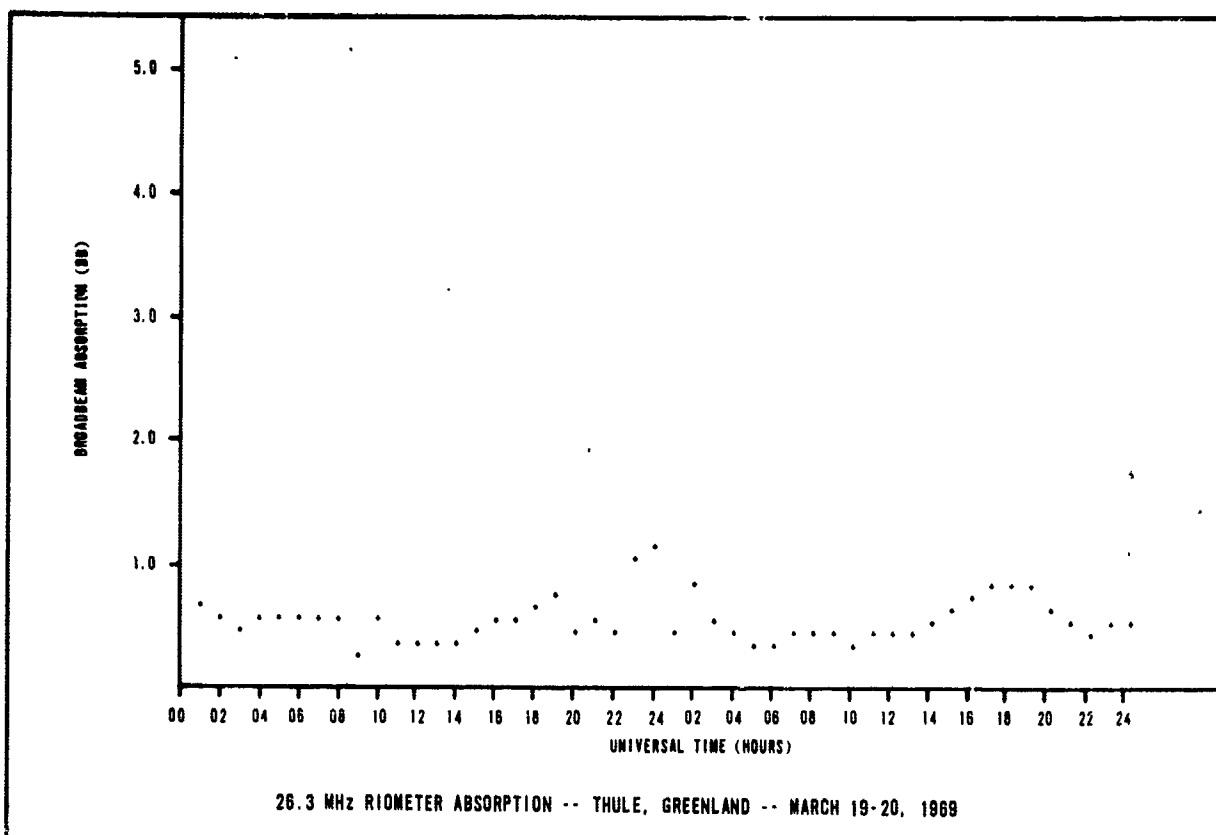


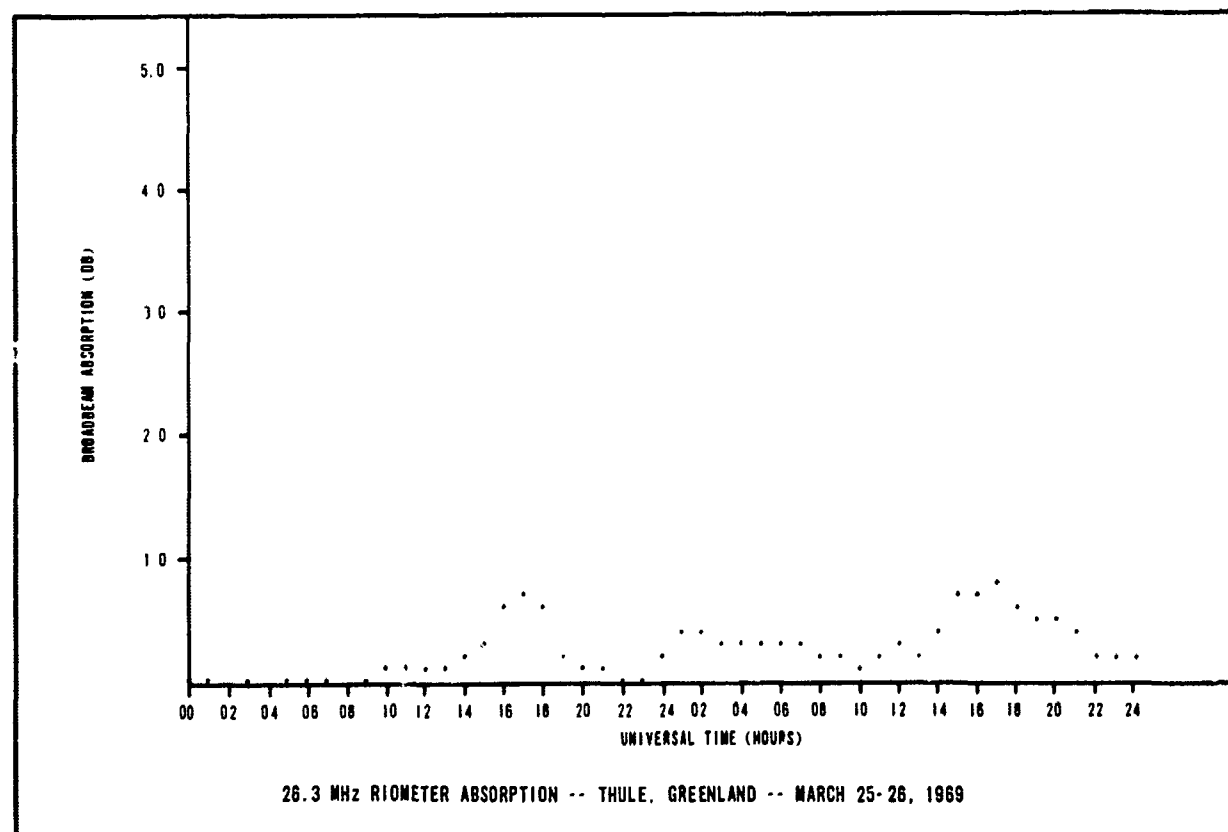
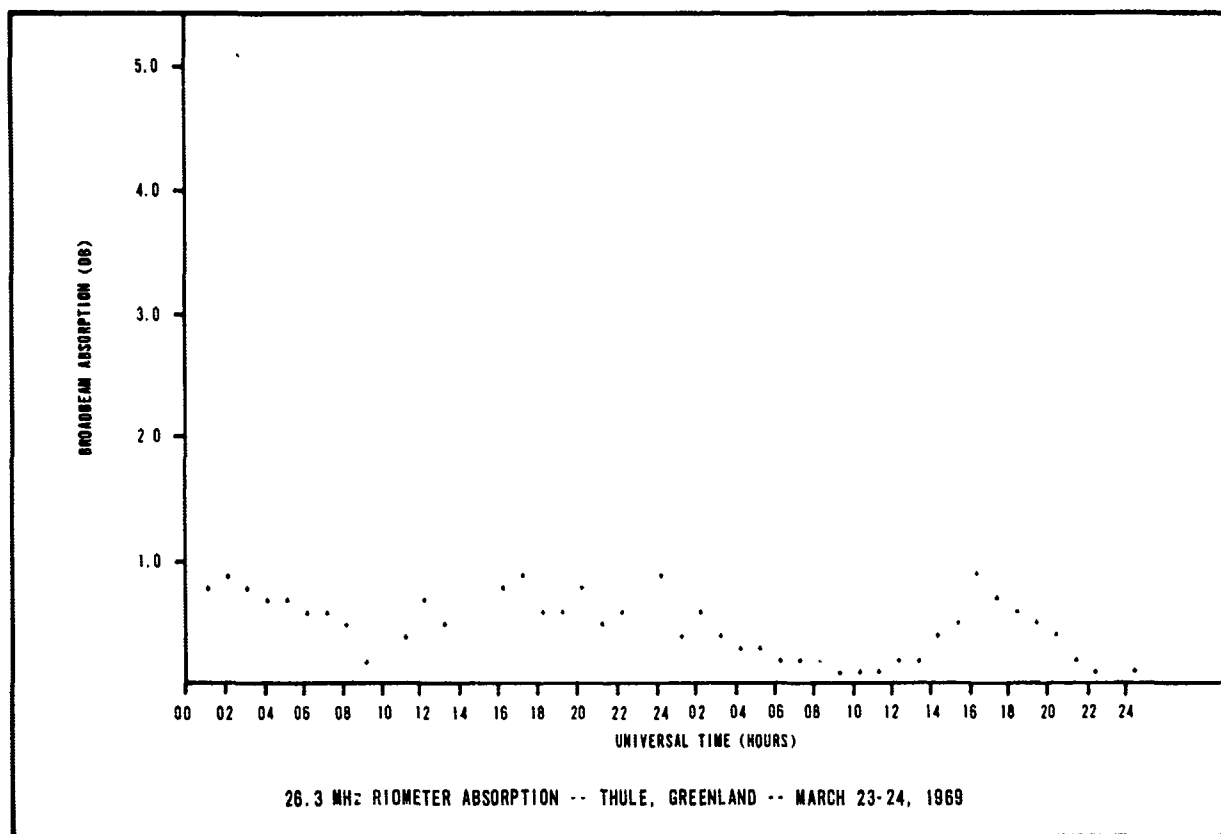


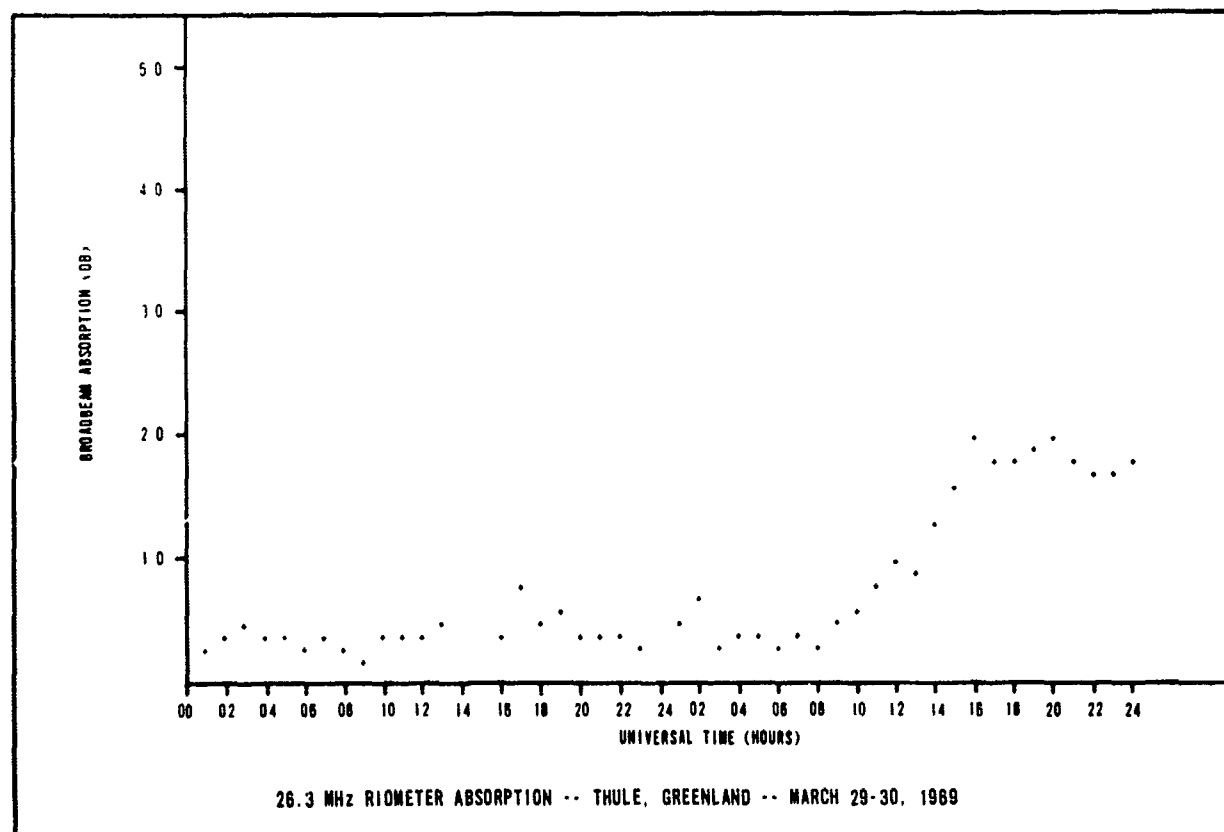
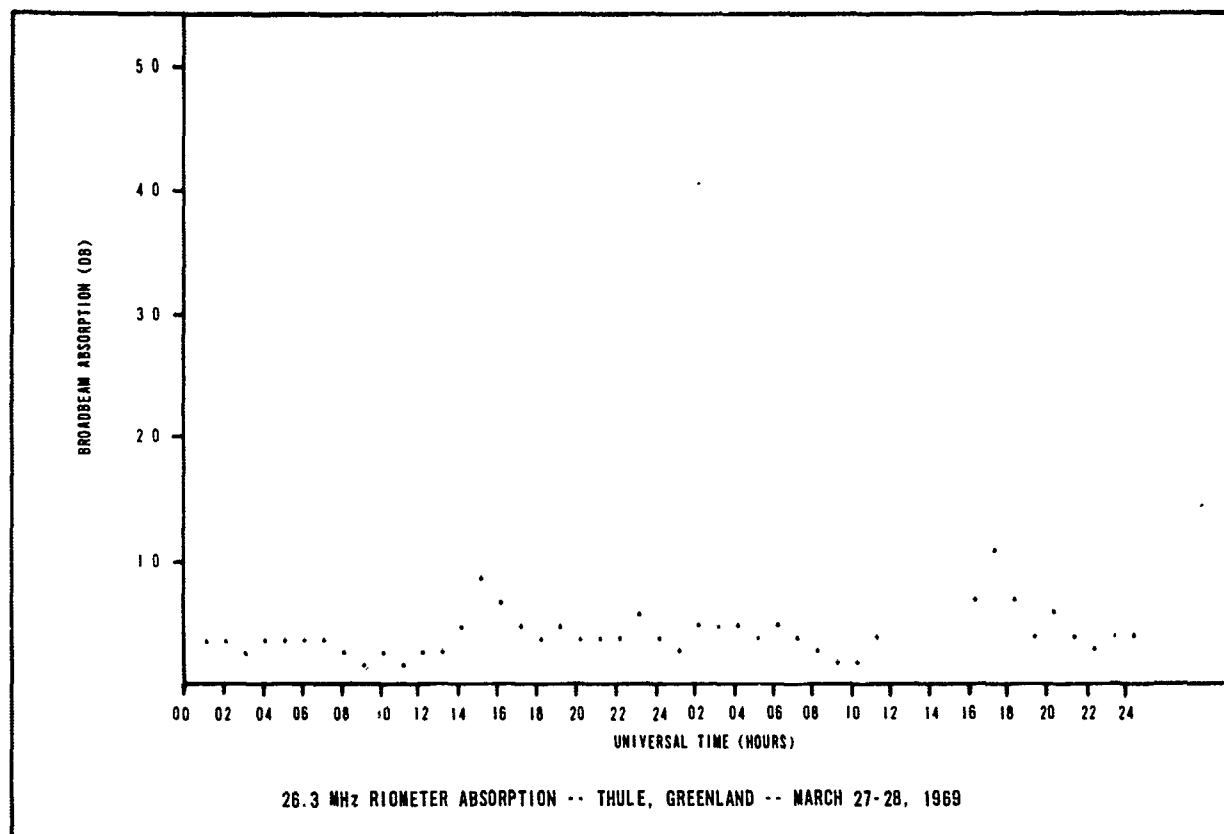


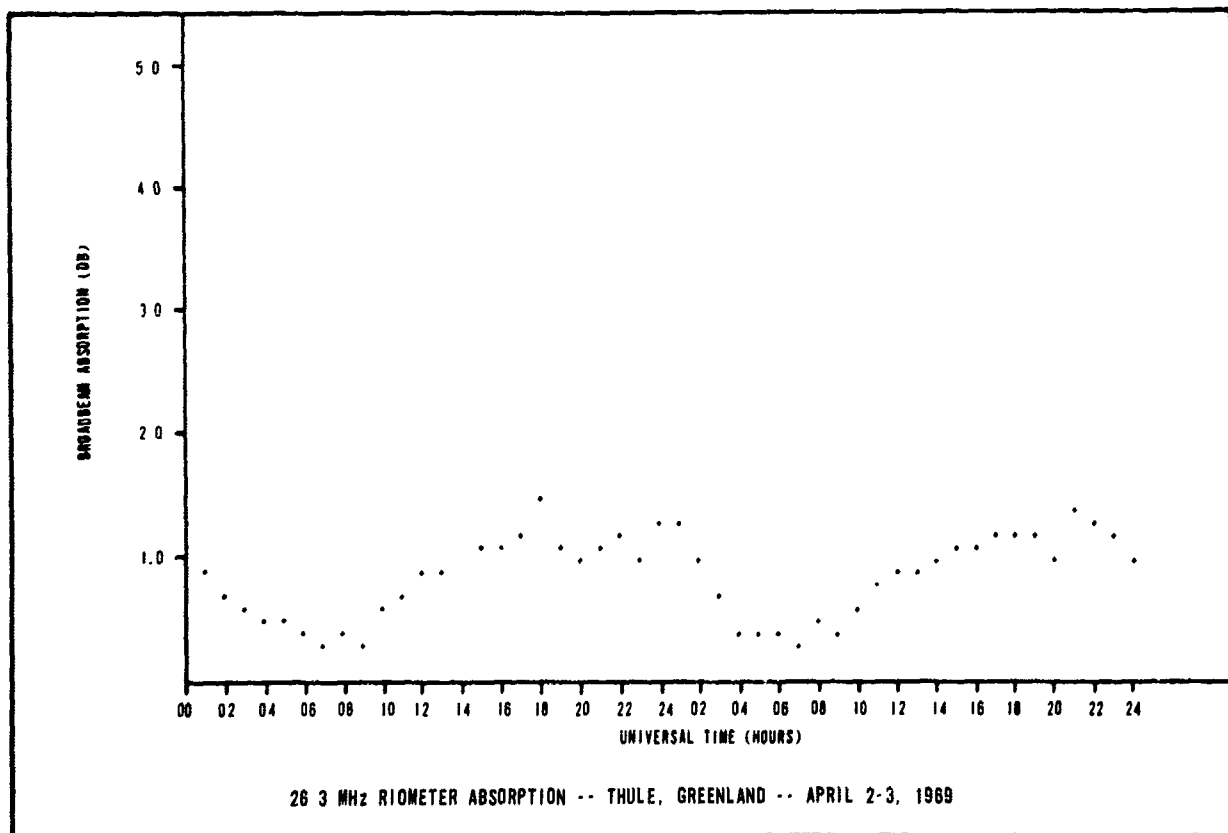
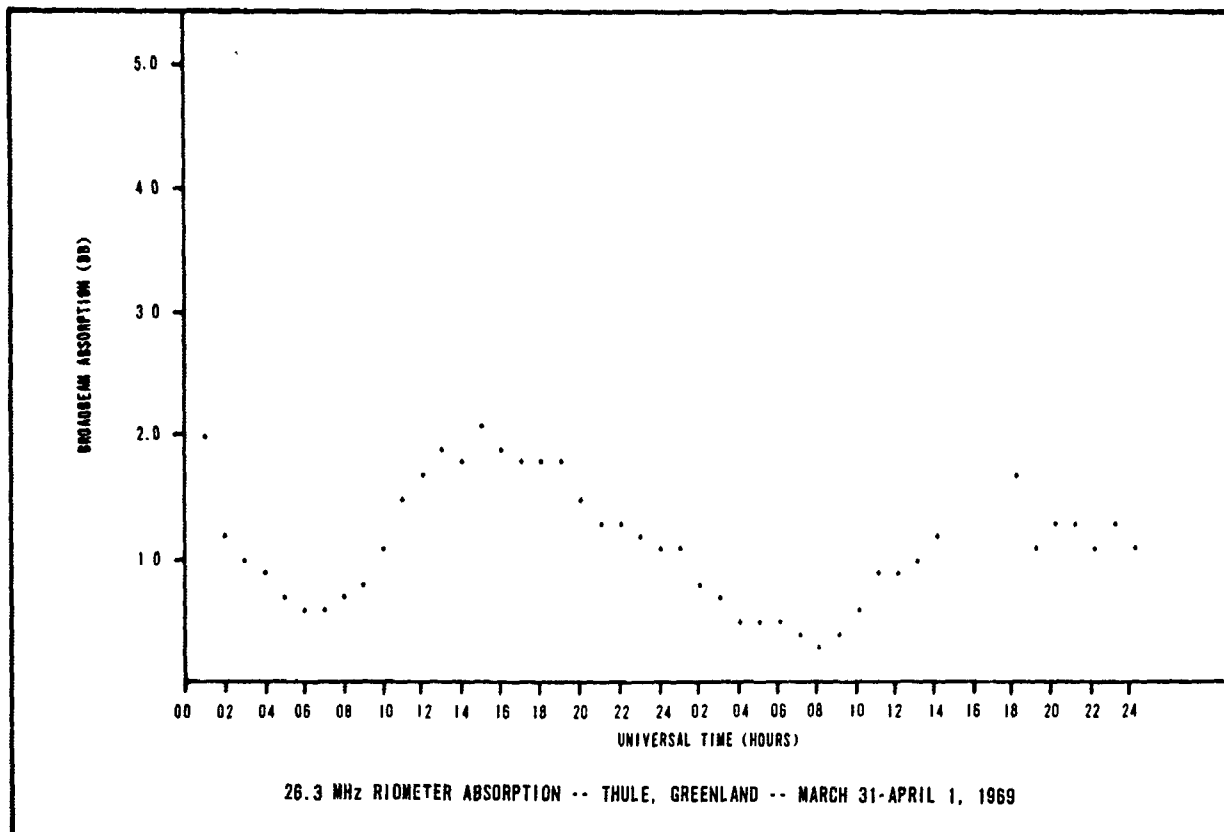


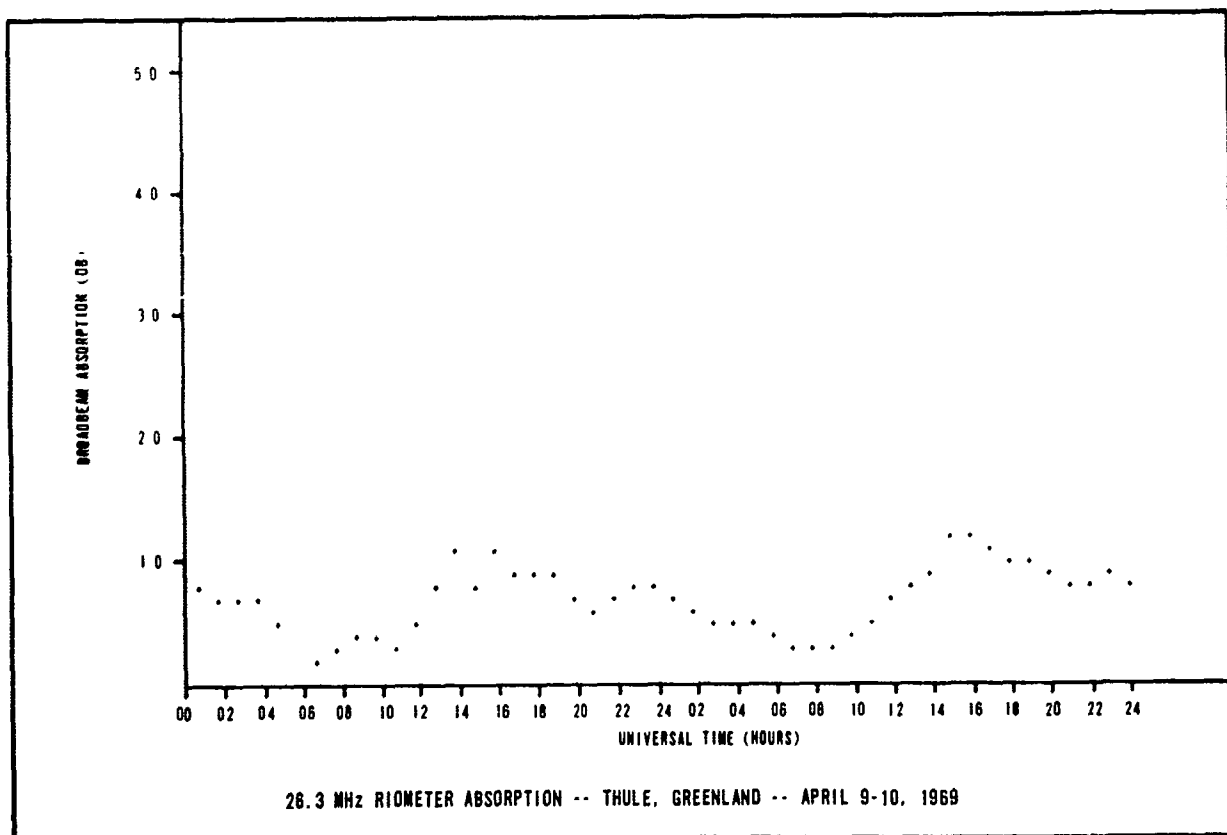
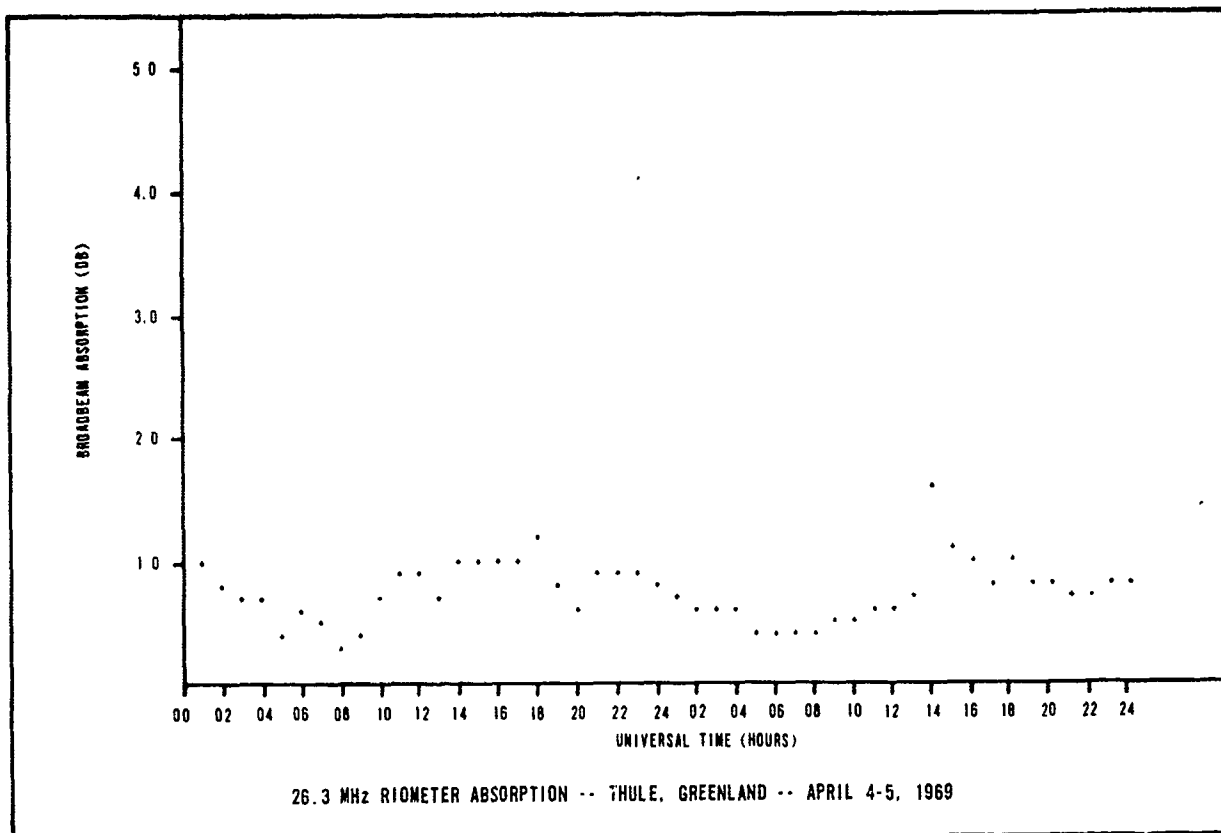


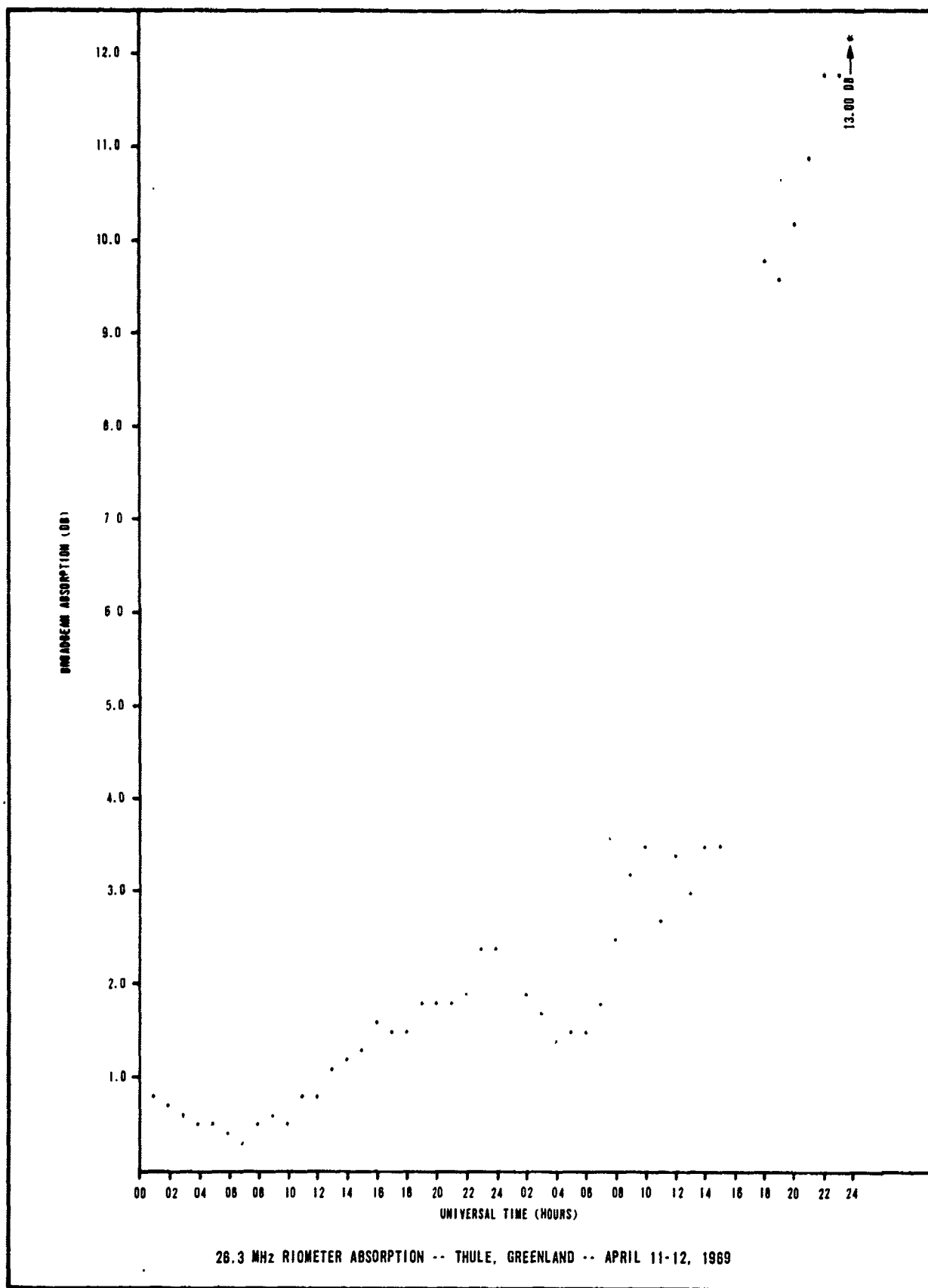


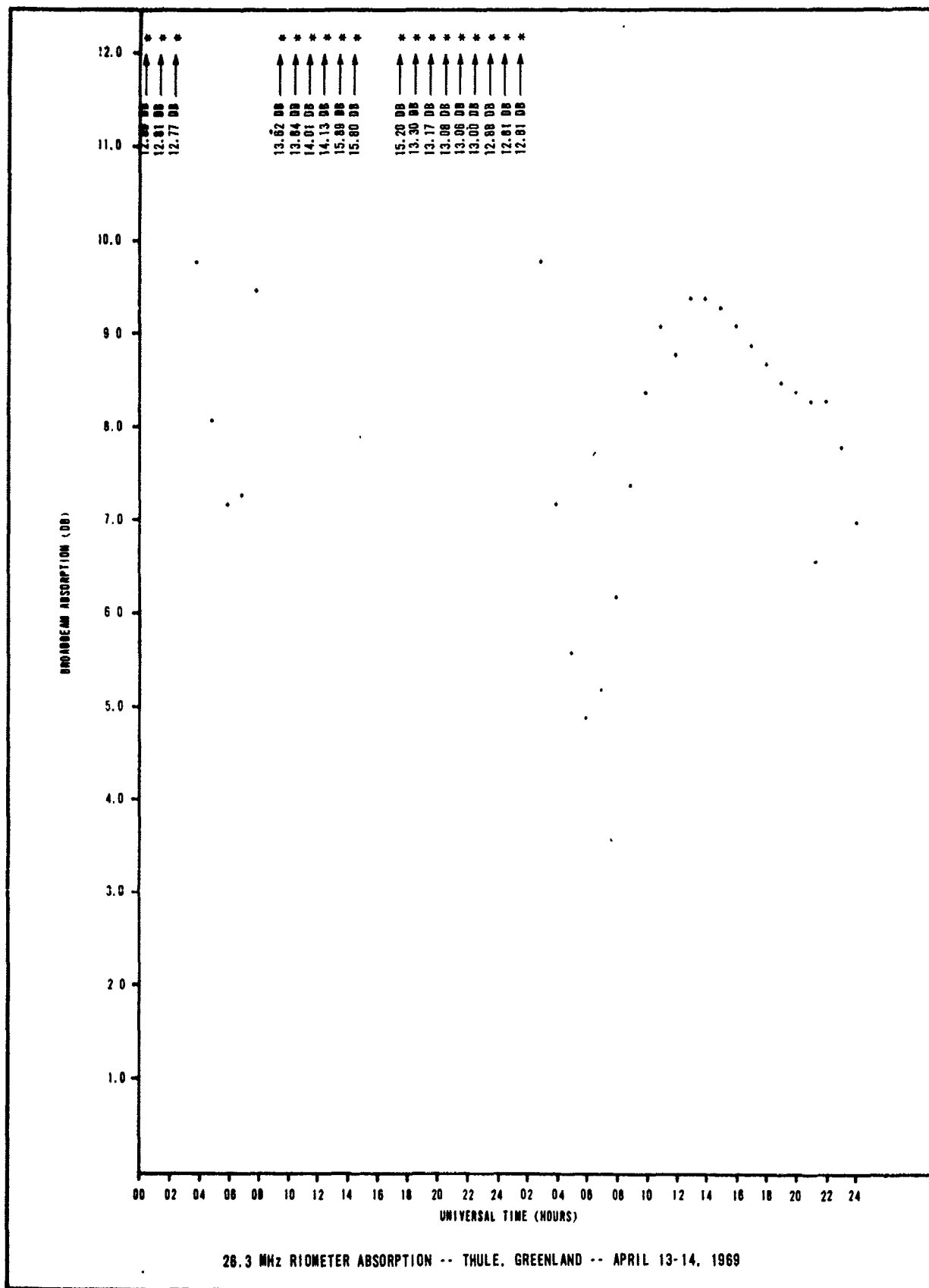


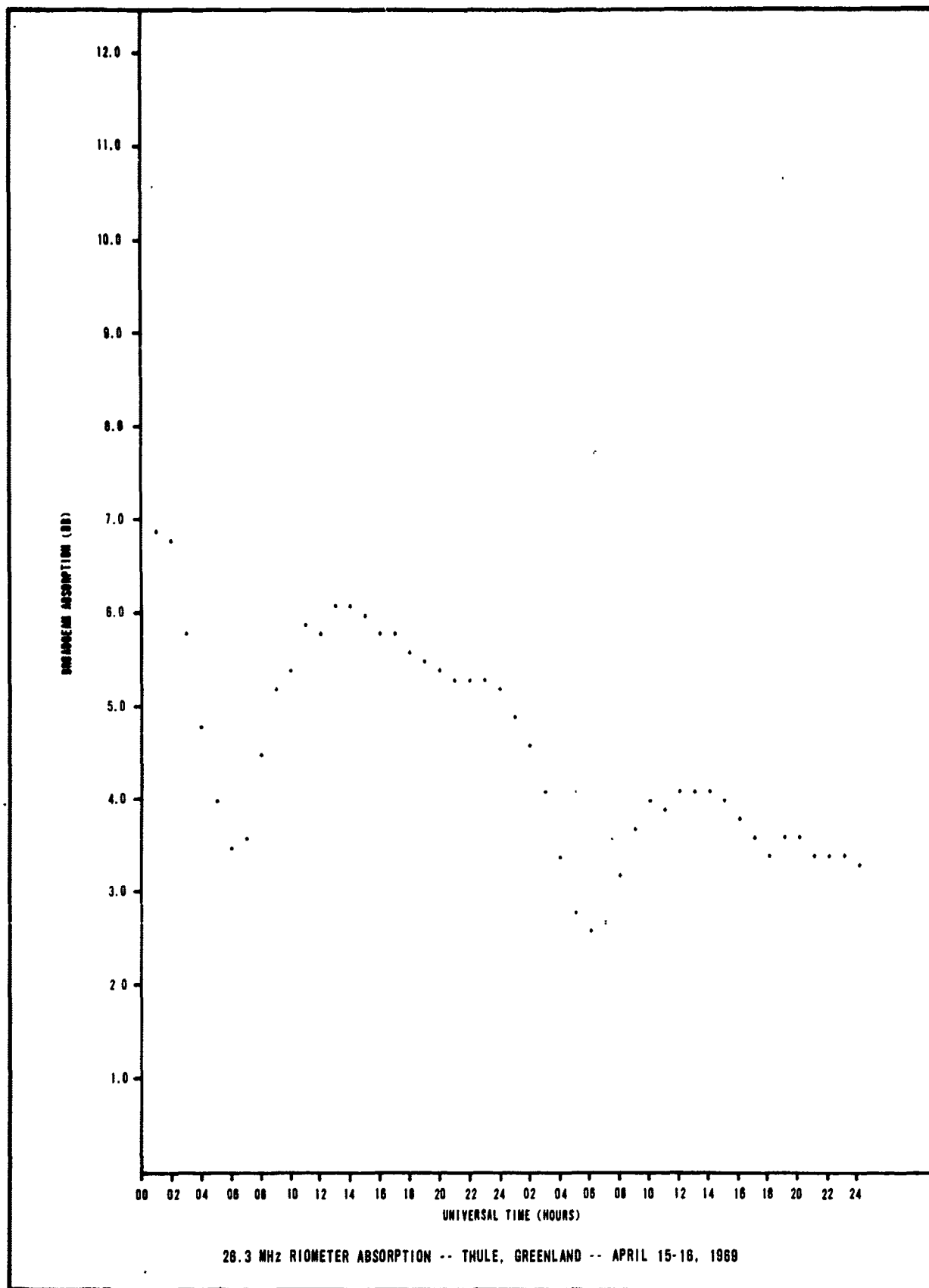




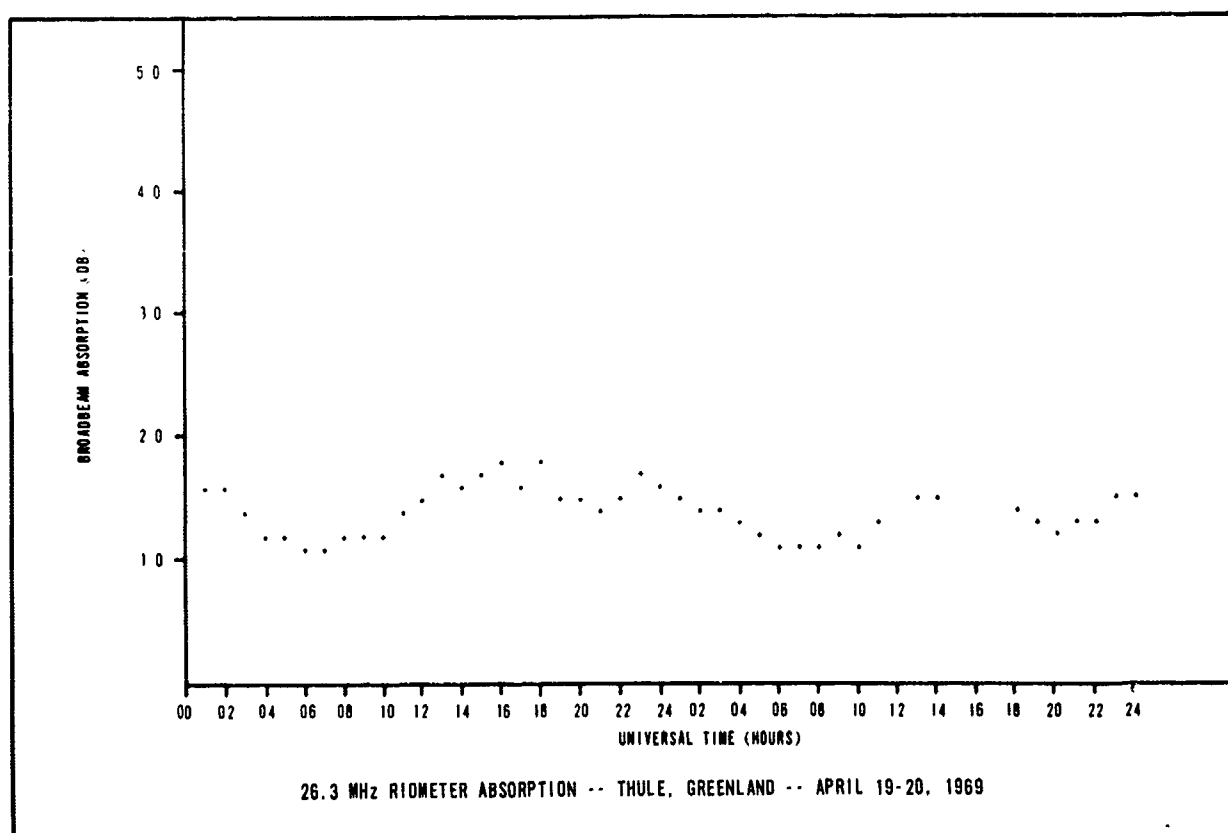
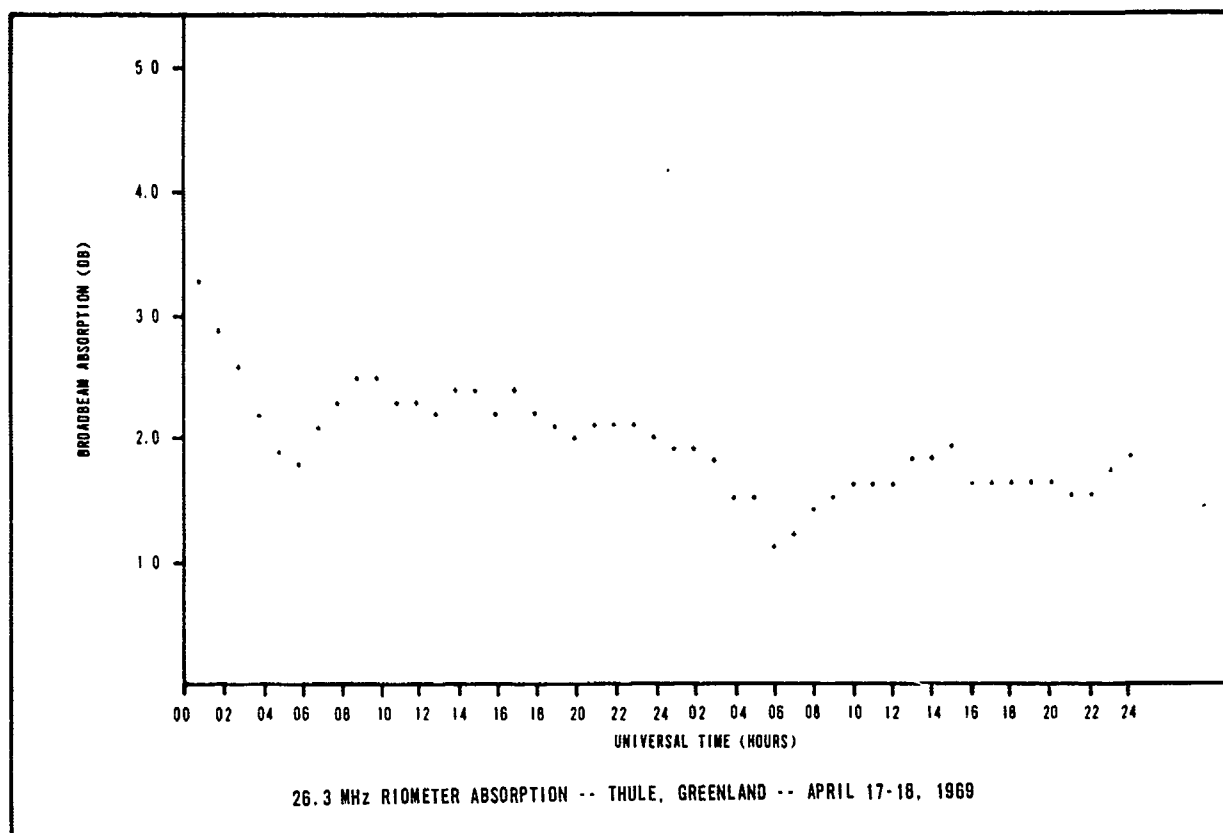


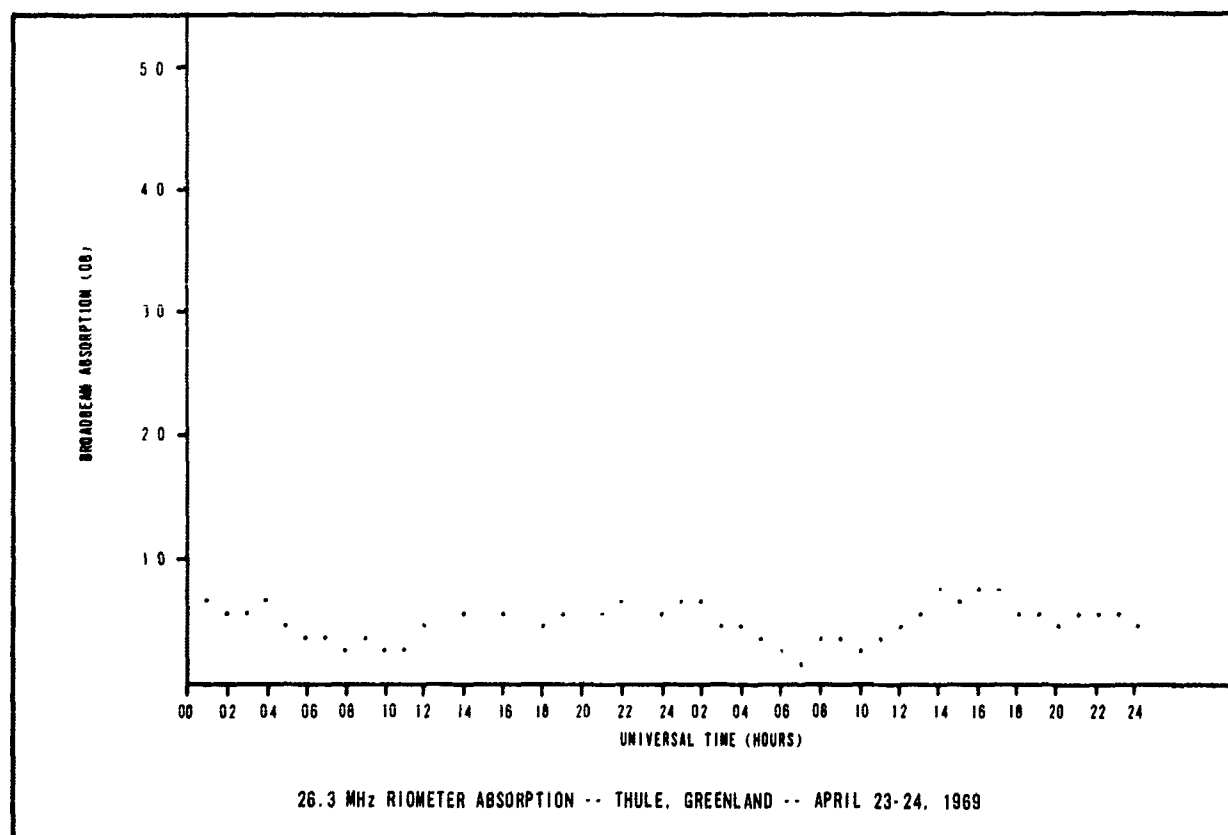
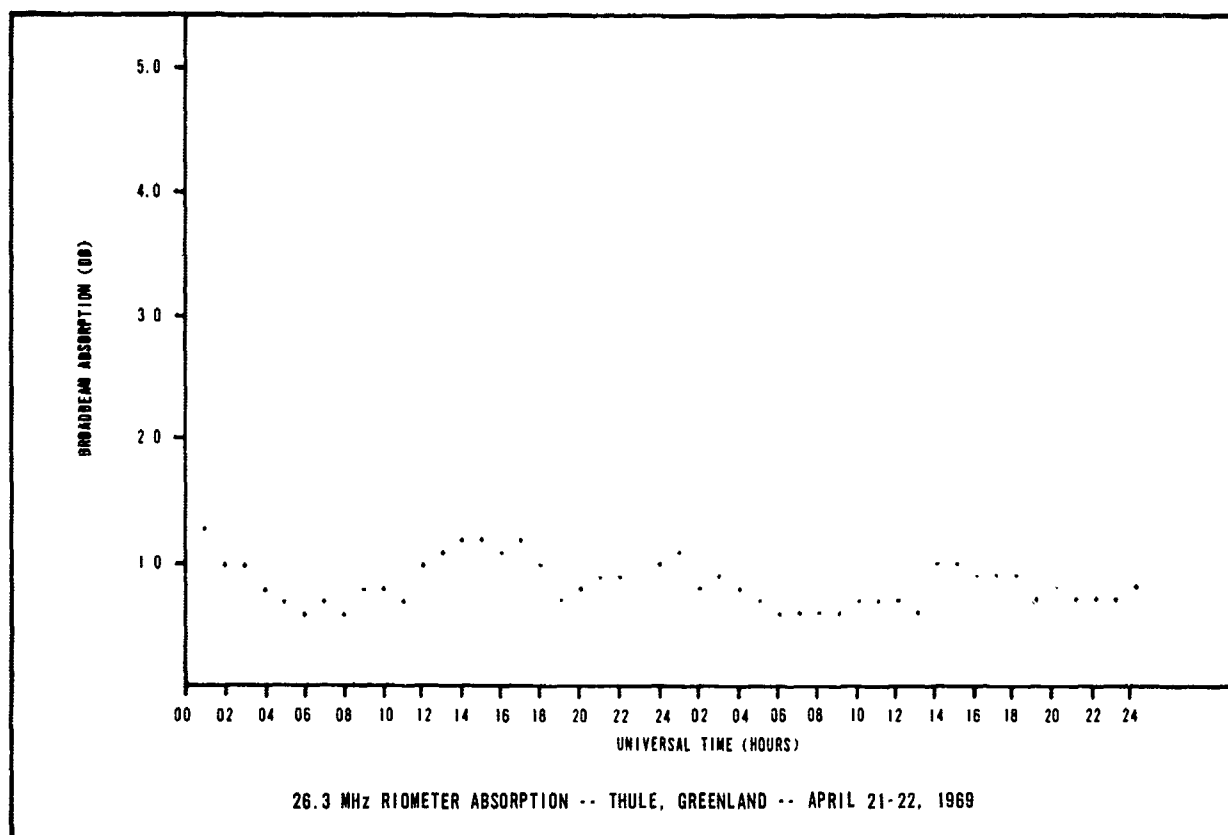


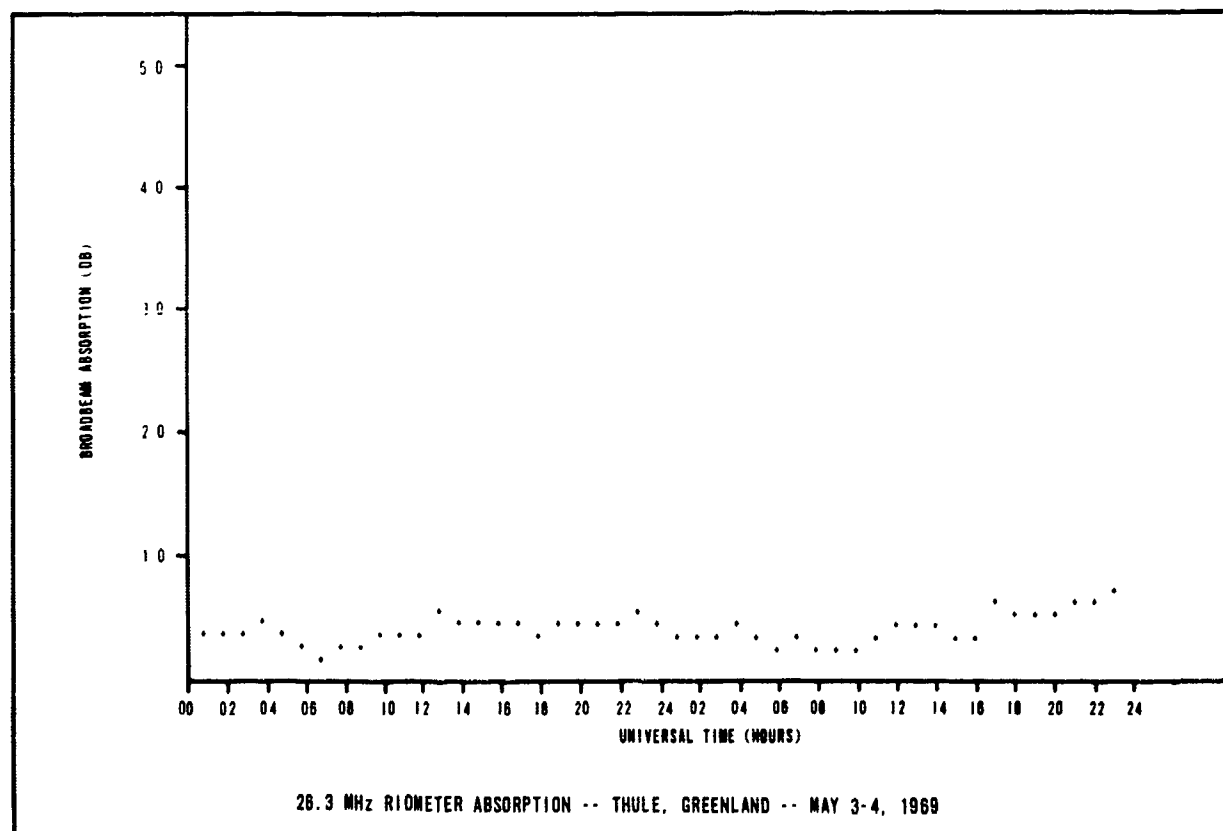
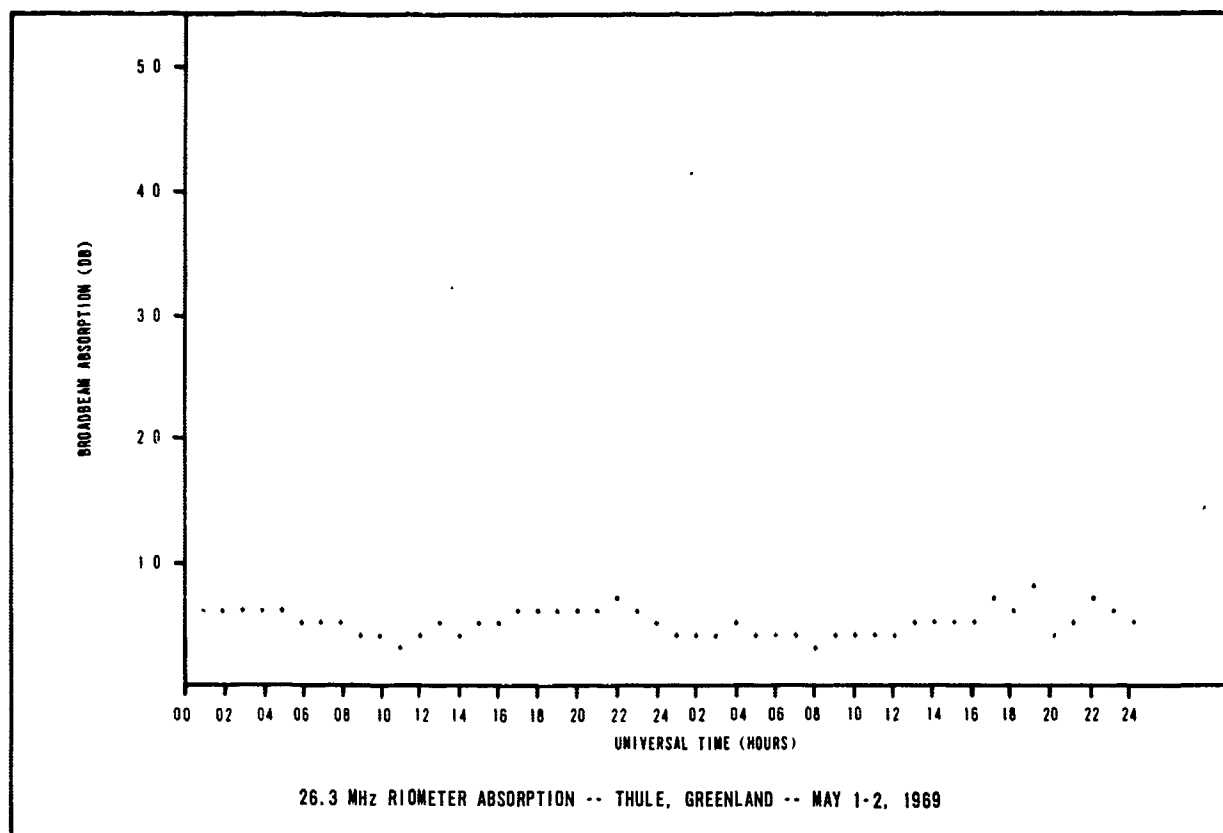


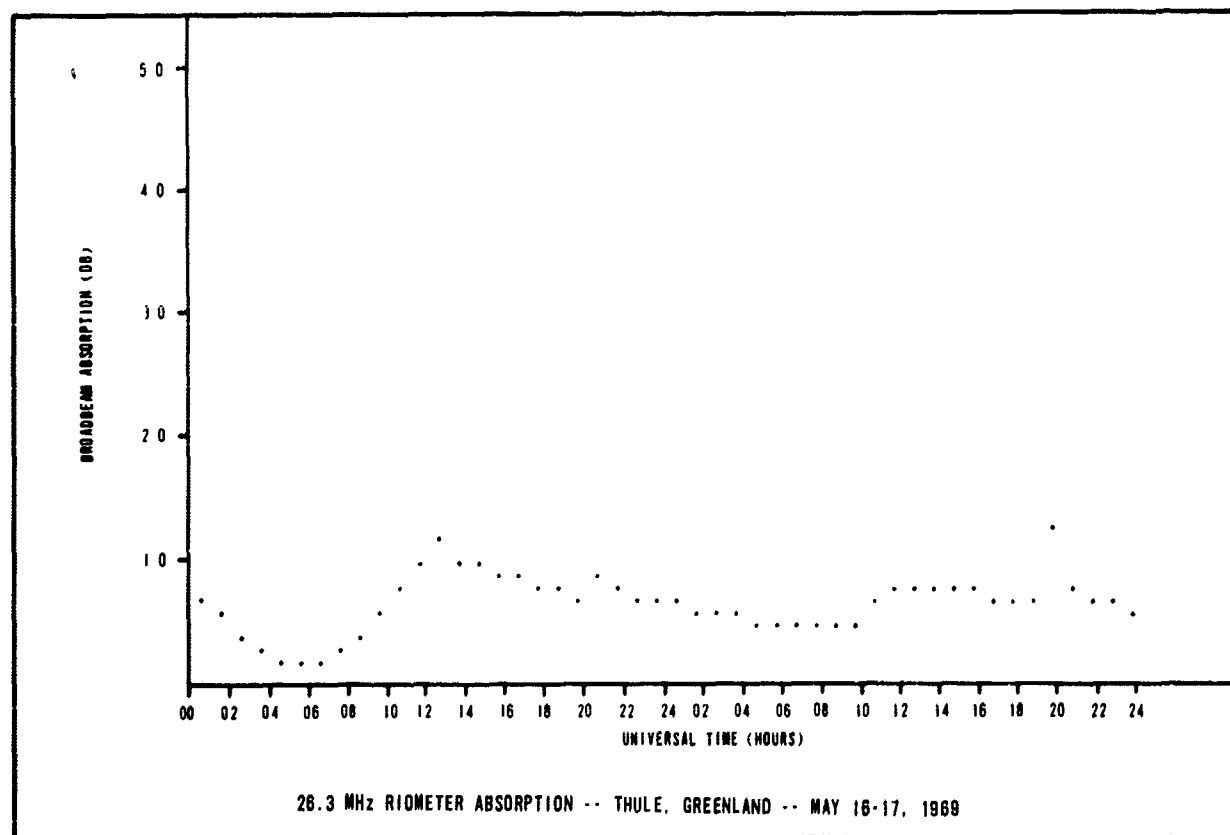
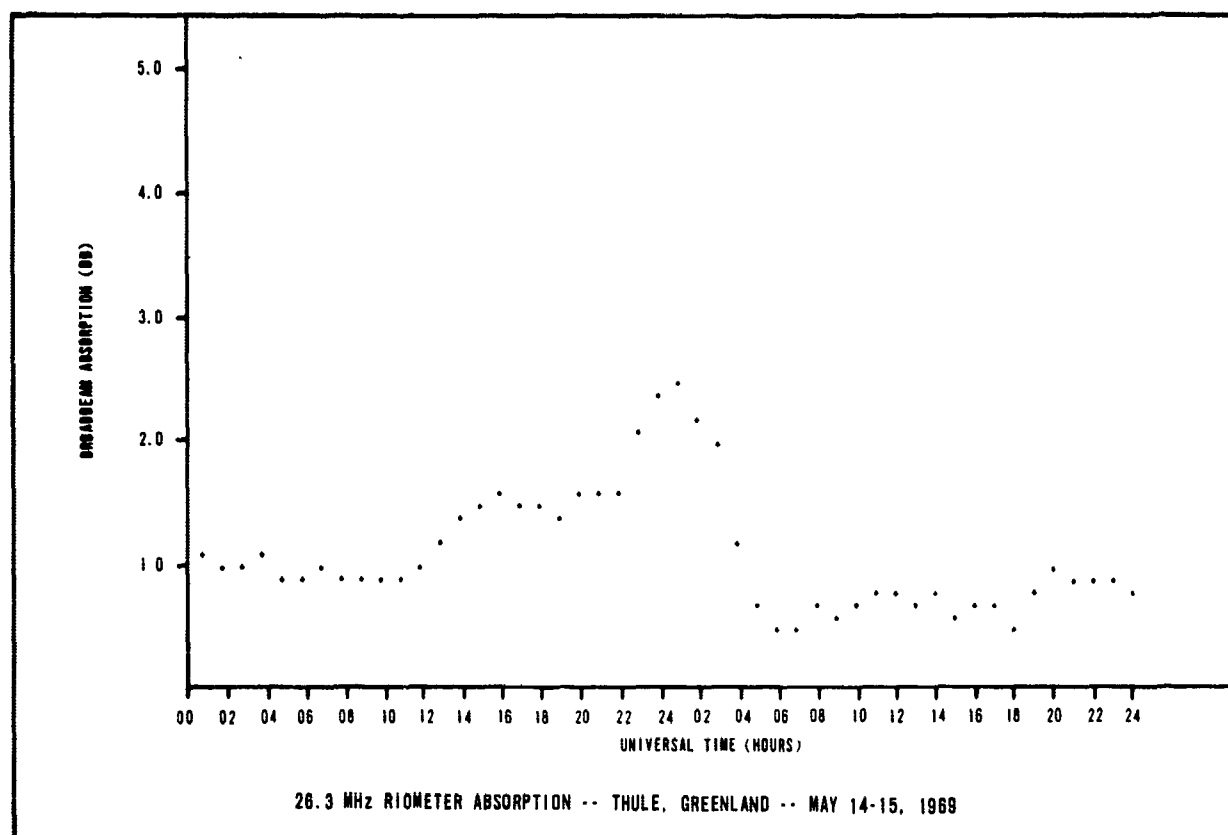


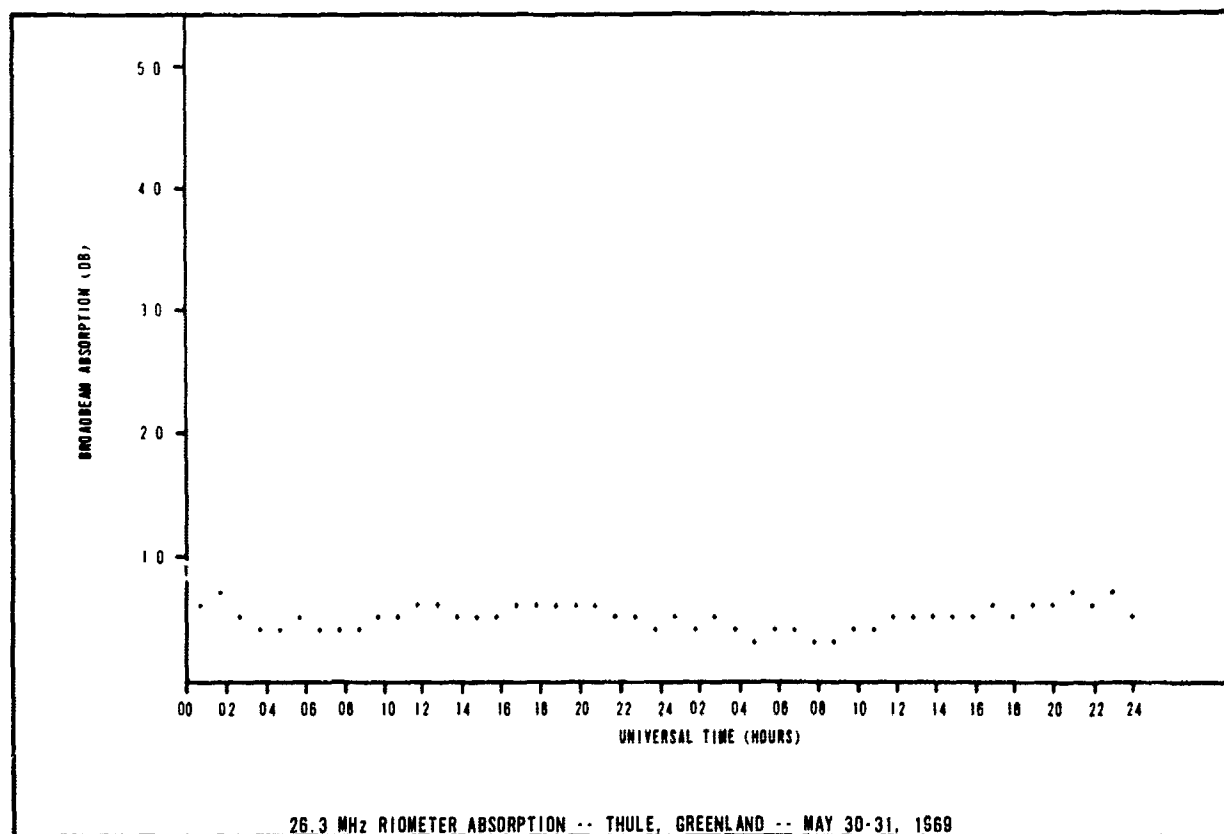
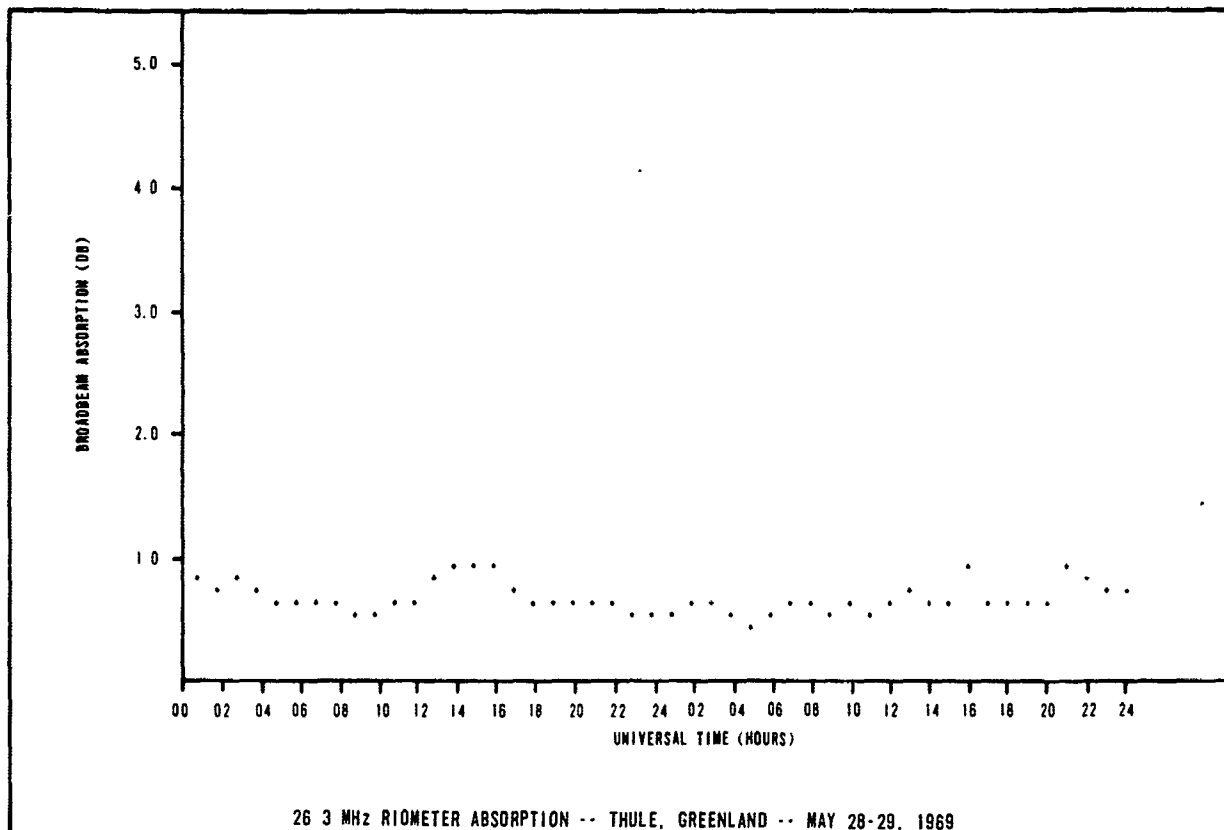


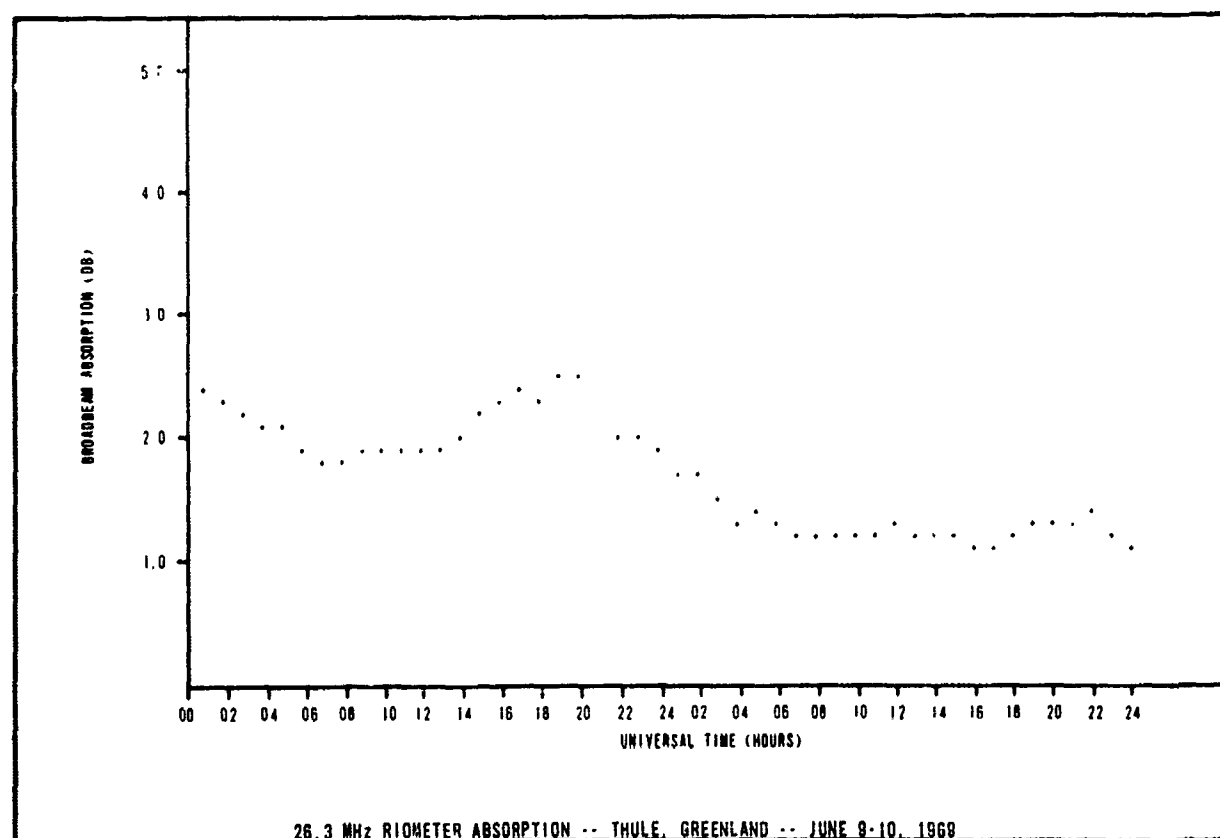
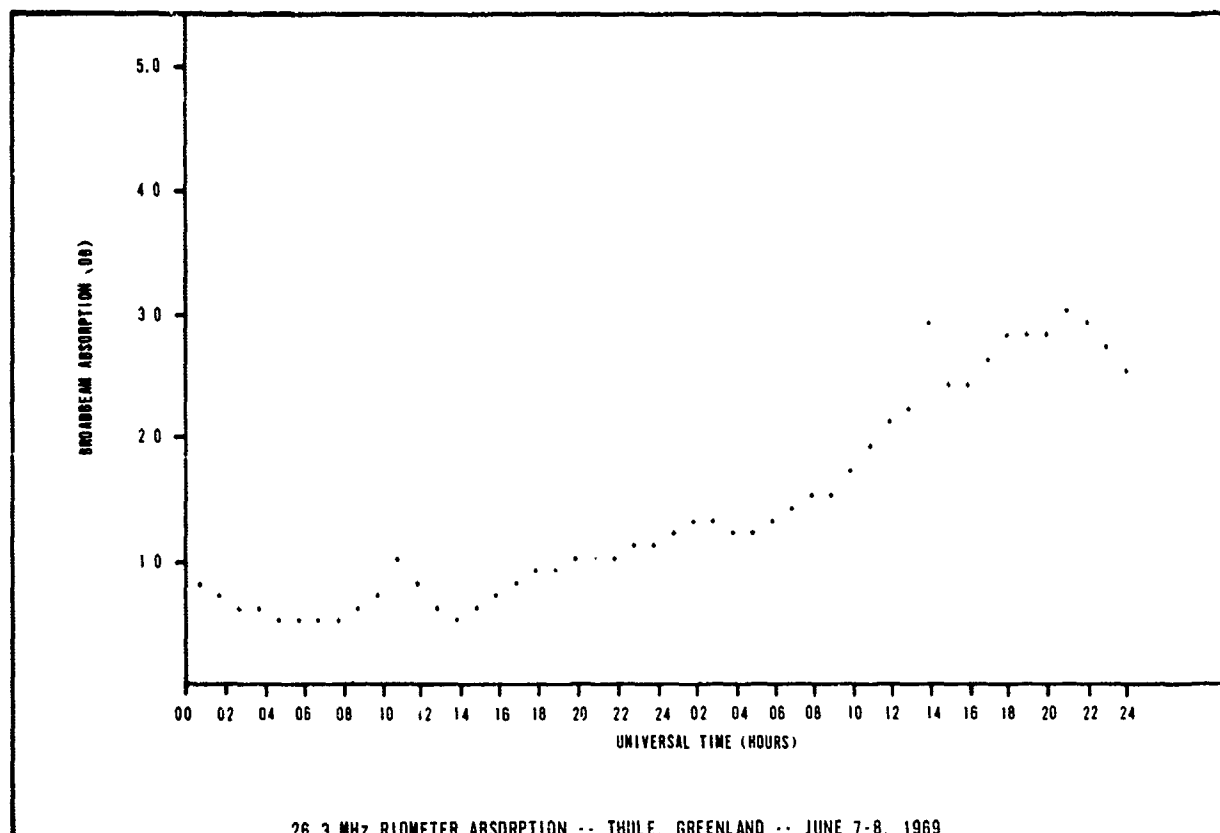


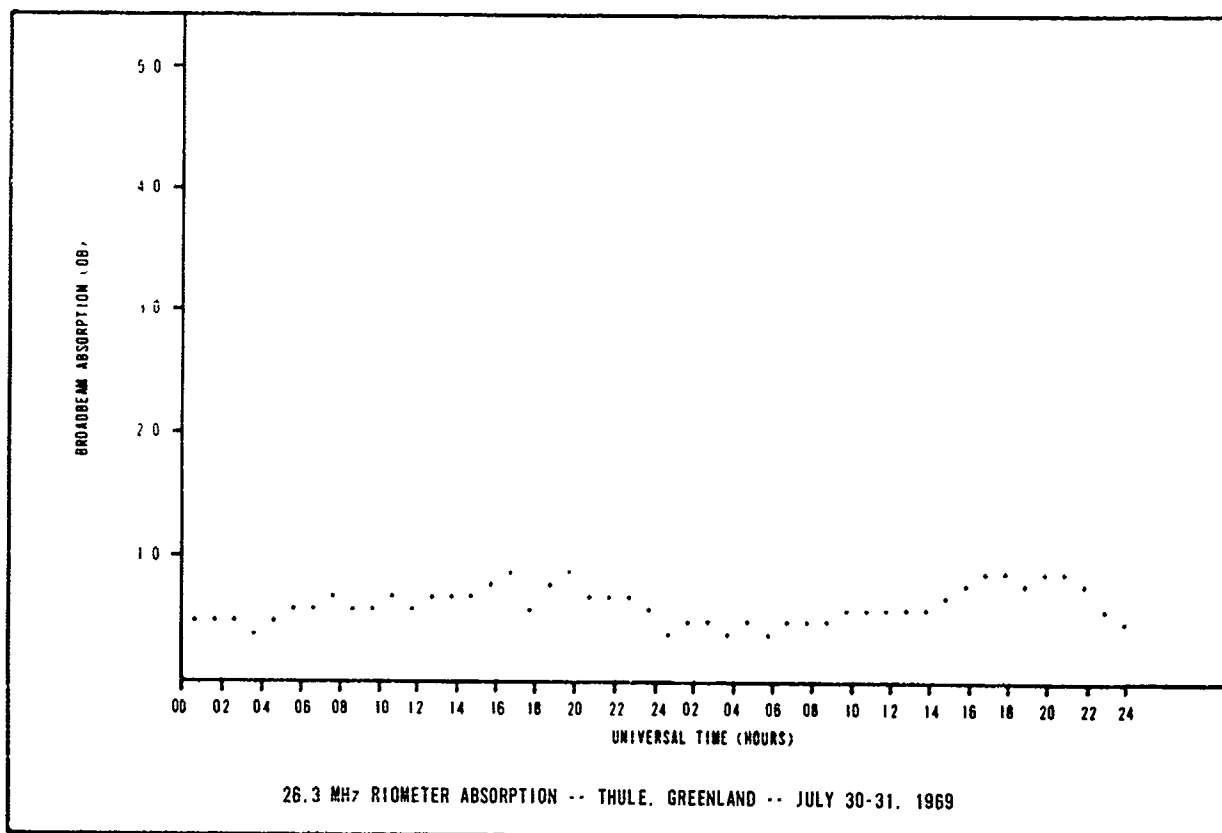
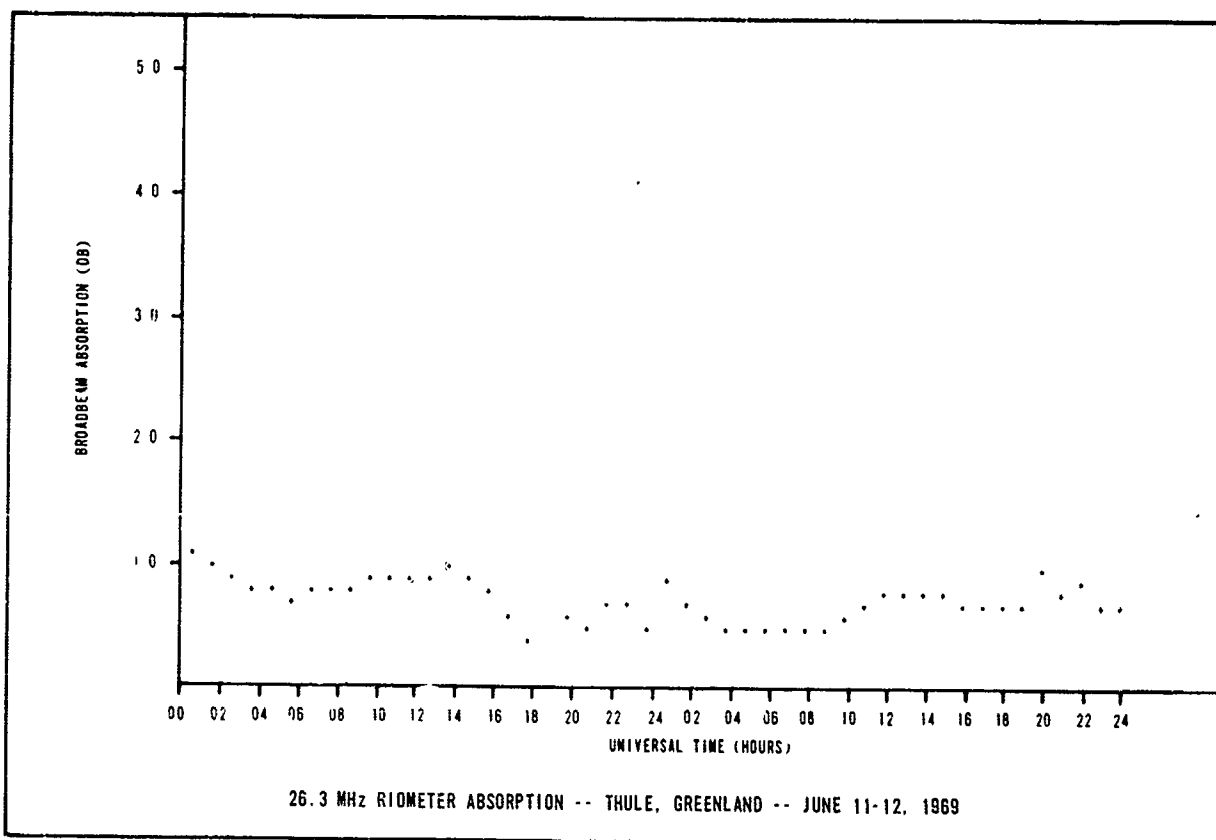


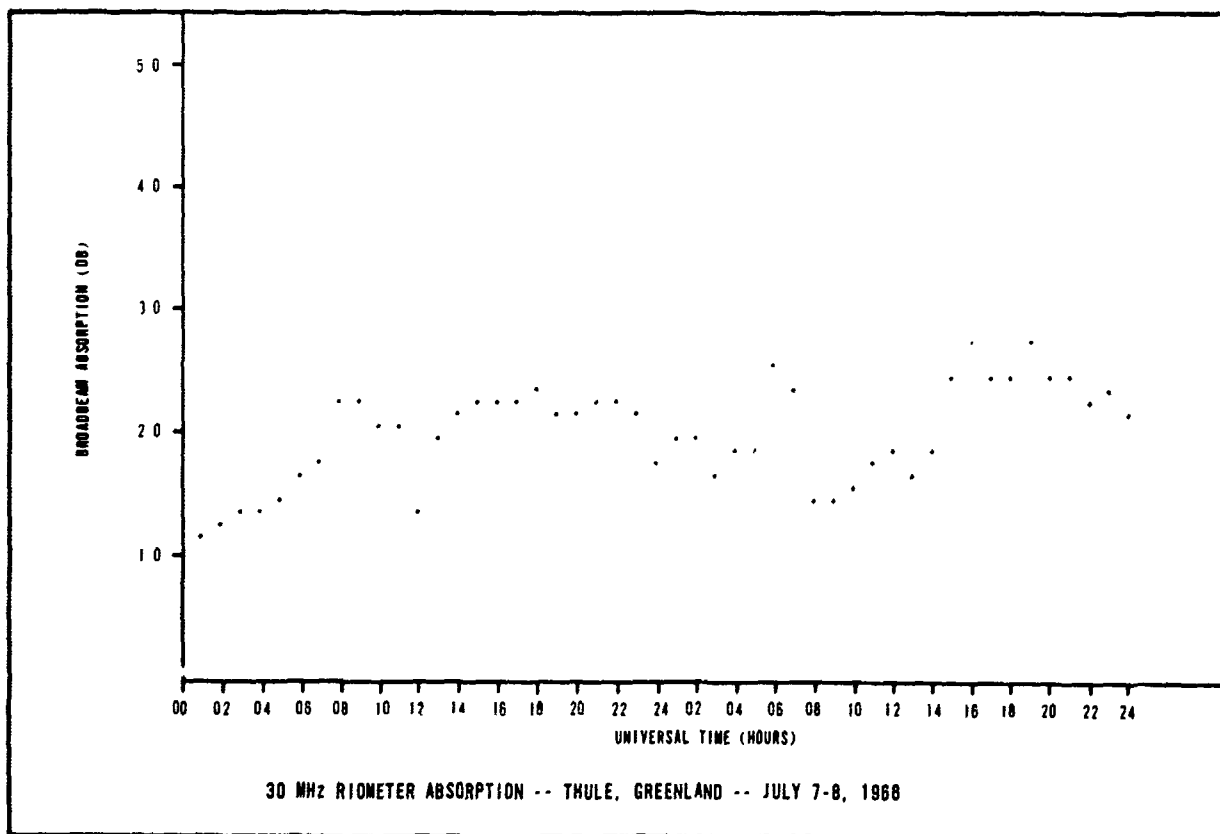
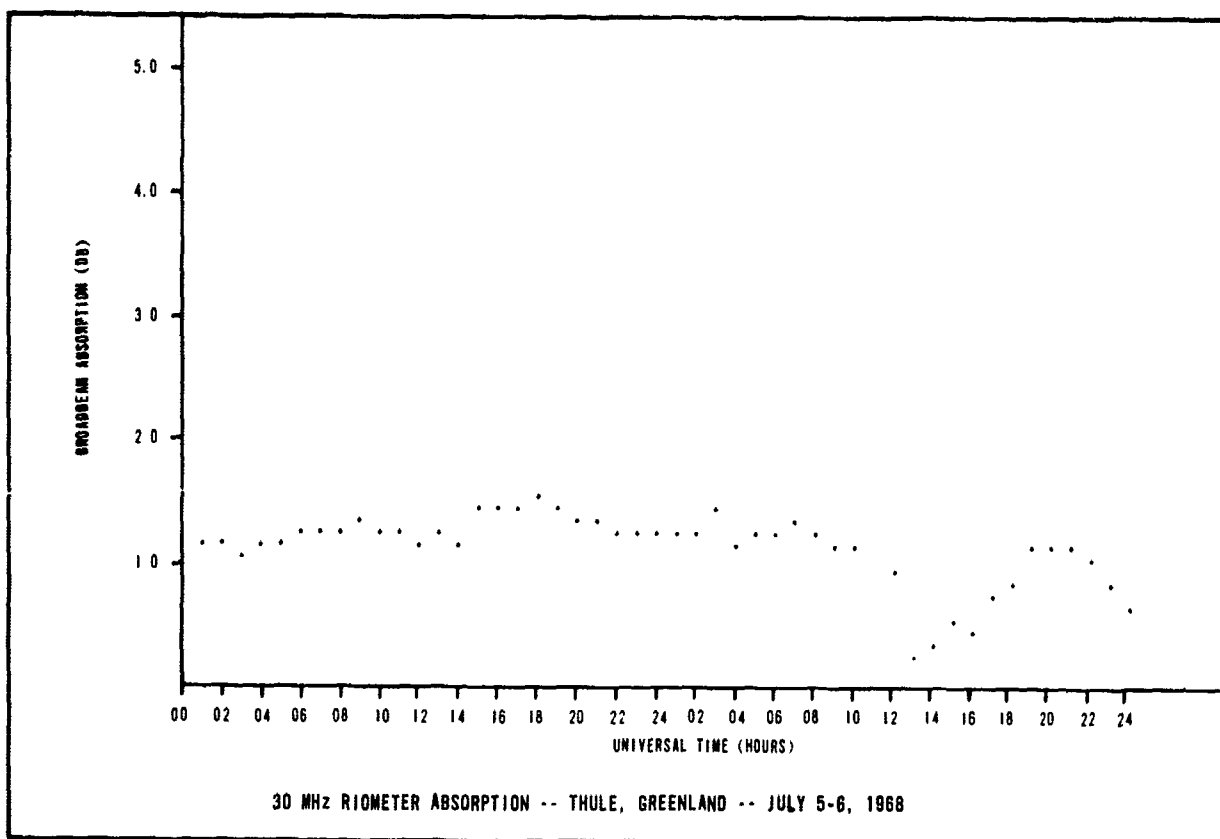




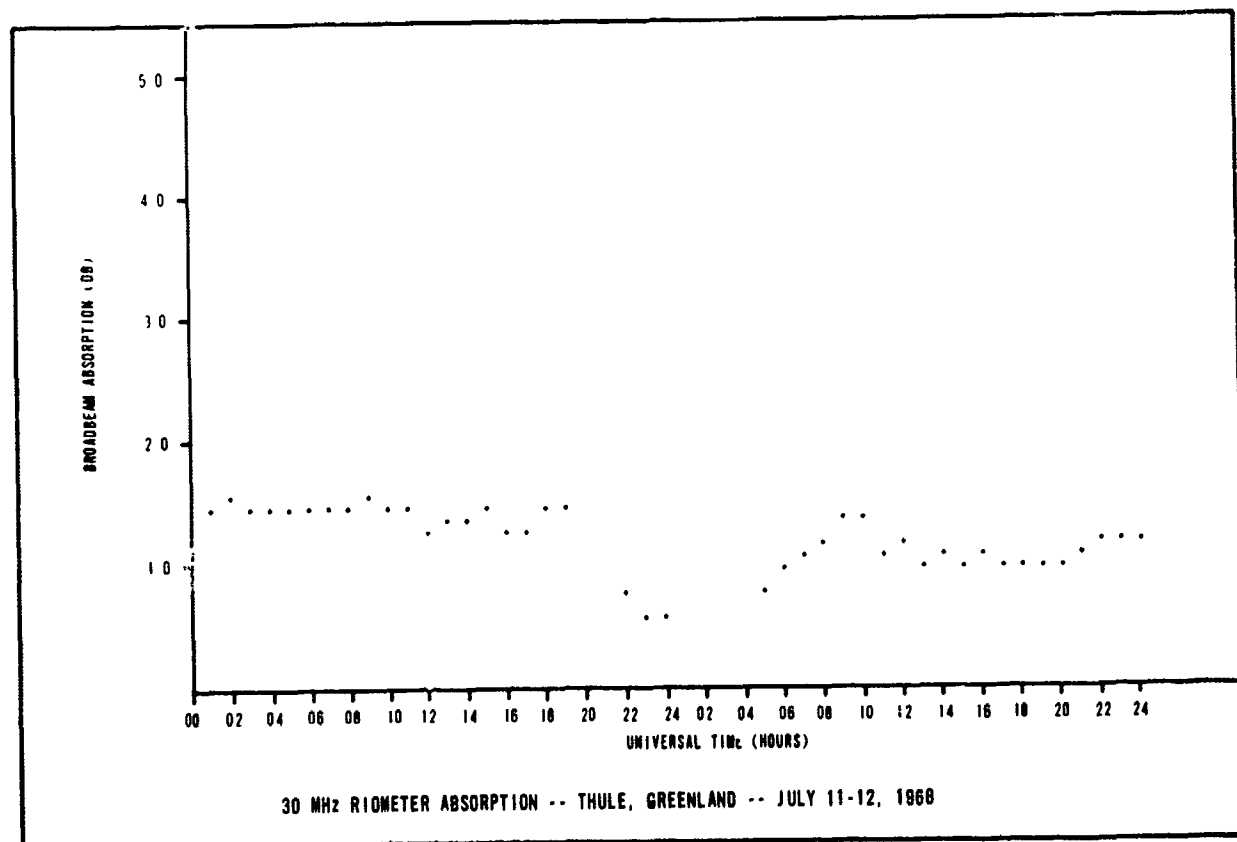
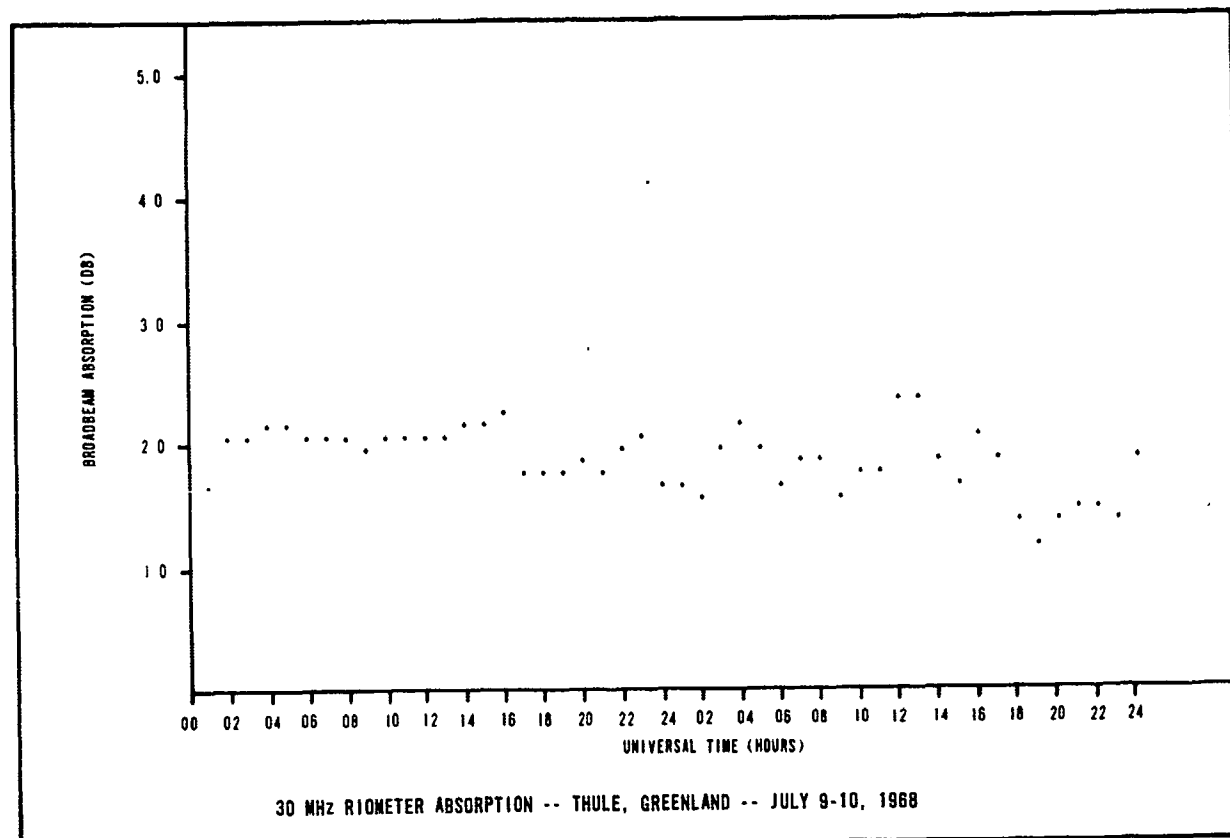


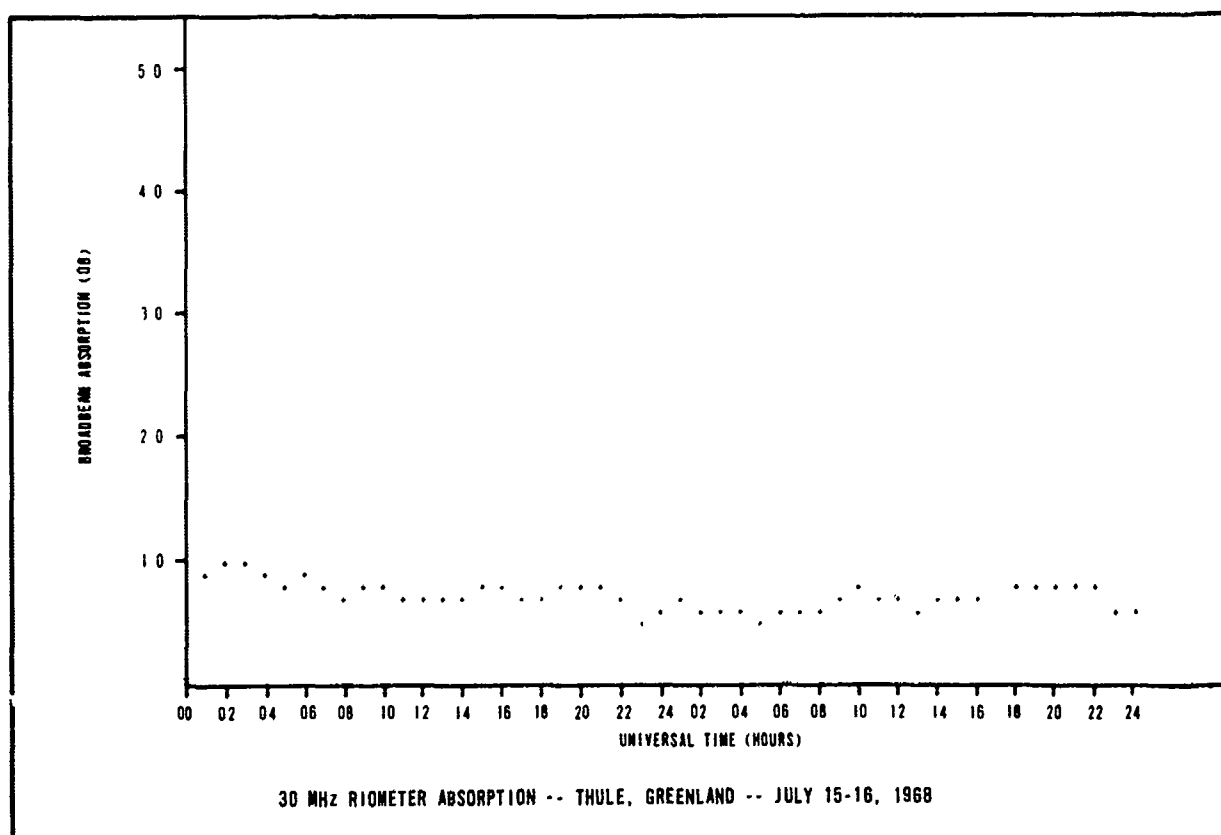
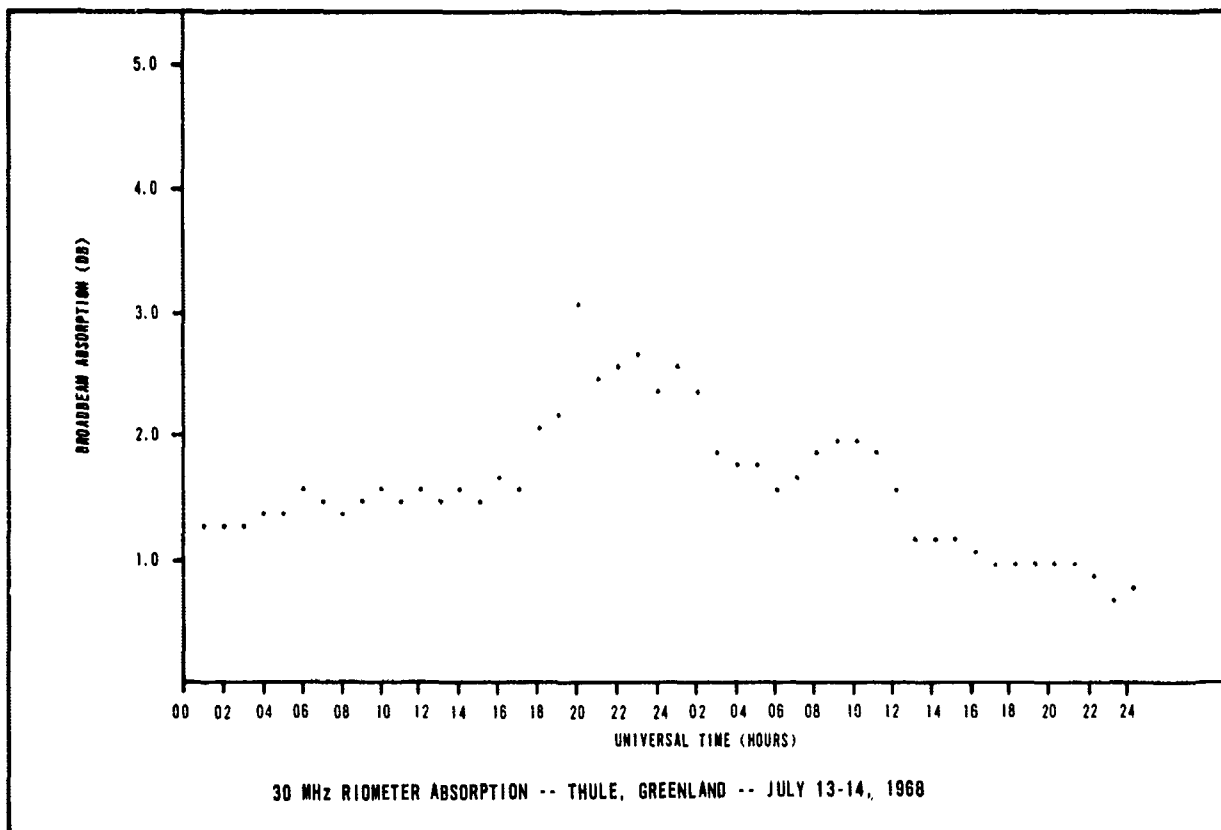


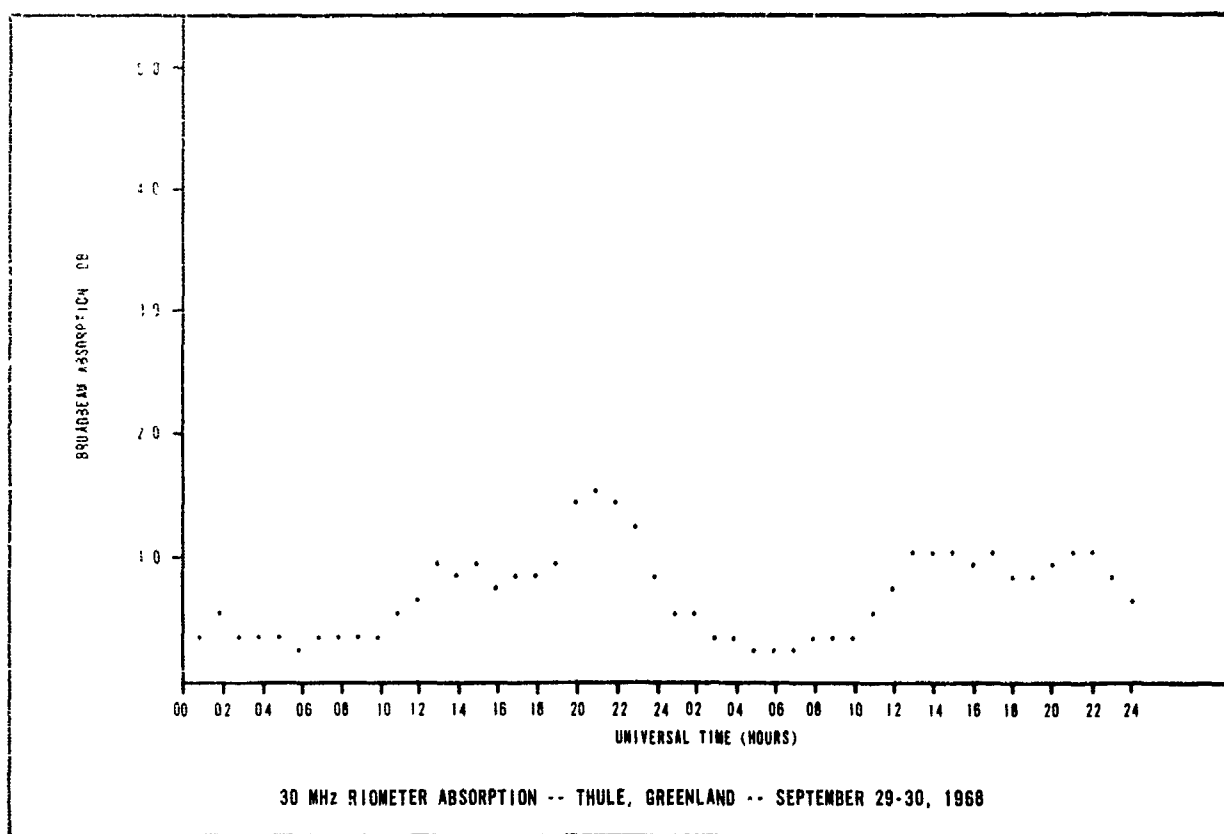
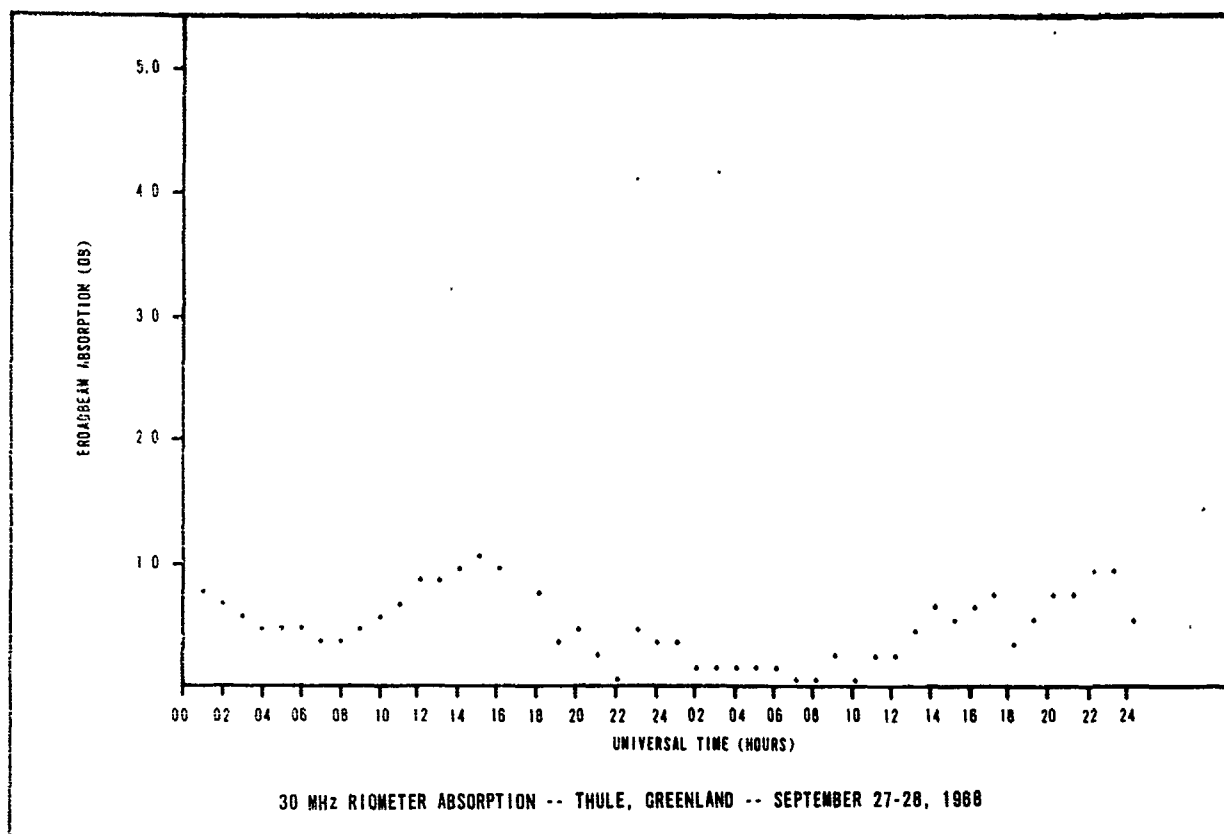


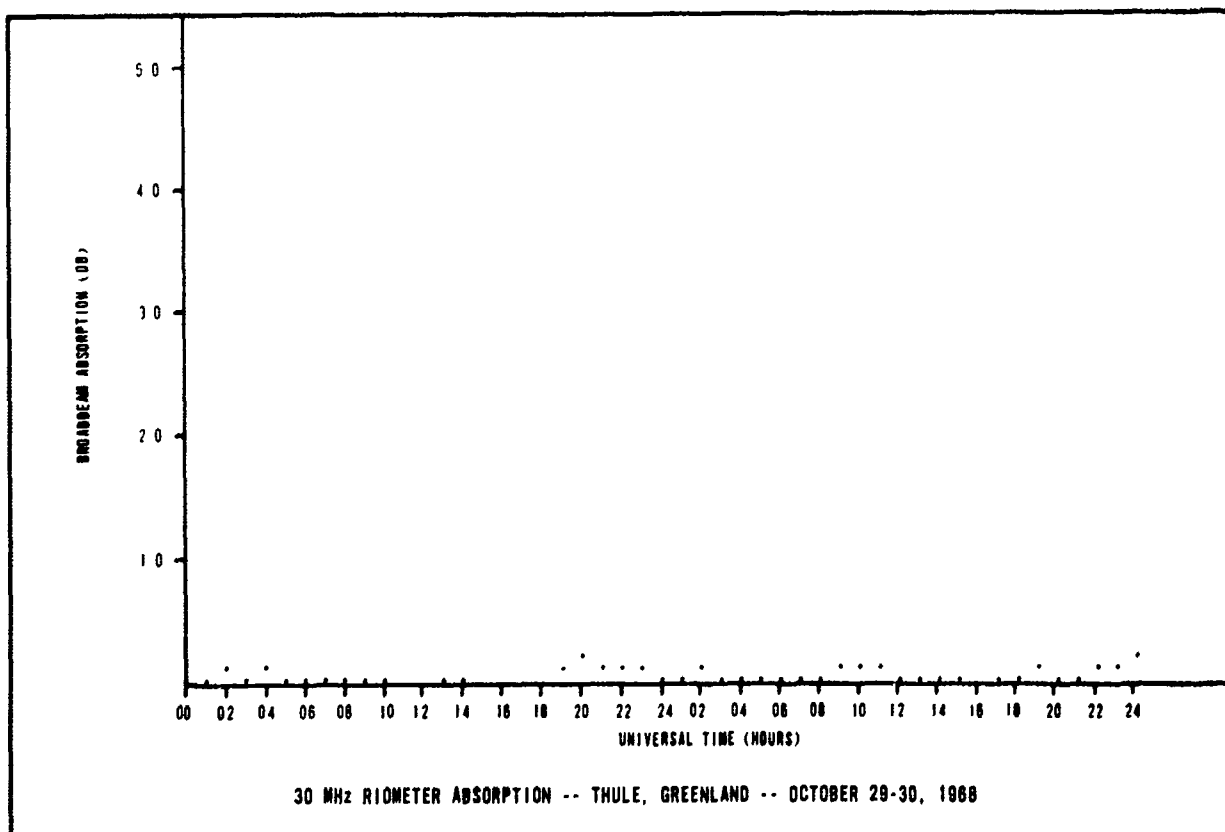
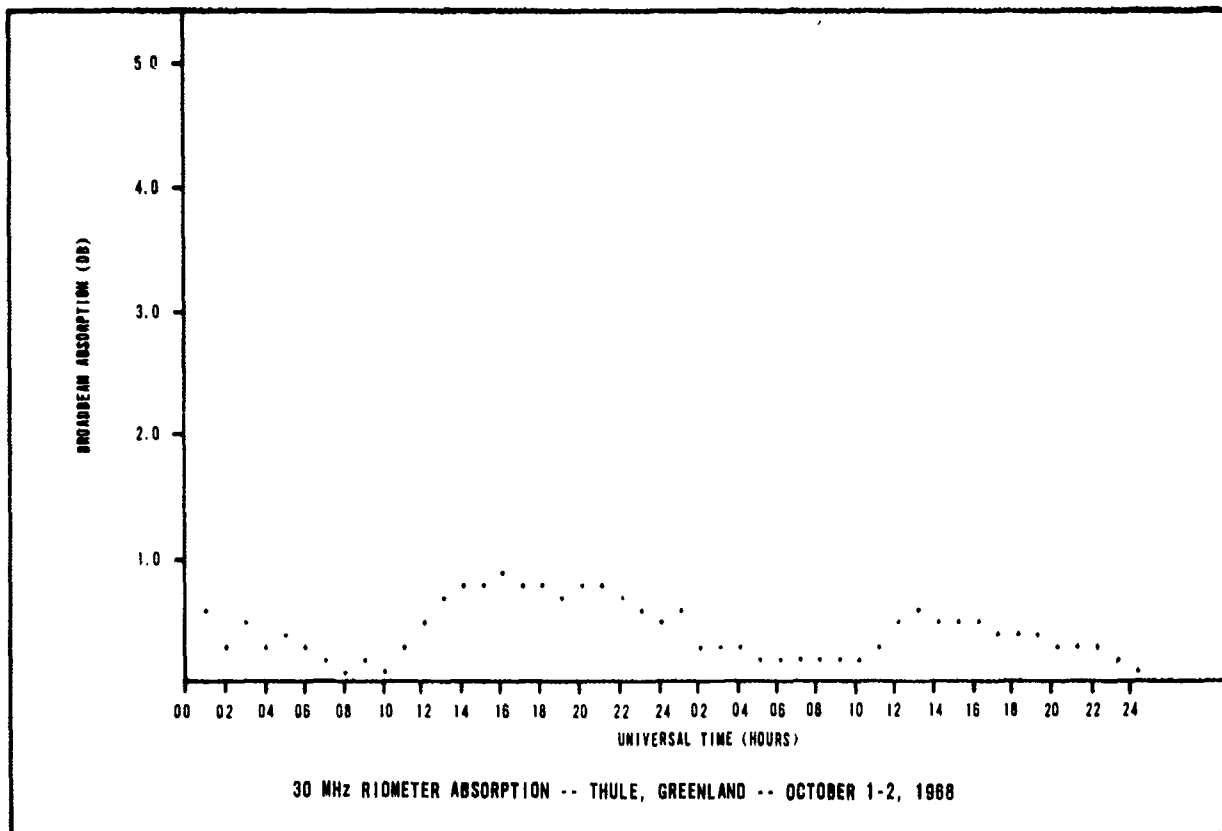


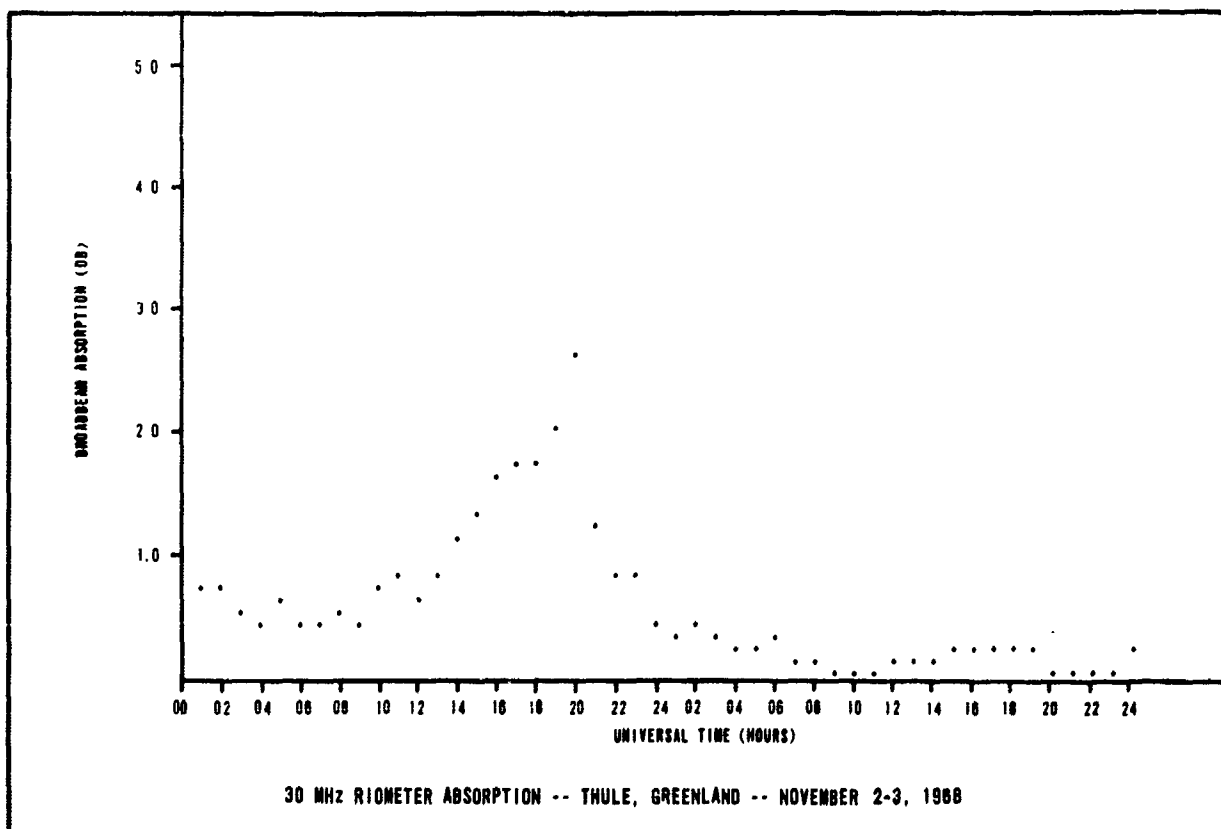
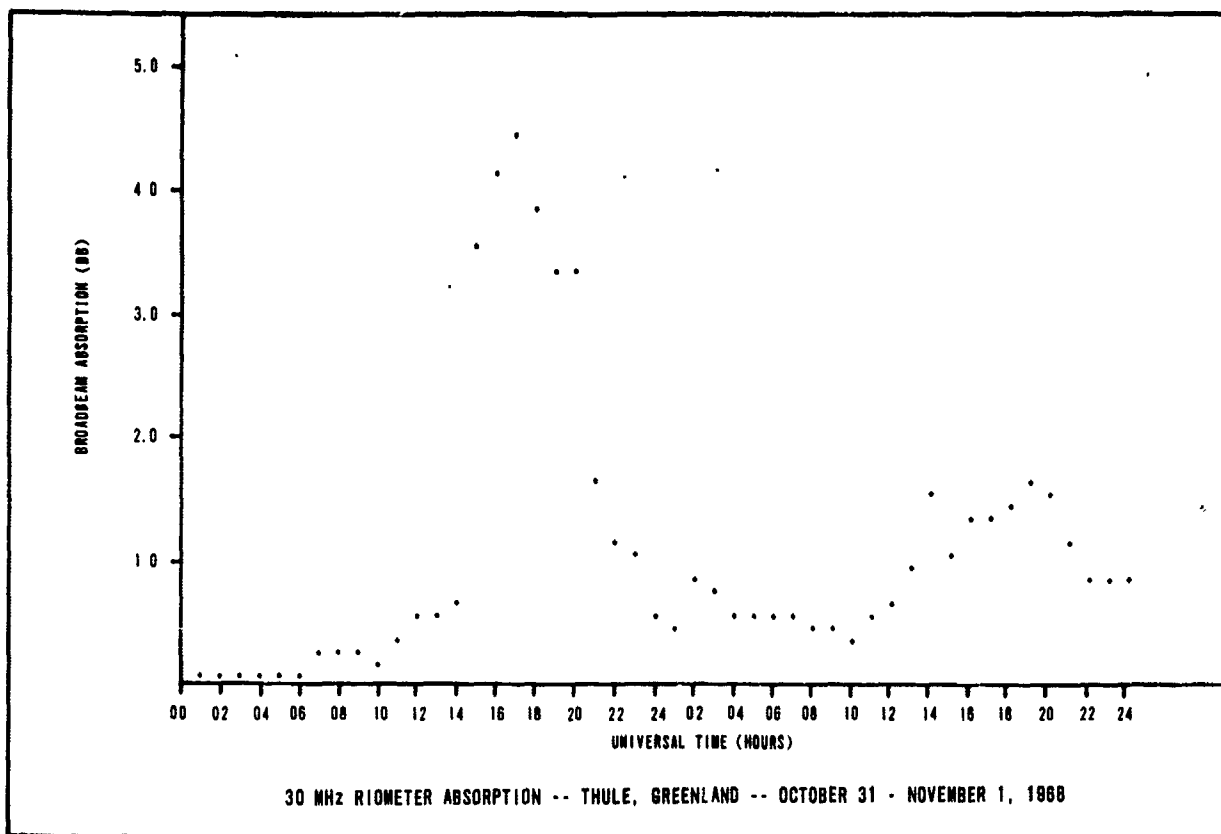


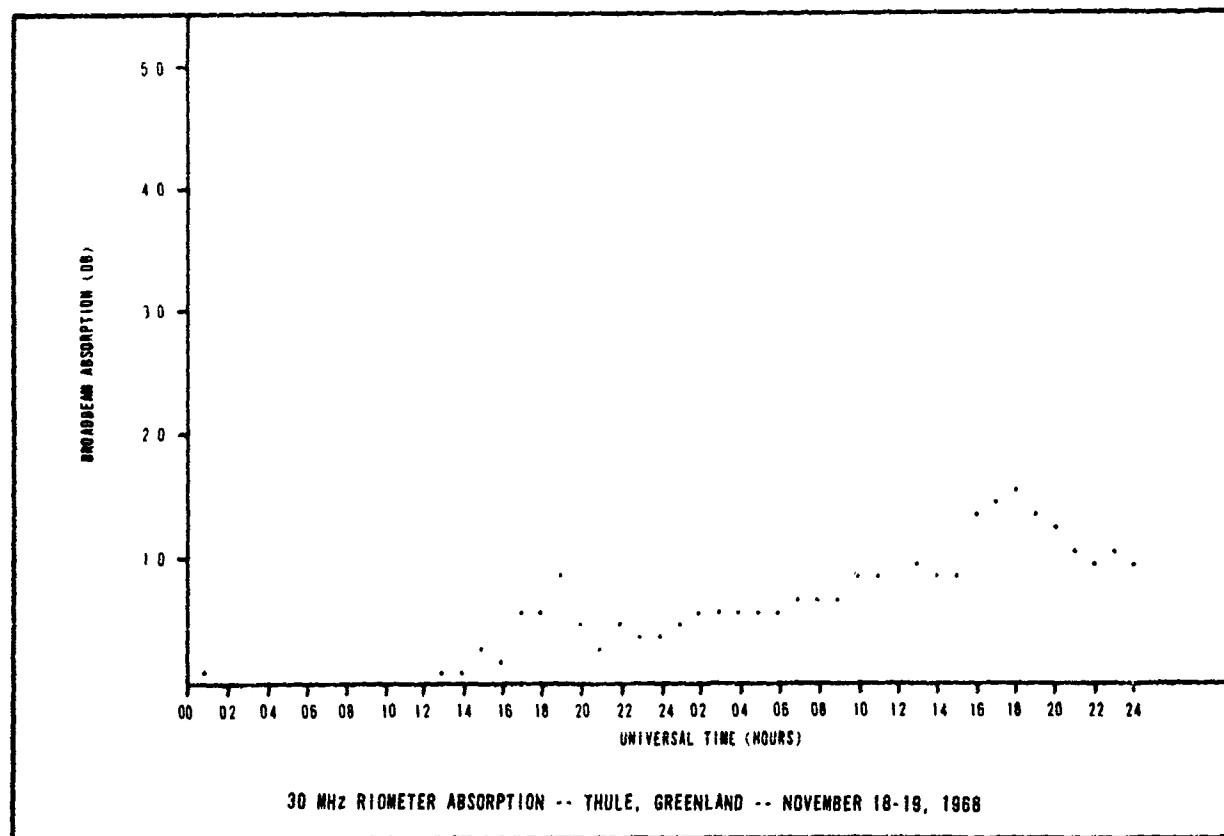
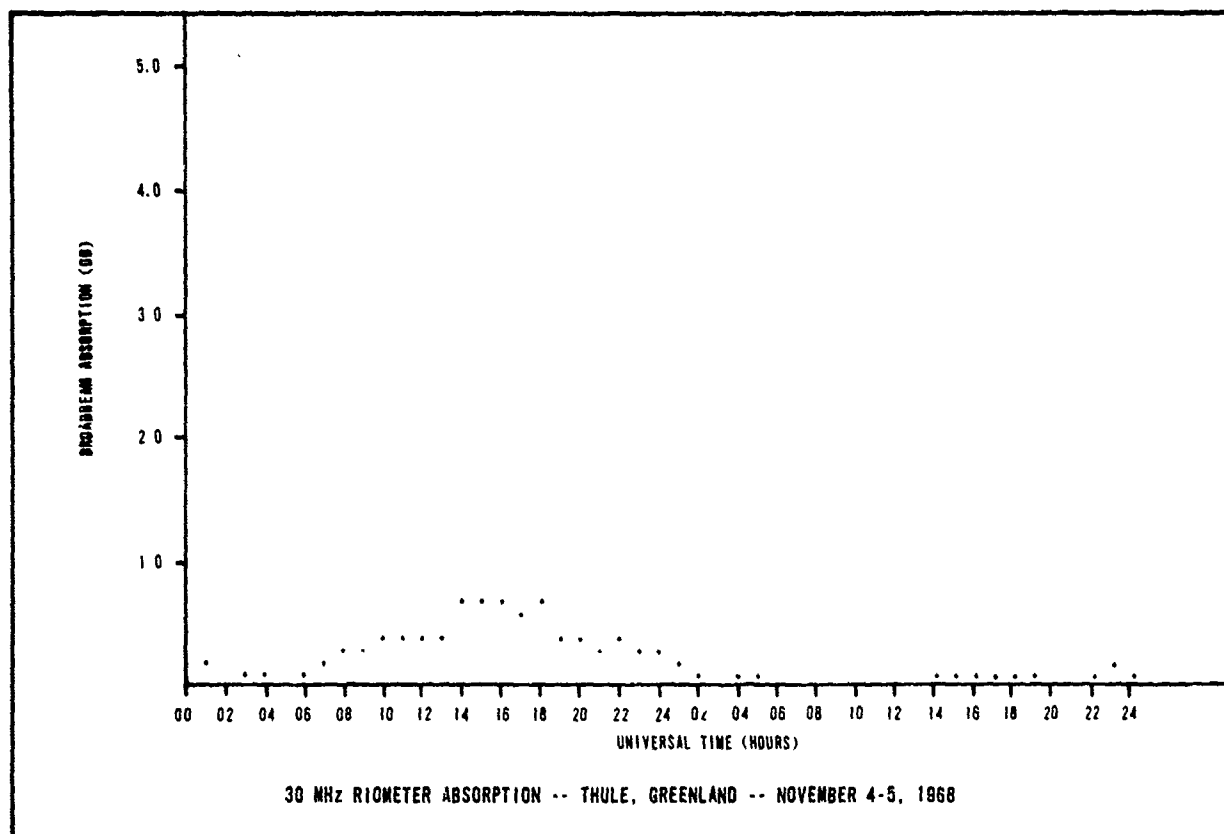


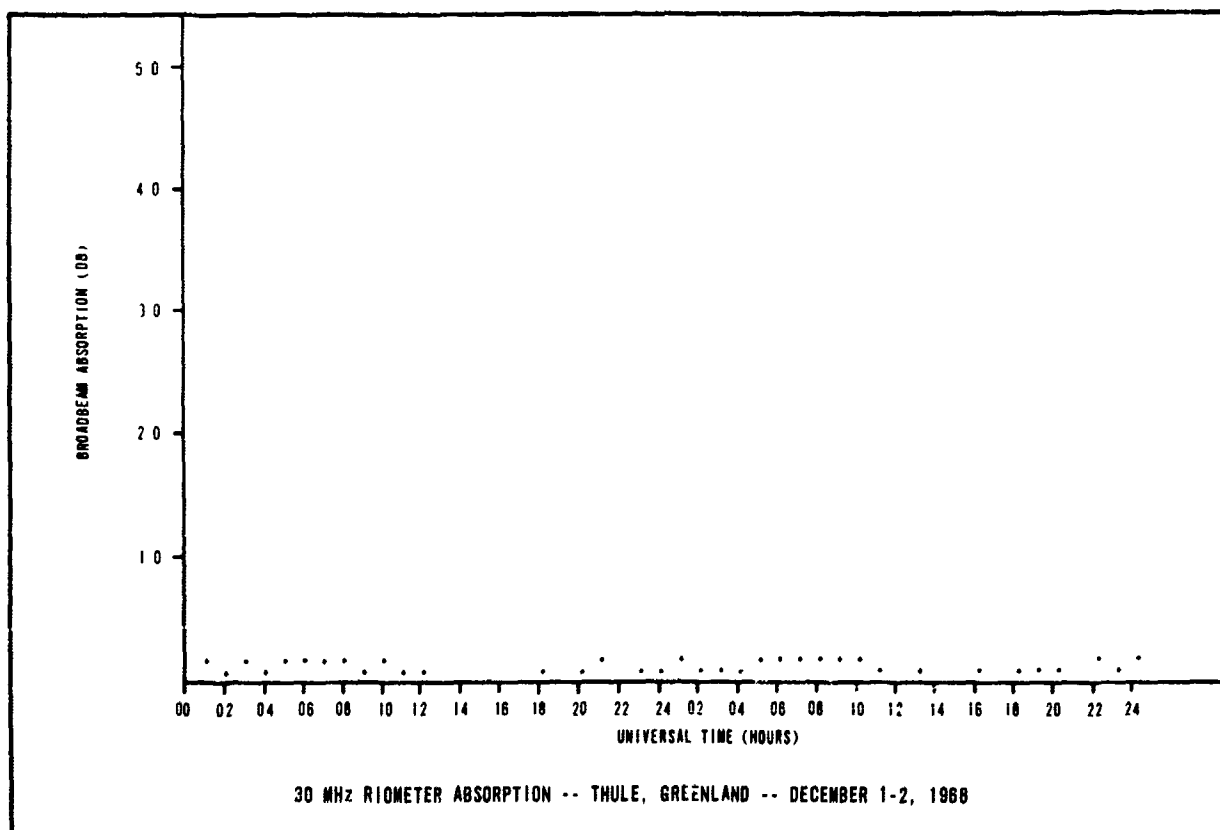
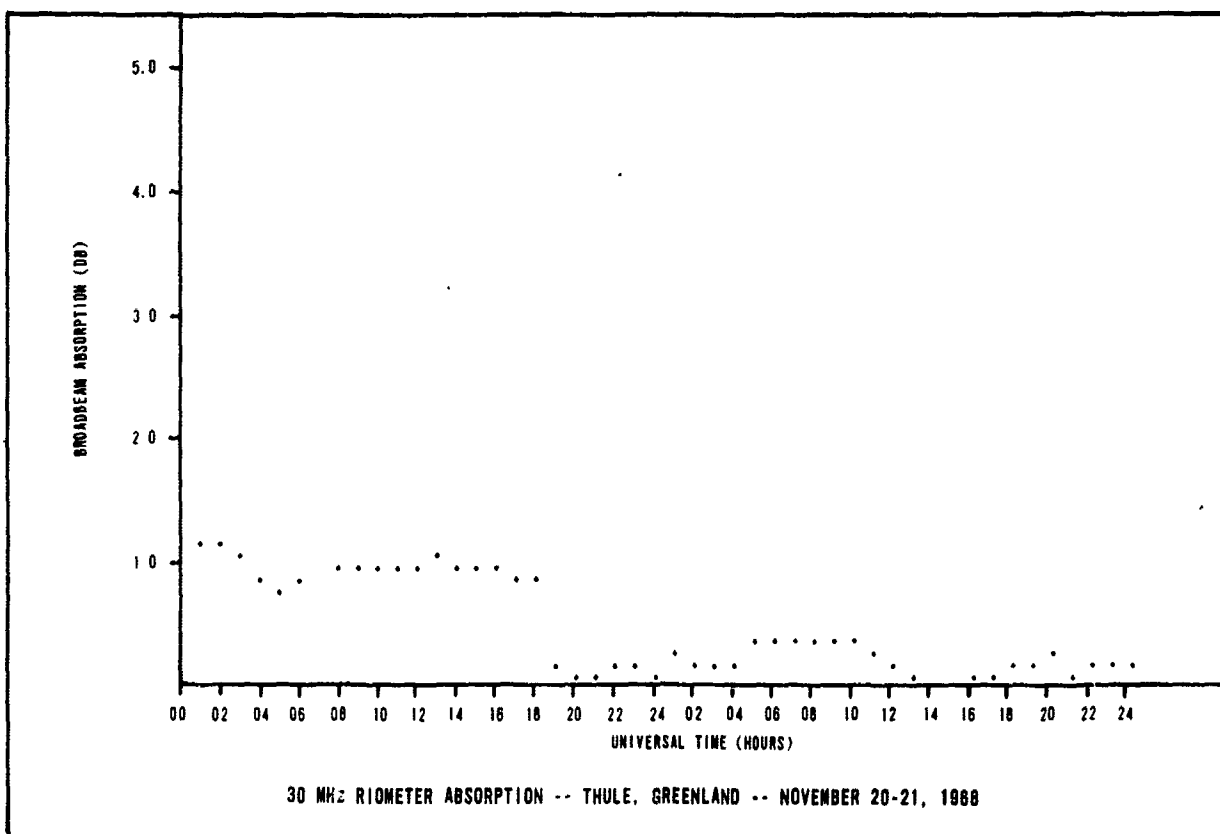


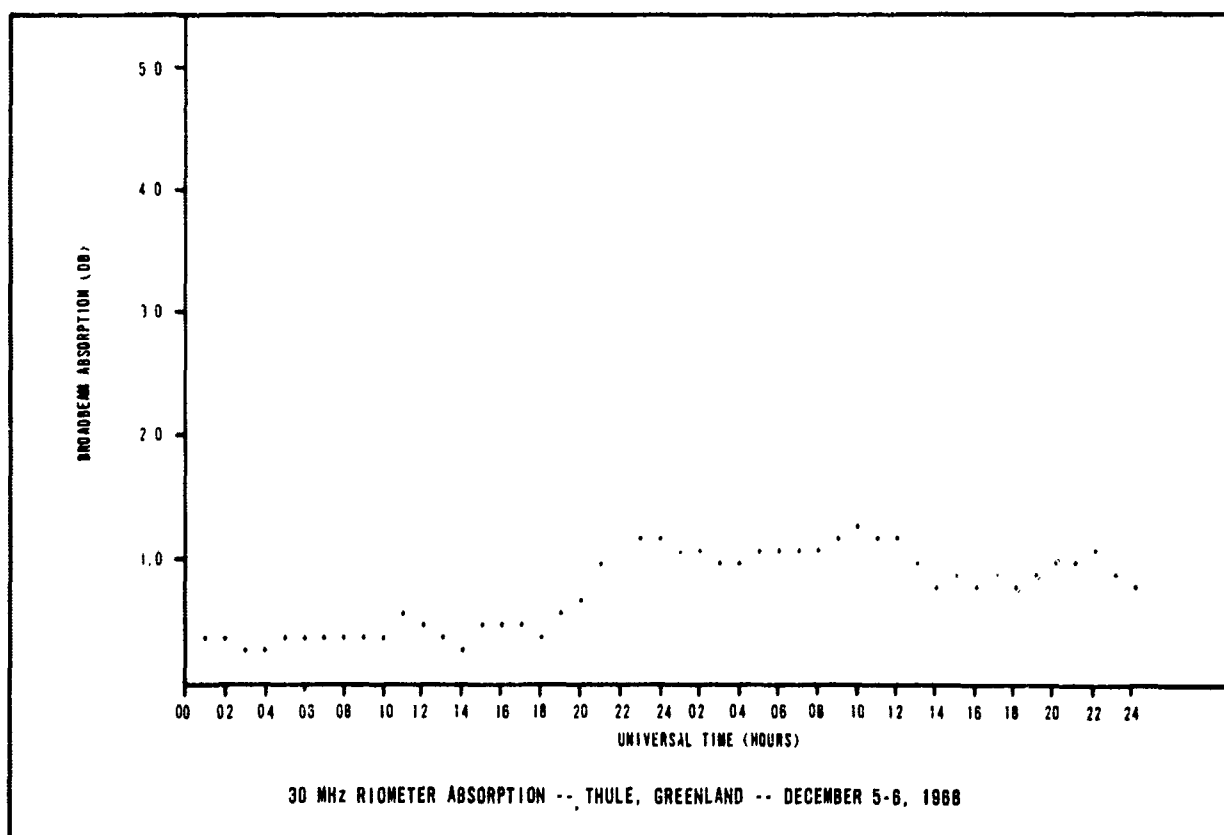
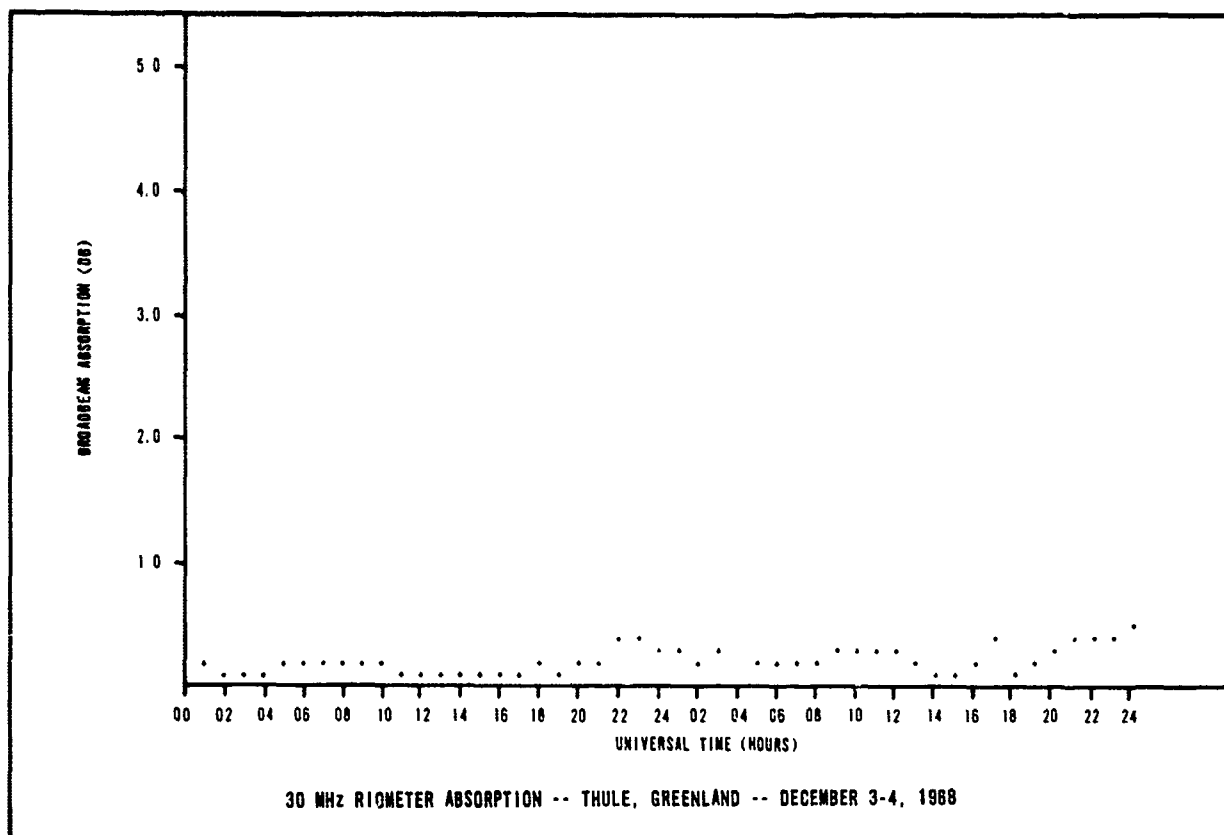




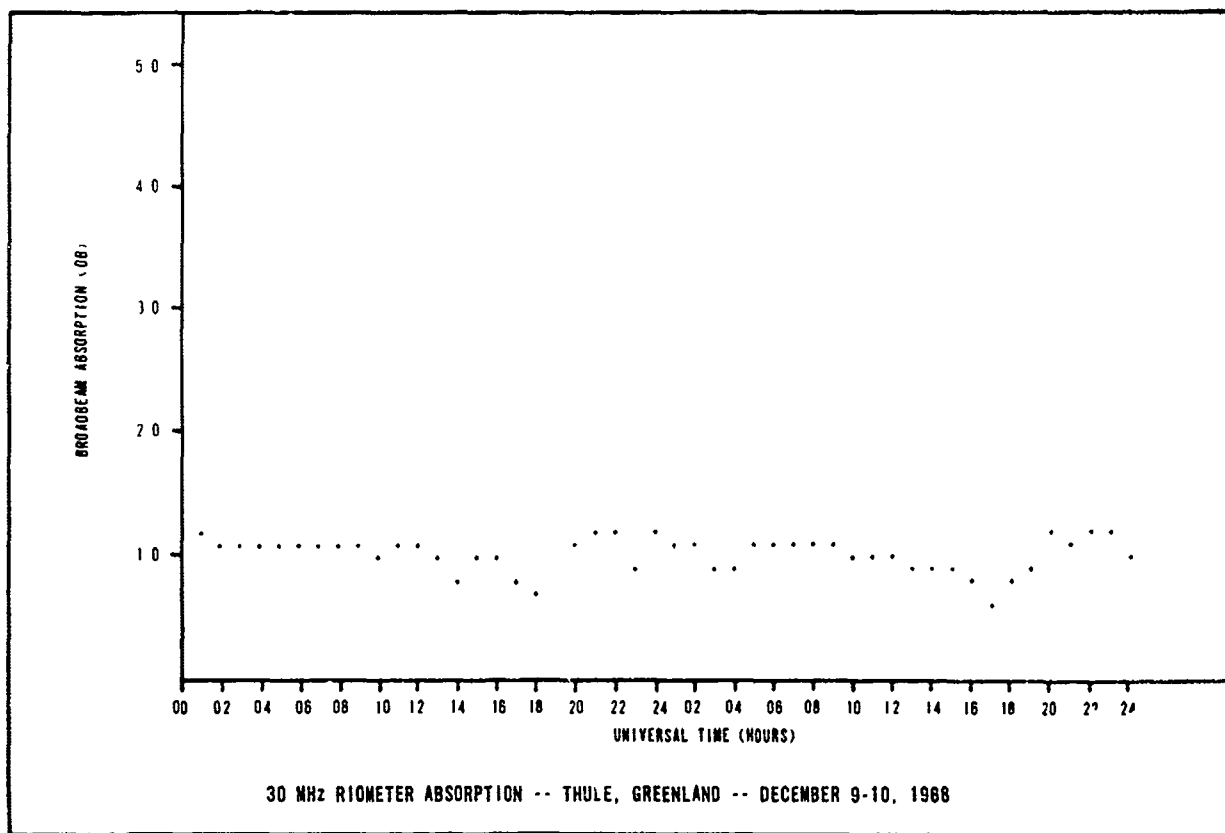
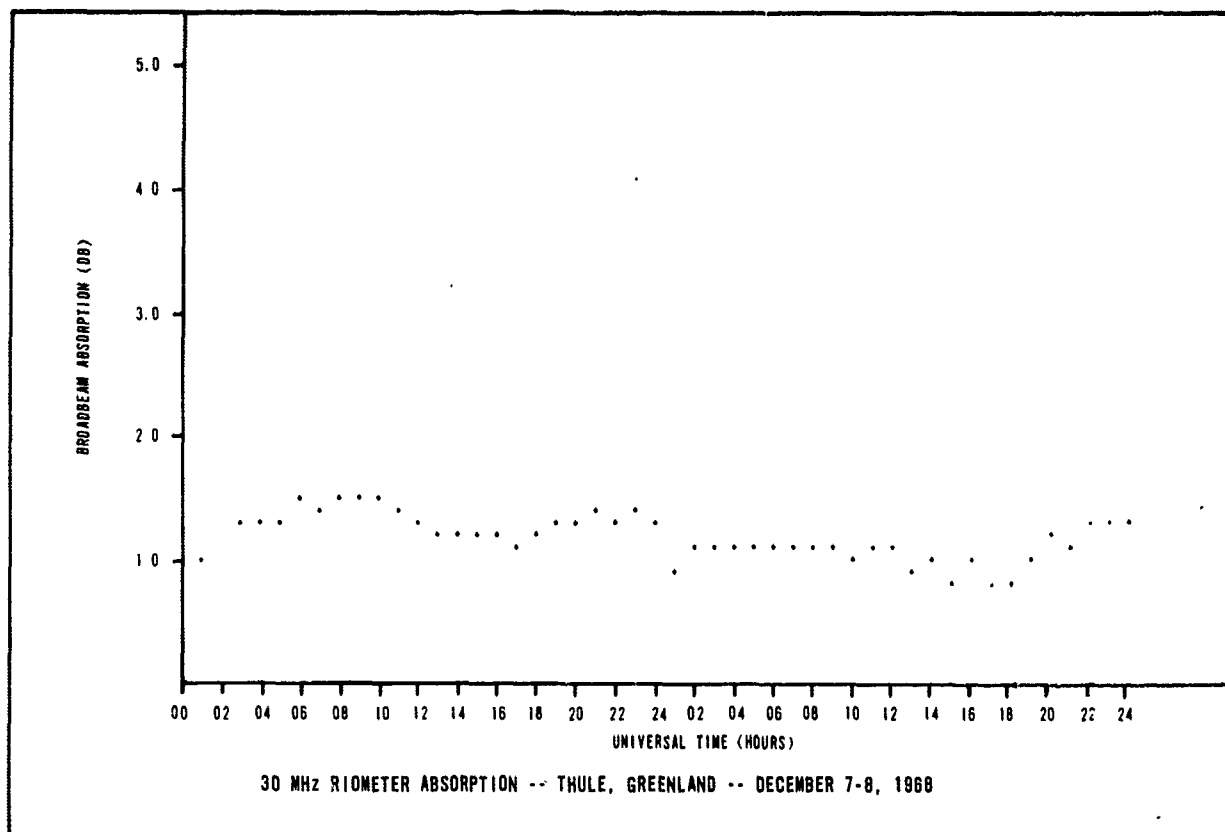


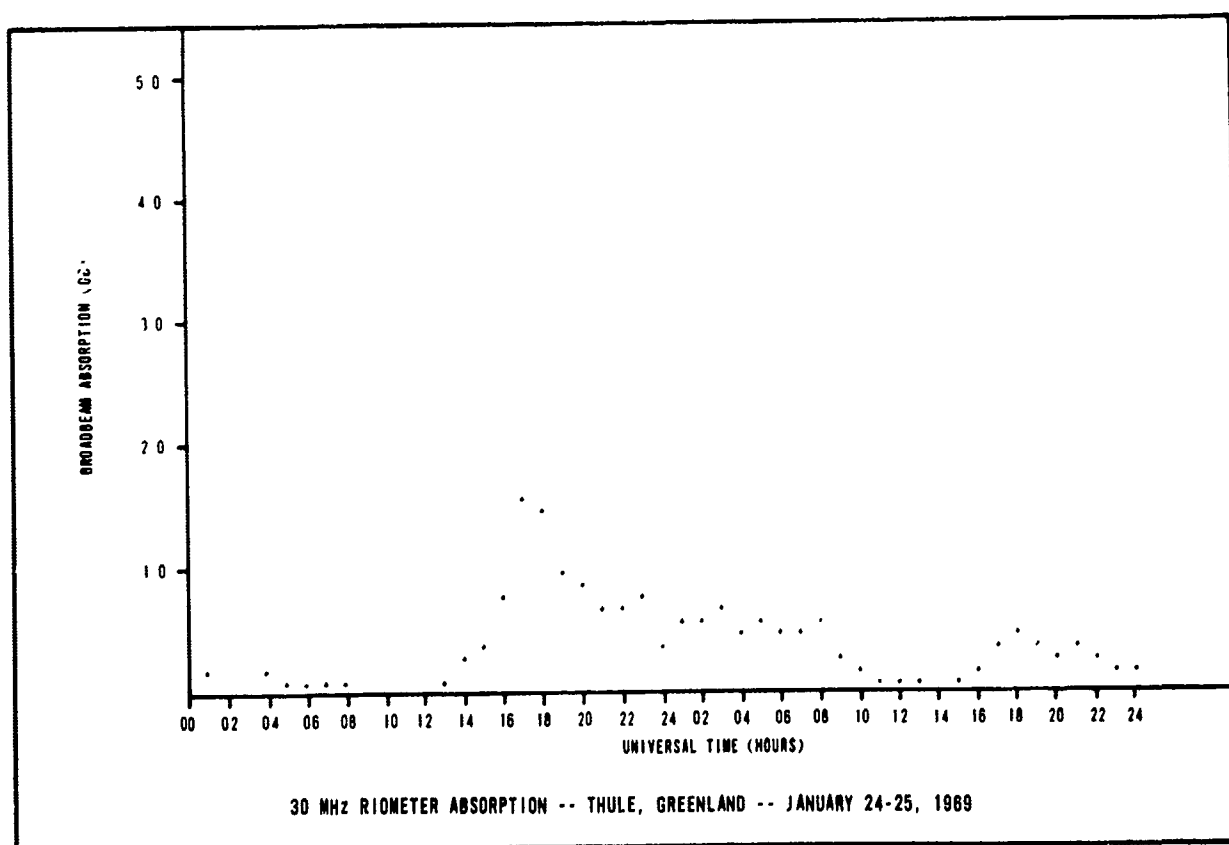
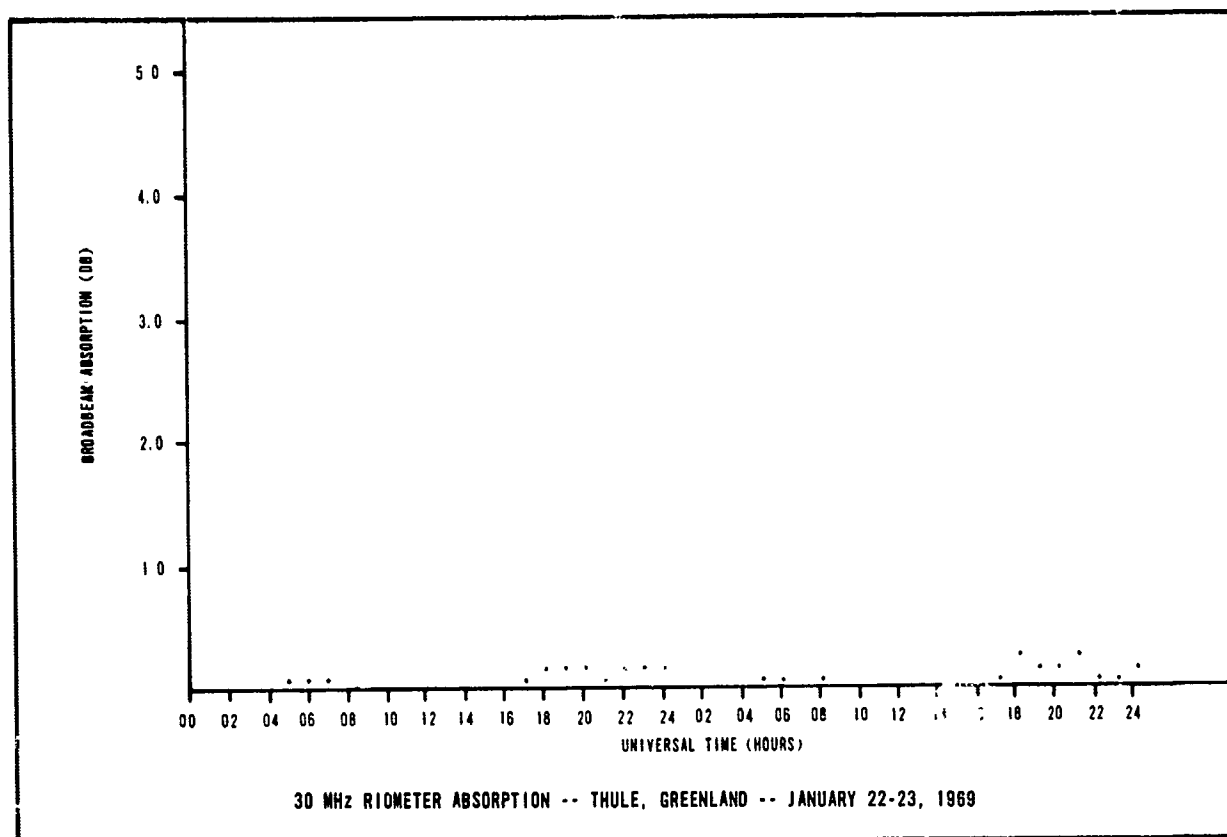


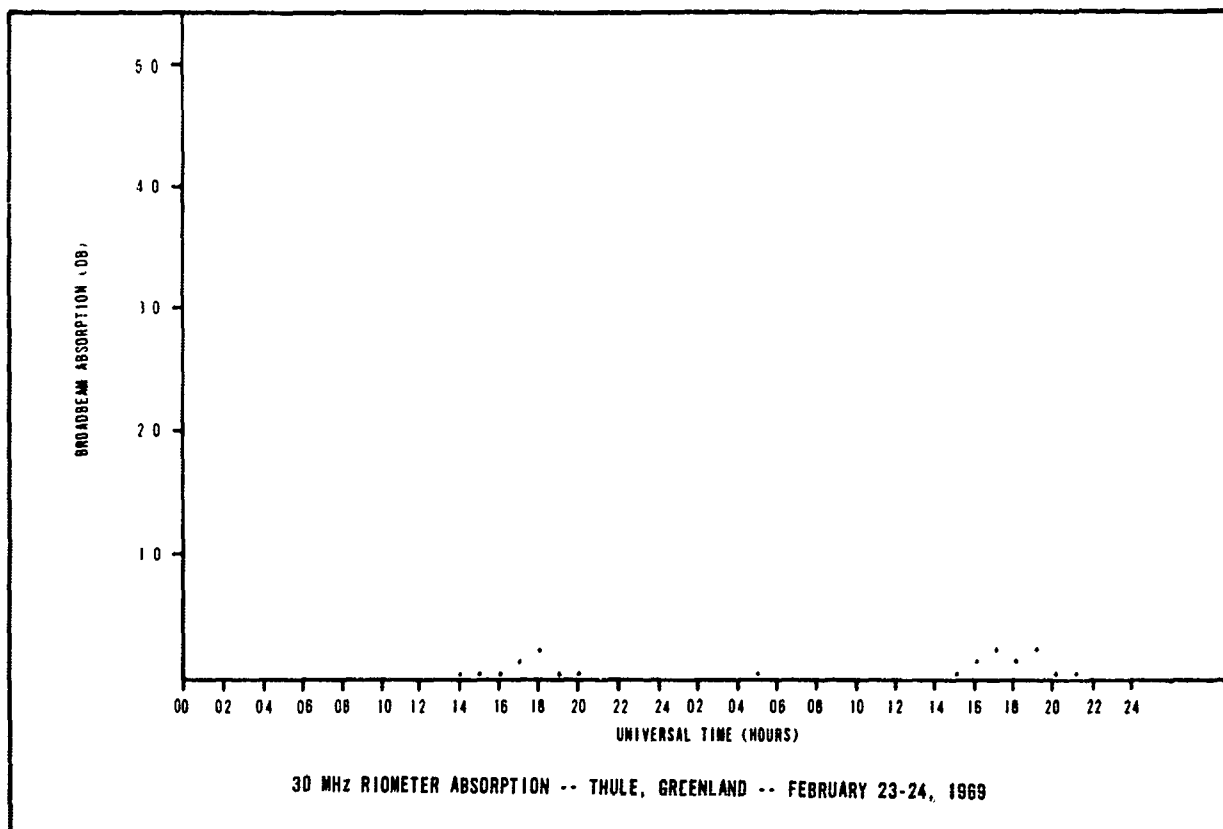
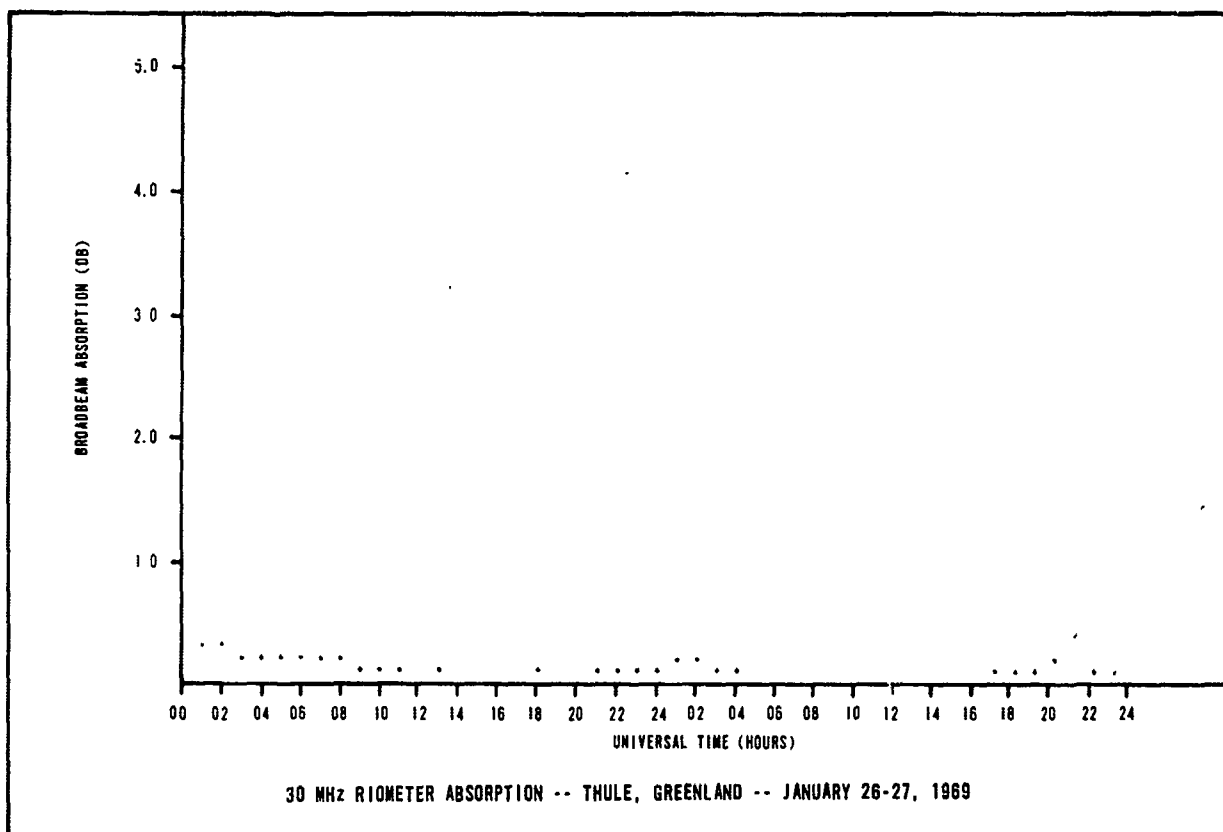


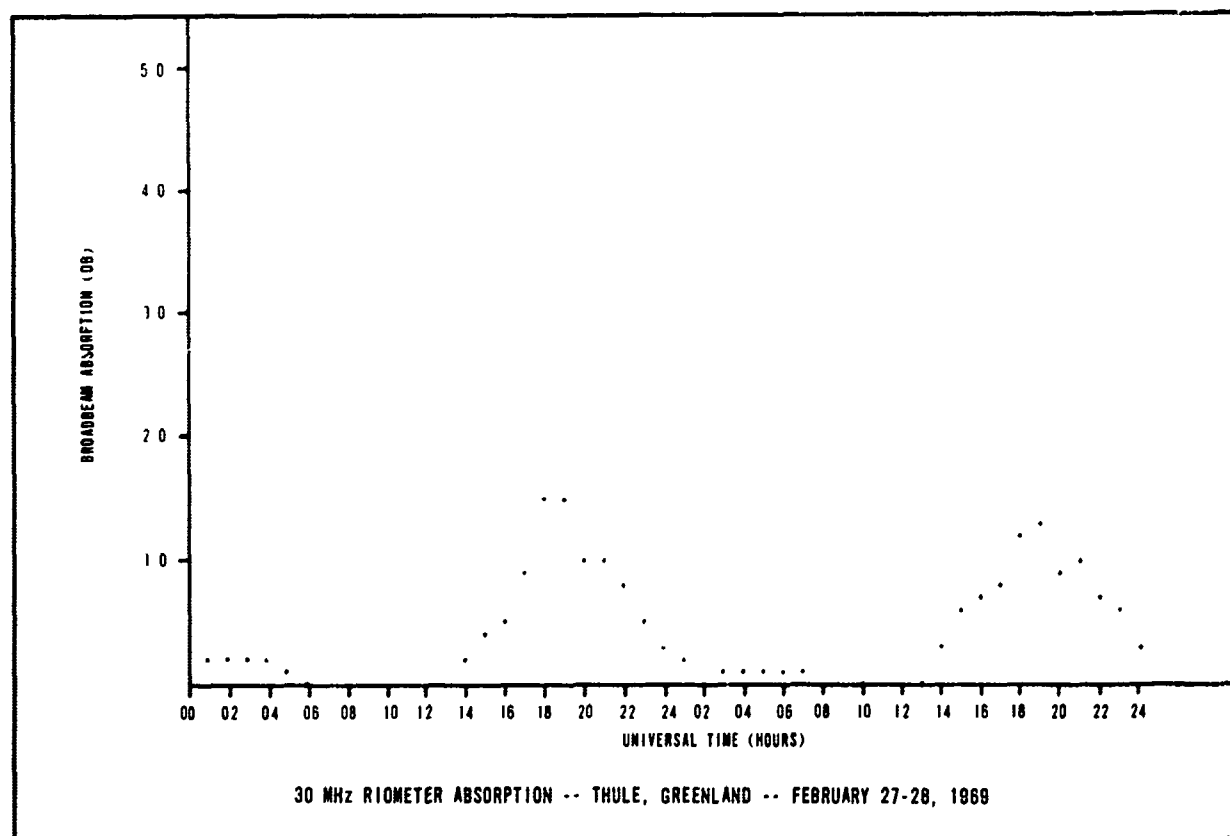
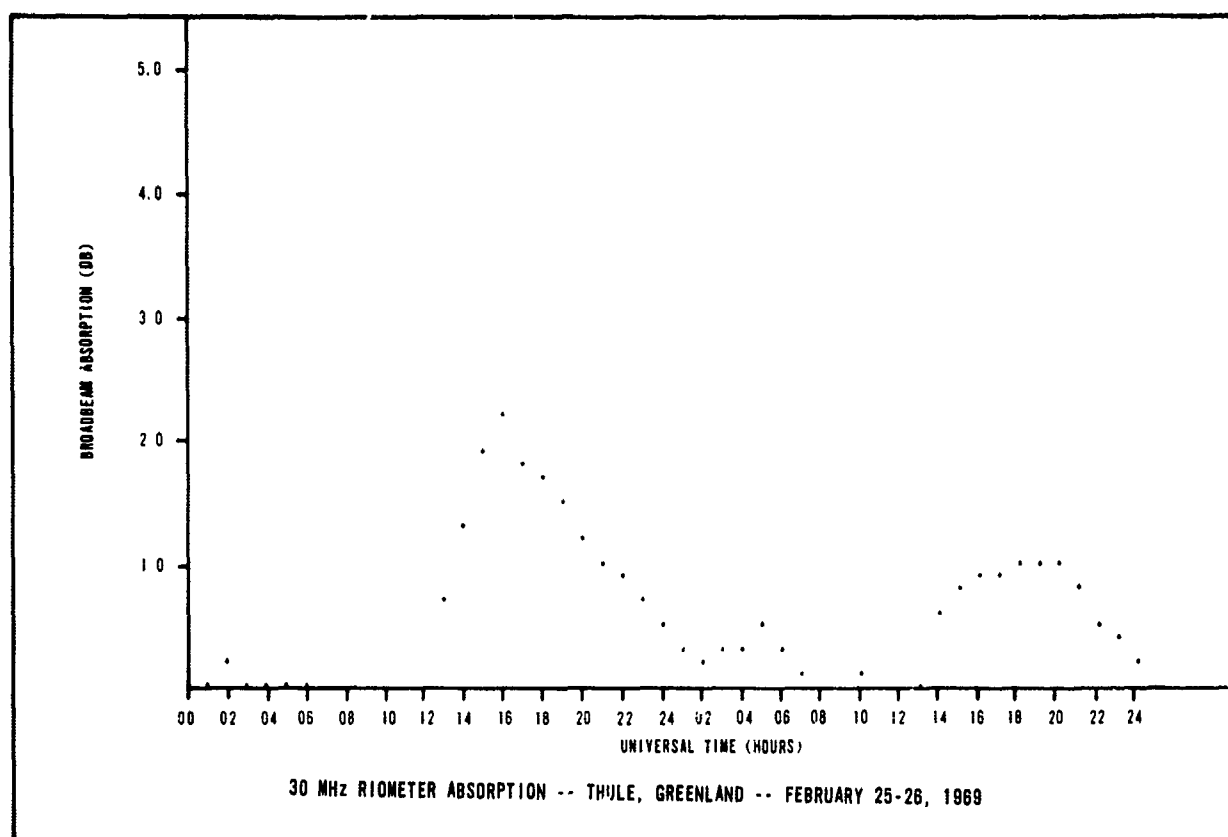


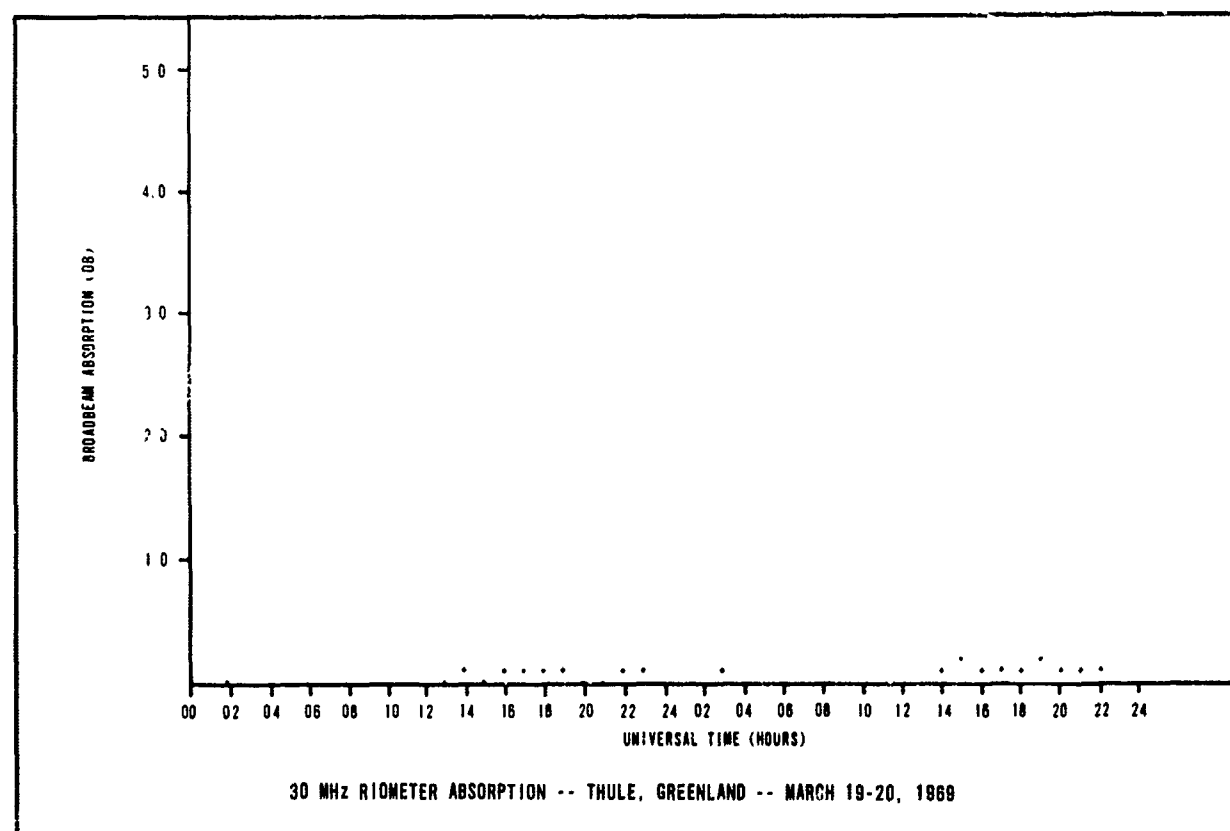
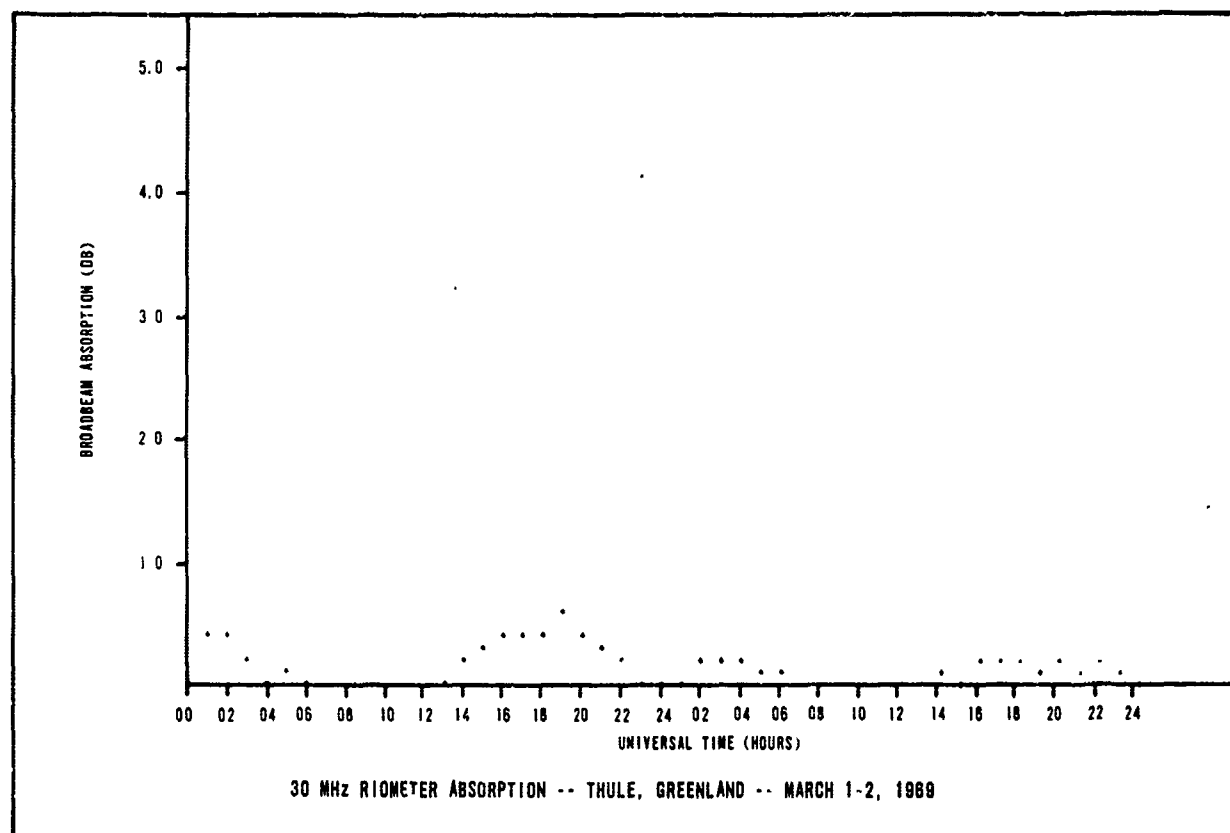


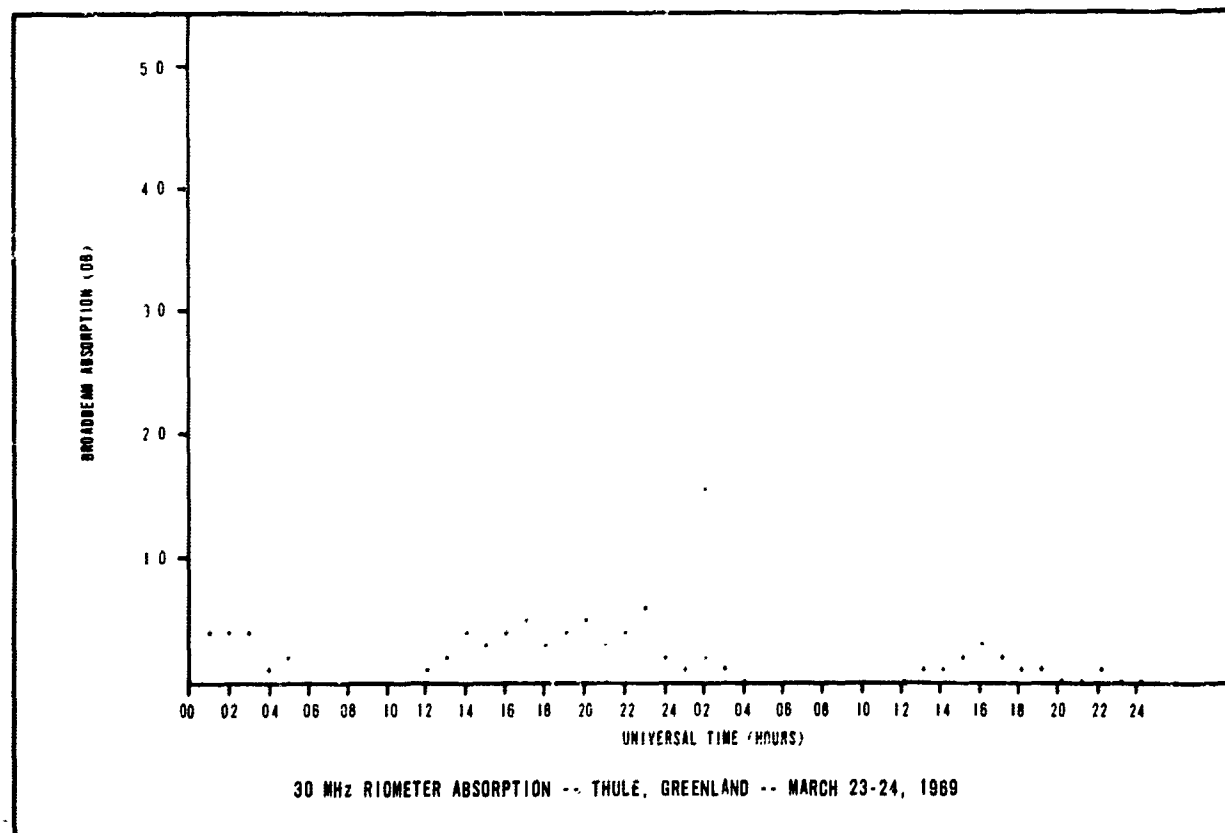
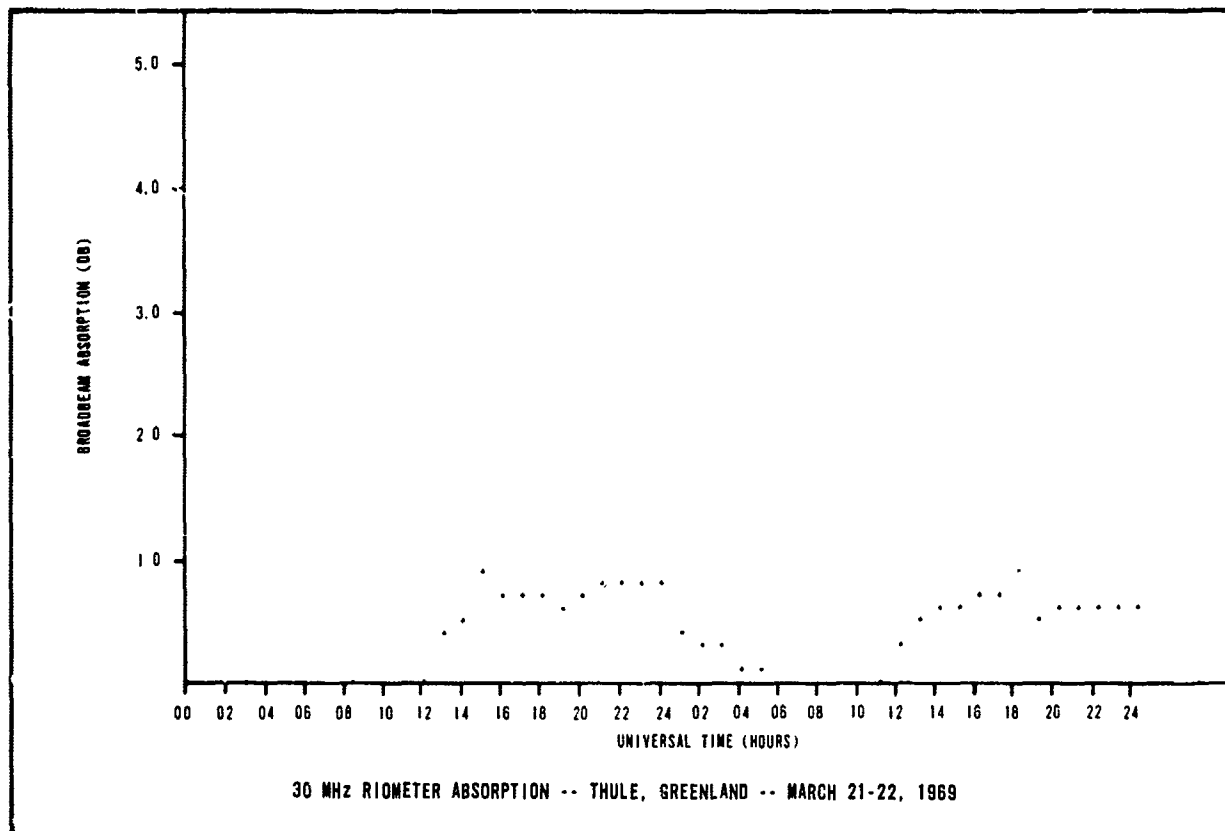


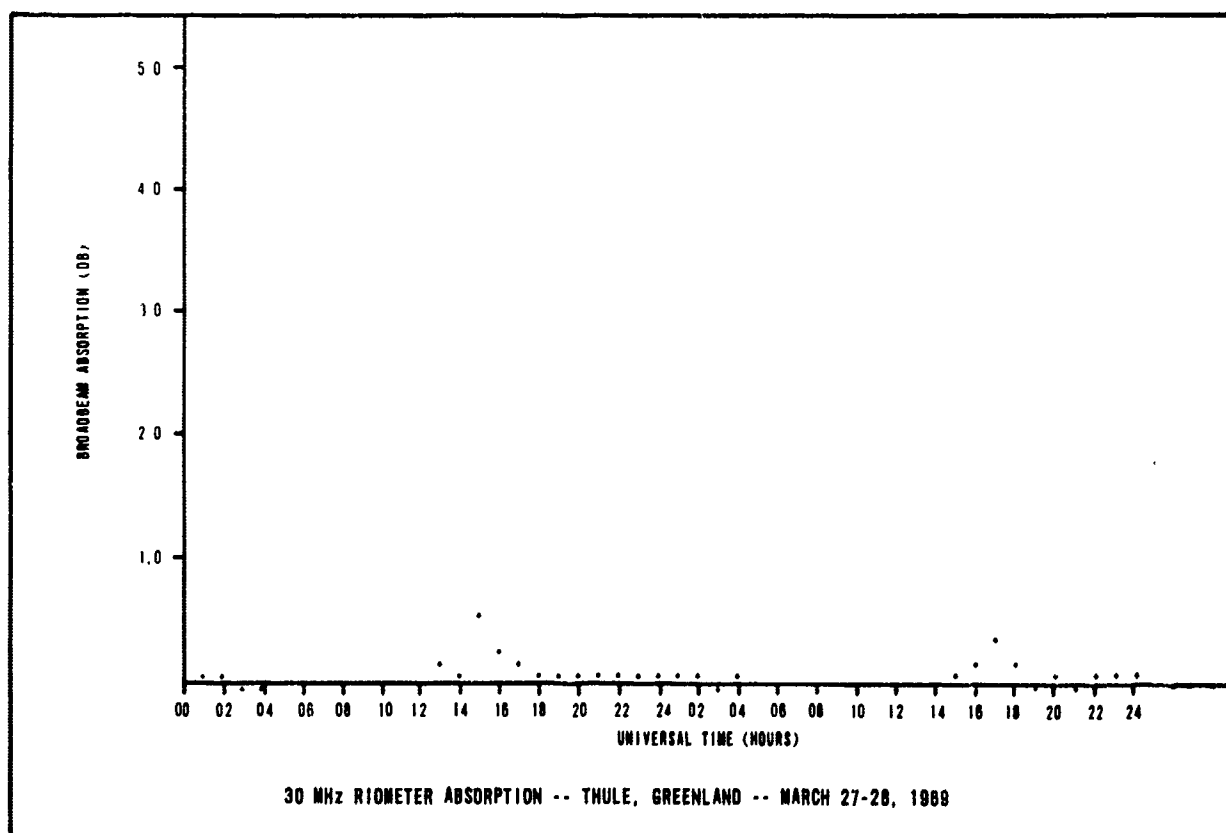
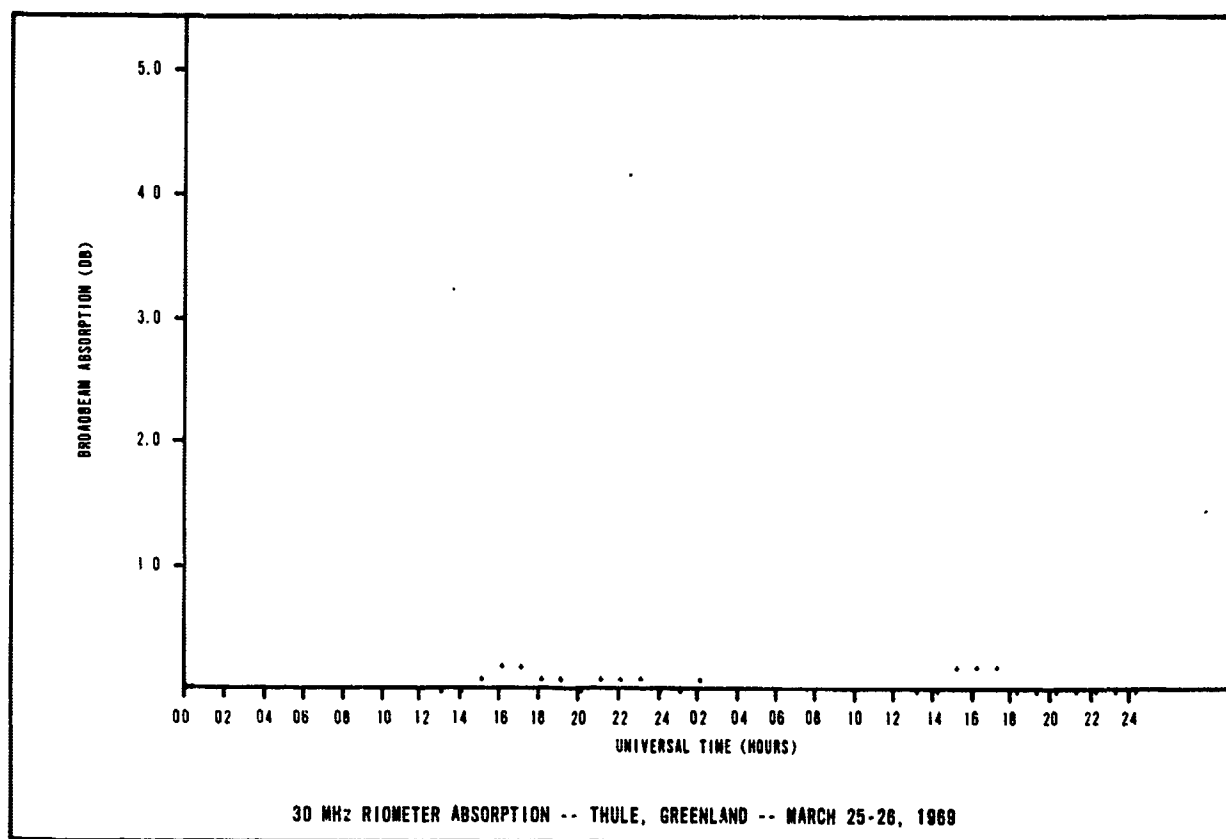






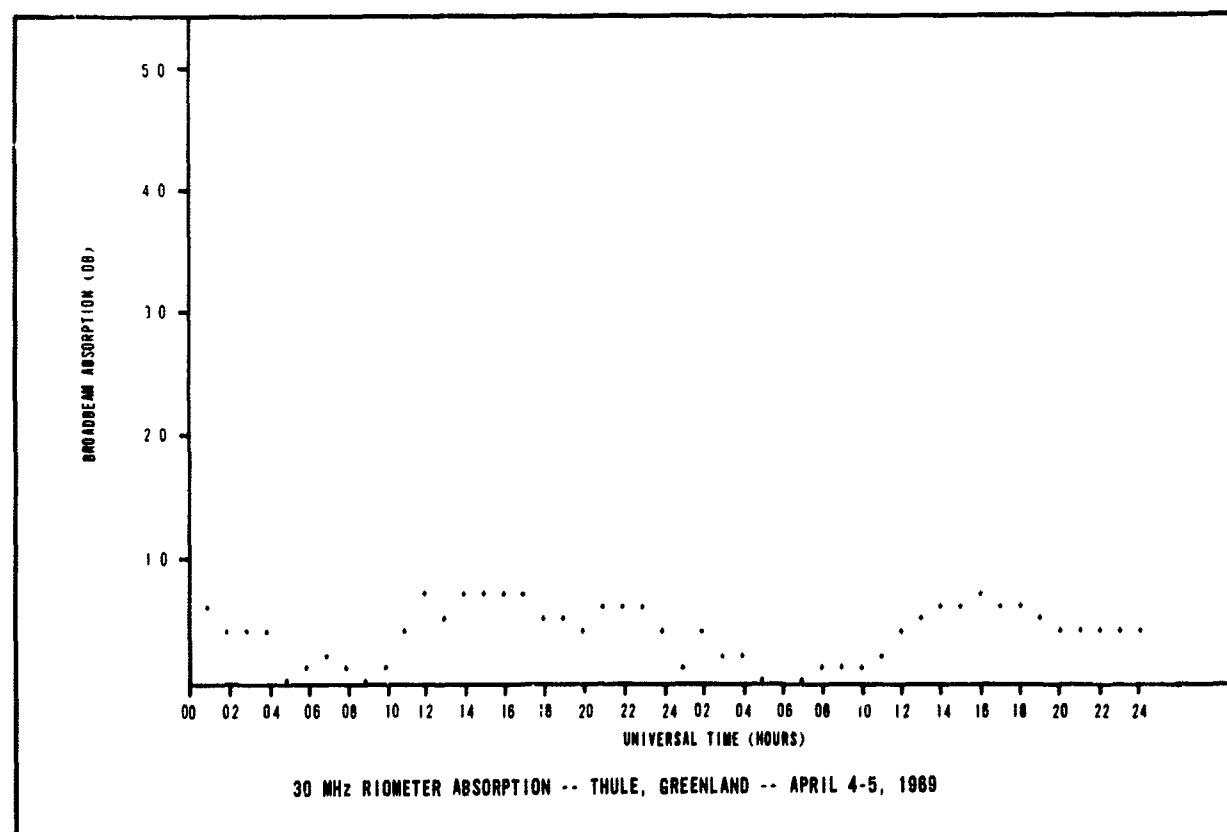
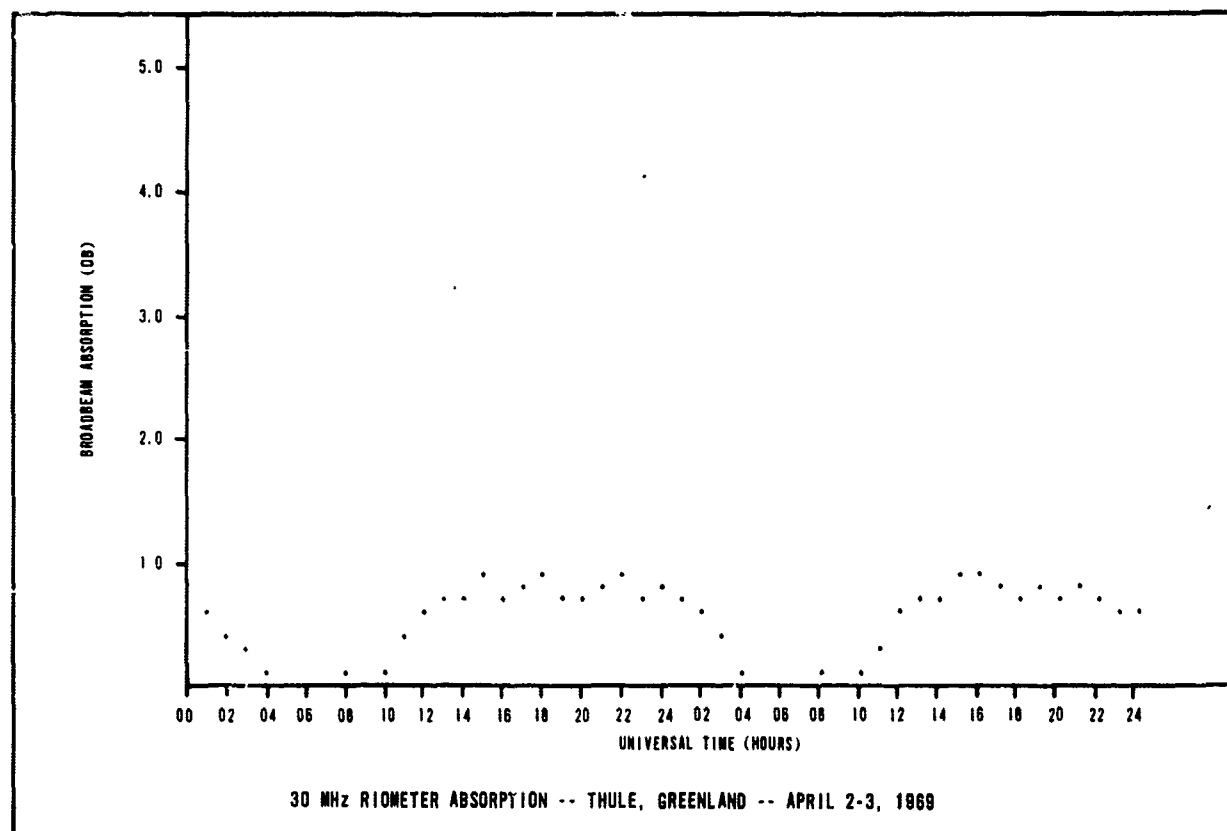


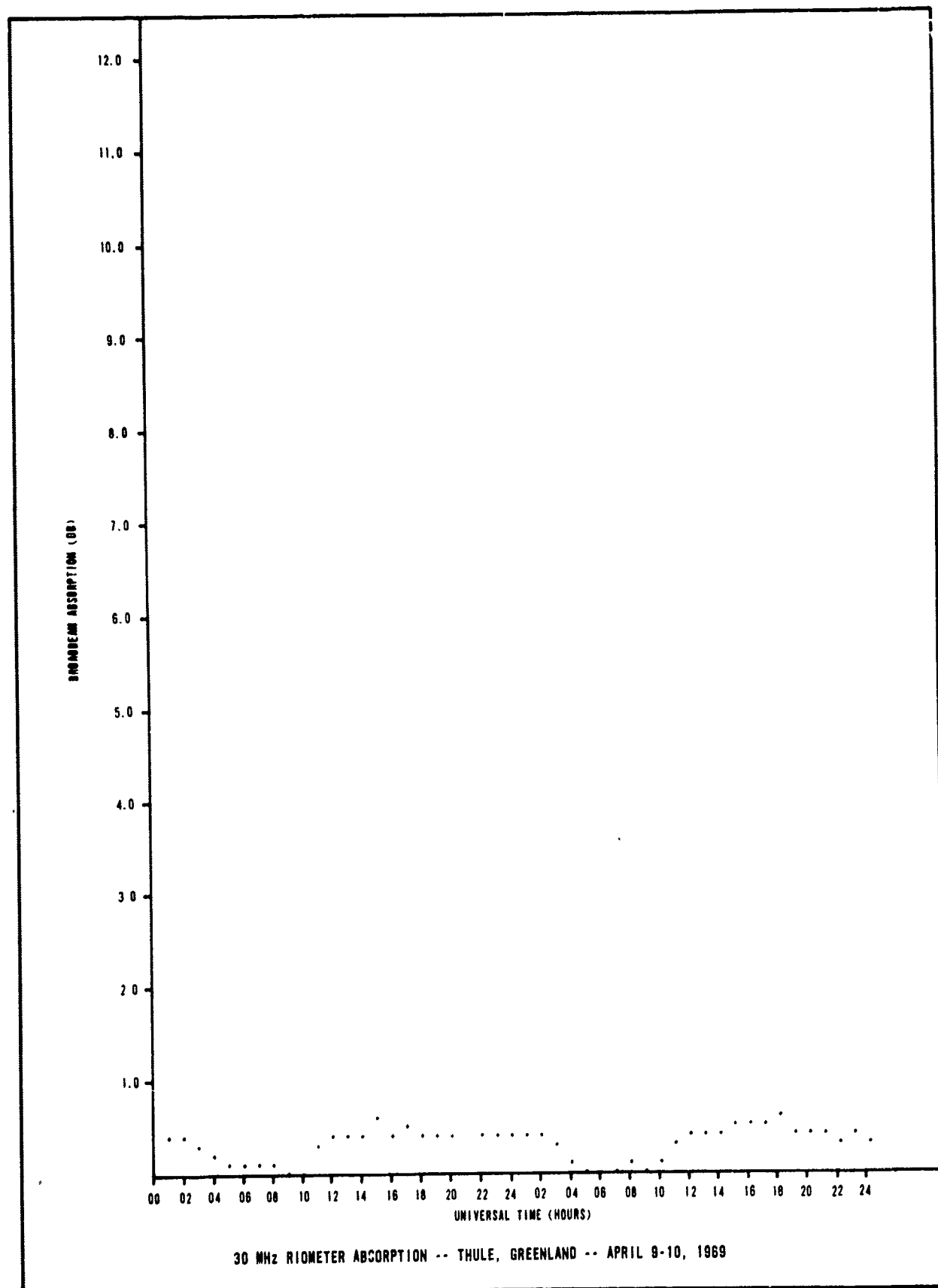


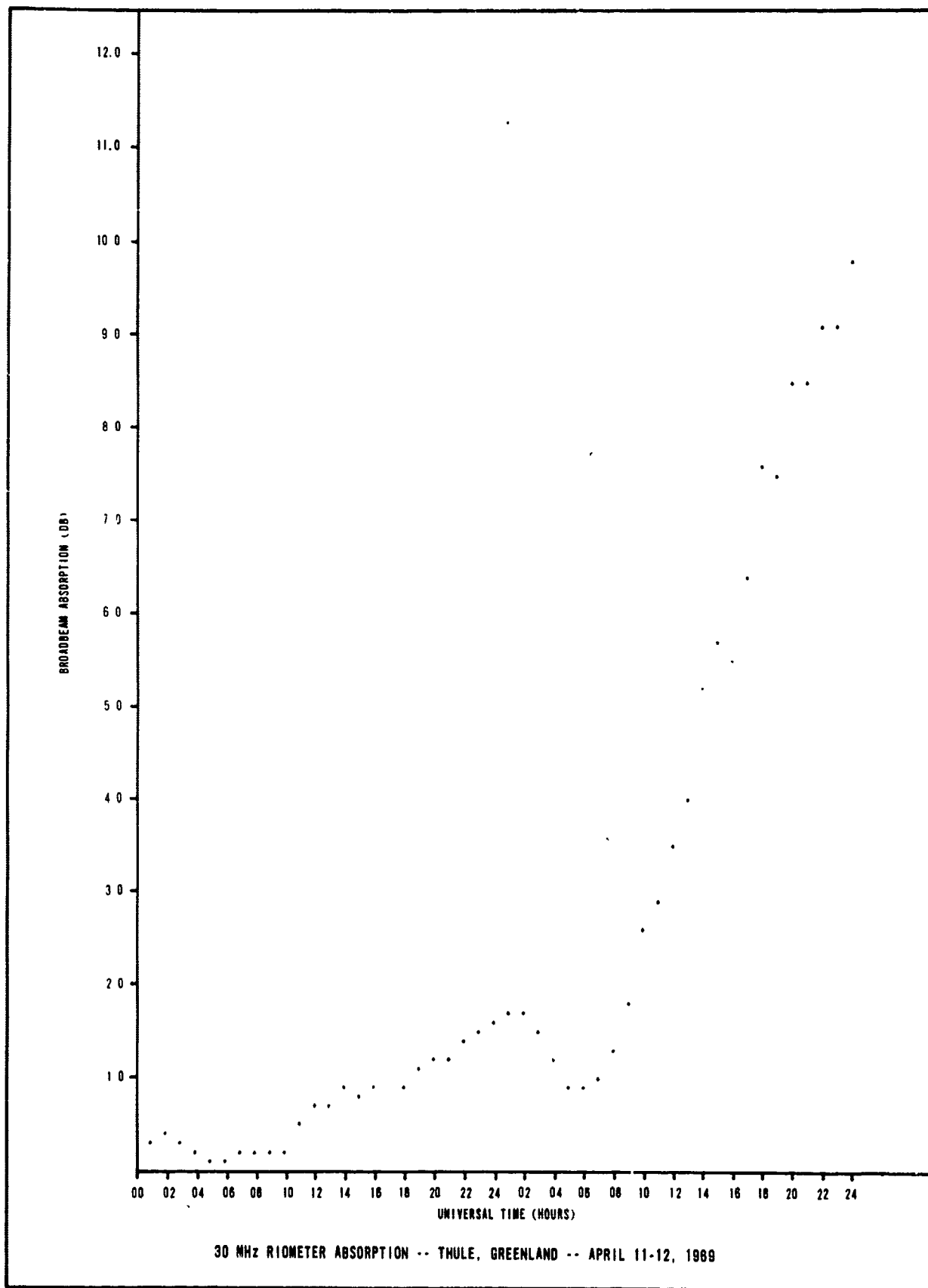


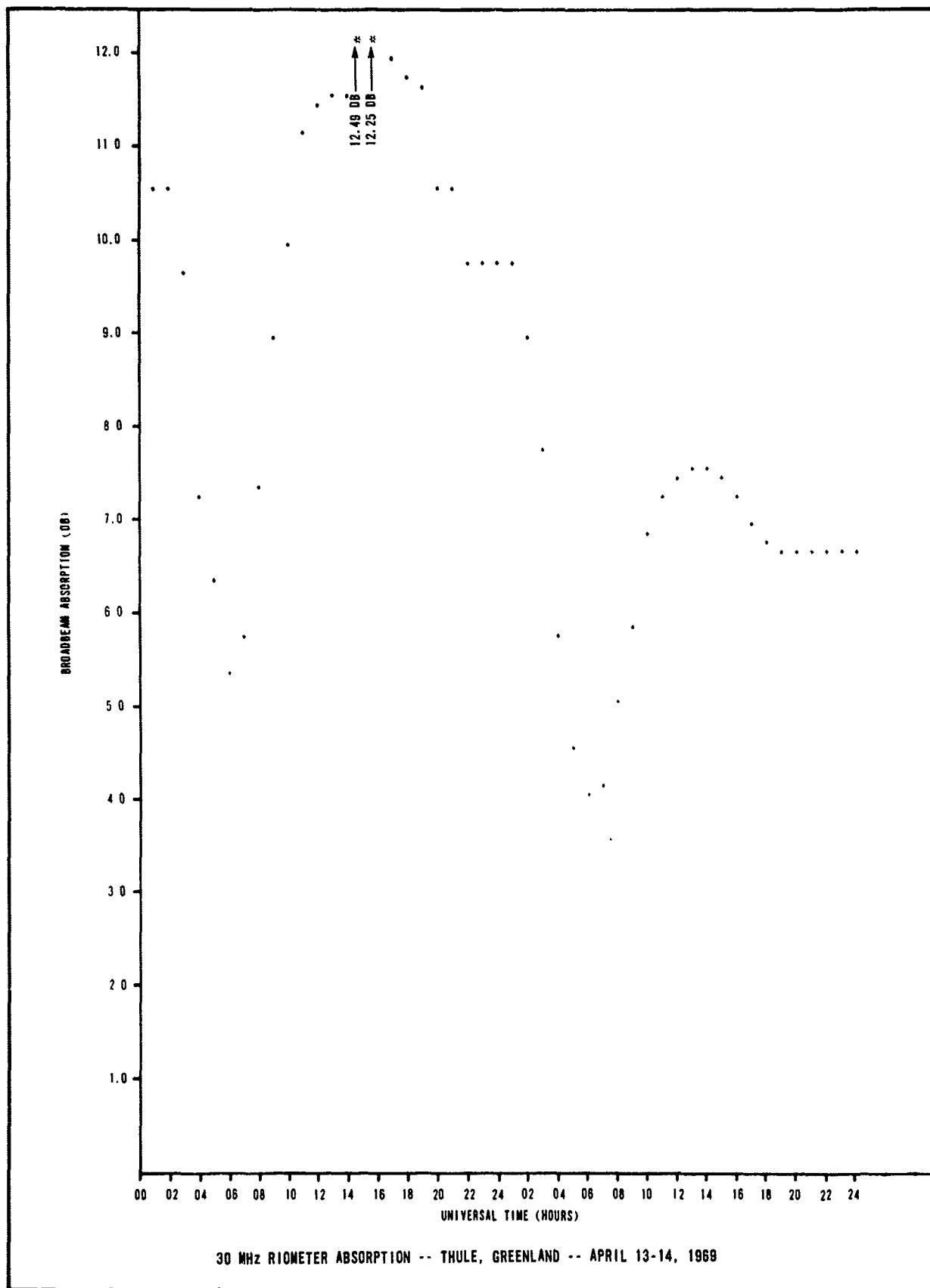




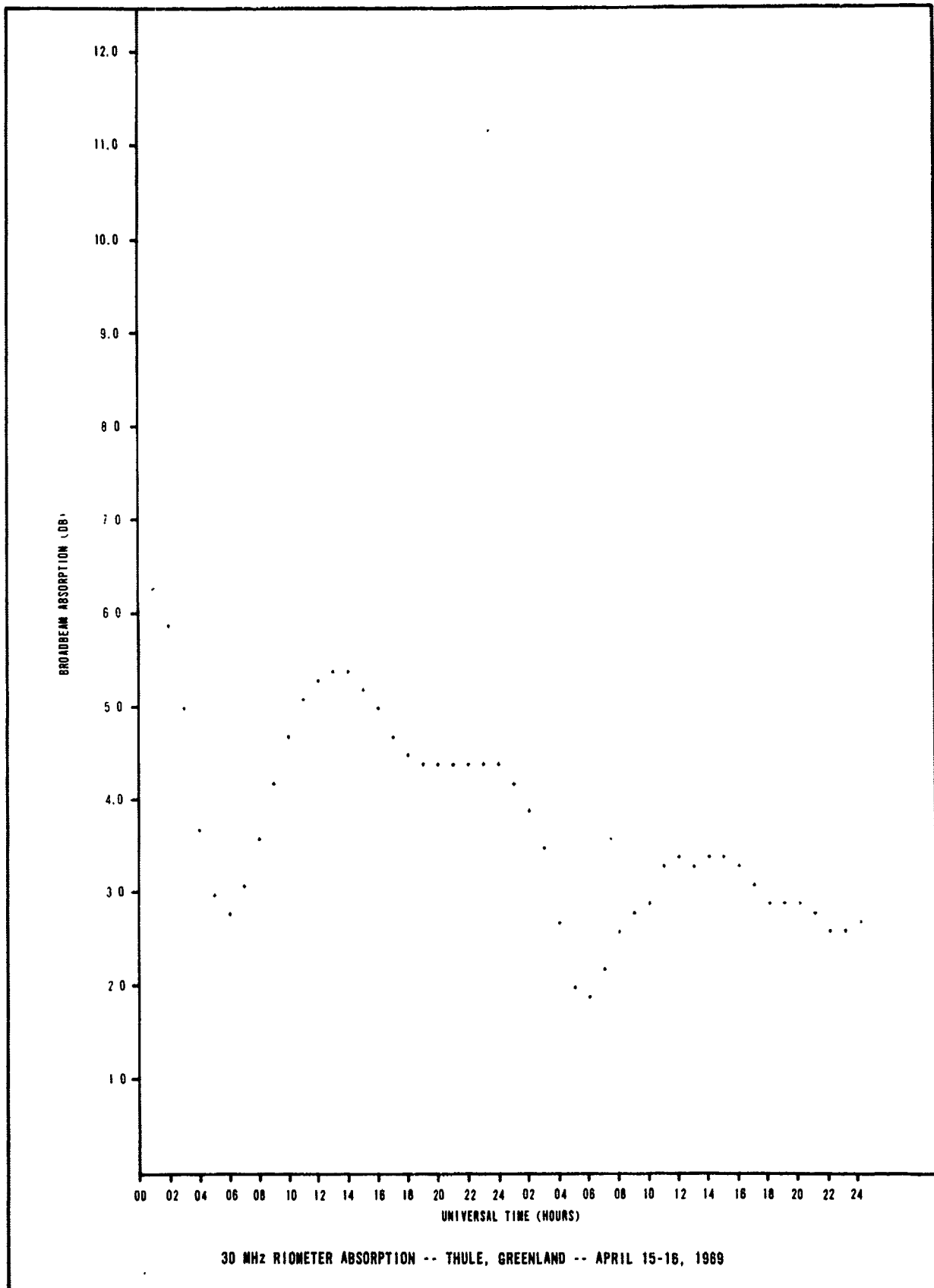


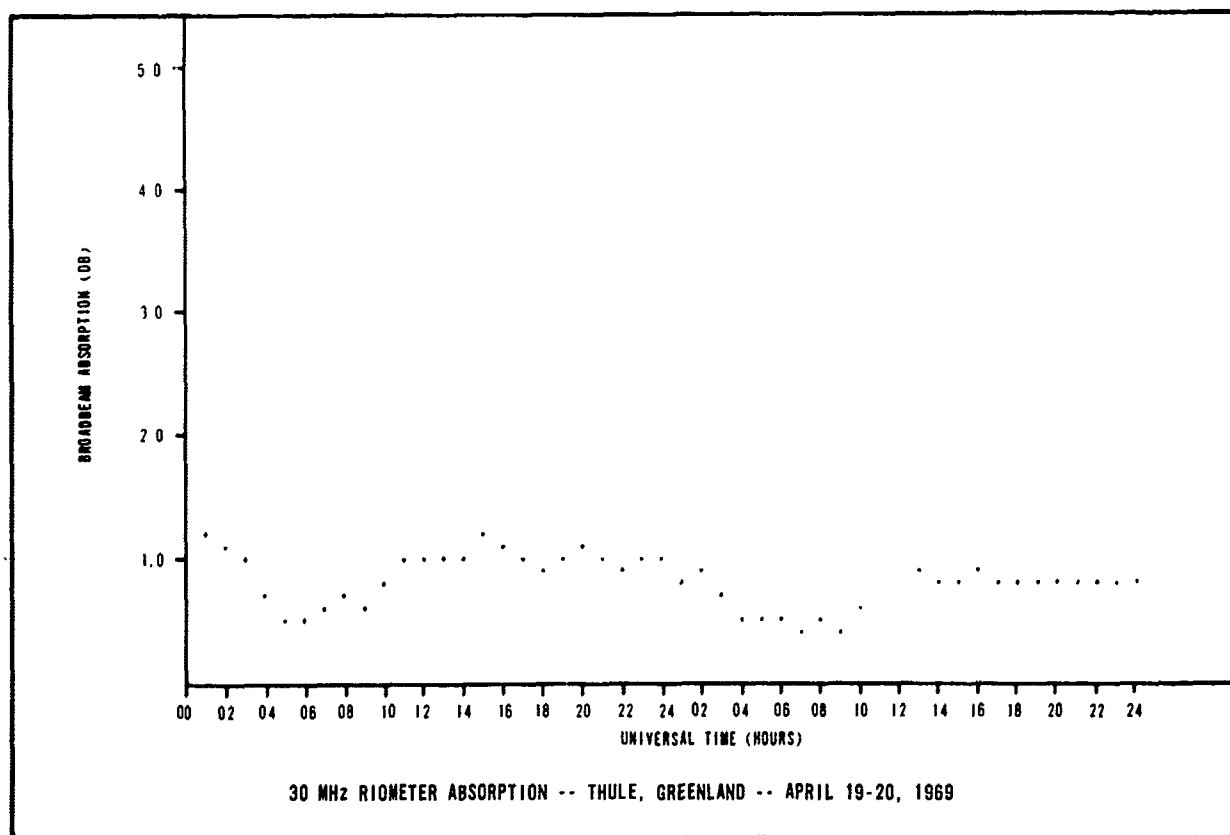
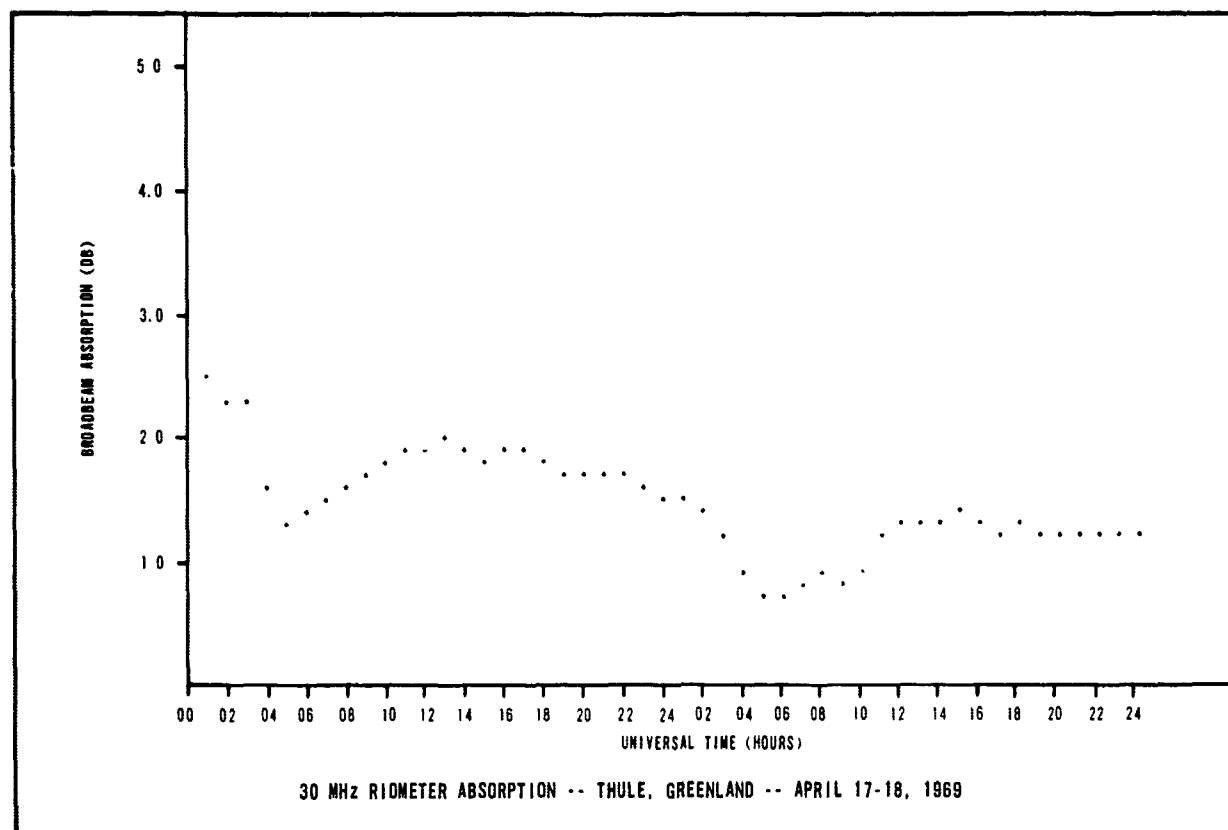


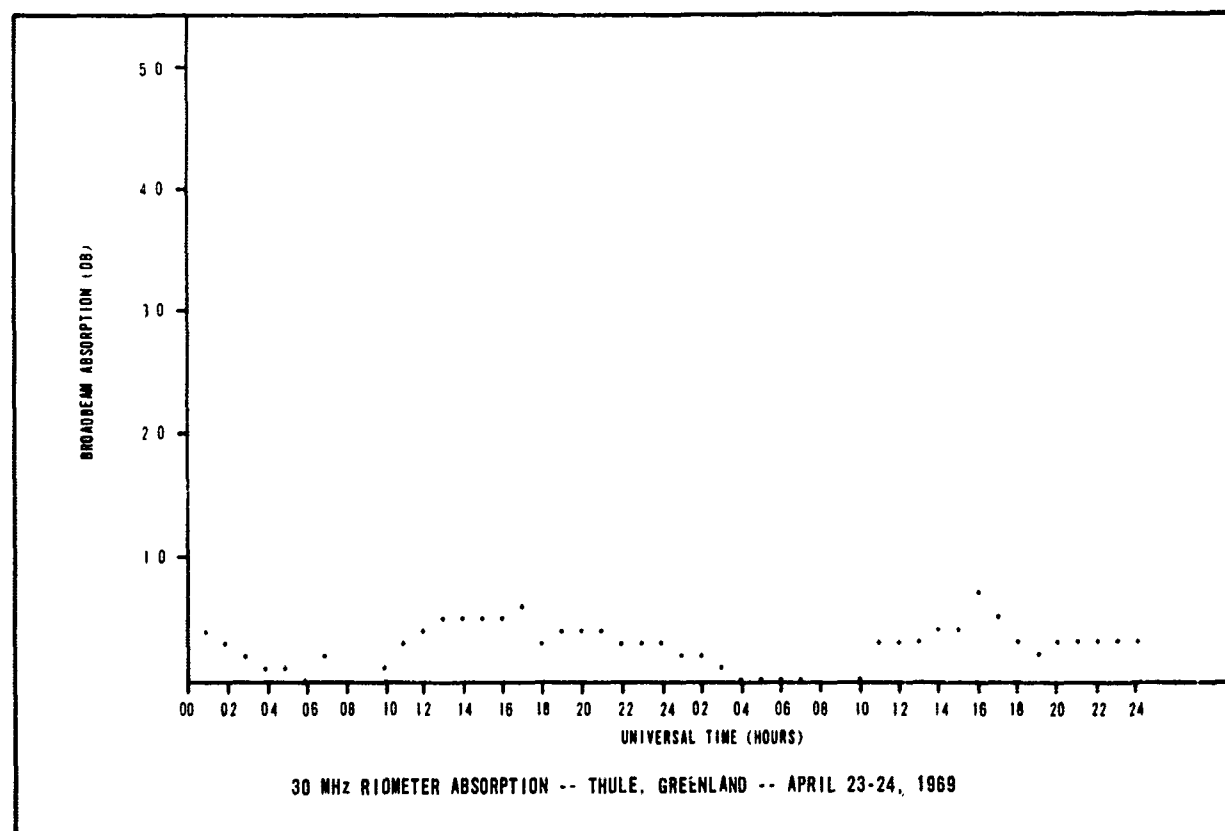
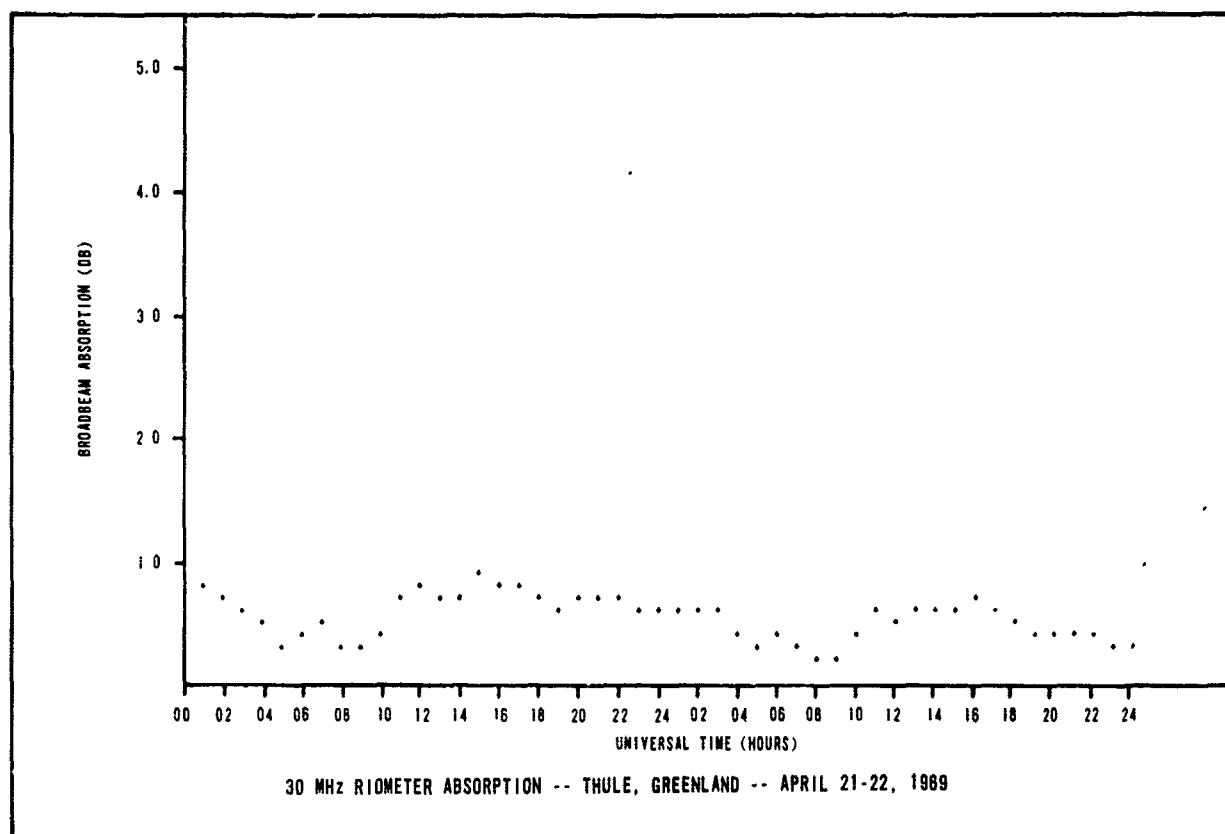


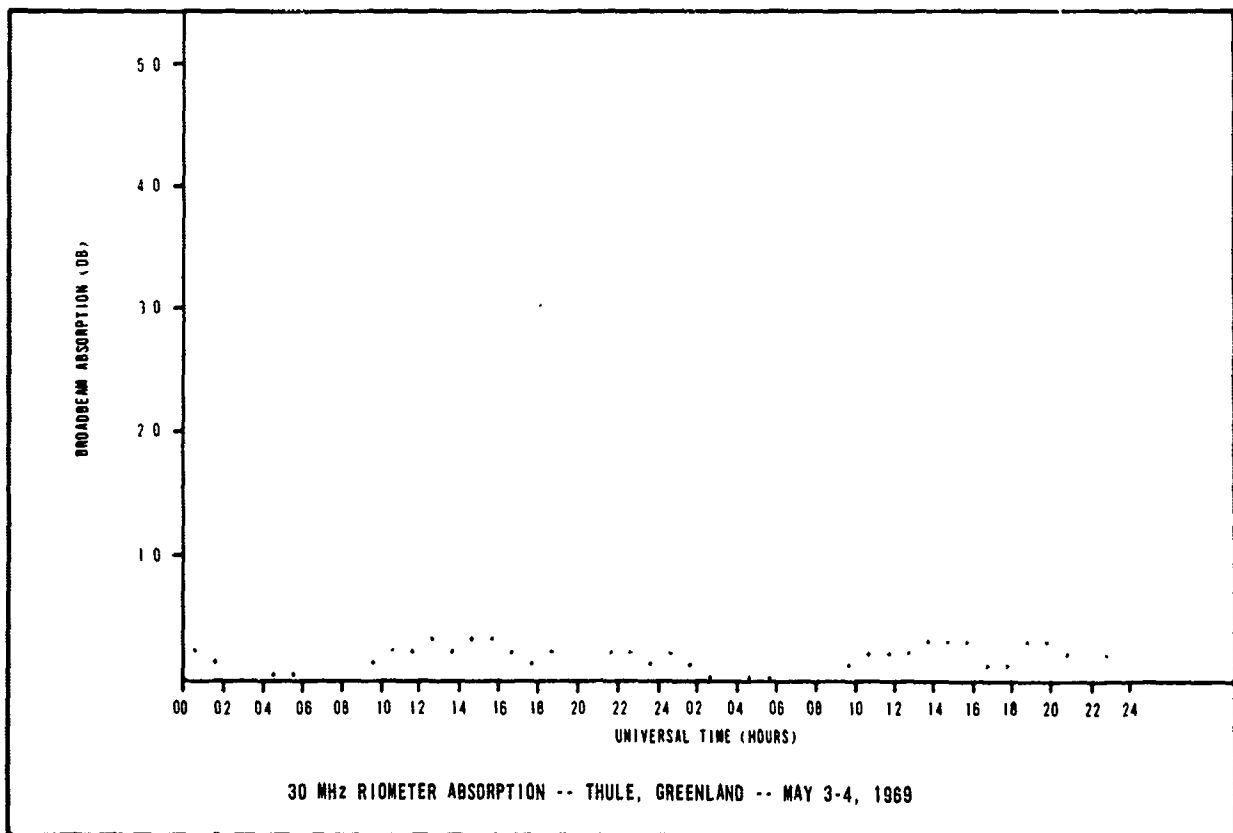
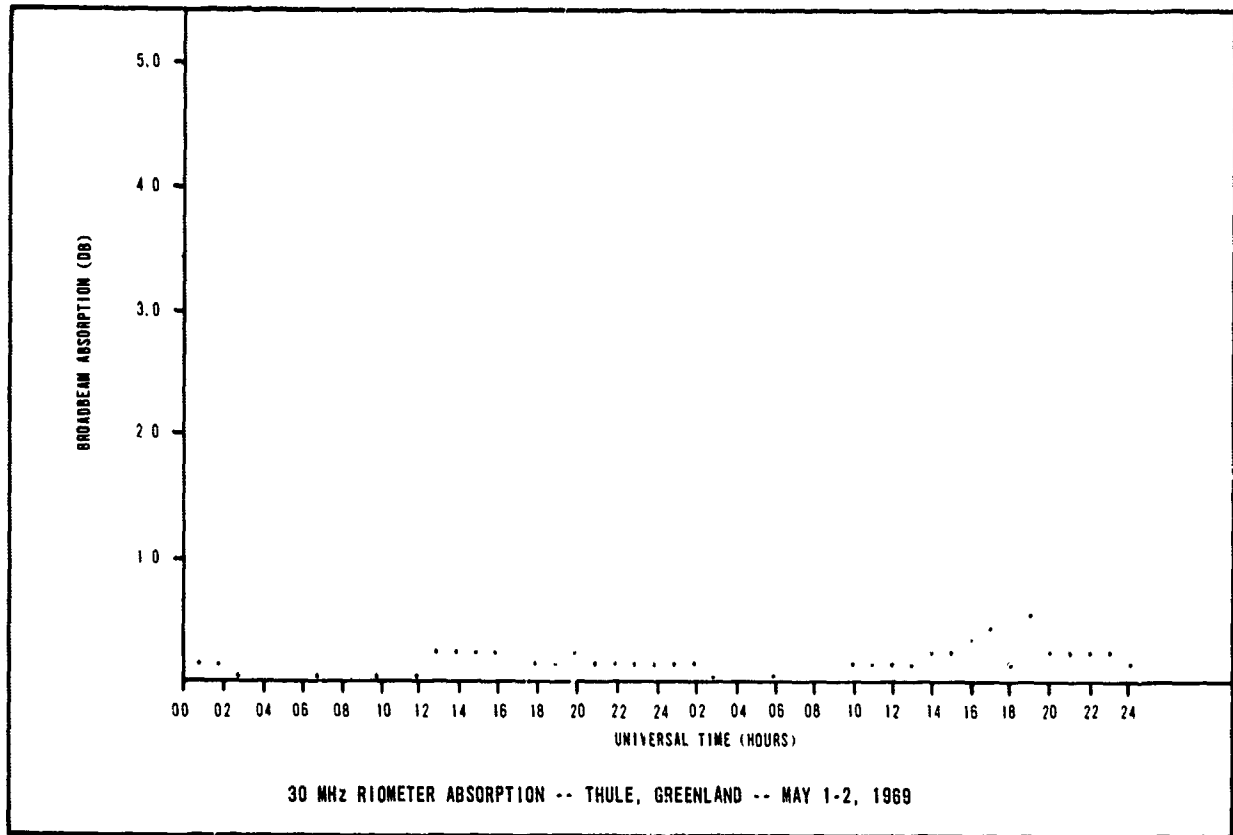


B-50

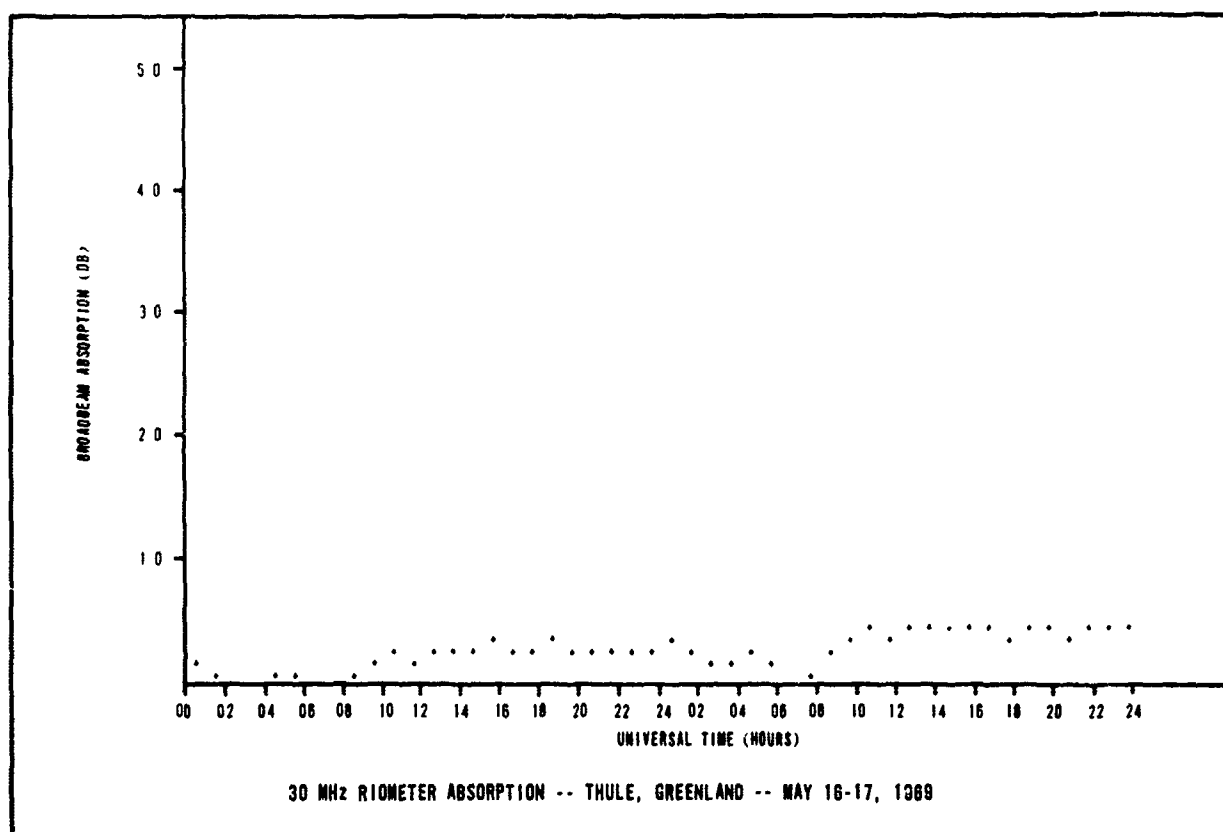
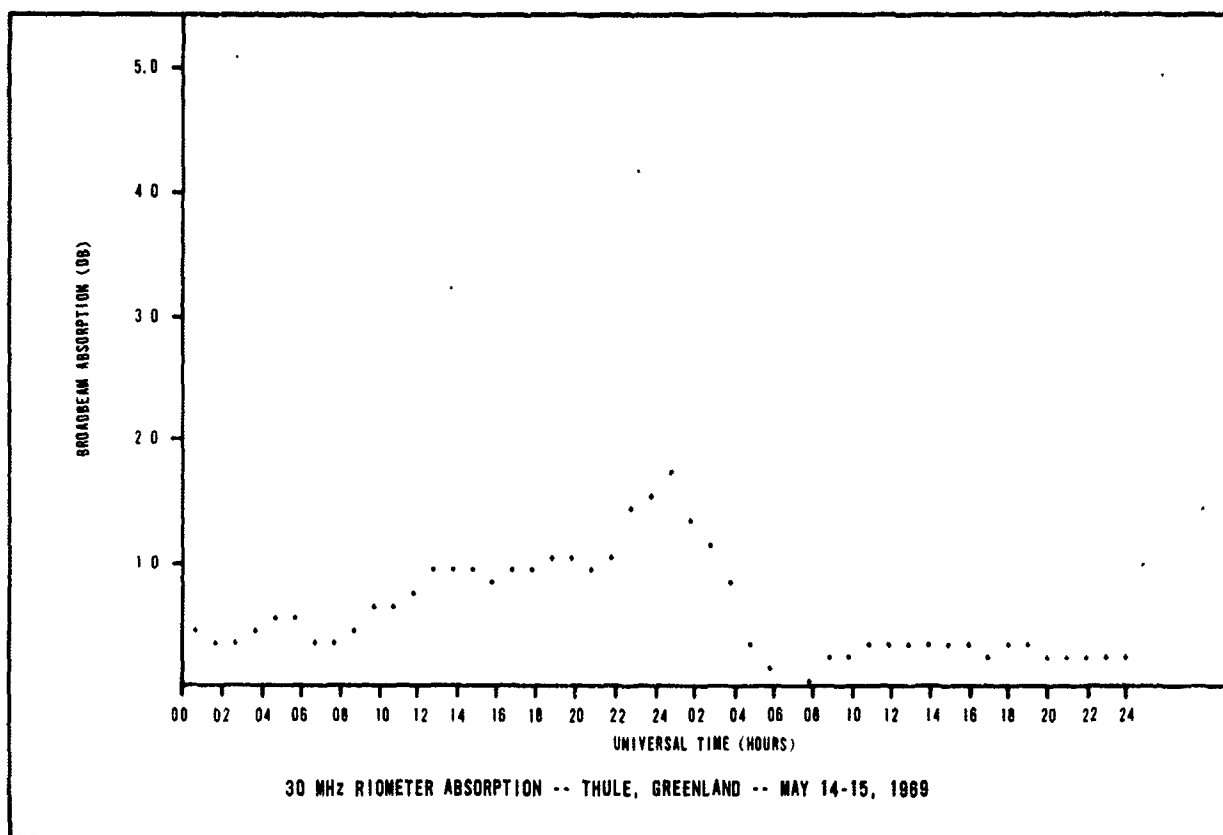


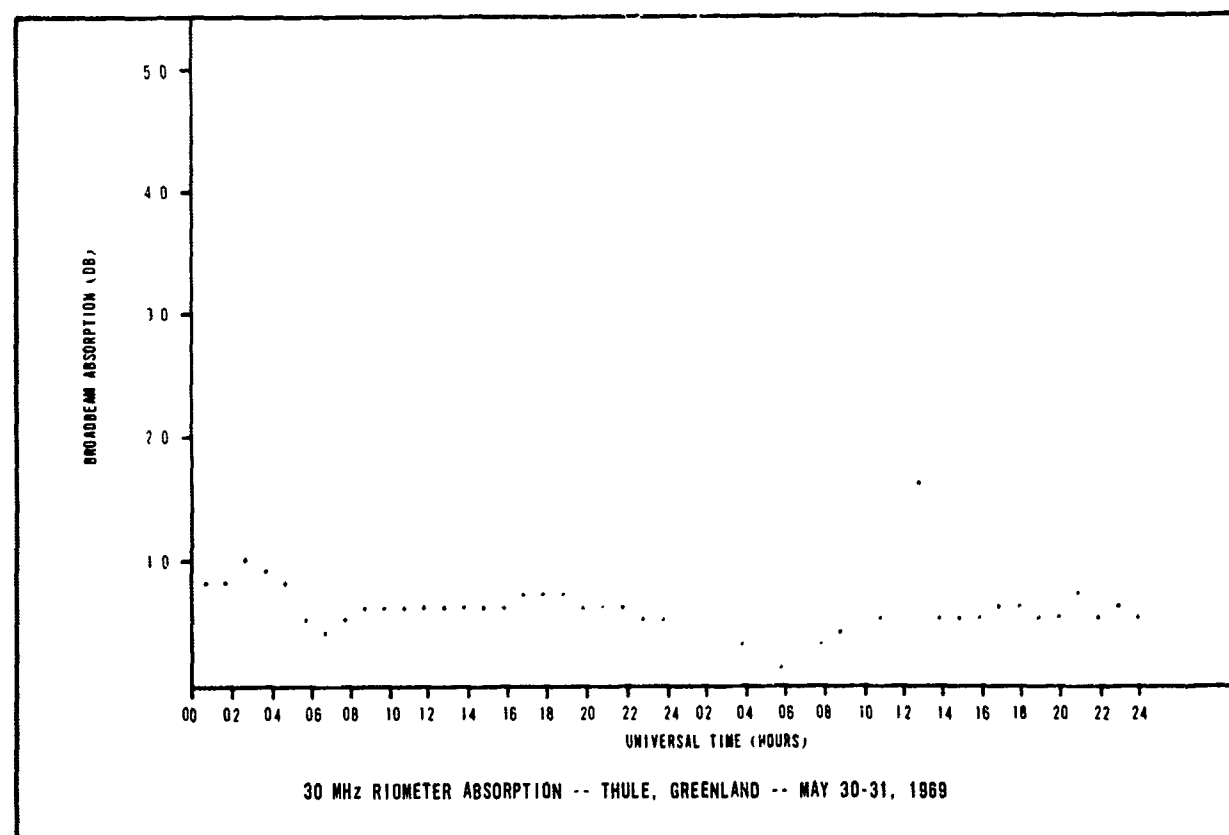
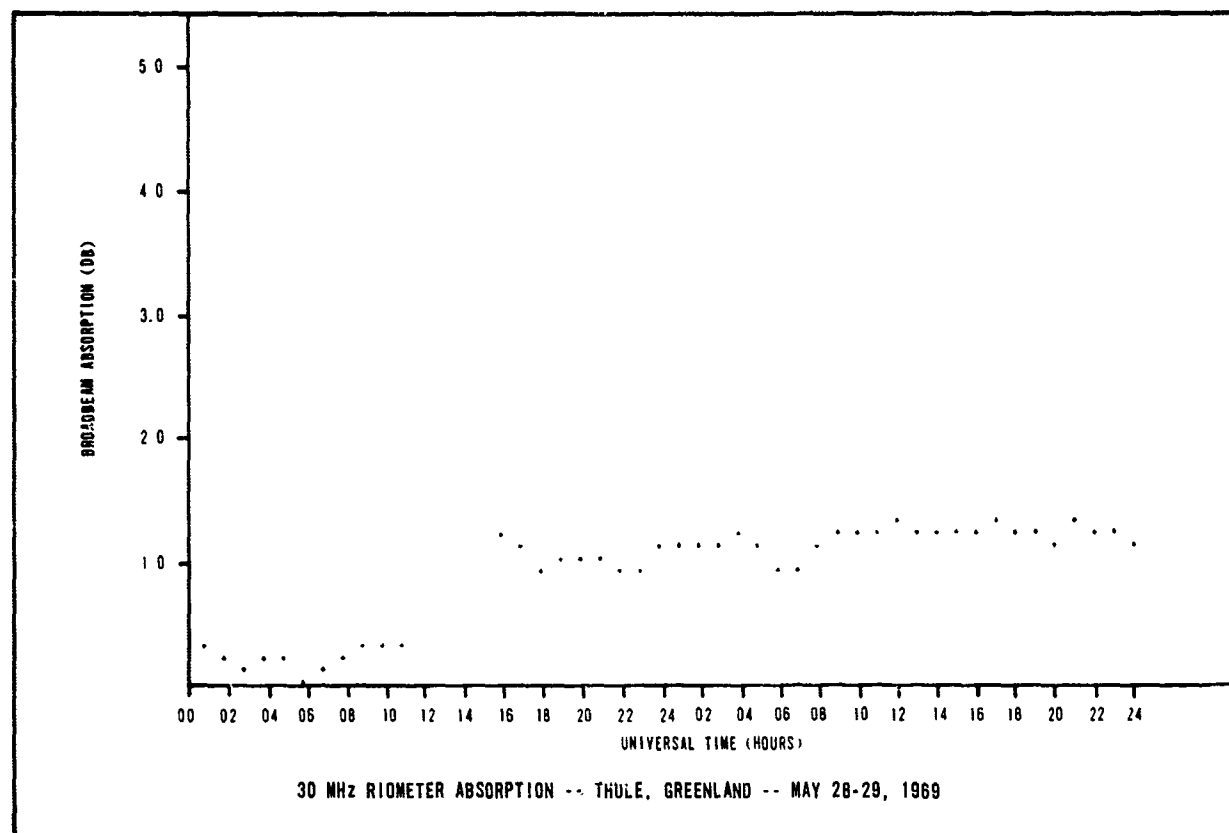


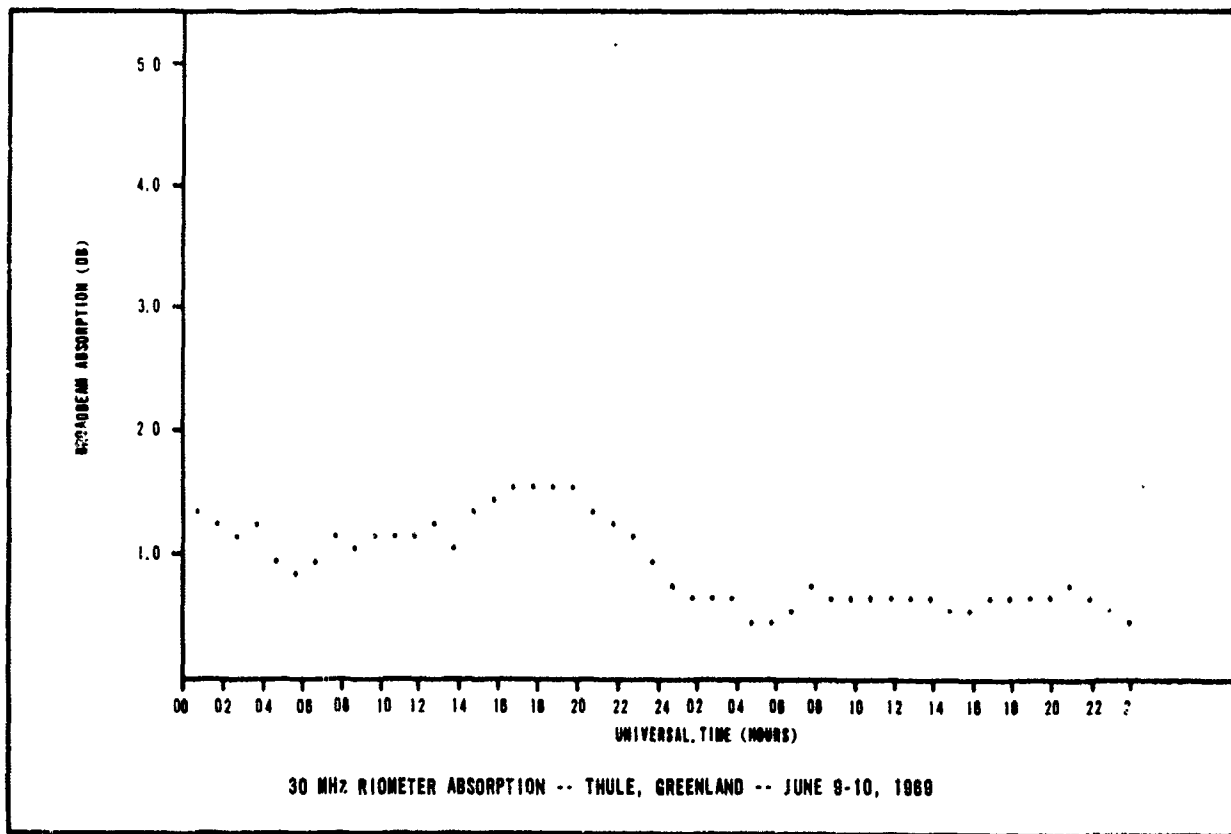
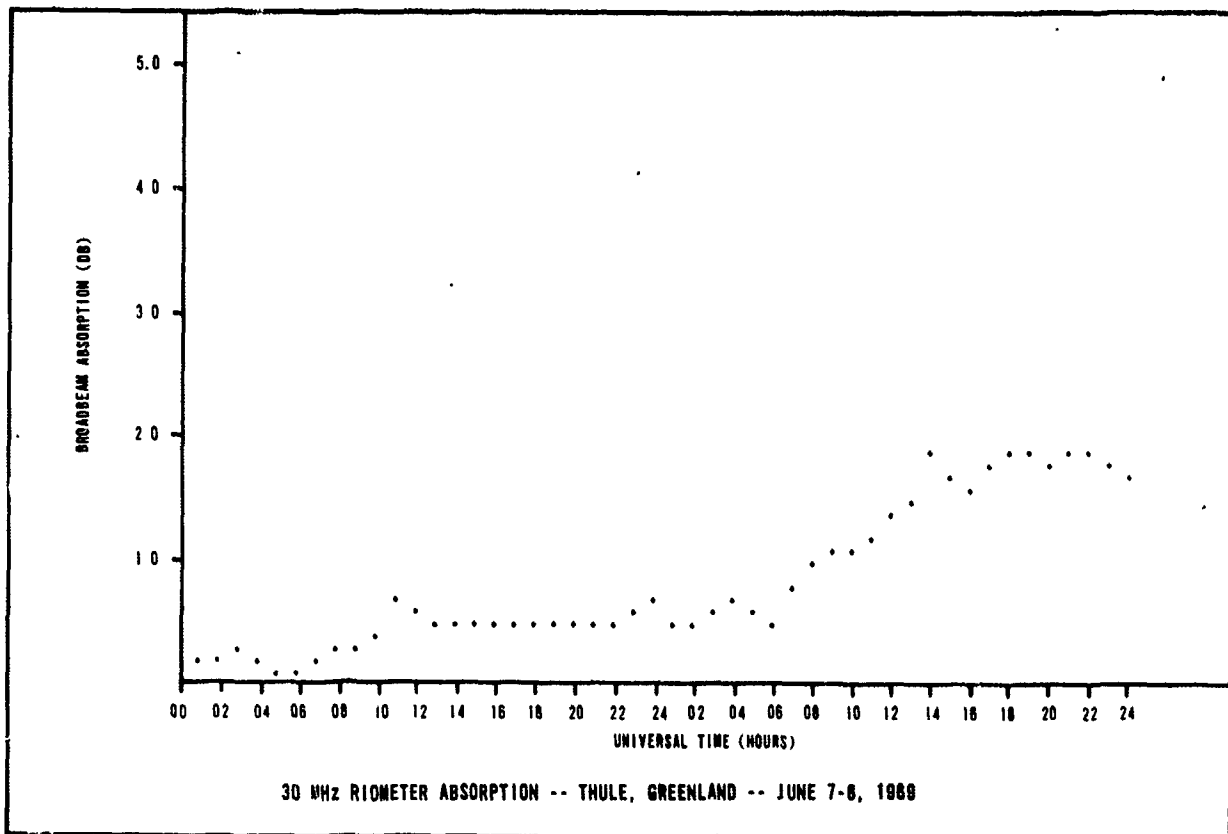


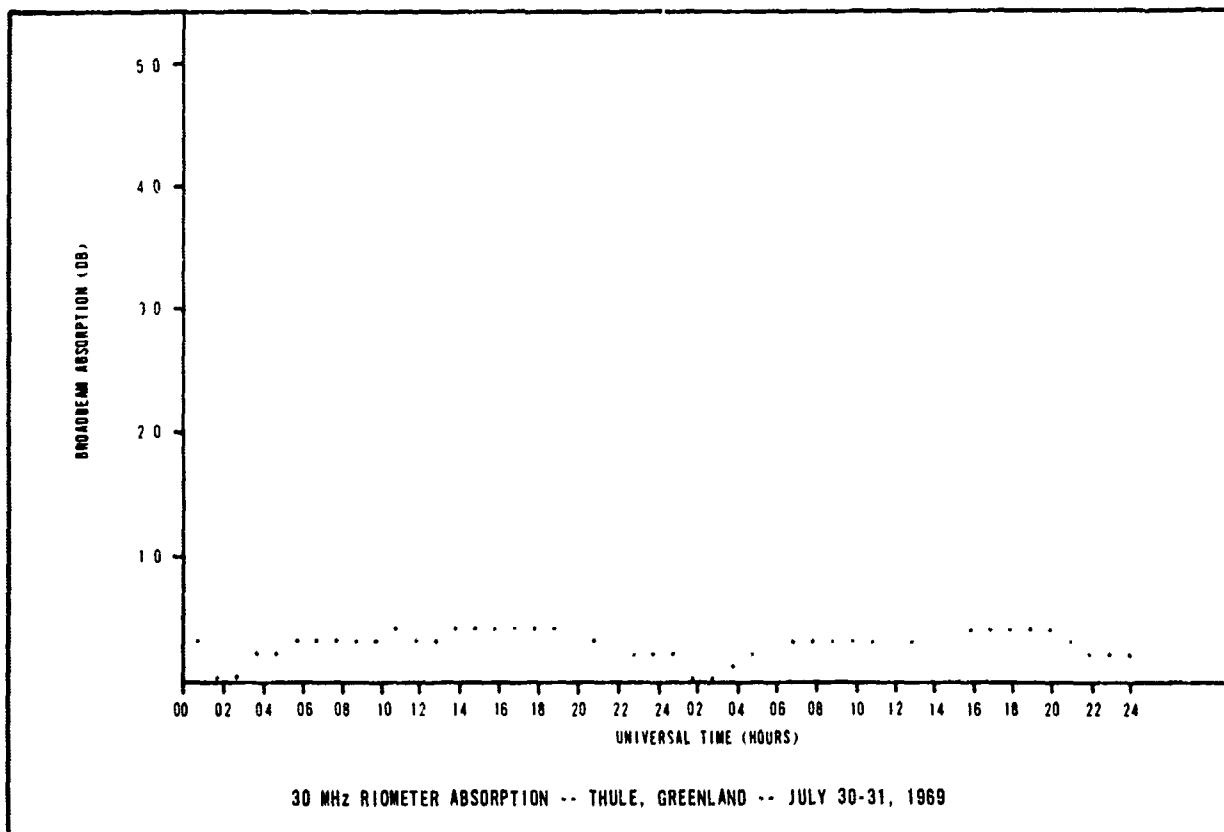
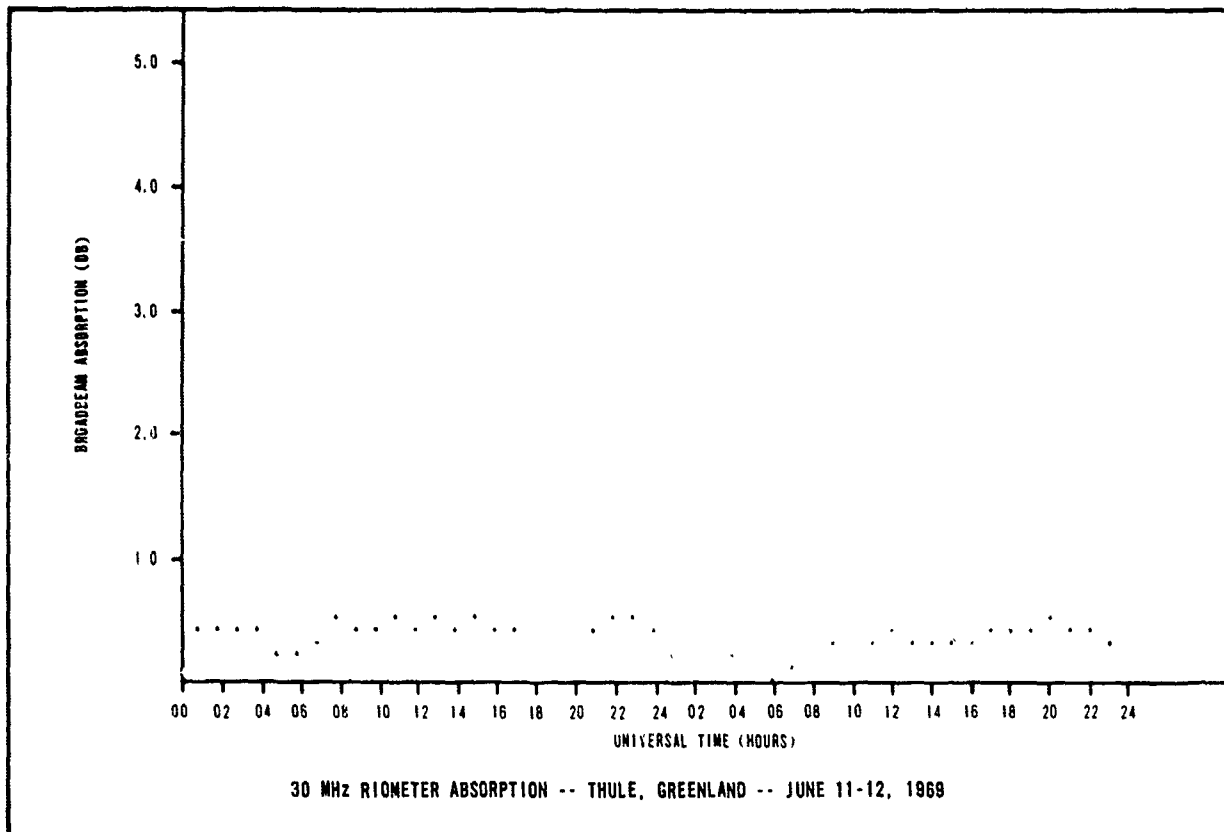


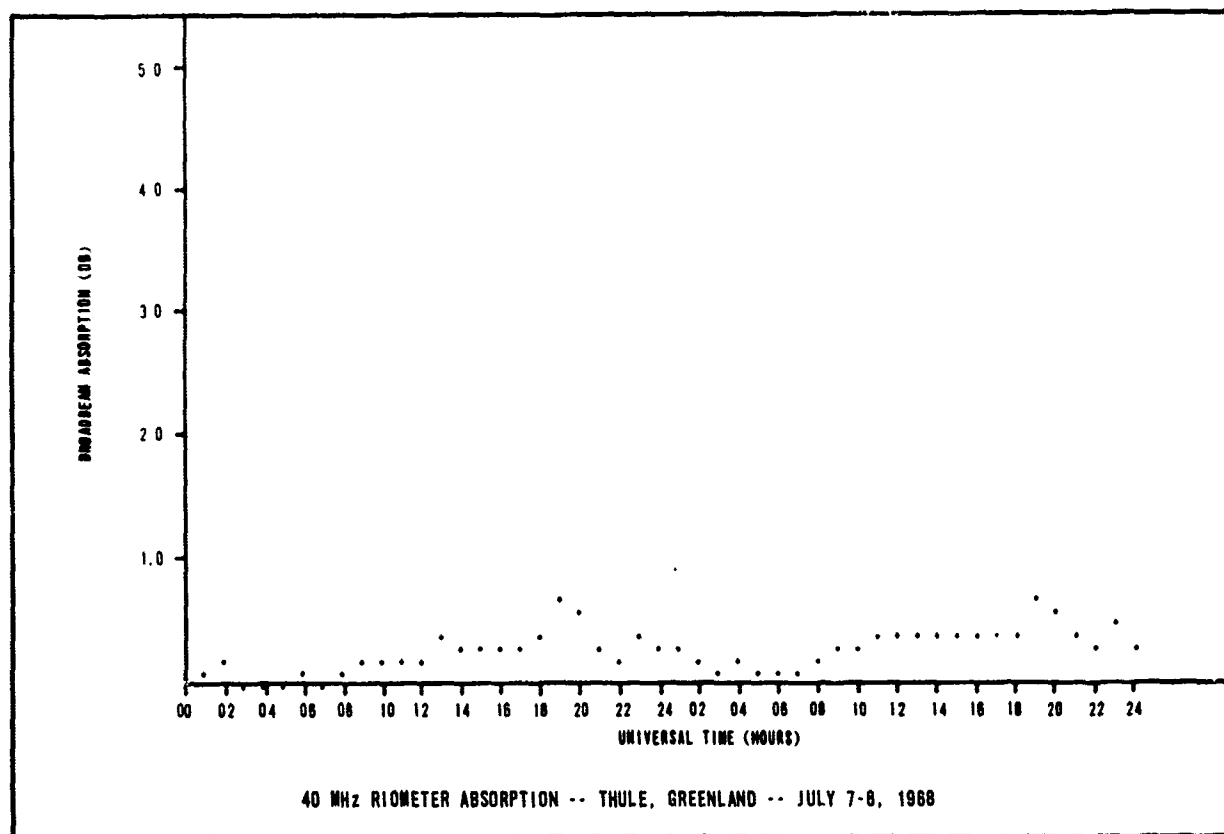
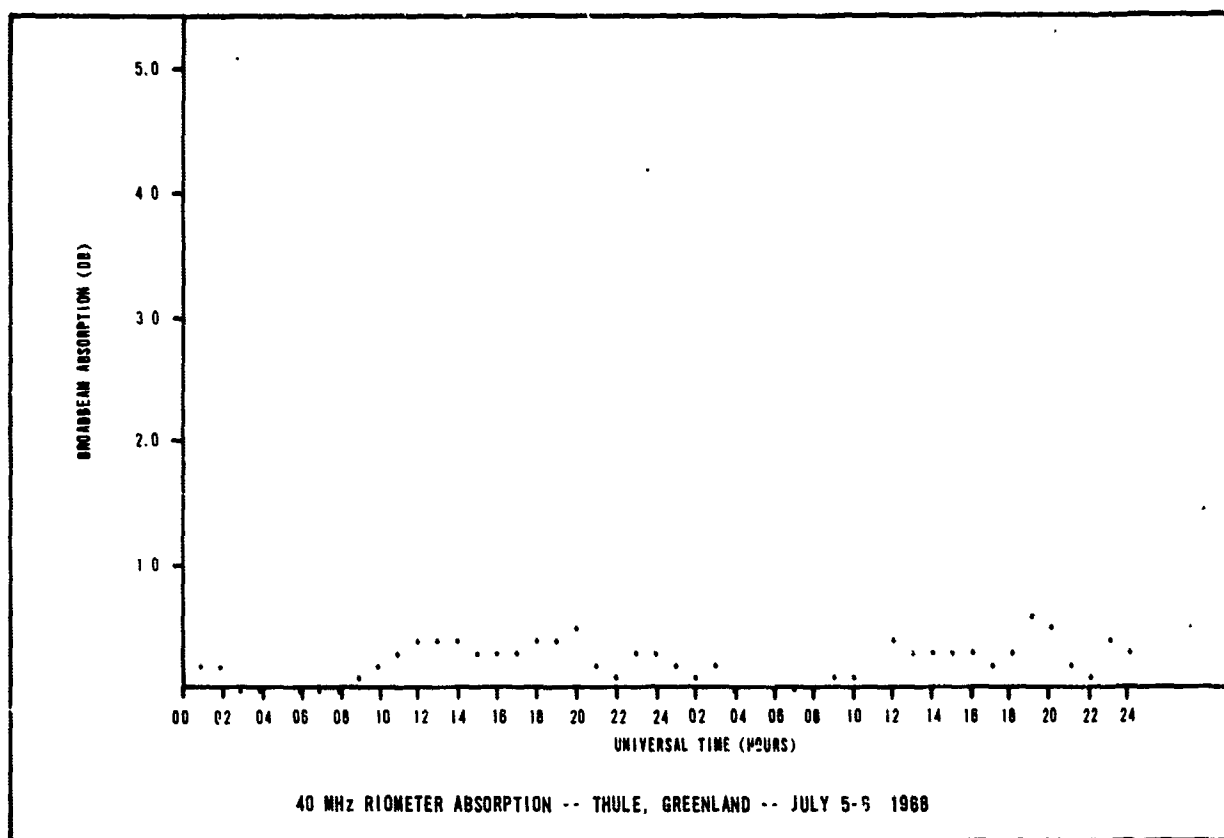


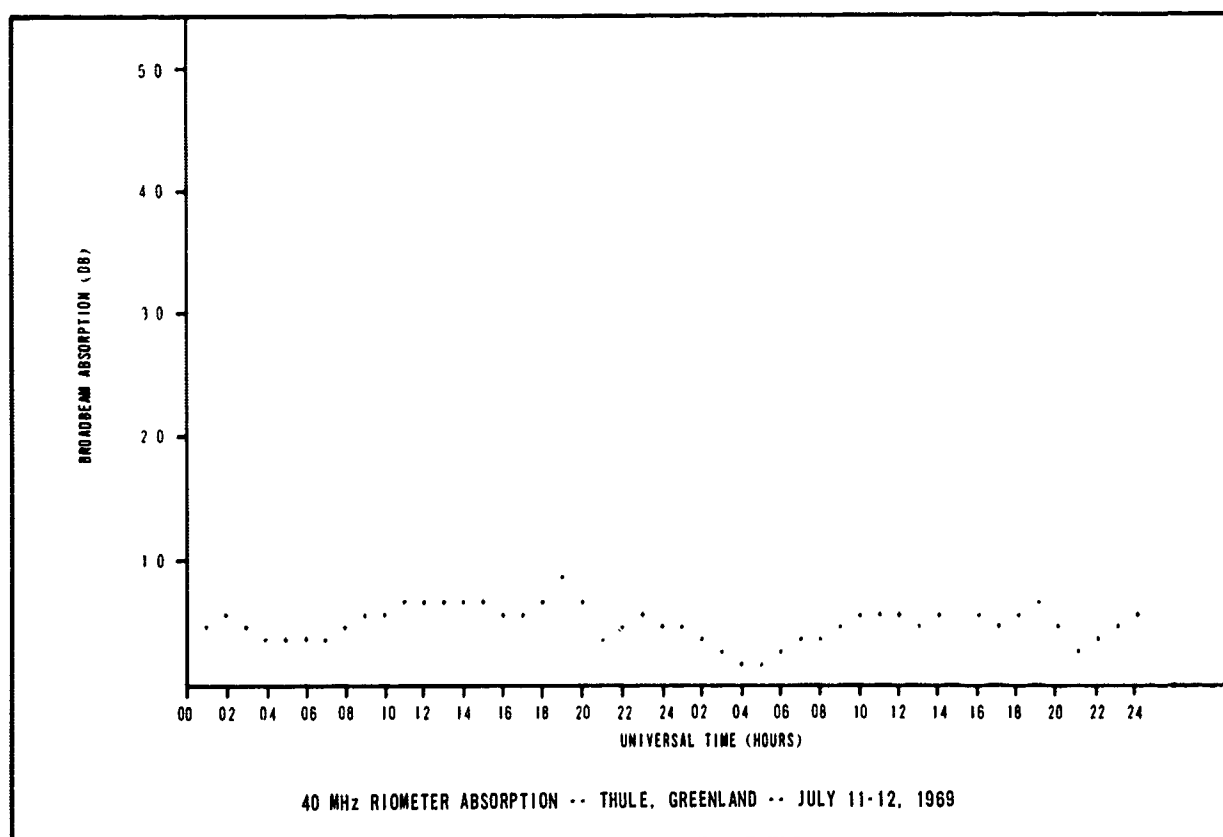
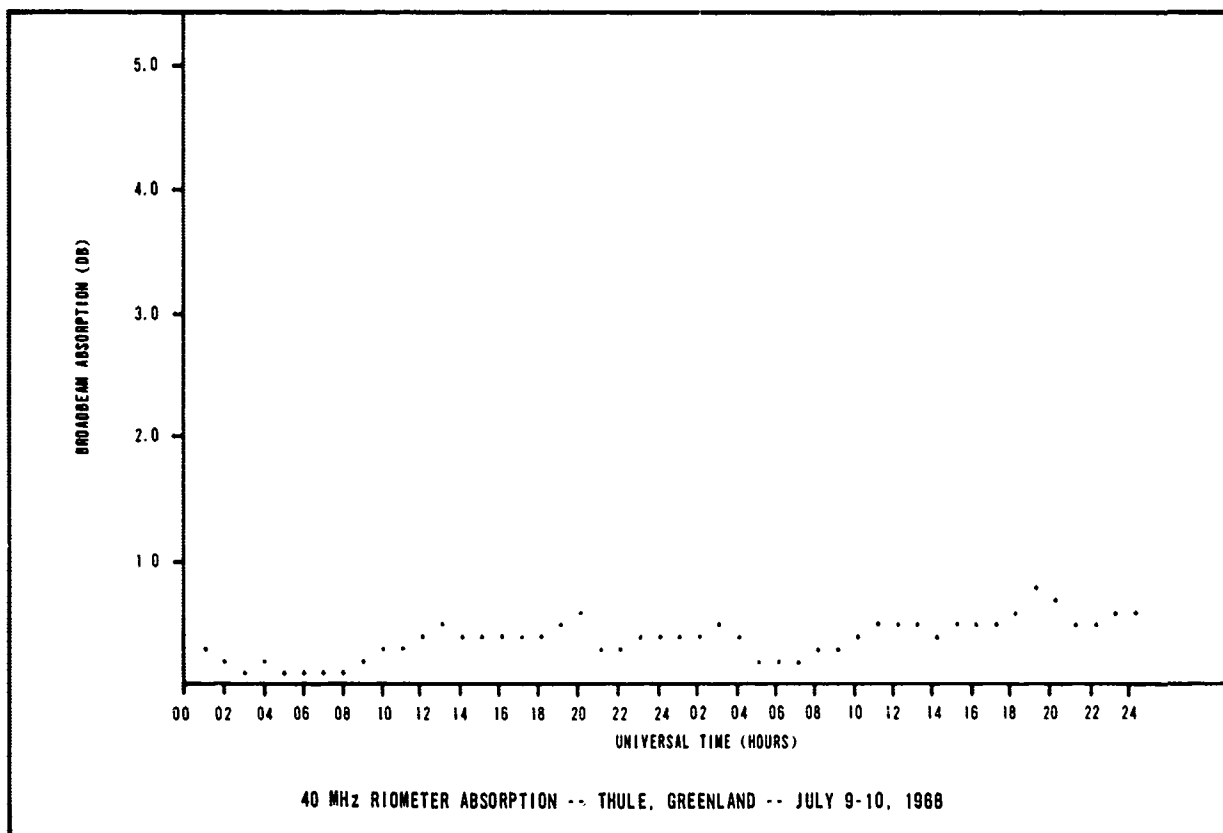




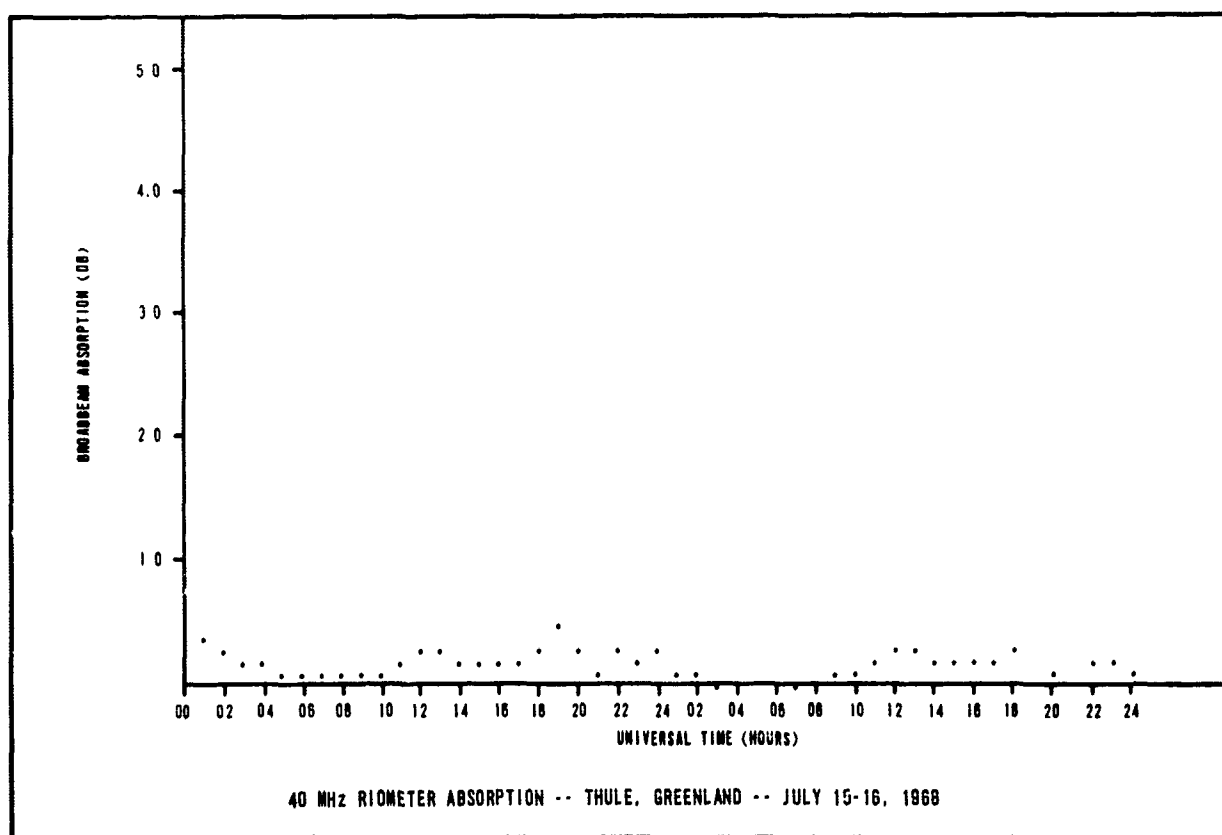
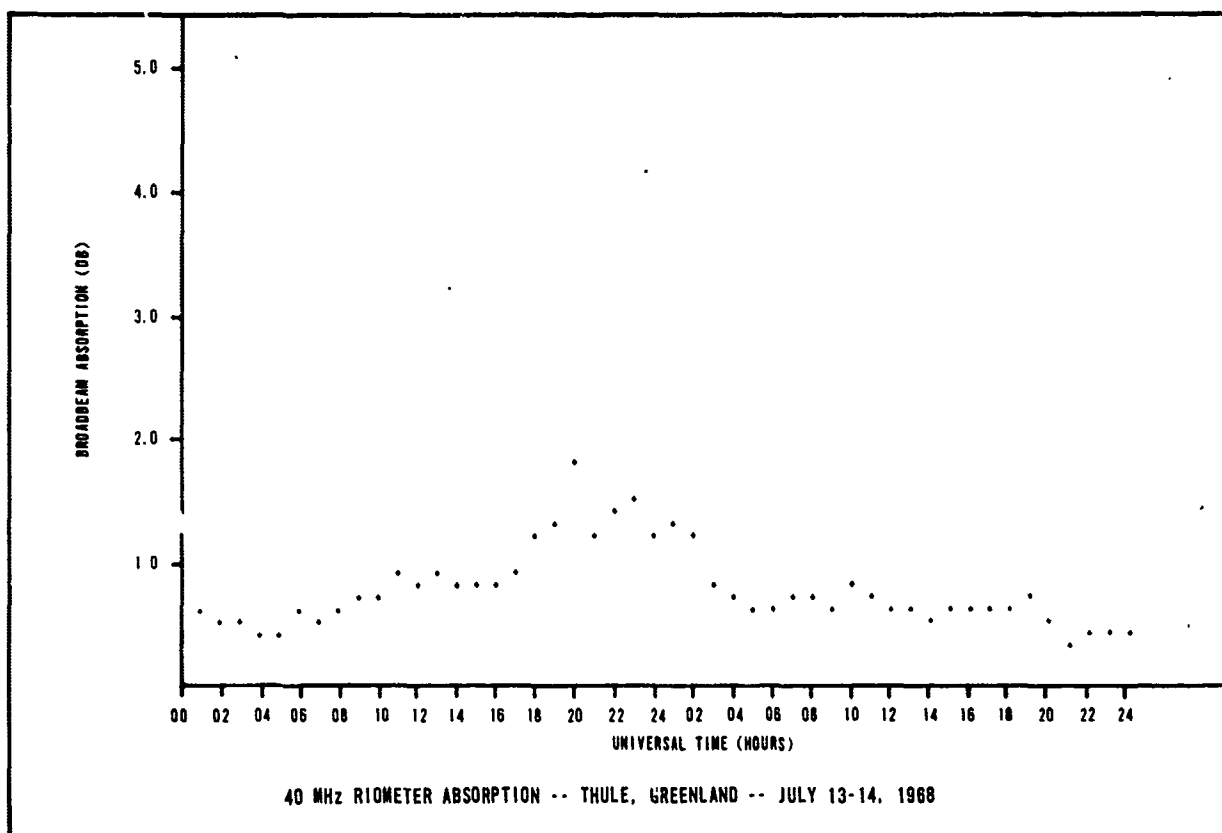


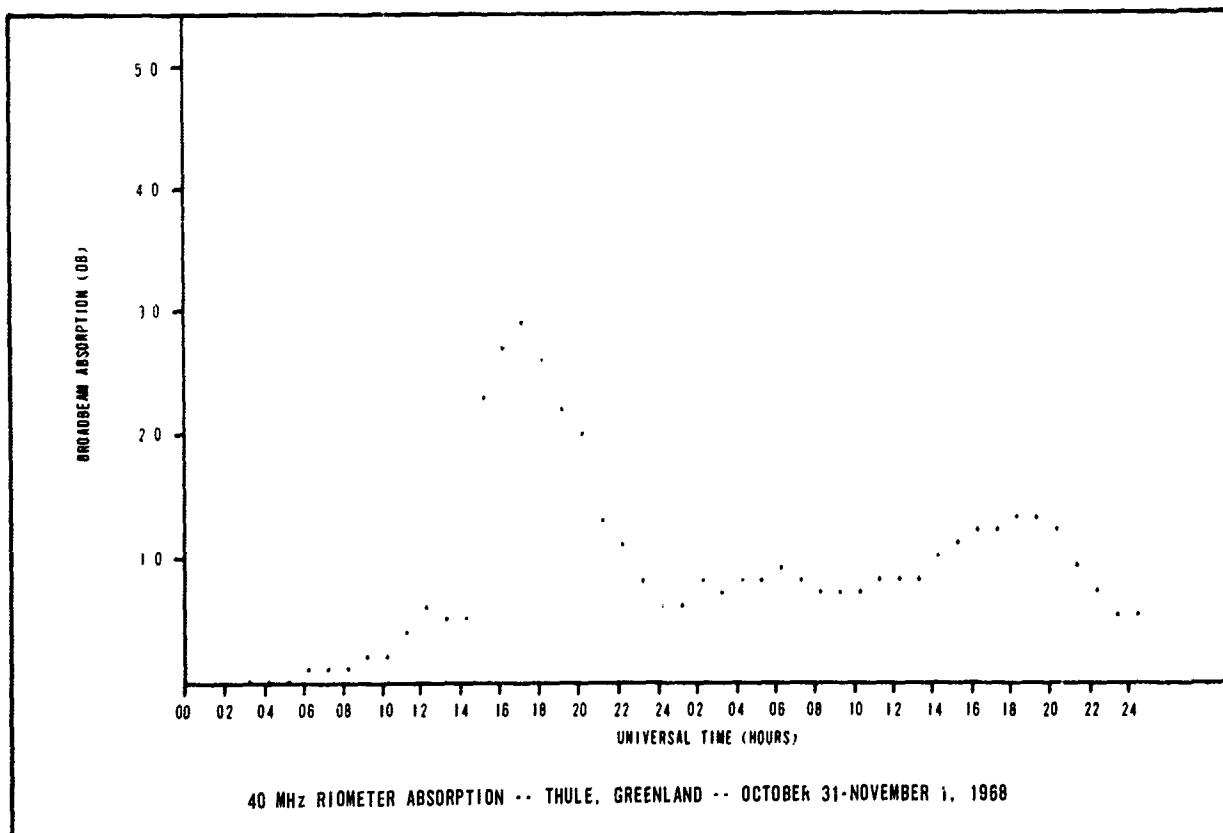
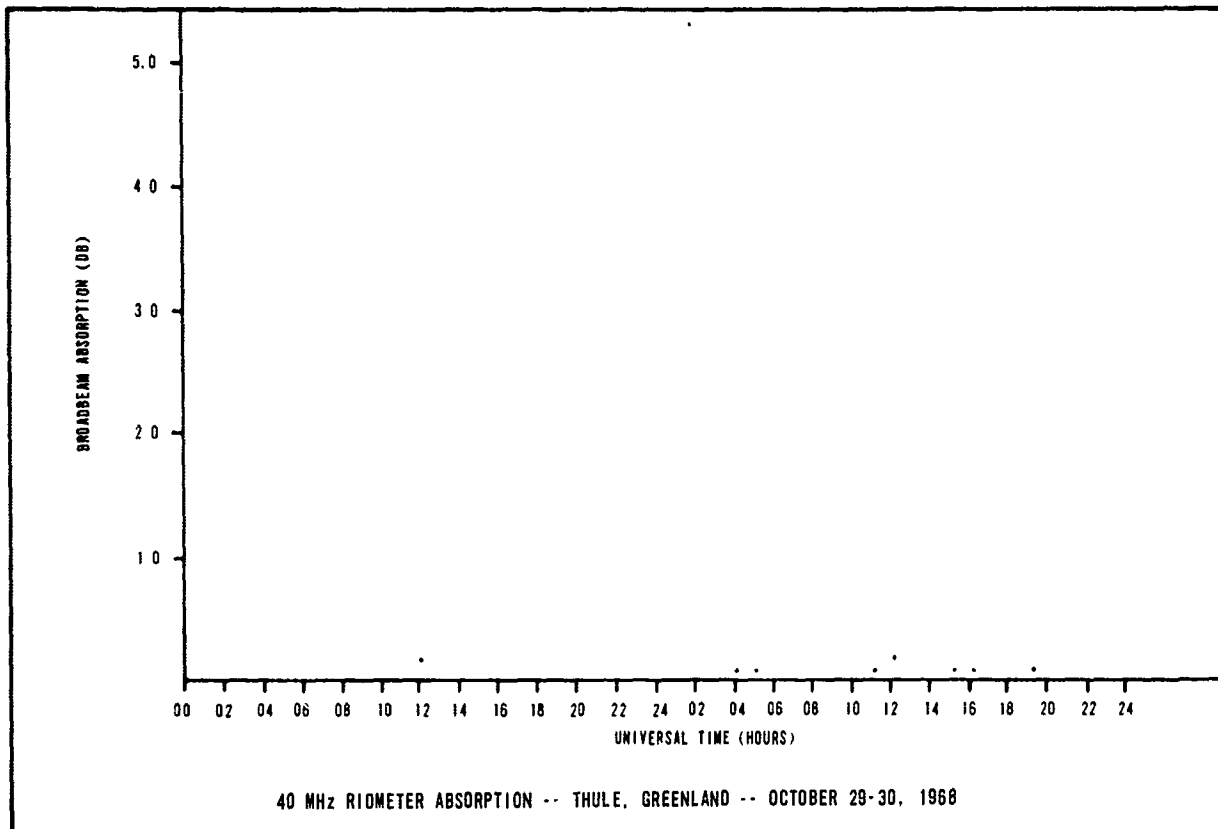




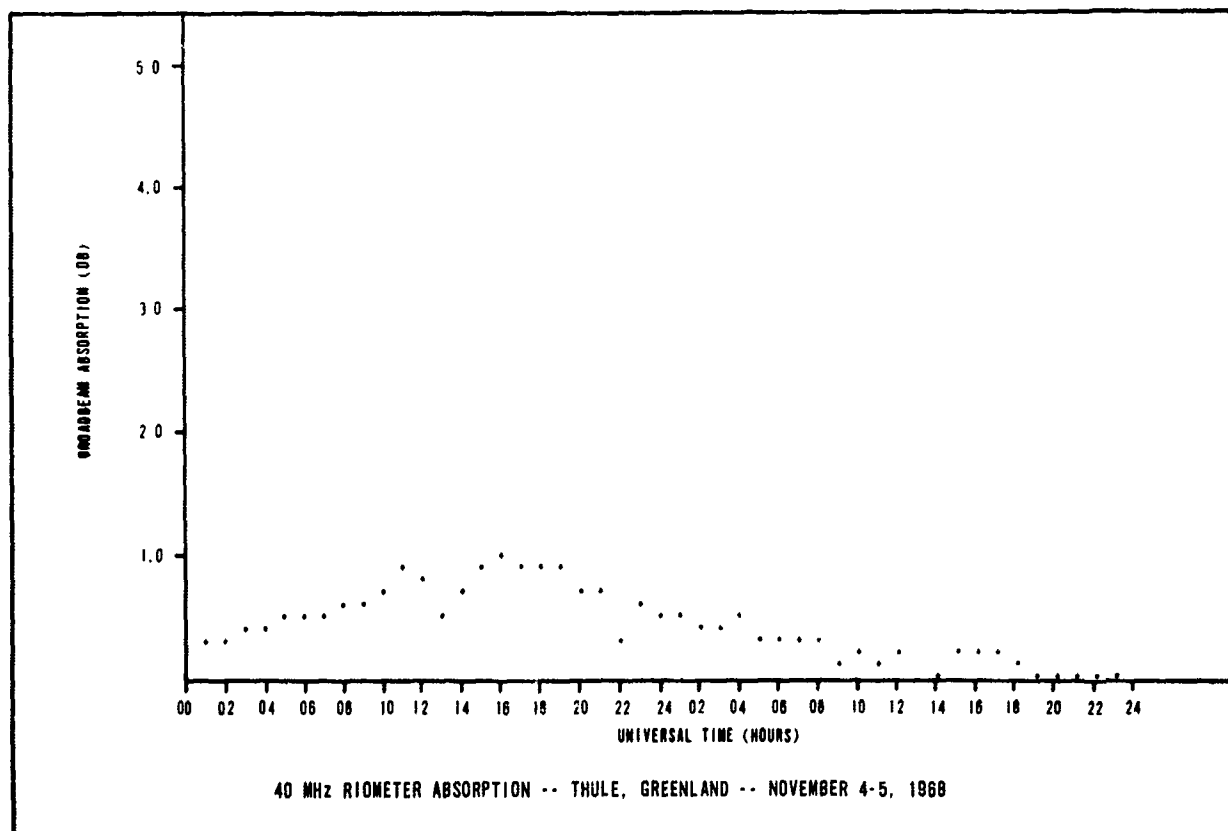
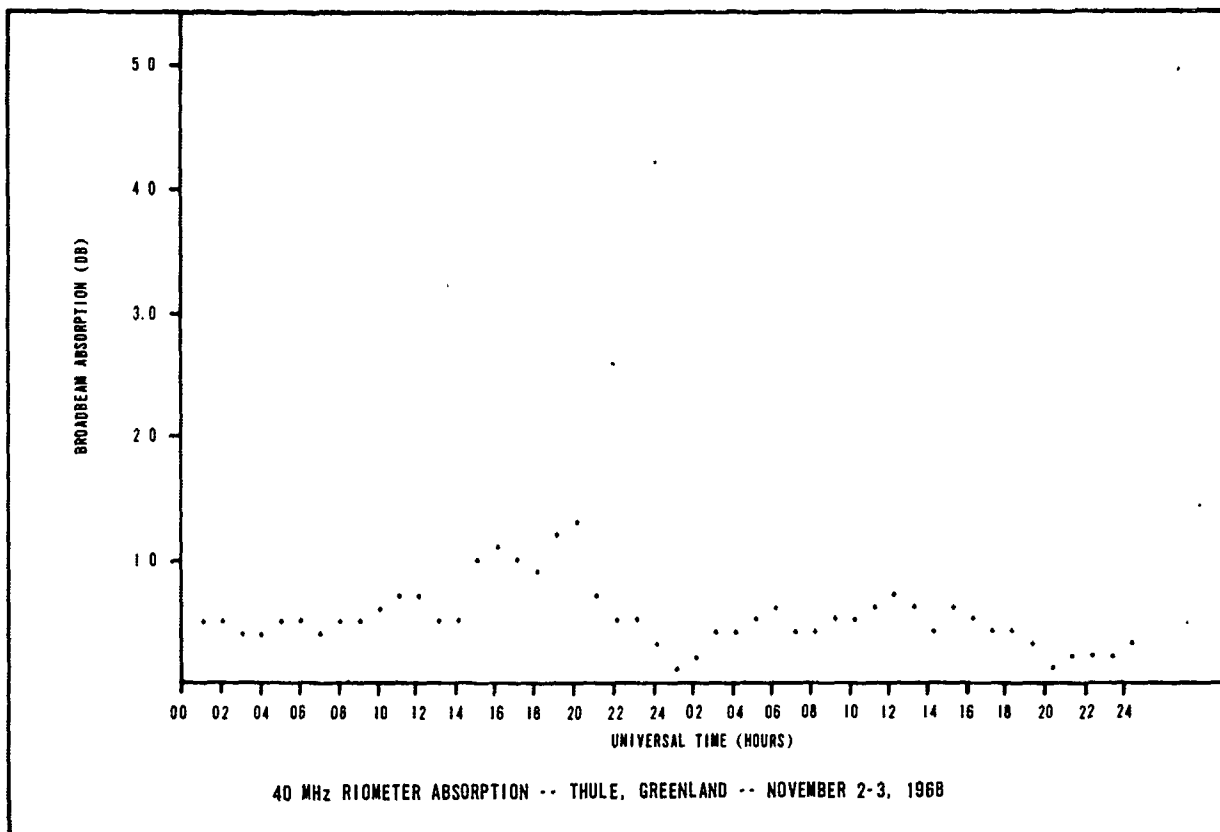


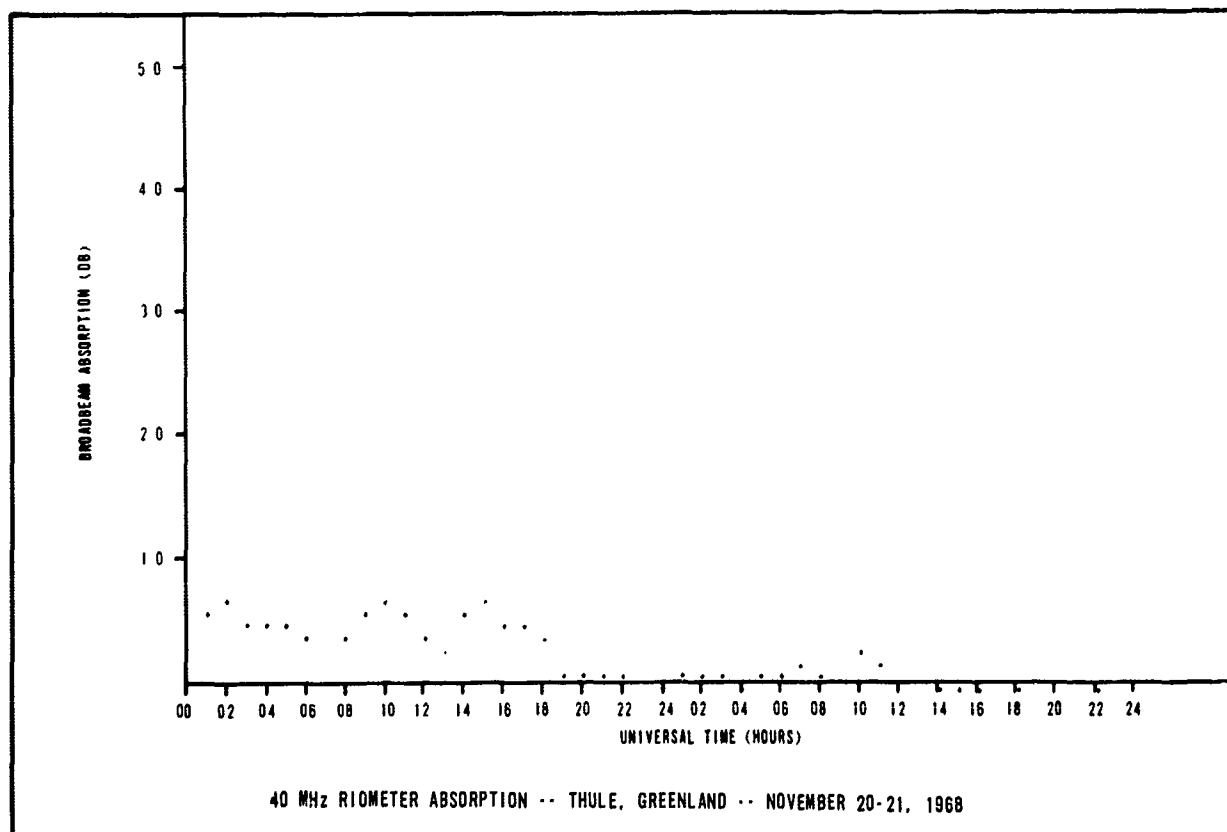
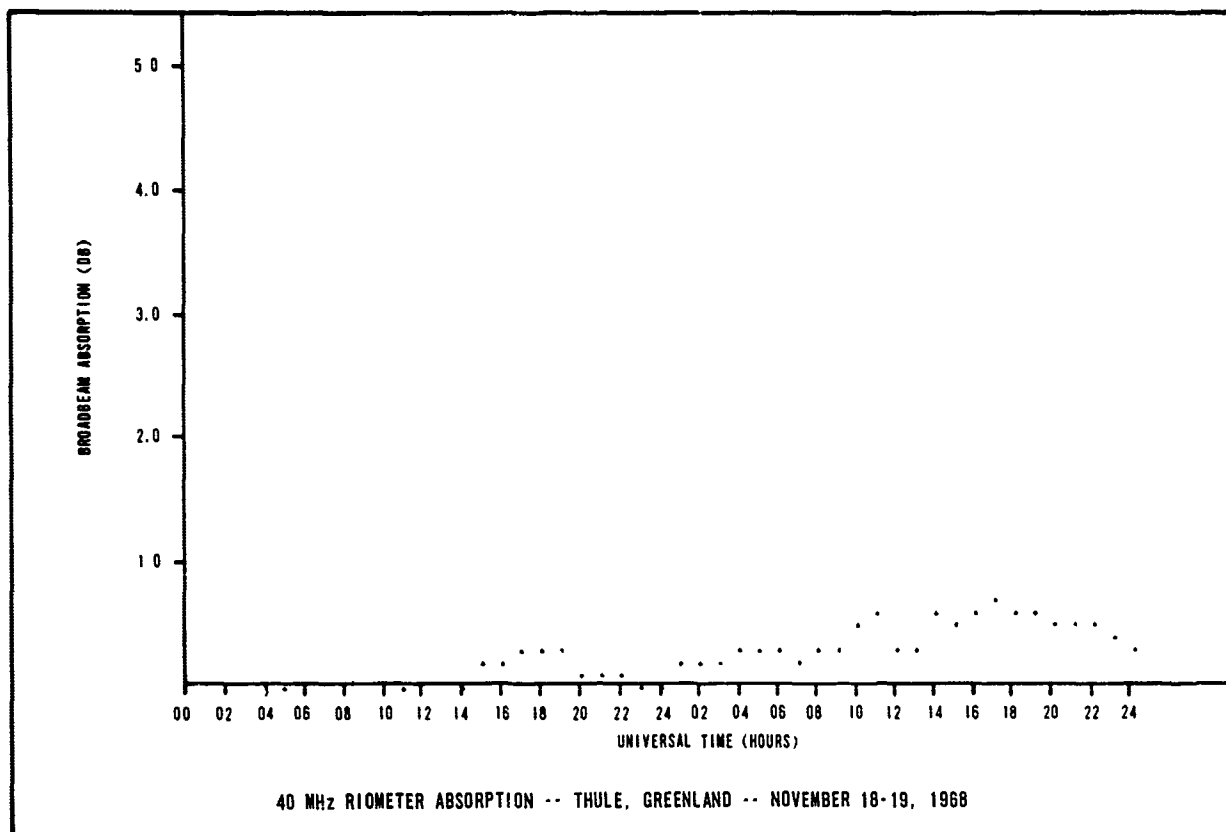
B-60

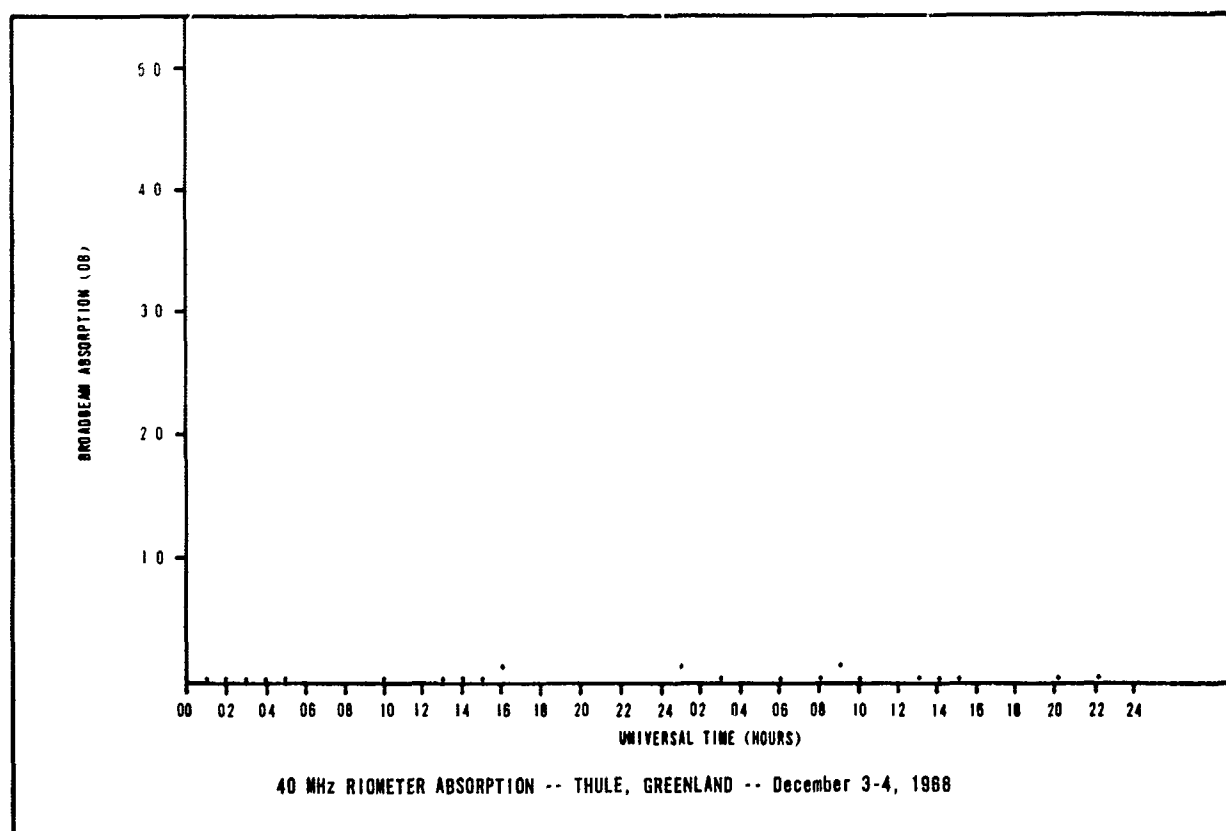
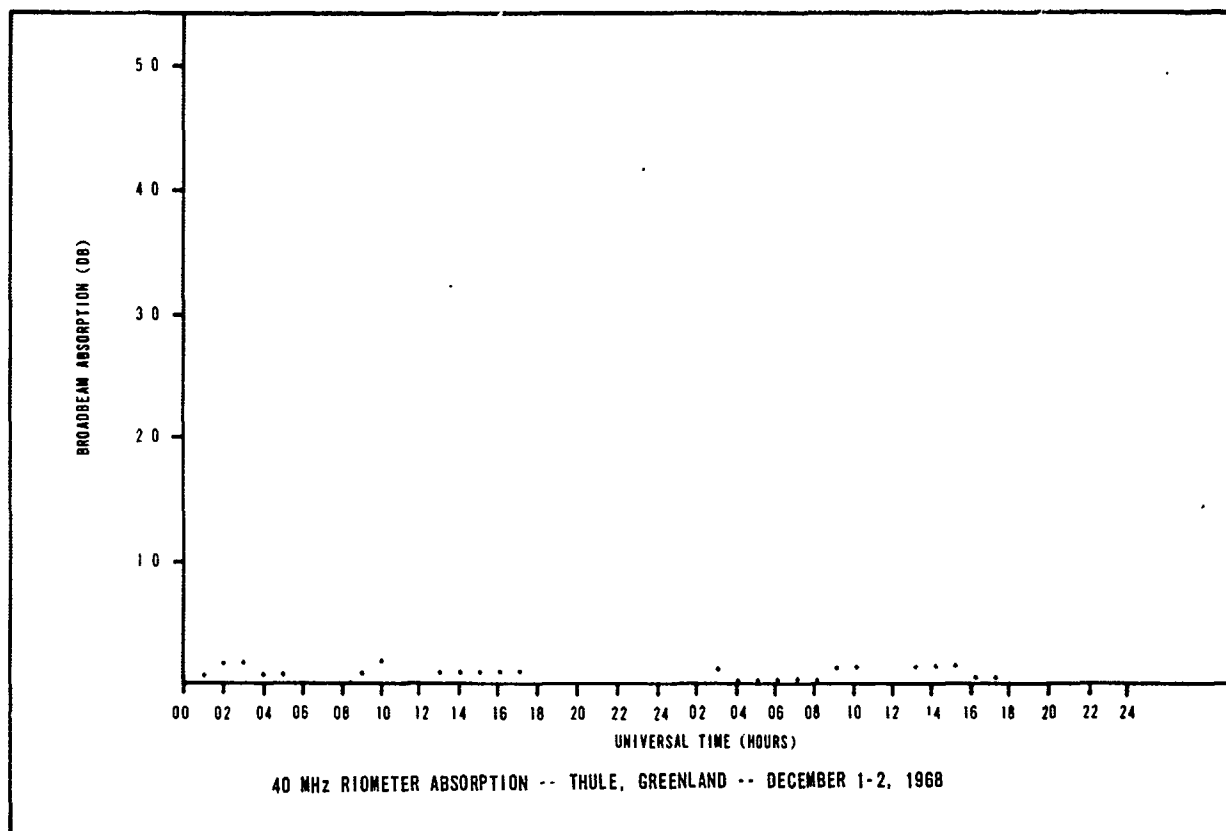


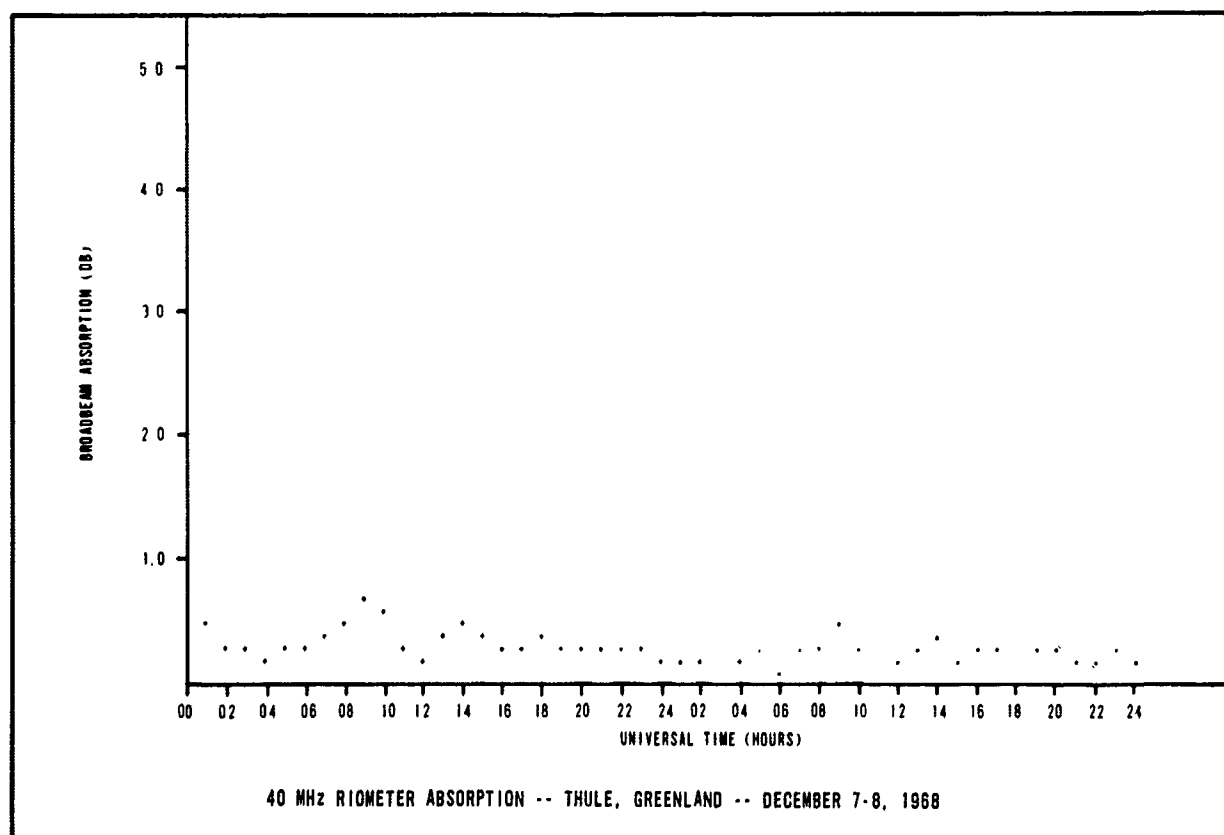
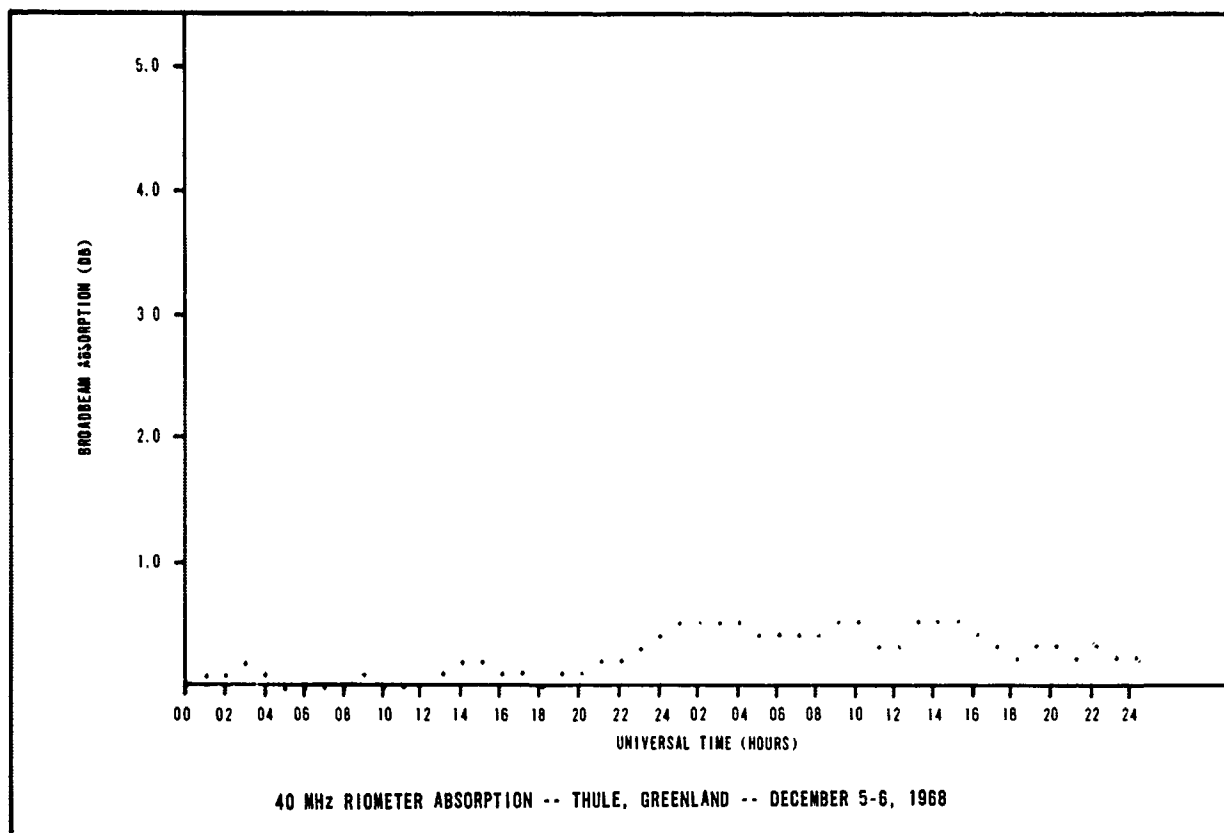


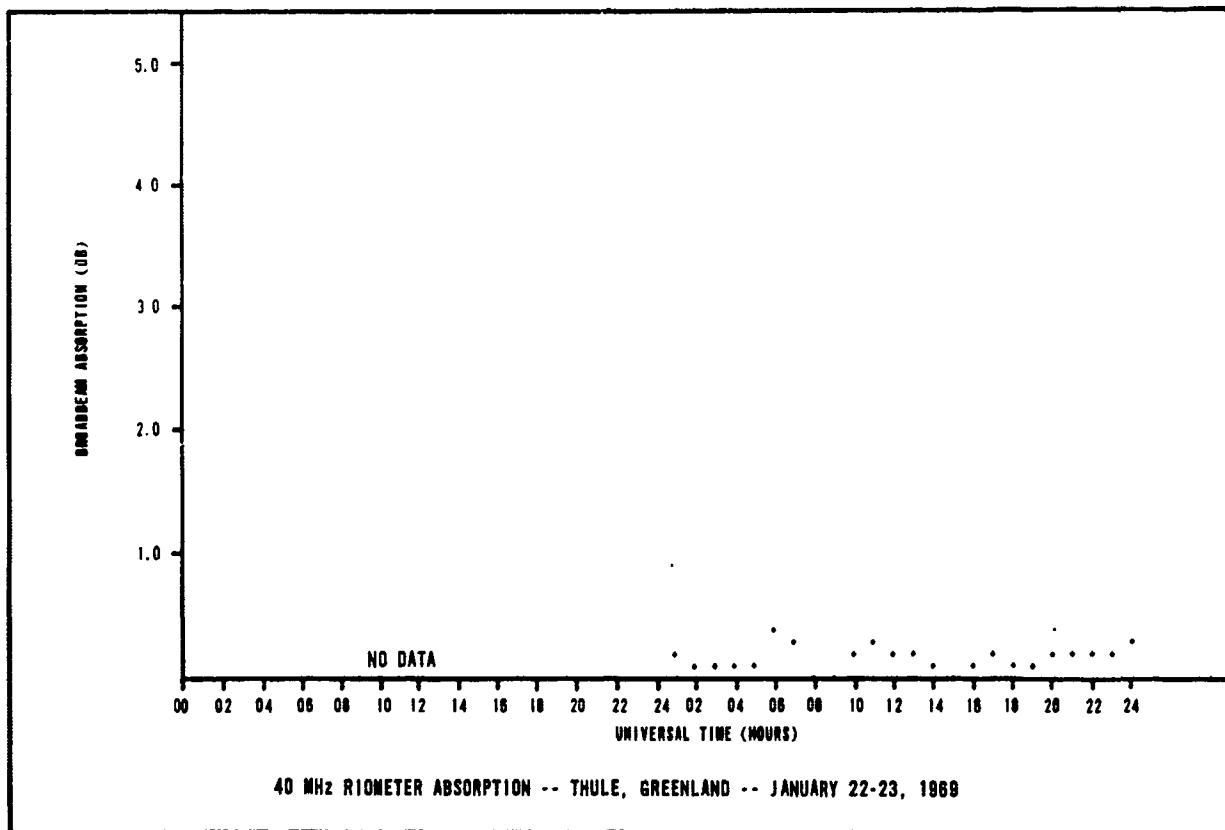
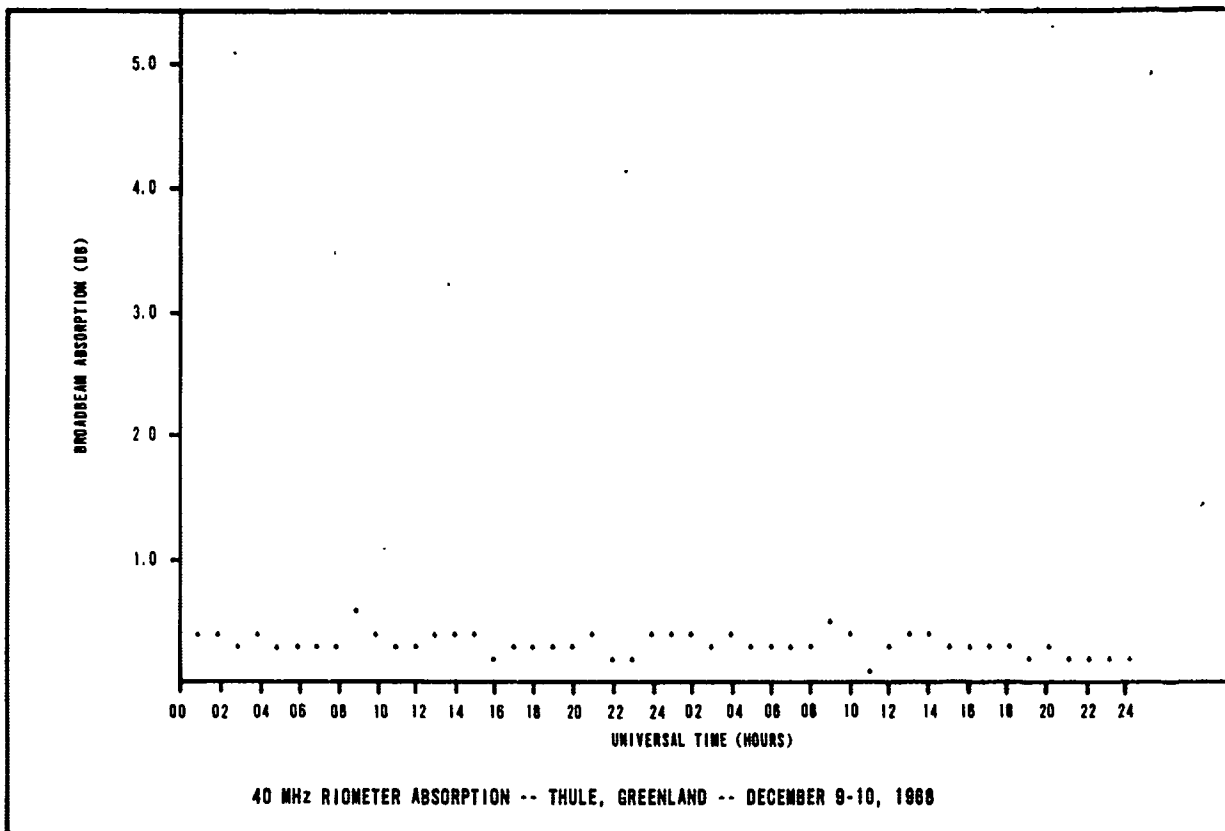


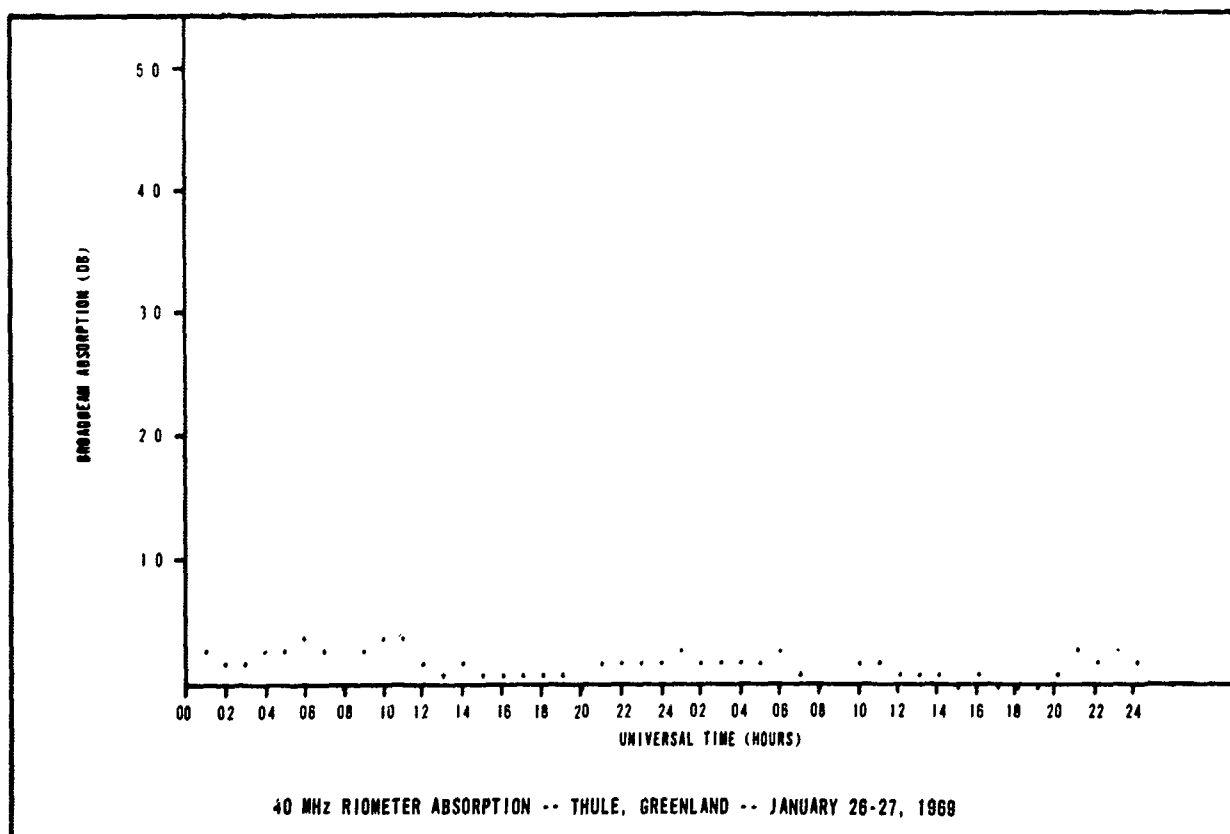
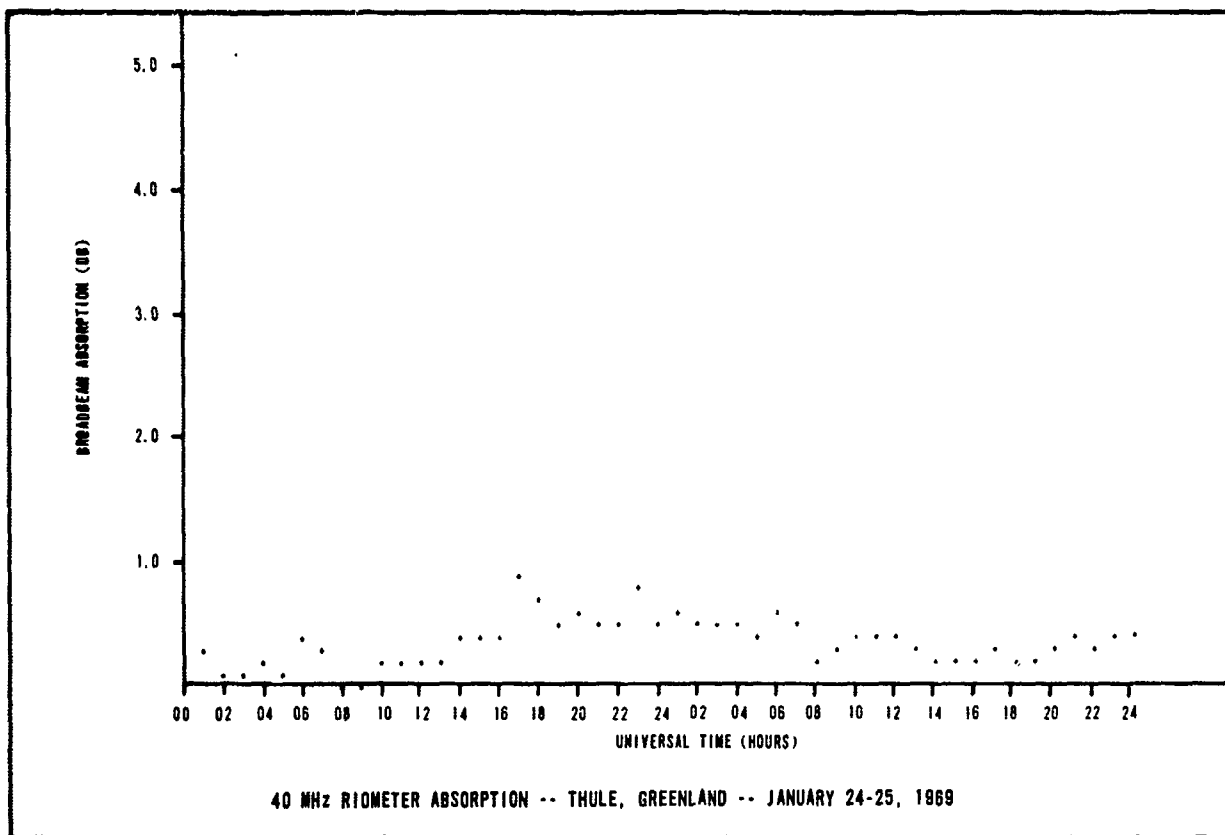


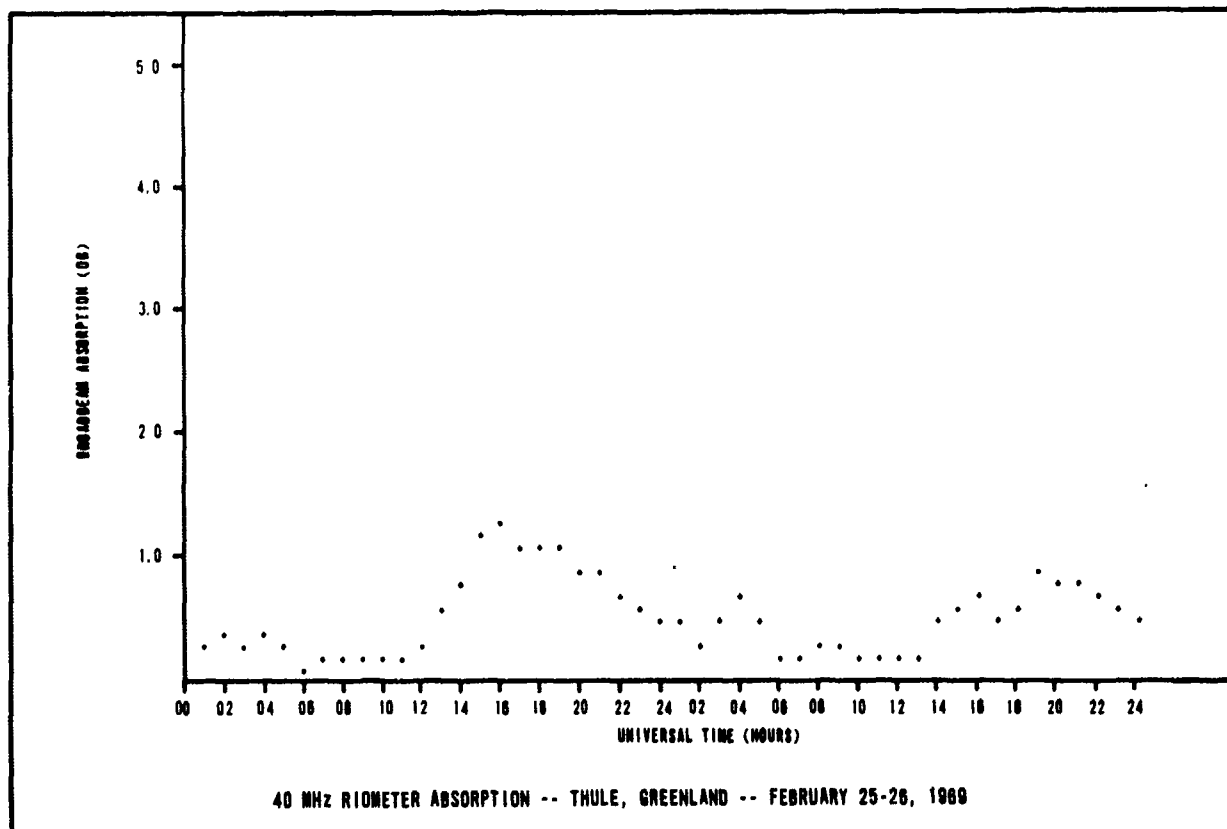
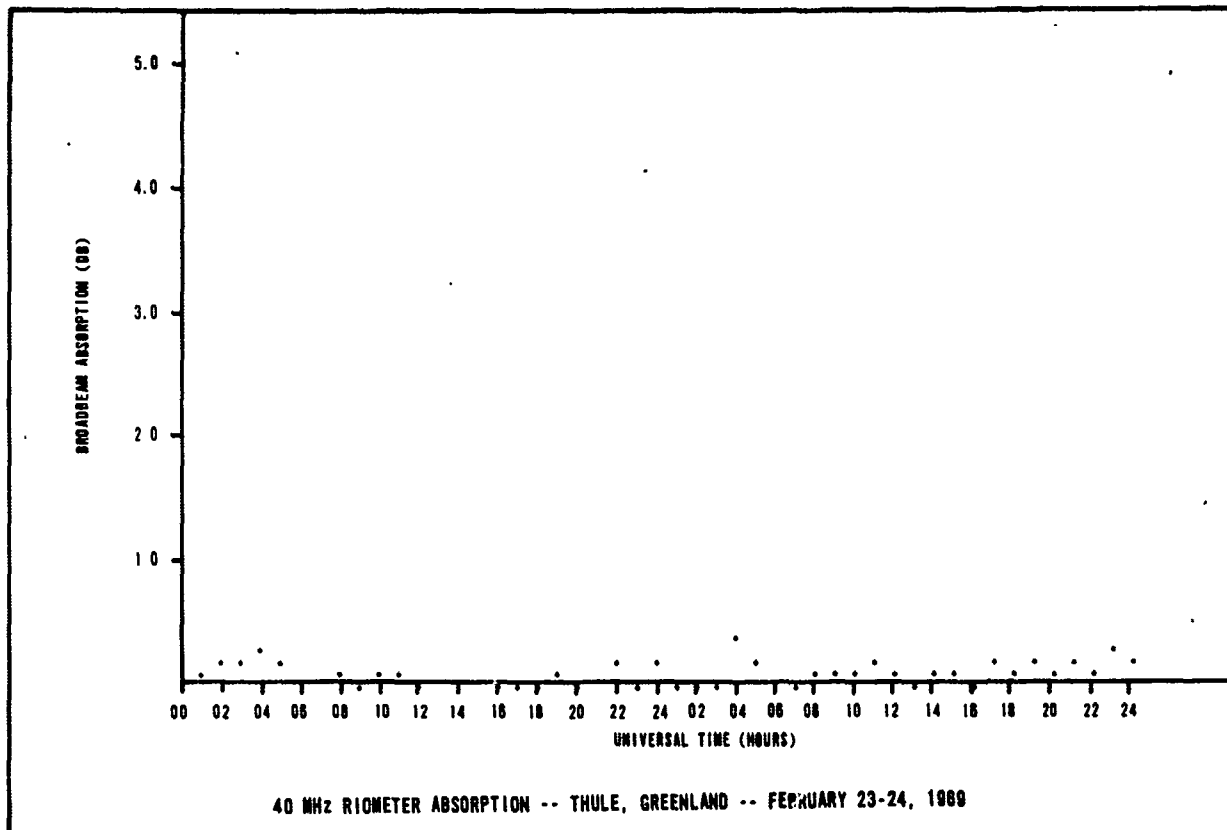


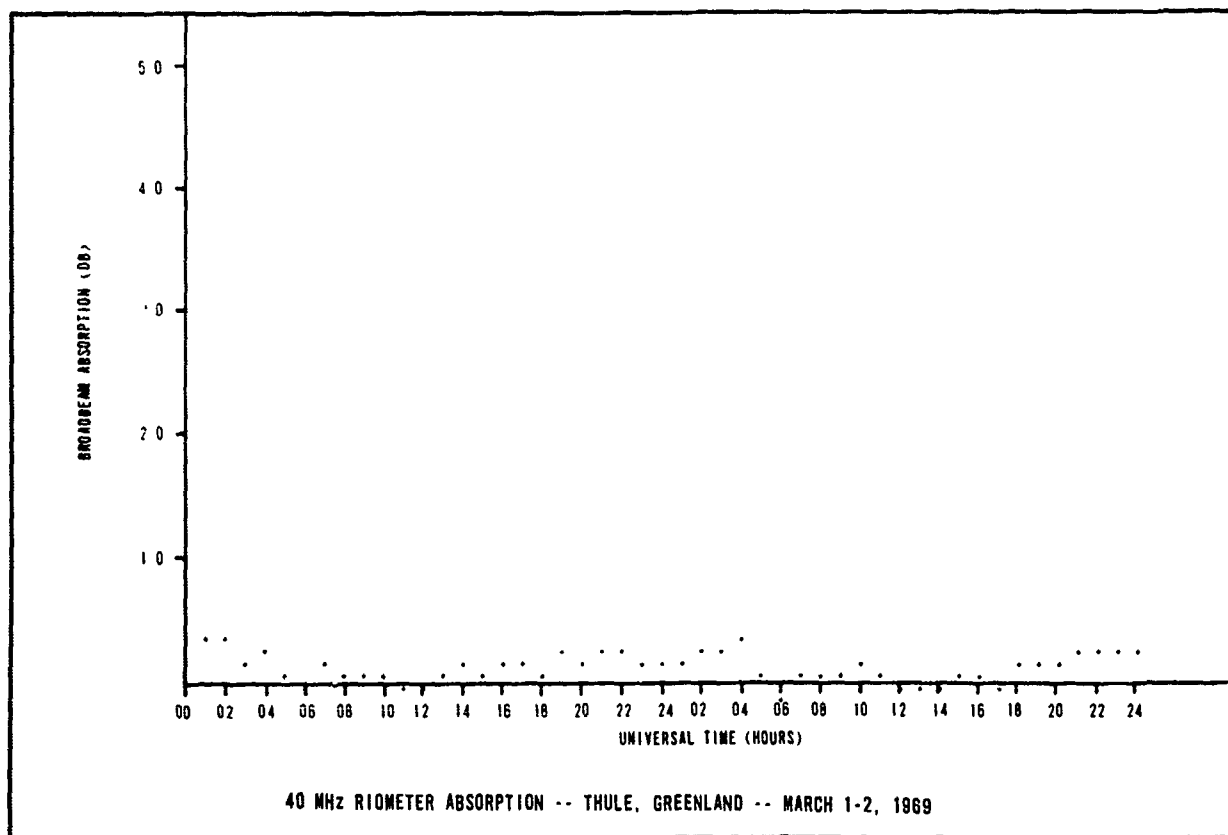
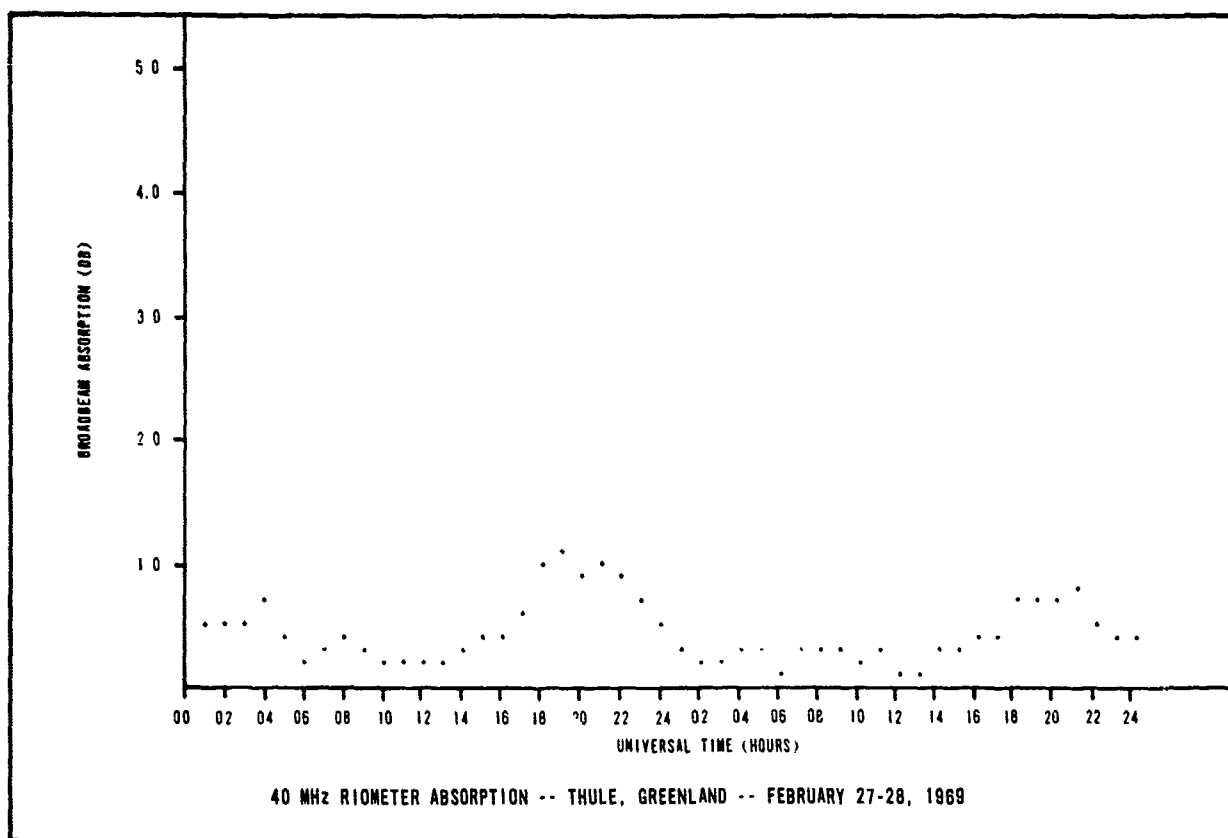




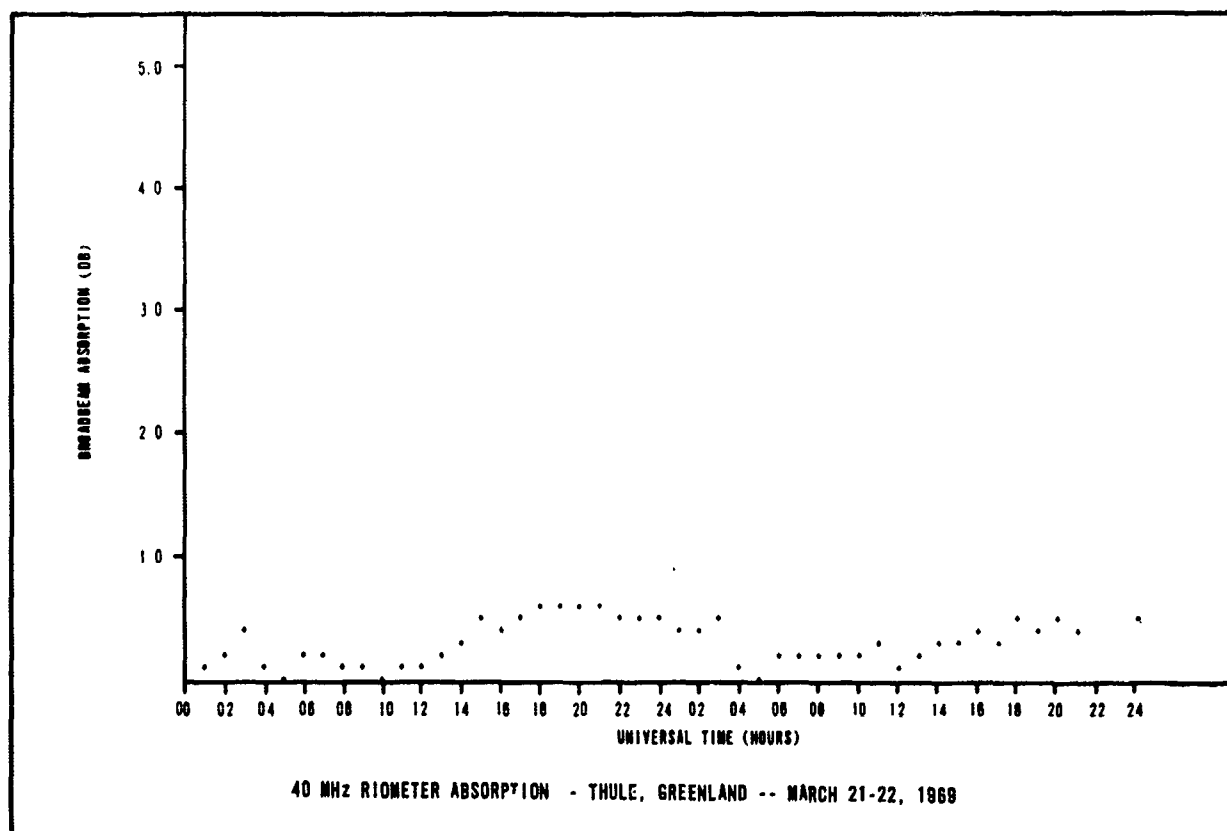
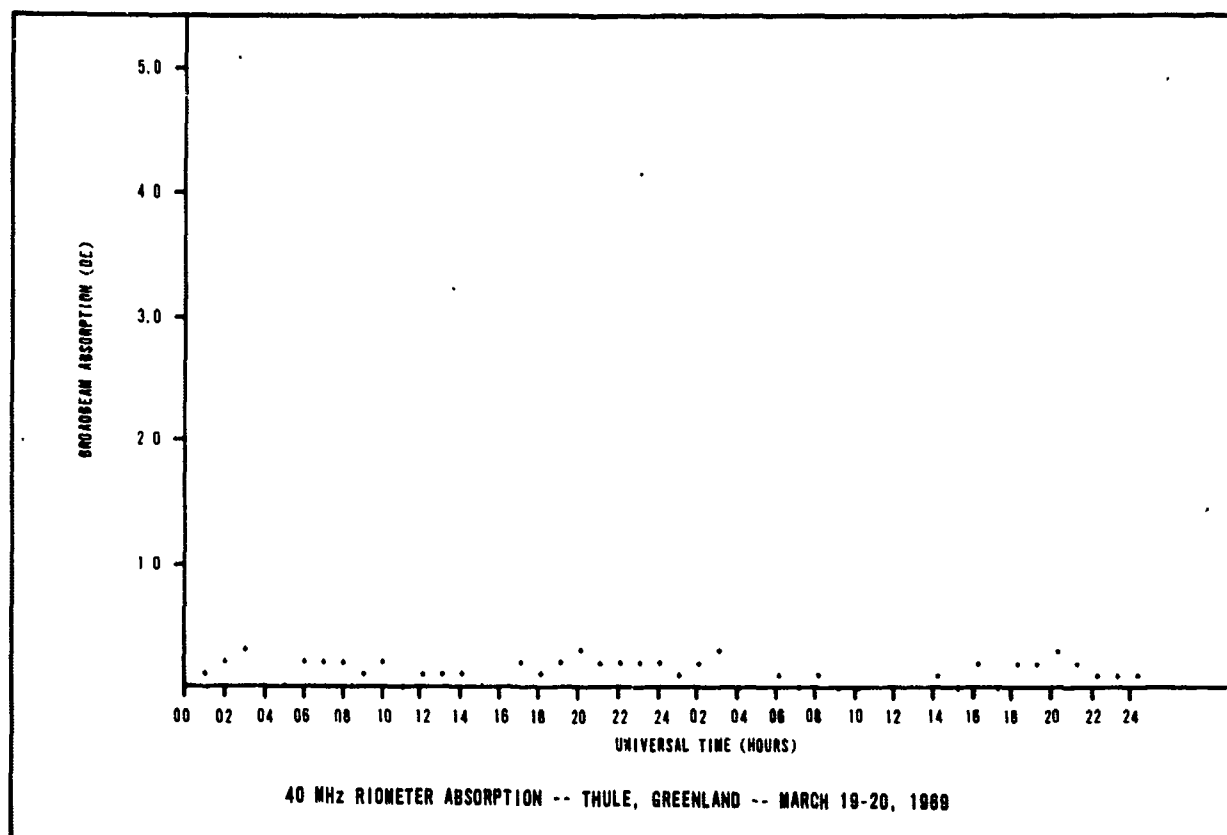


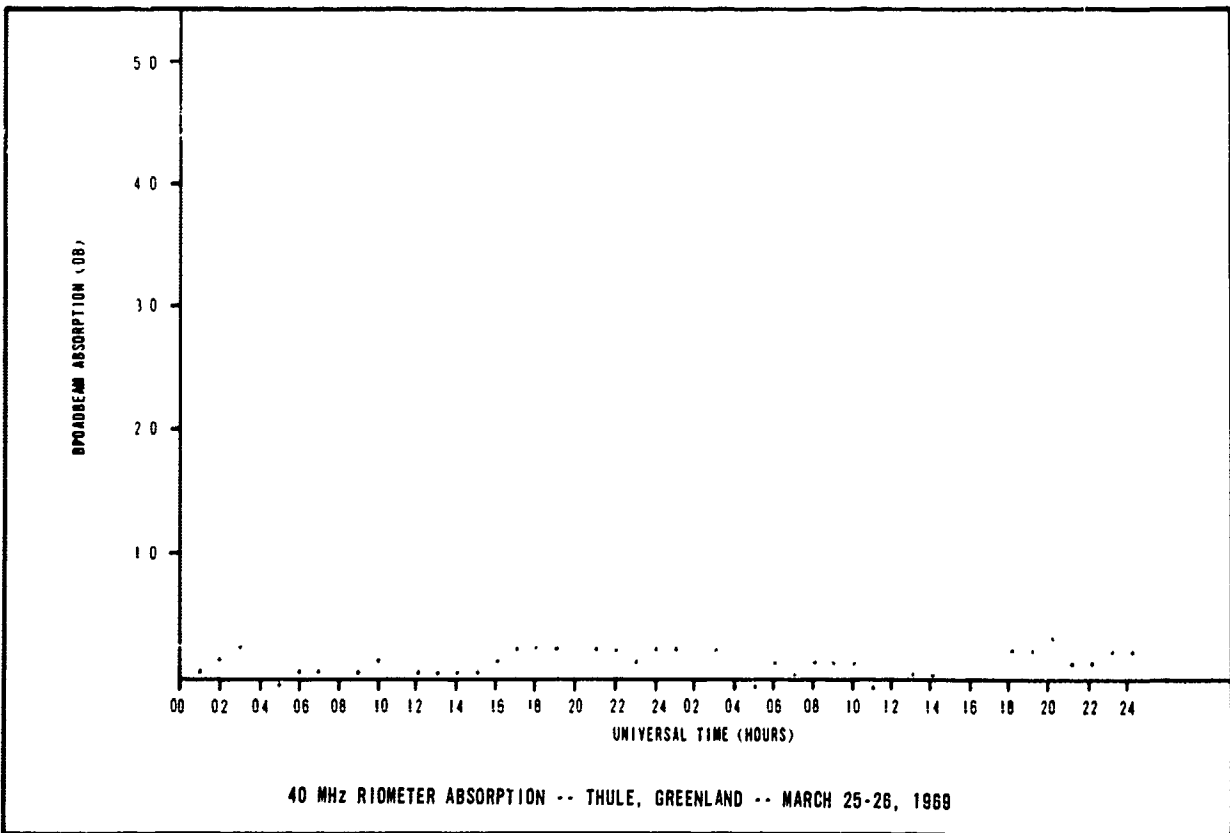
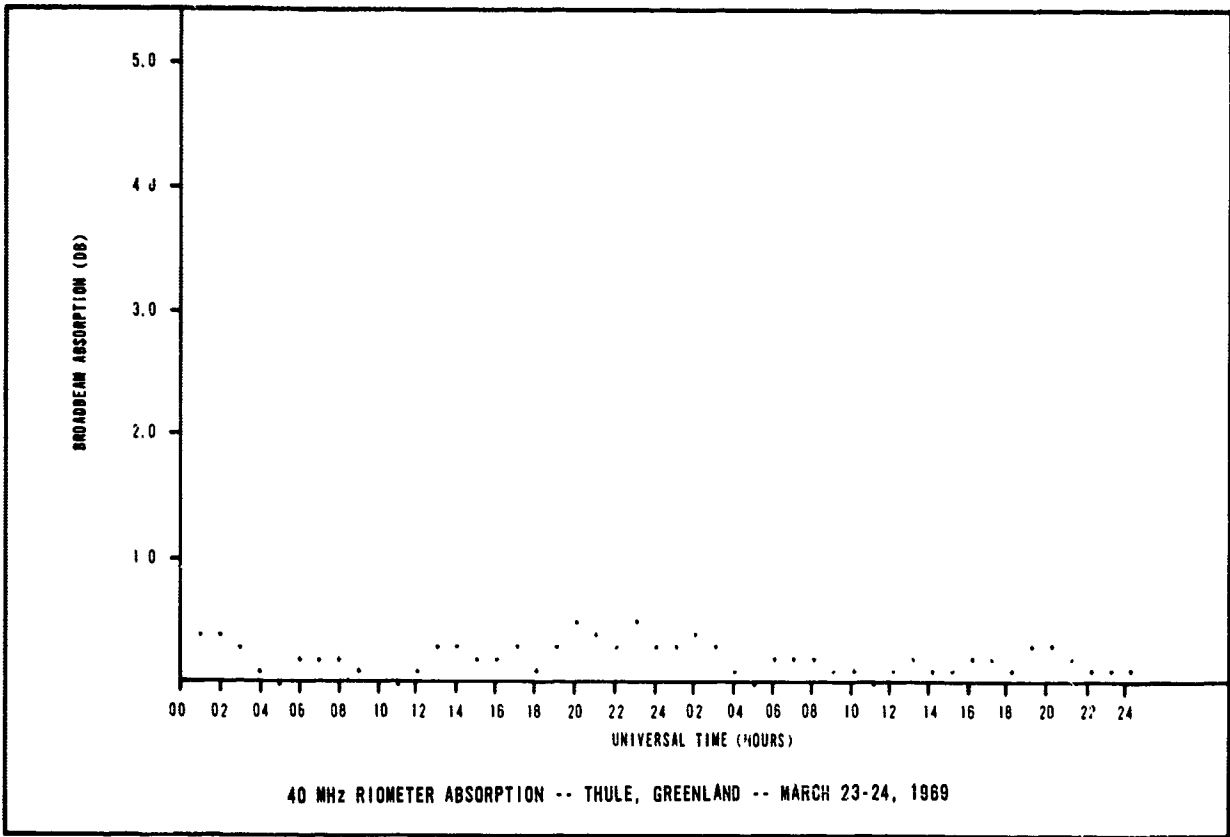


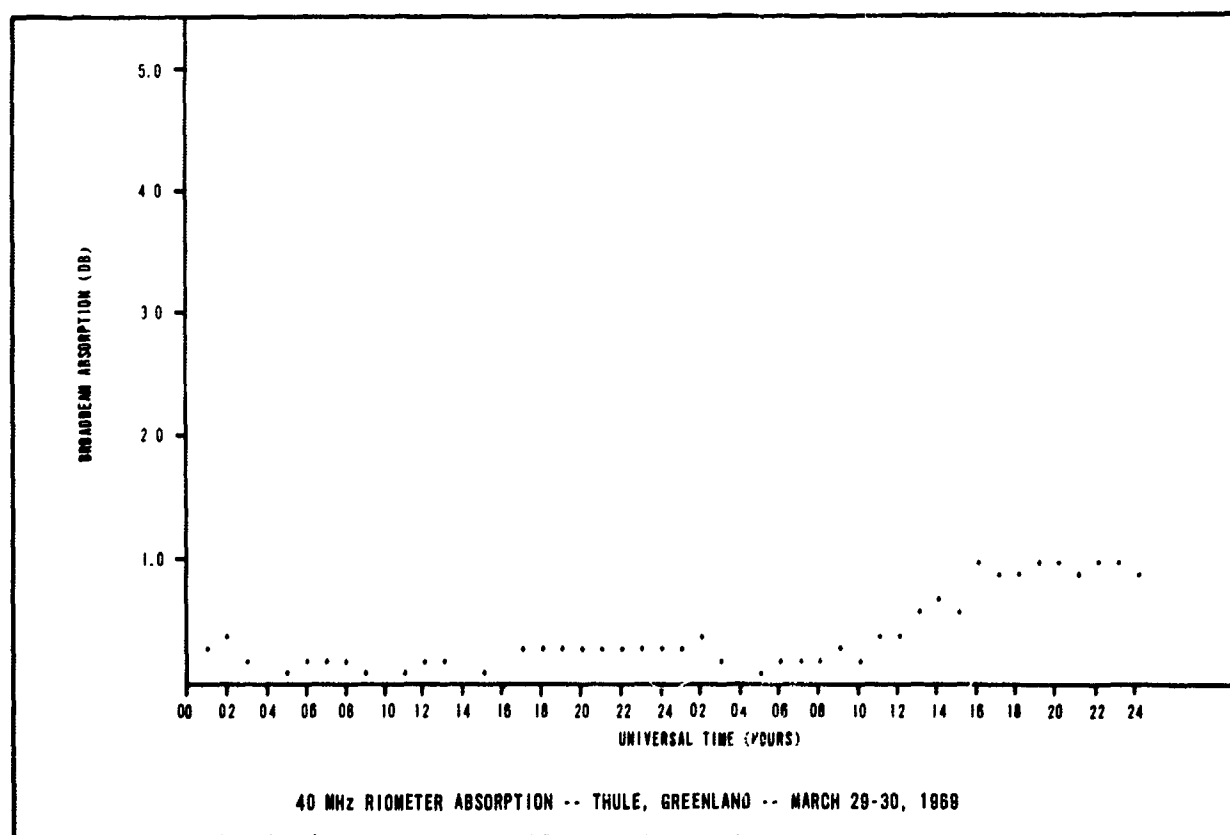
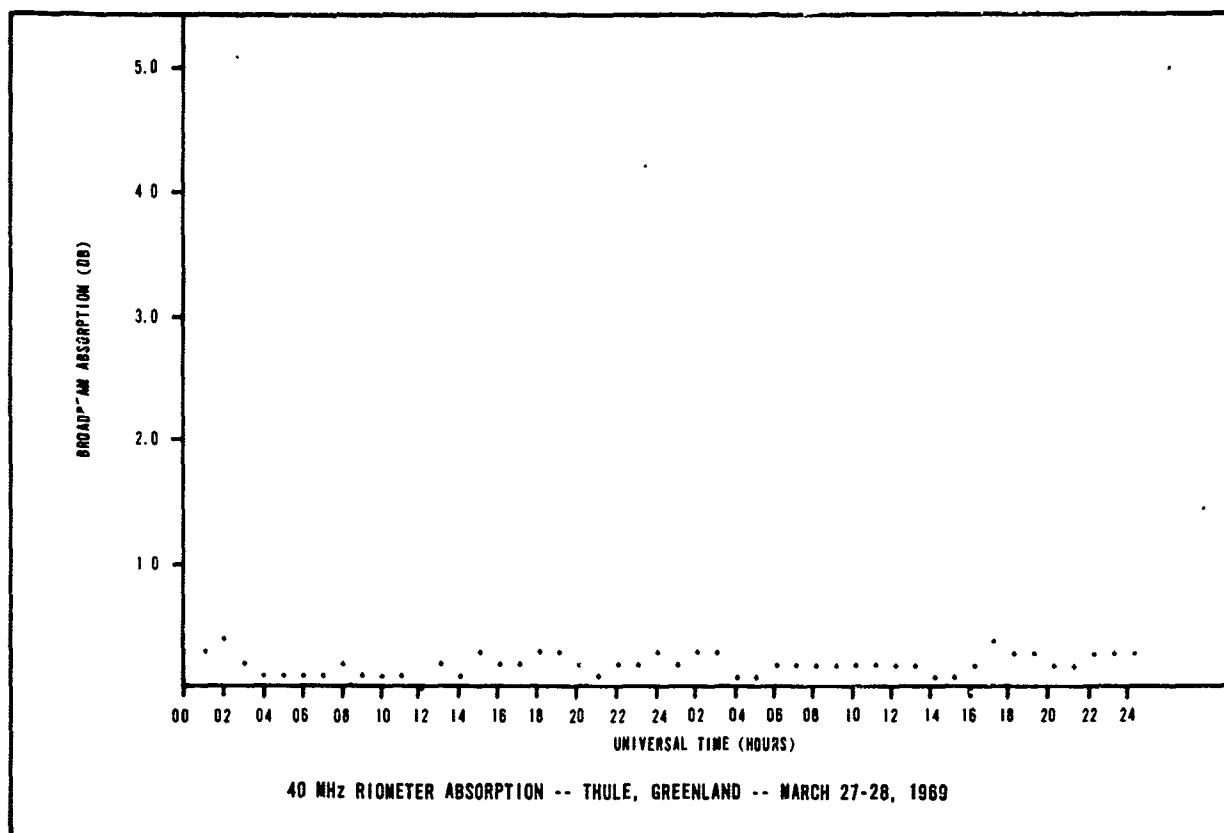


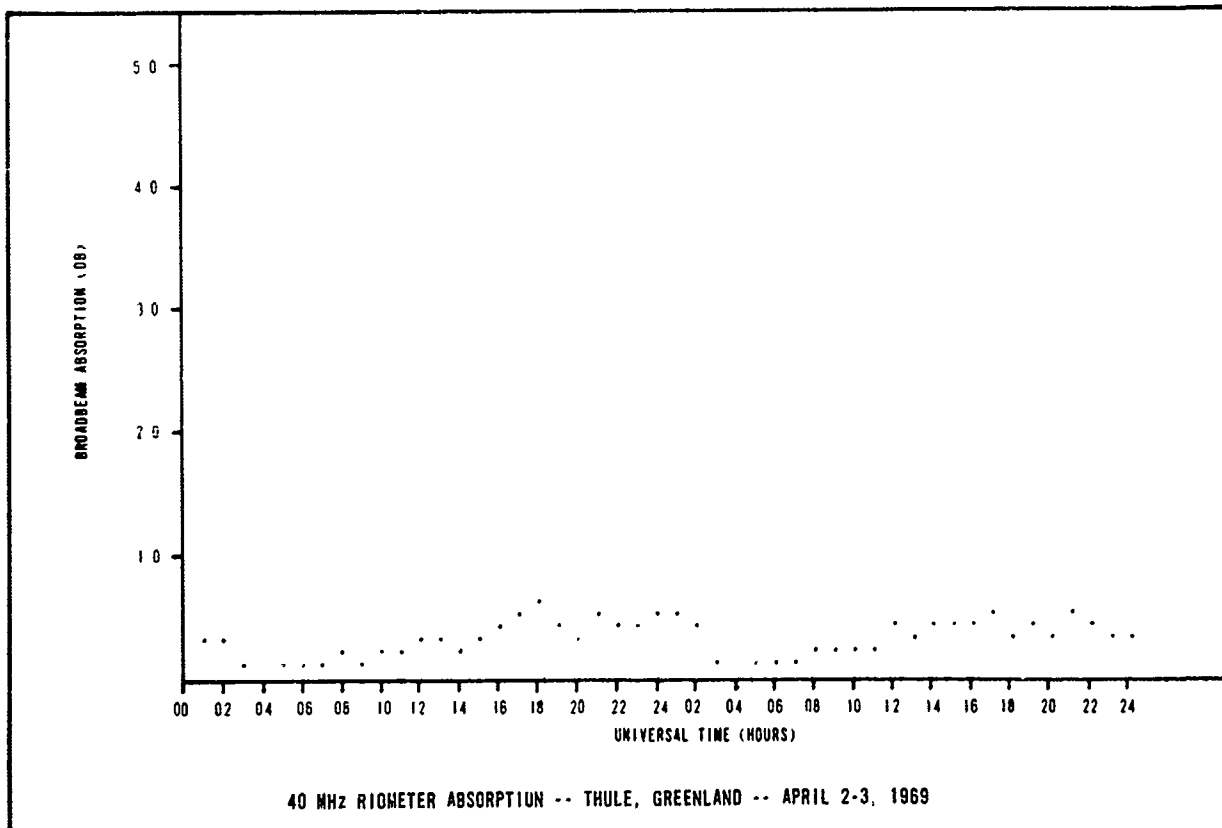
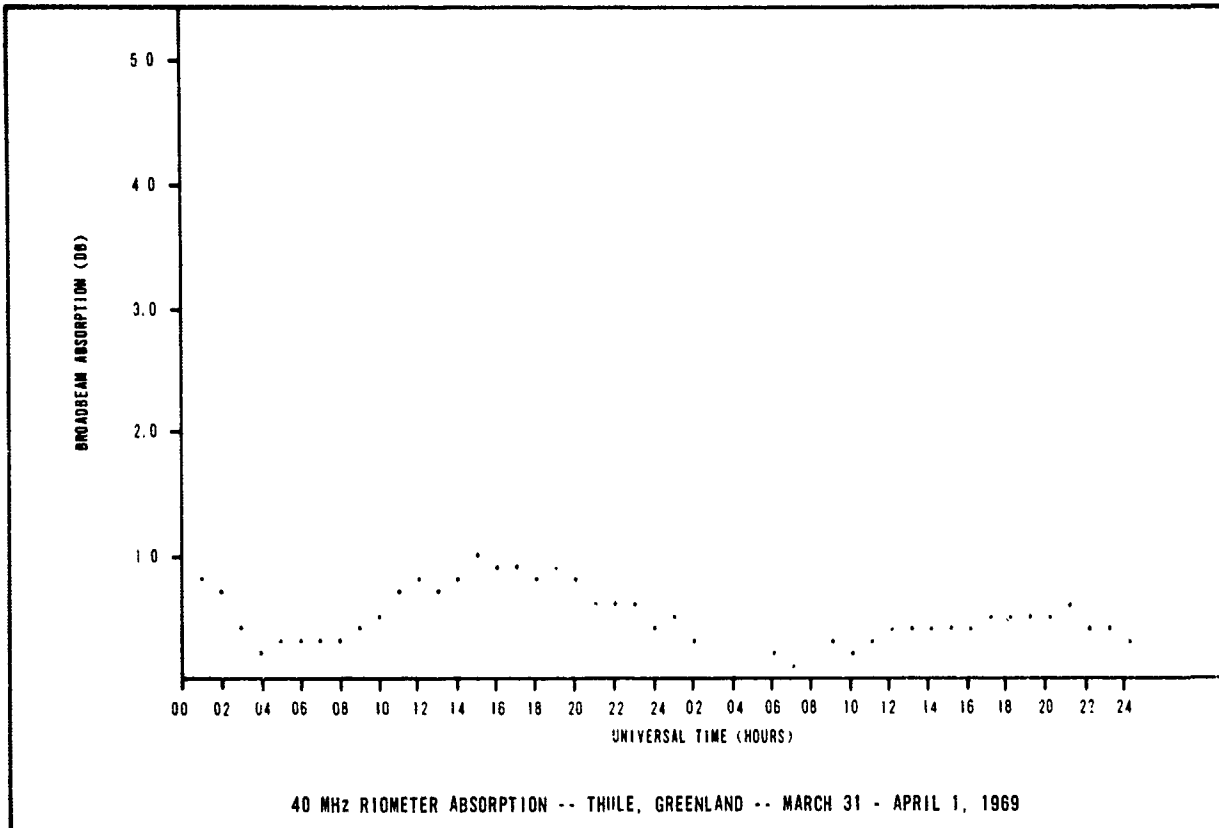


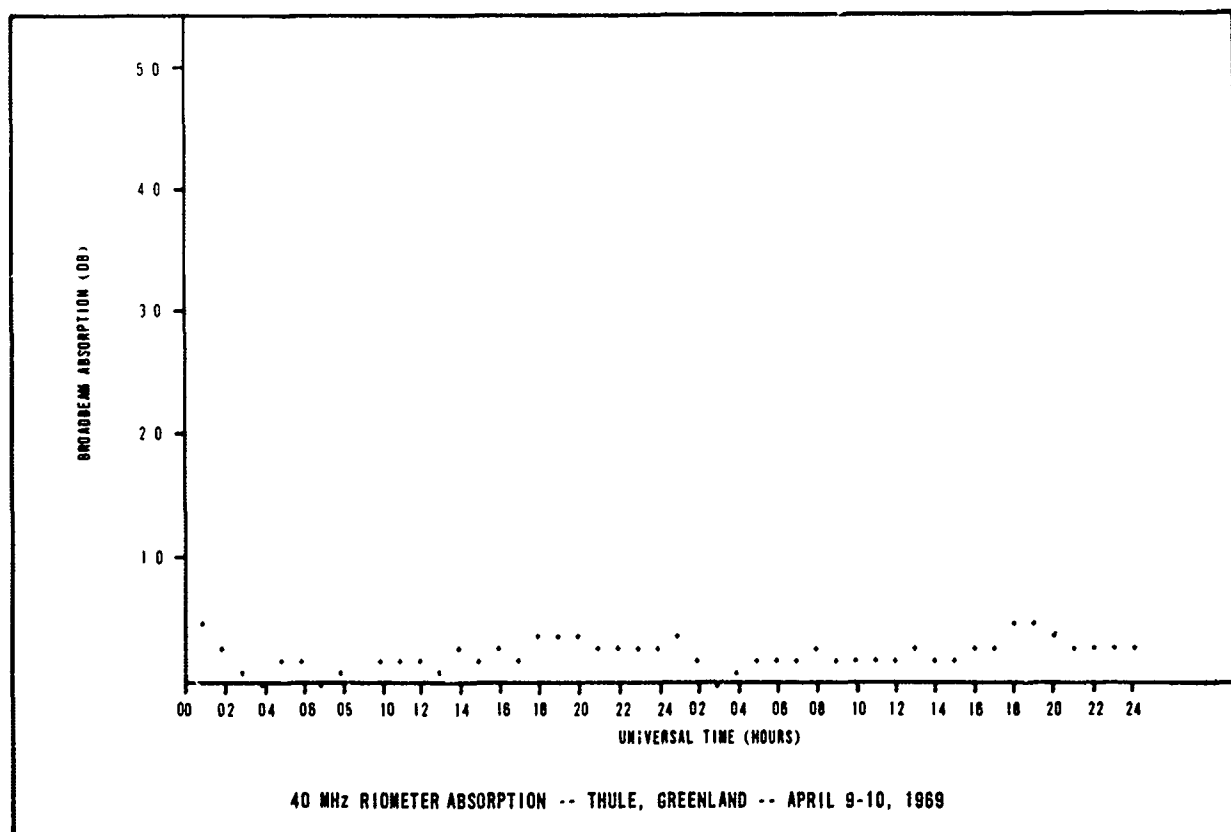
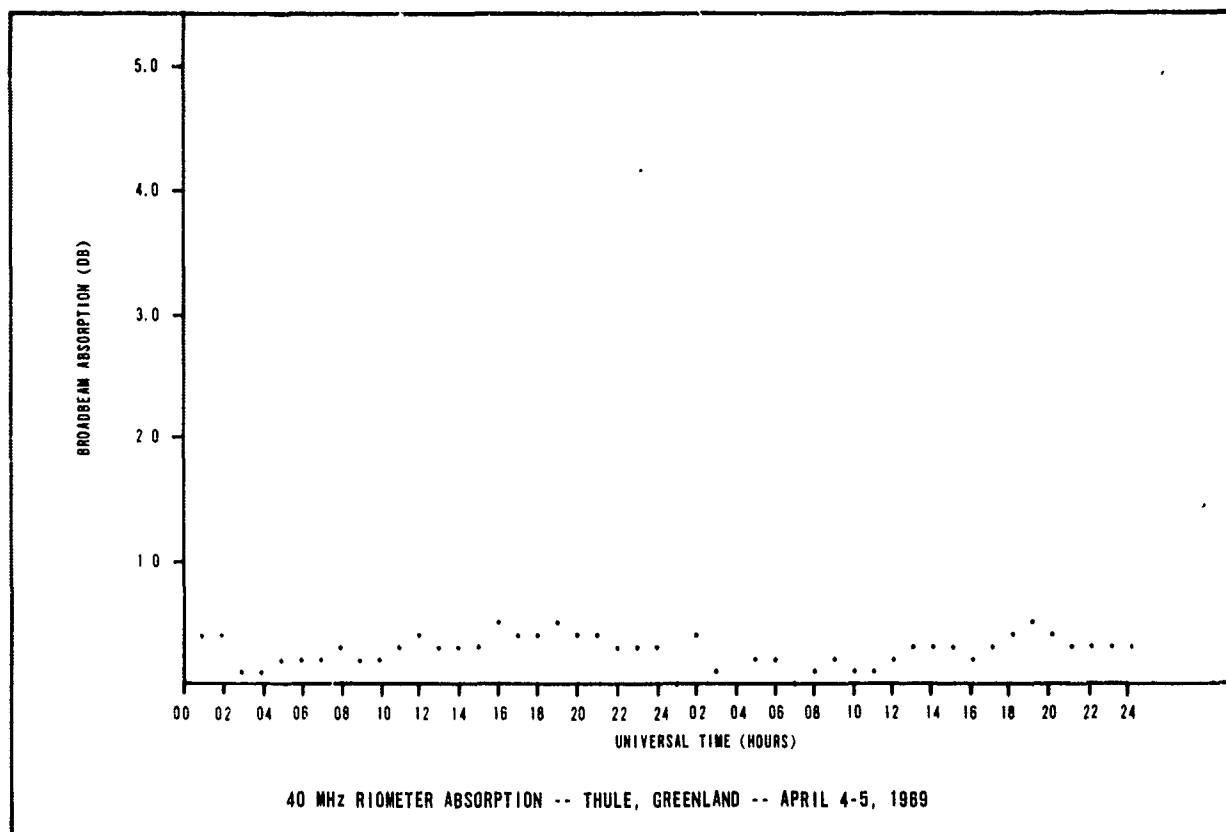


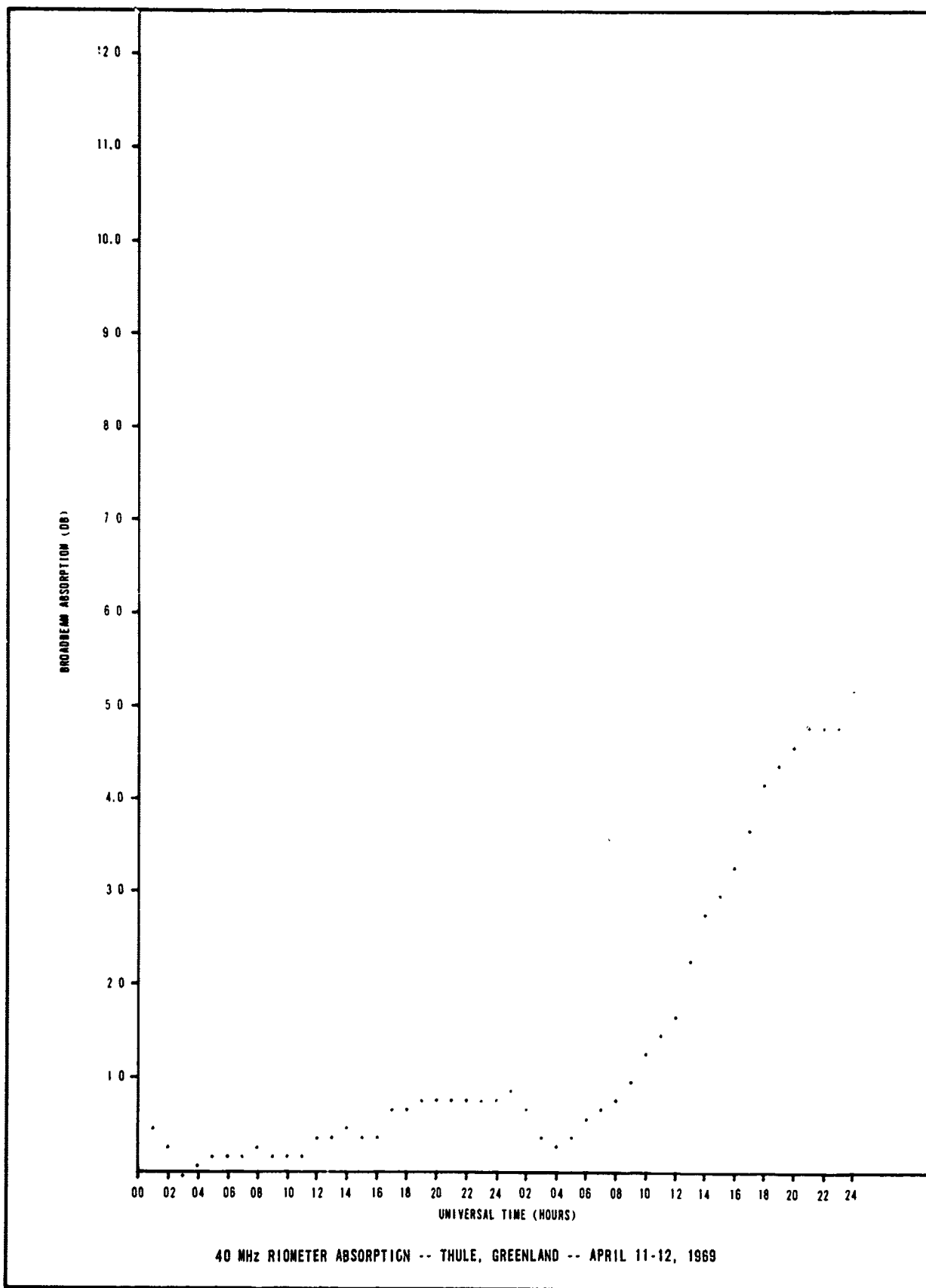


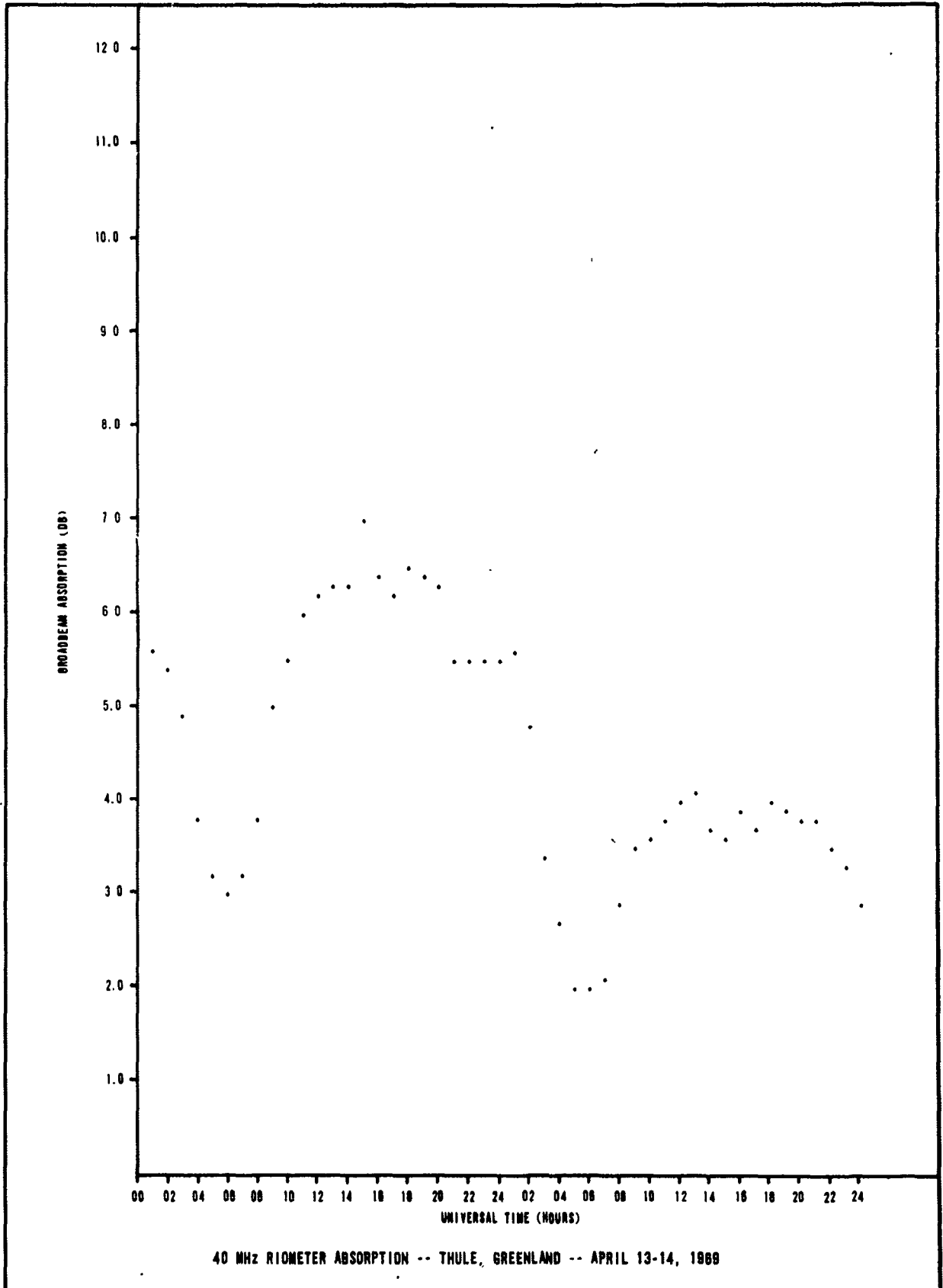


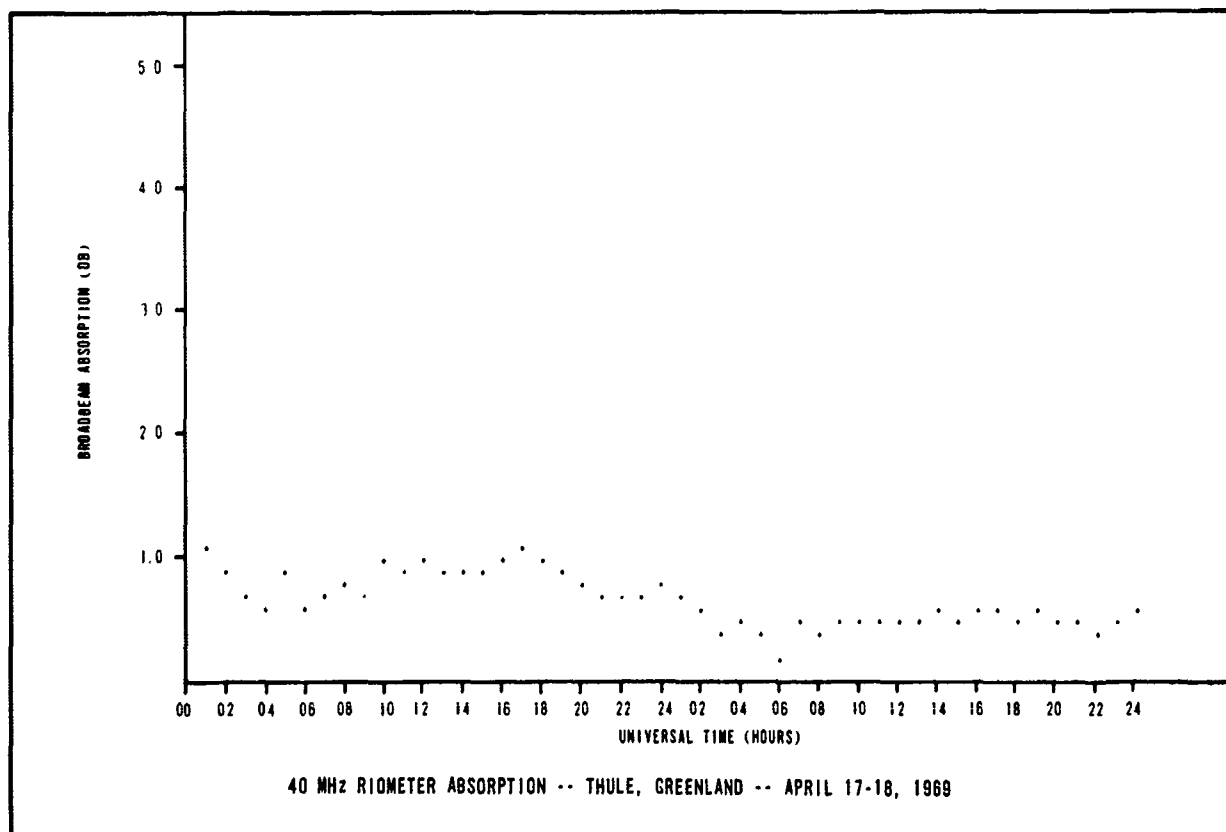
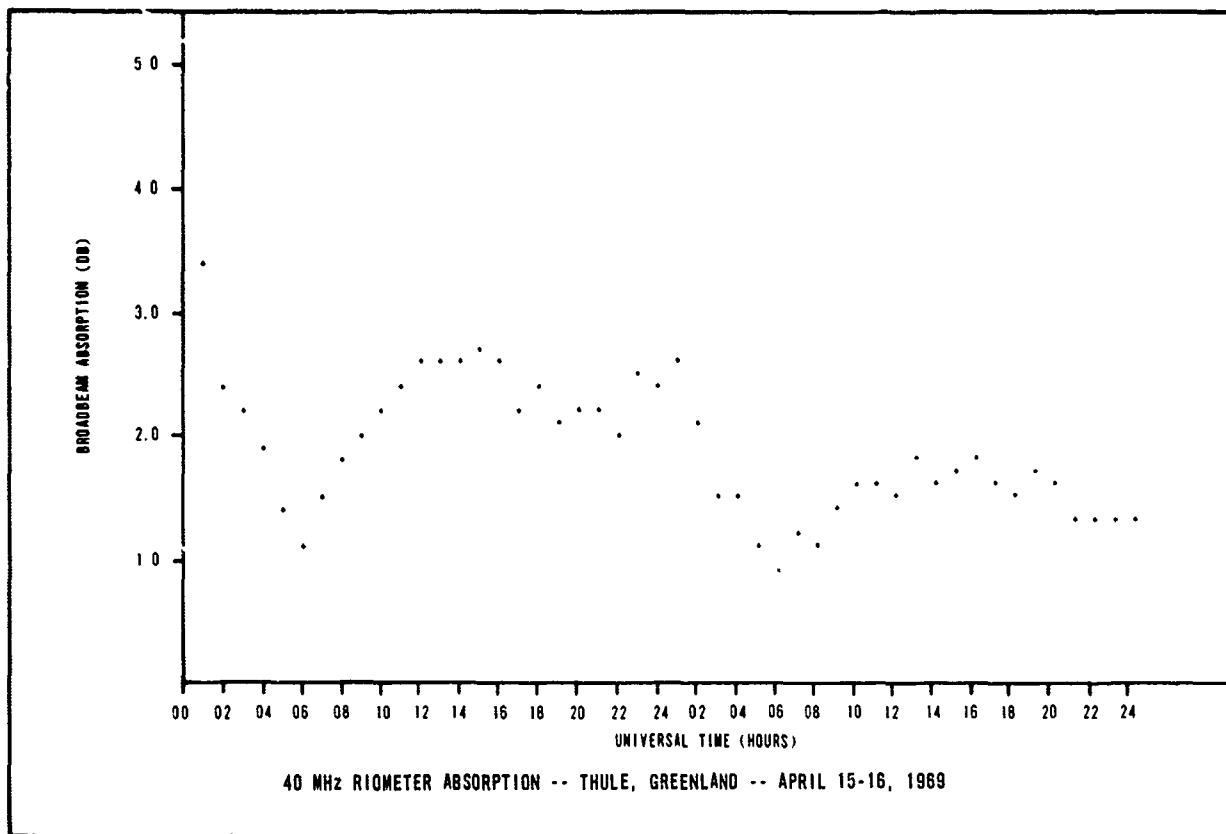




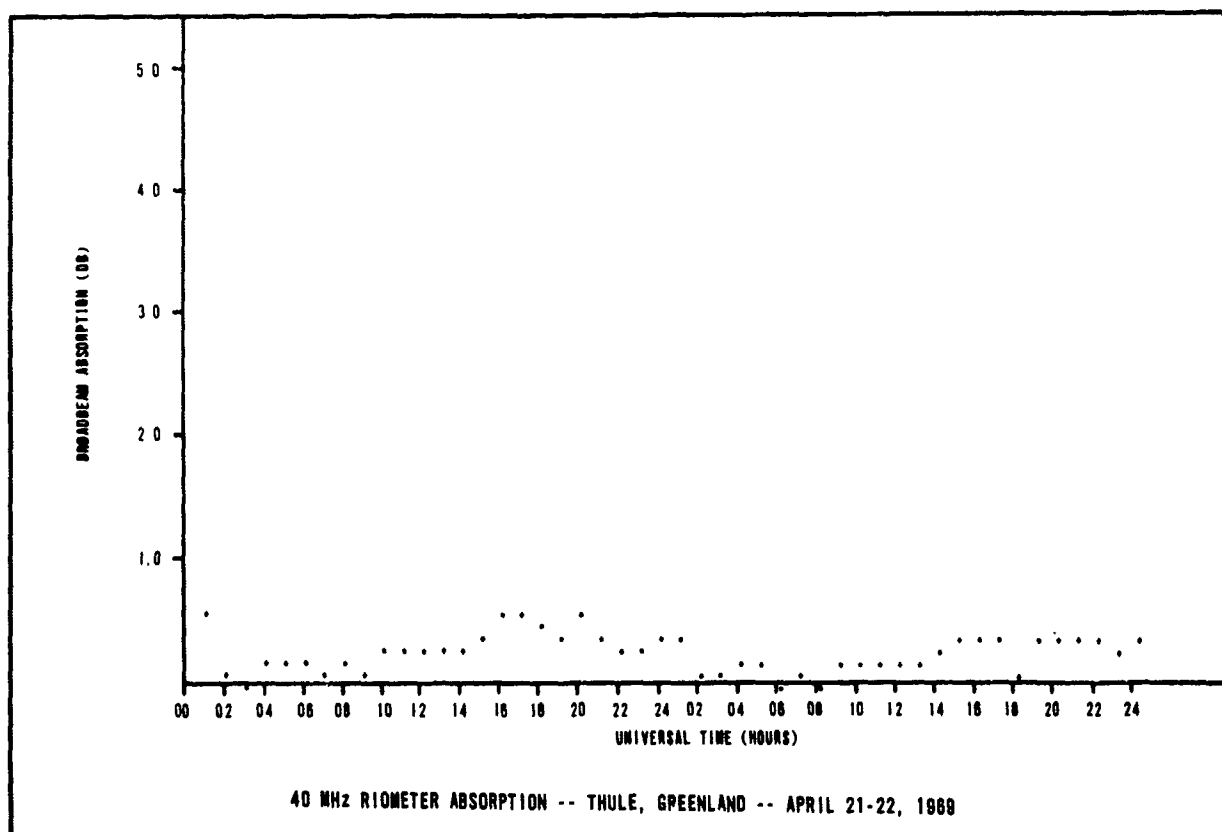
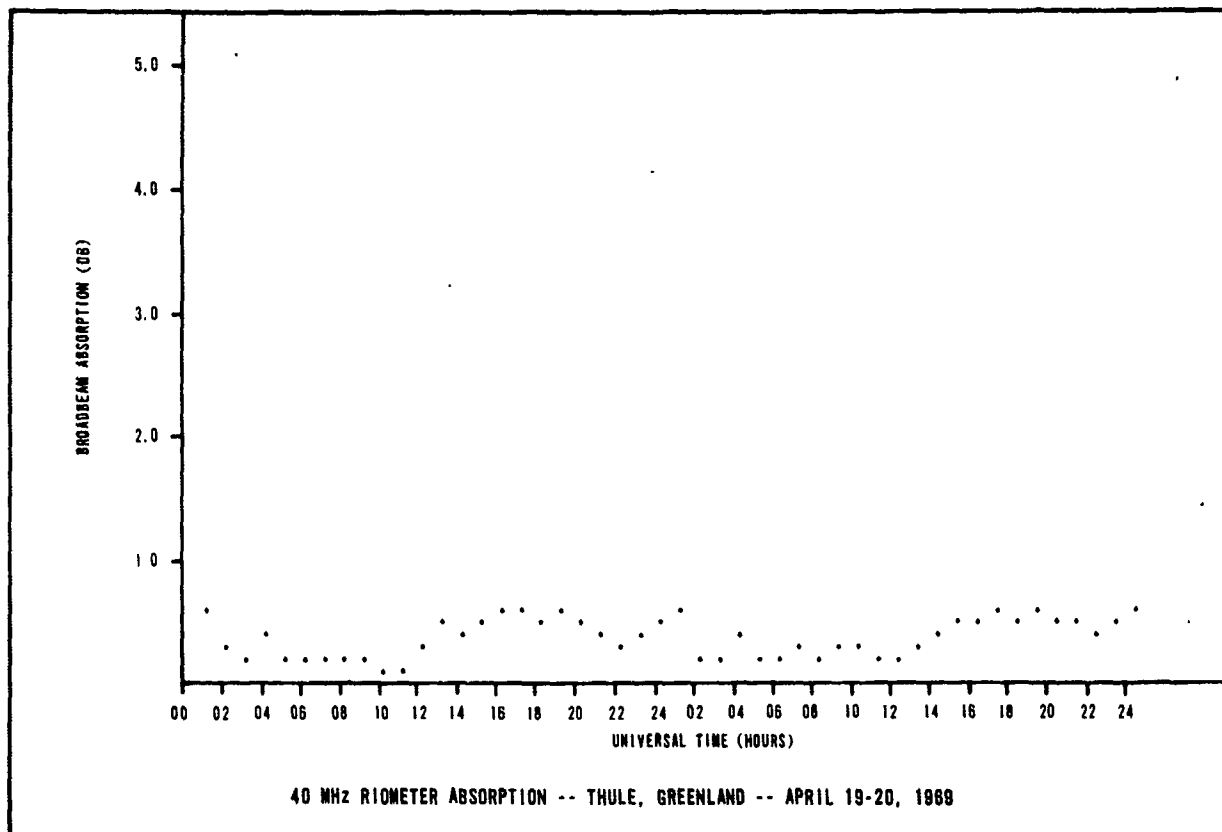


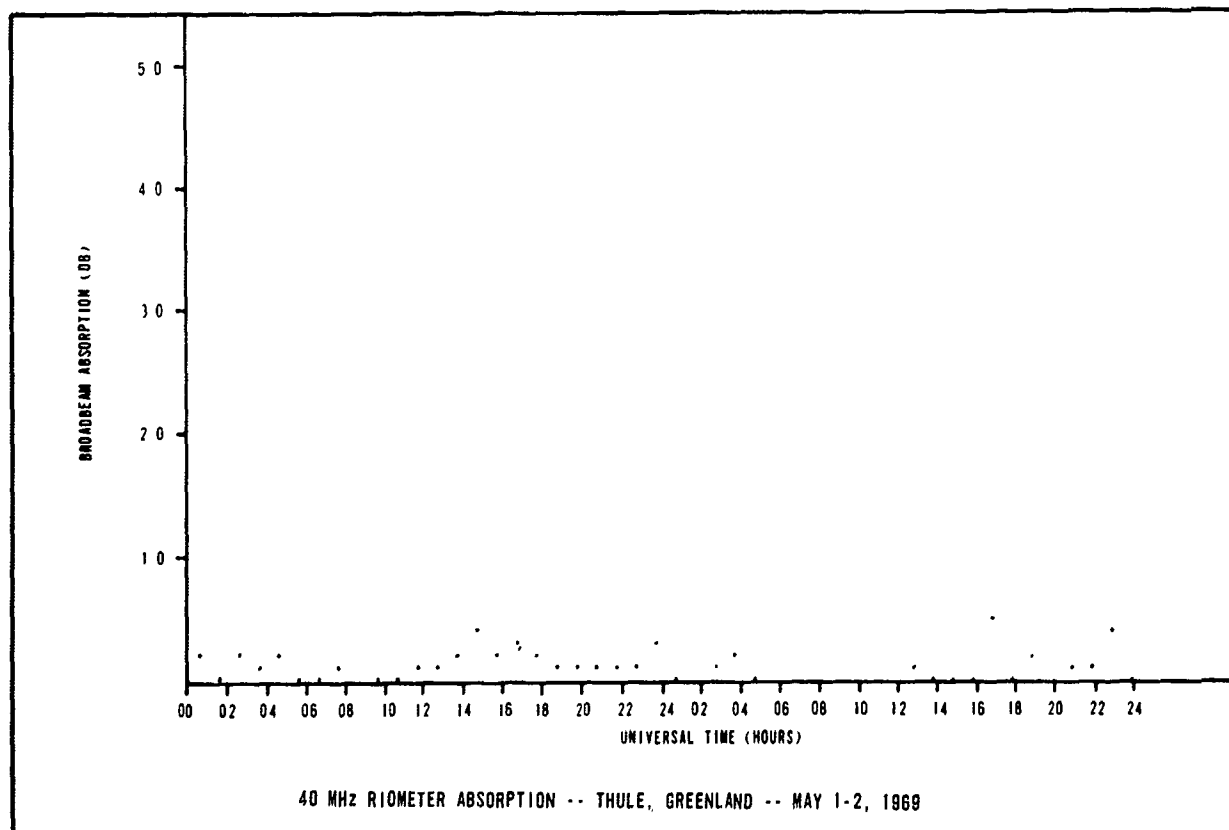
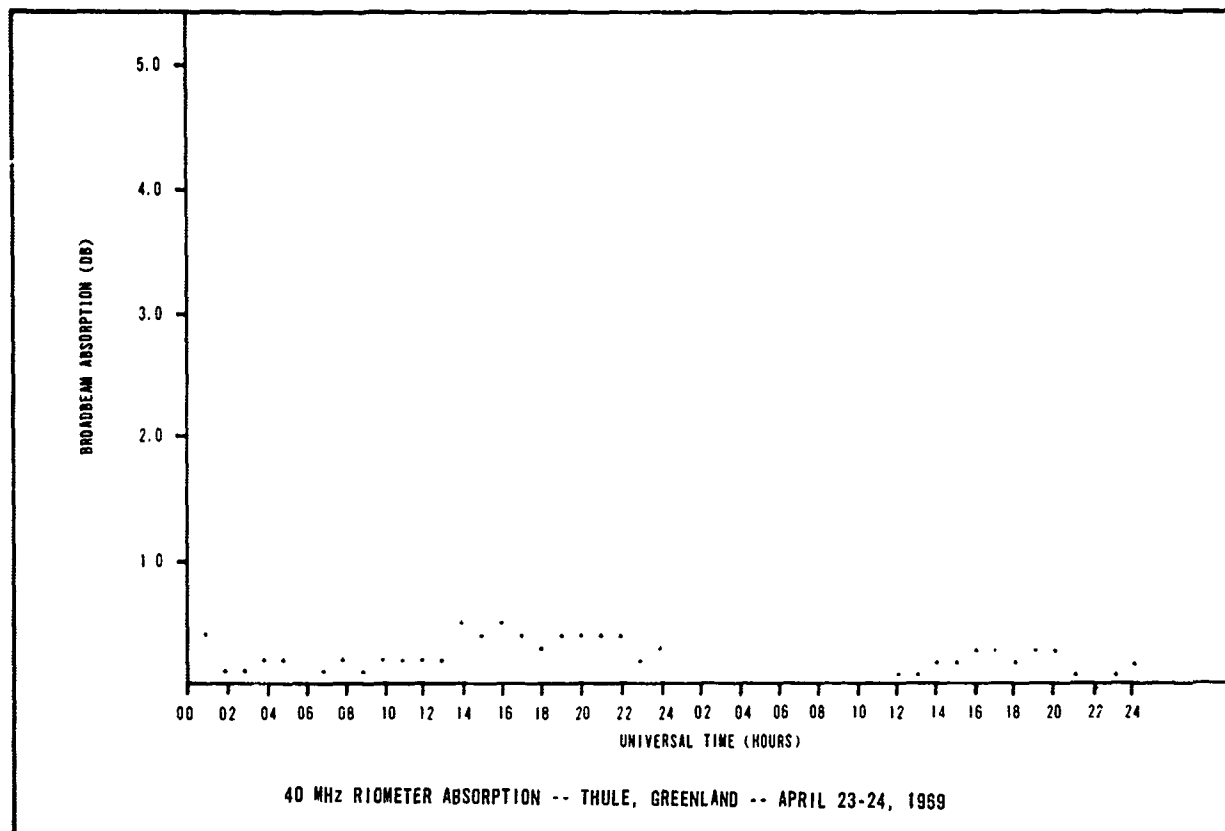


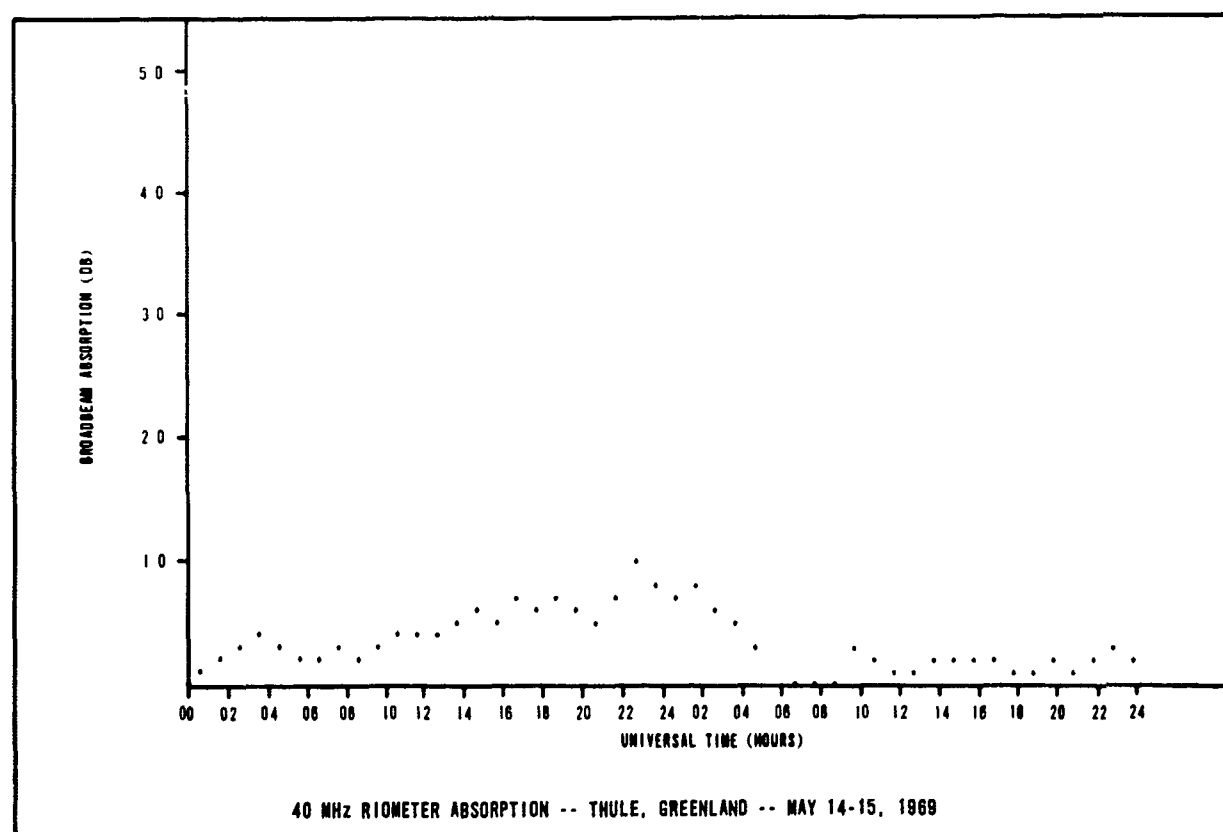
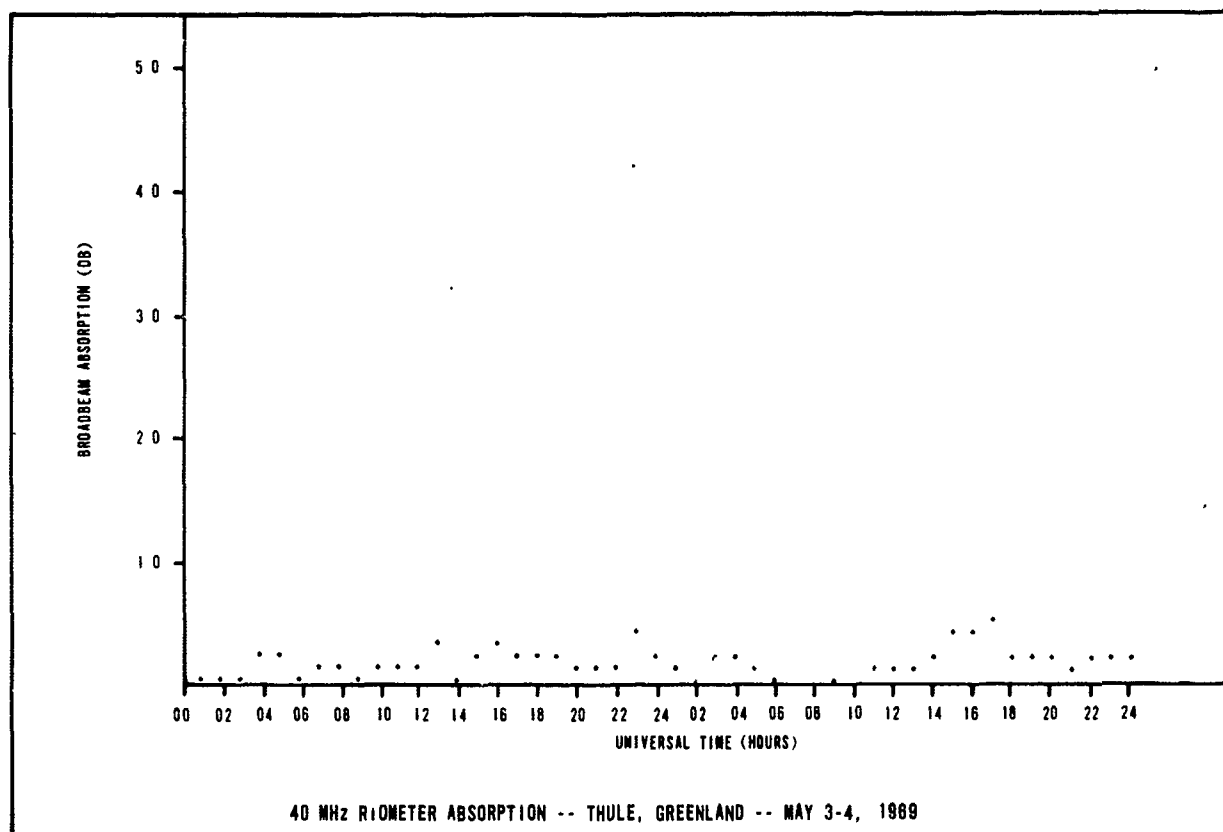


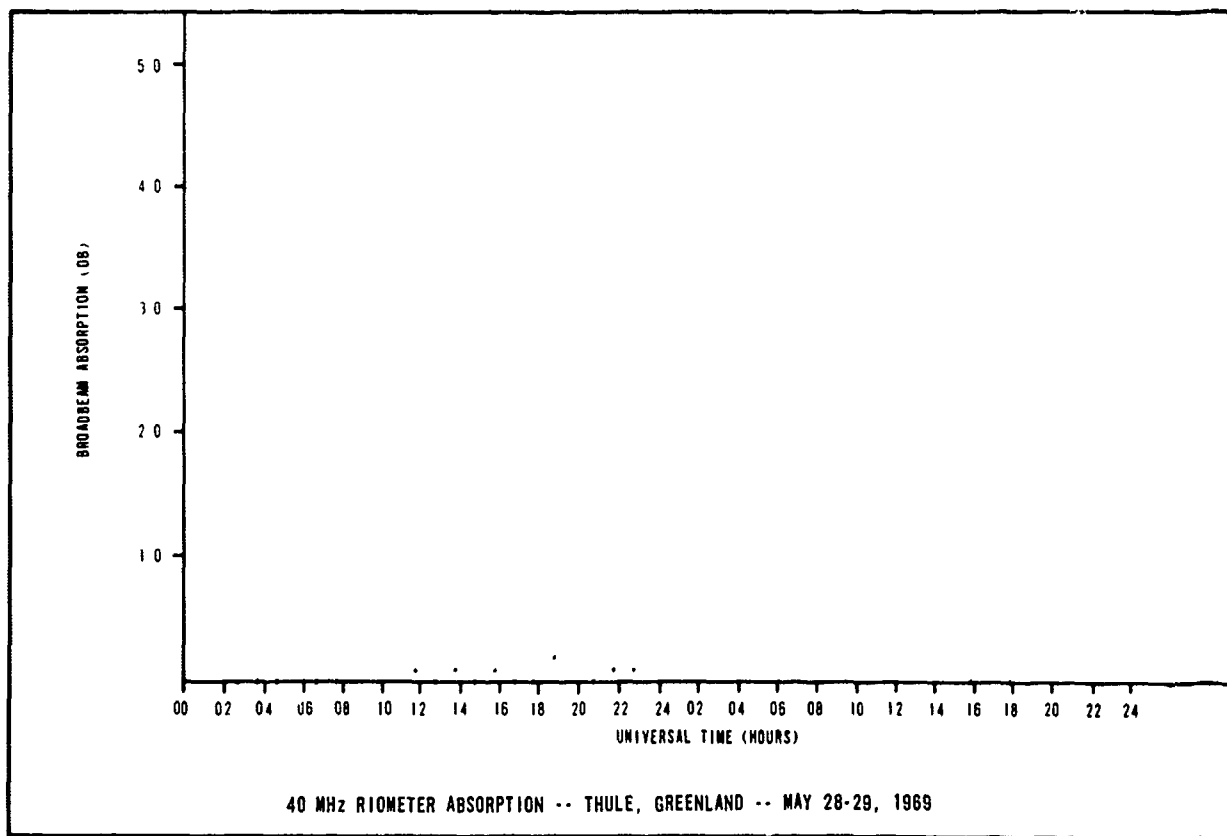
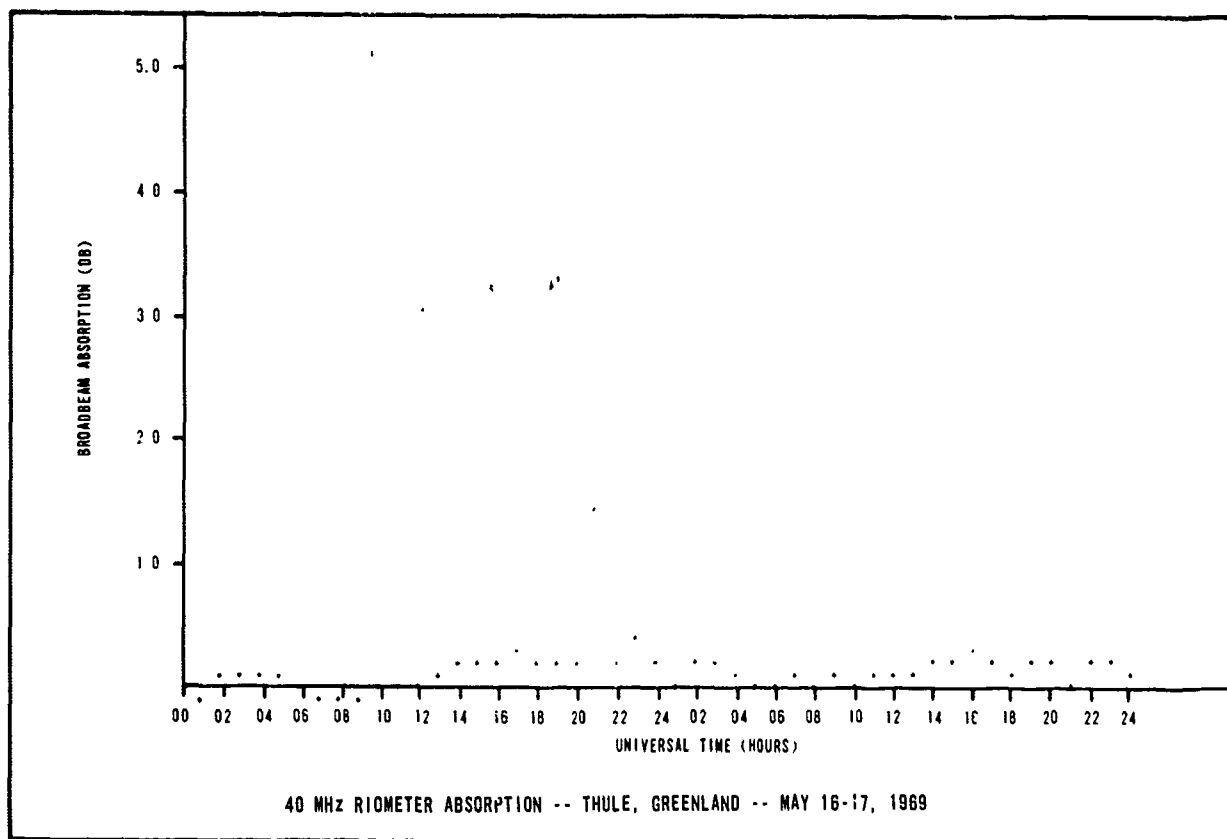


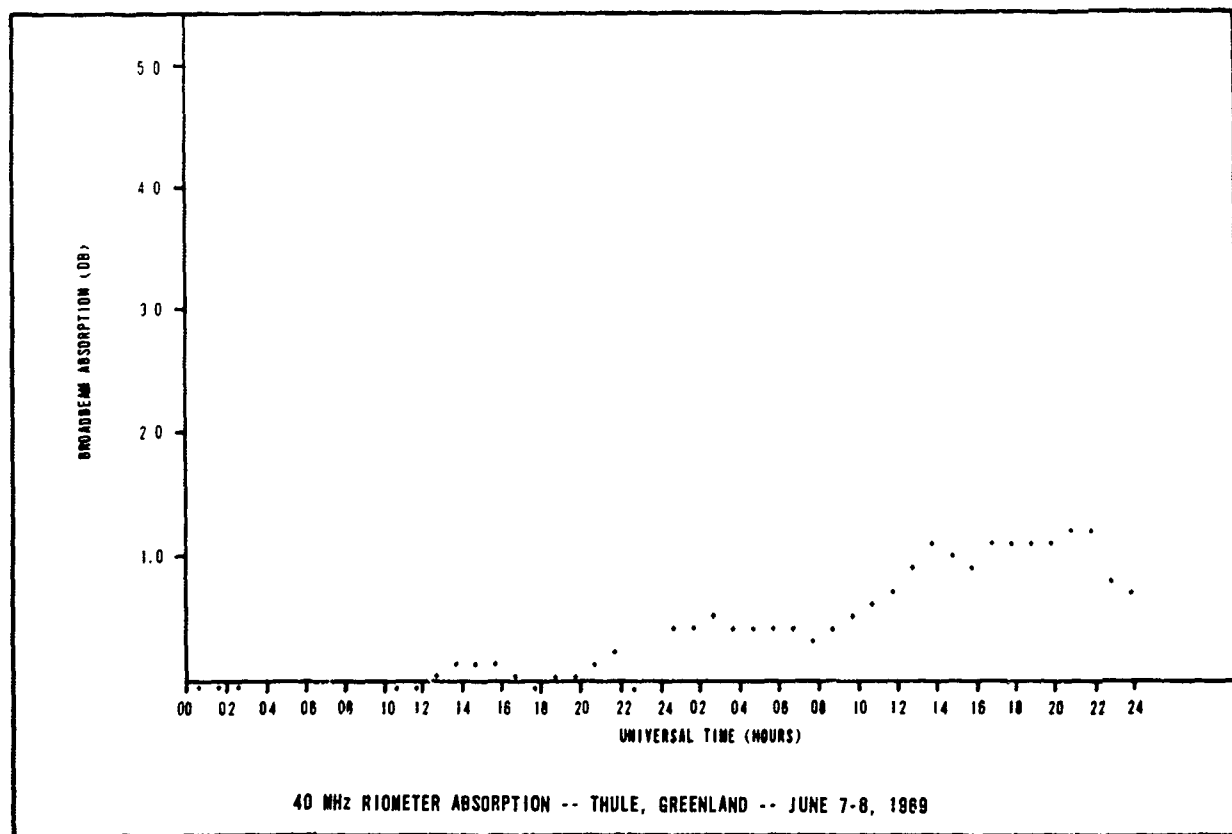
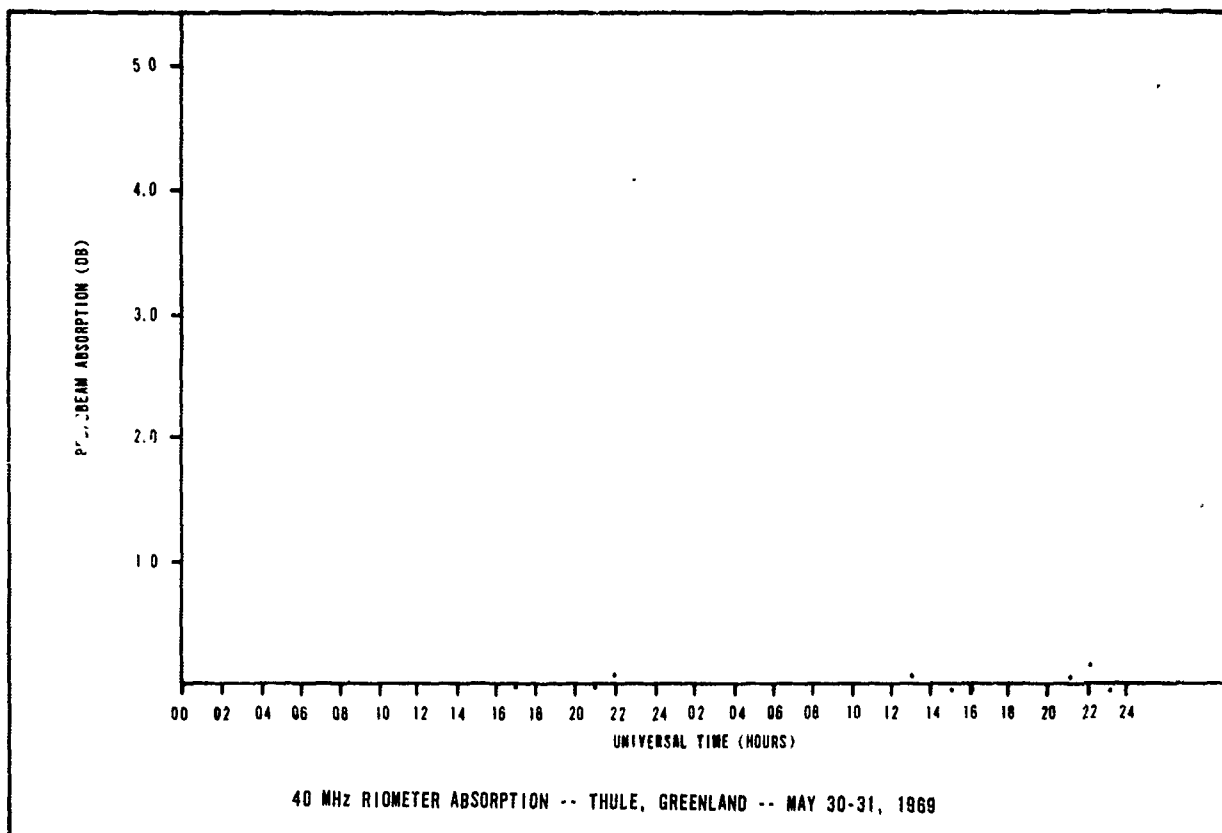


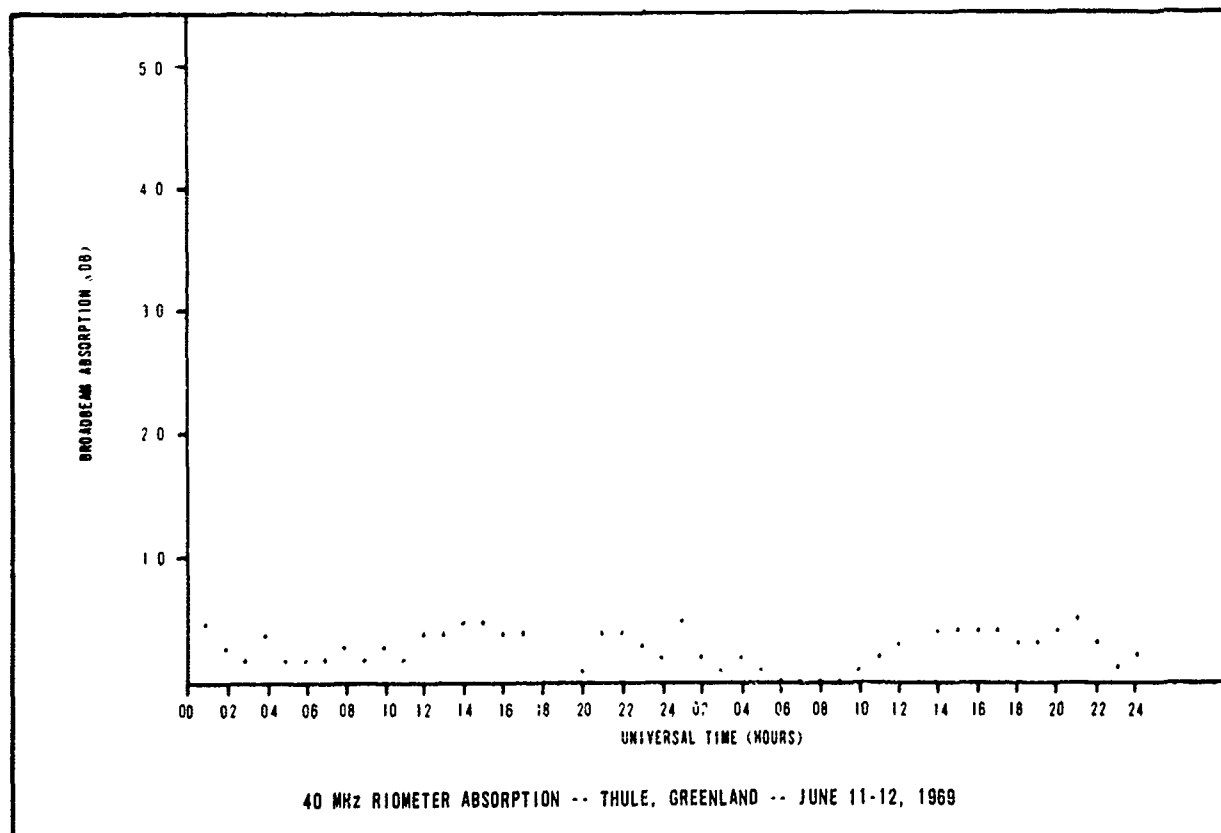
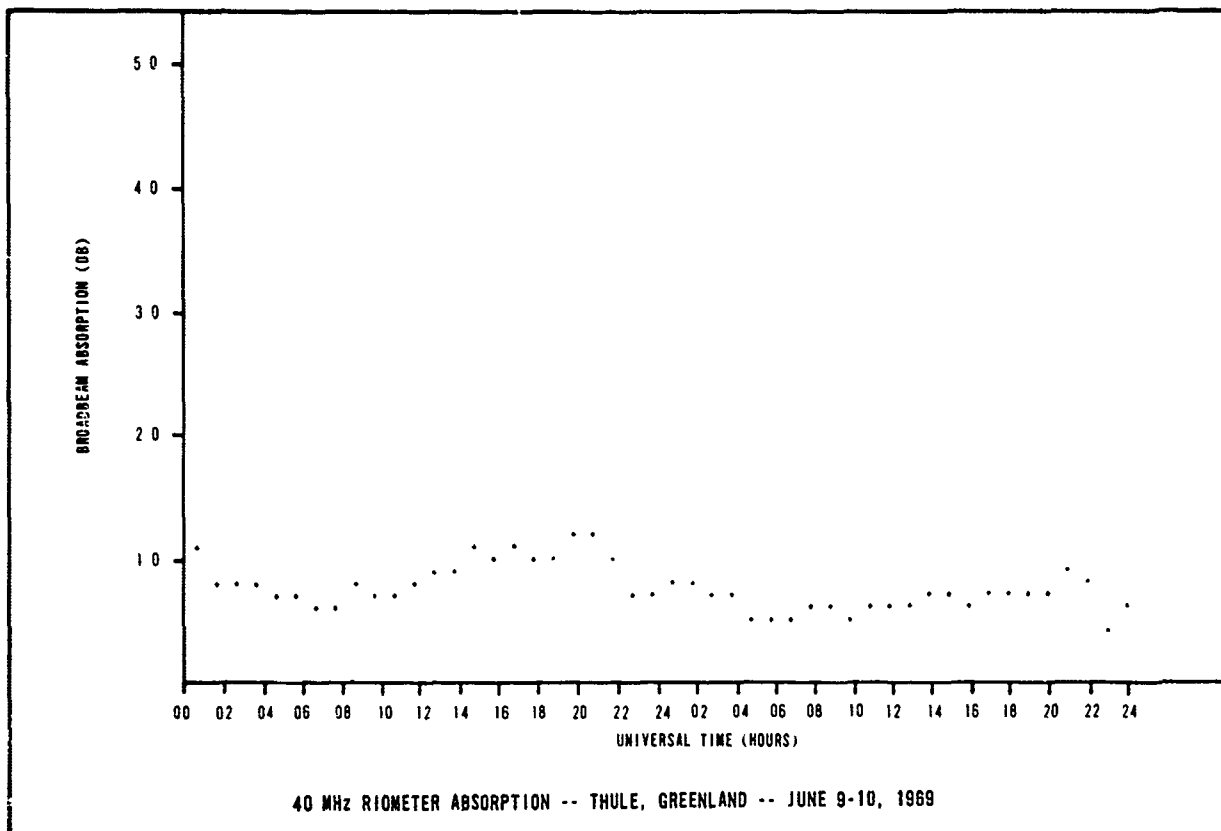


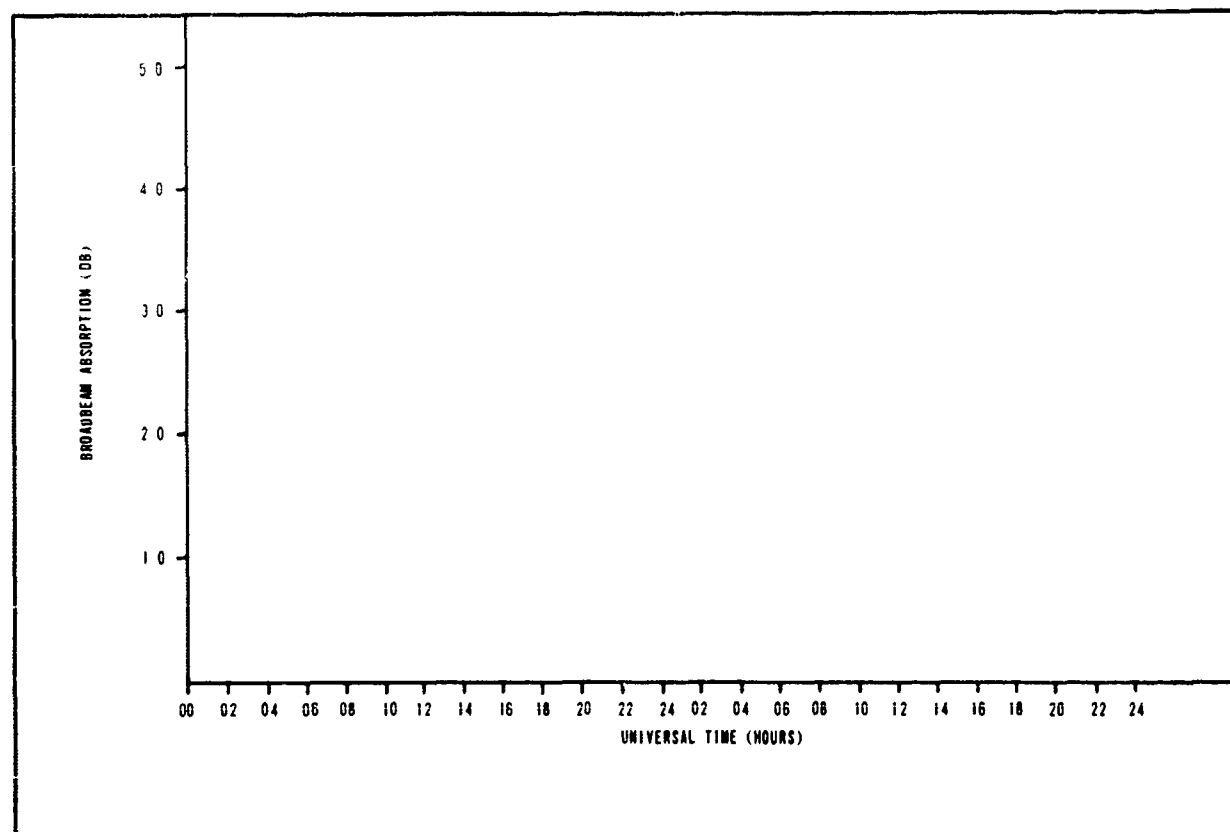
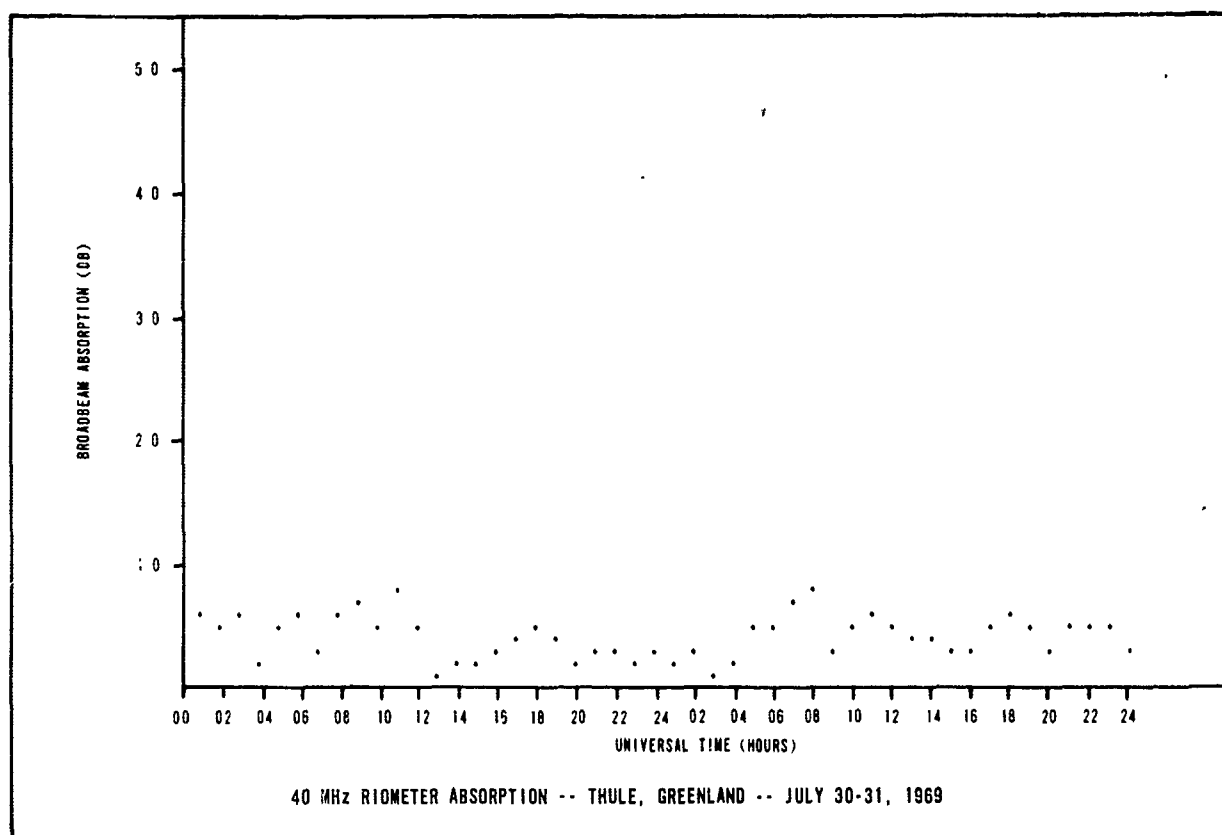


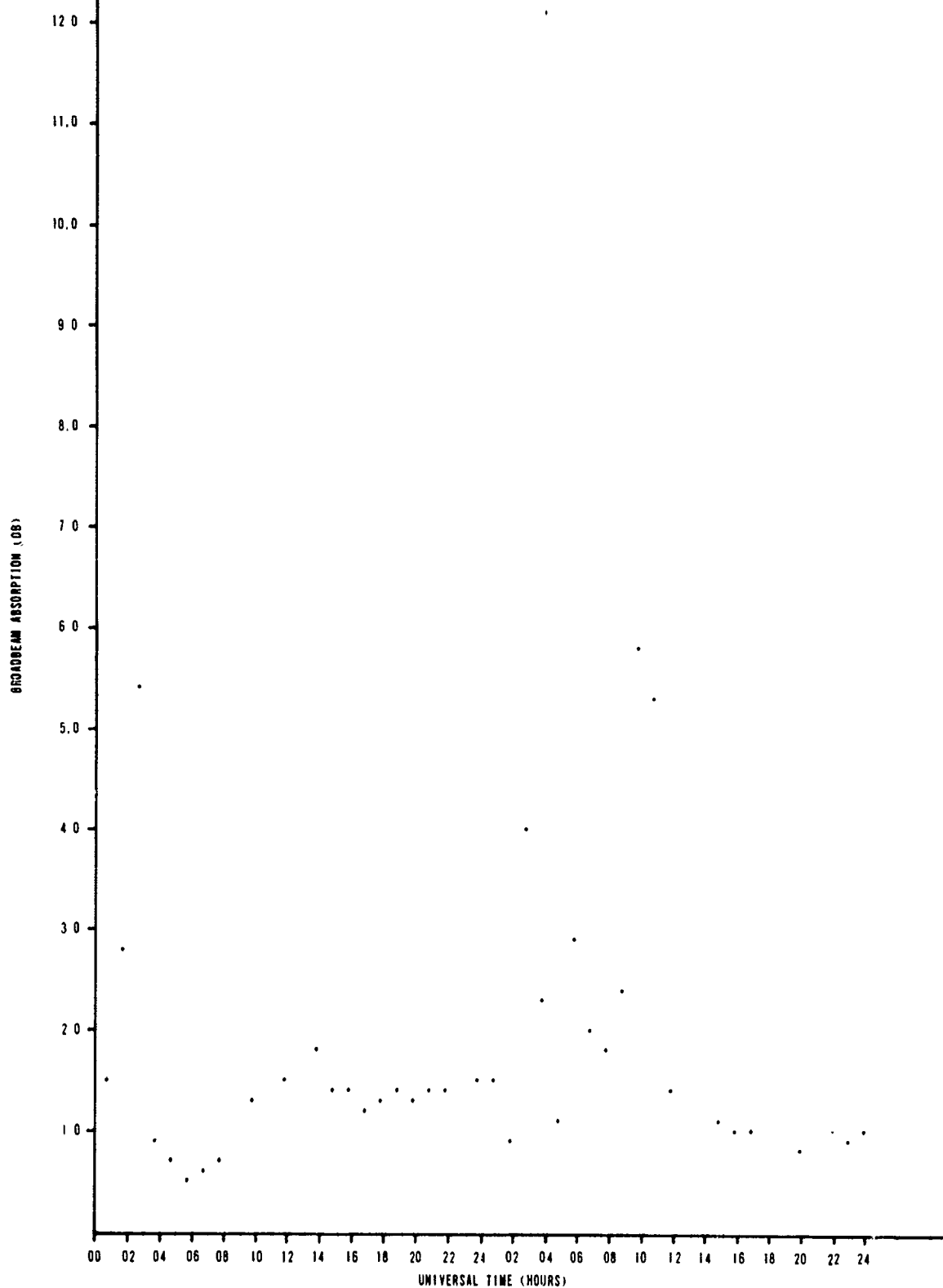






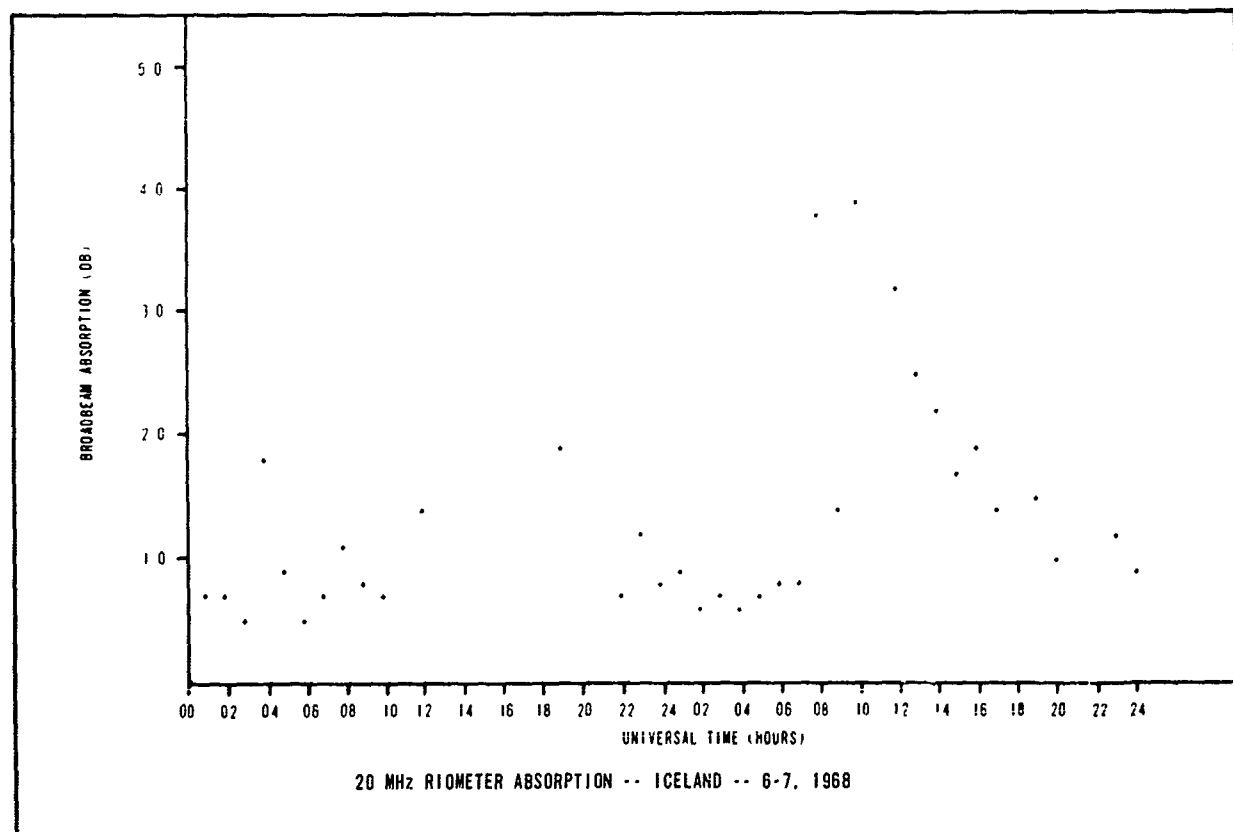
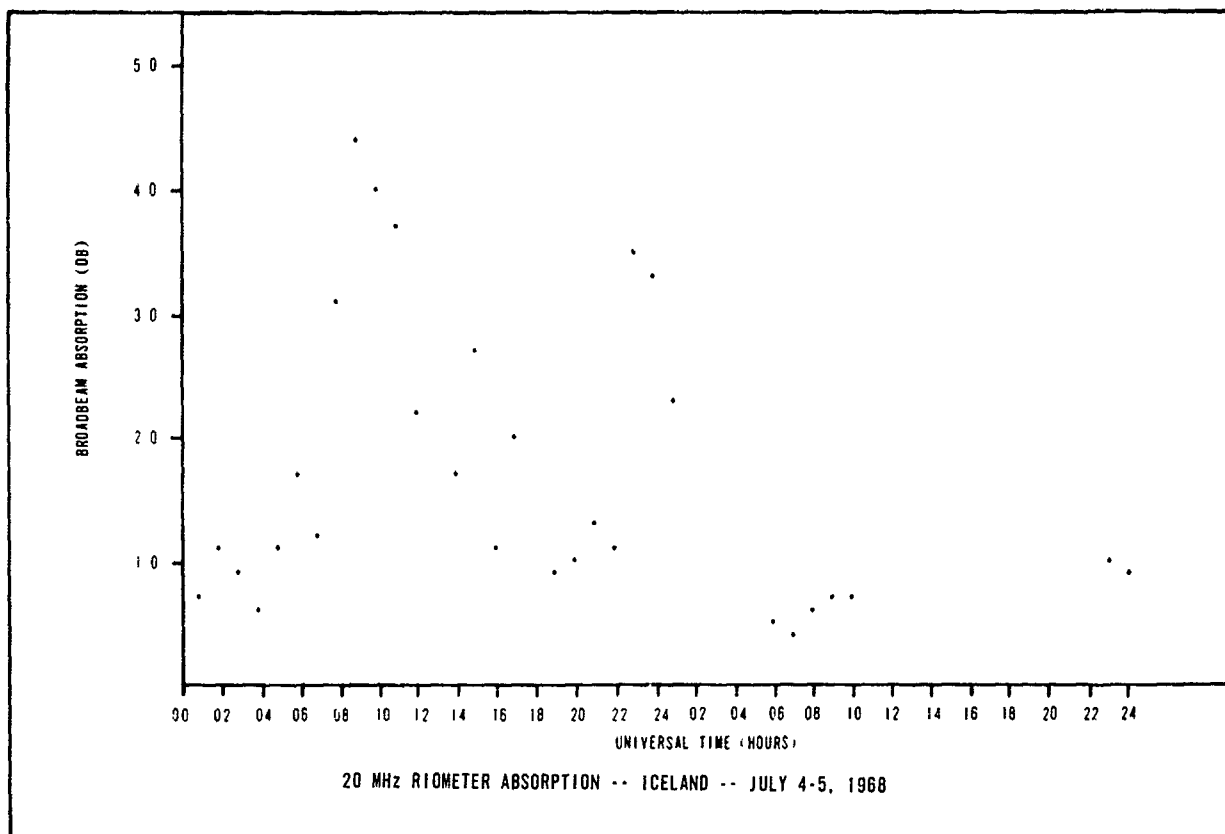


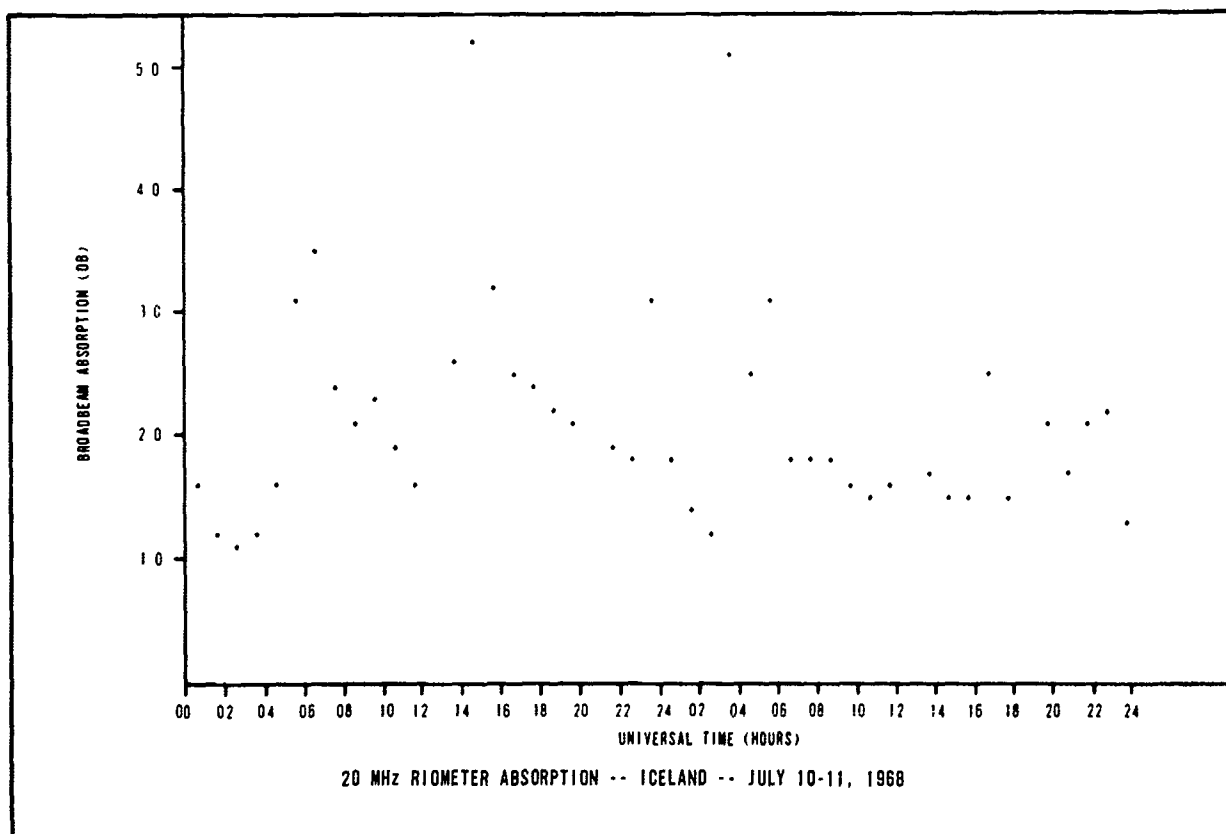
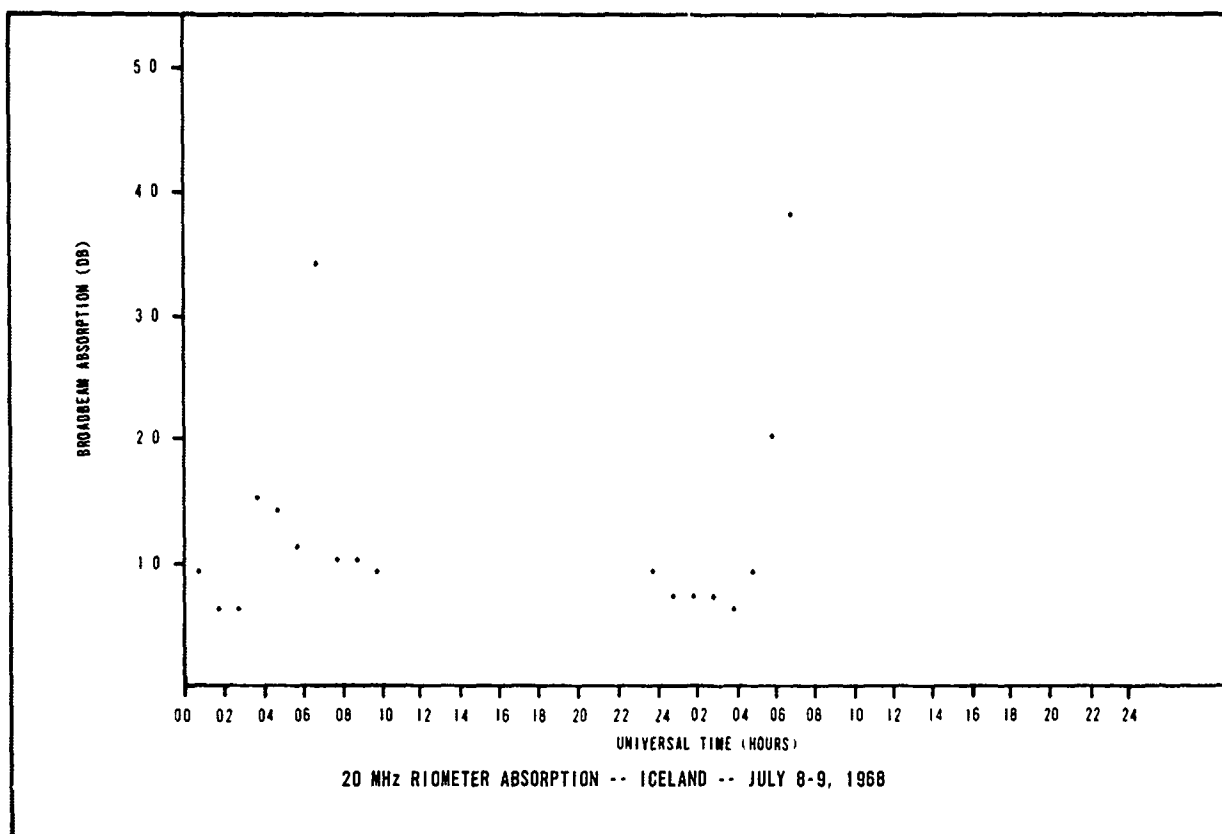


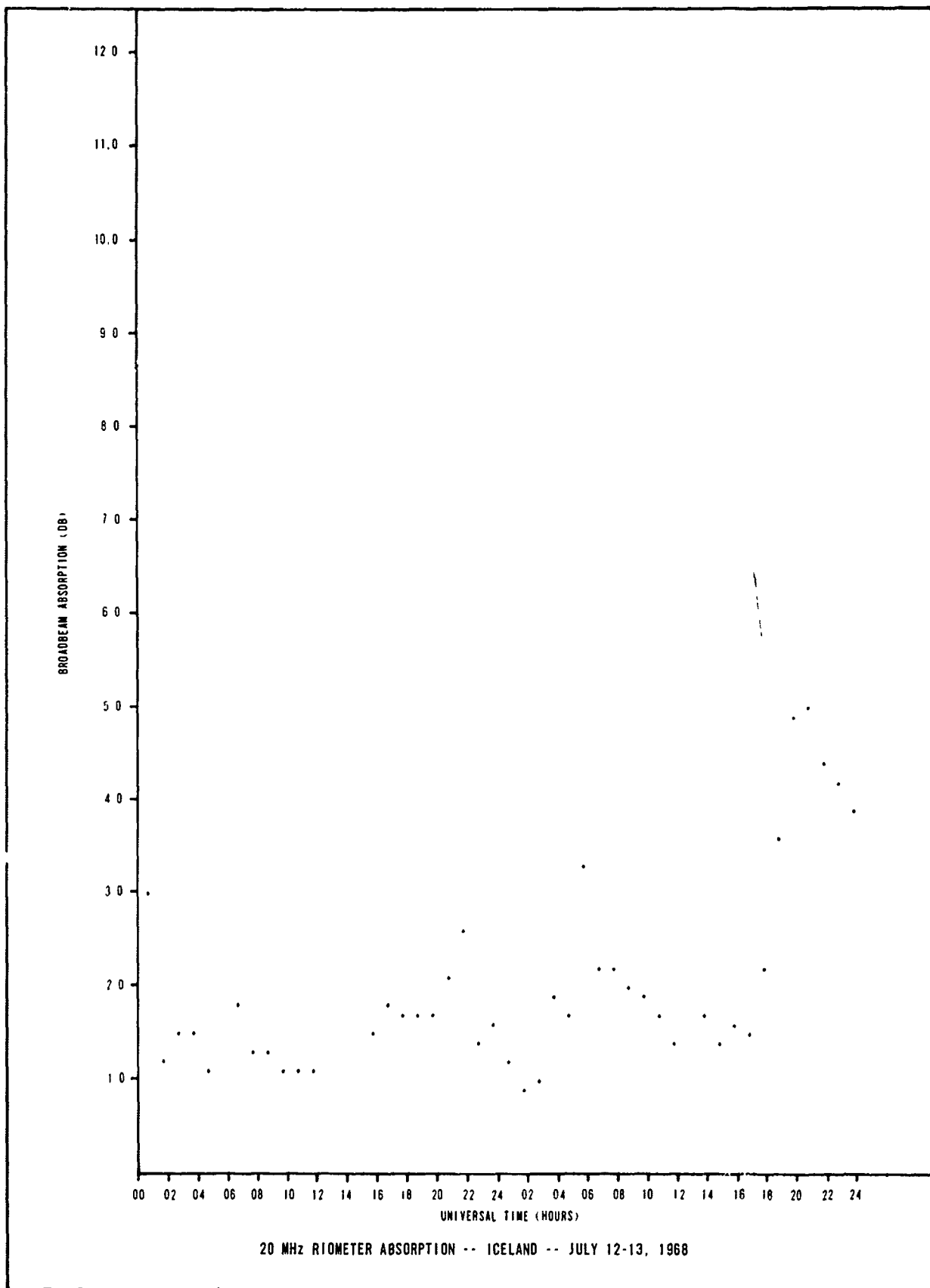


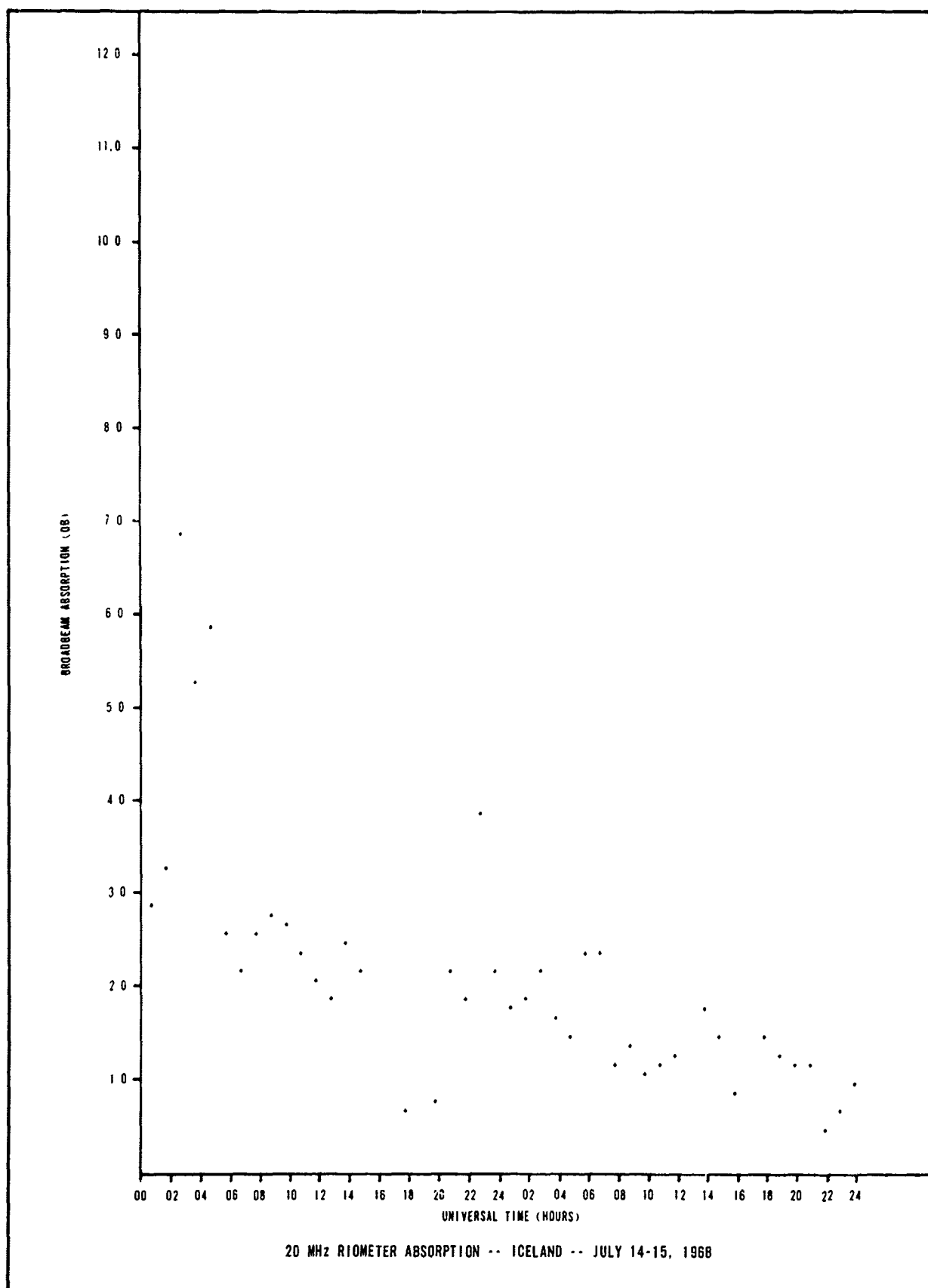
20 MHz RIOMETER ABSORPTION -- ICELAND -- JULY 2-3, 1968

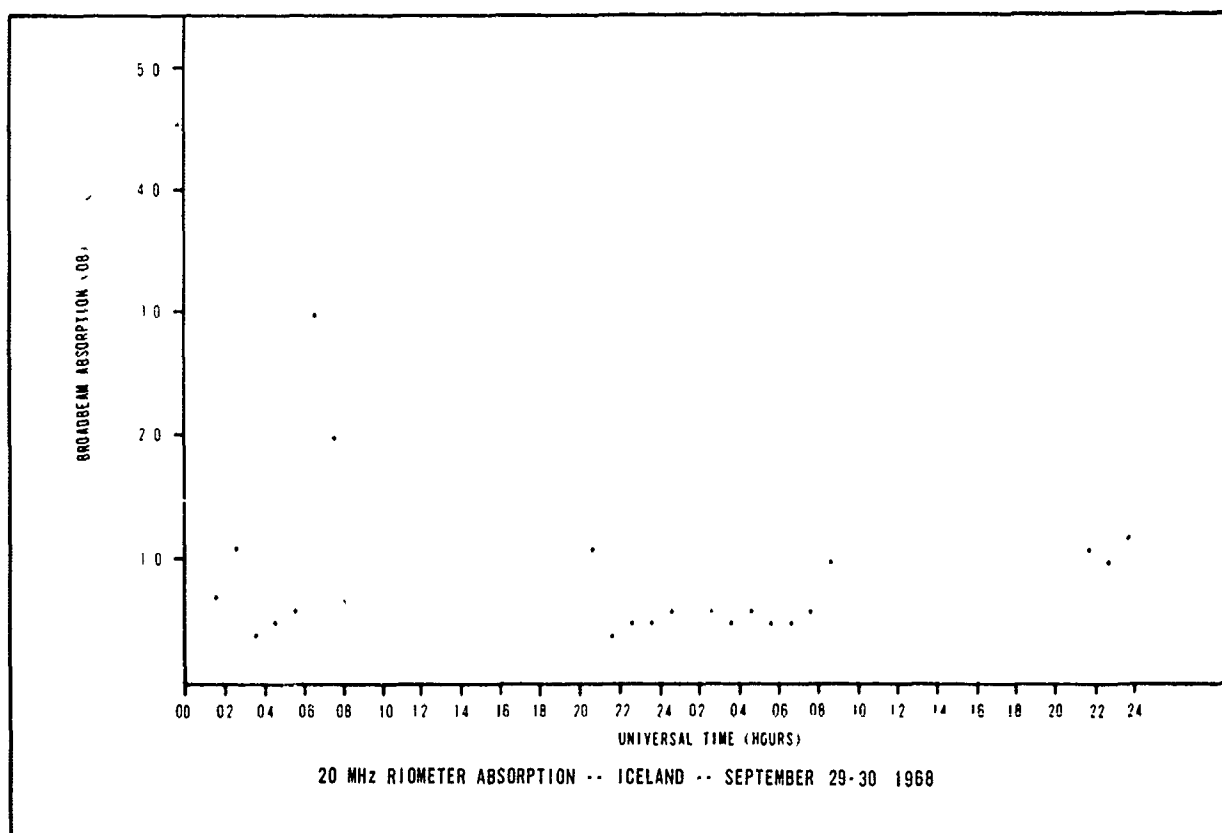
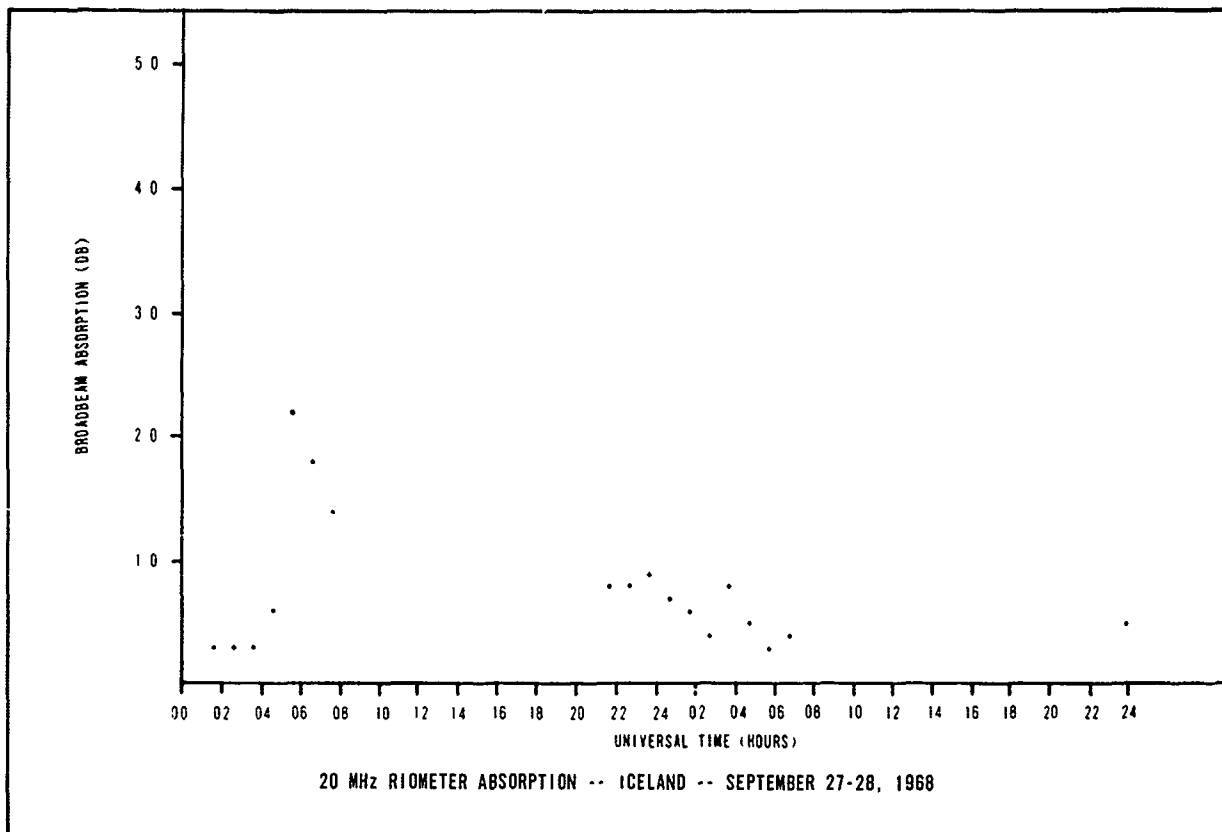


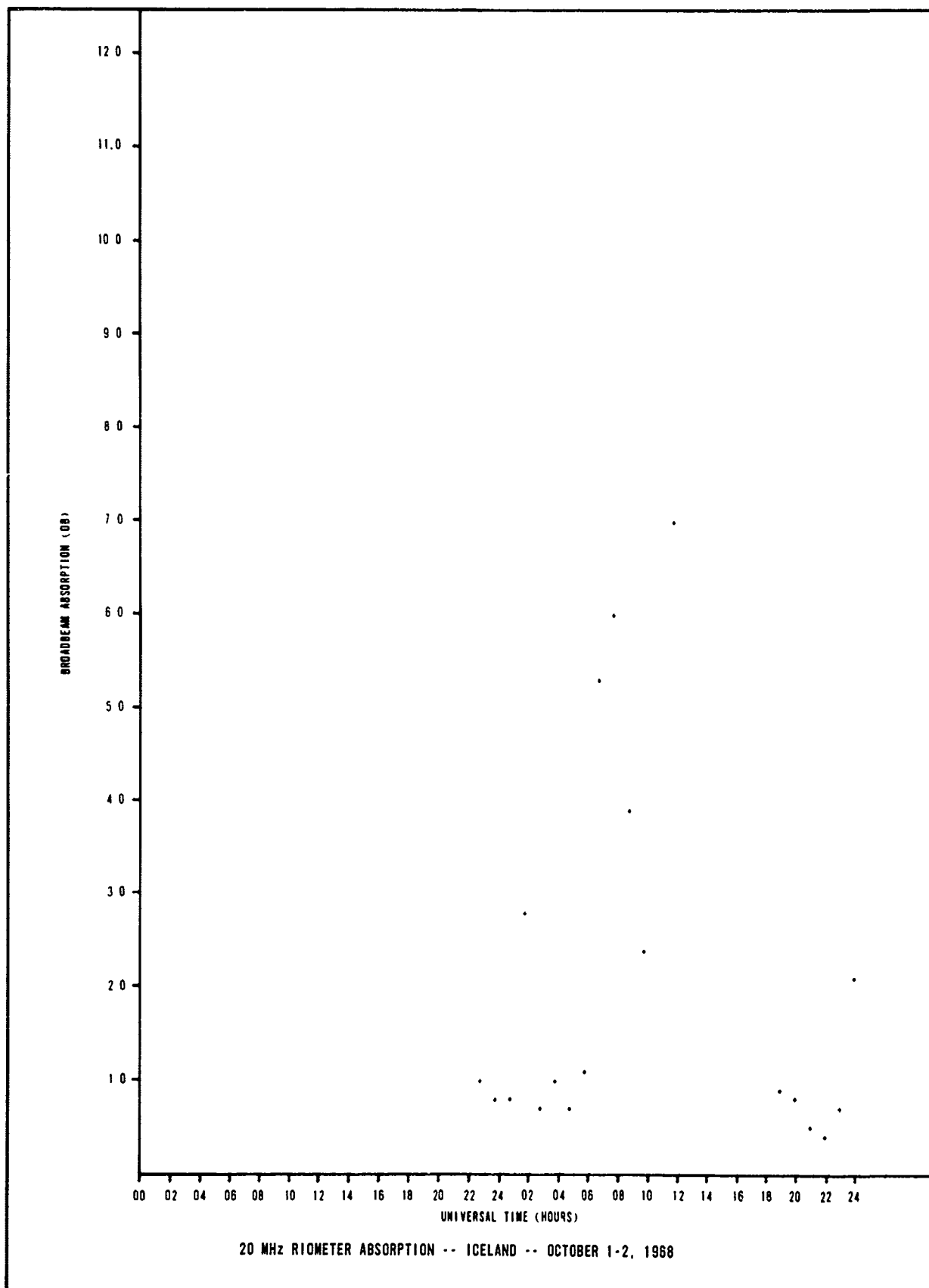


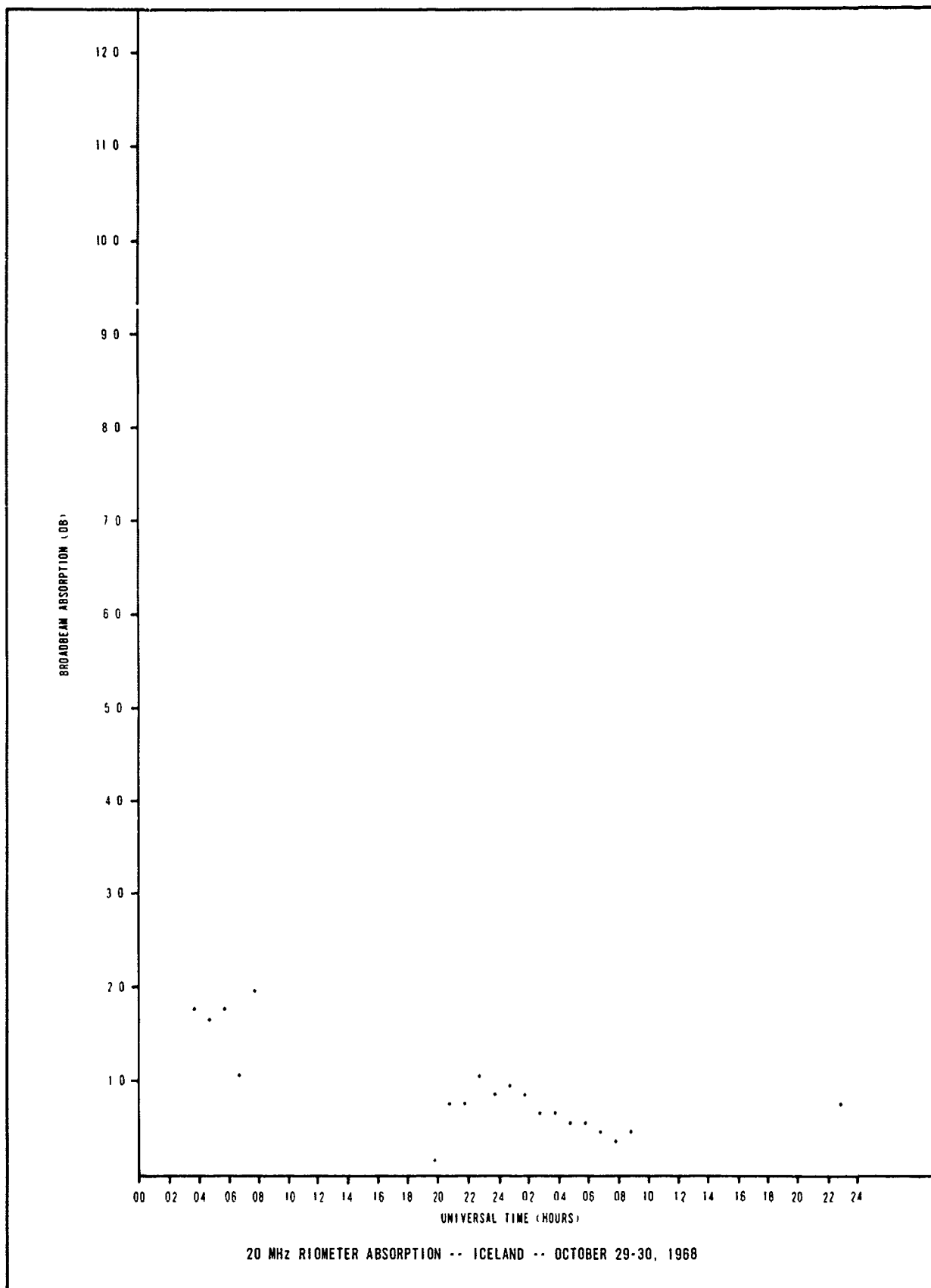


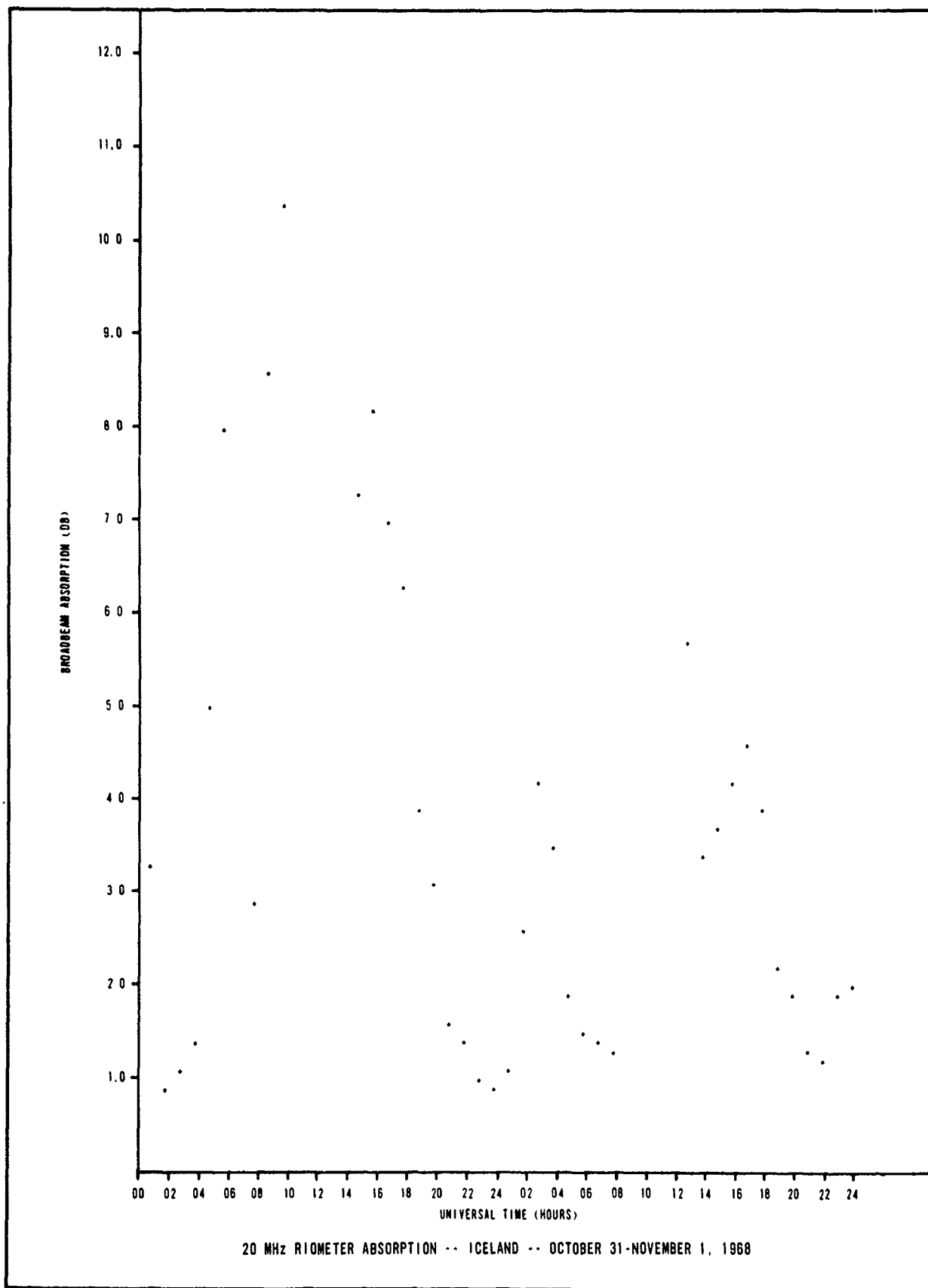






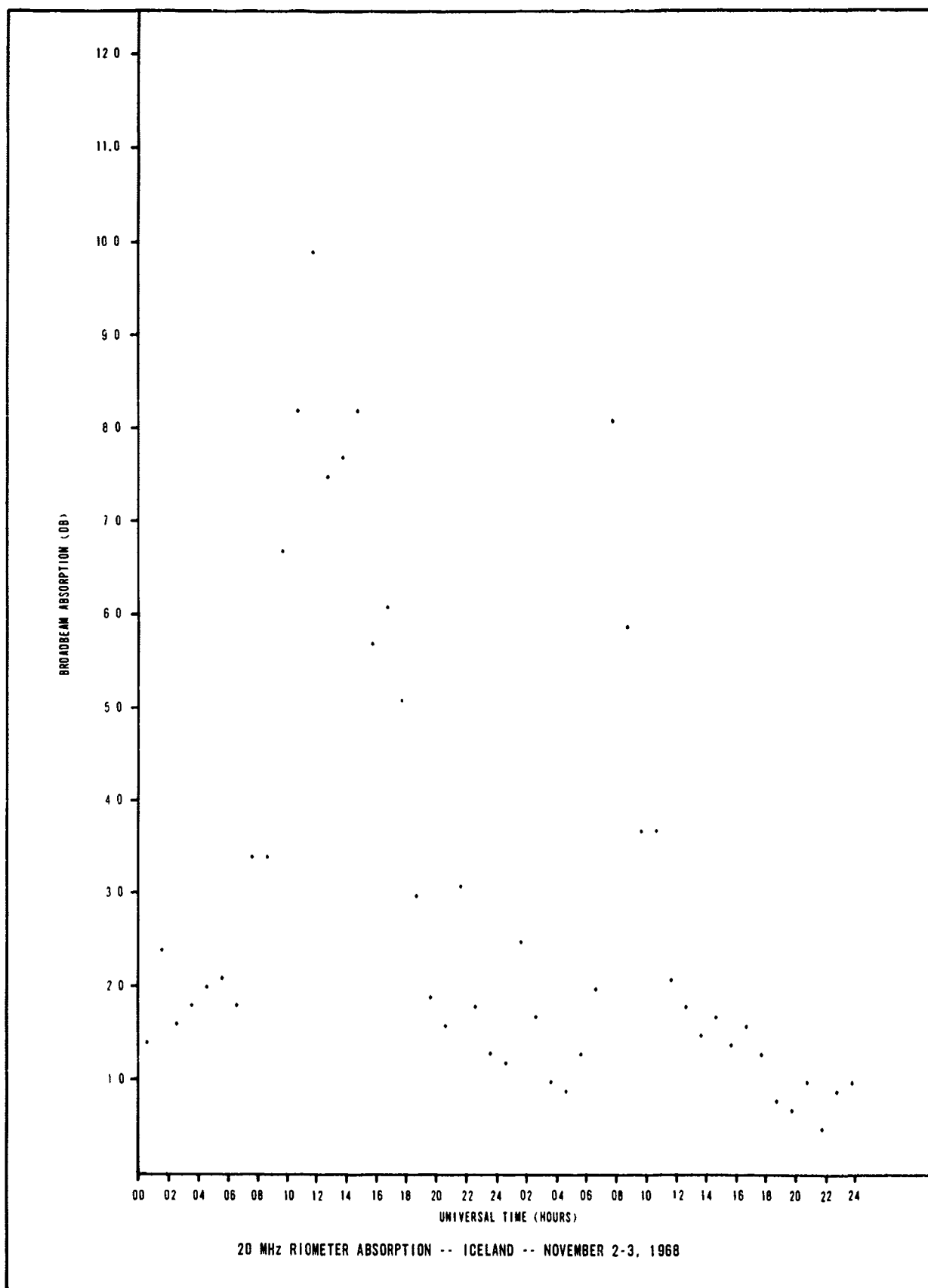


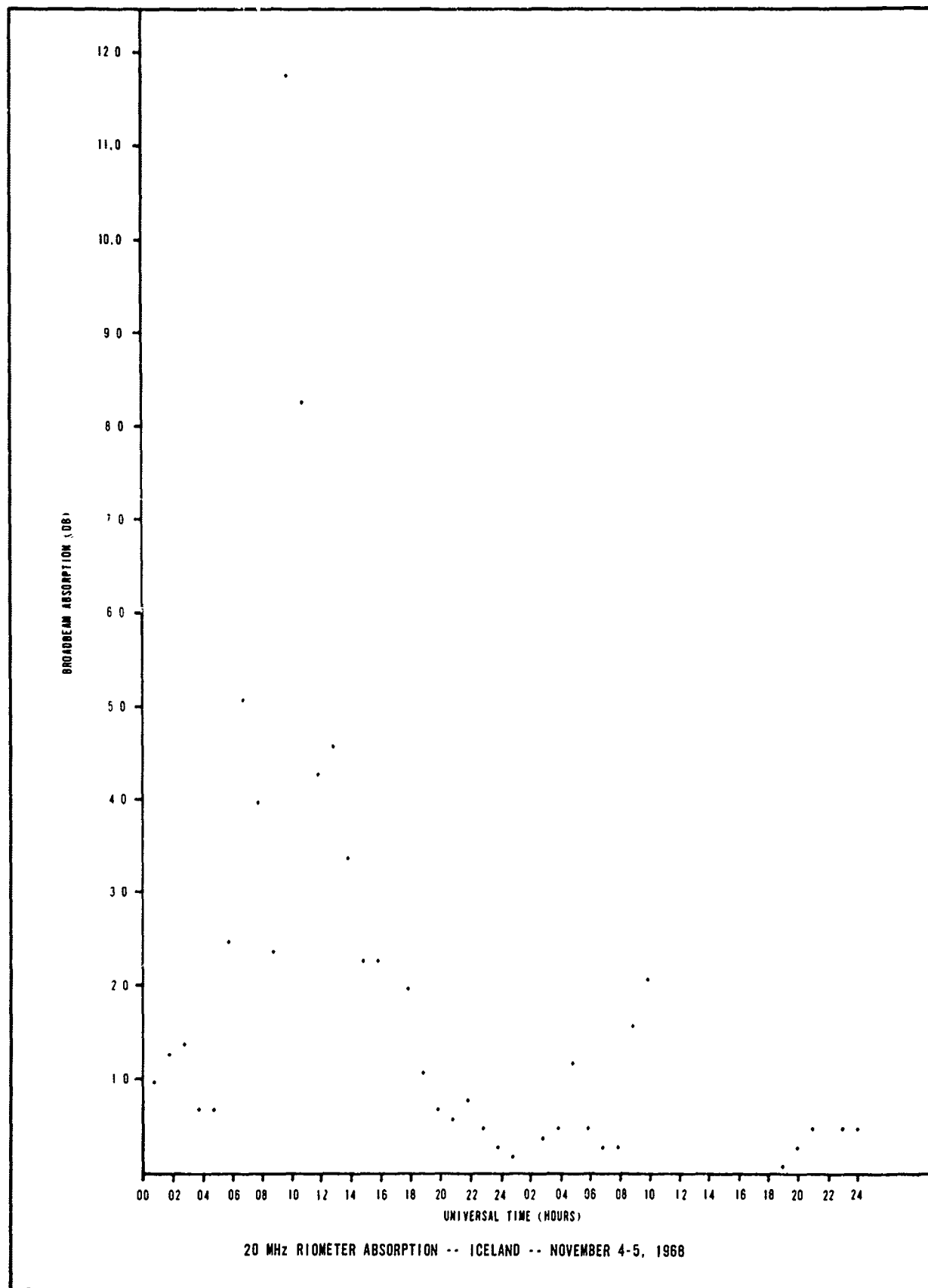




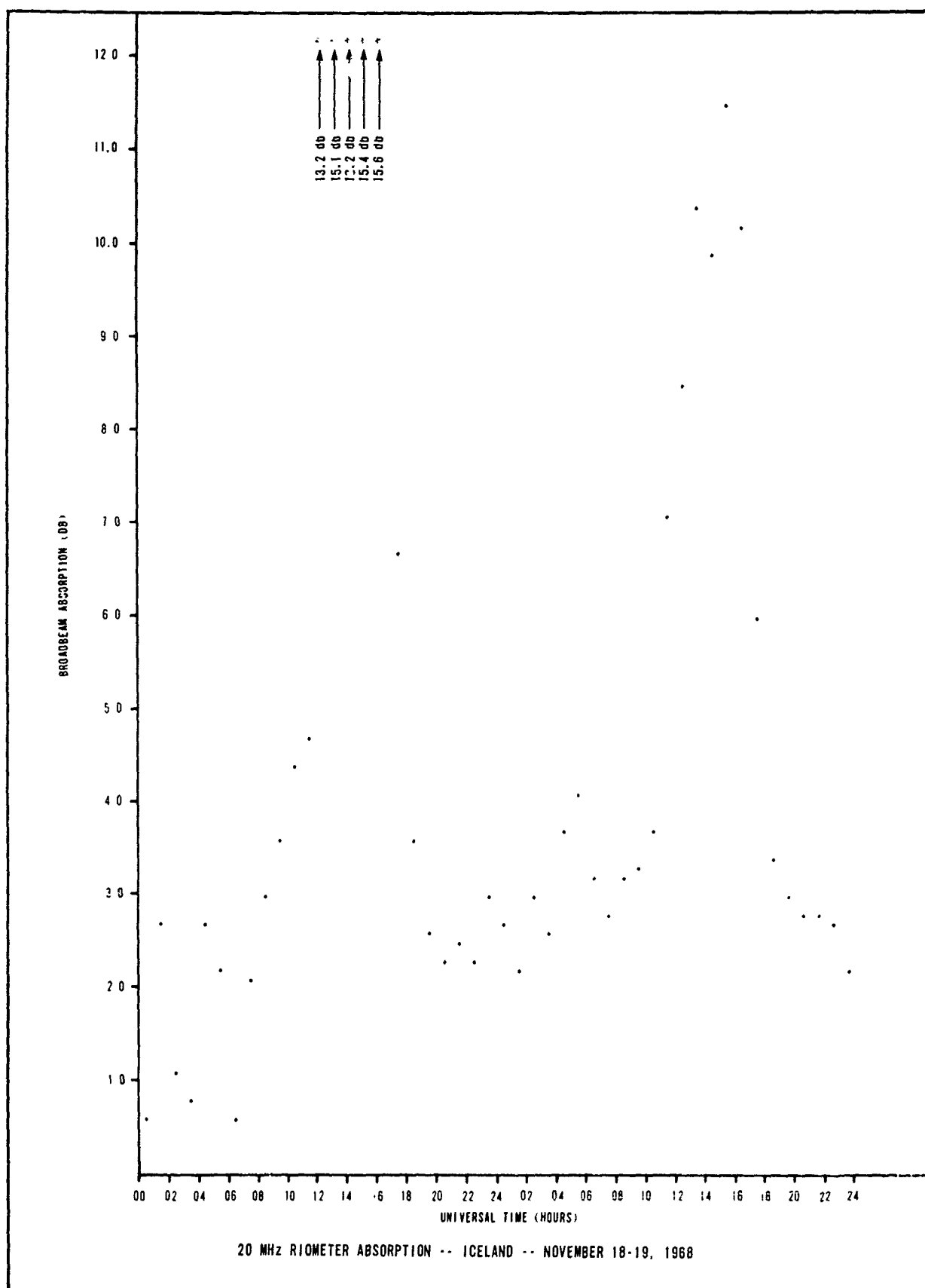
B-94

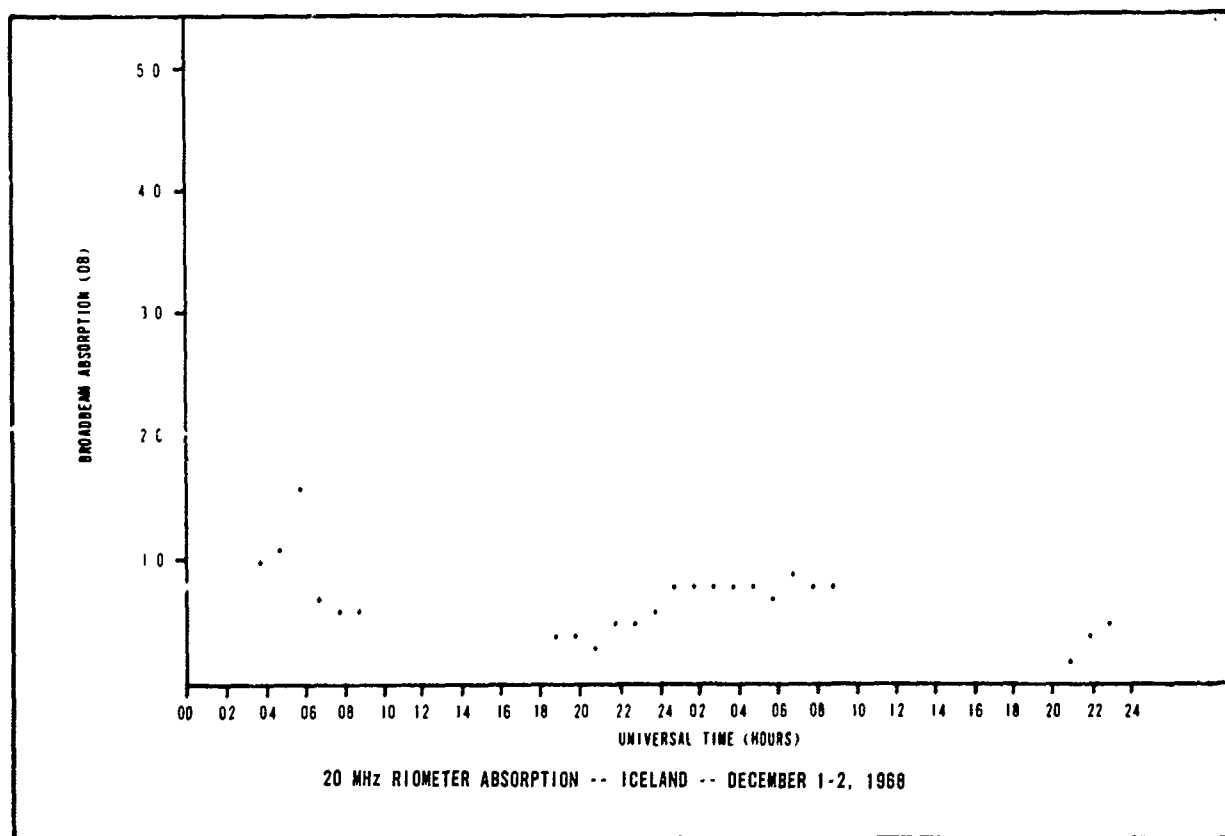
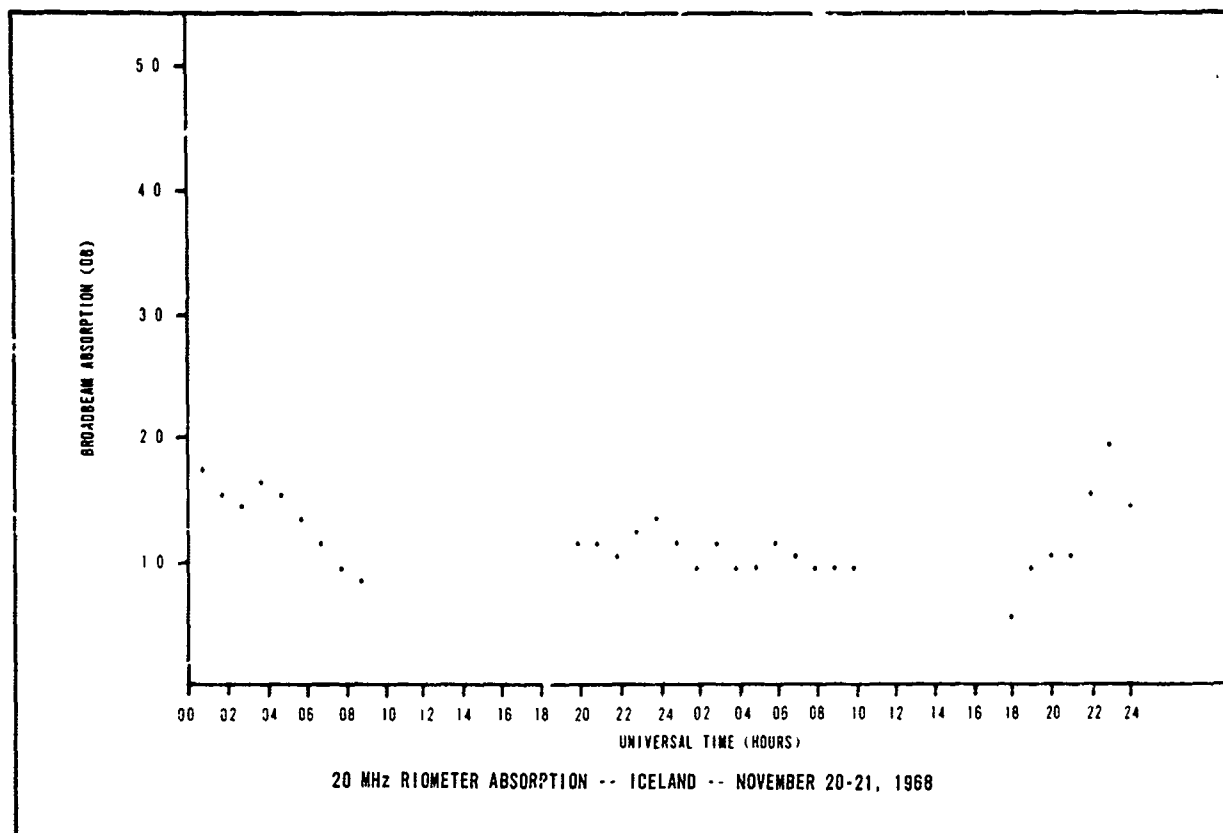


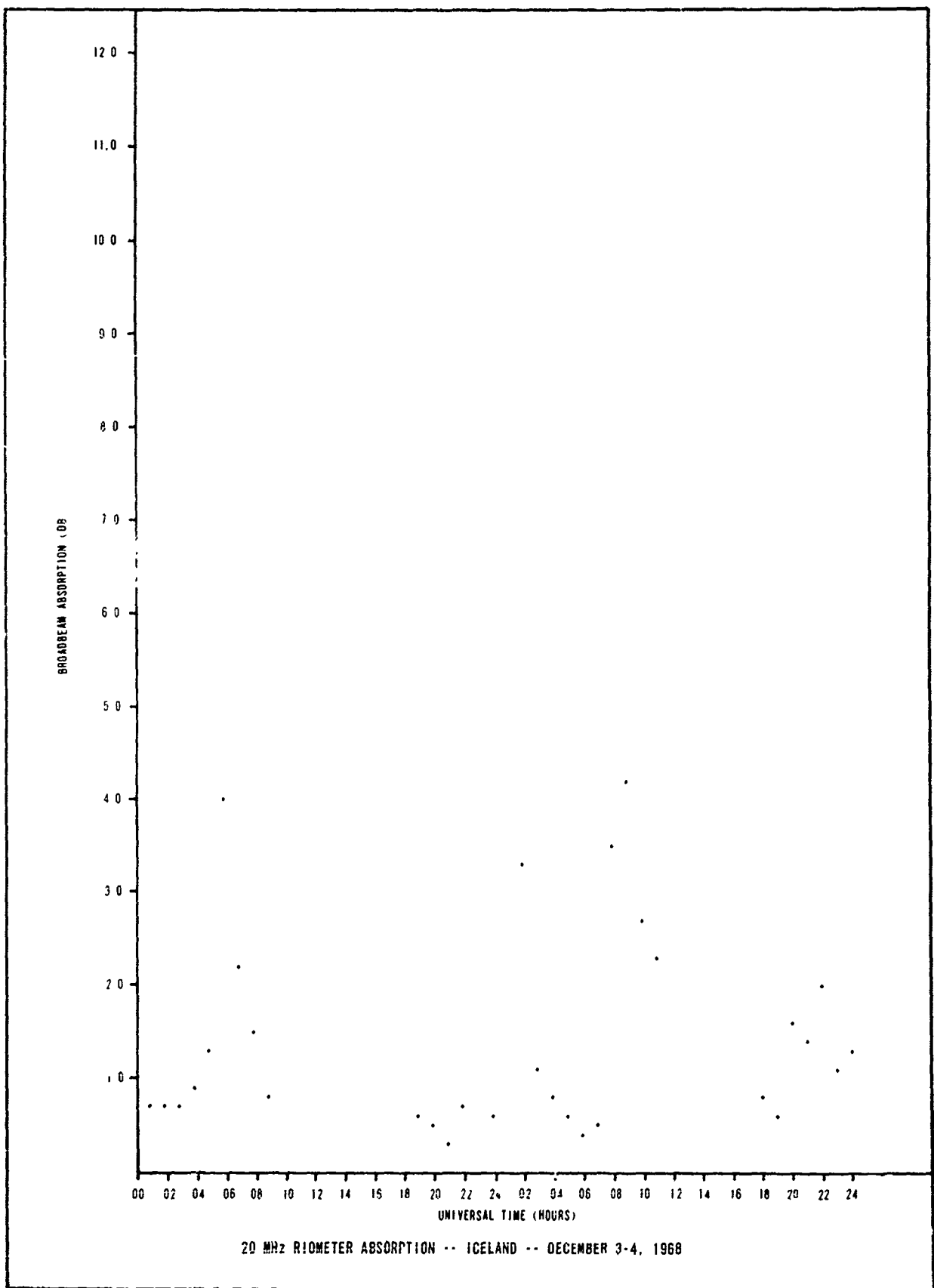


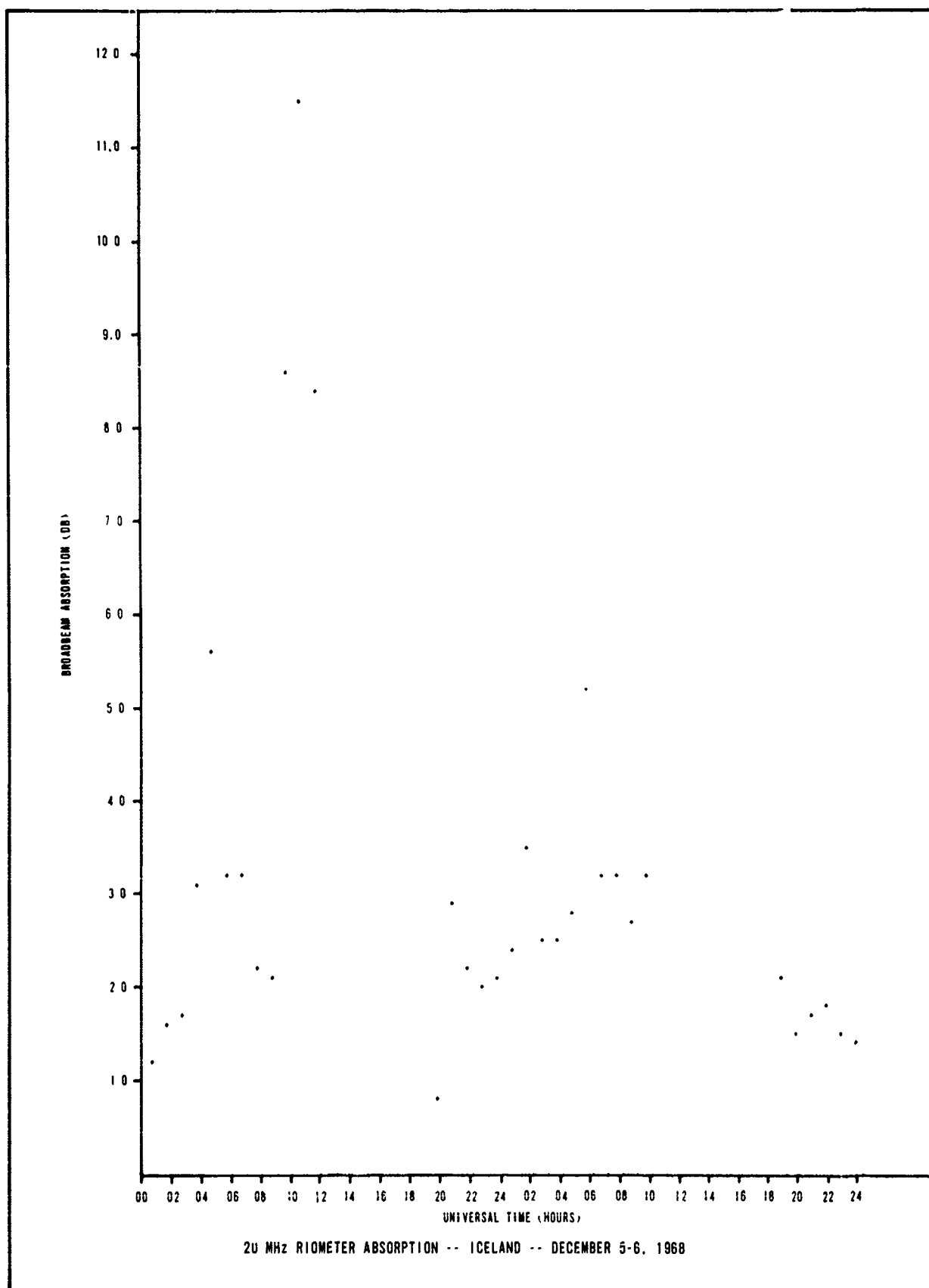


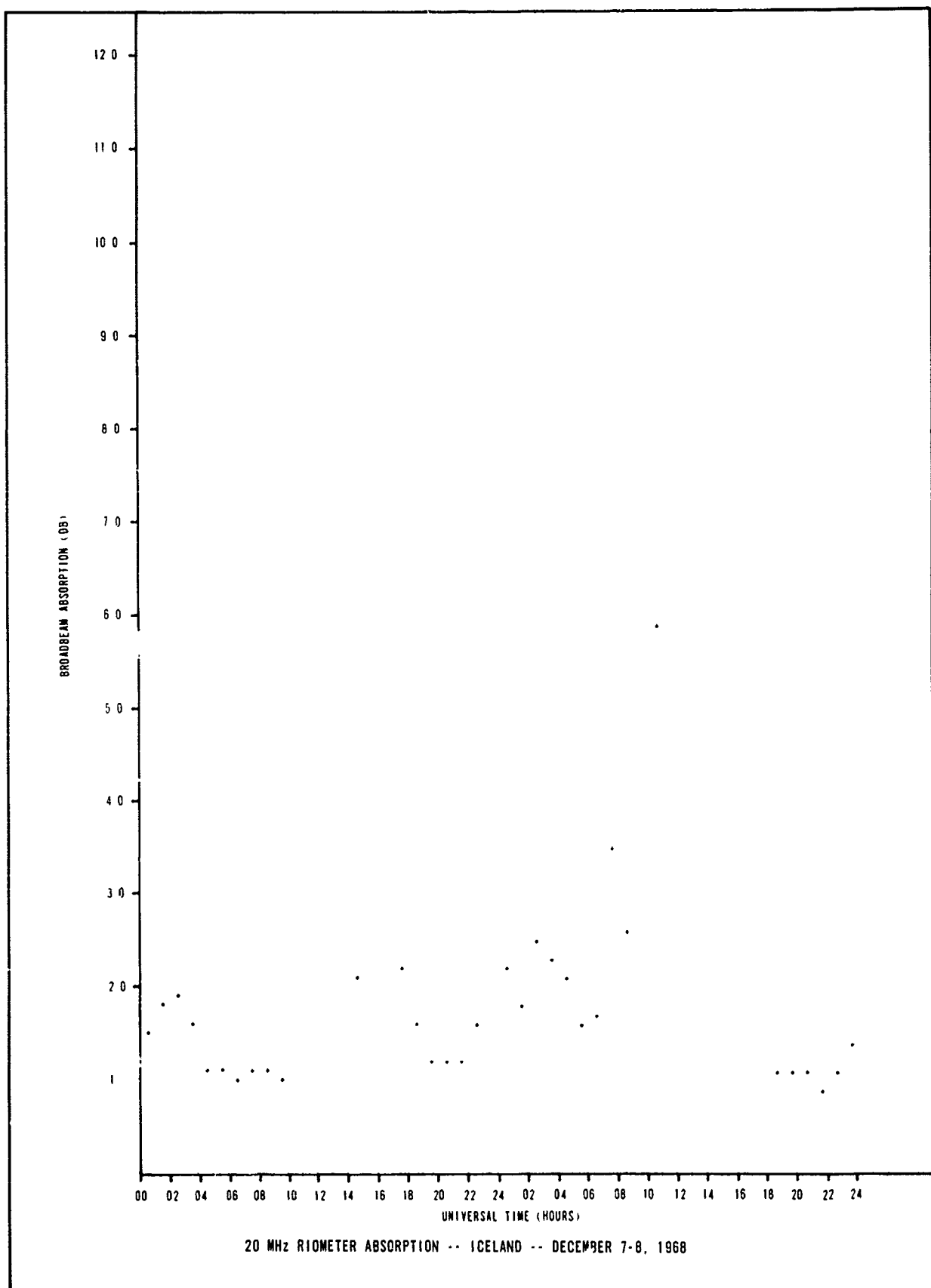
B-96

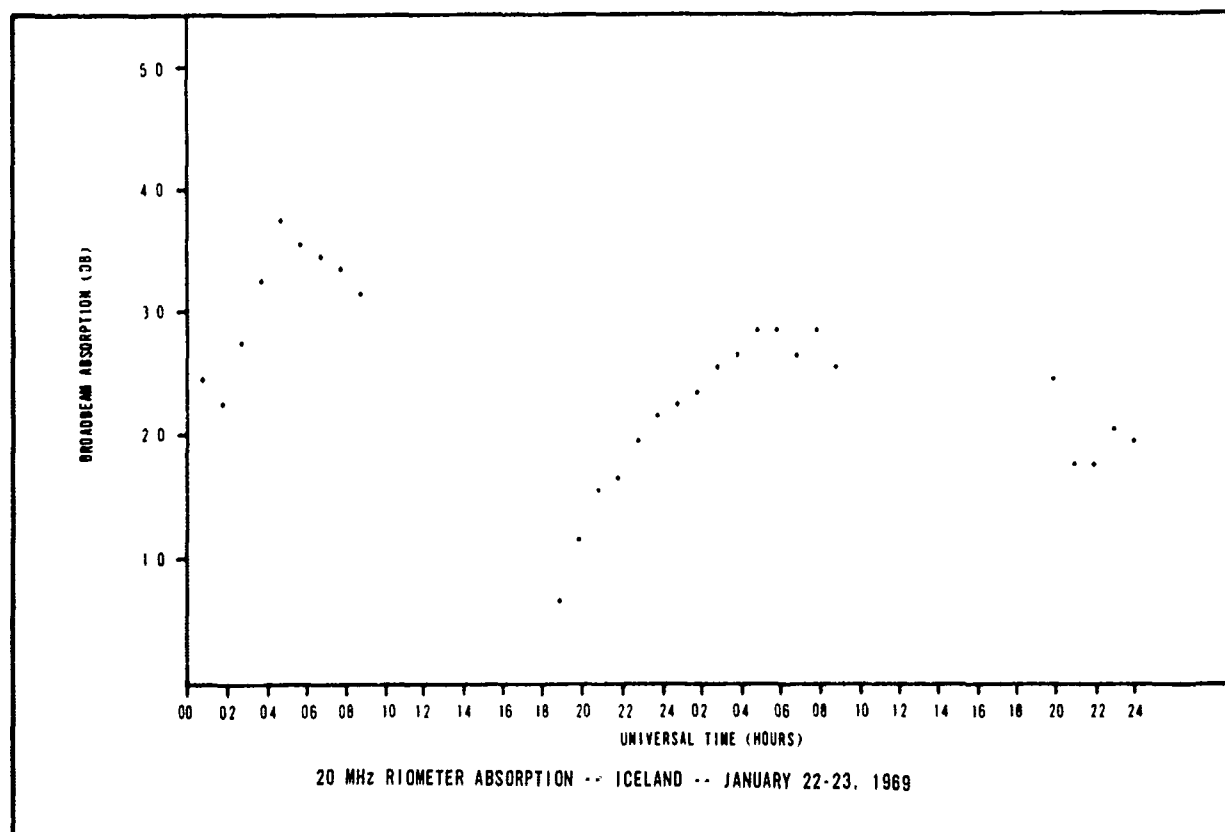
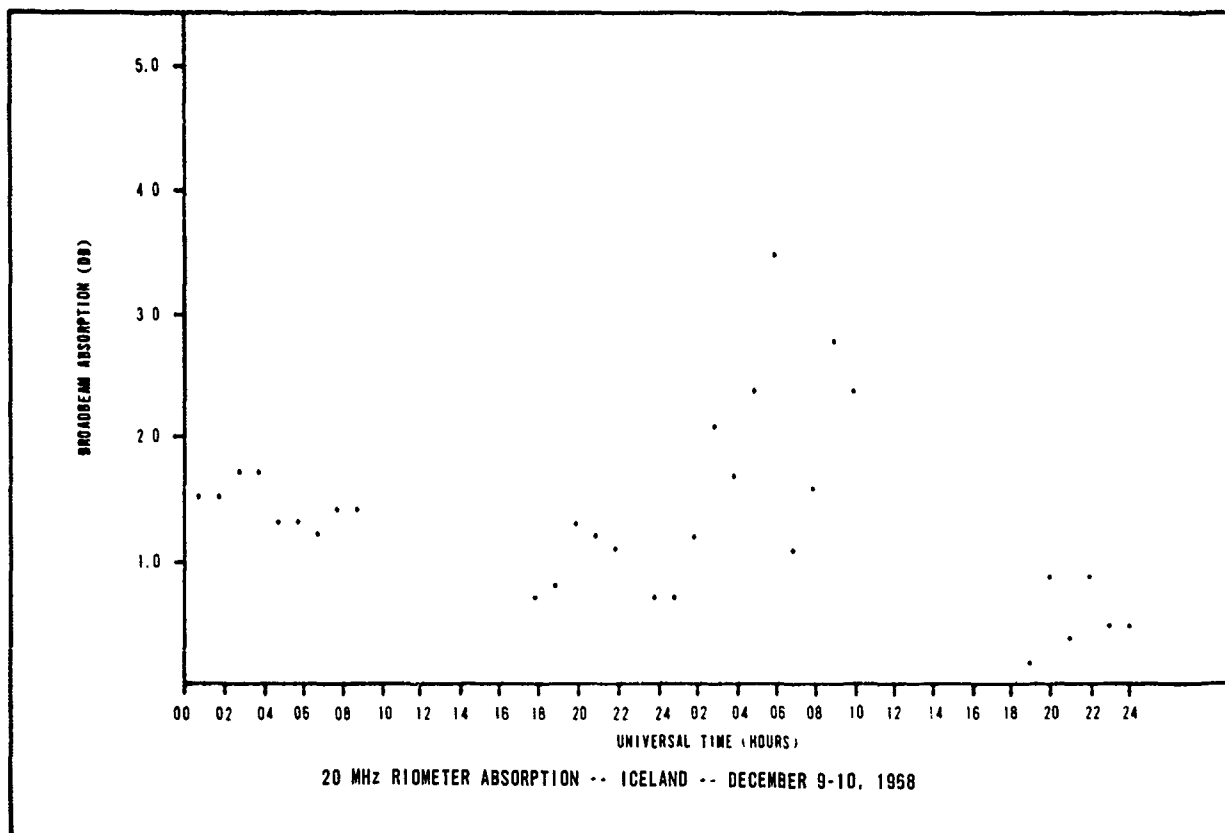




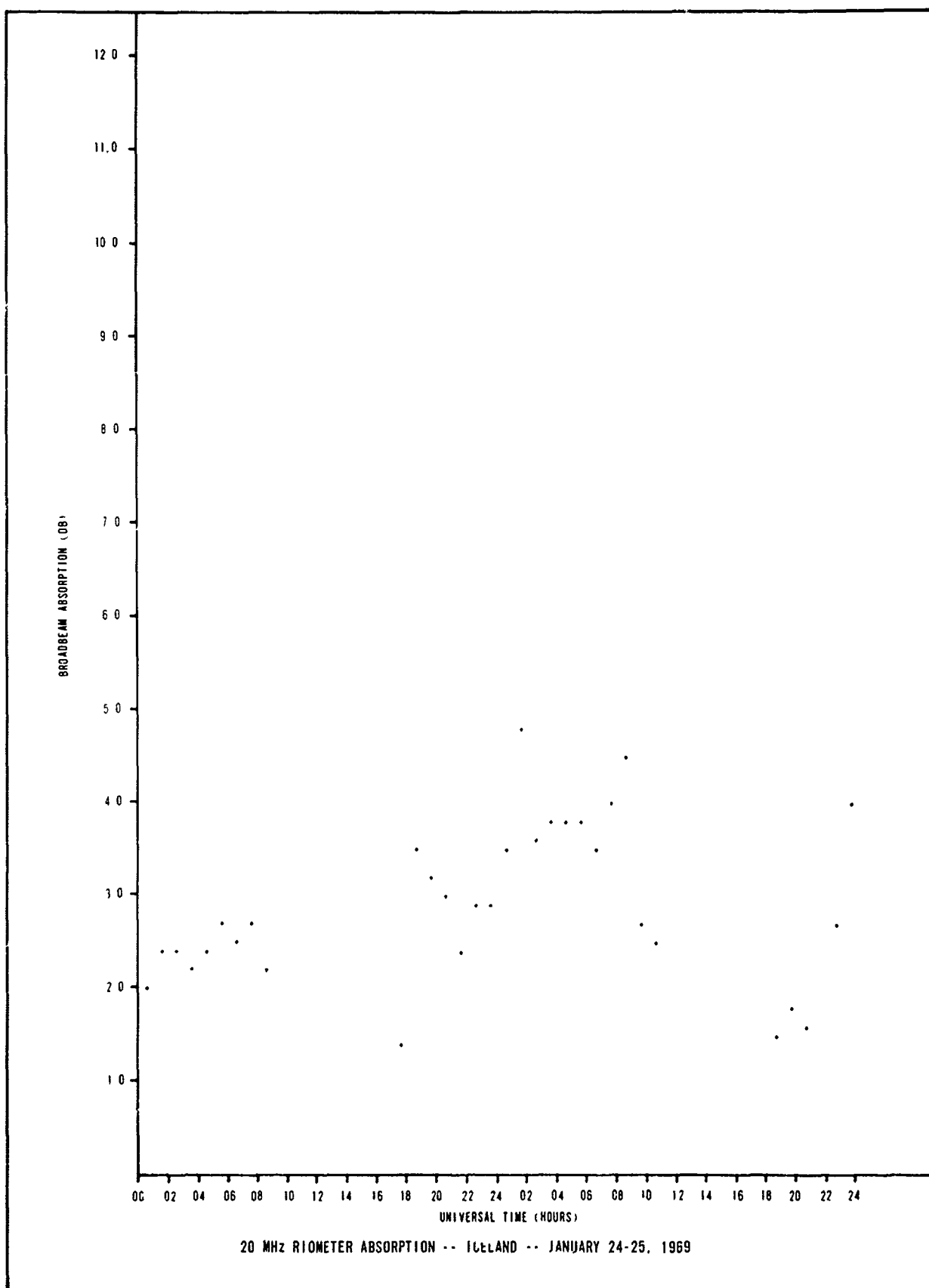


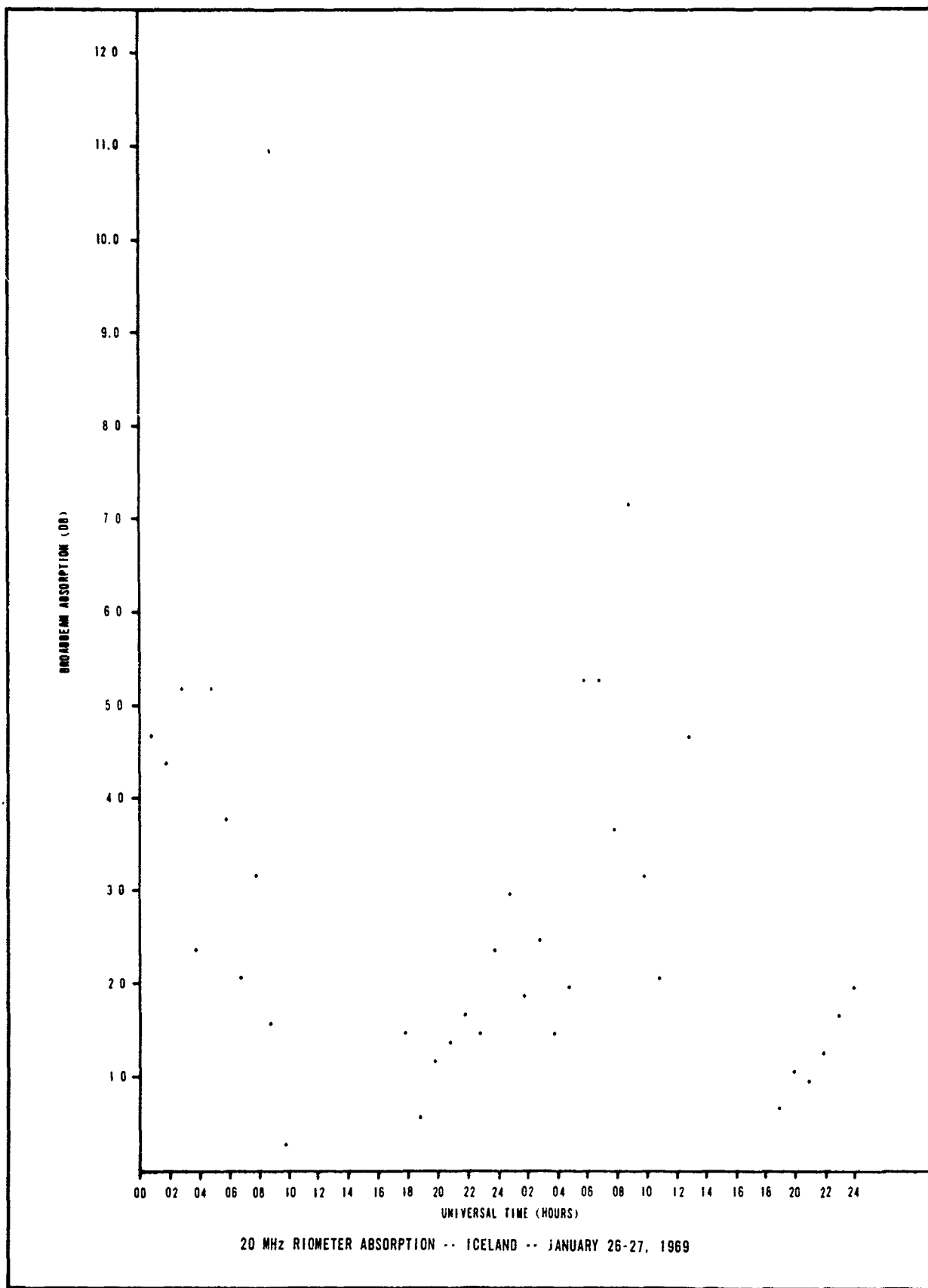




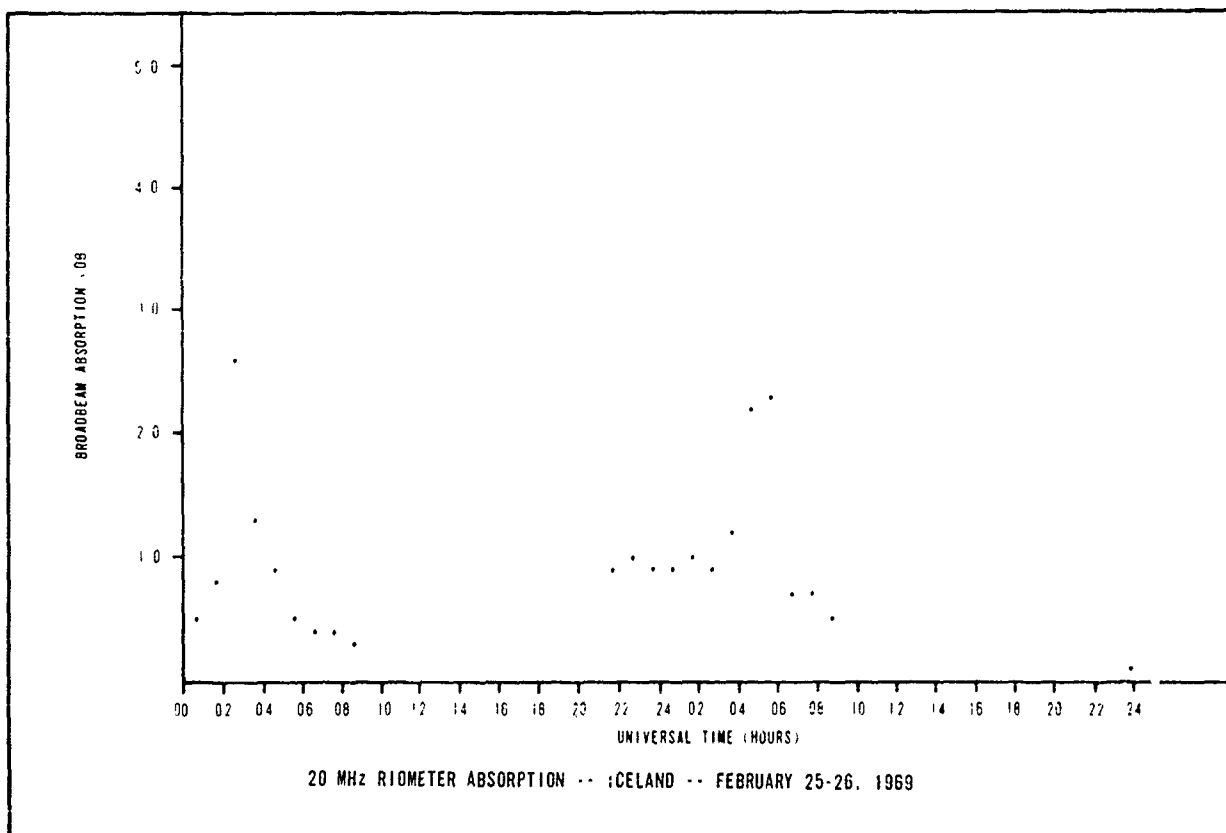
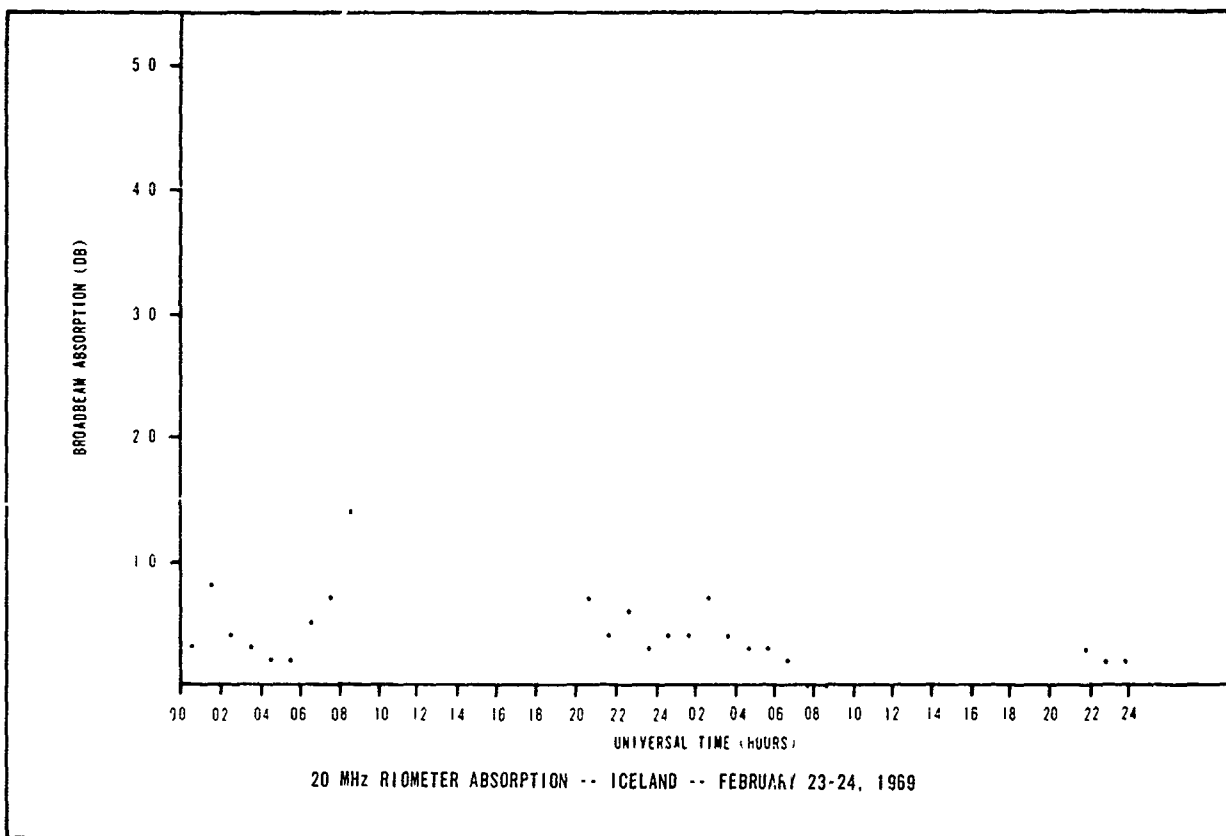


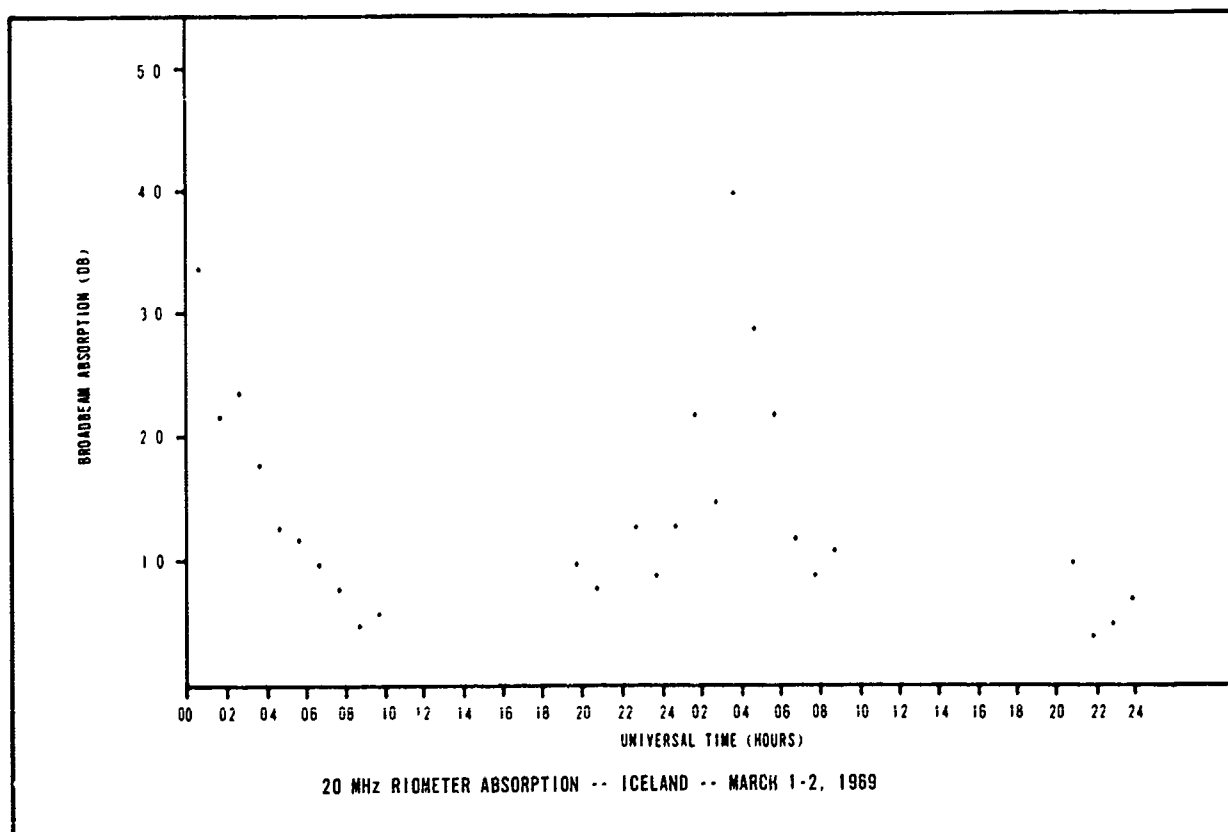
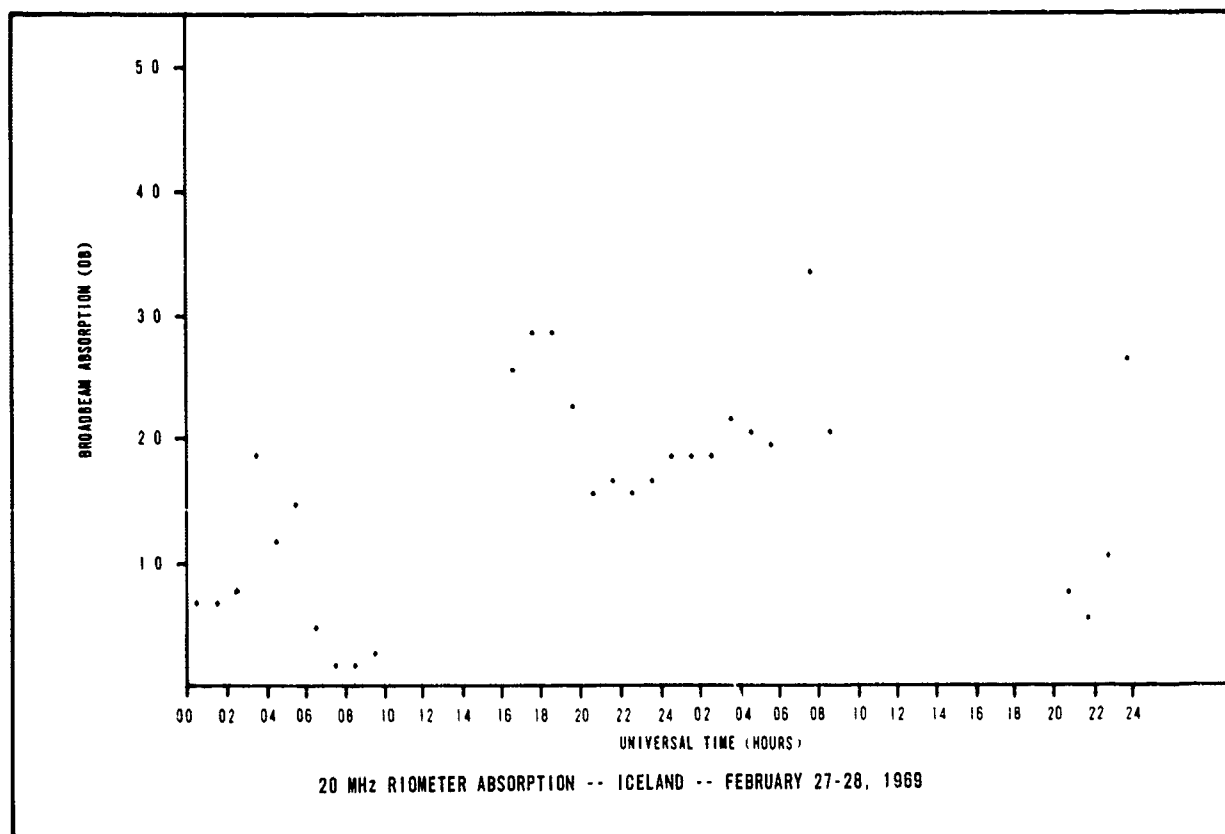


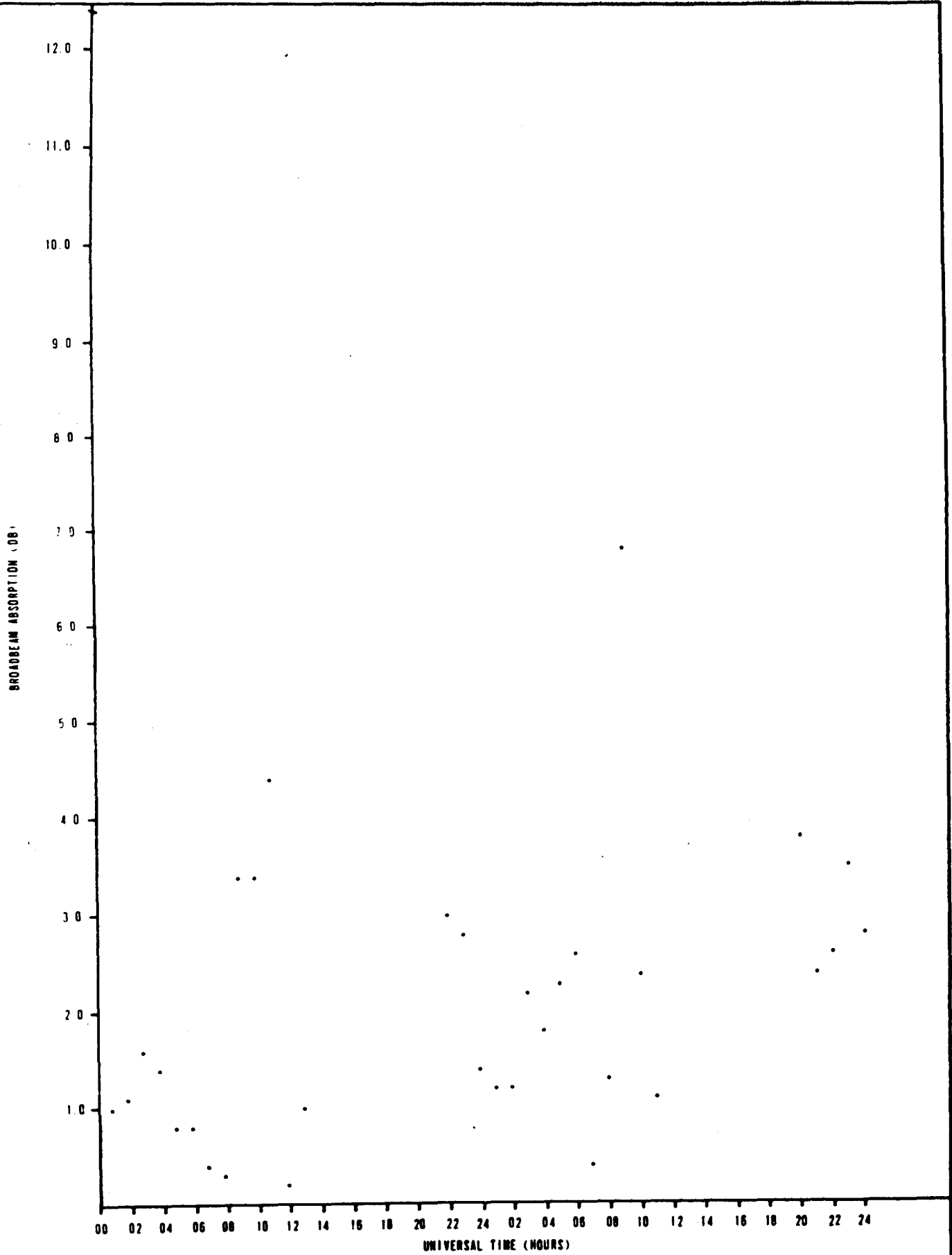




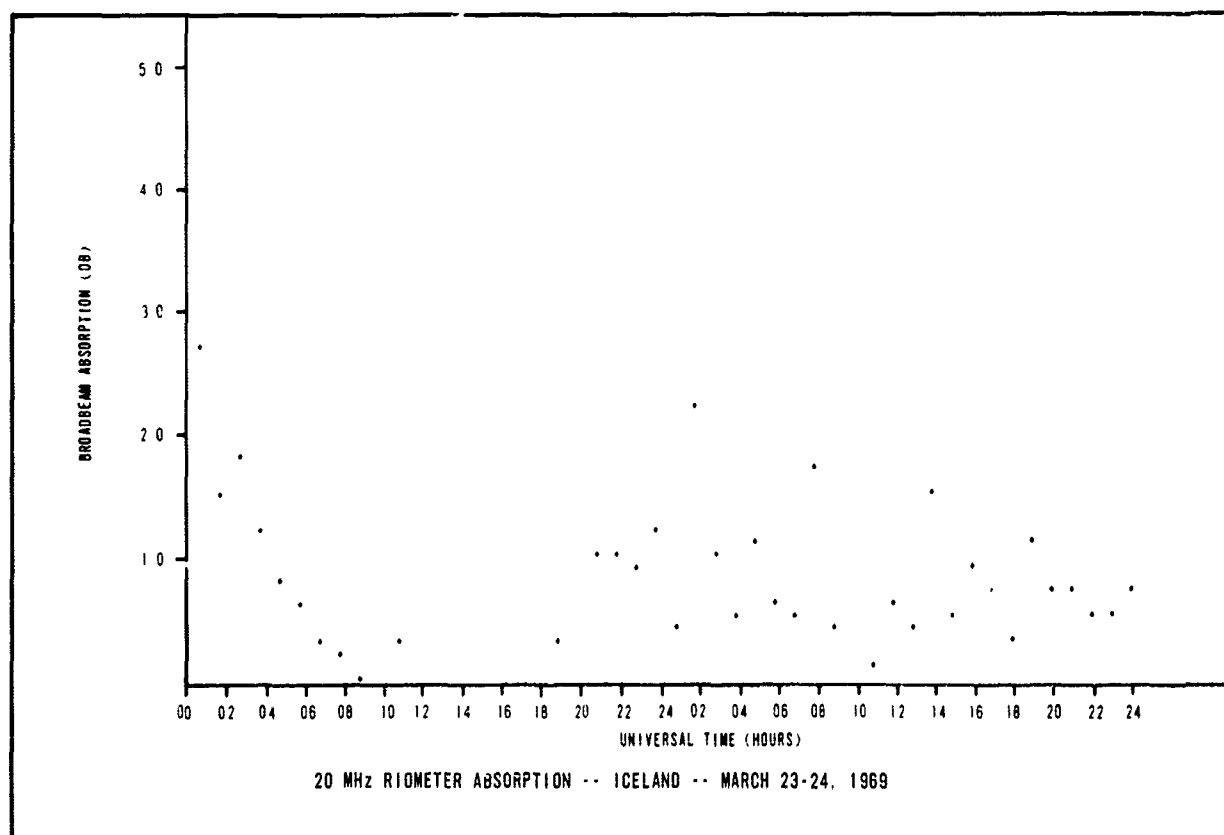
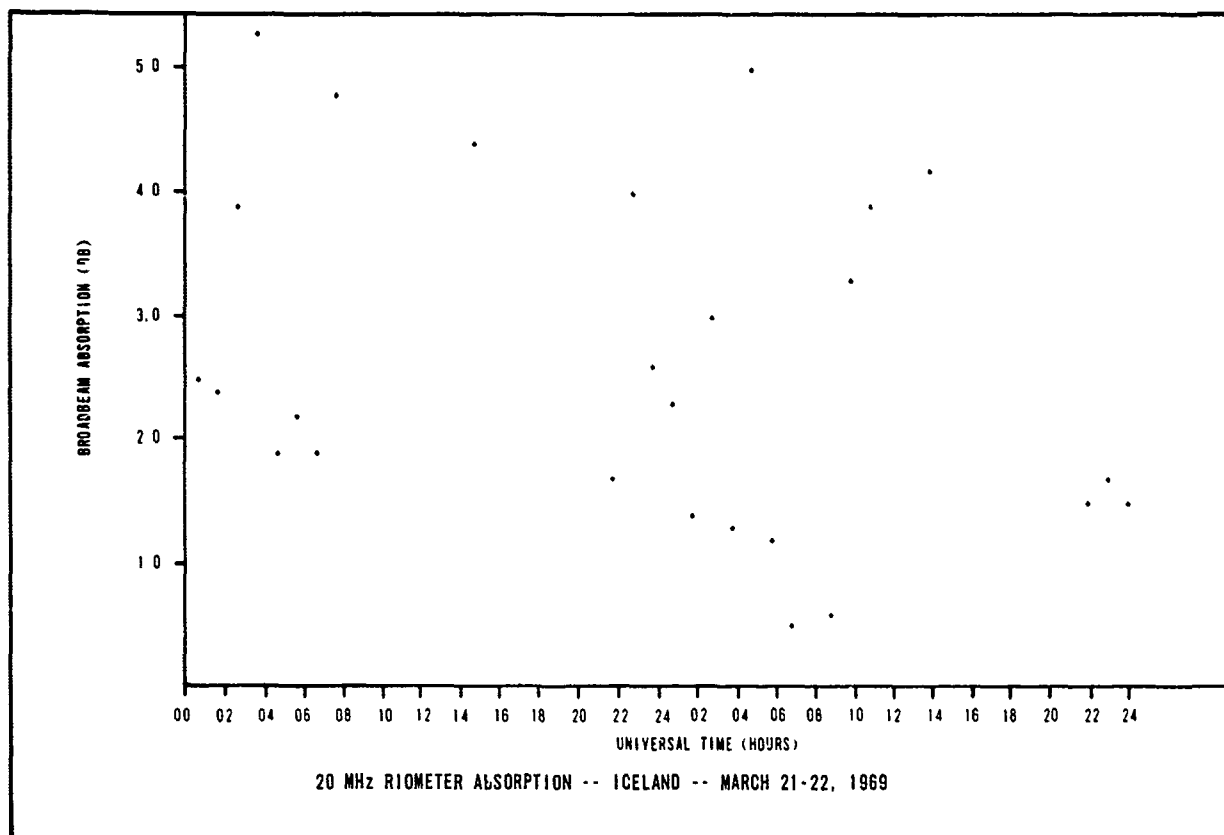
B-104

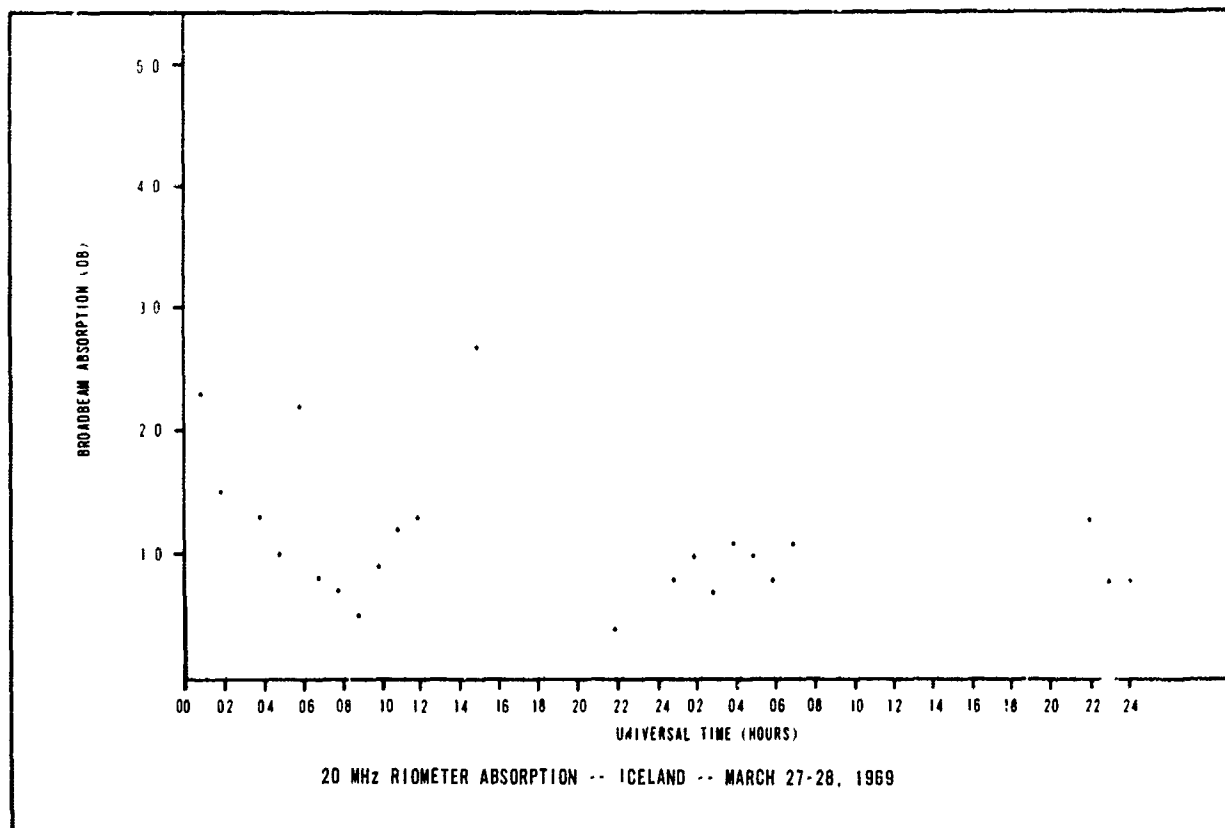
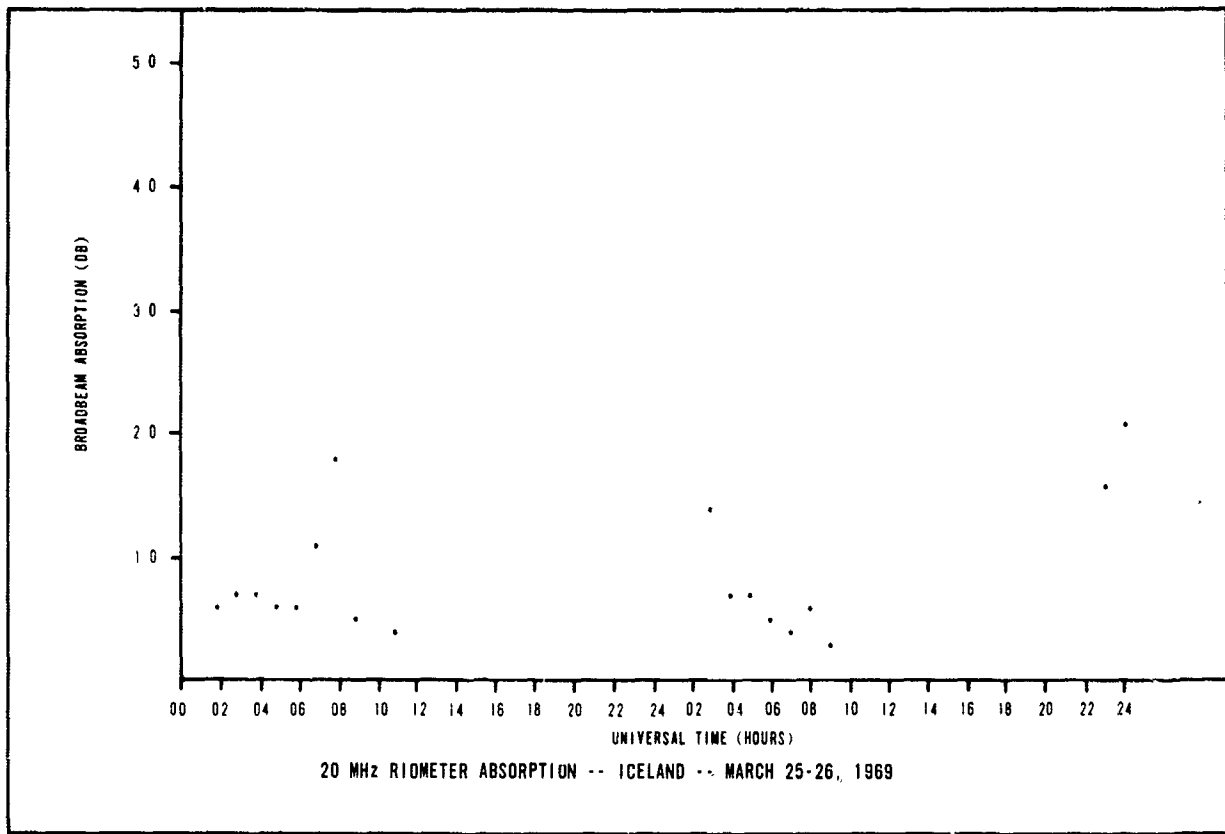


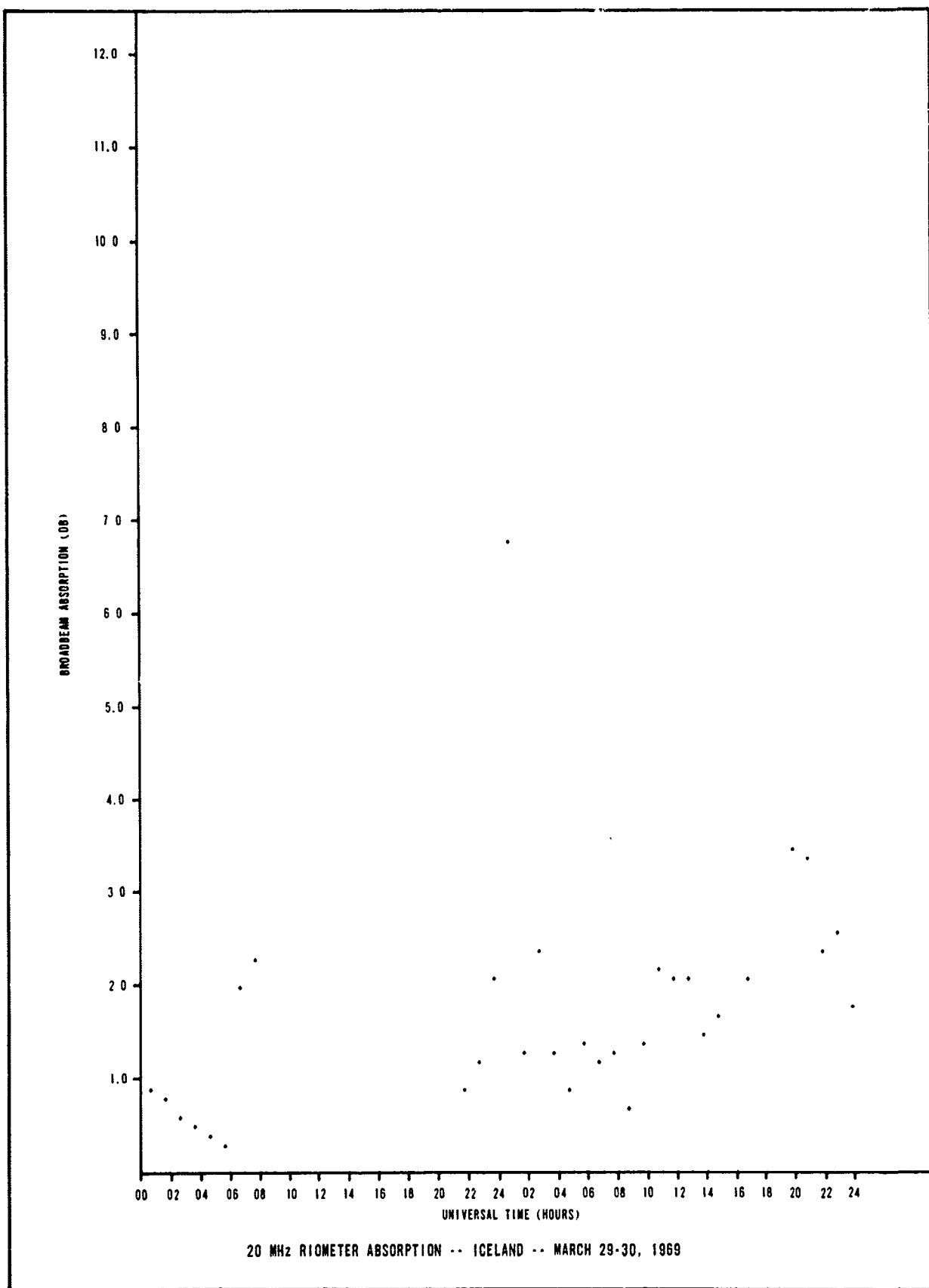




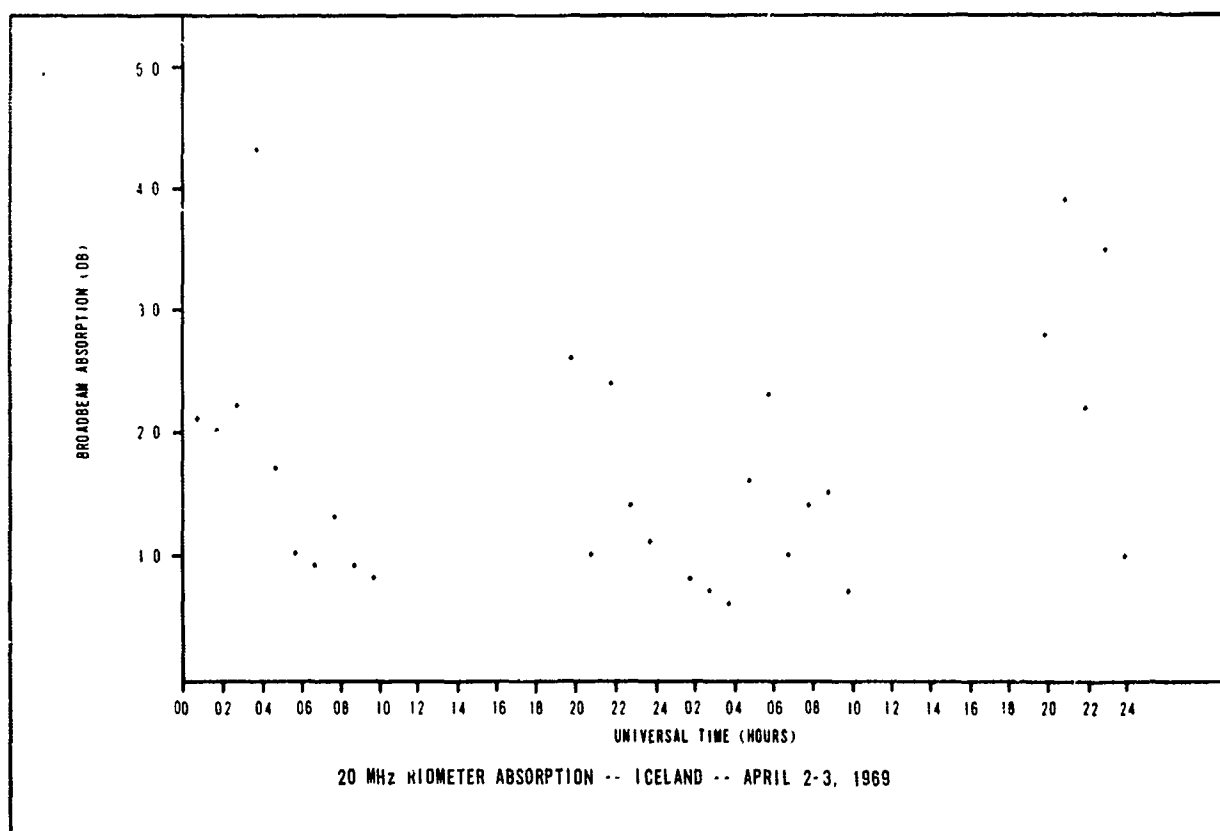
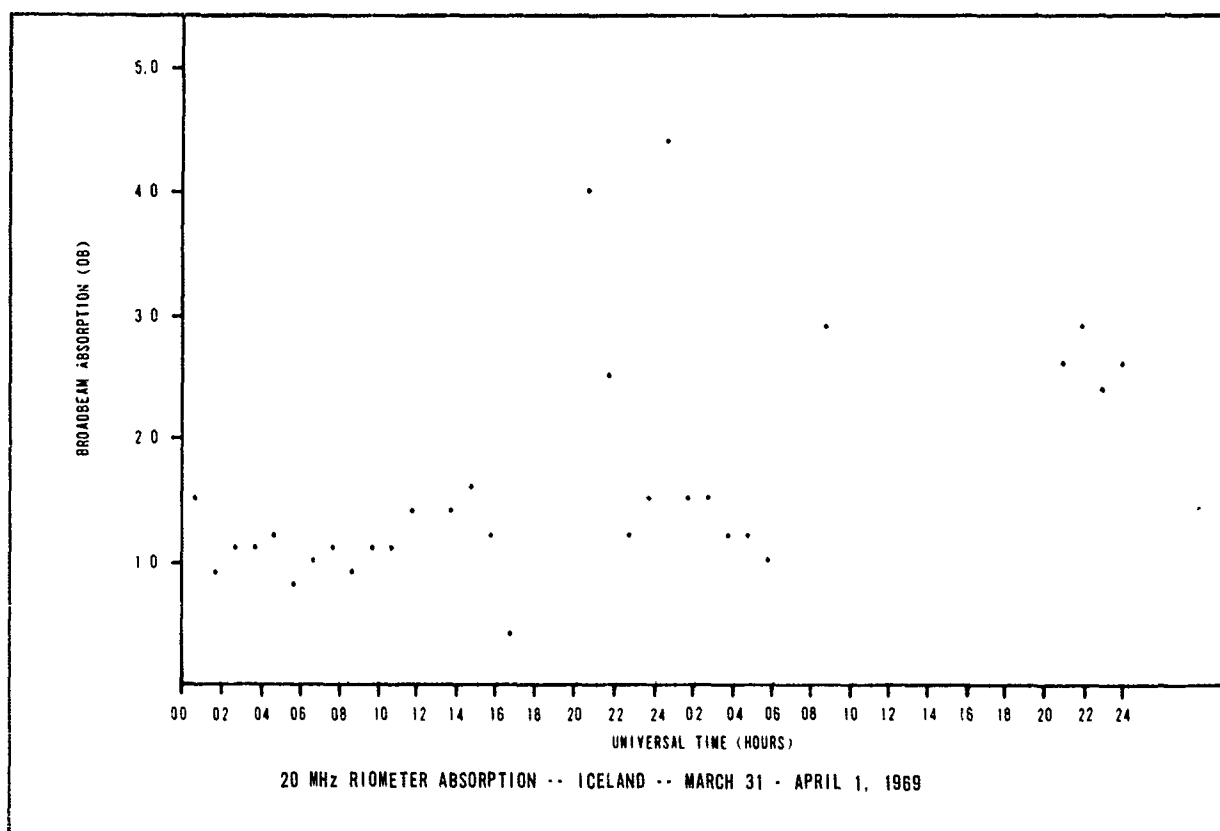
20 MHz RIOMETER ABSORPTION -- ICELAND -- MARCH 19-20, 1969

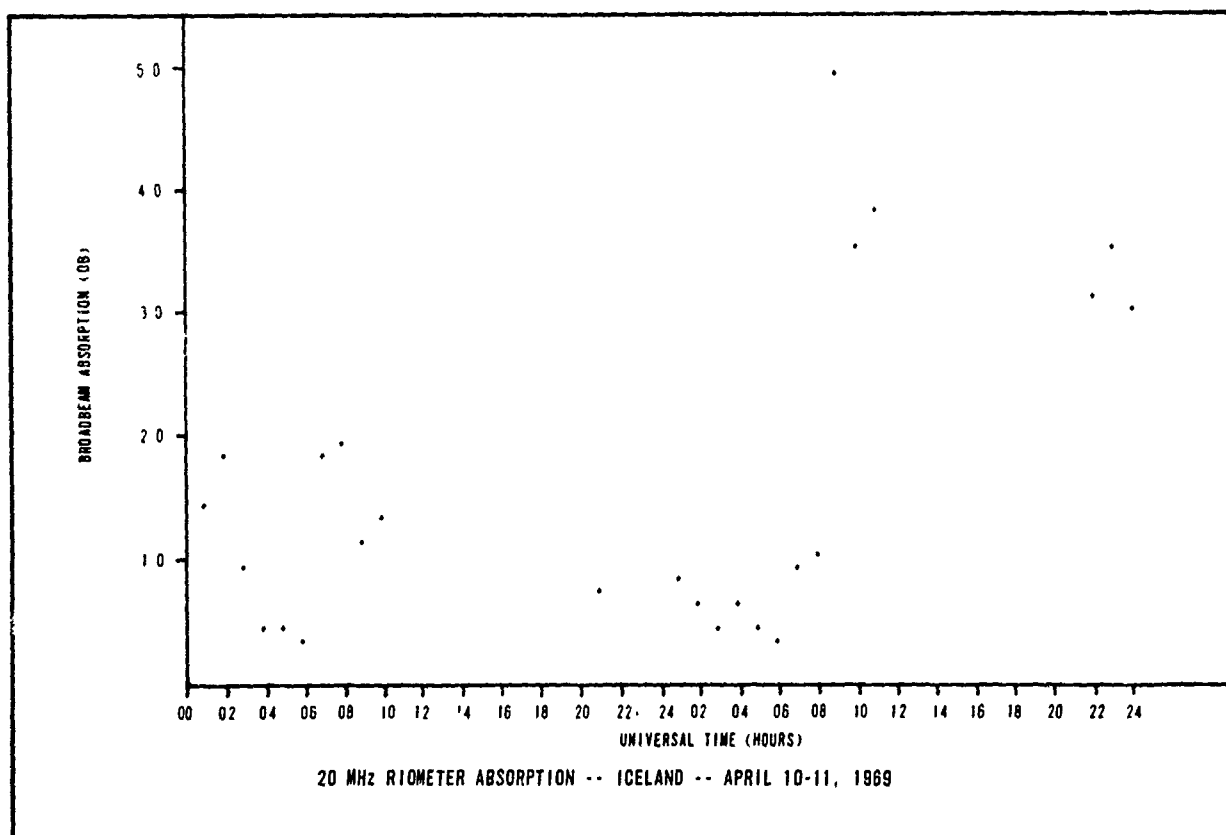
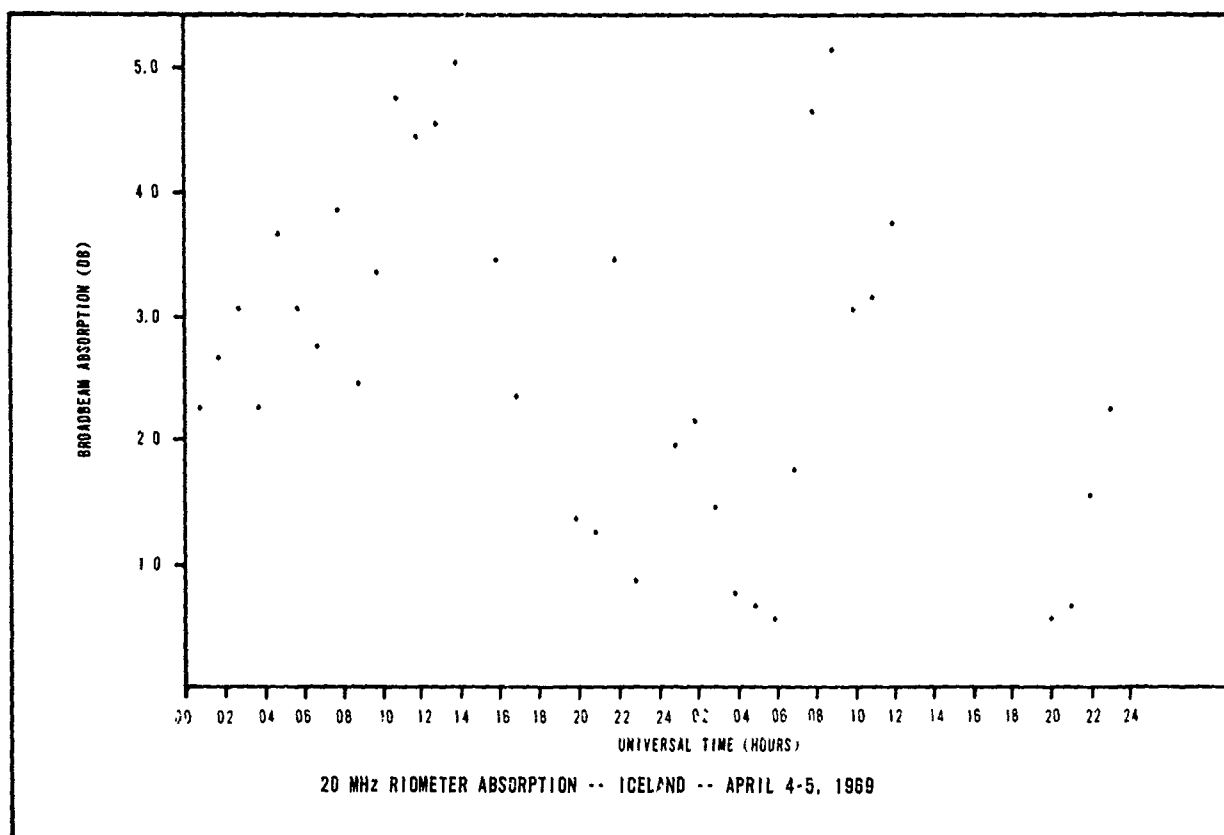


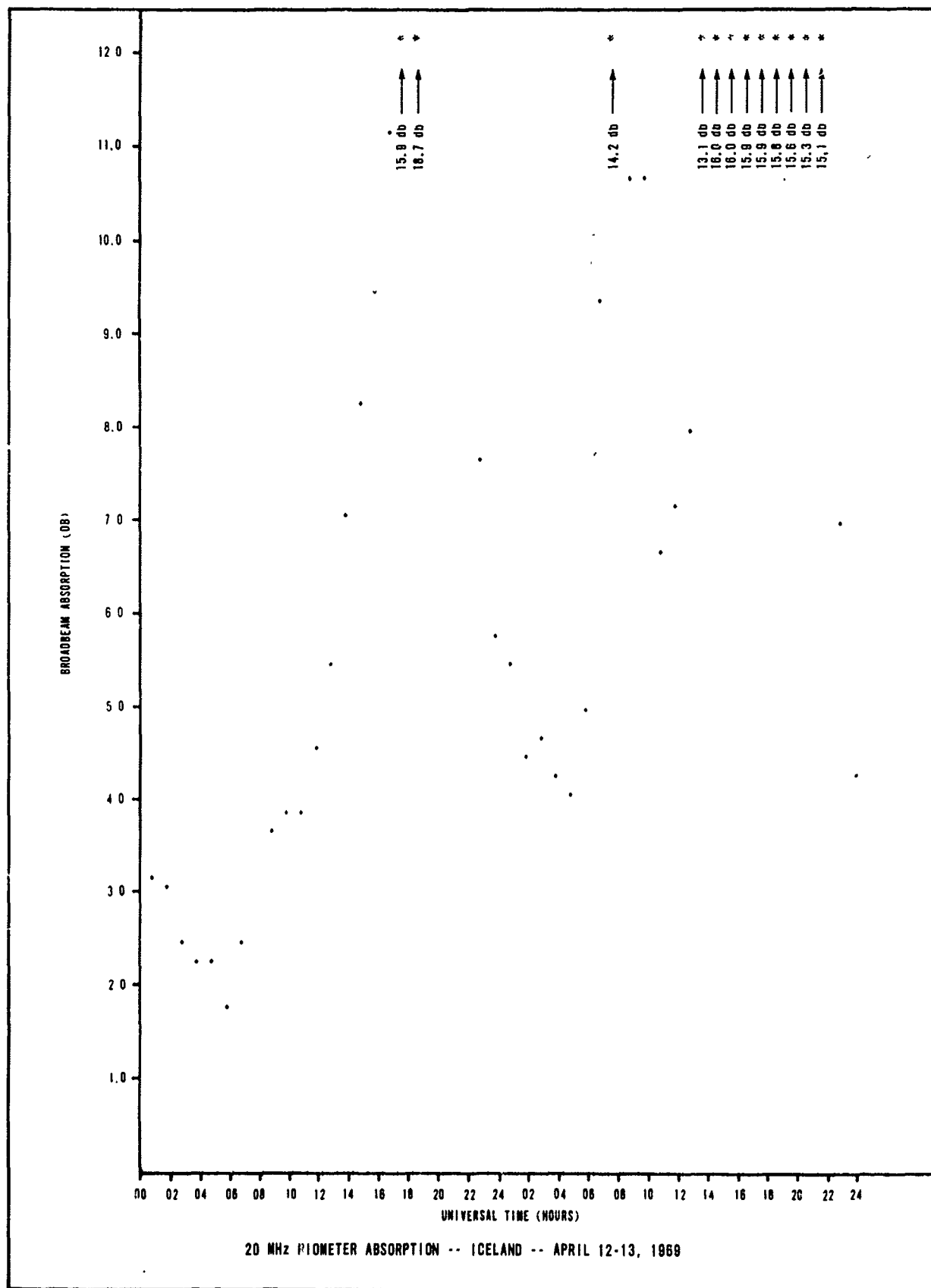


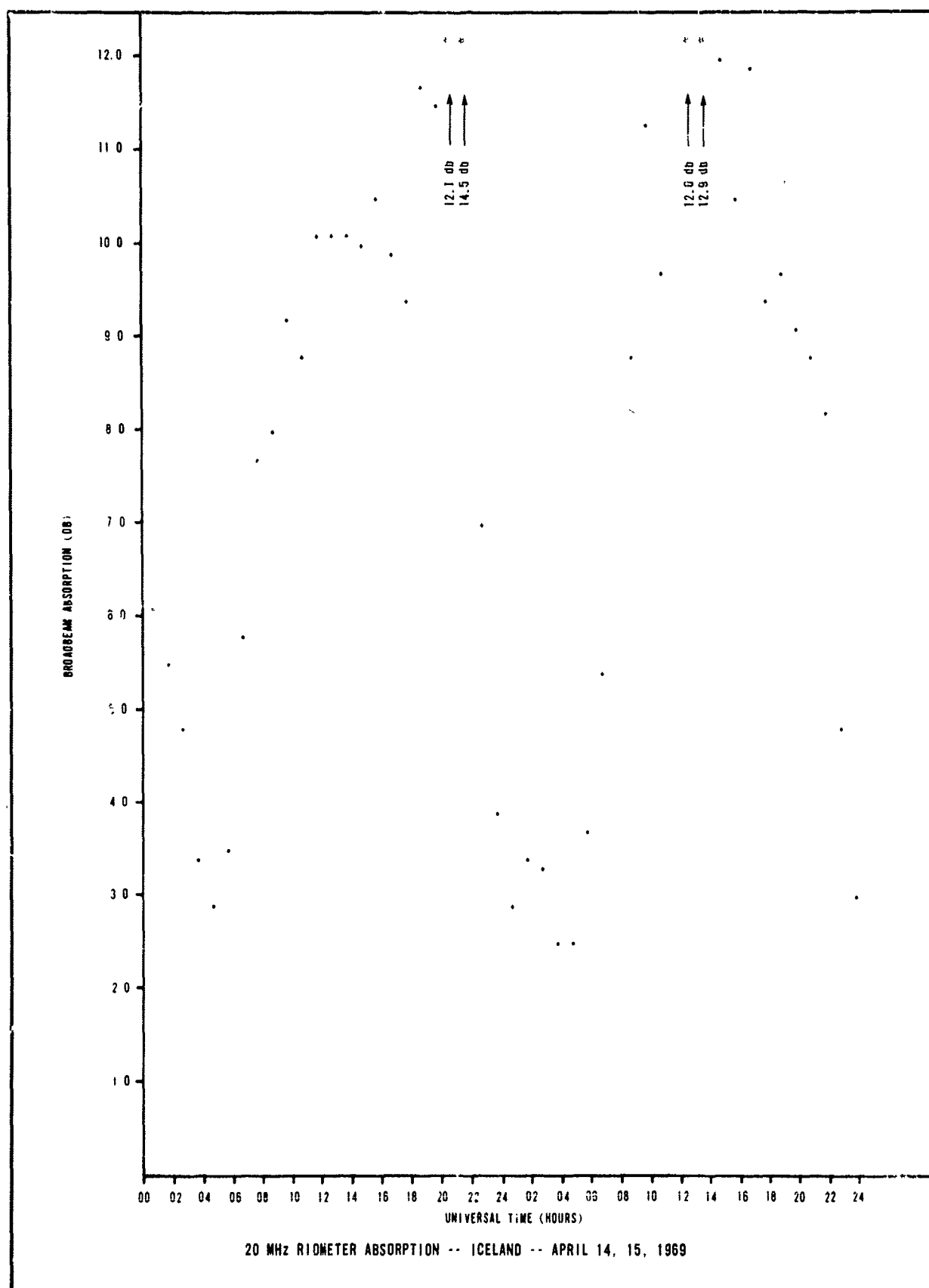


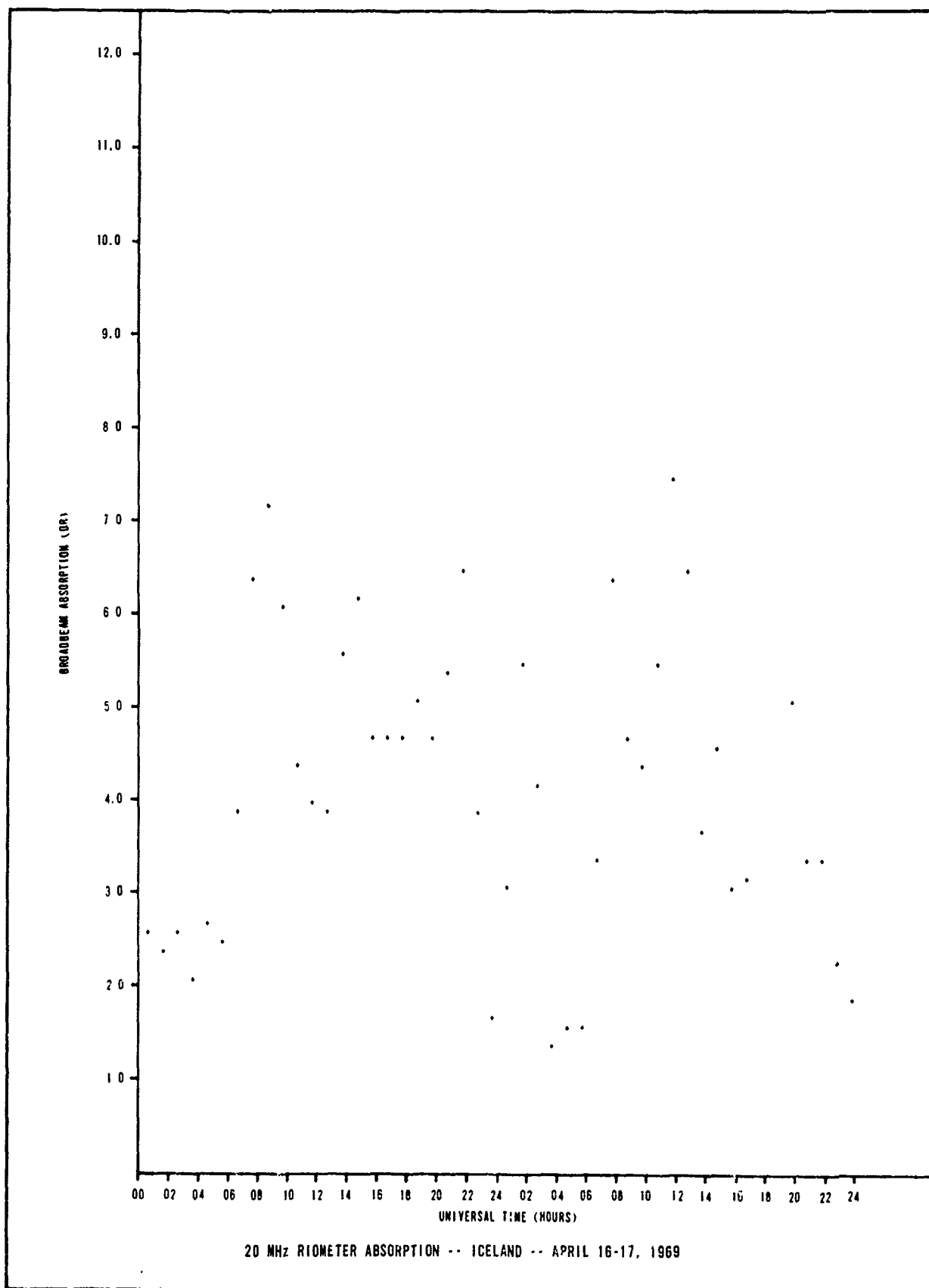


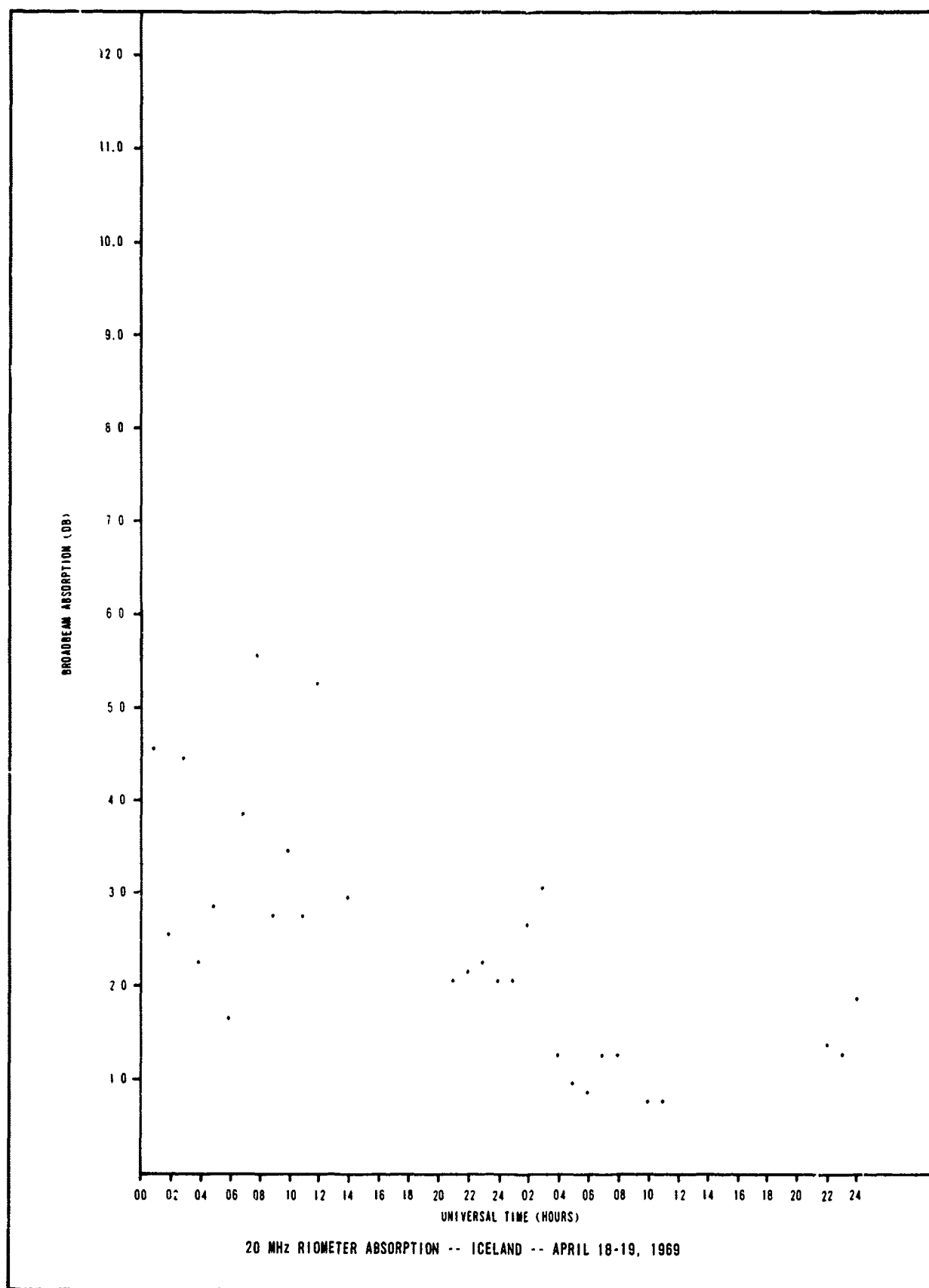




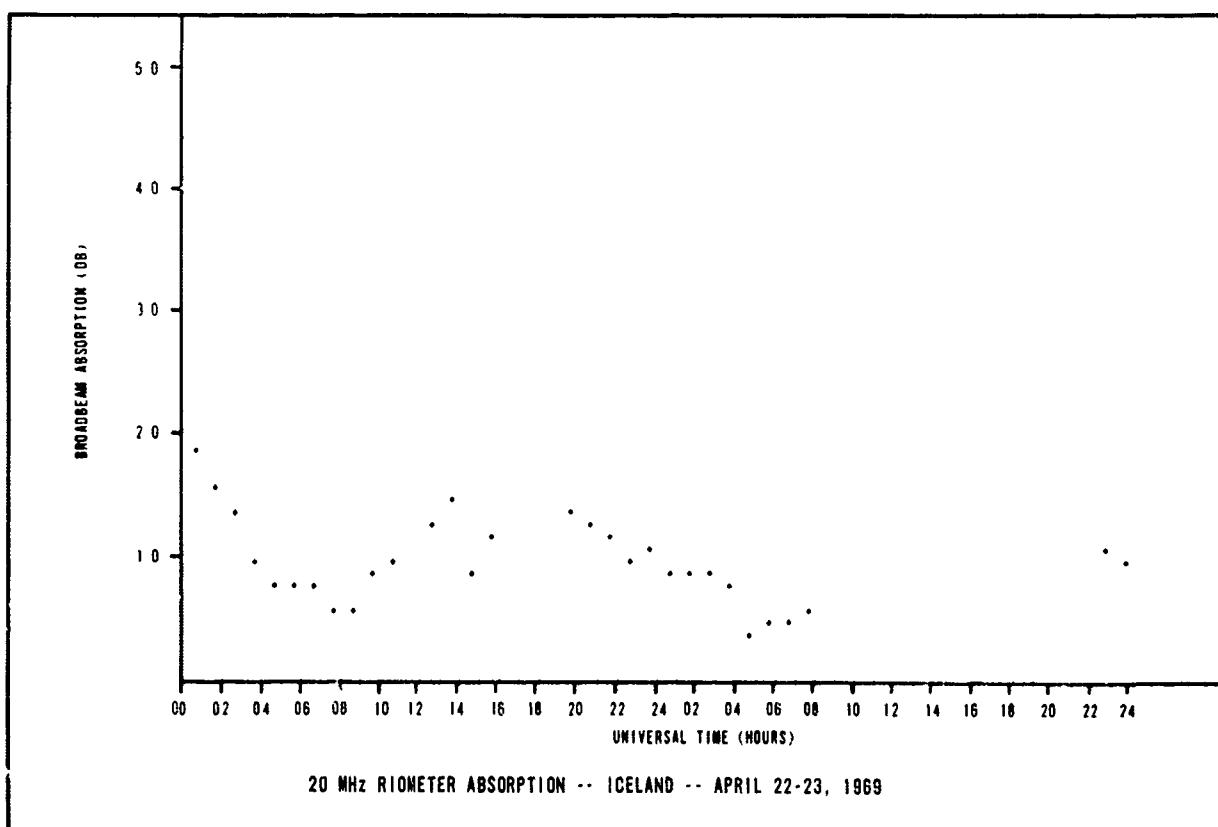
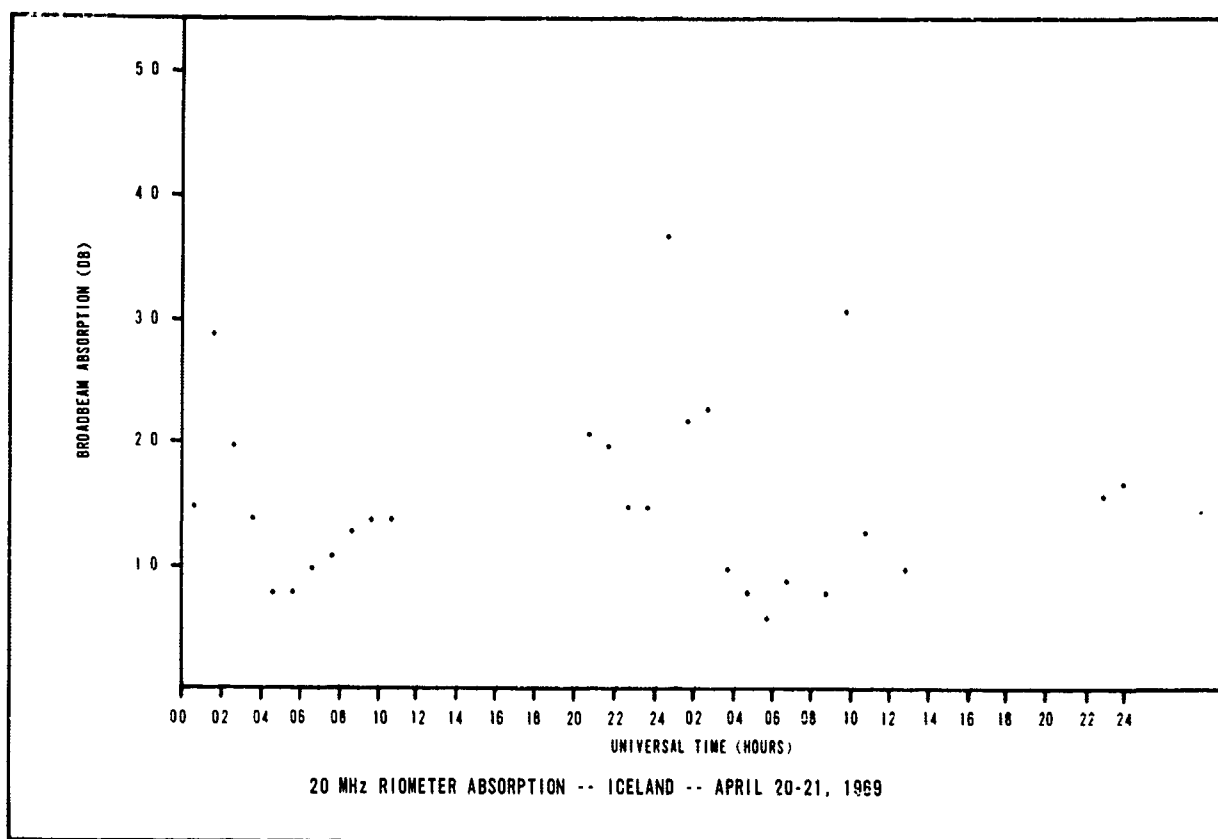


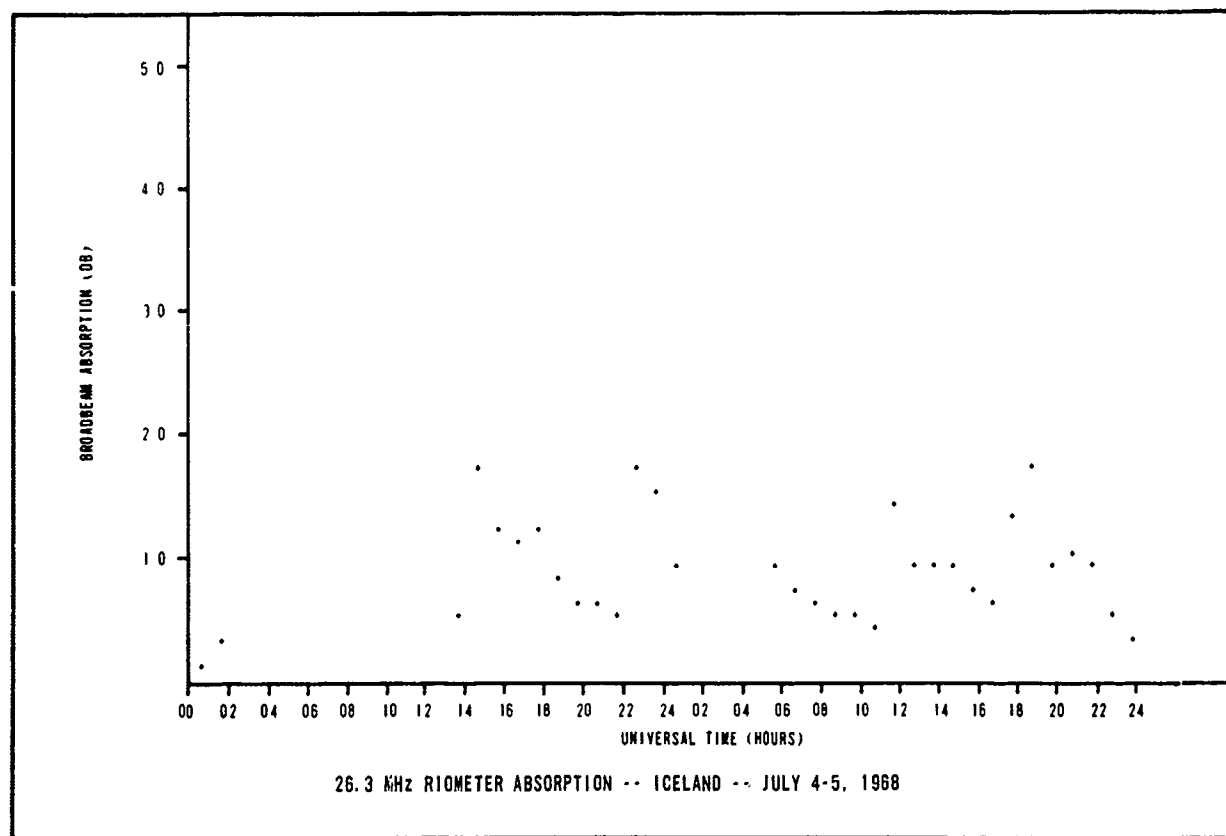
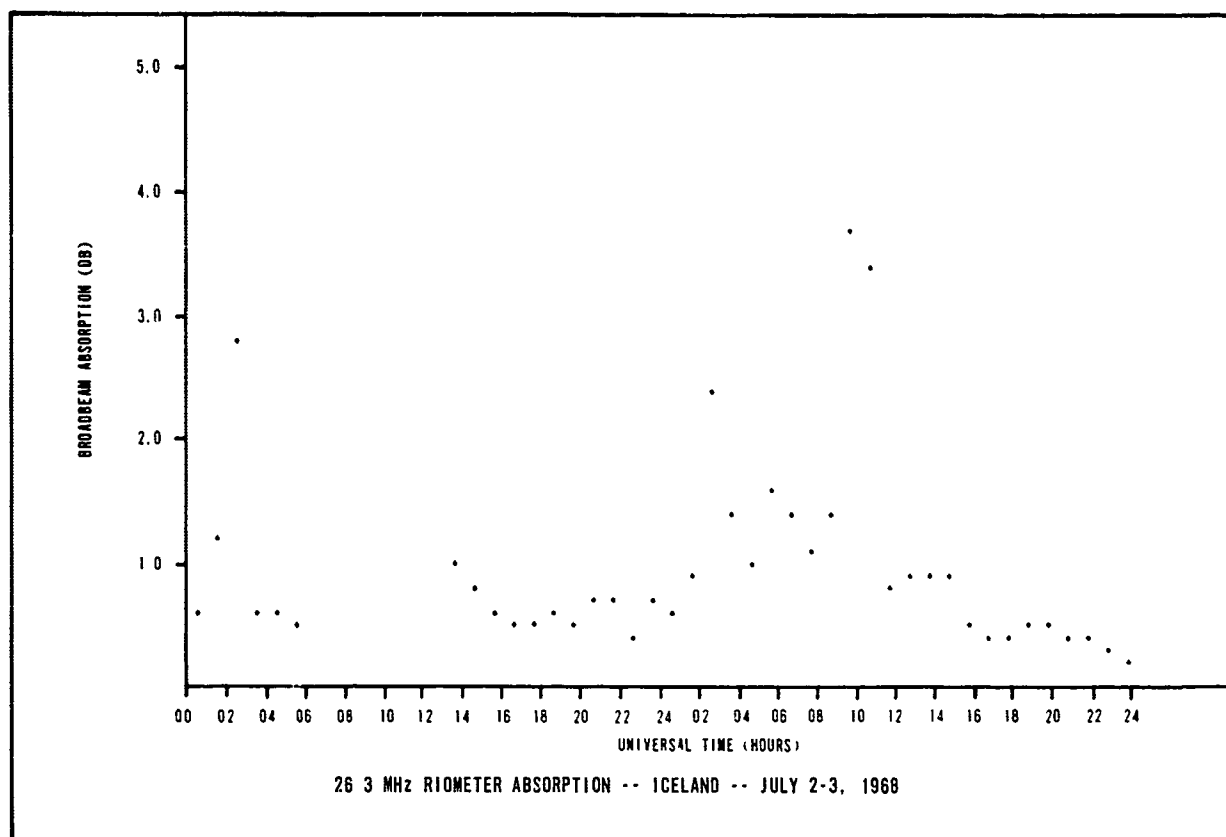




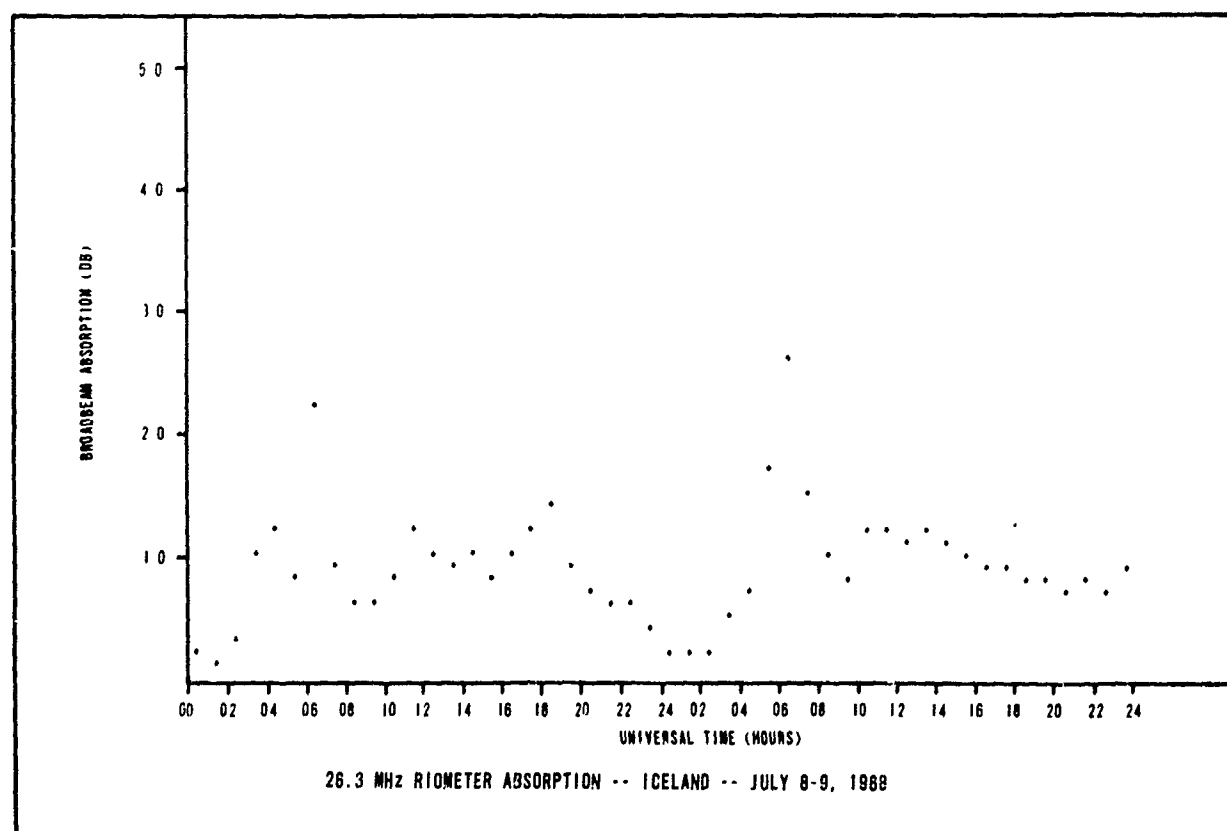
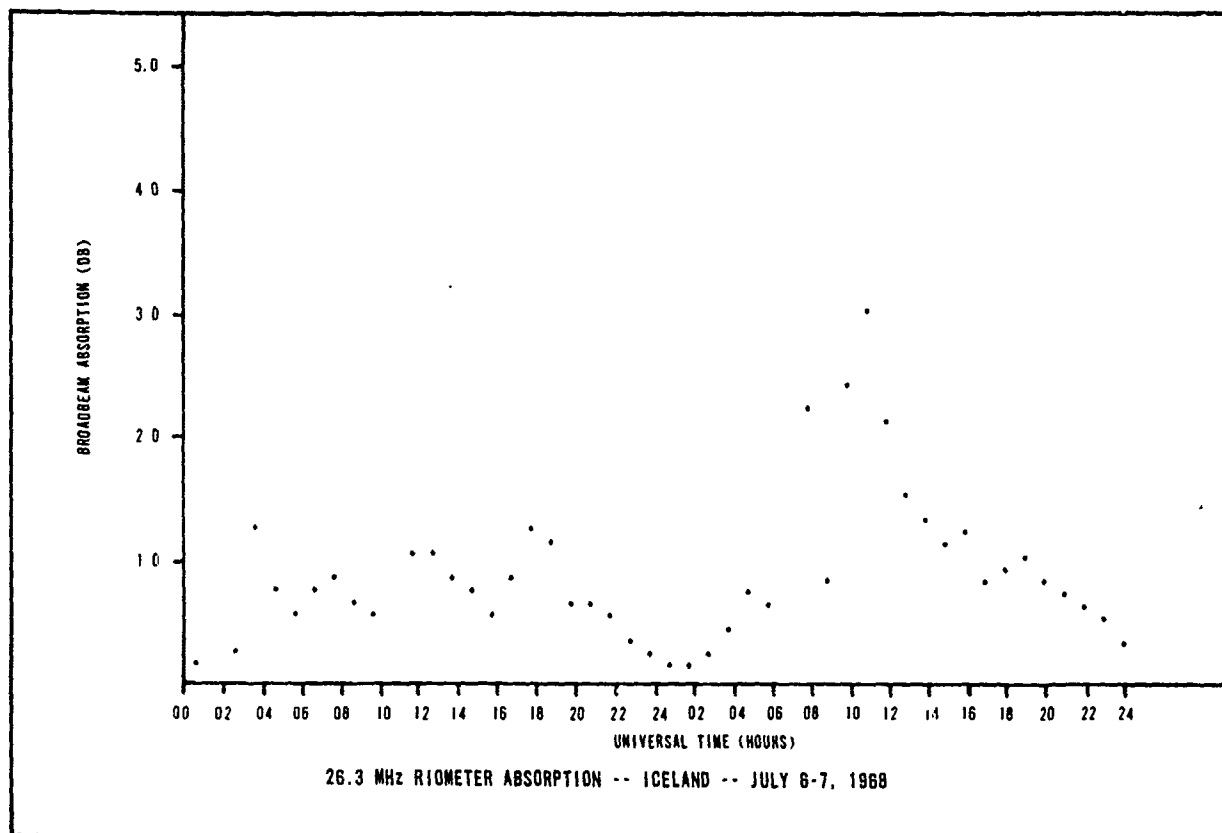


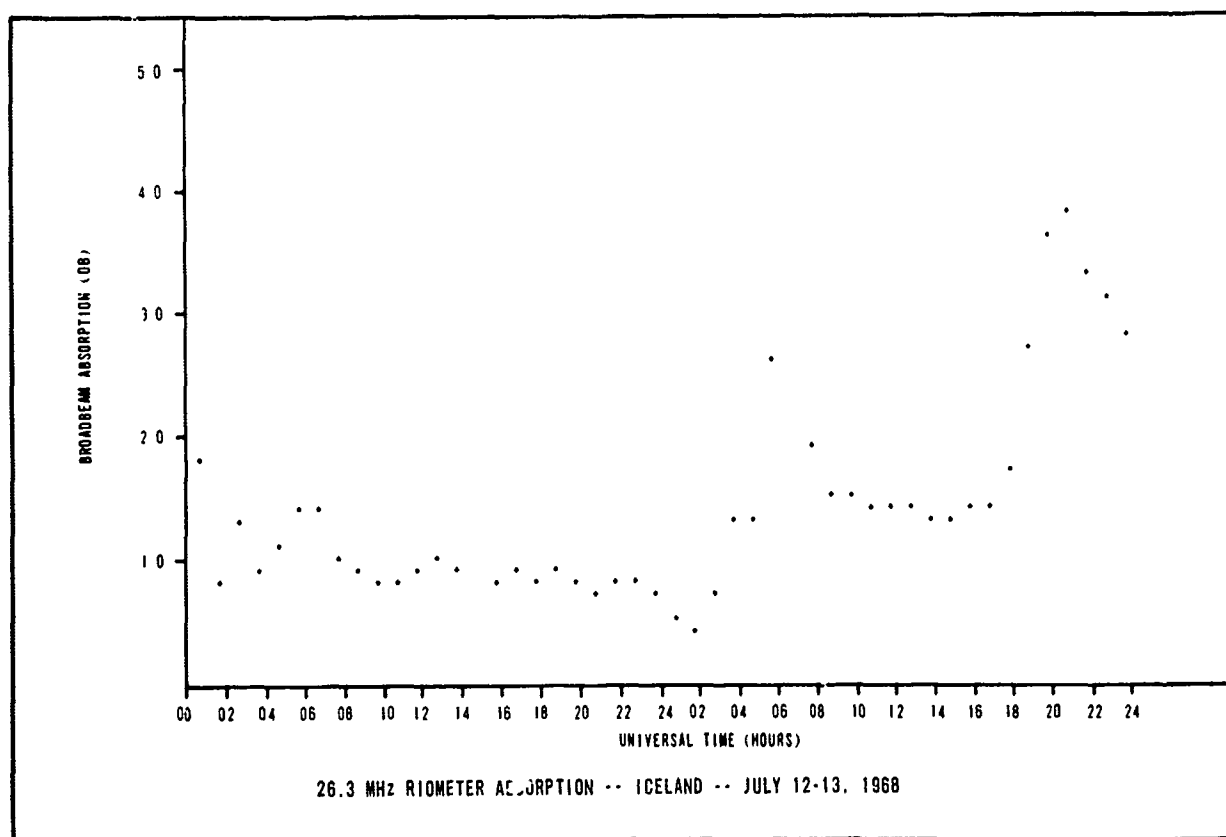
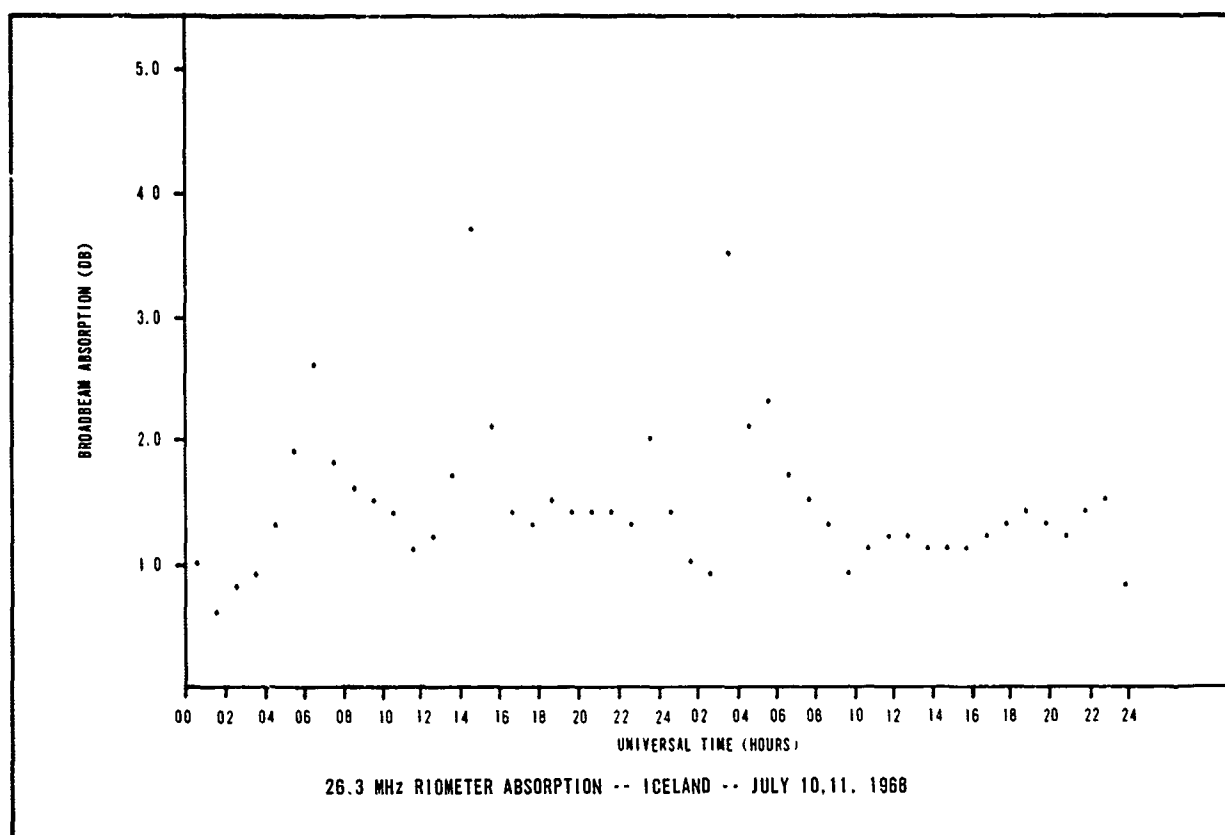
B-116

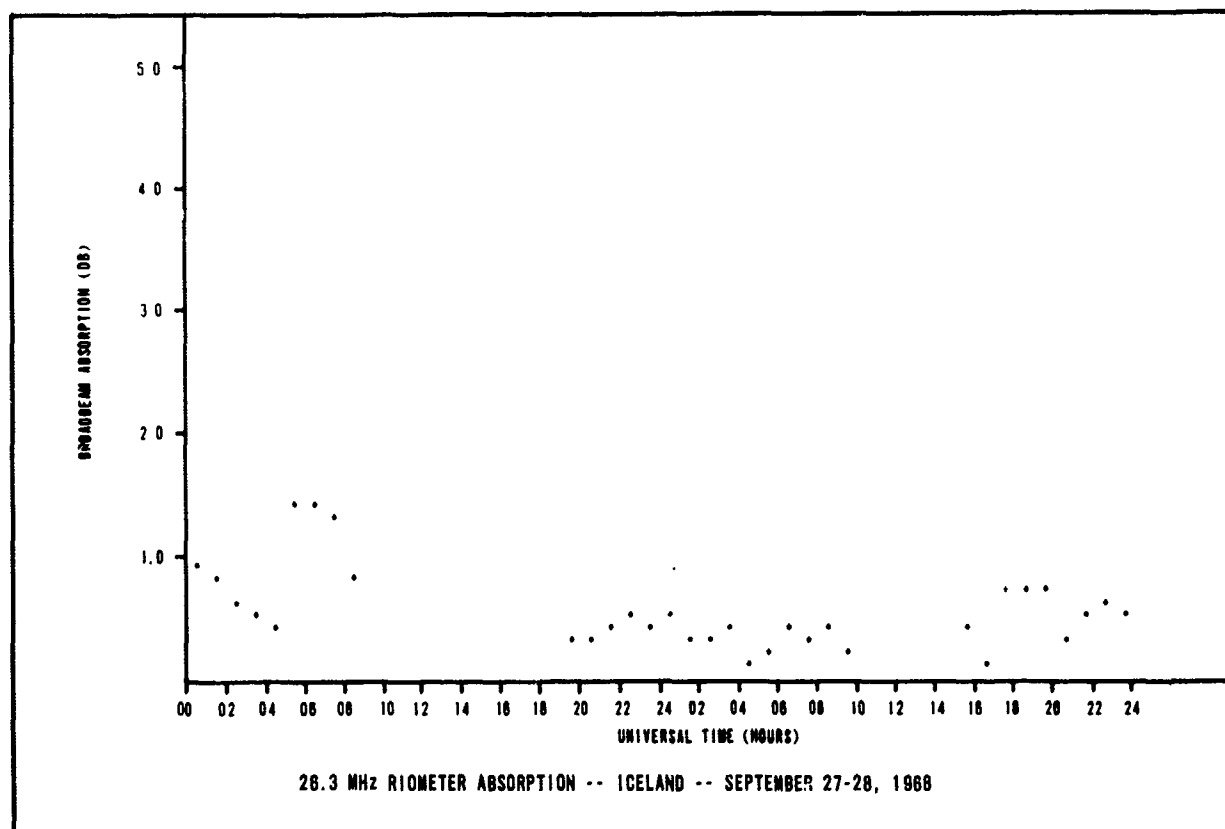
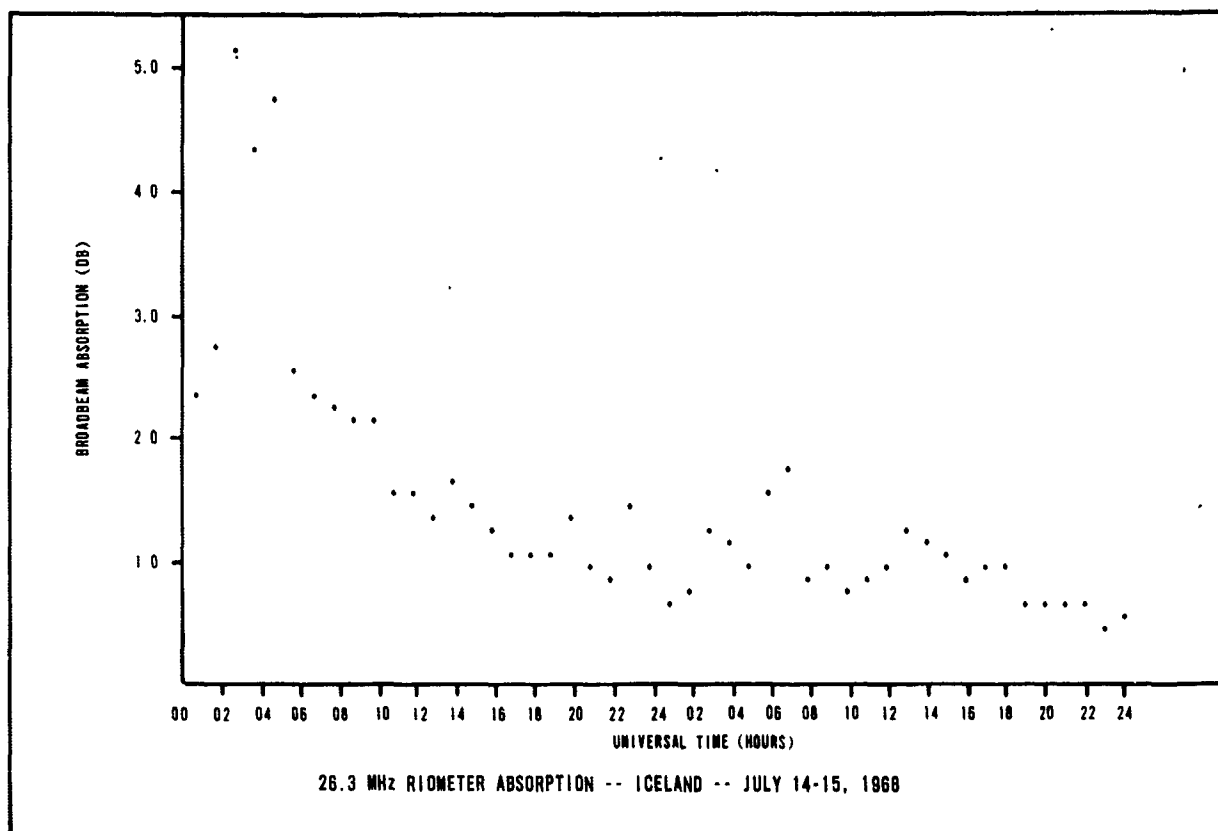


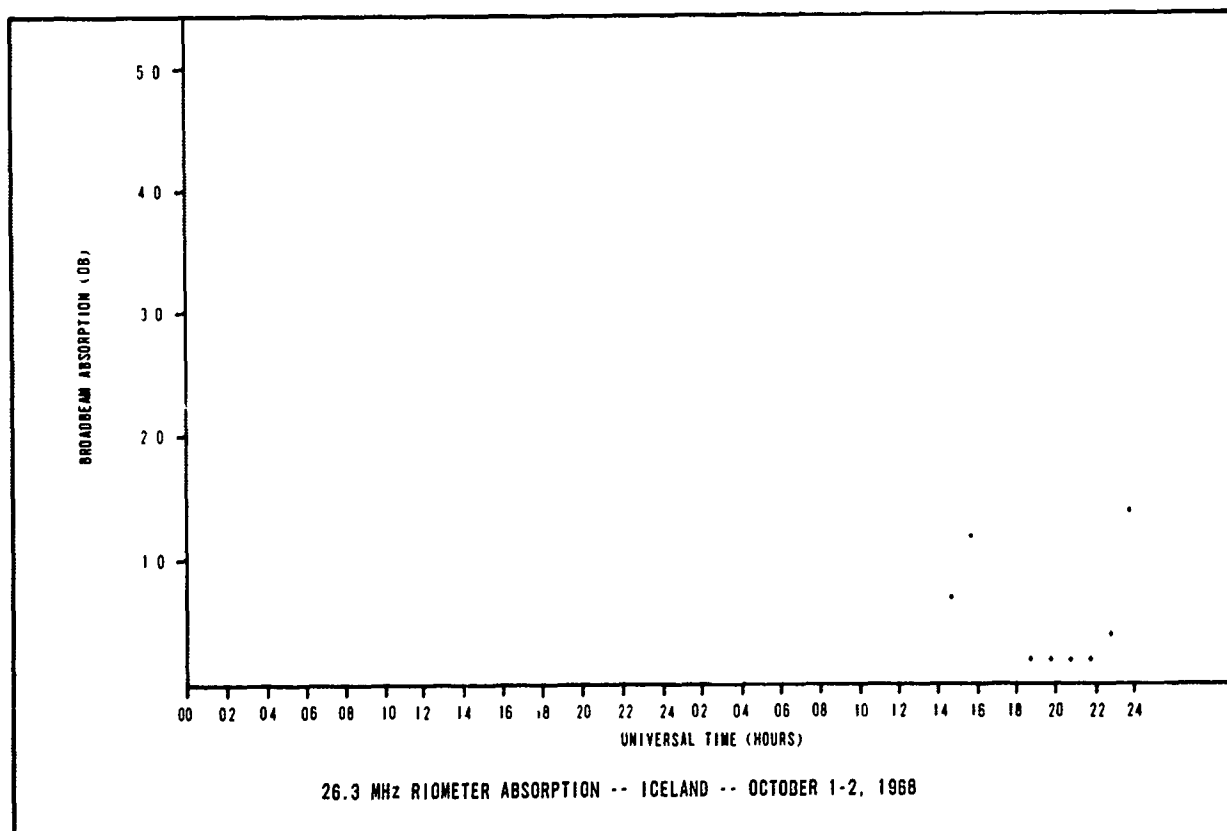
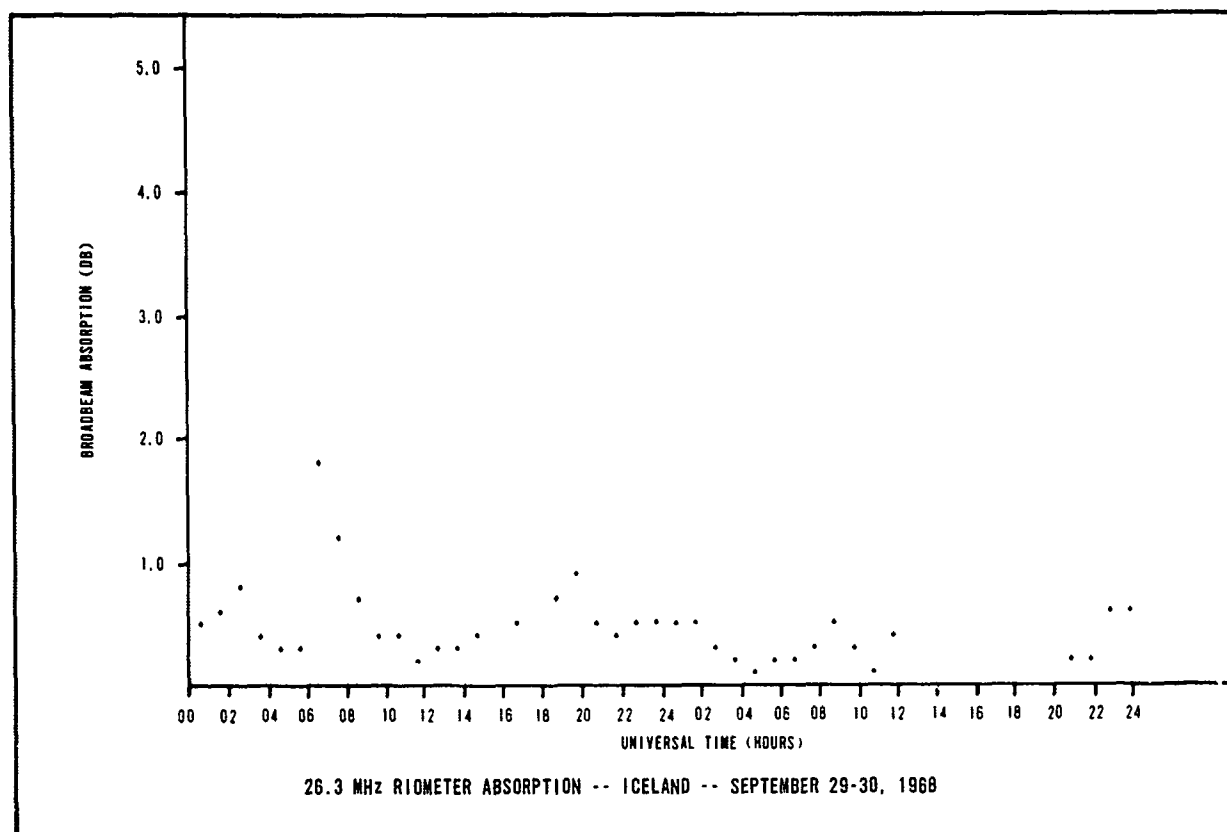


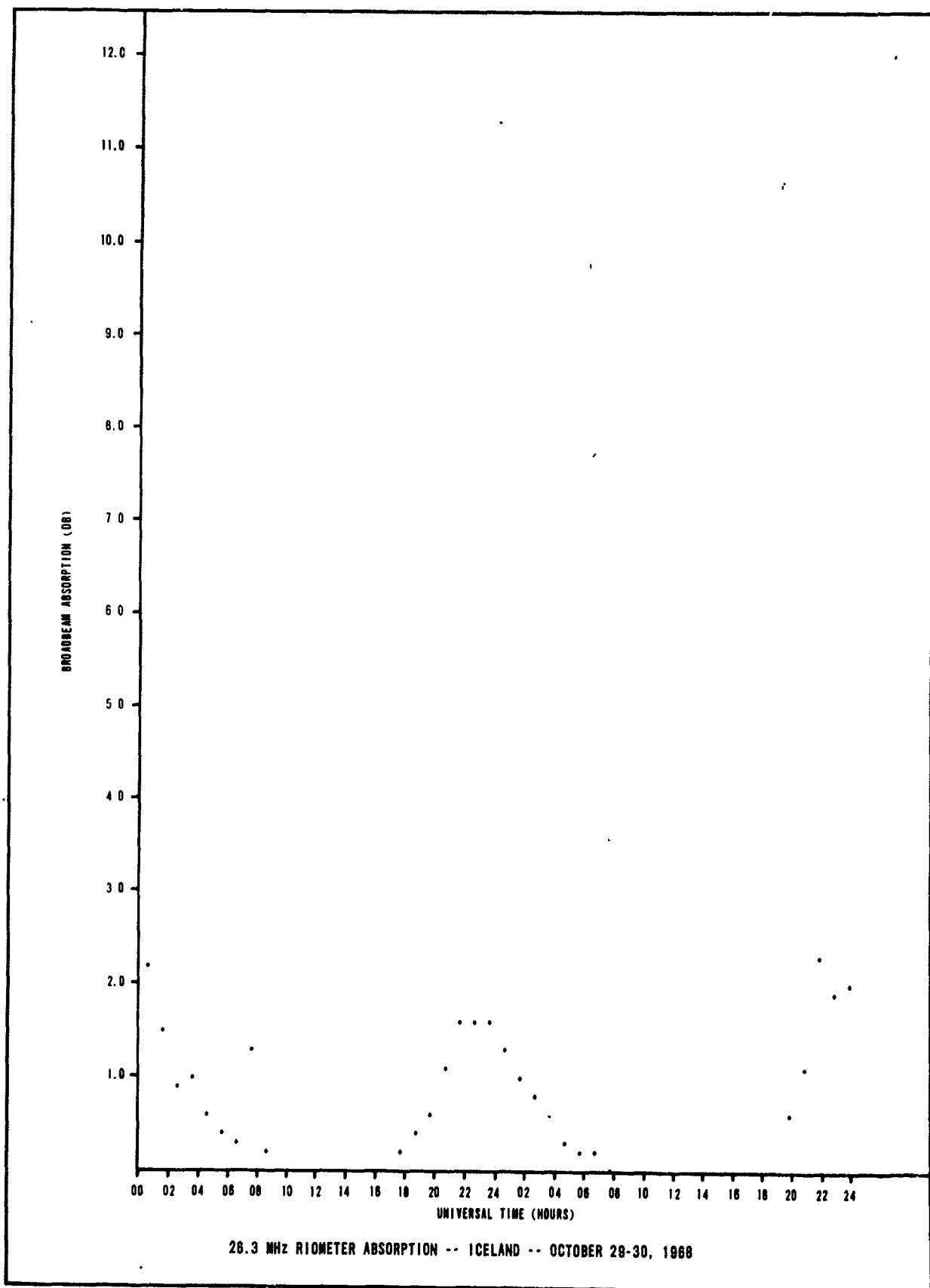


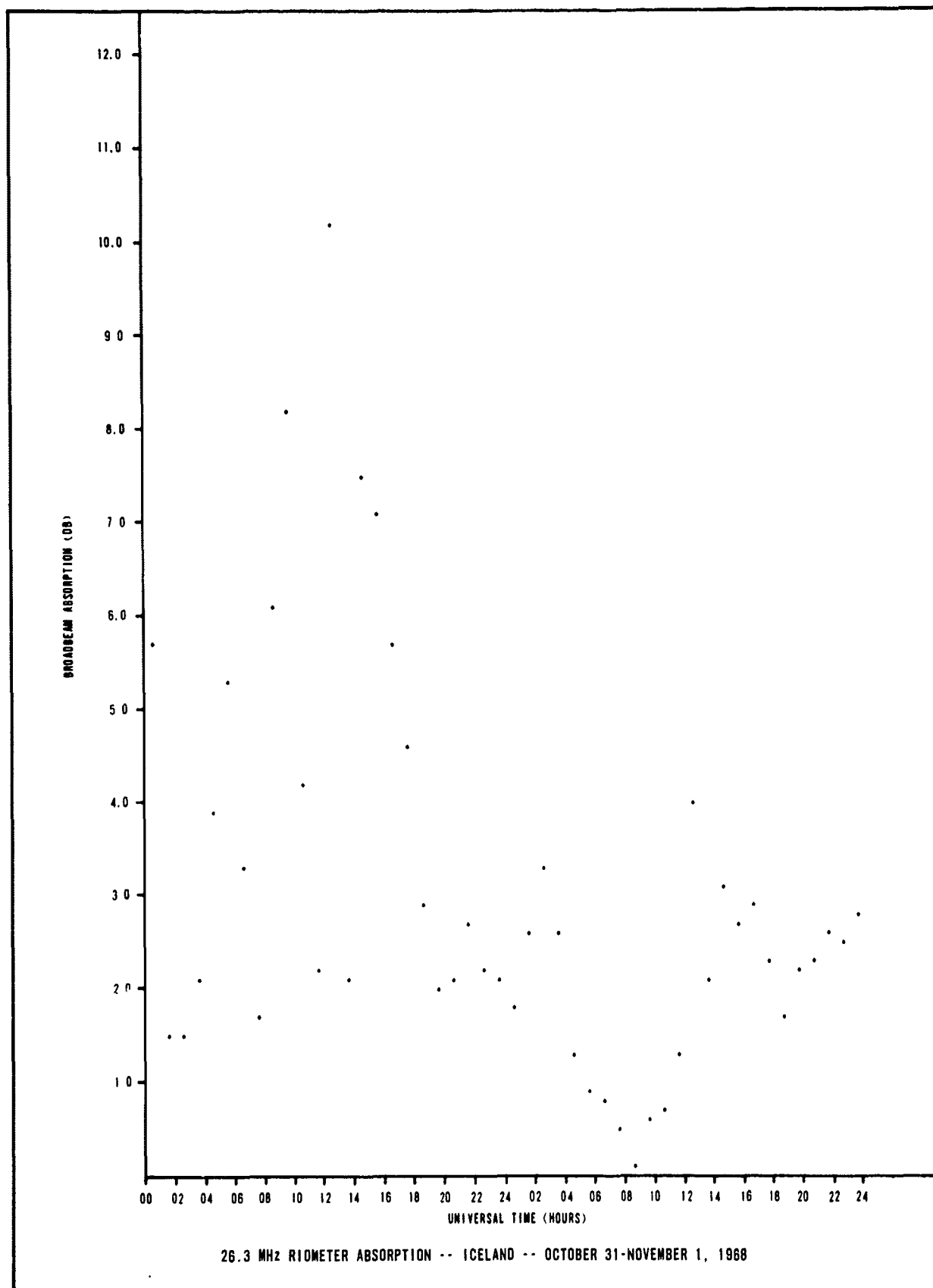


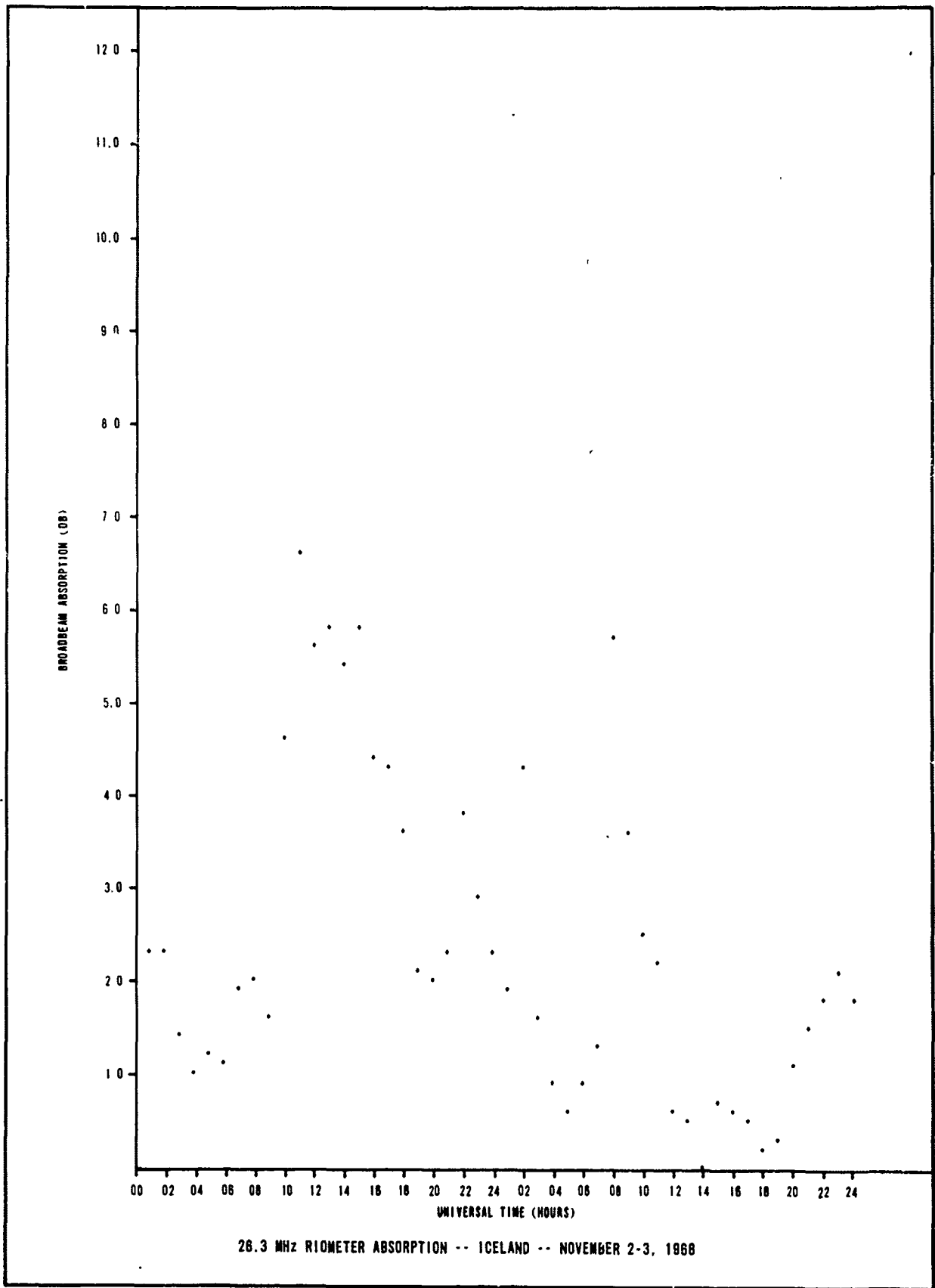


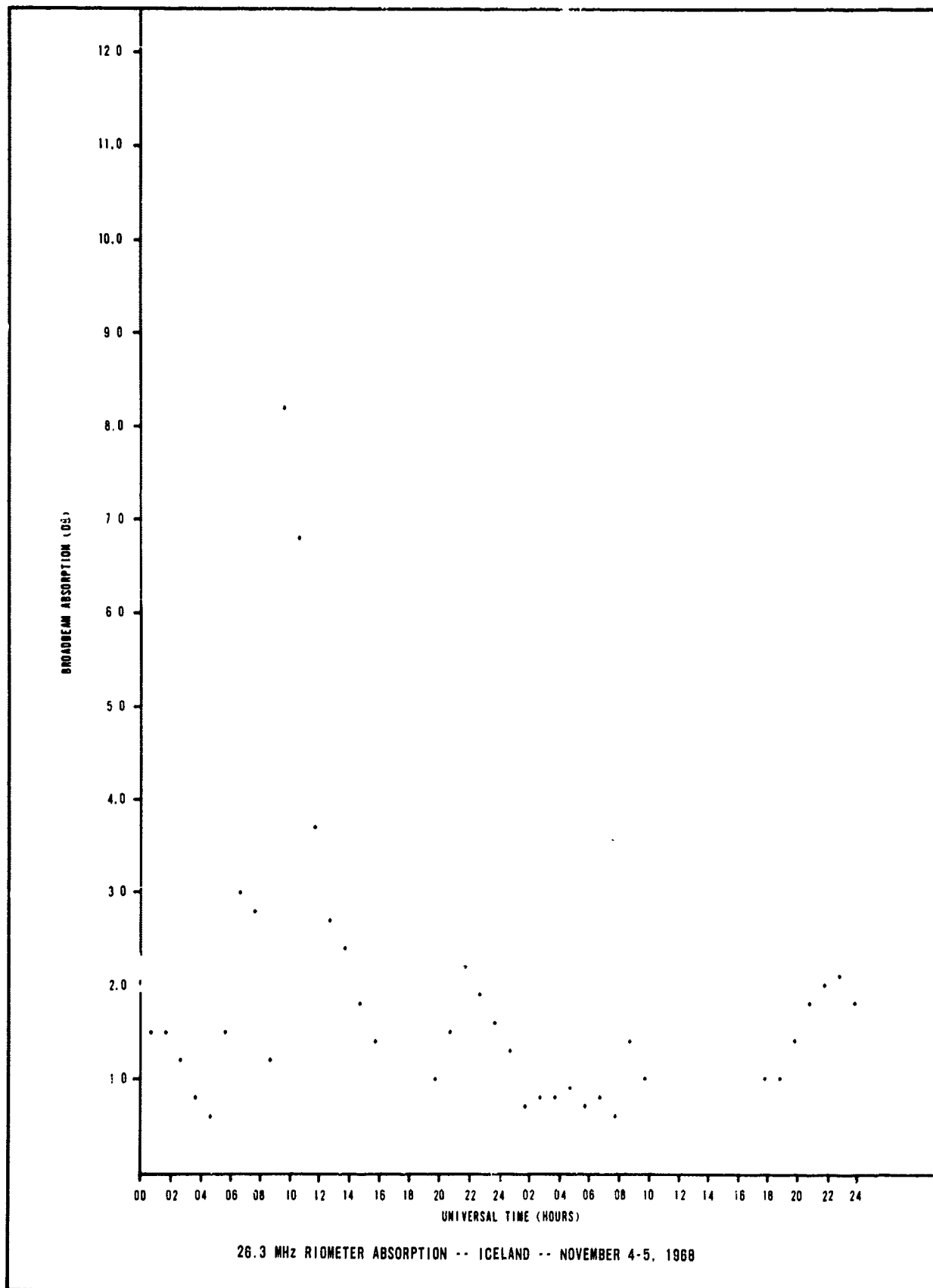




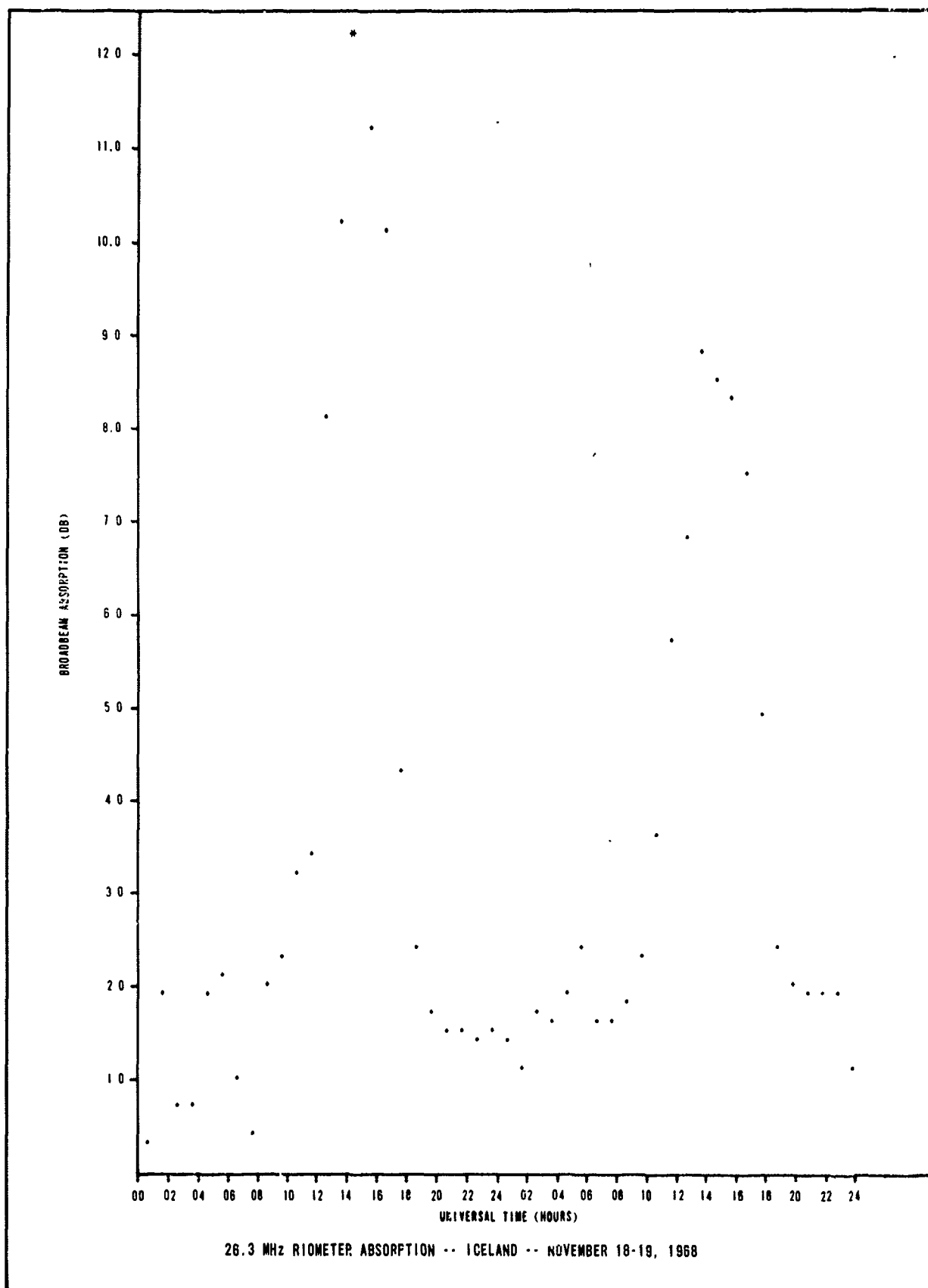


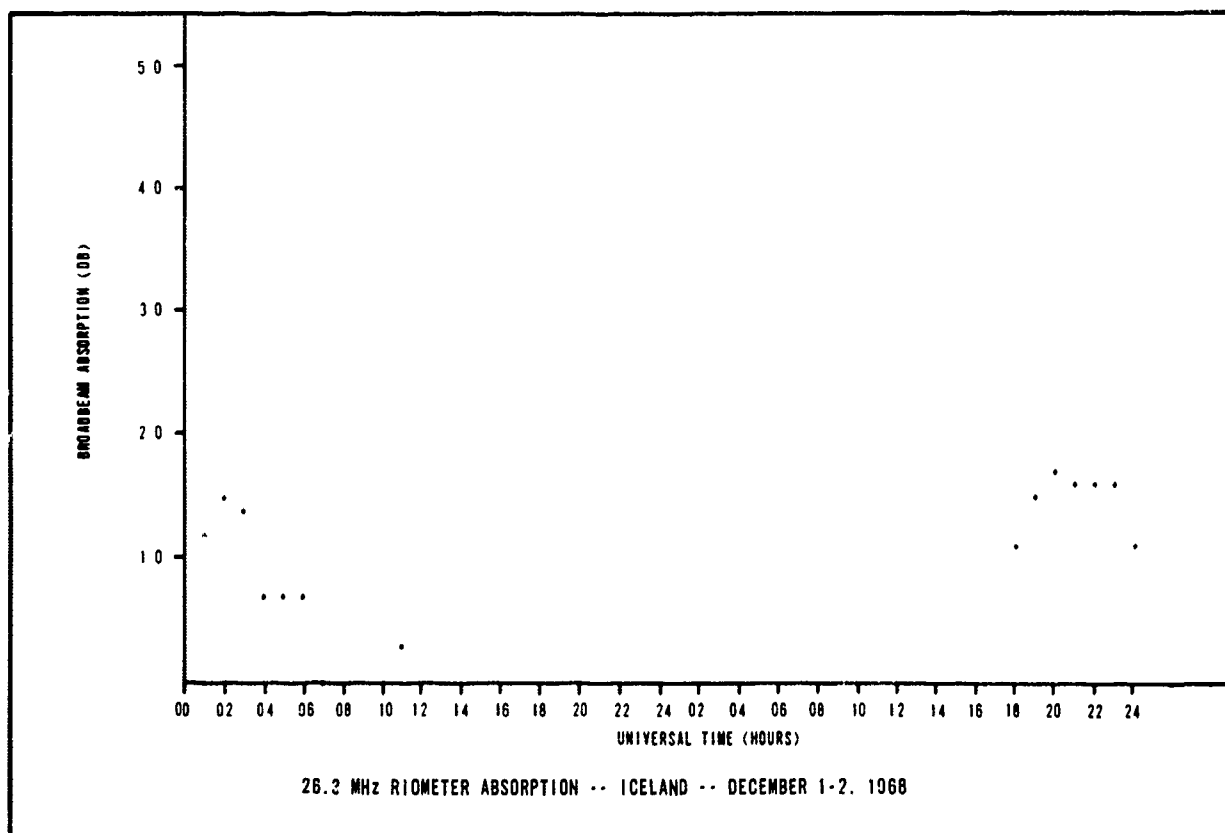
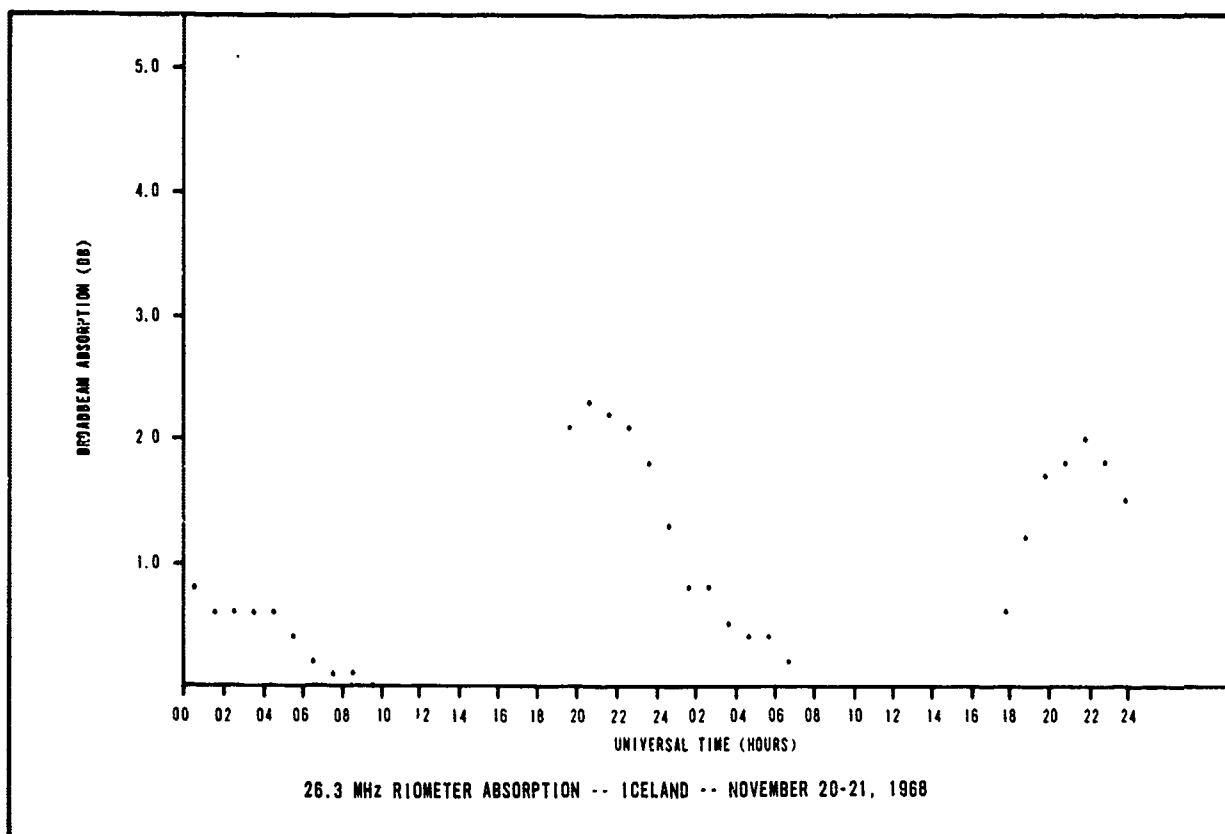


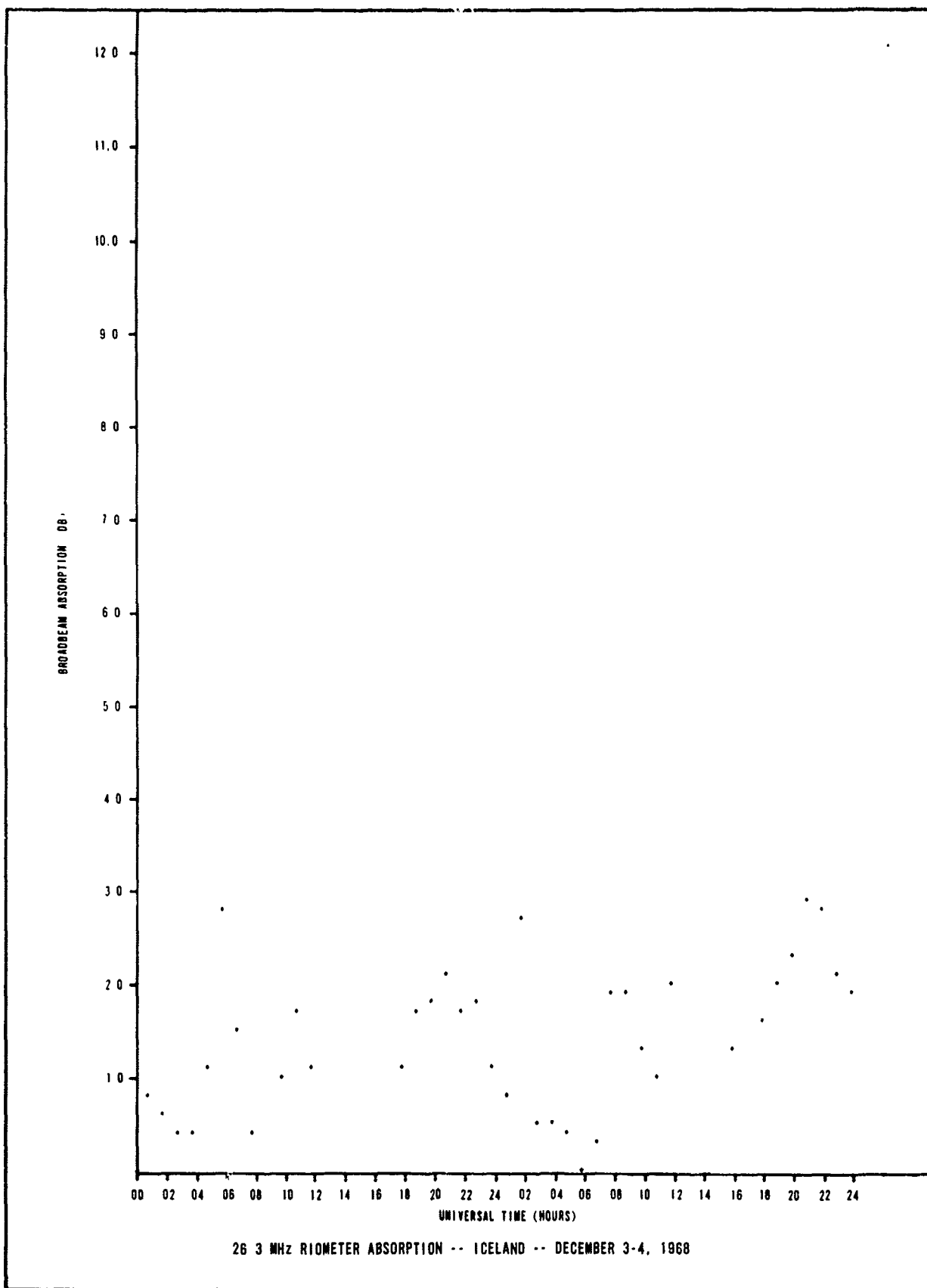


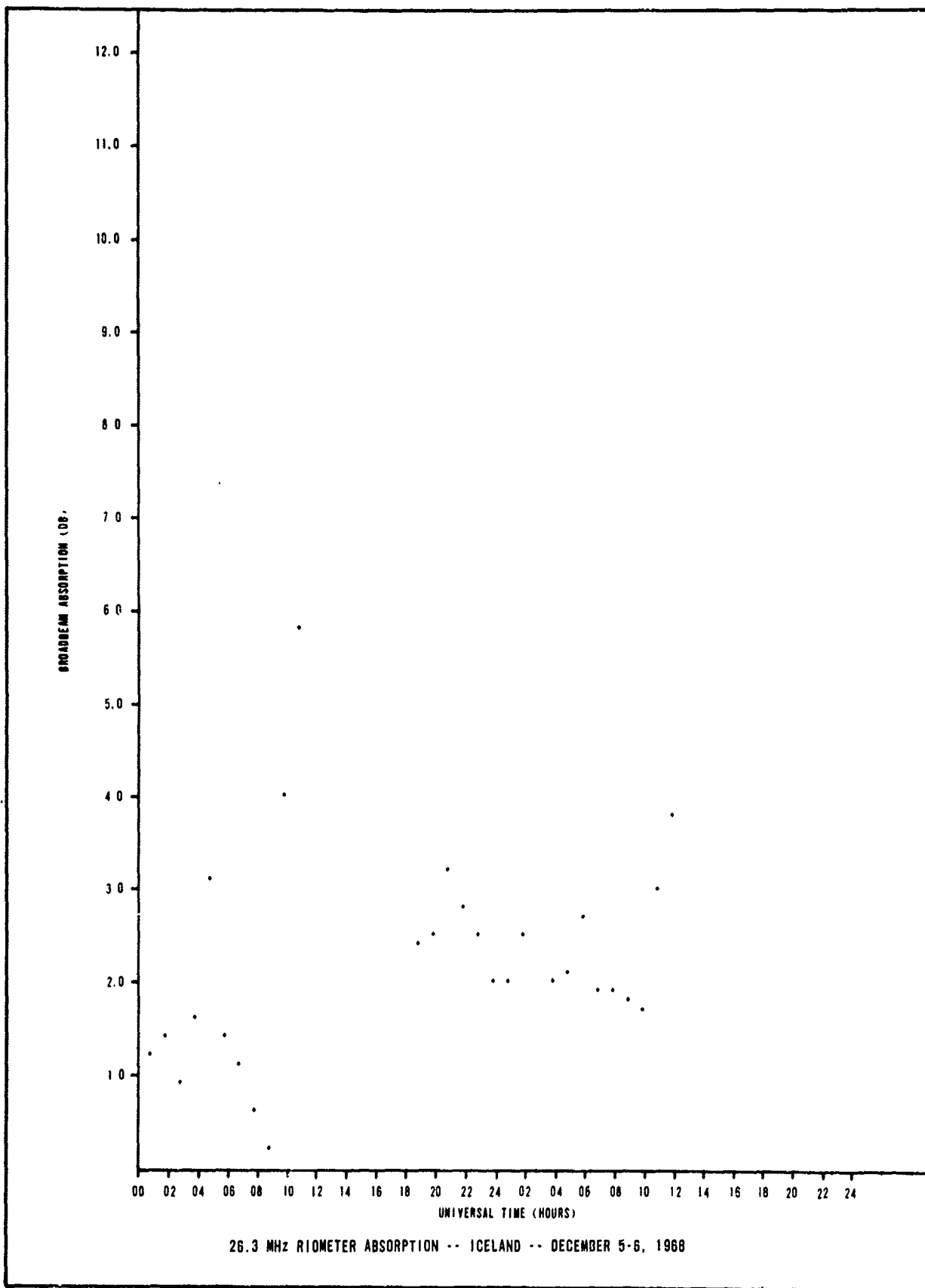


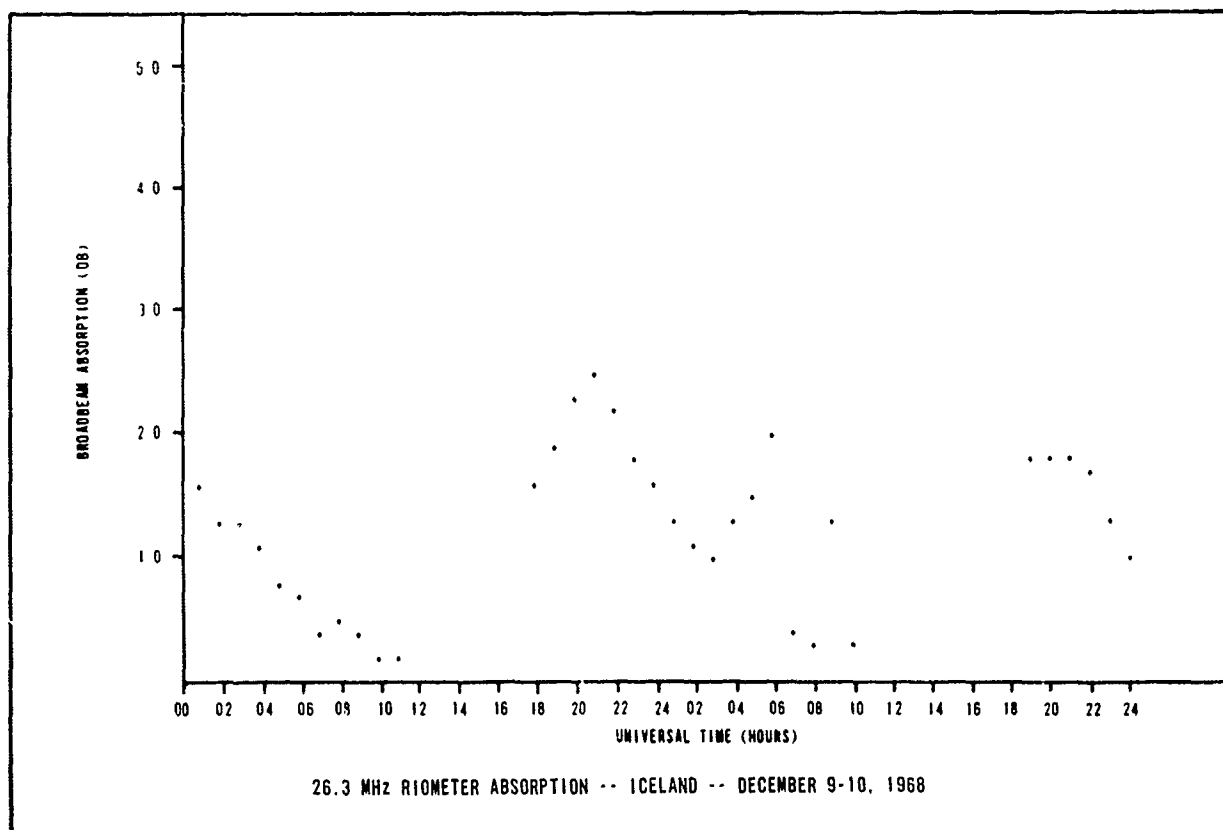
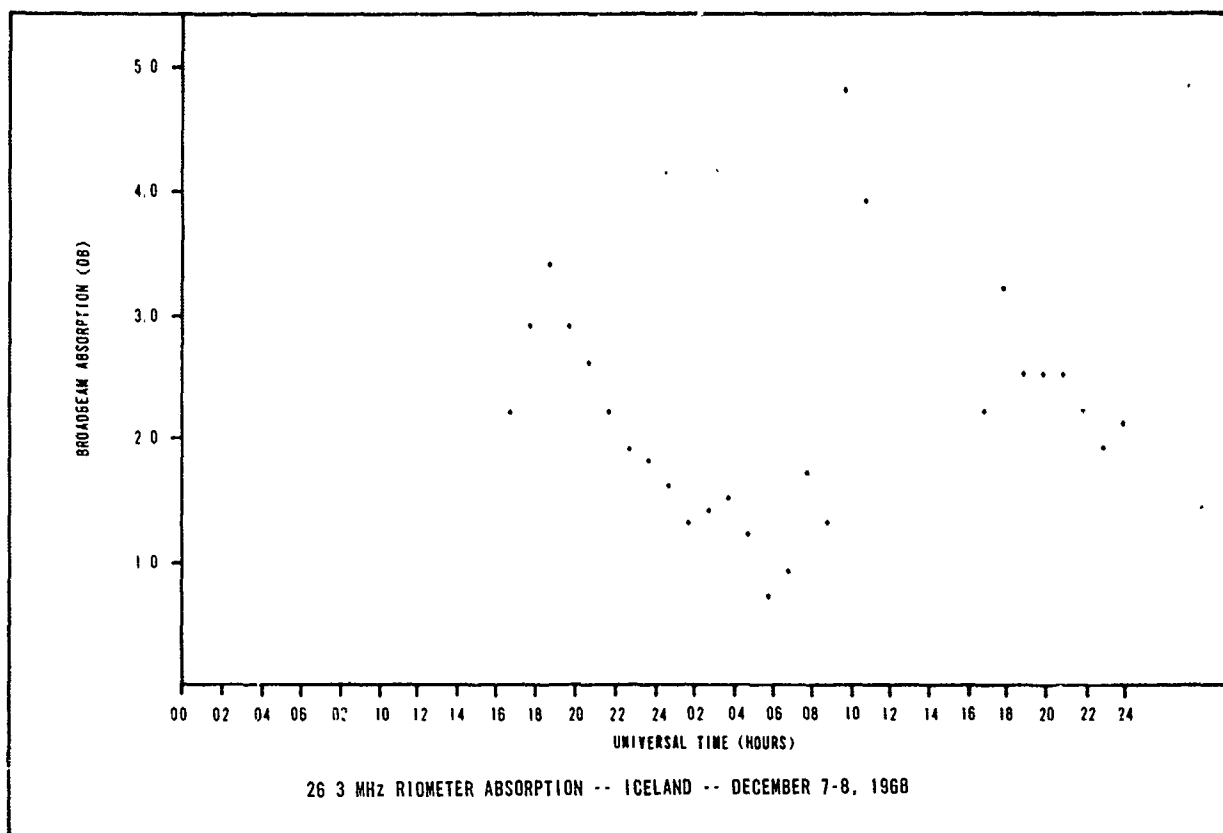


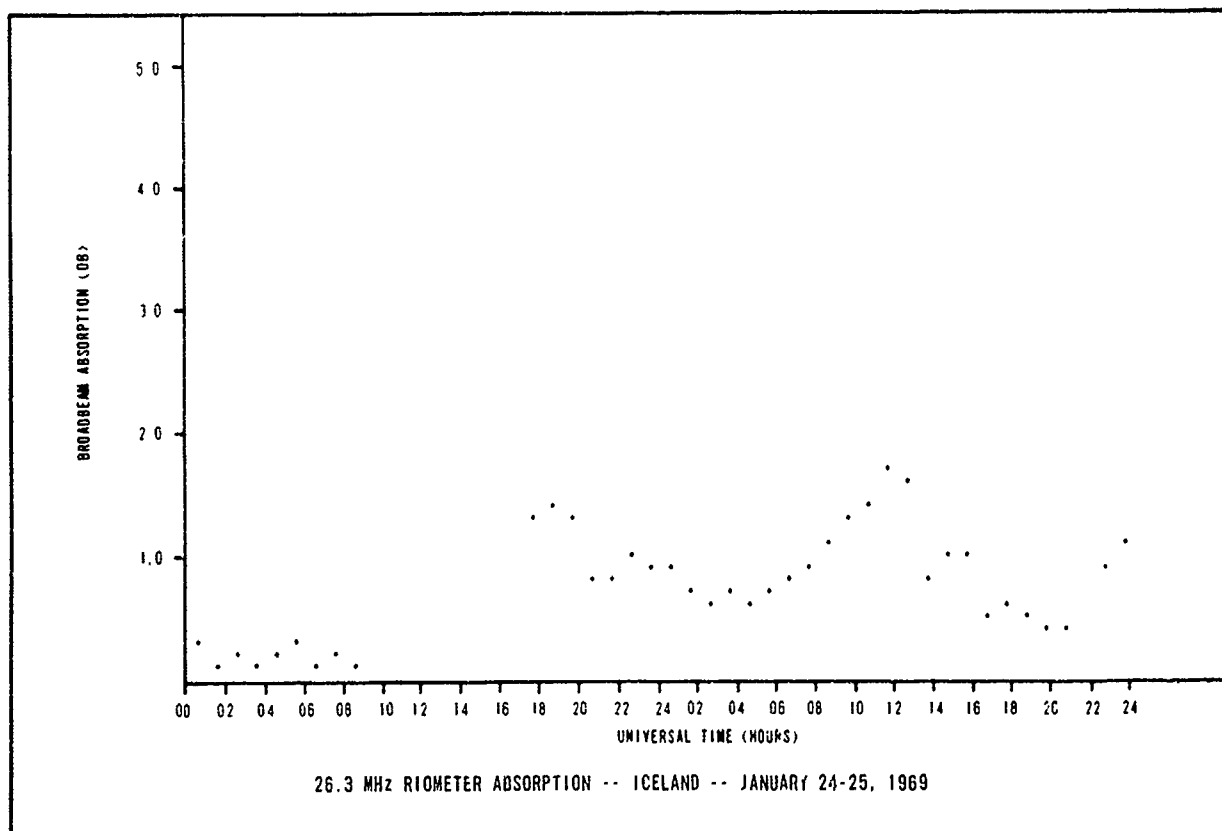
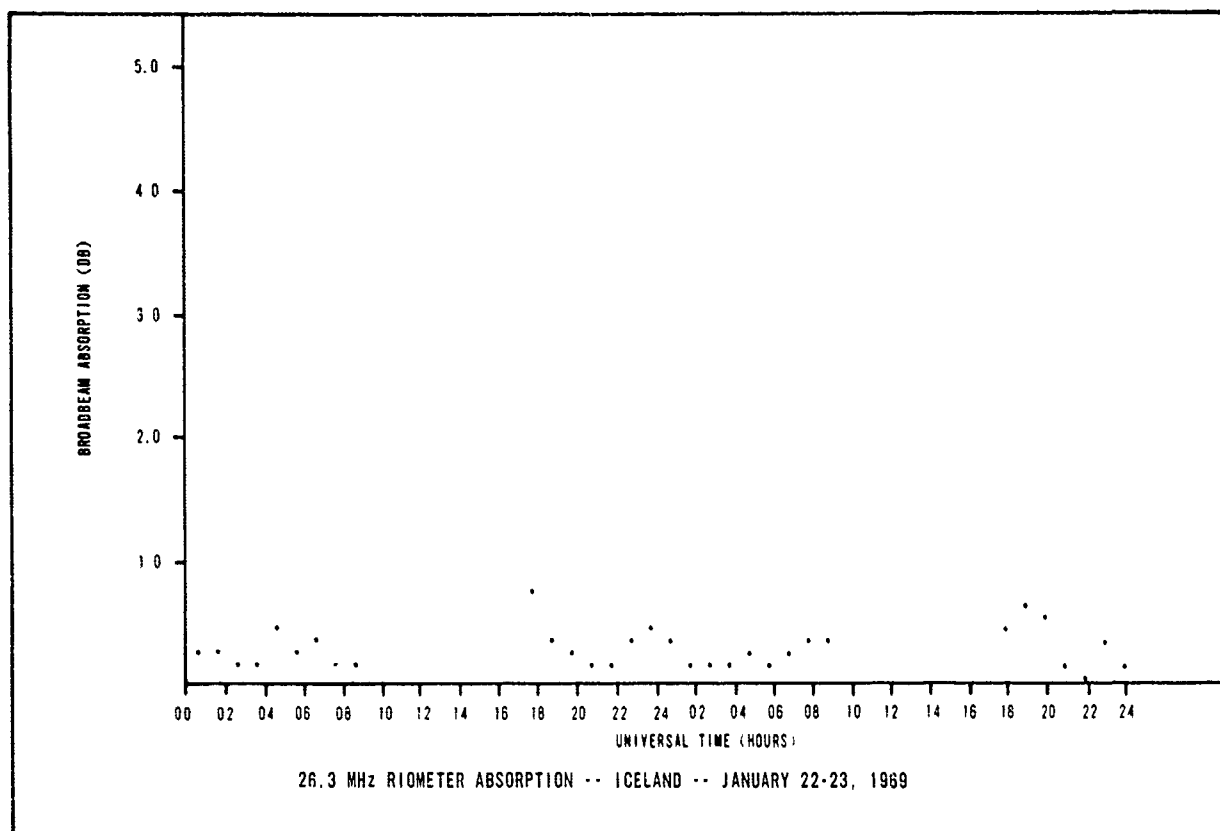


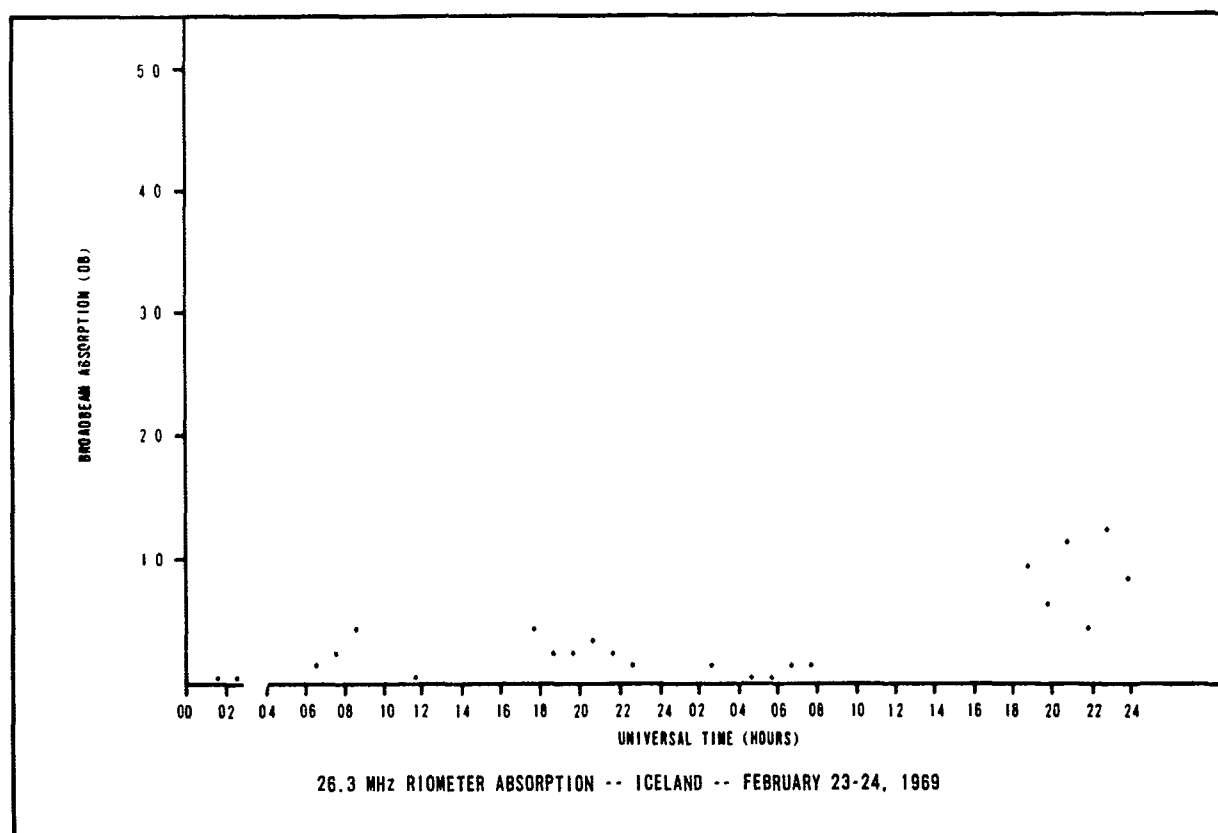
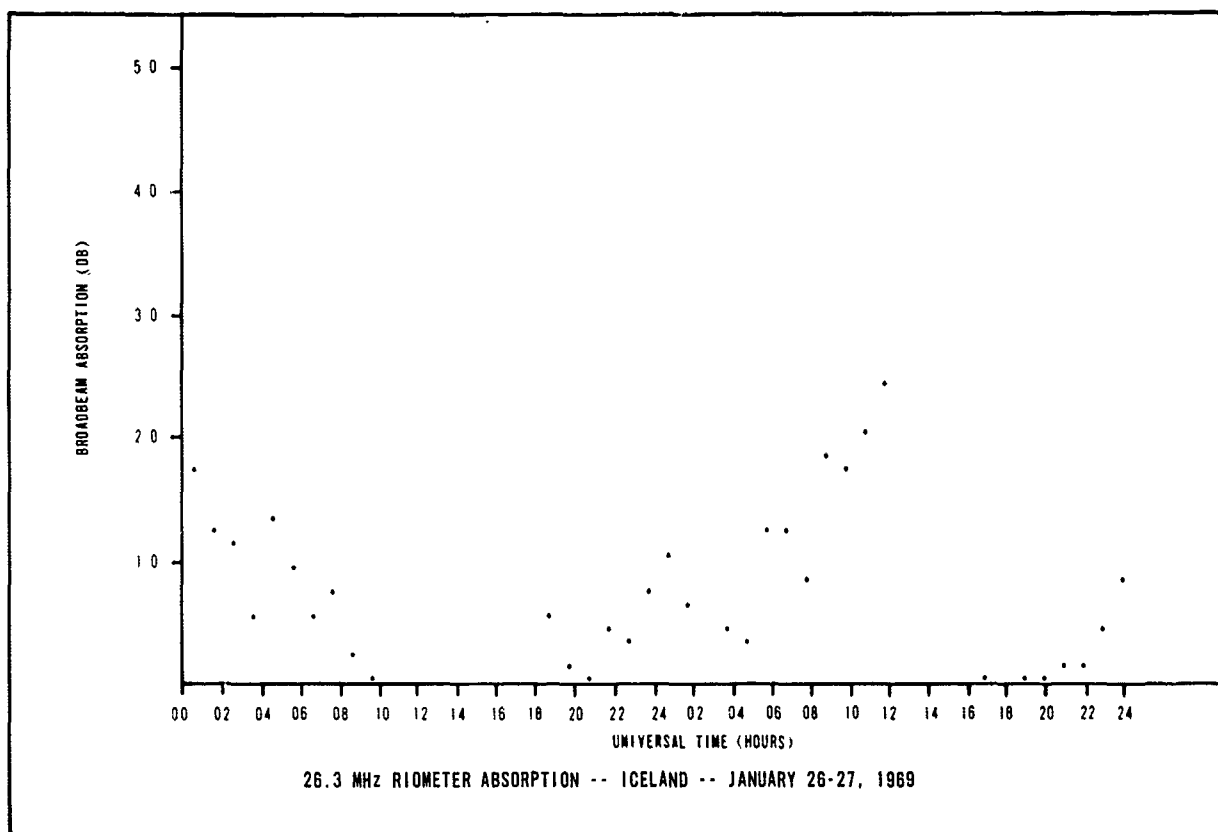


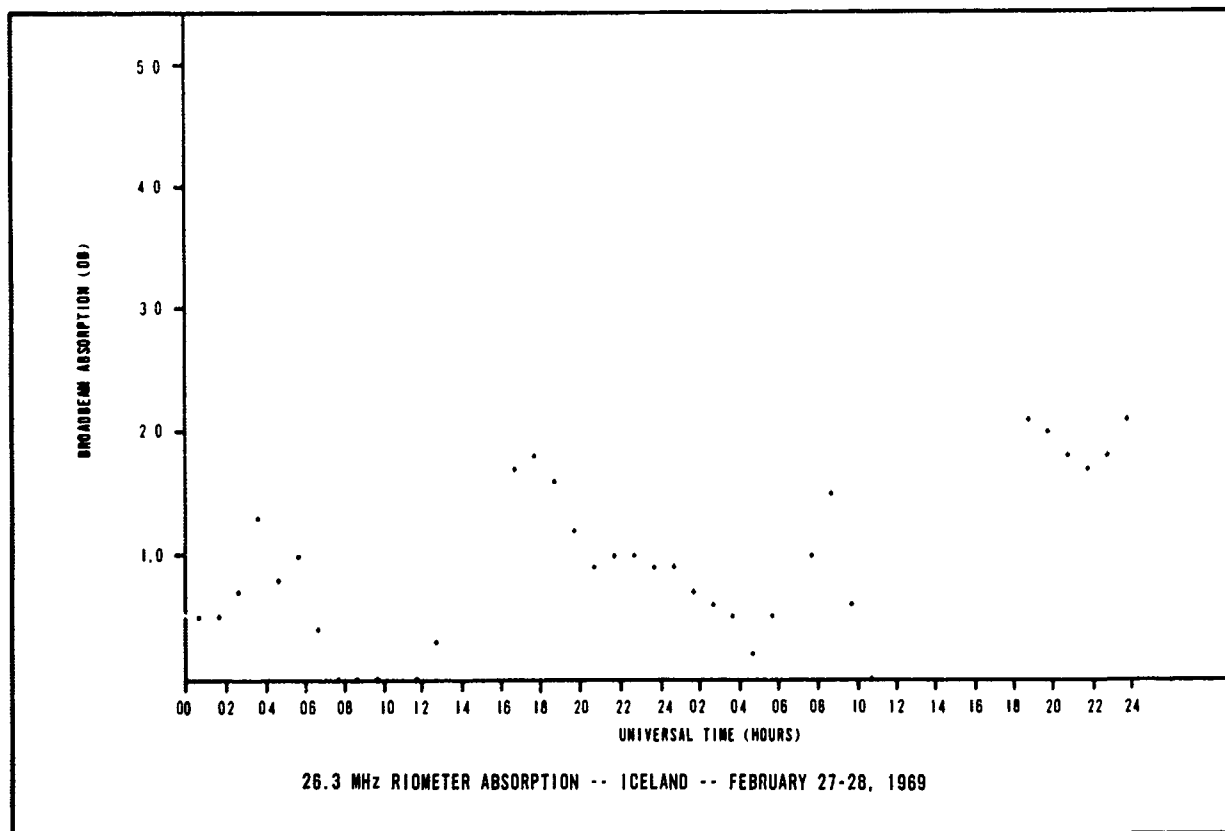
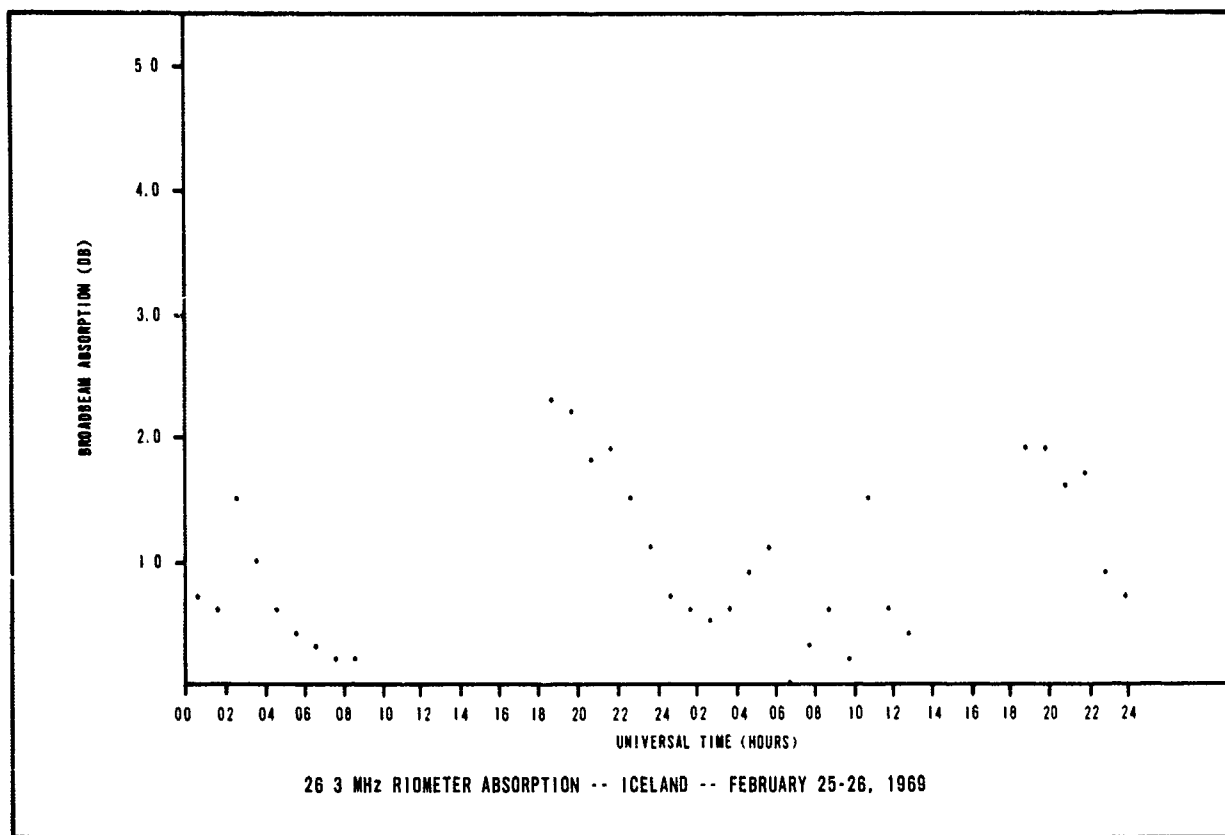




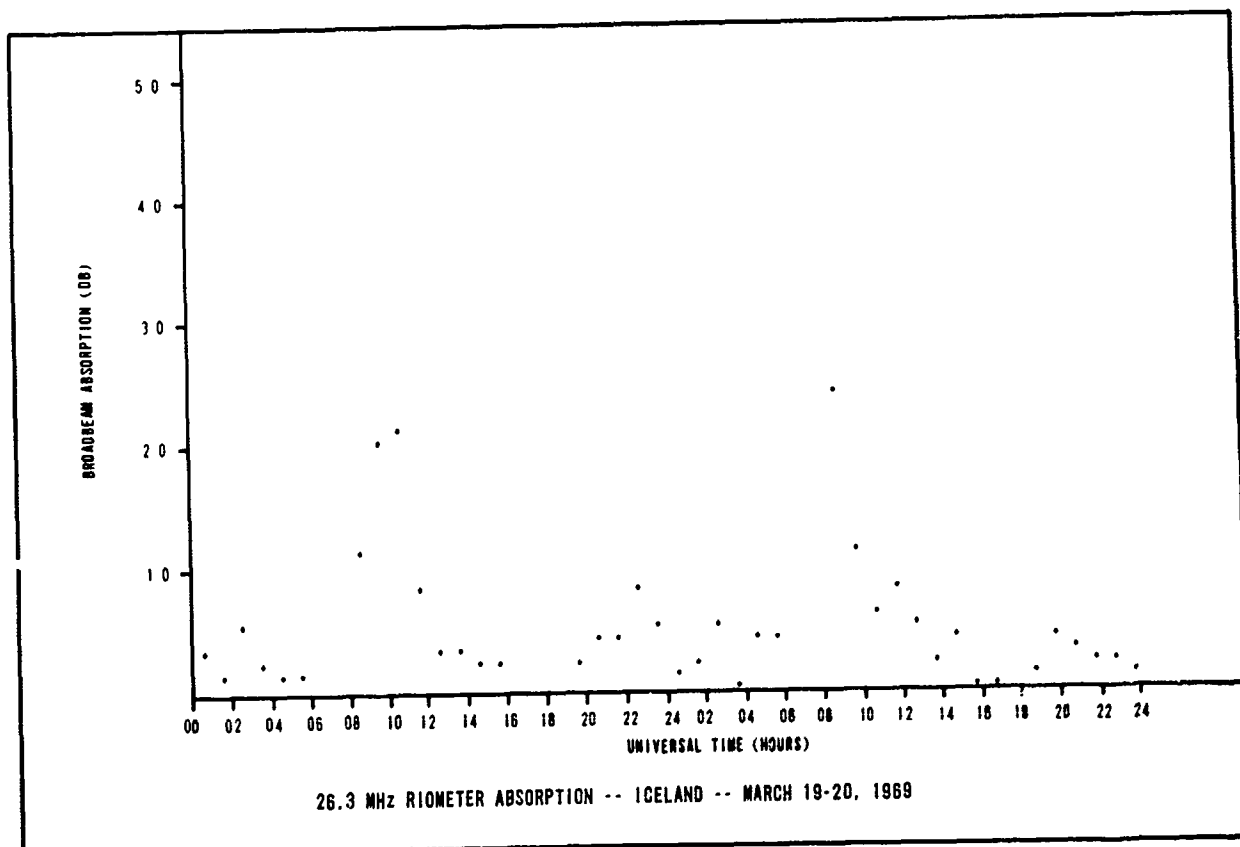
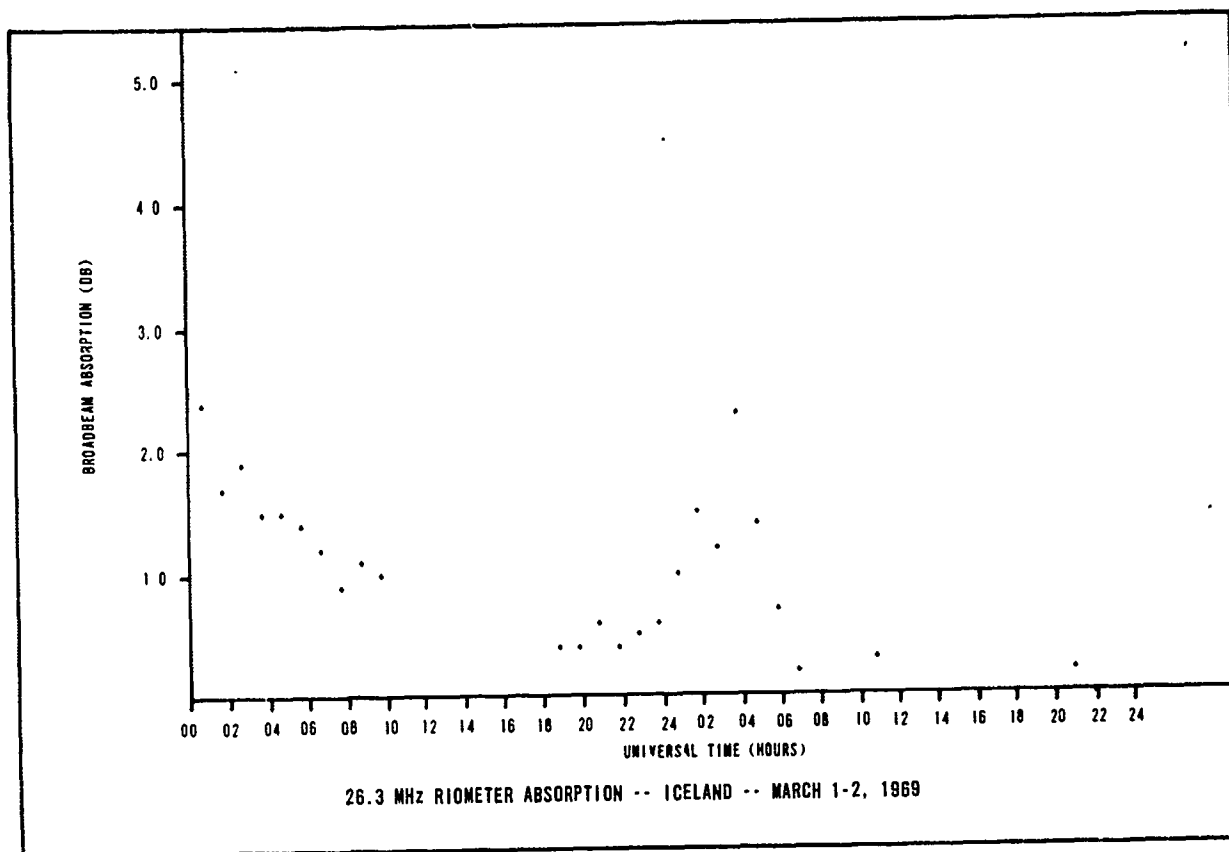


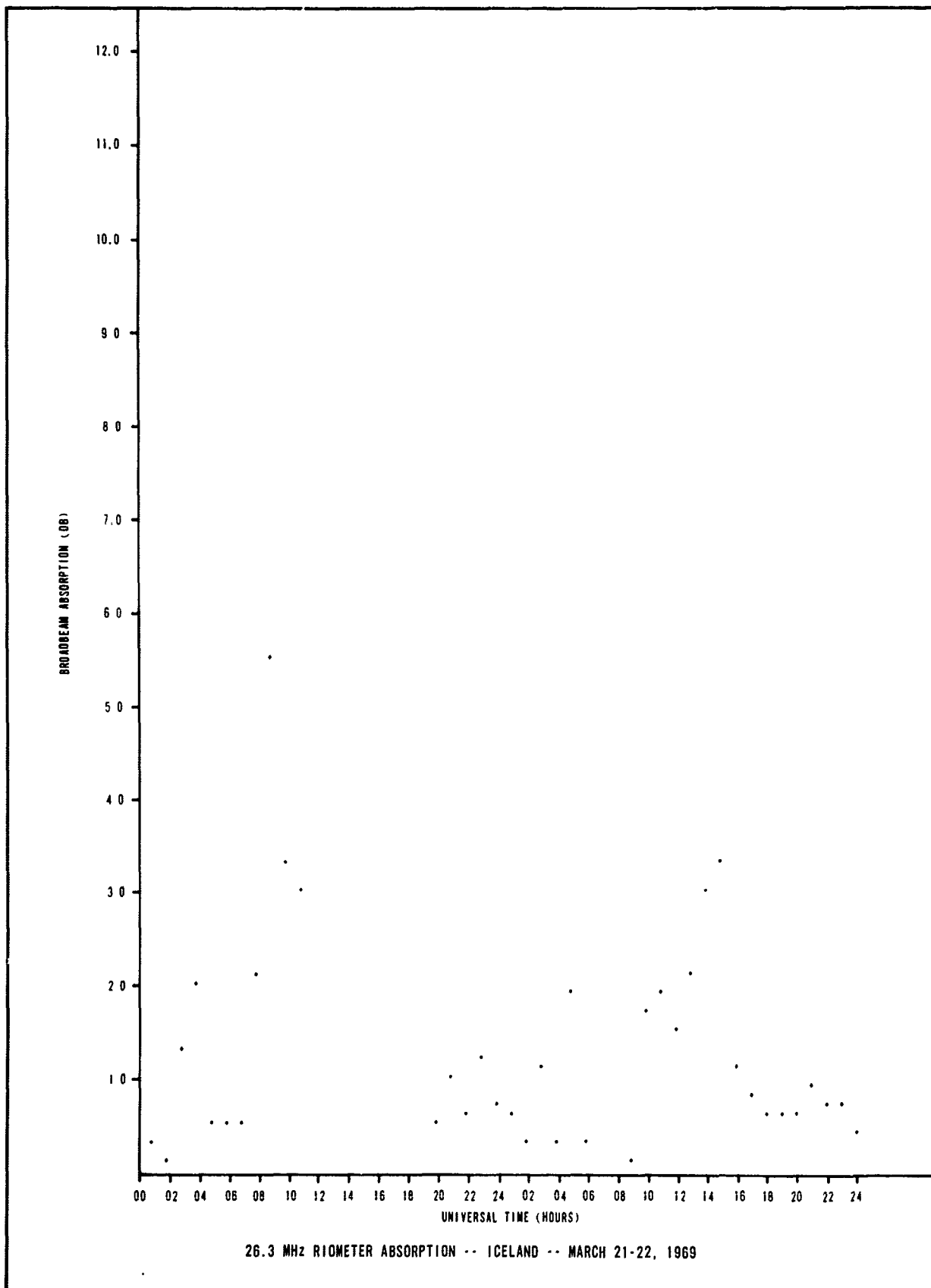


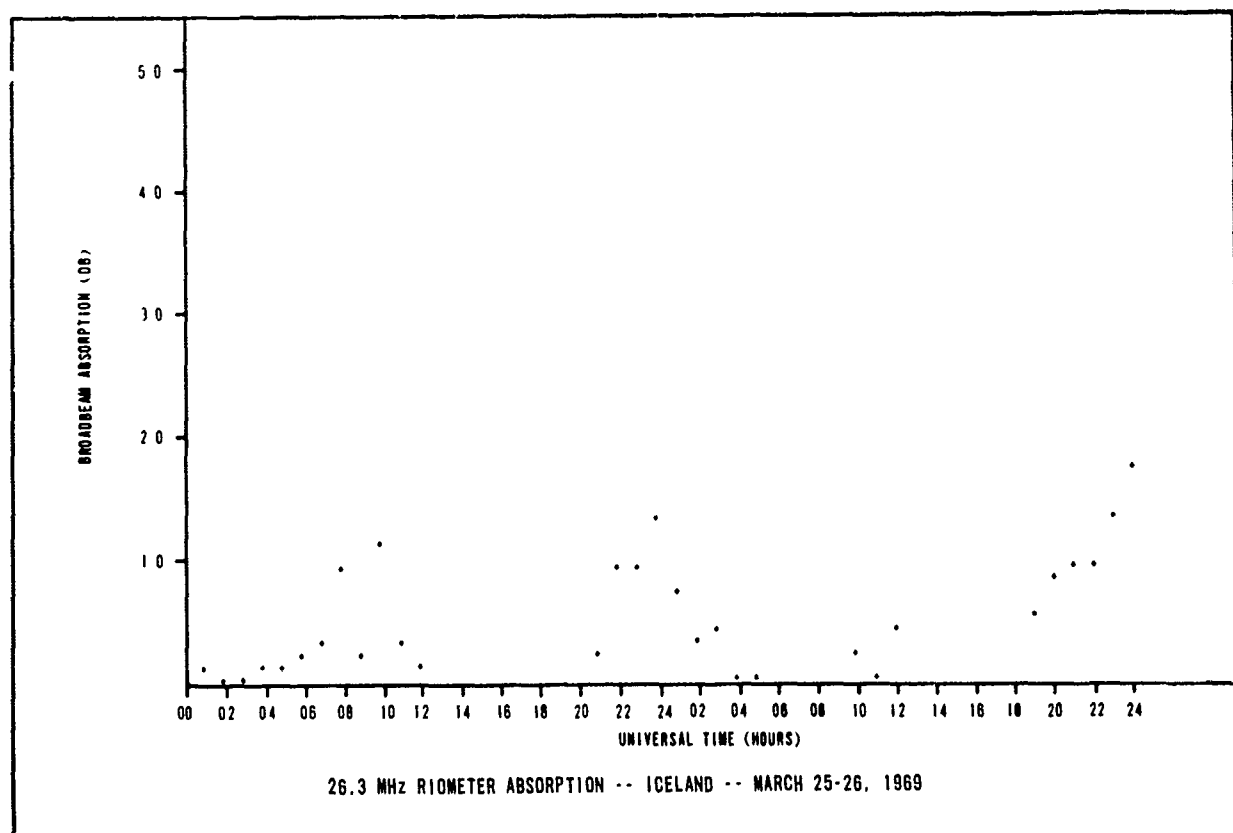
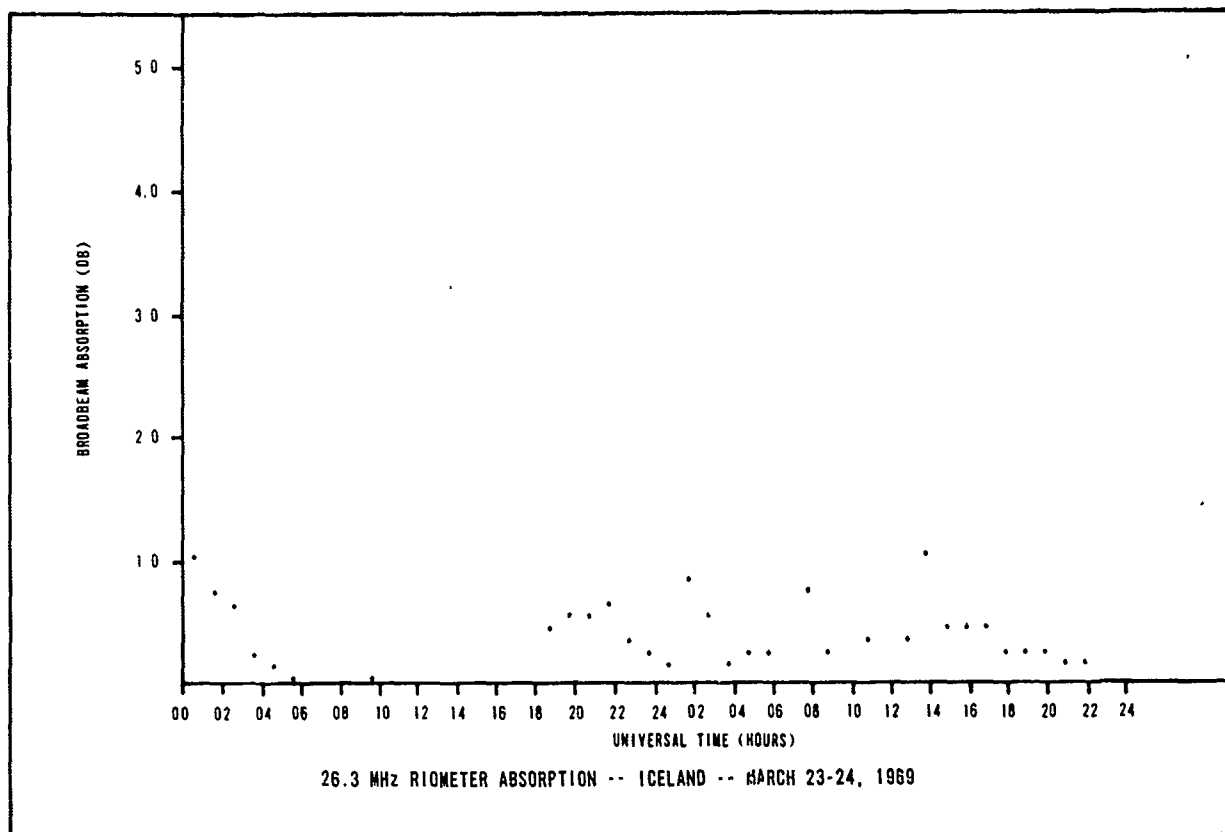


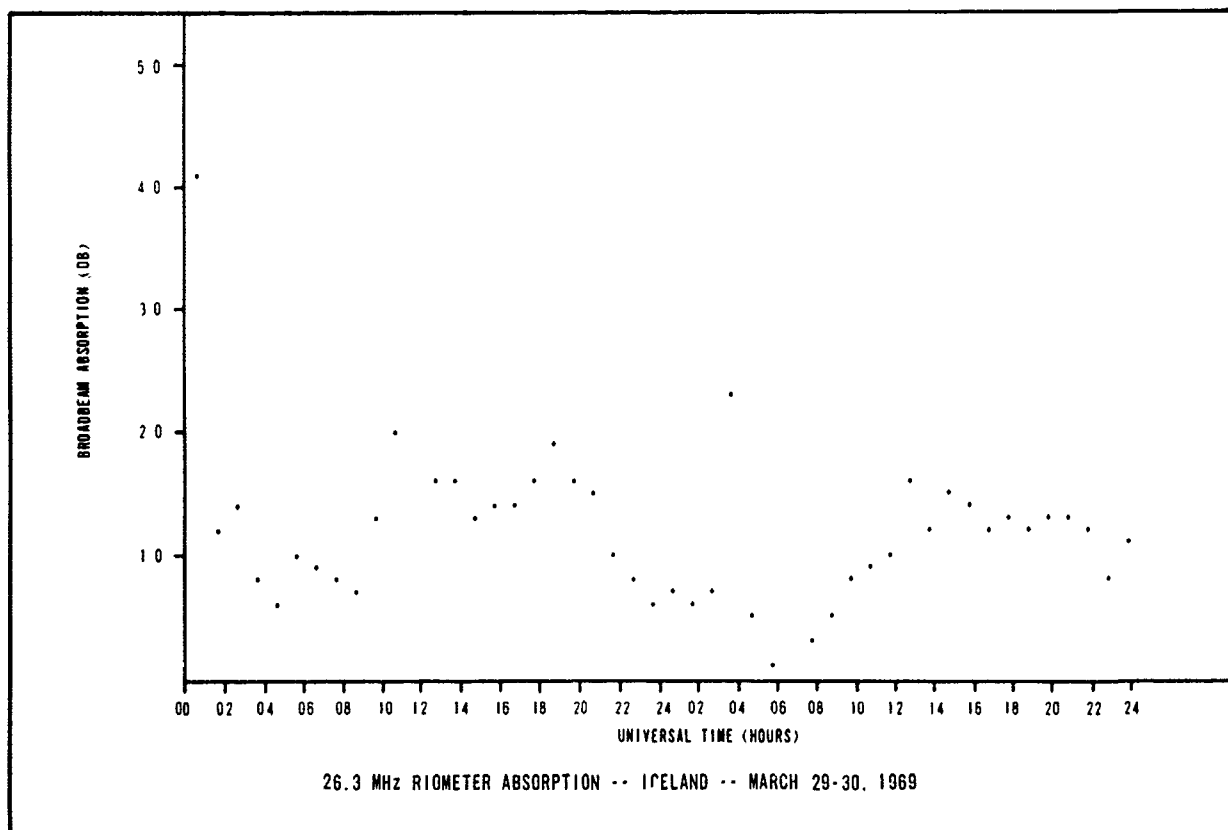
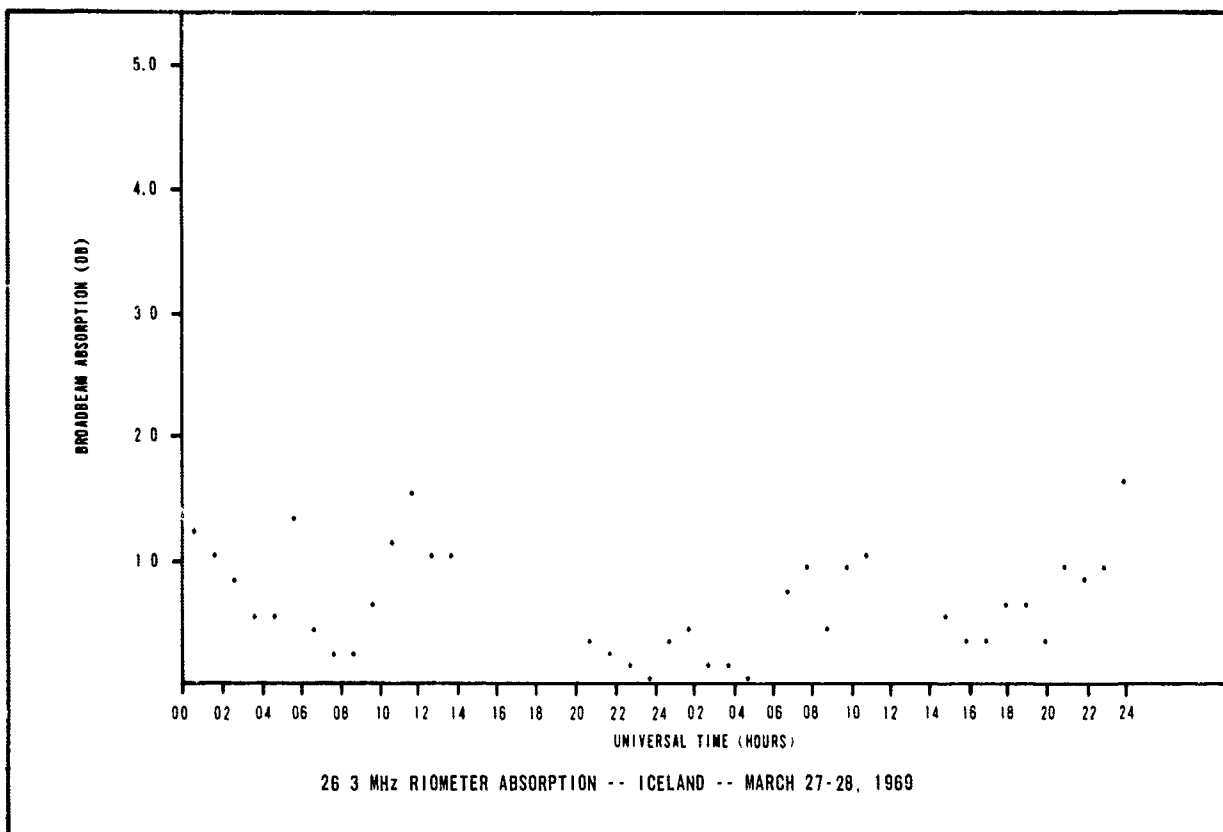


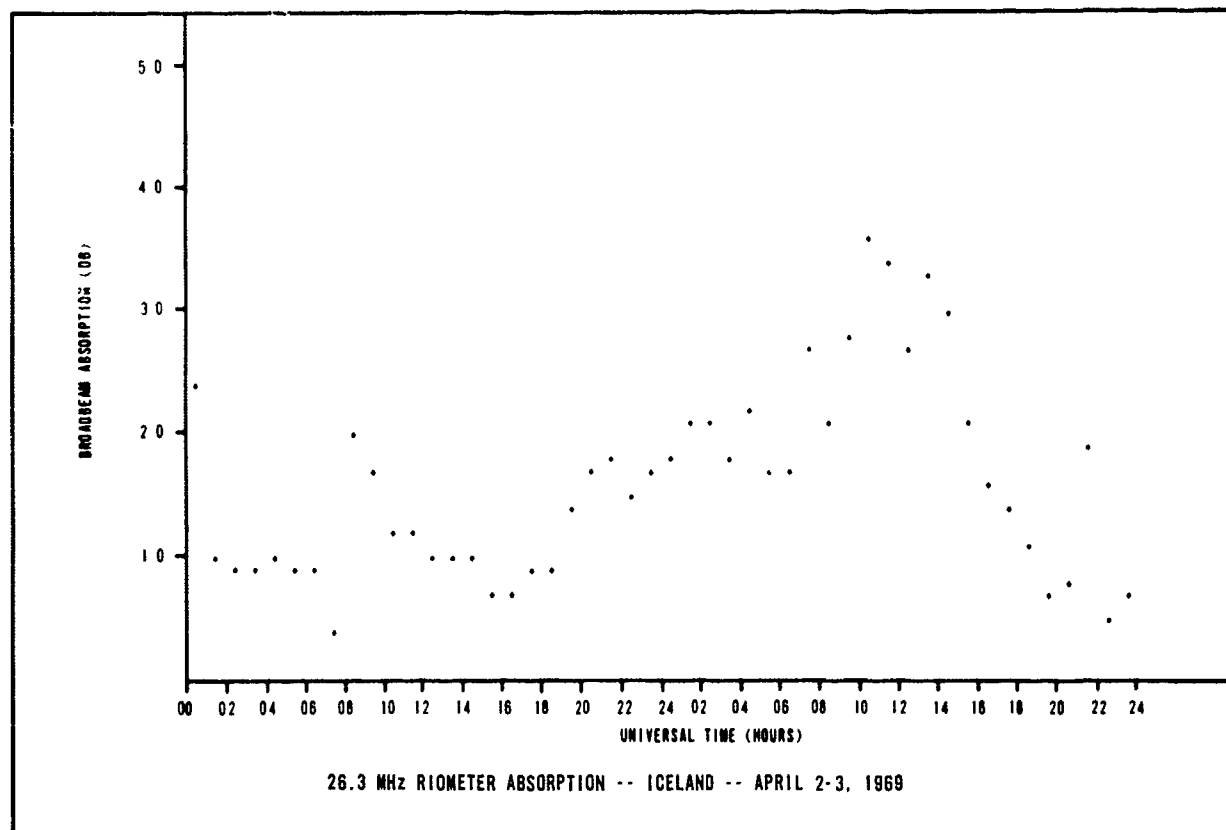
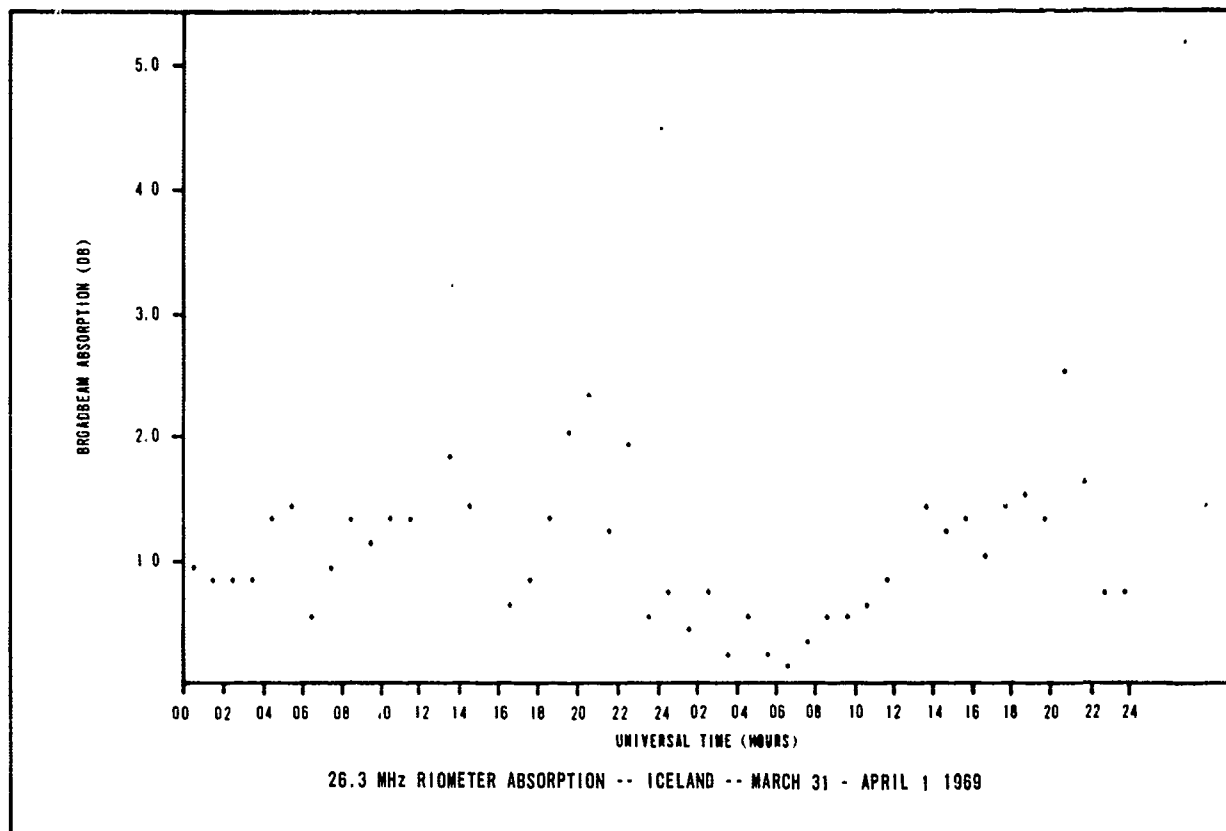


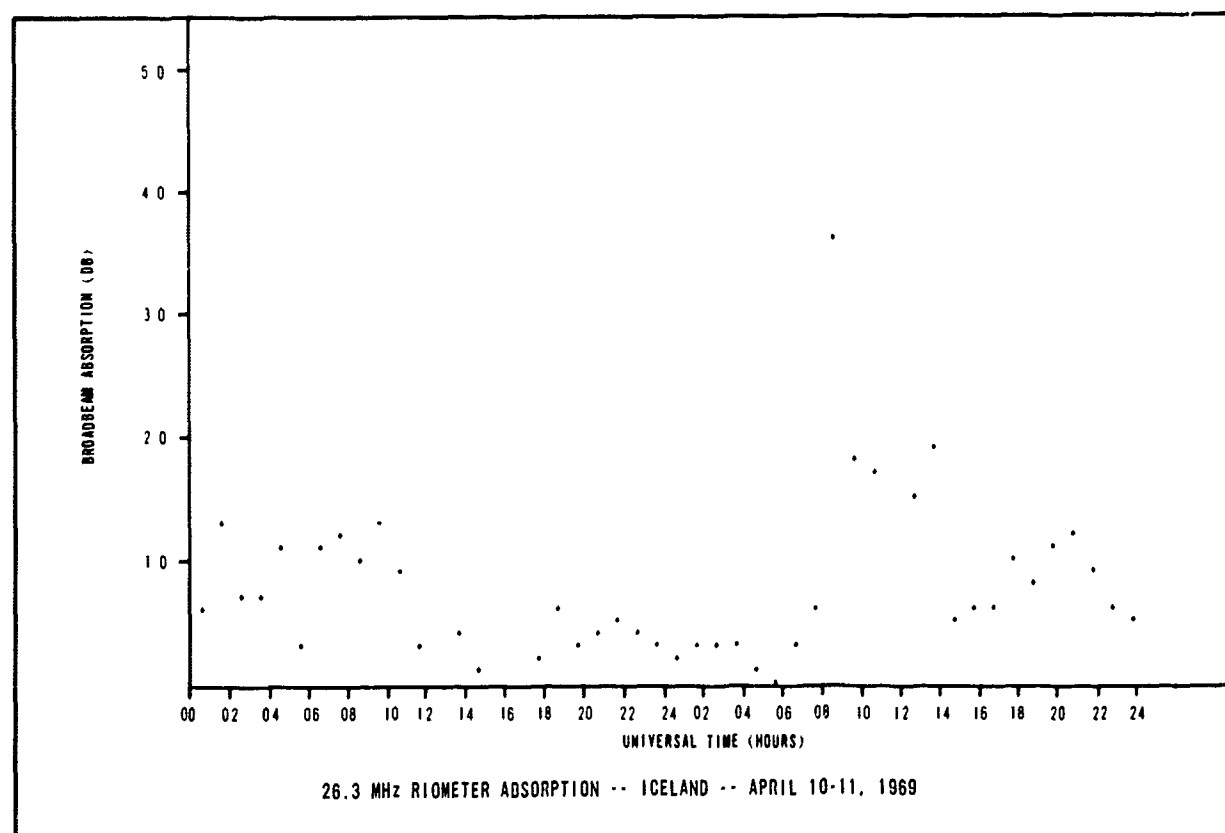
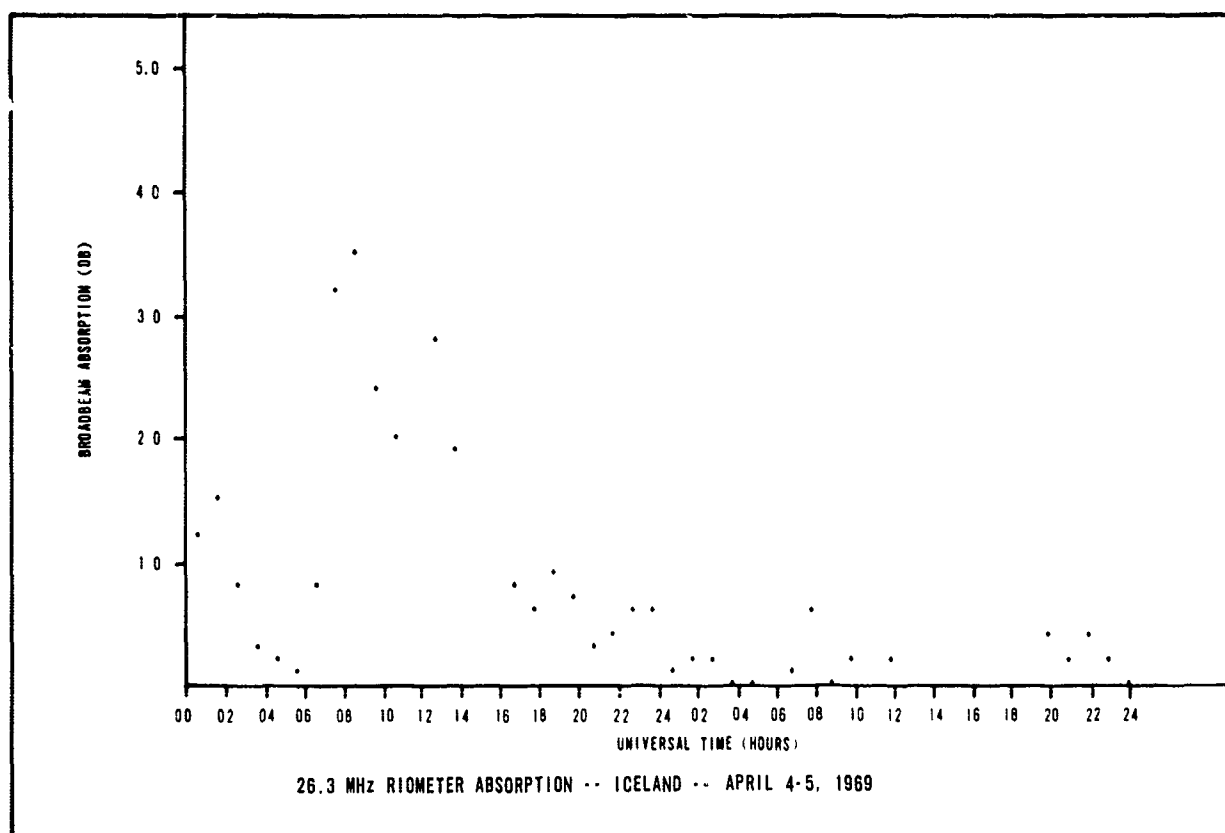


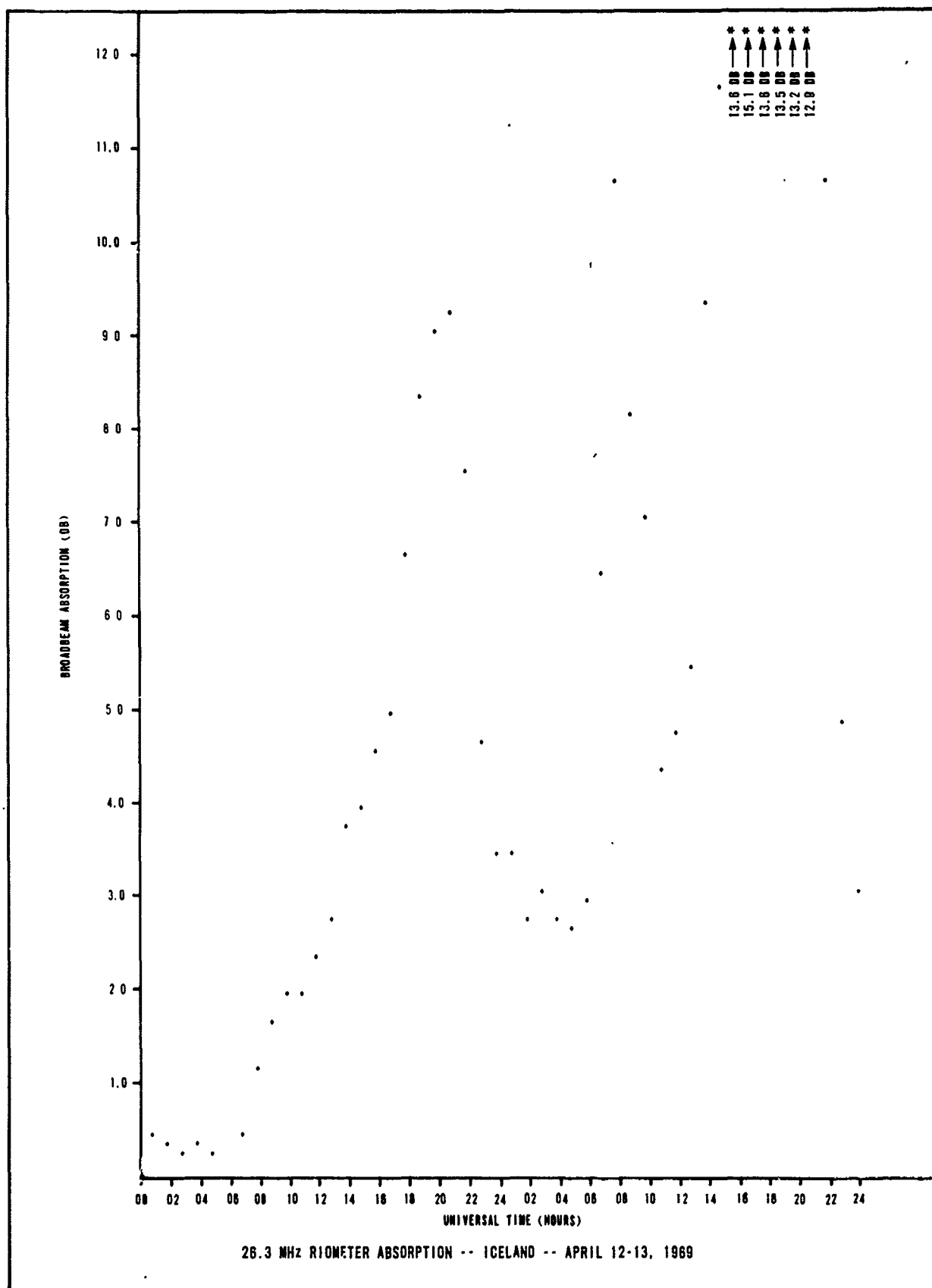


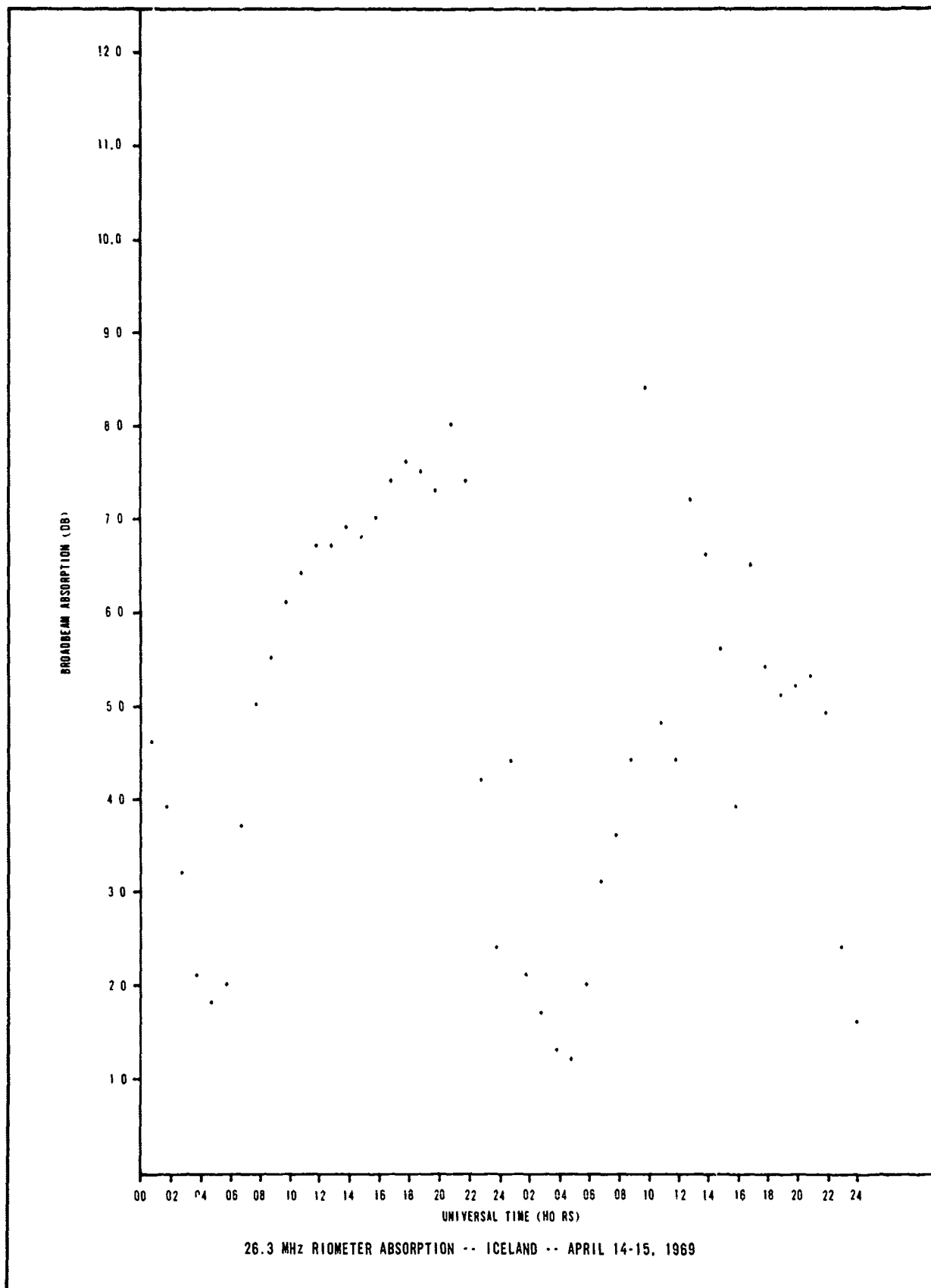




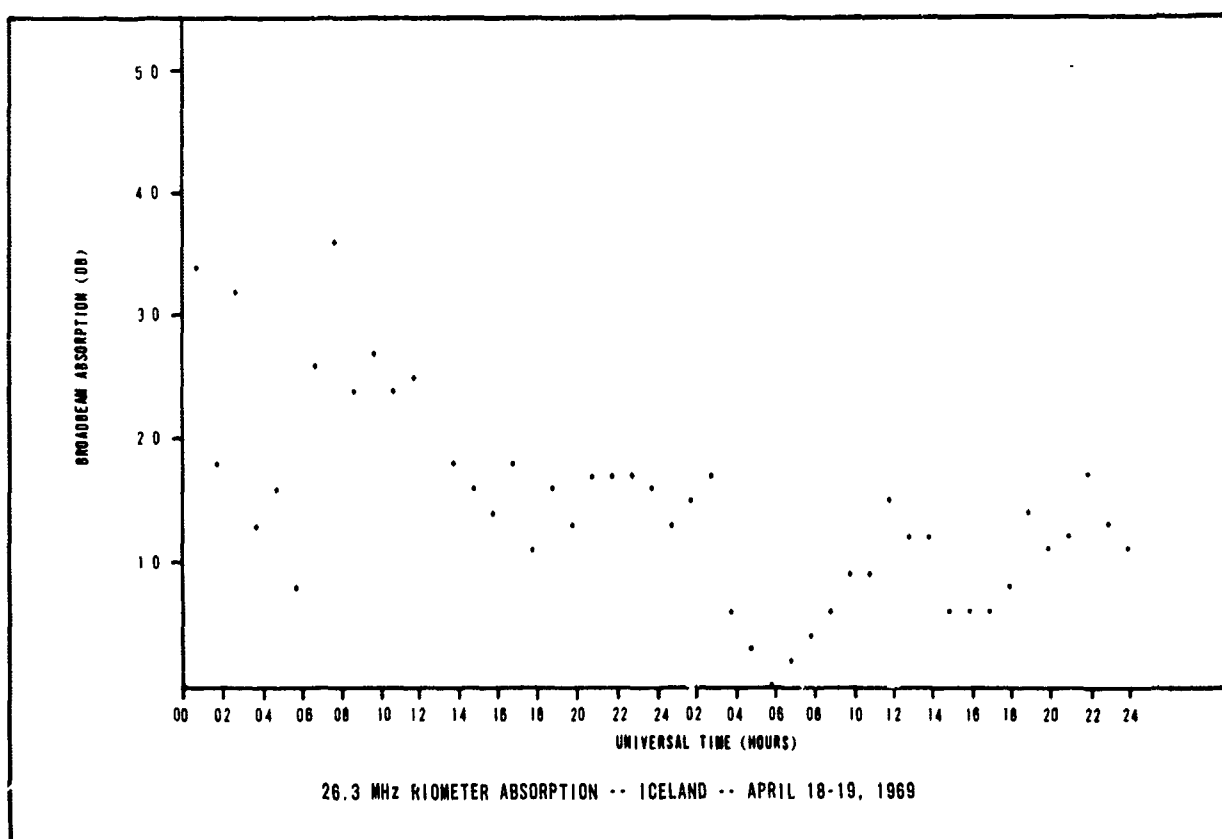
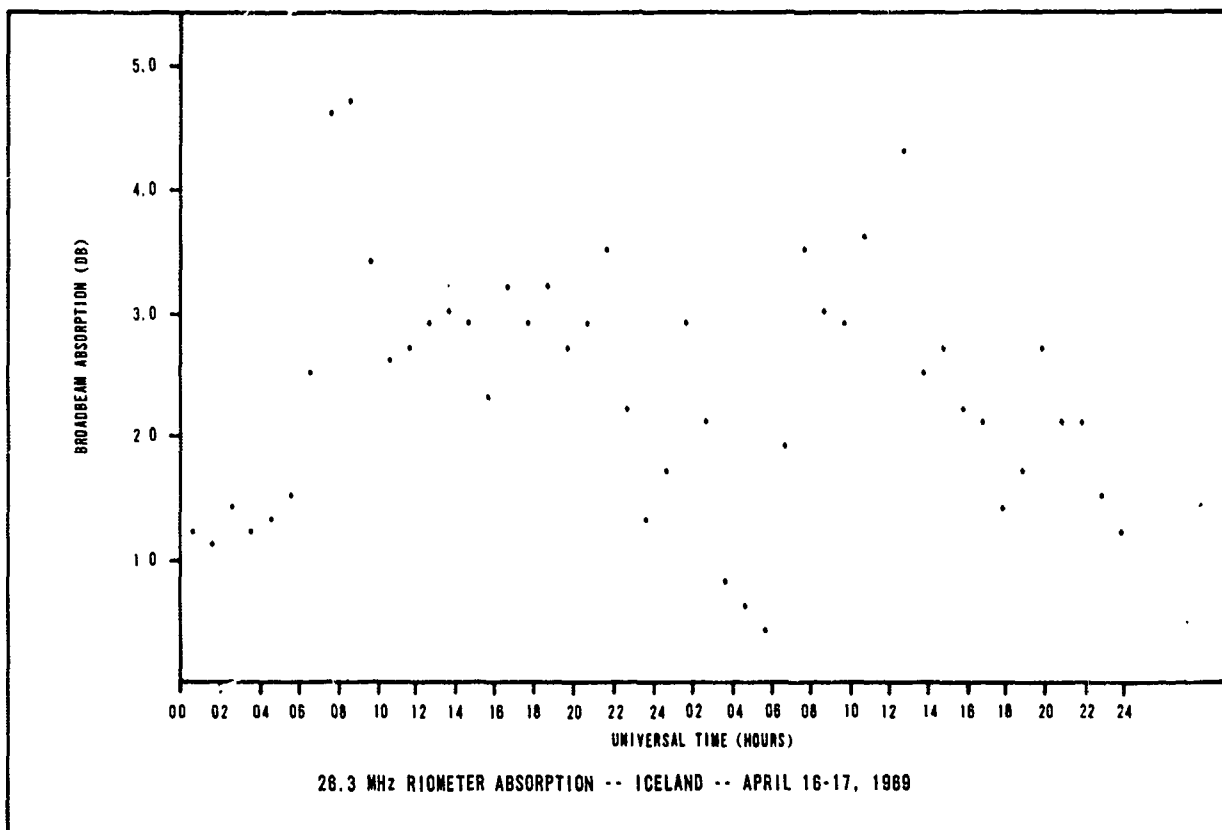


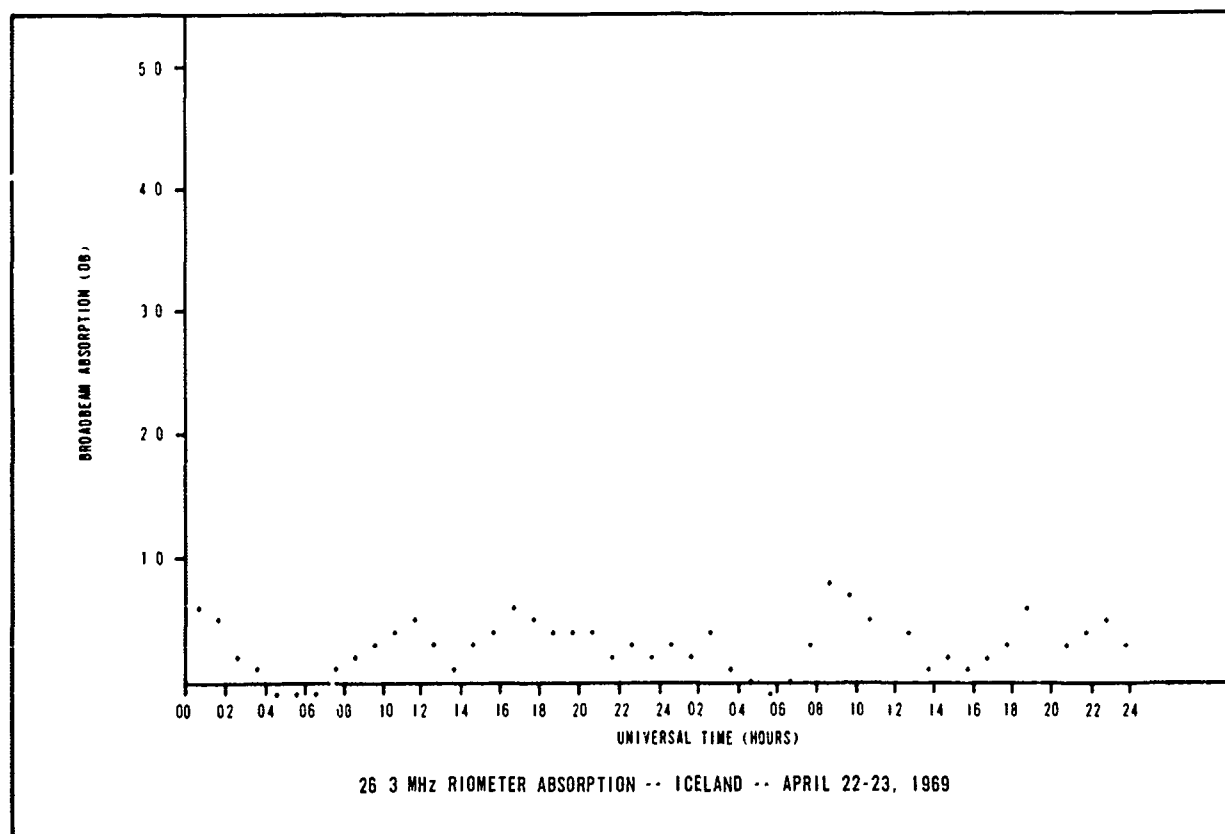
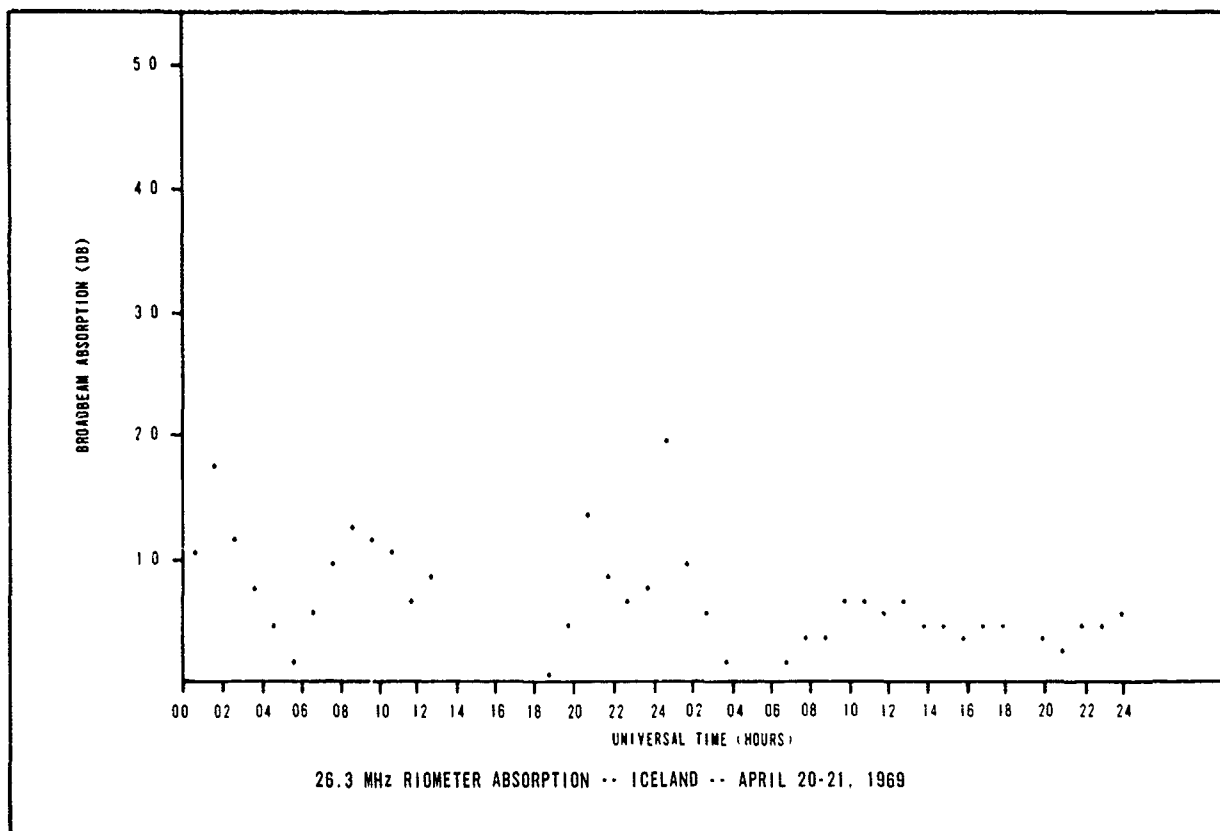


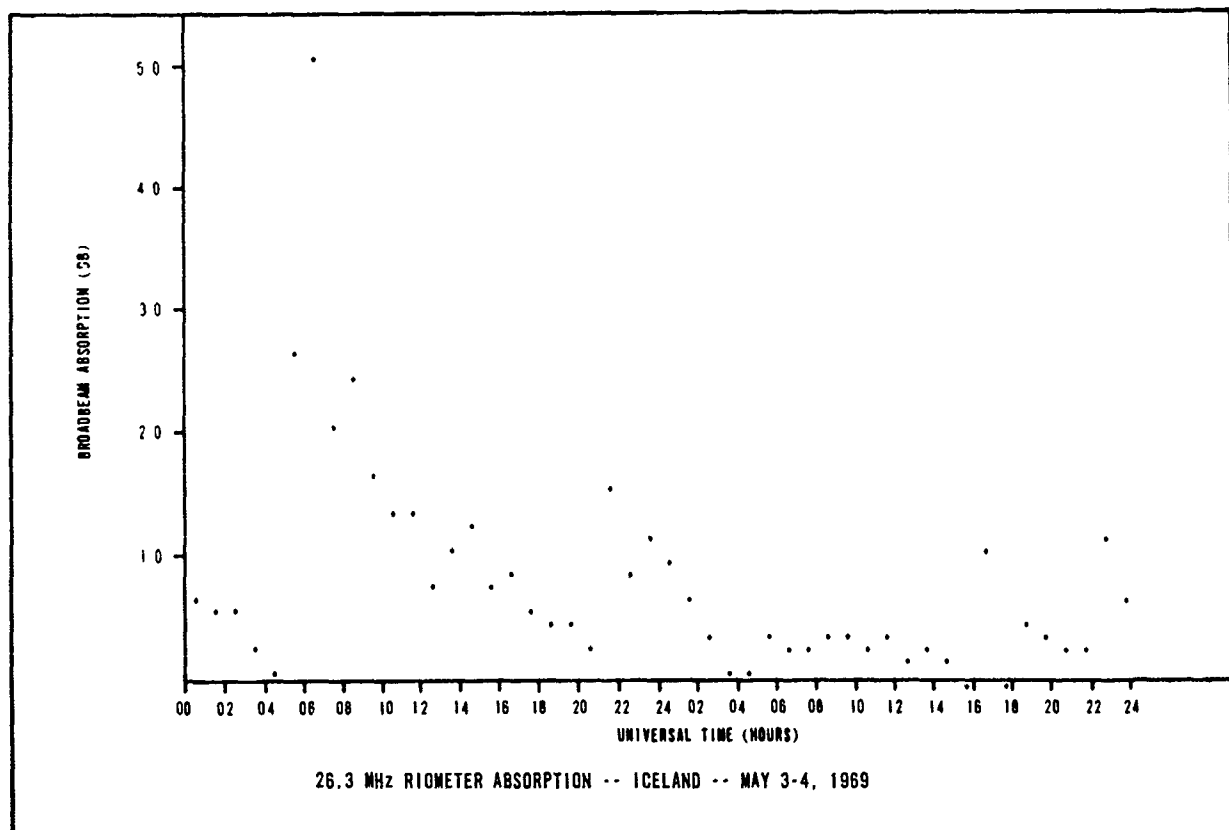
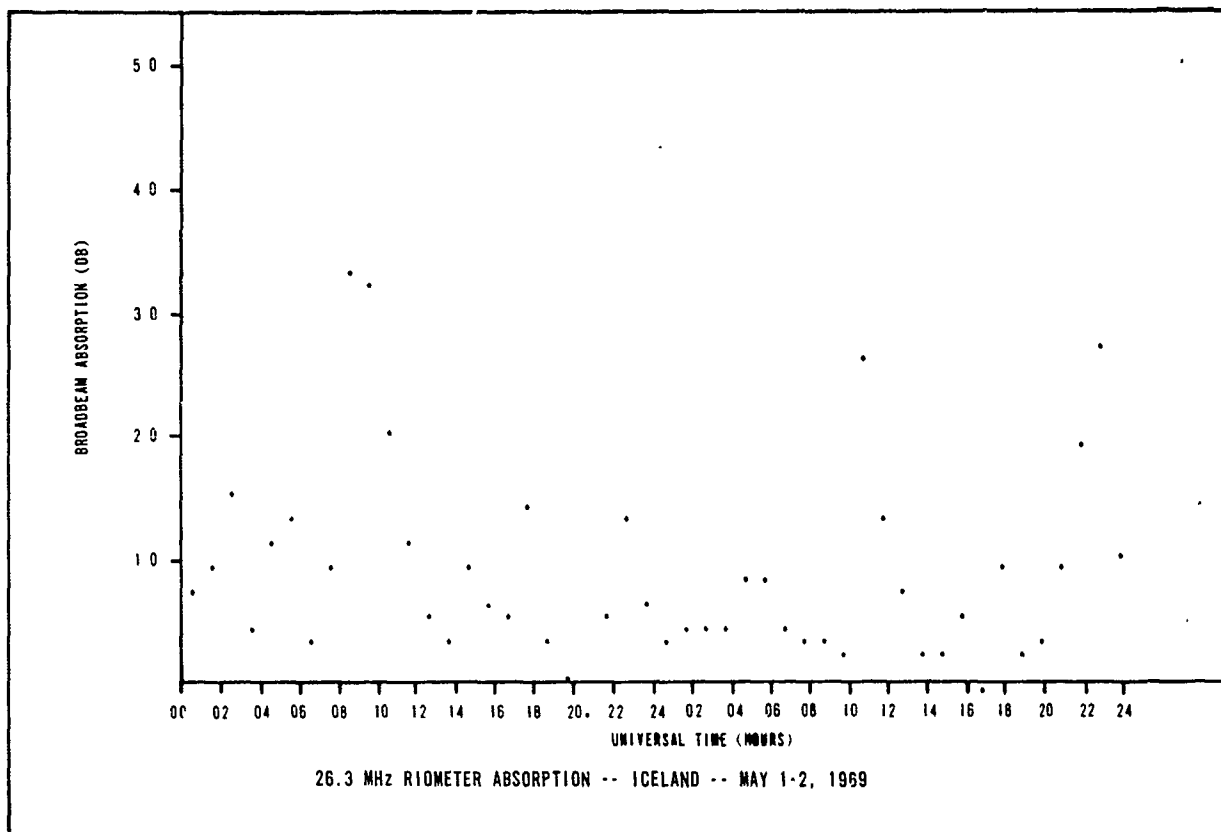


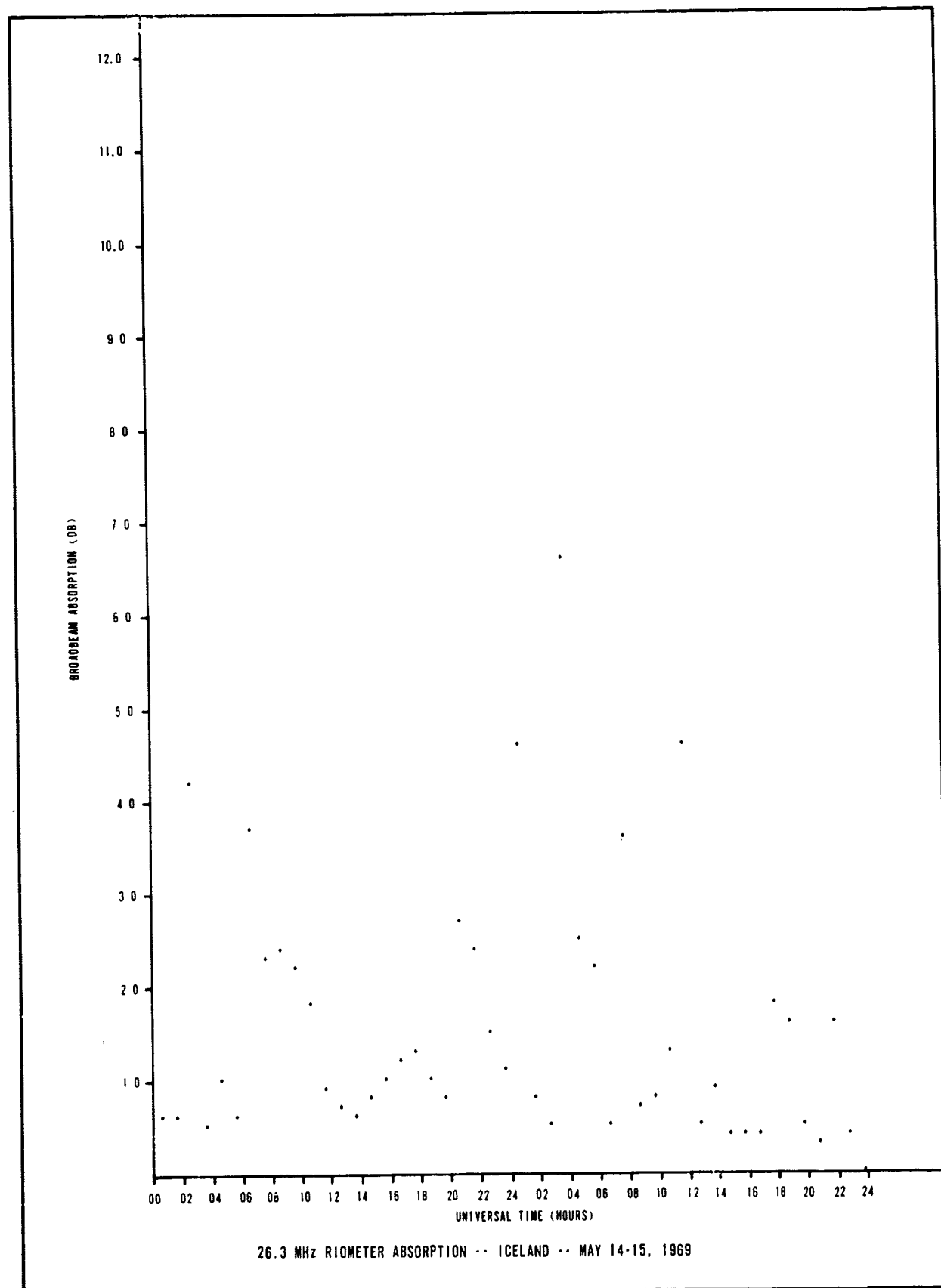




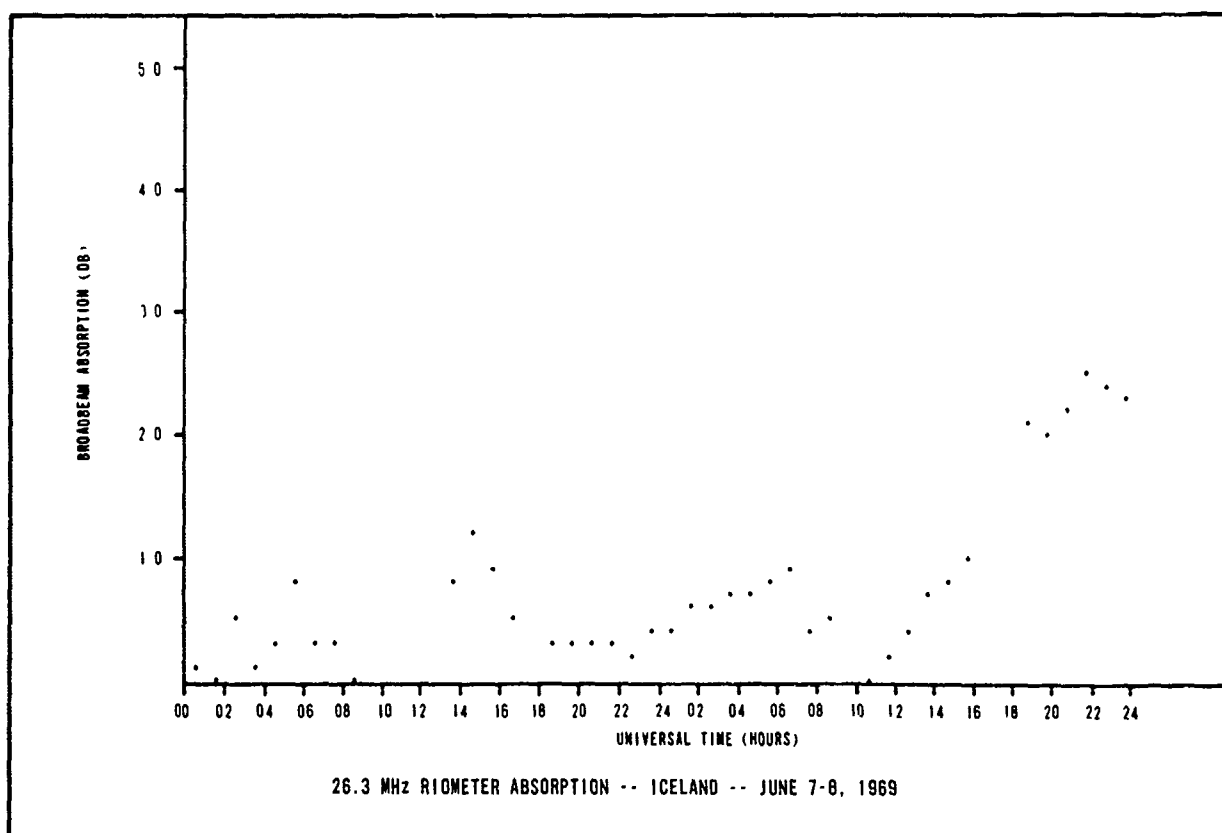
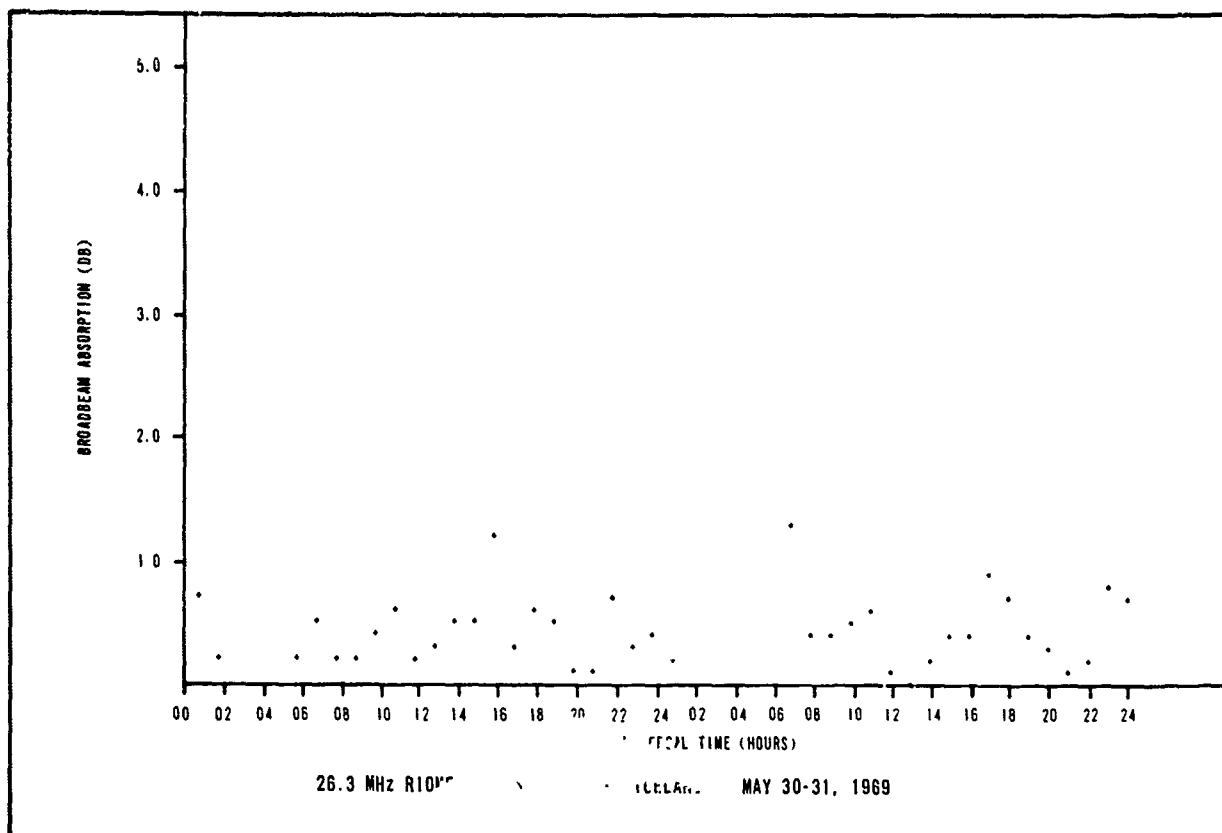


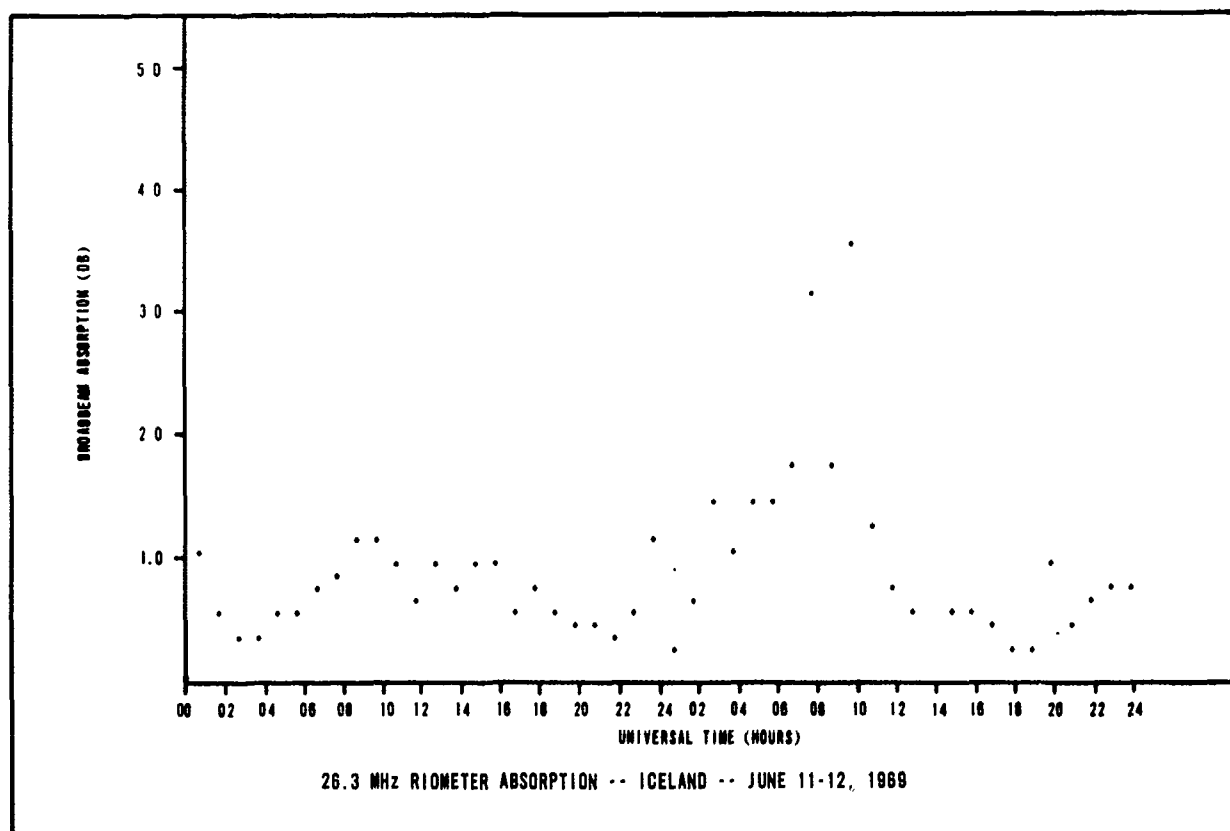
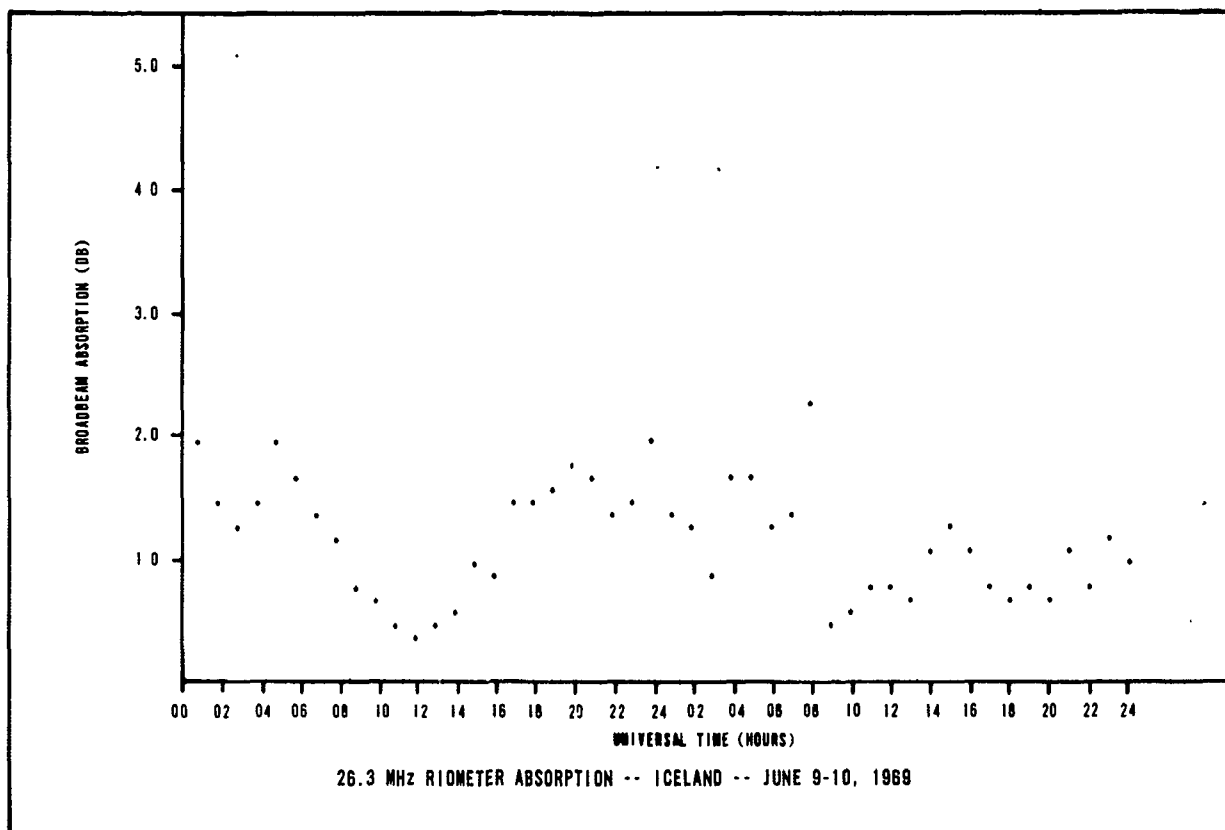


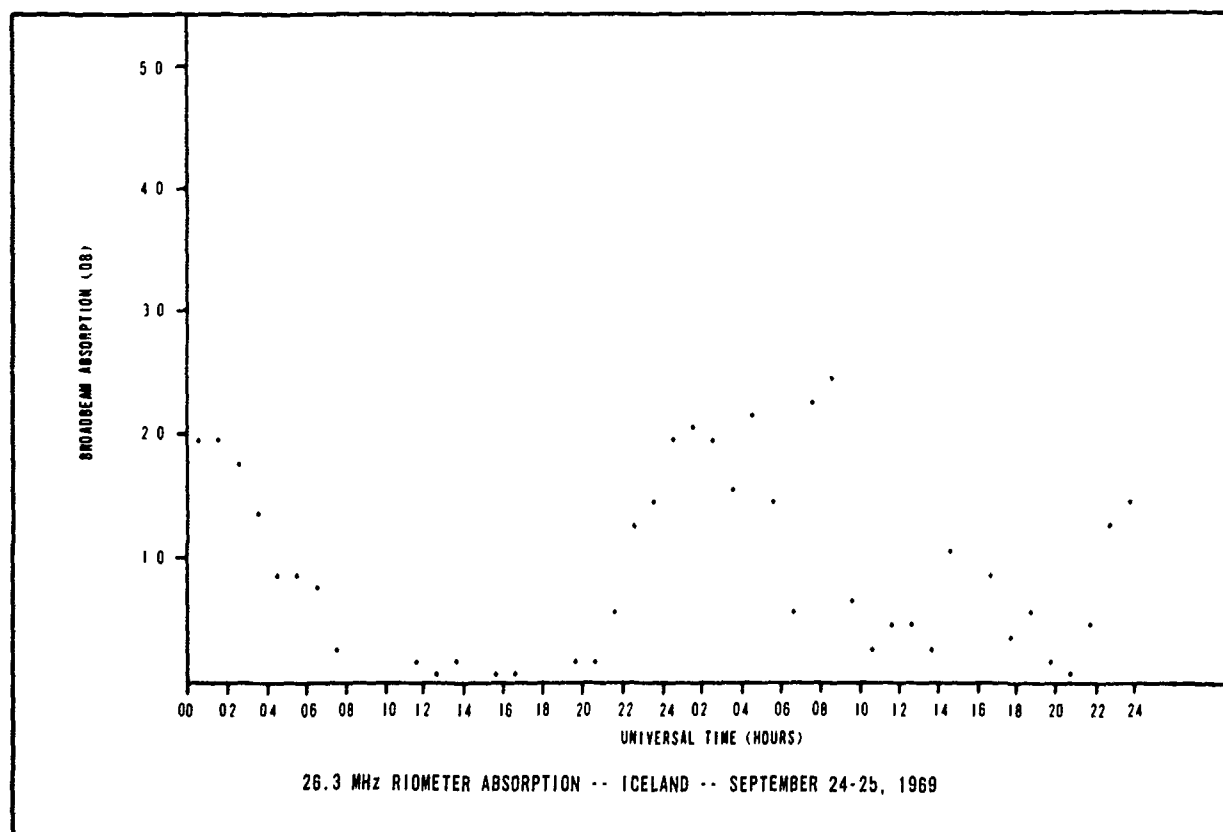
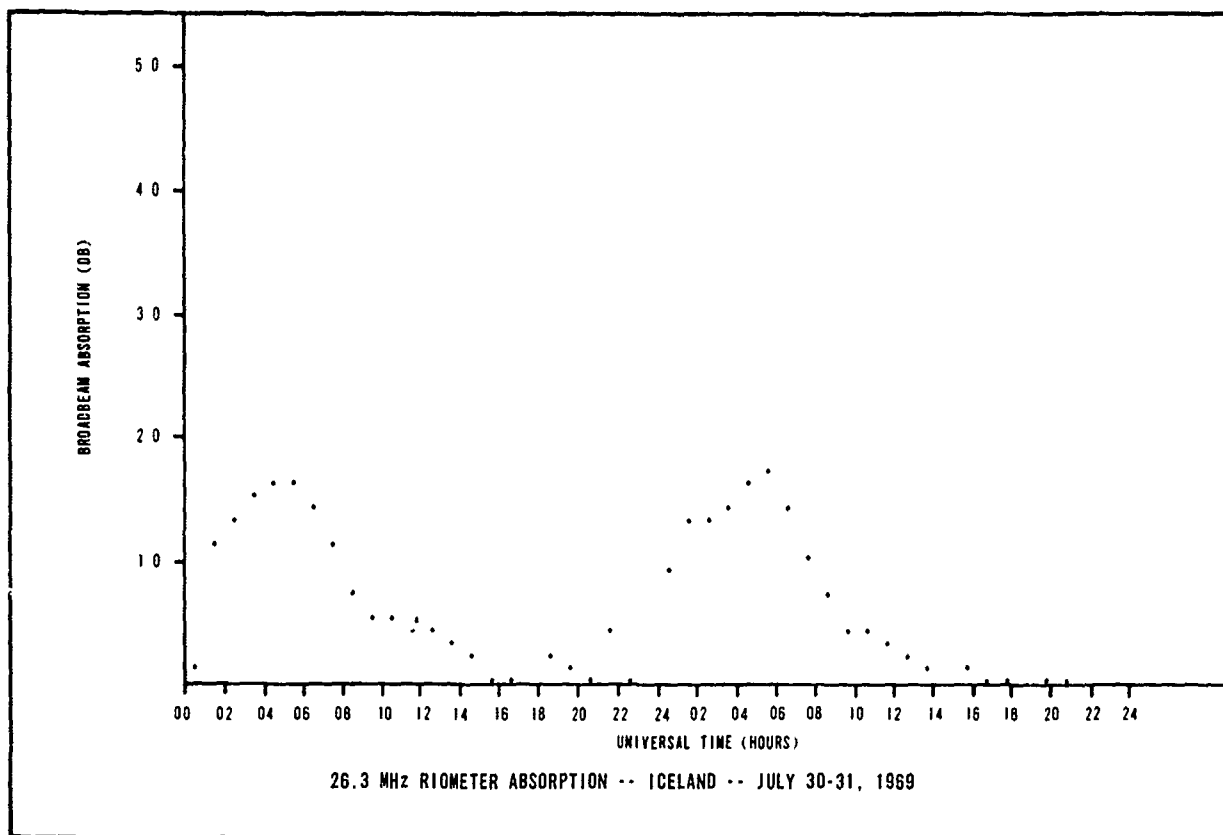




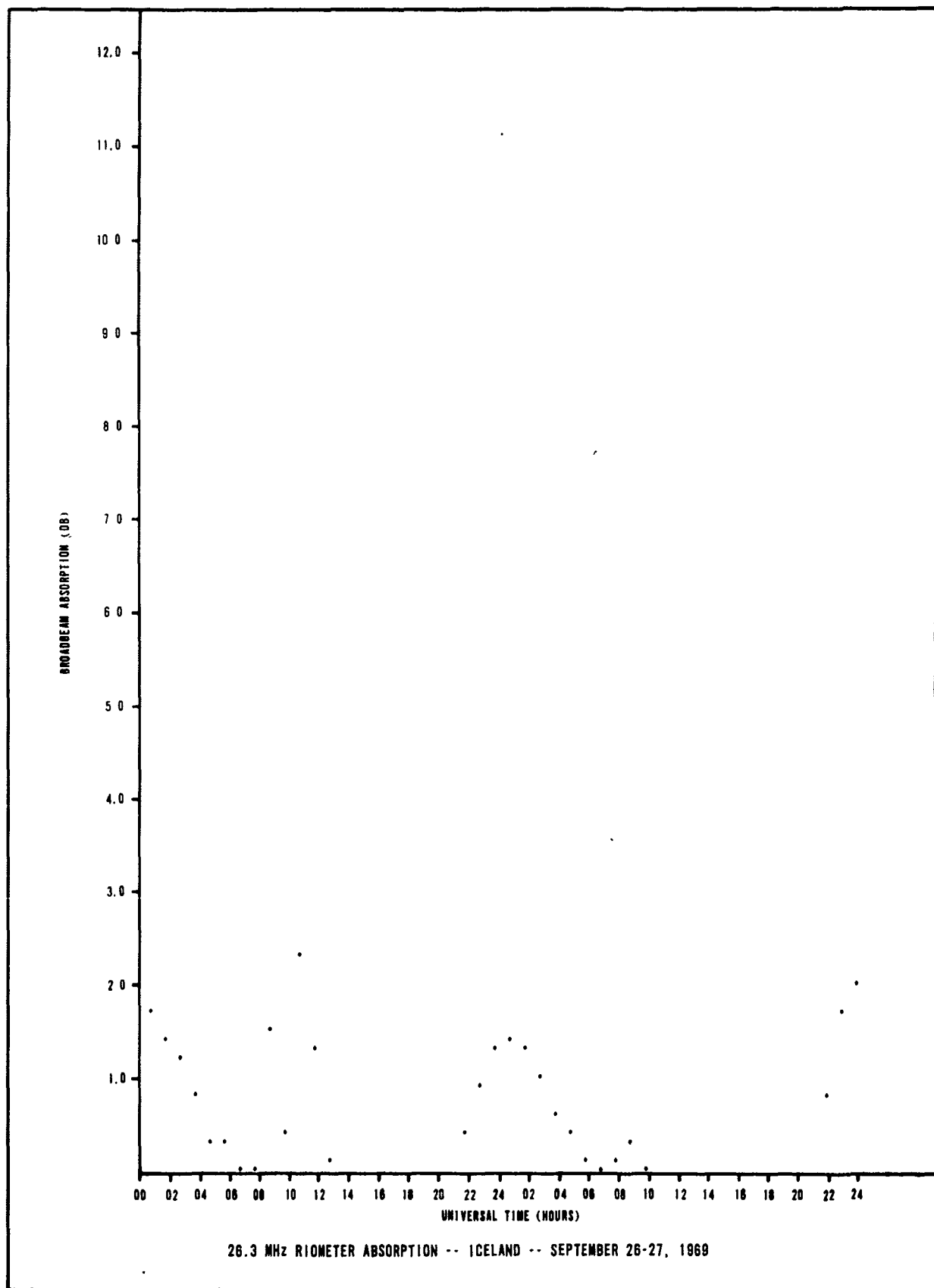


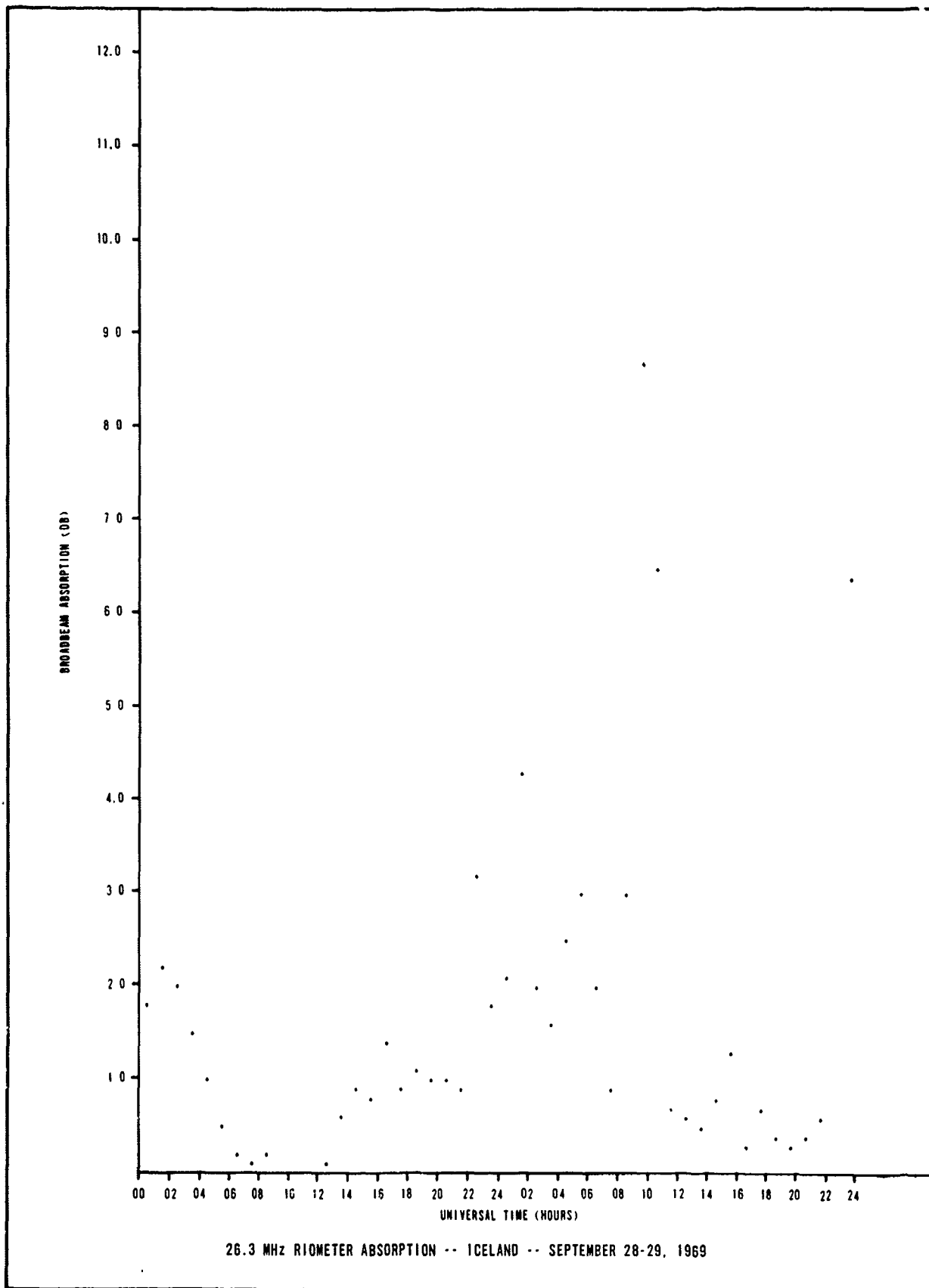


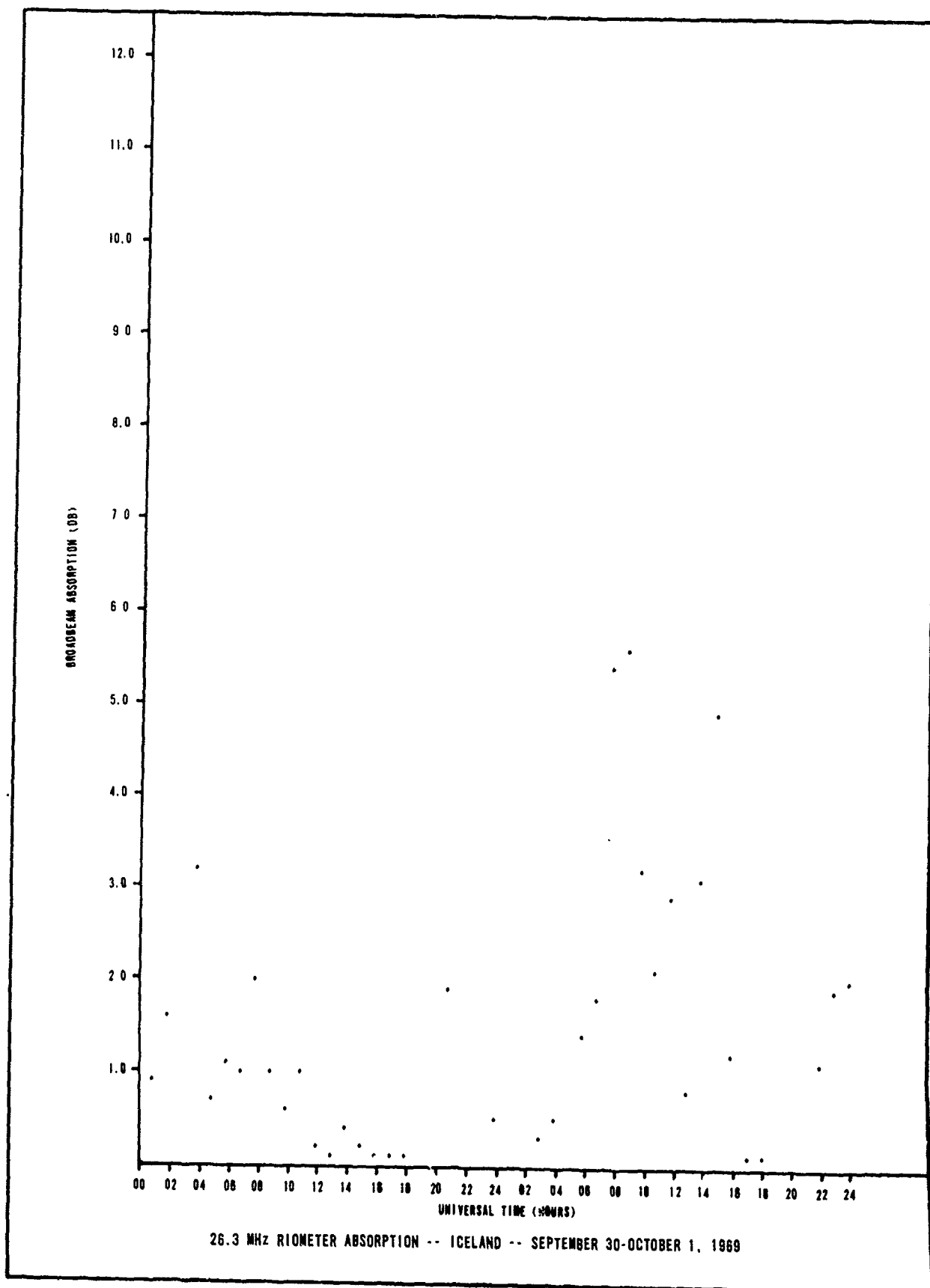


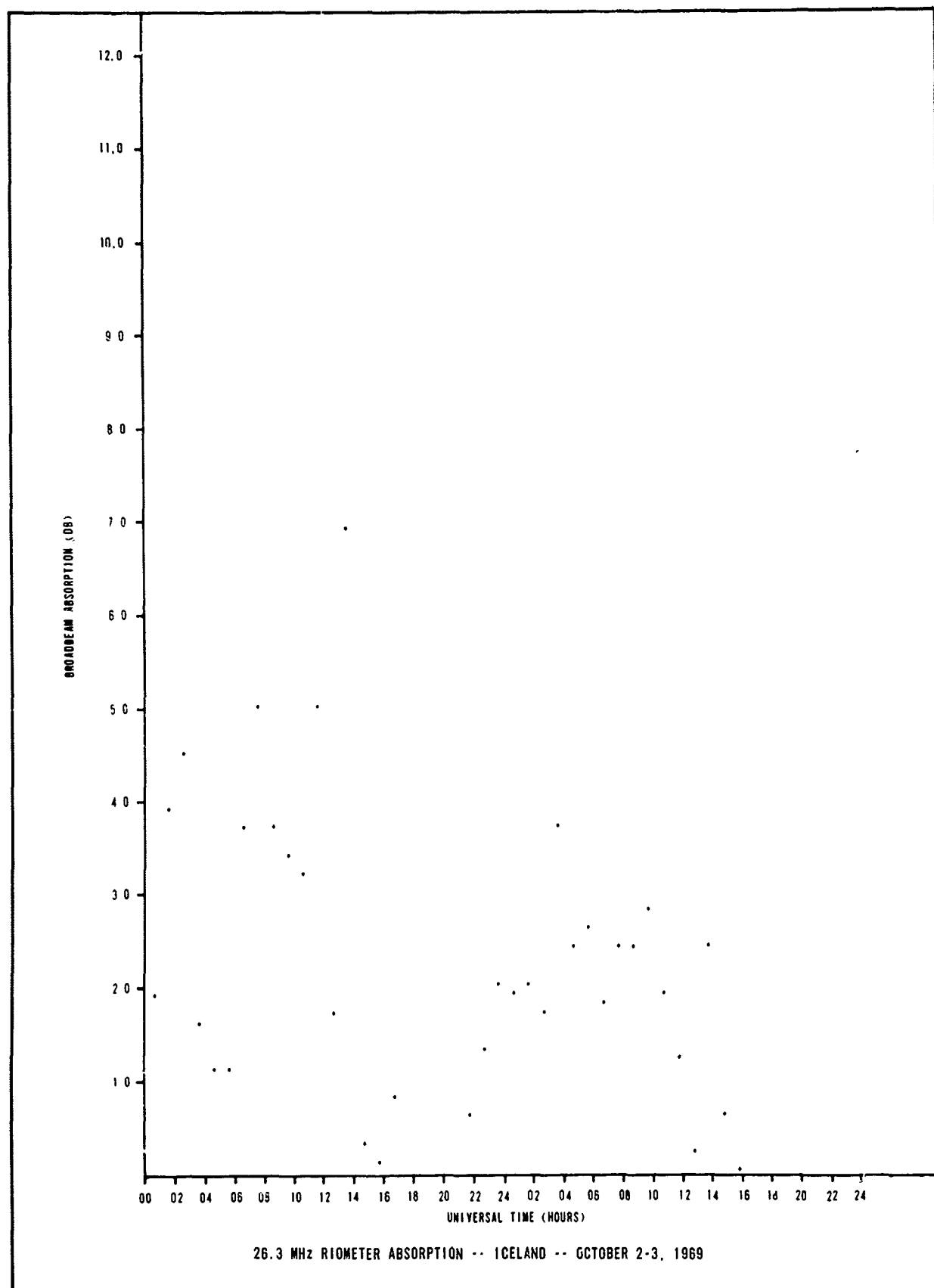


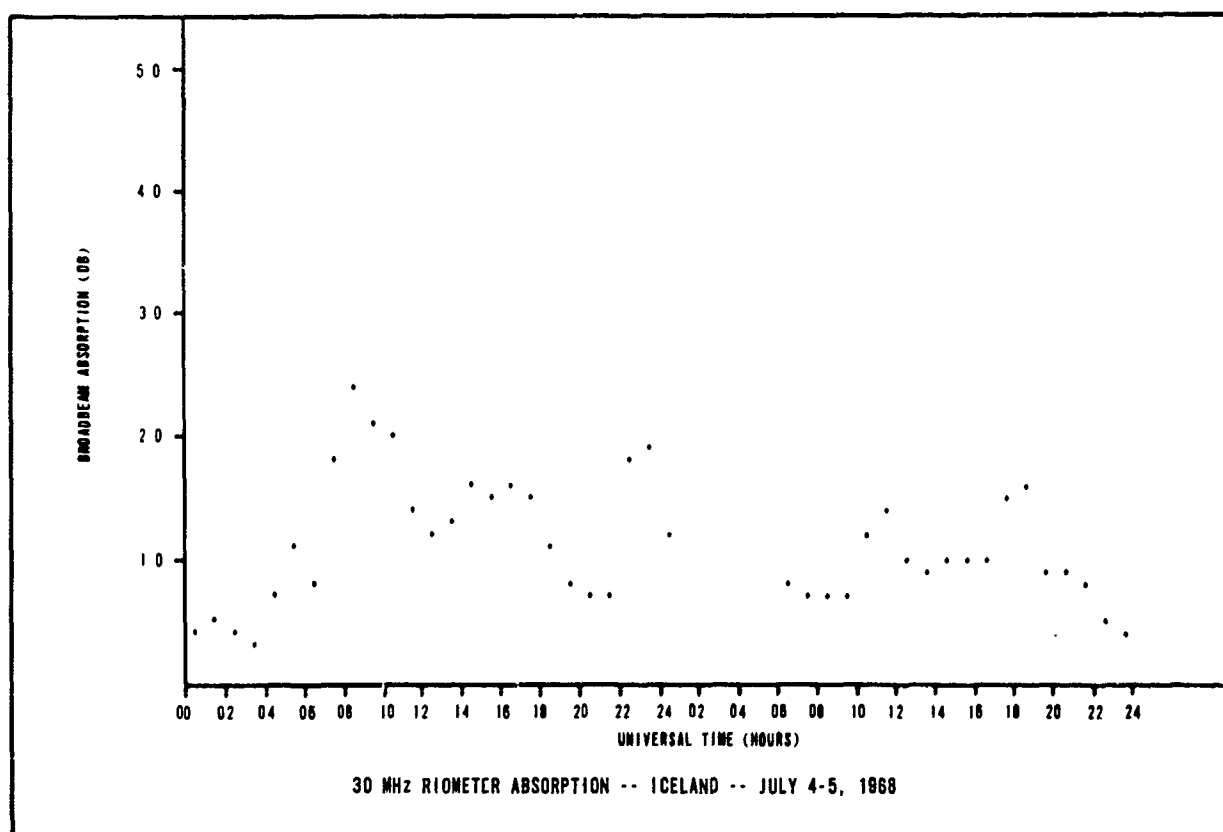
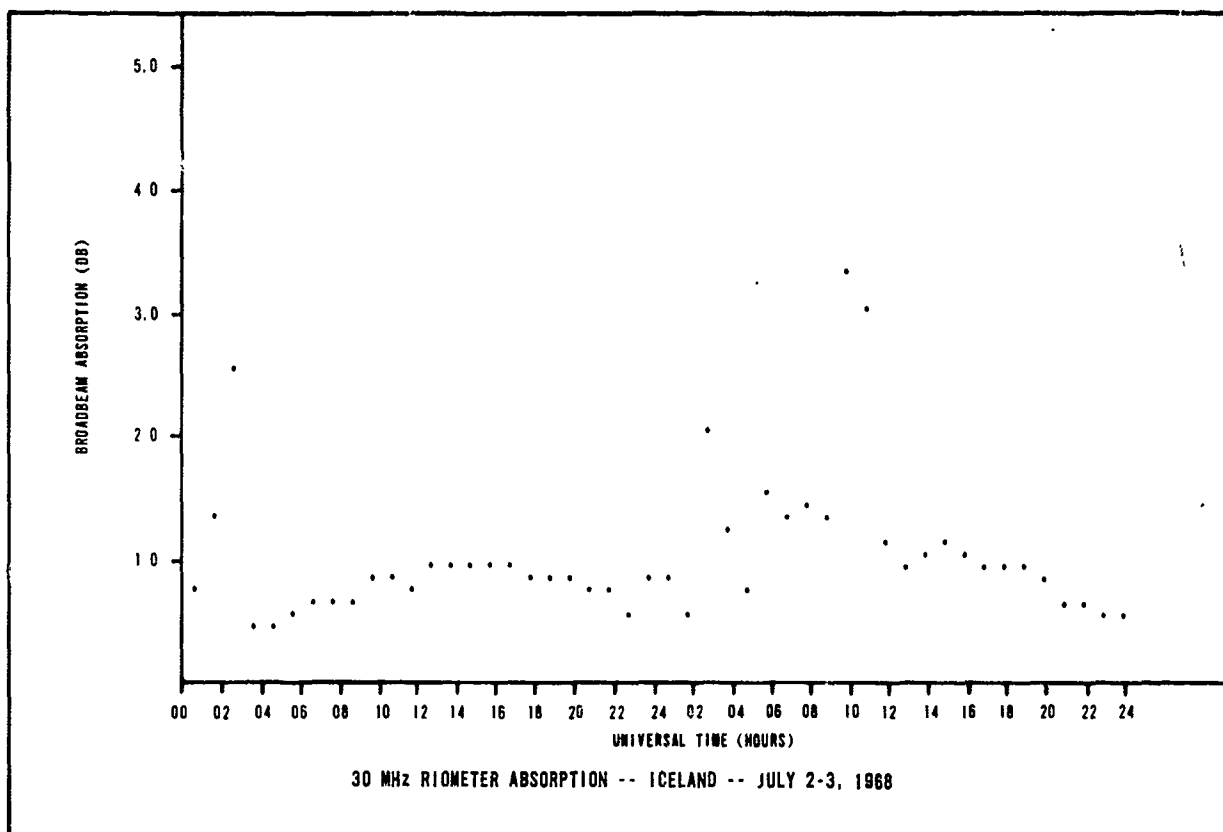


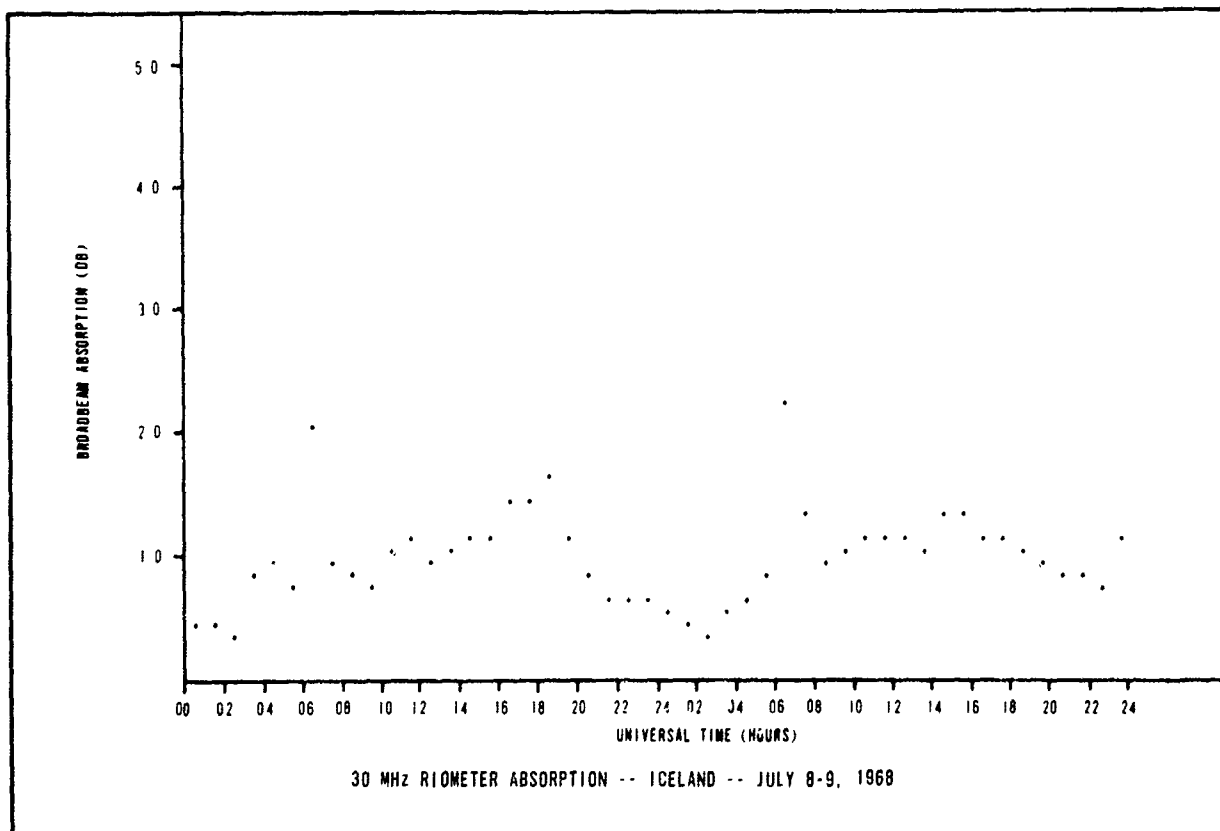
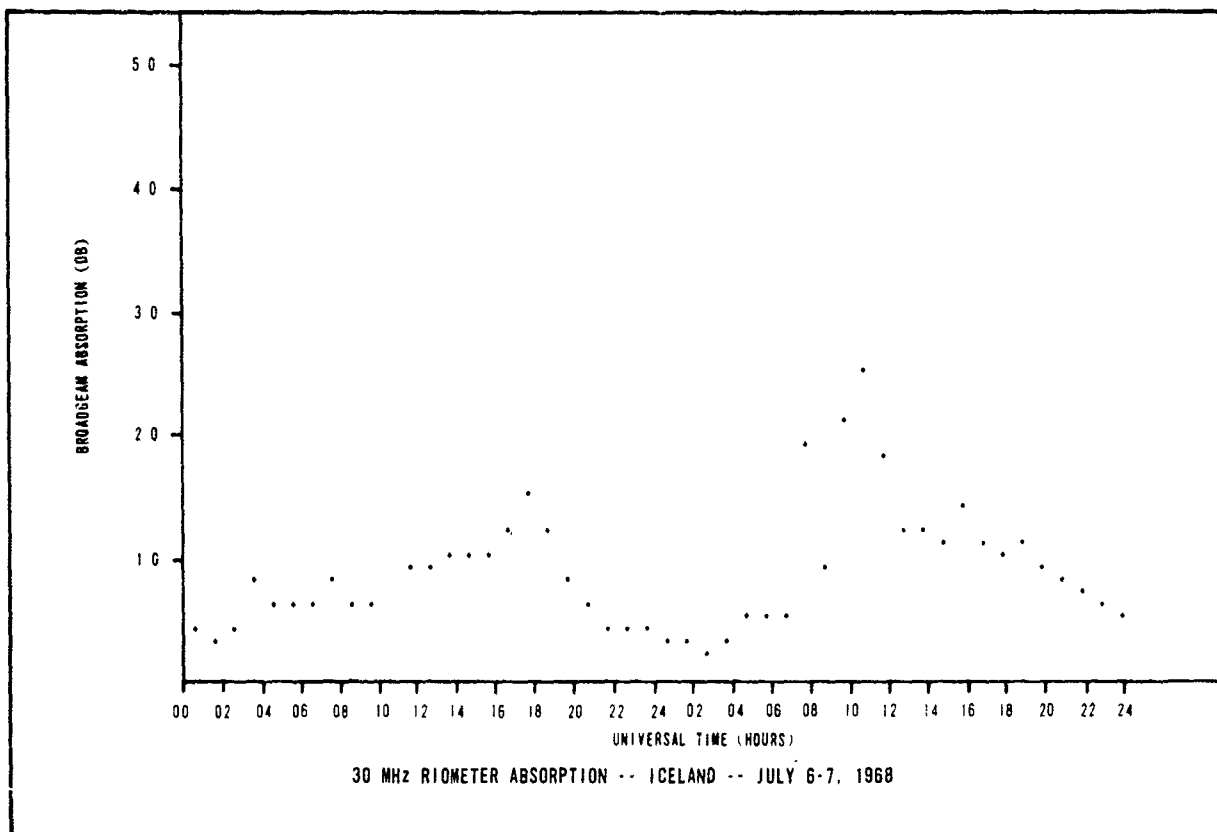


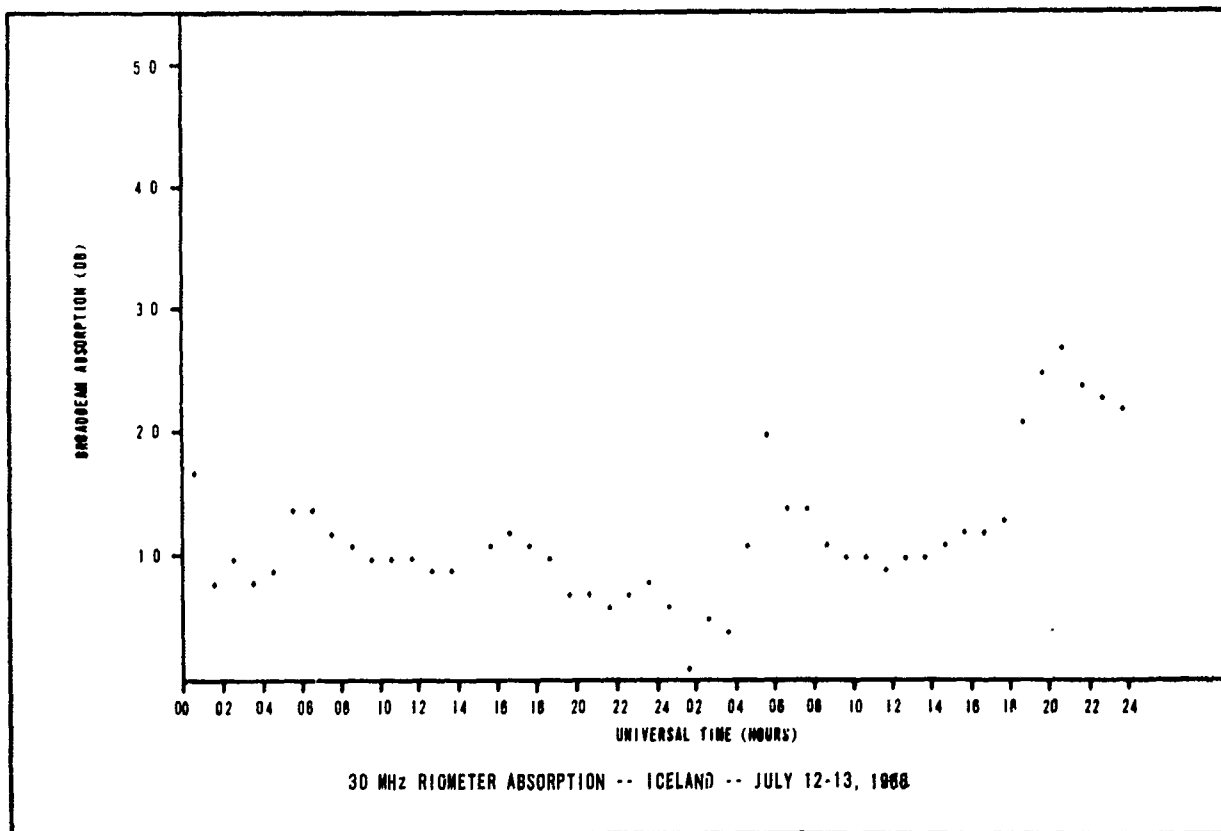
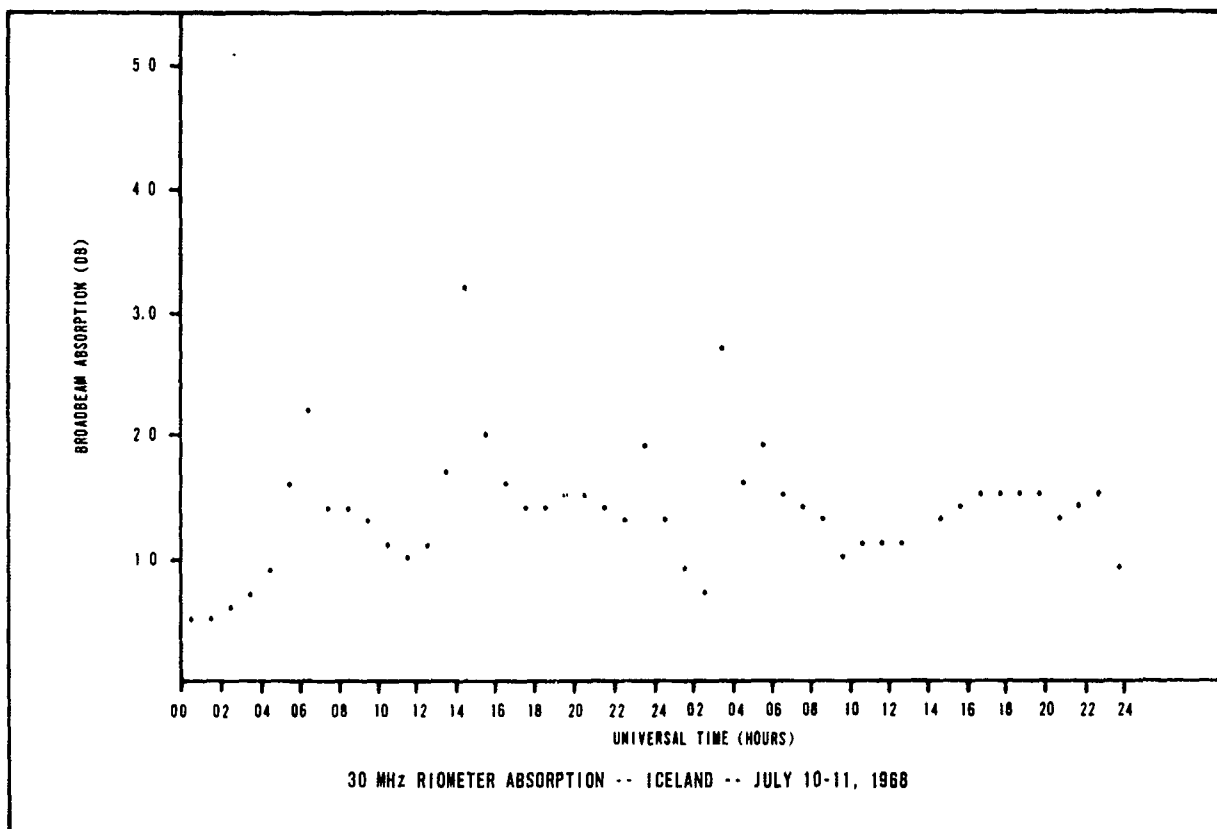


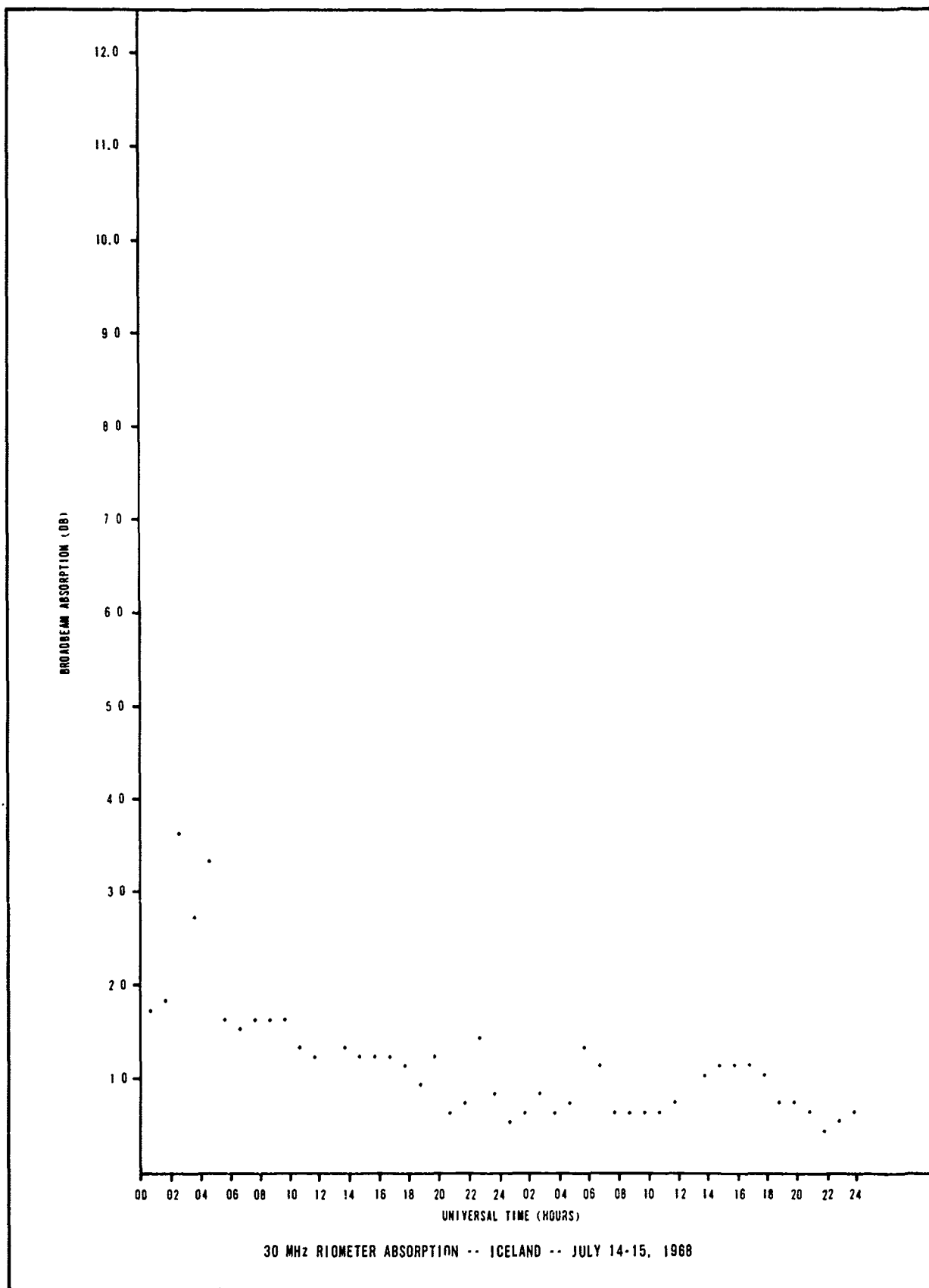








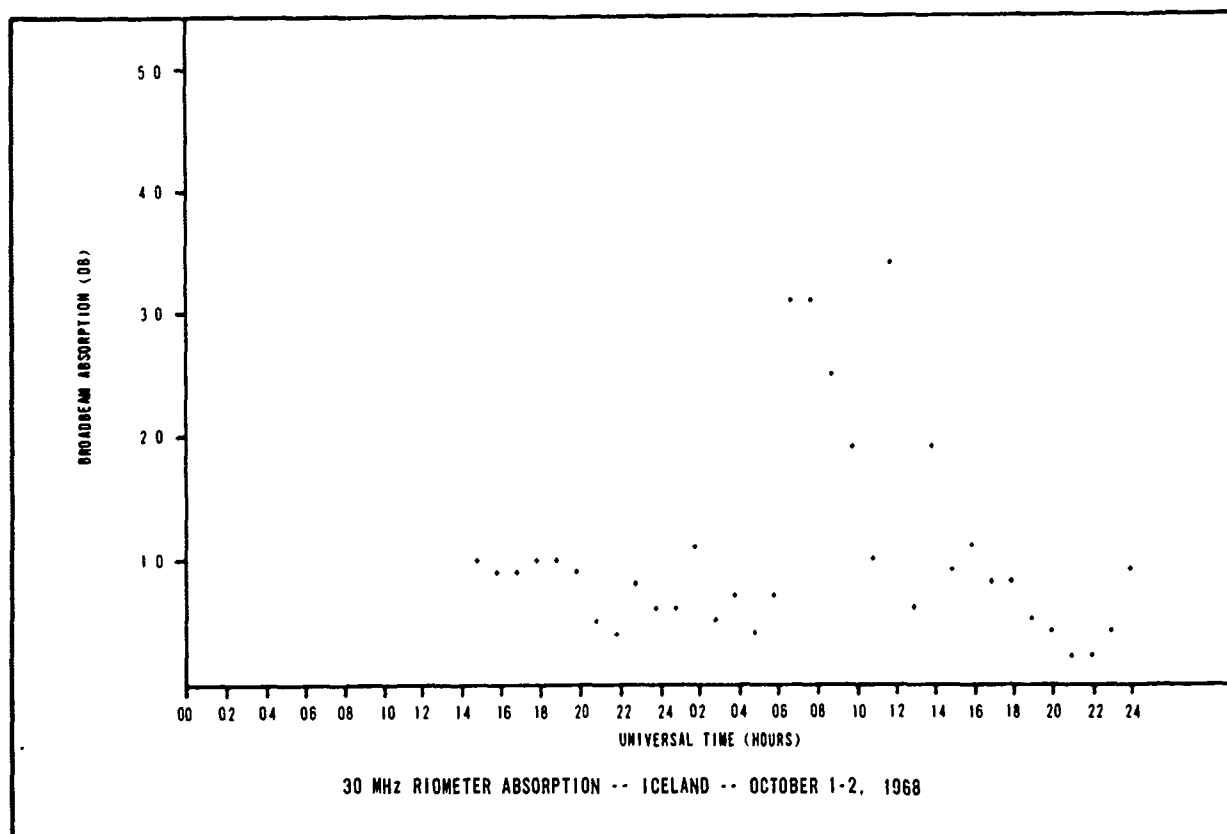
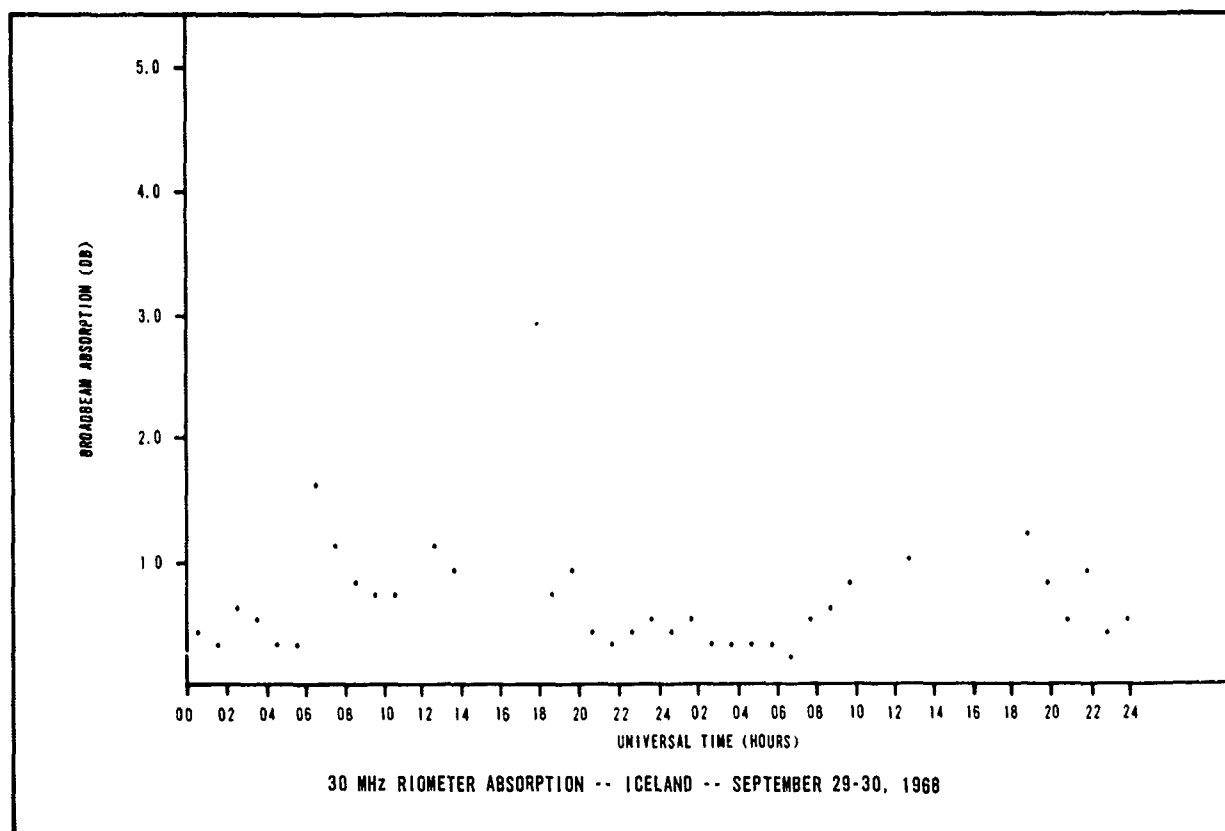


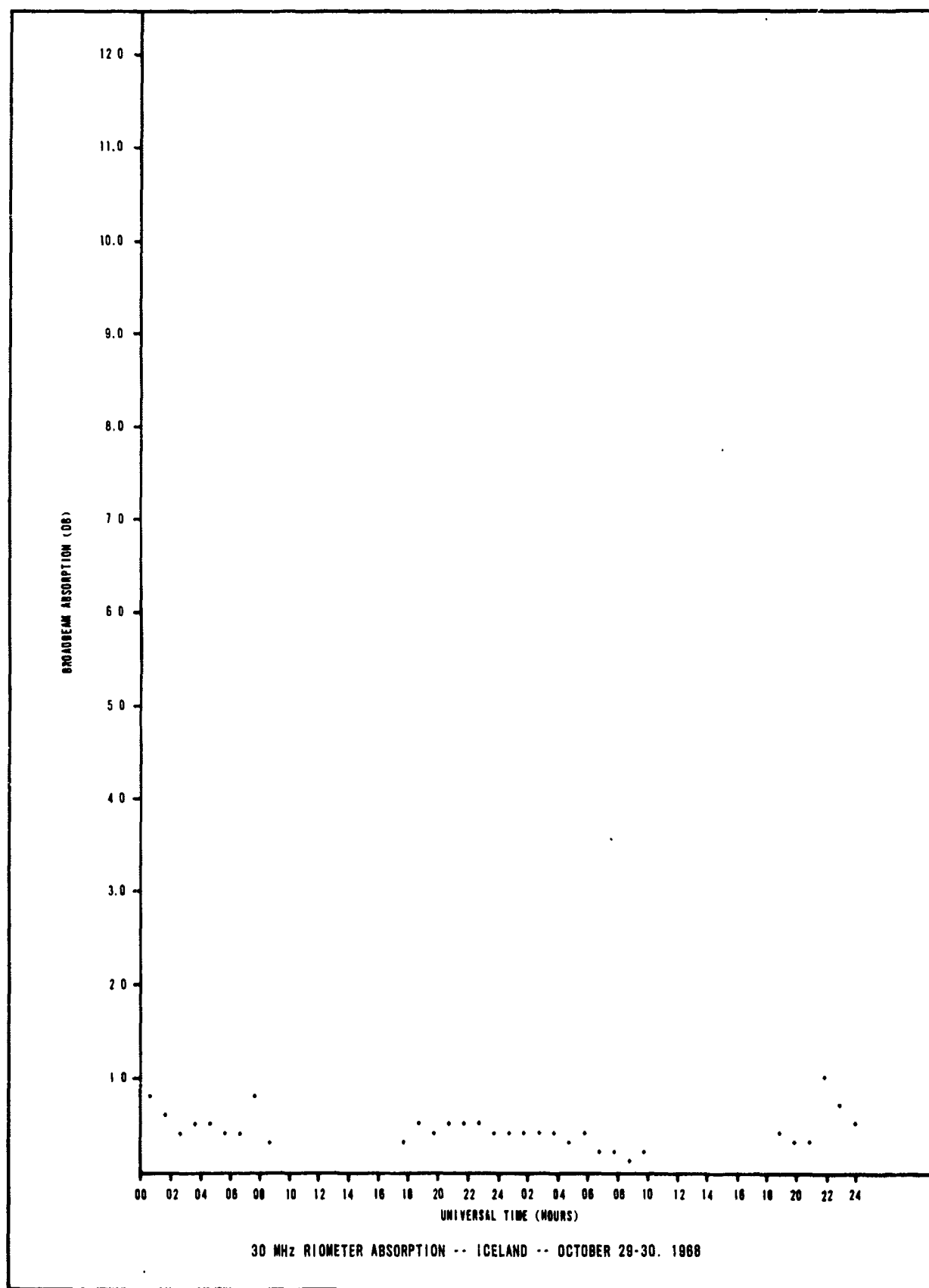


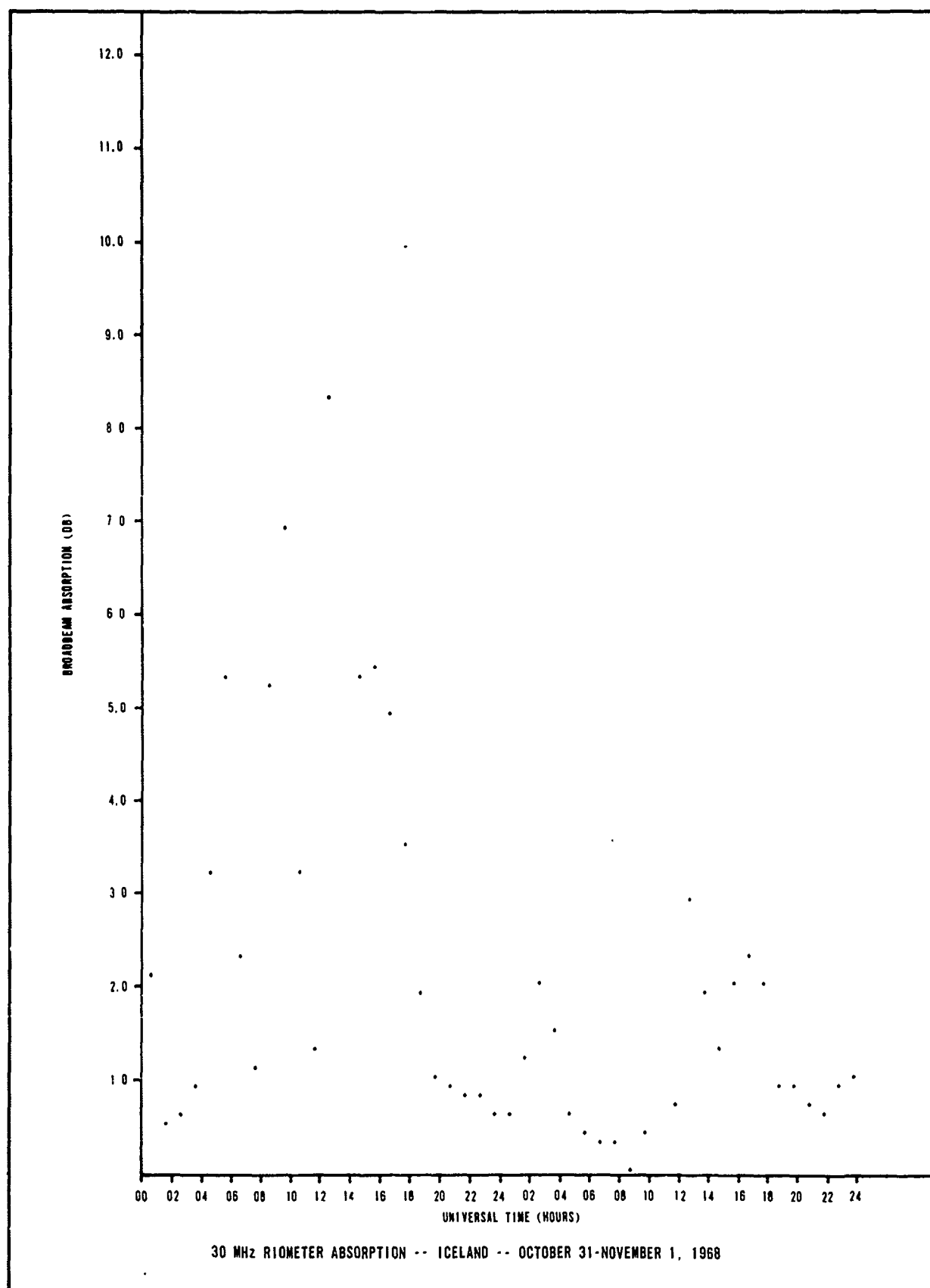
B-158

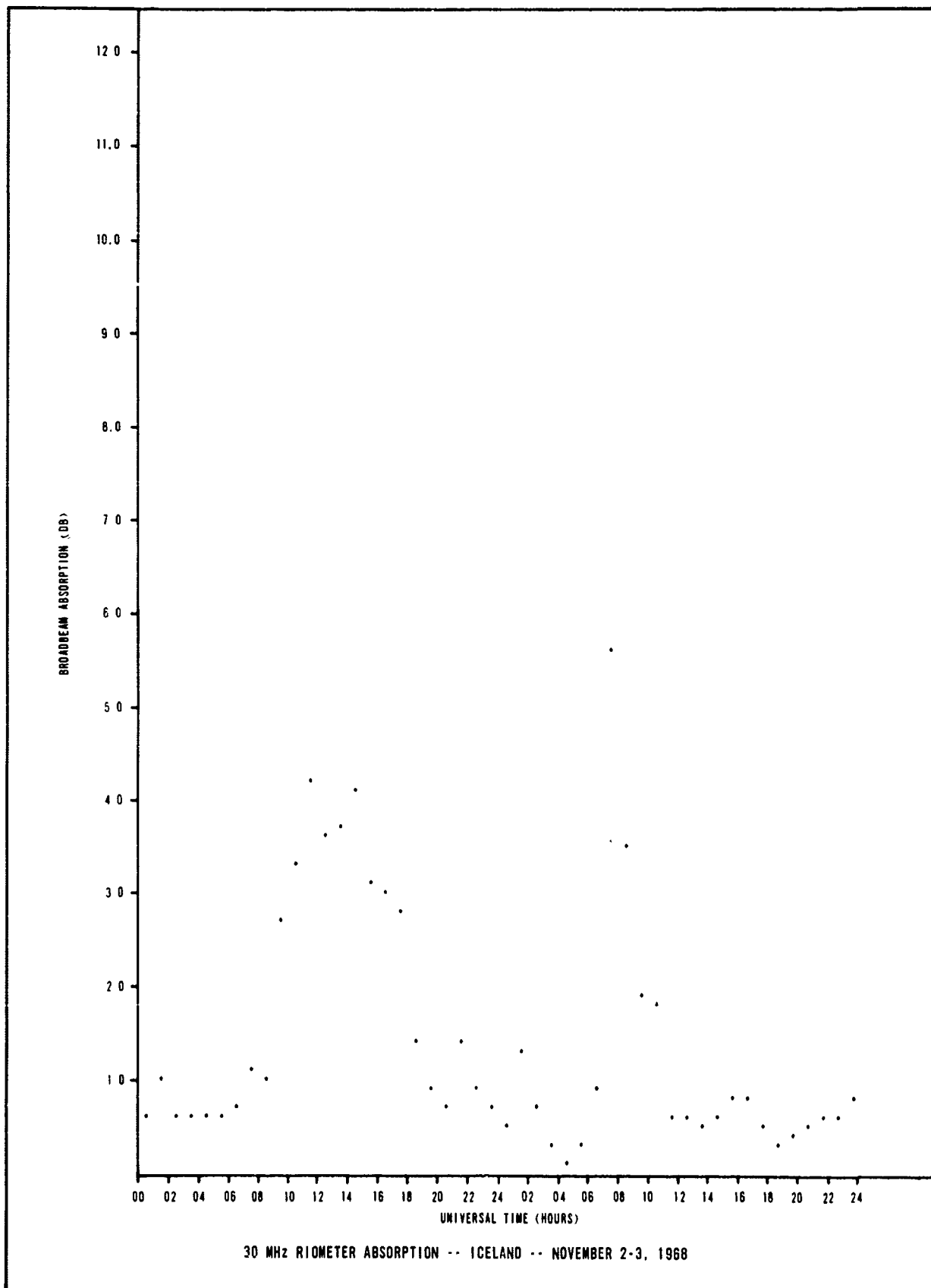


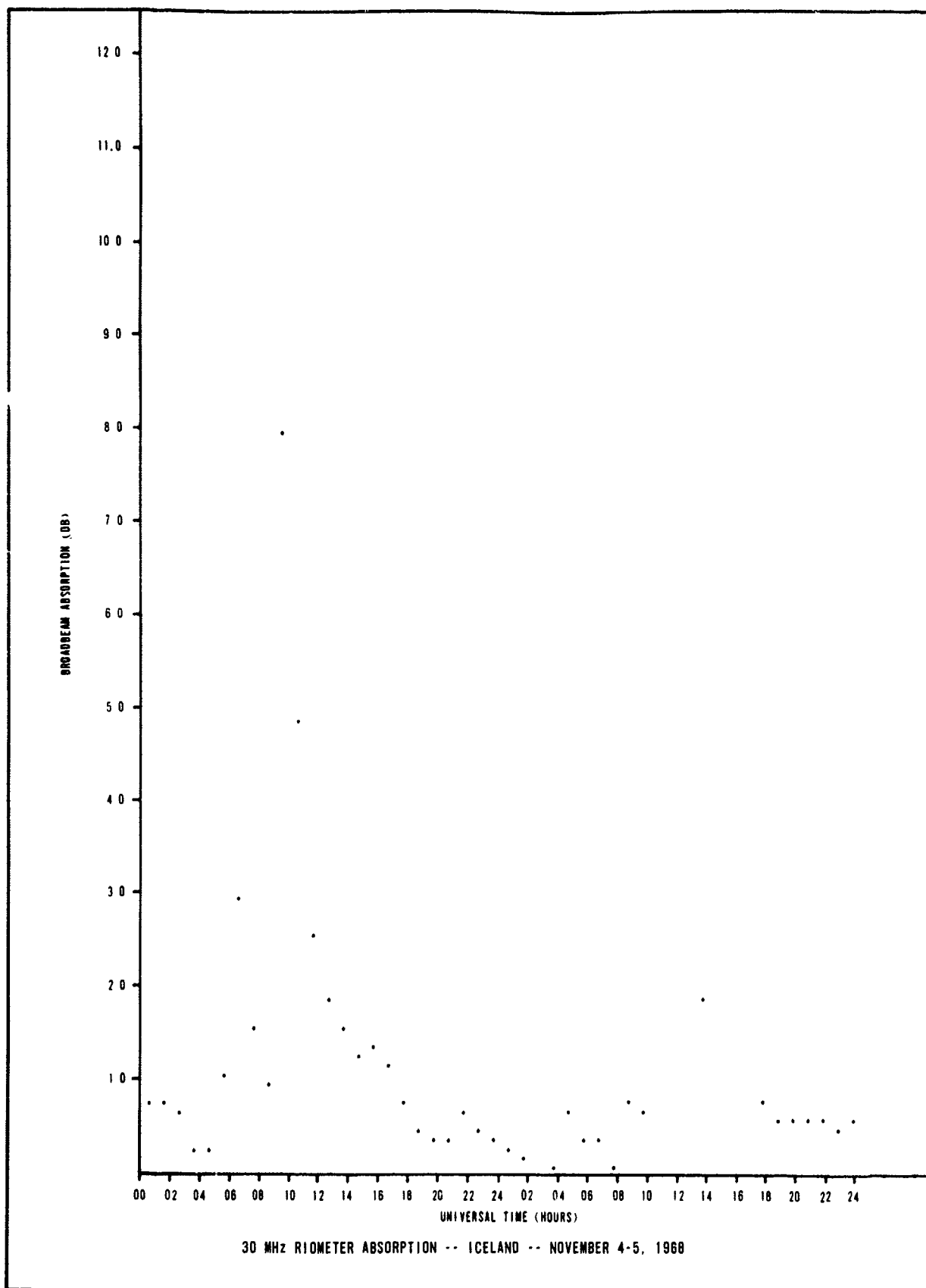


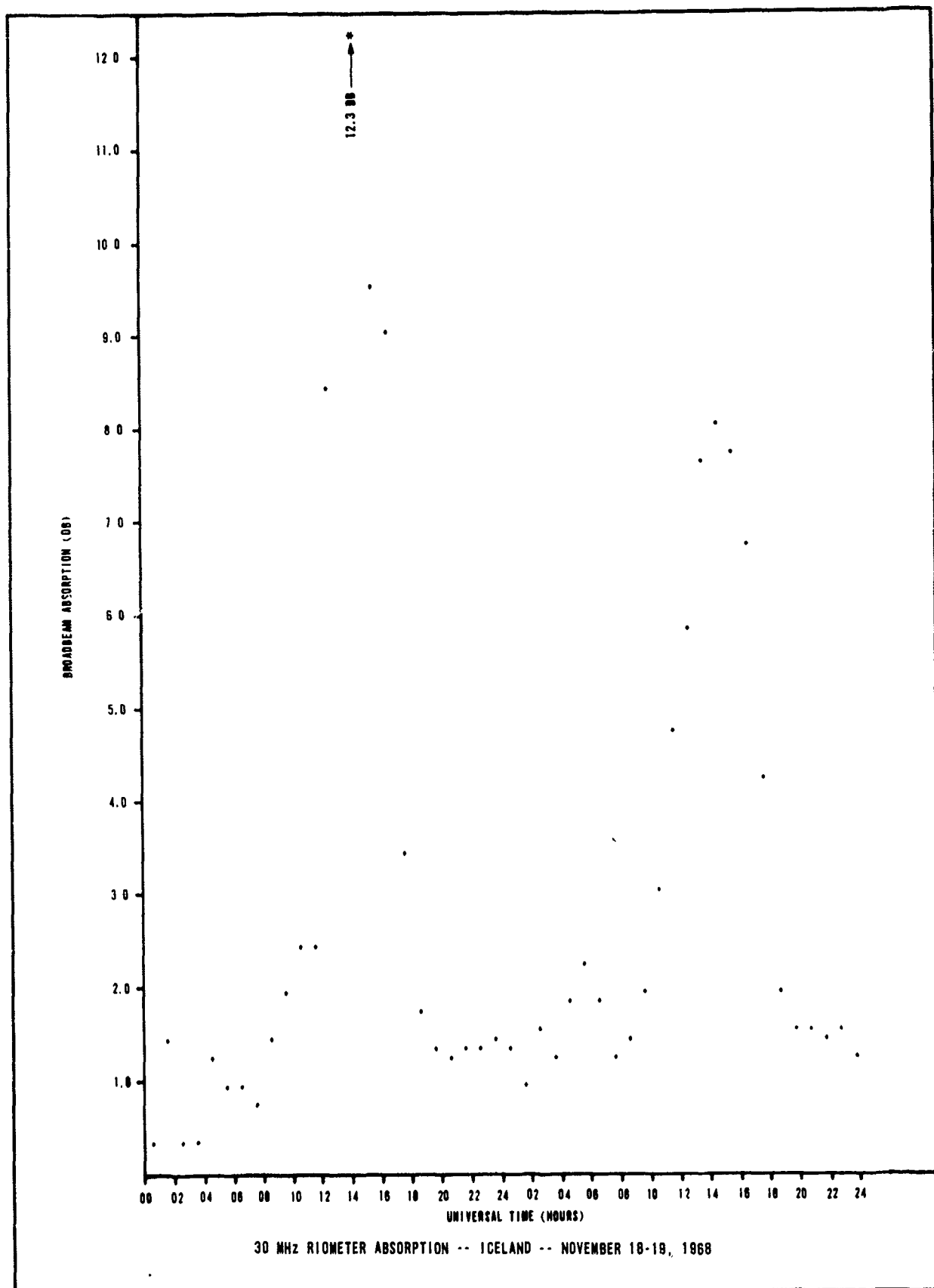


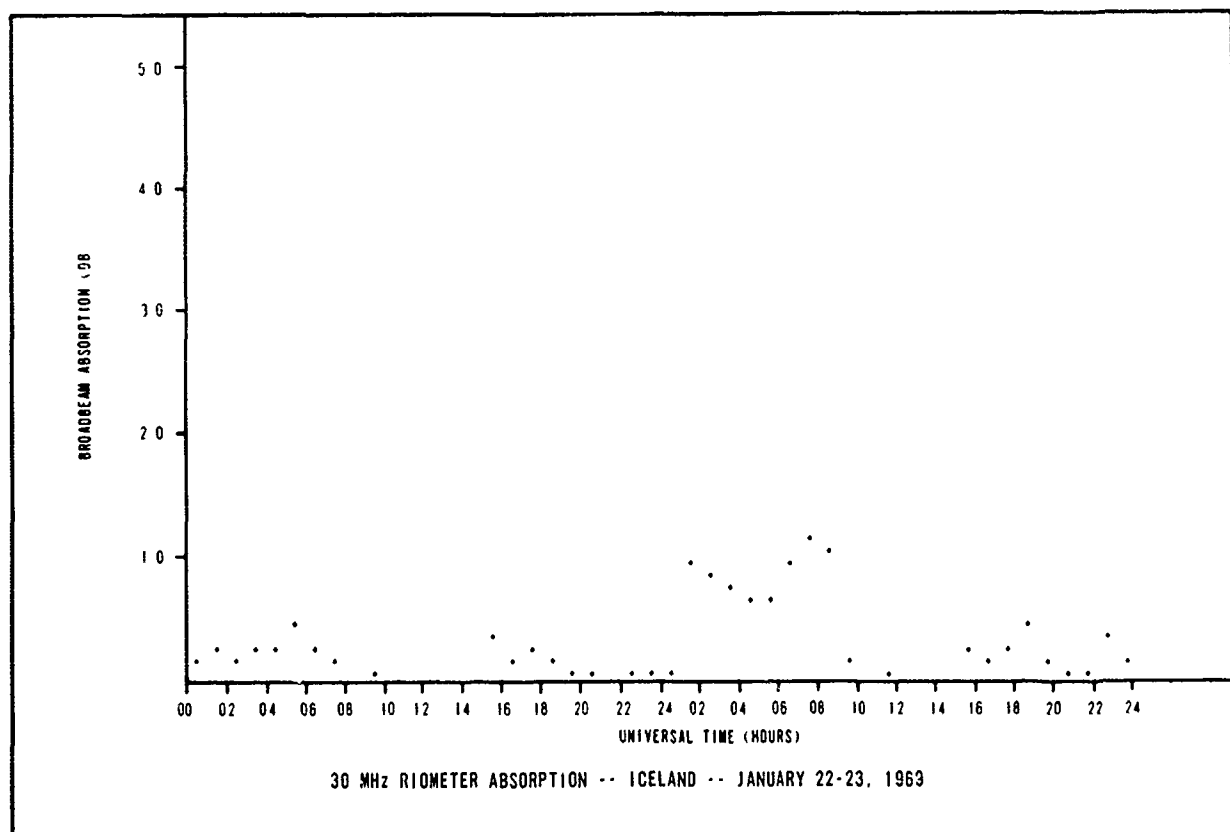
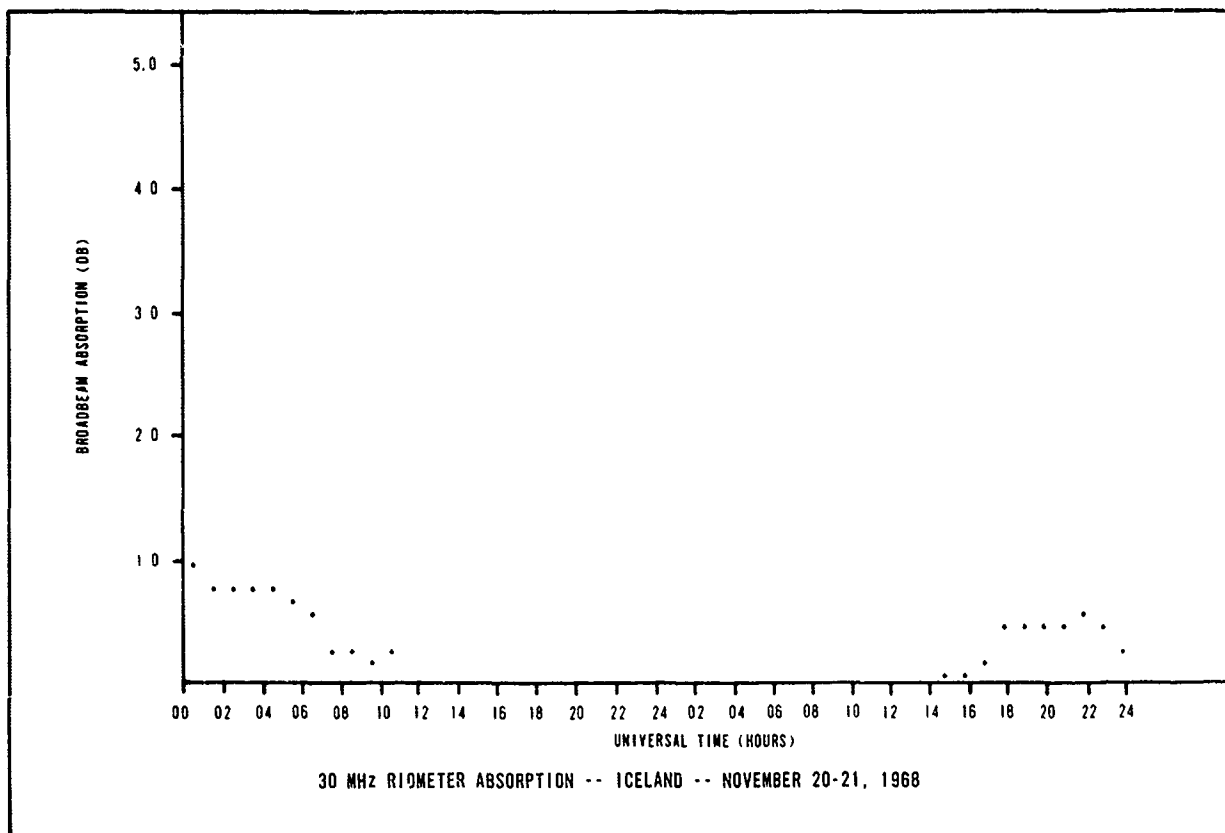




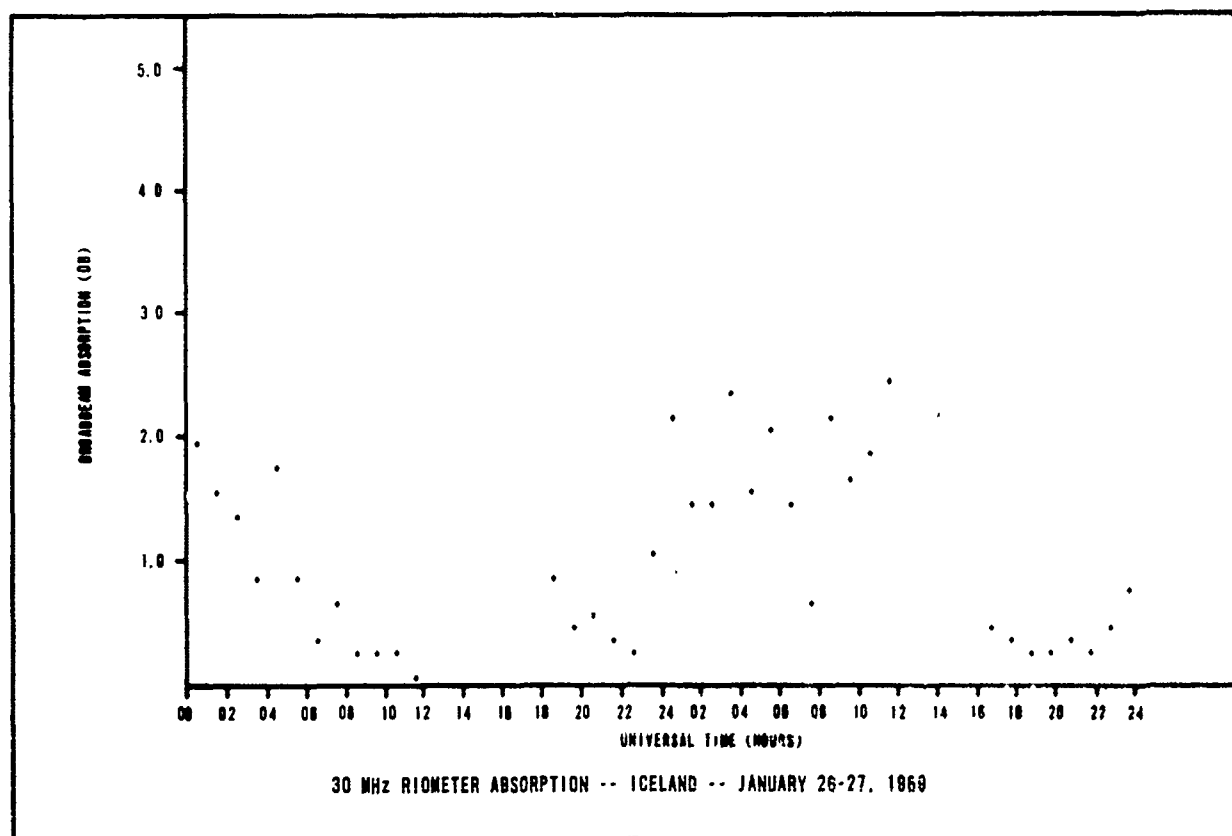
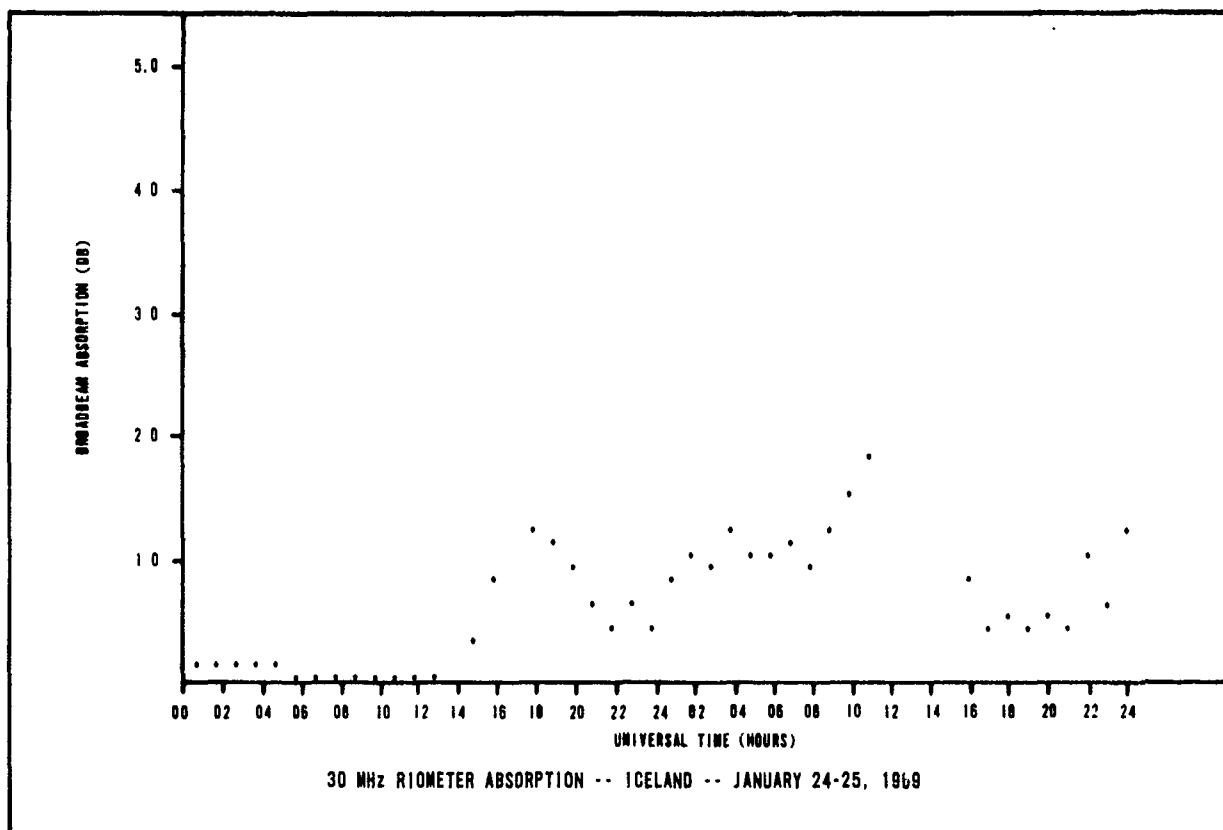


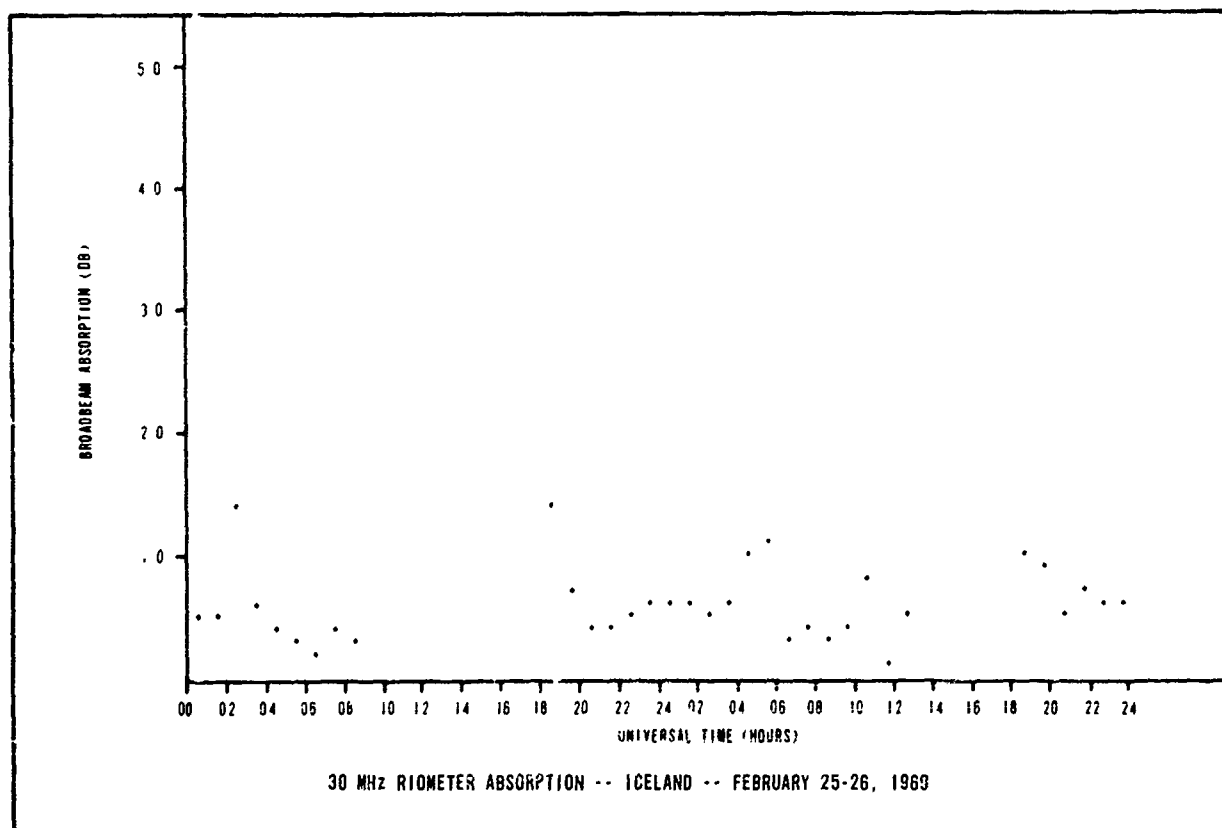
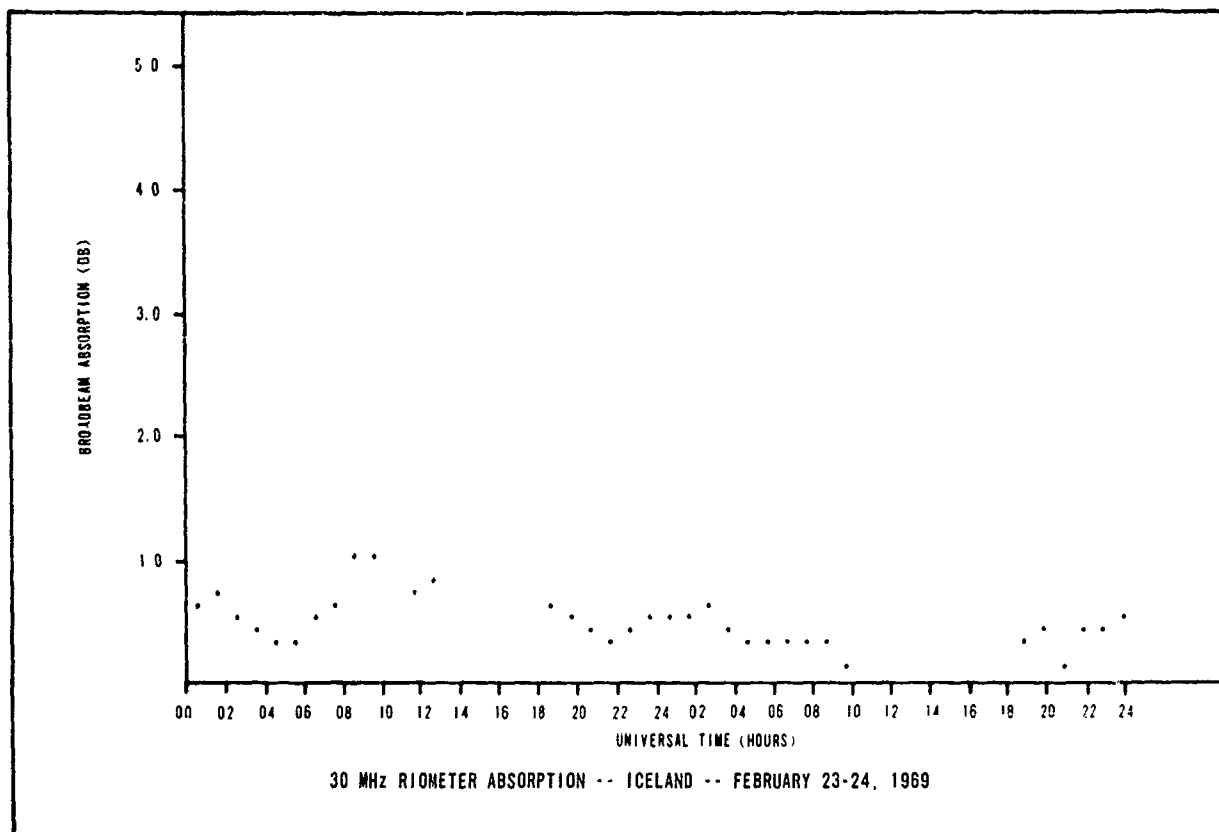


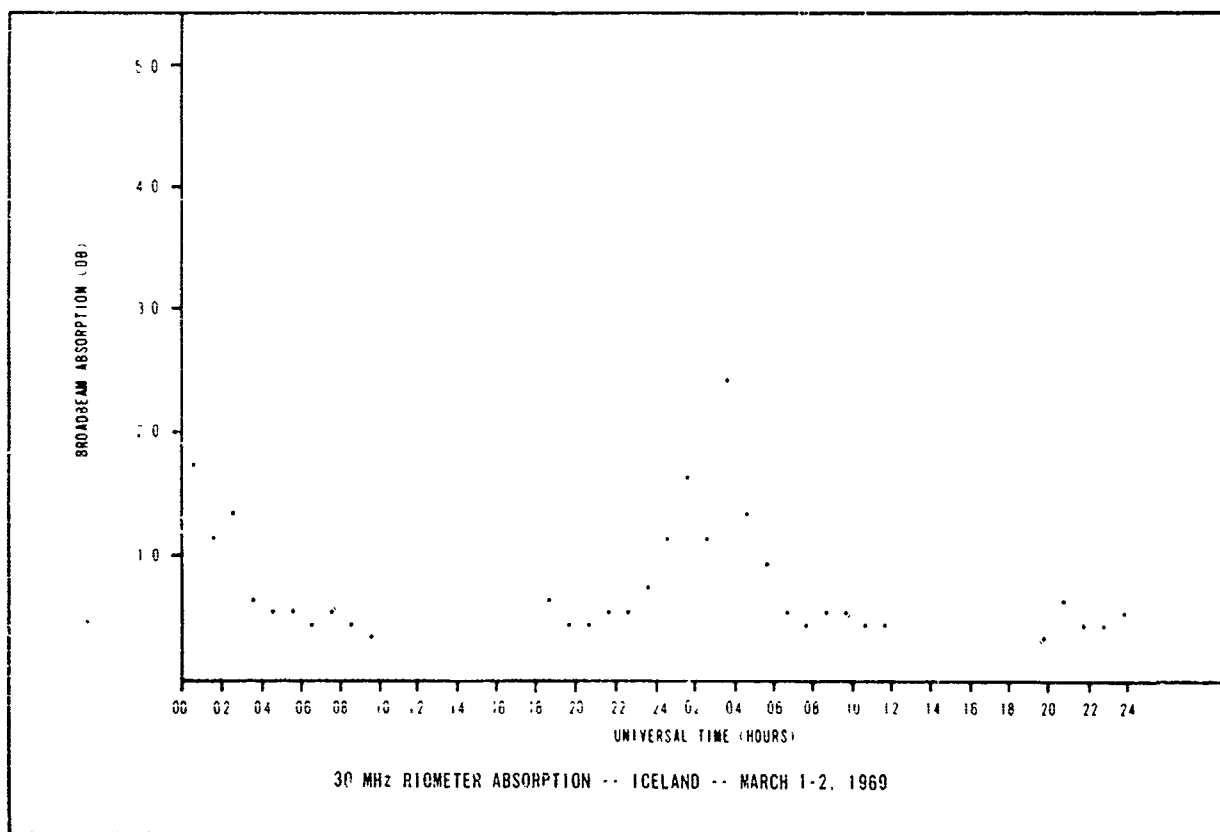
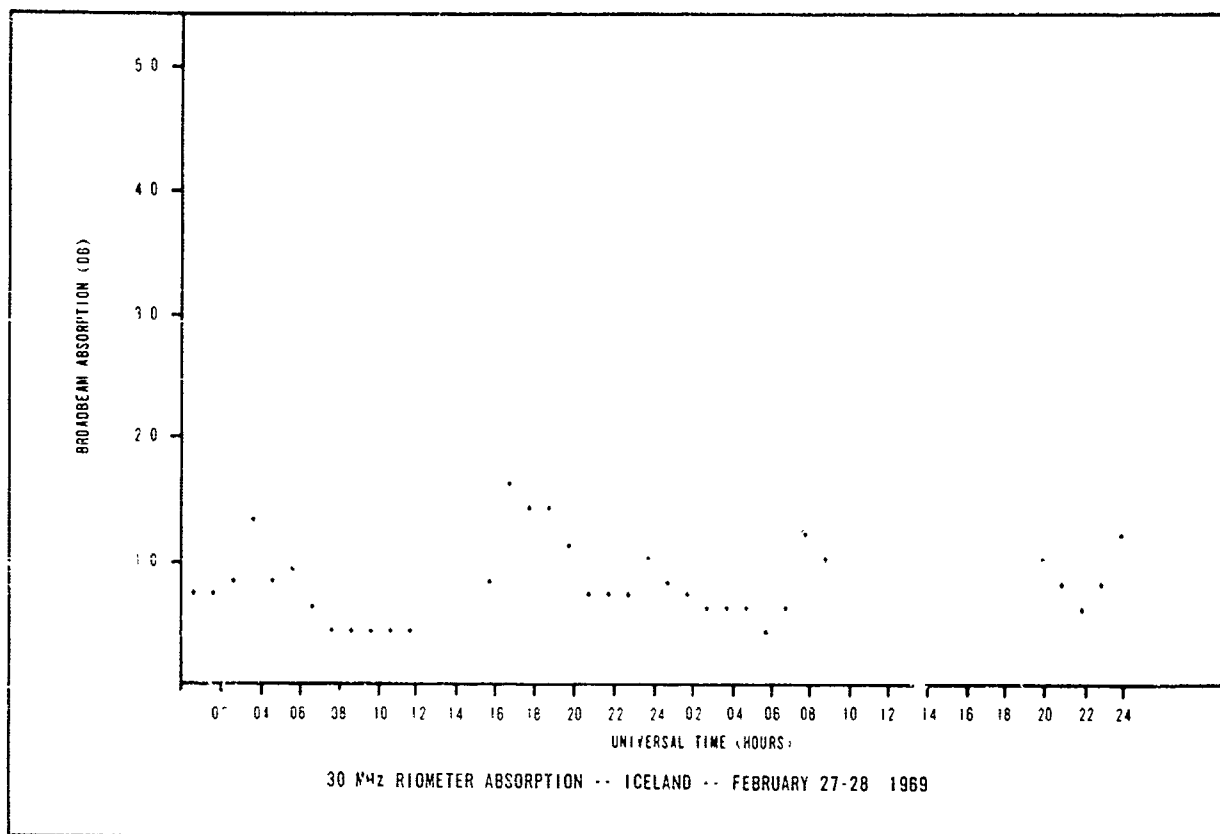


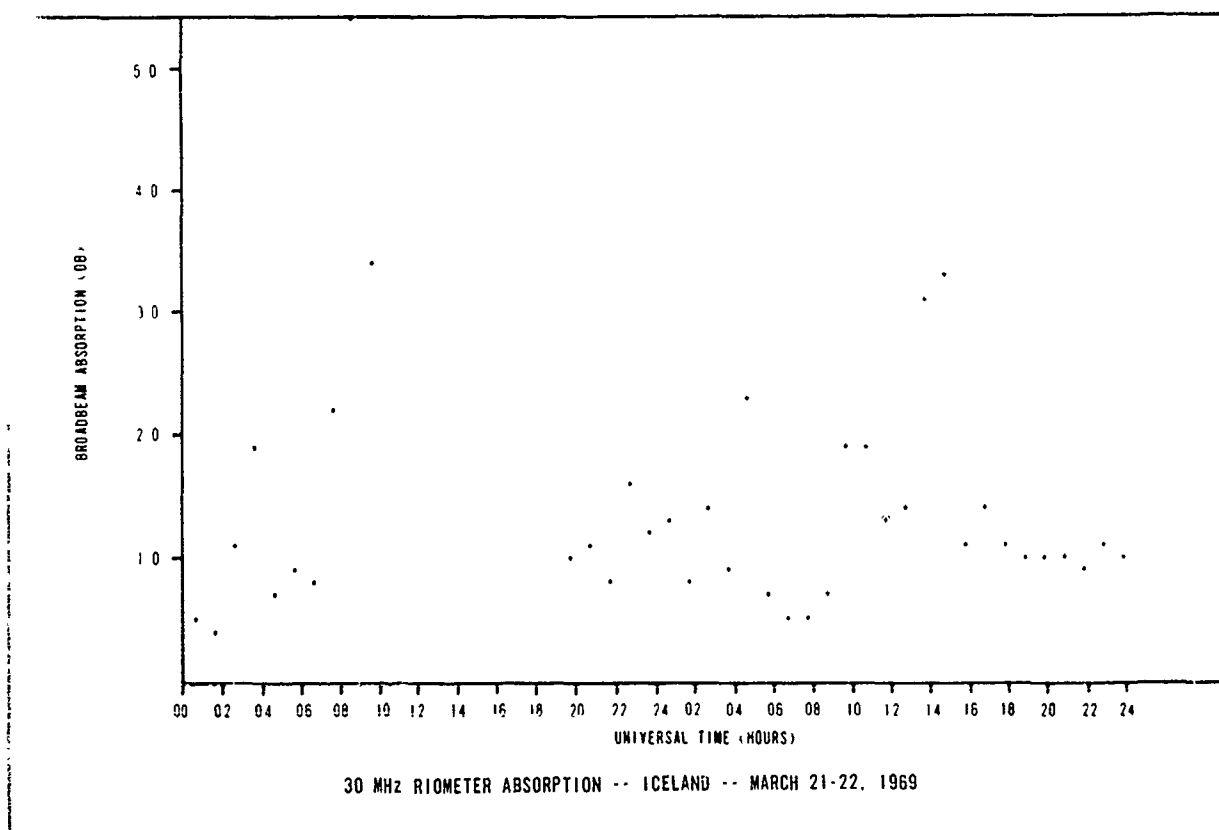
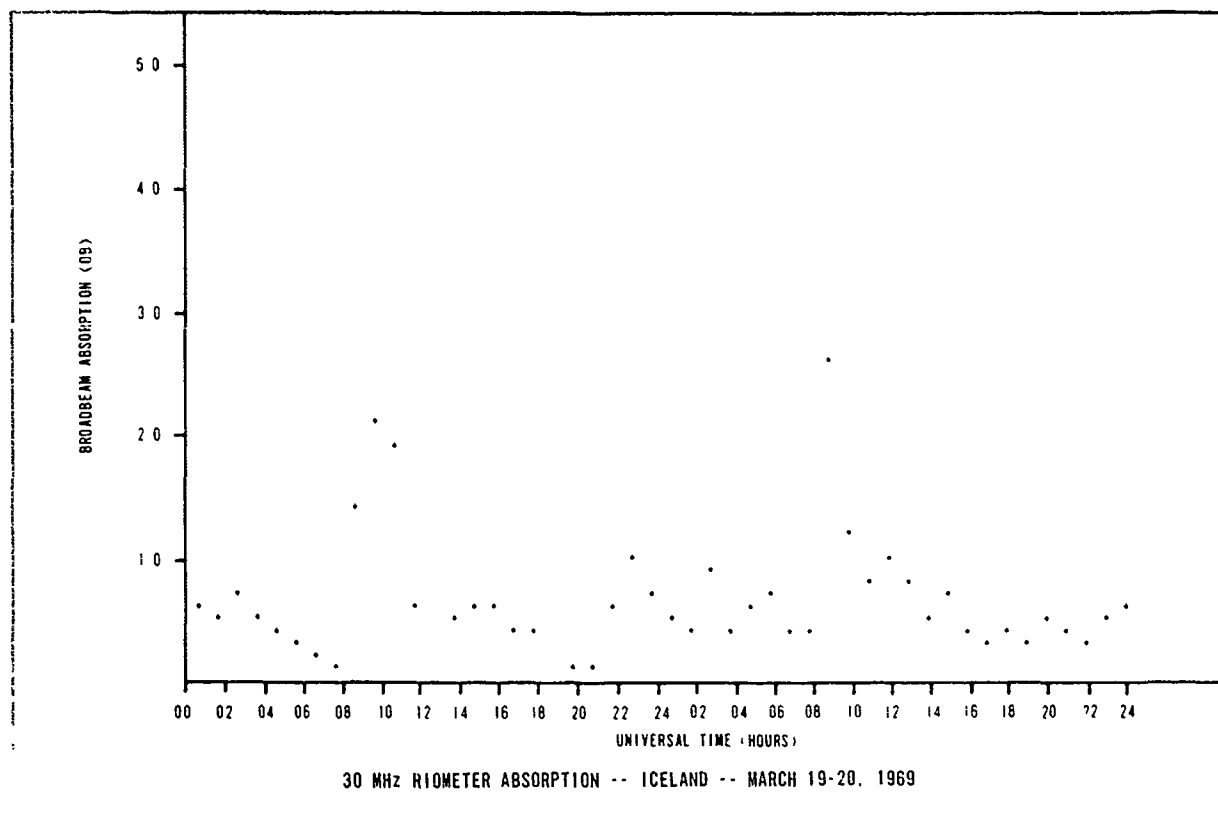


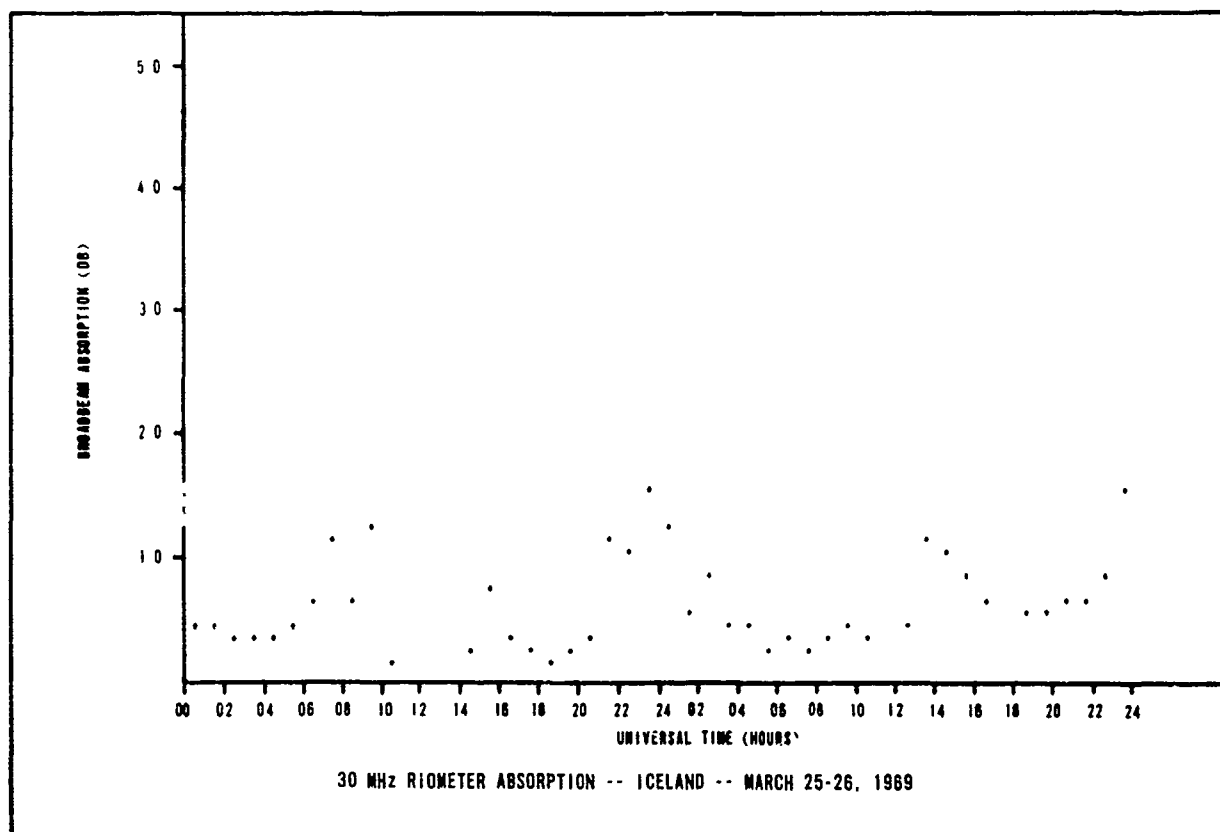
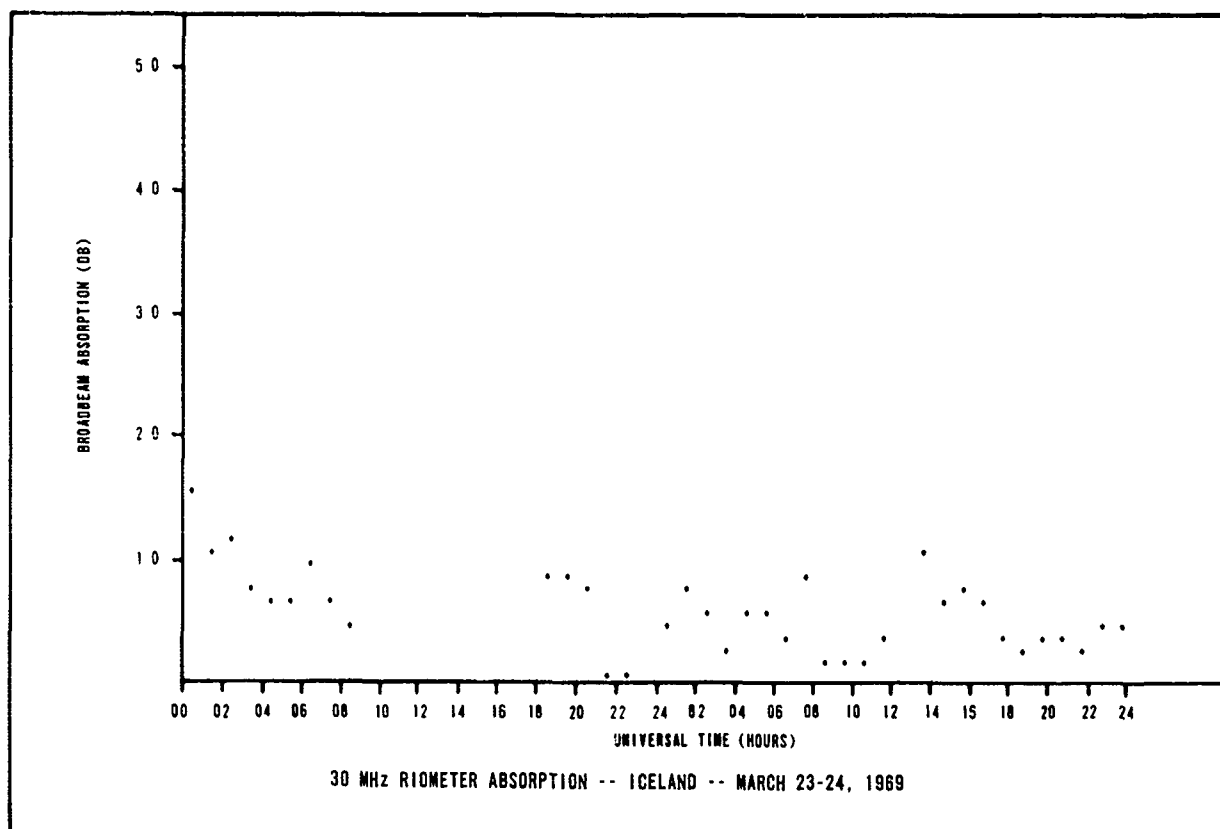


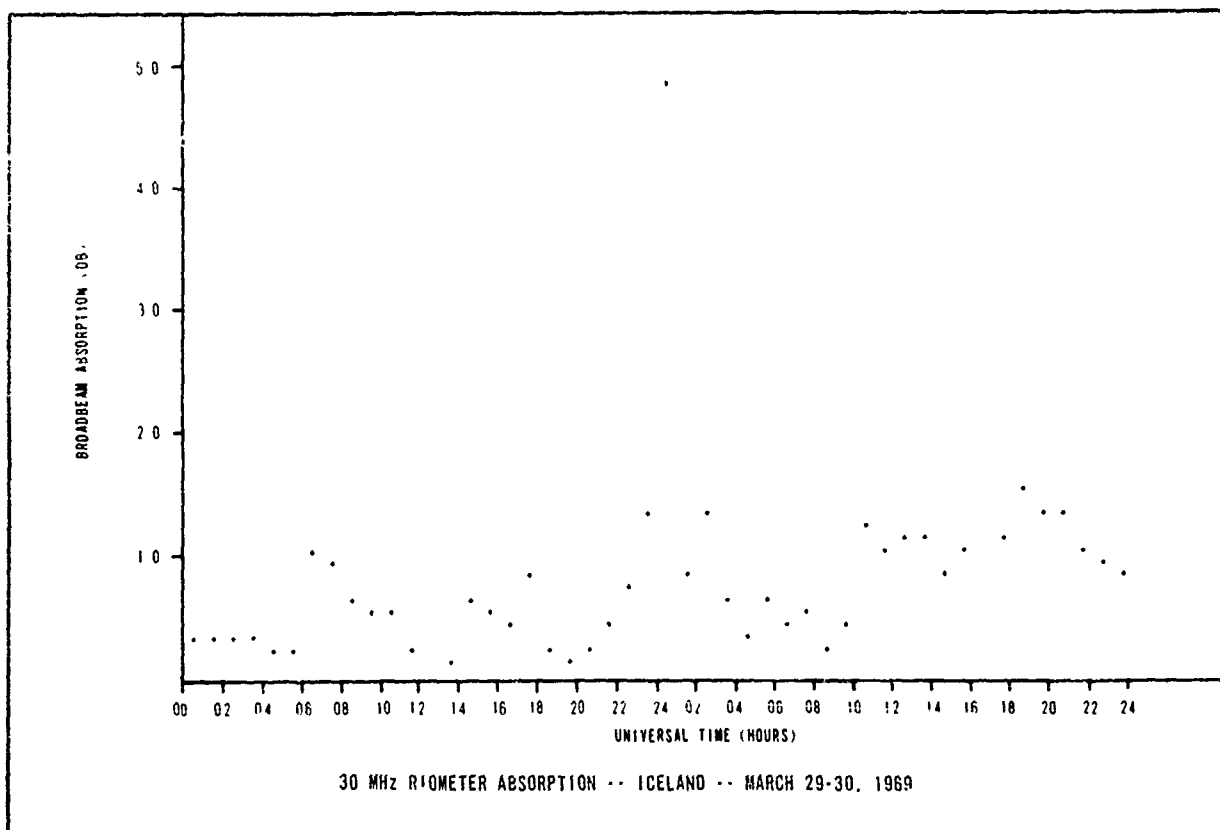
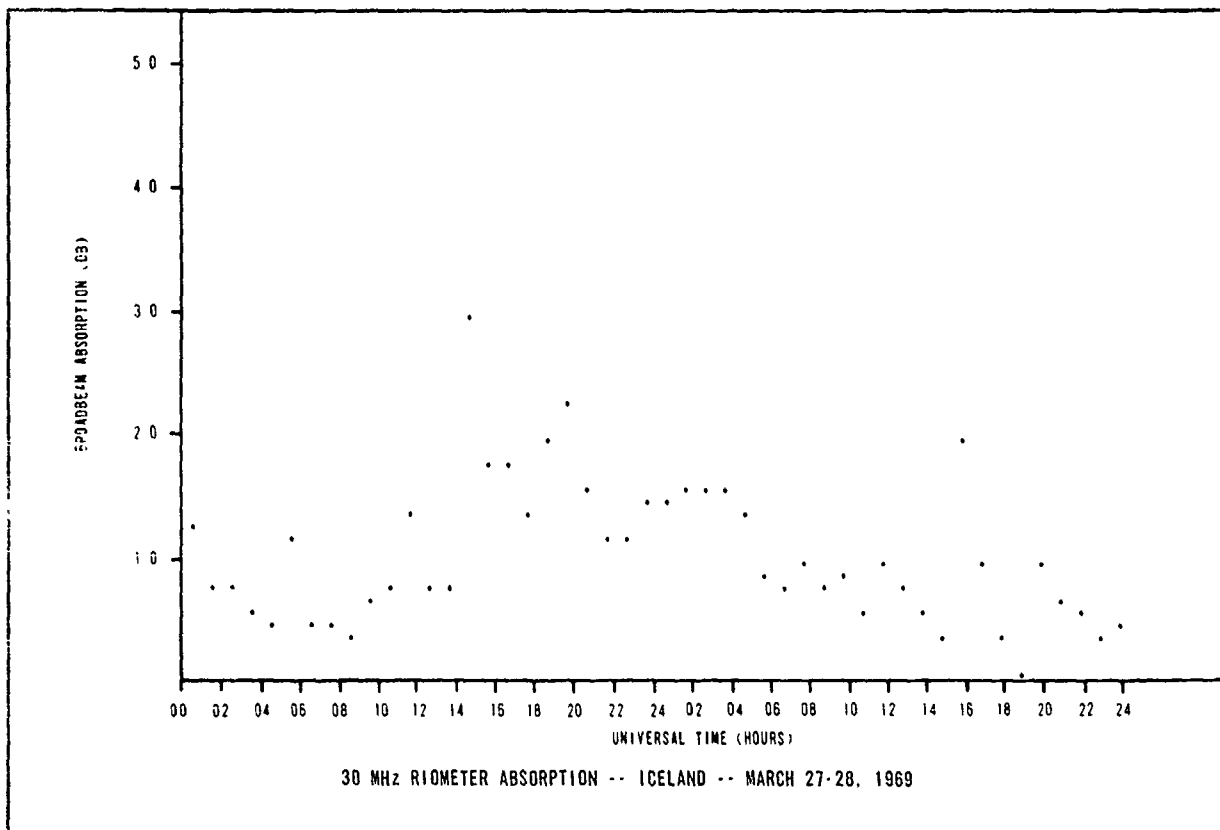


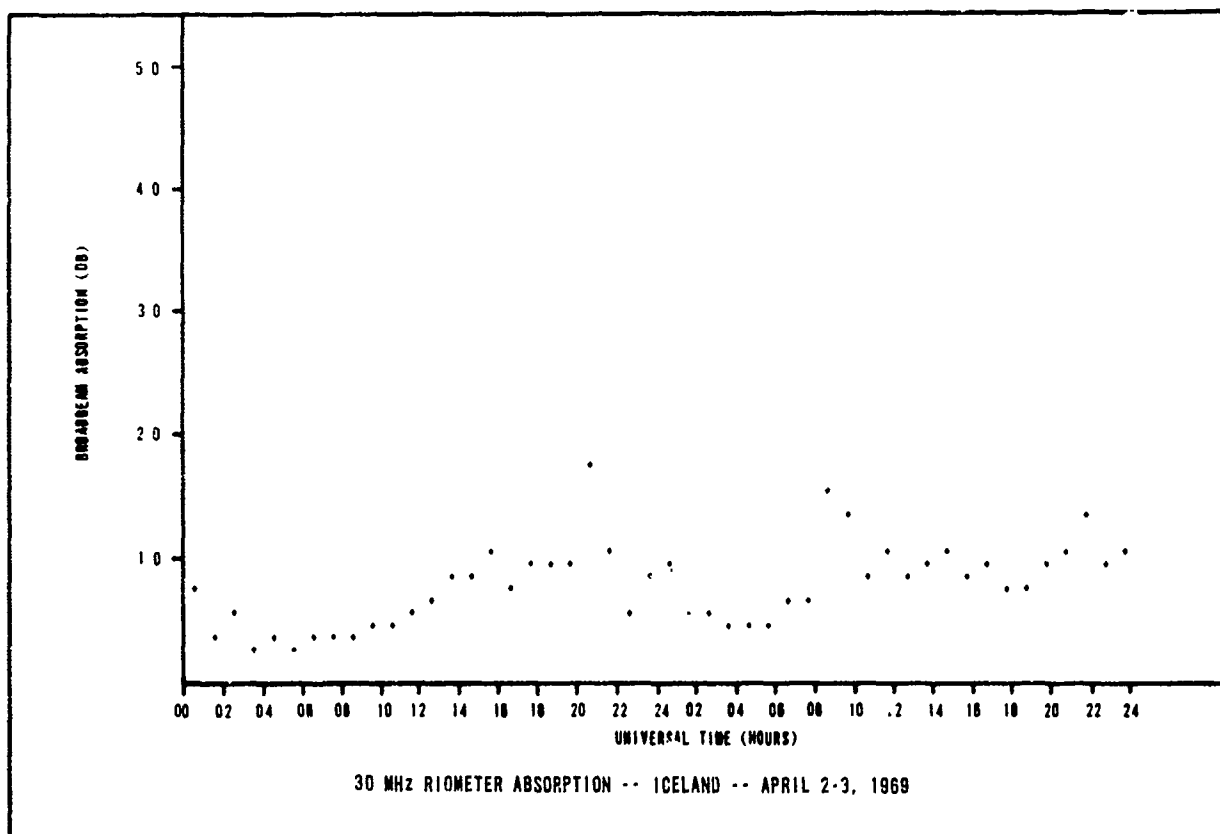
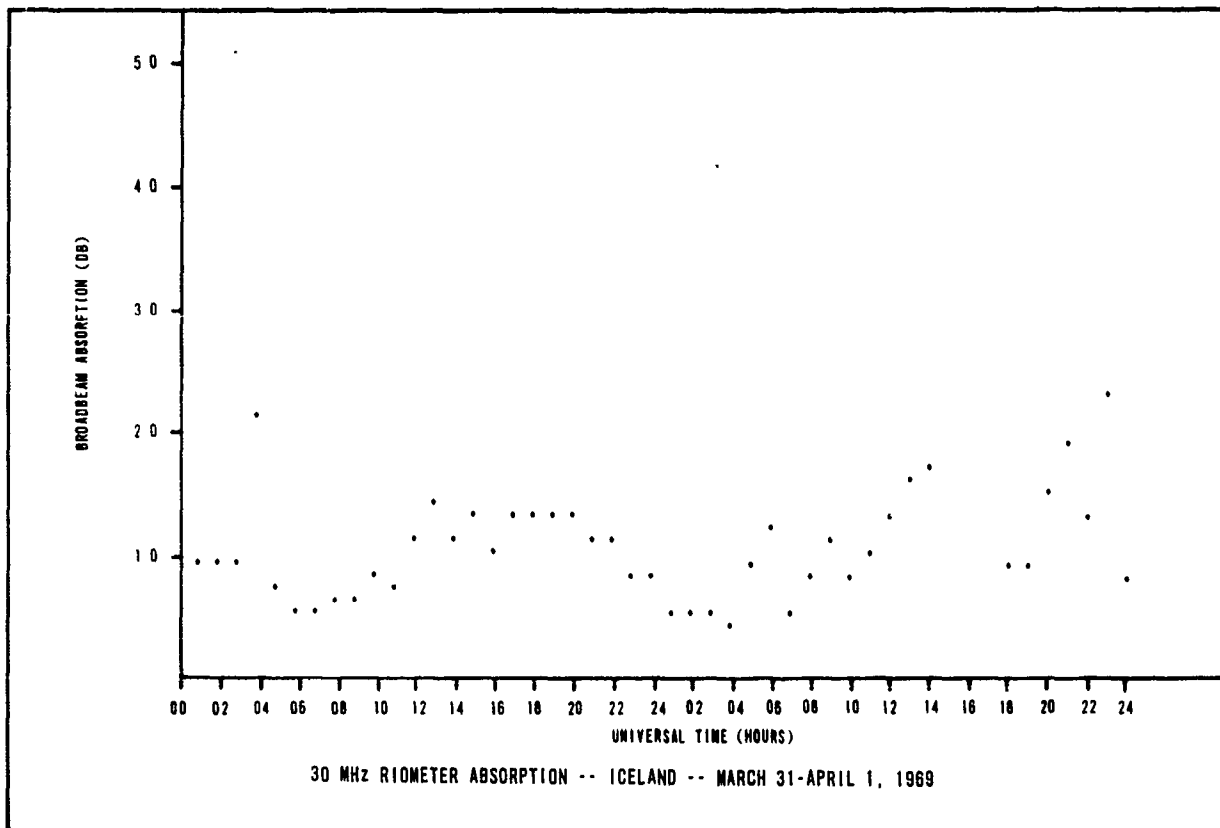


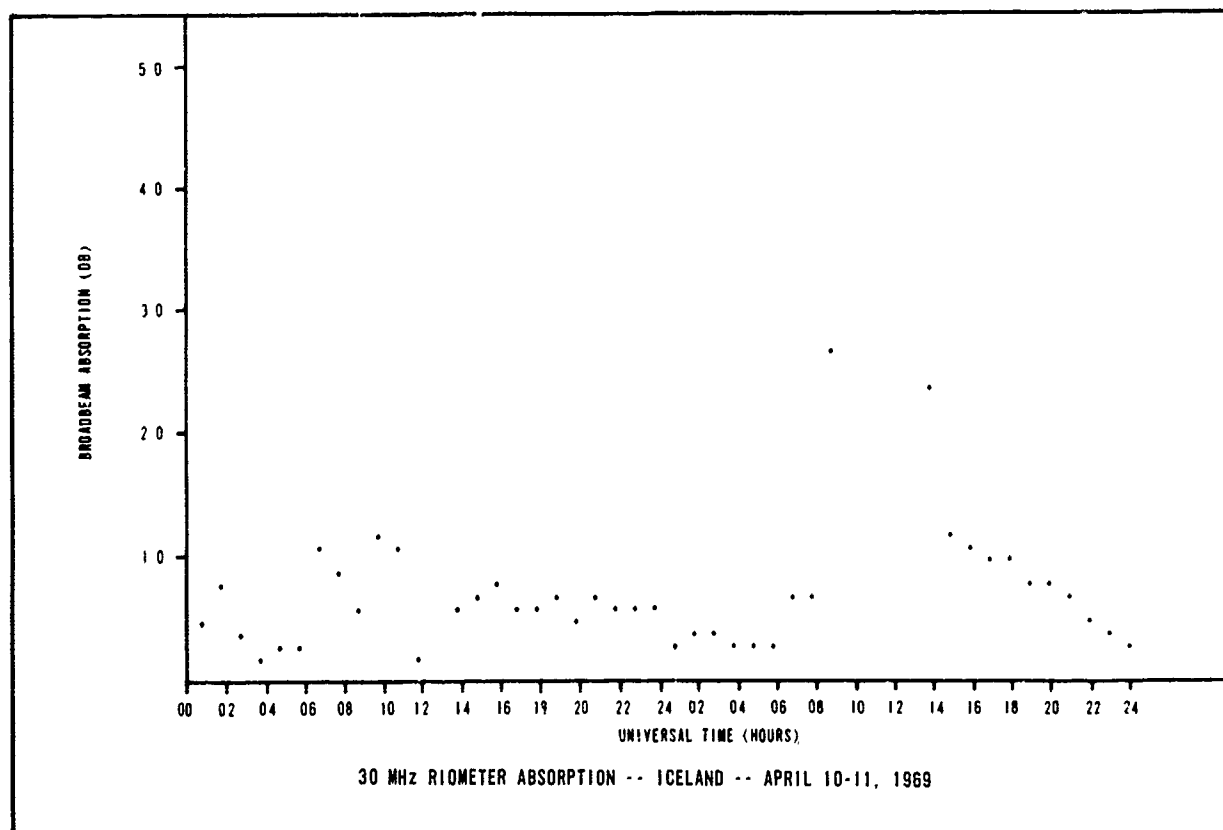
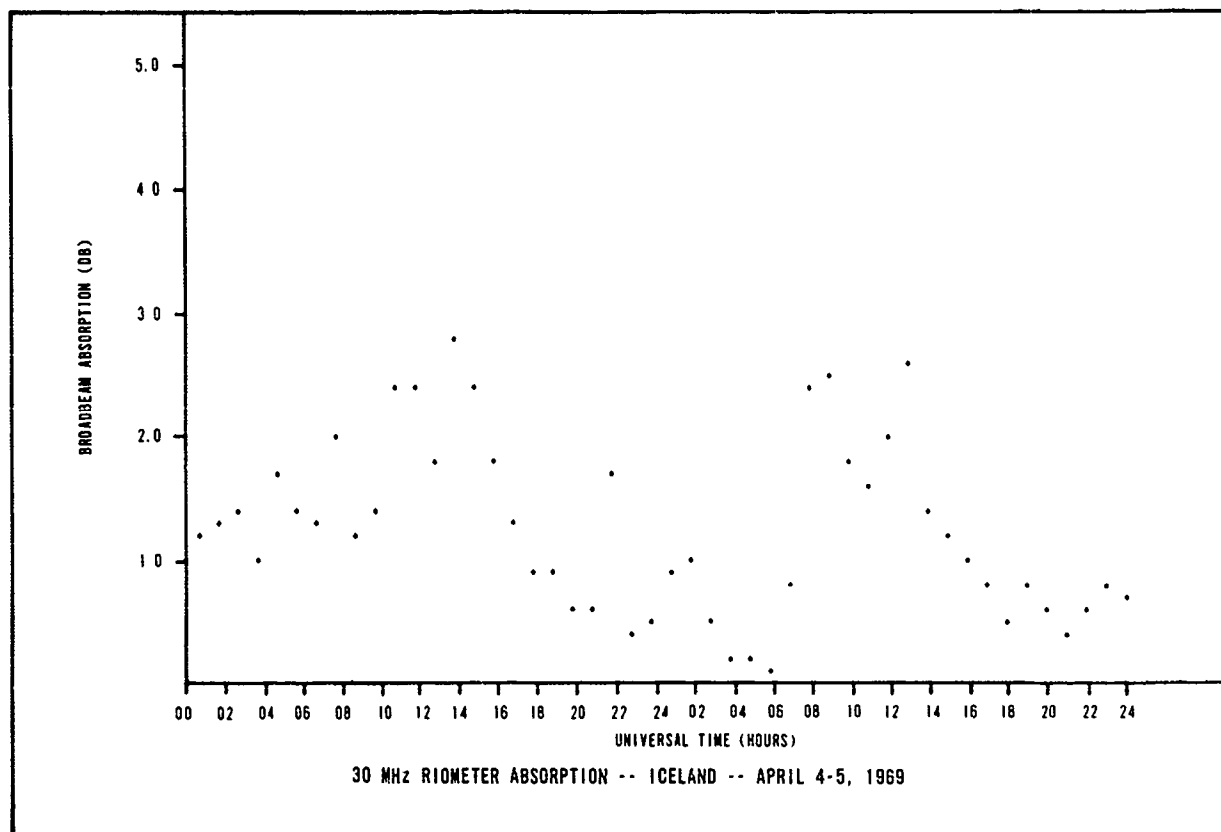




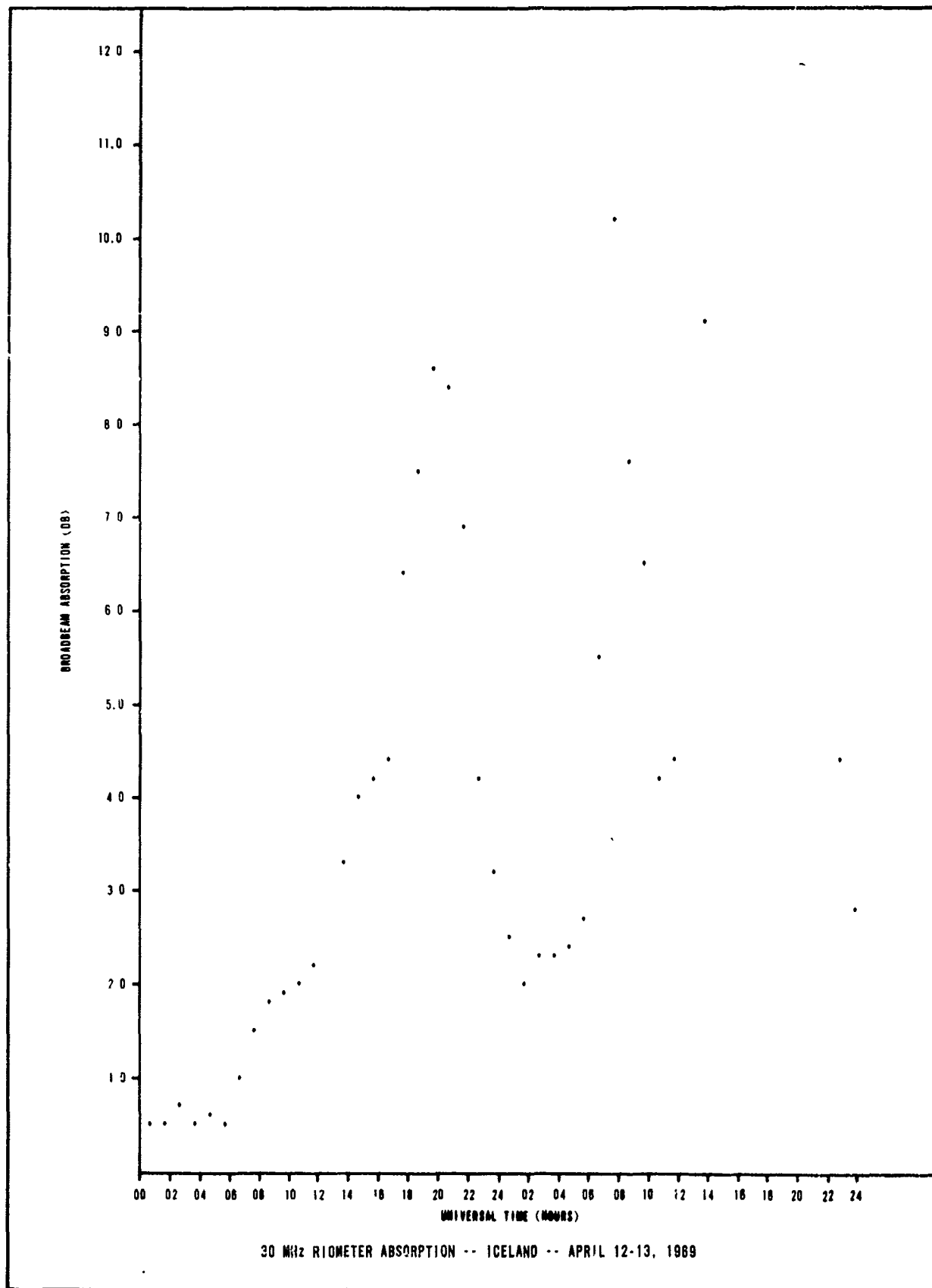


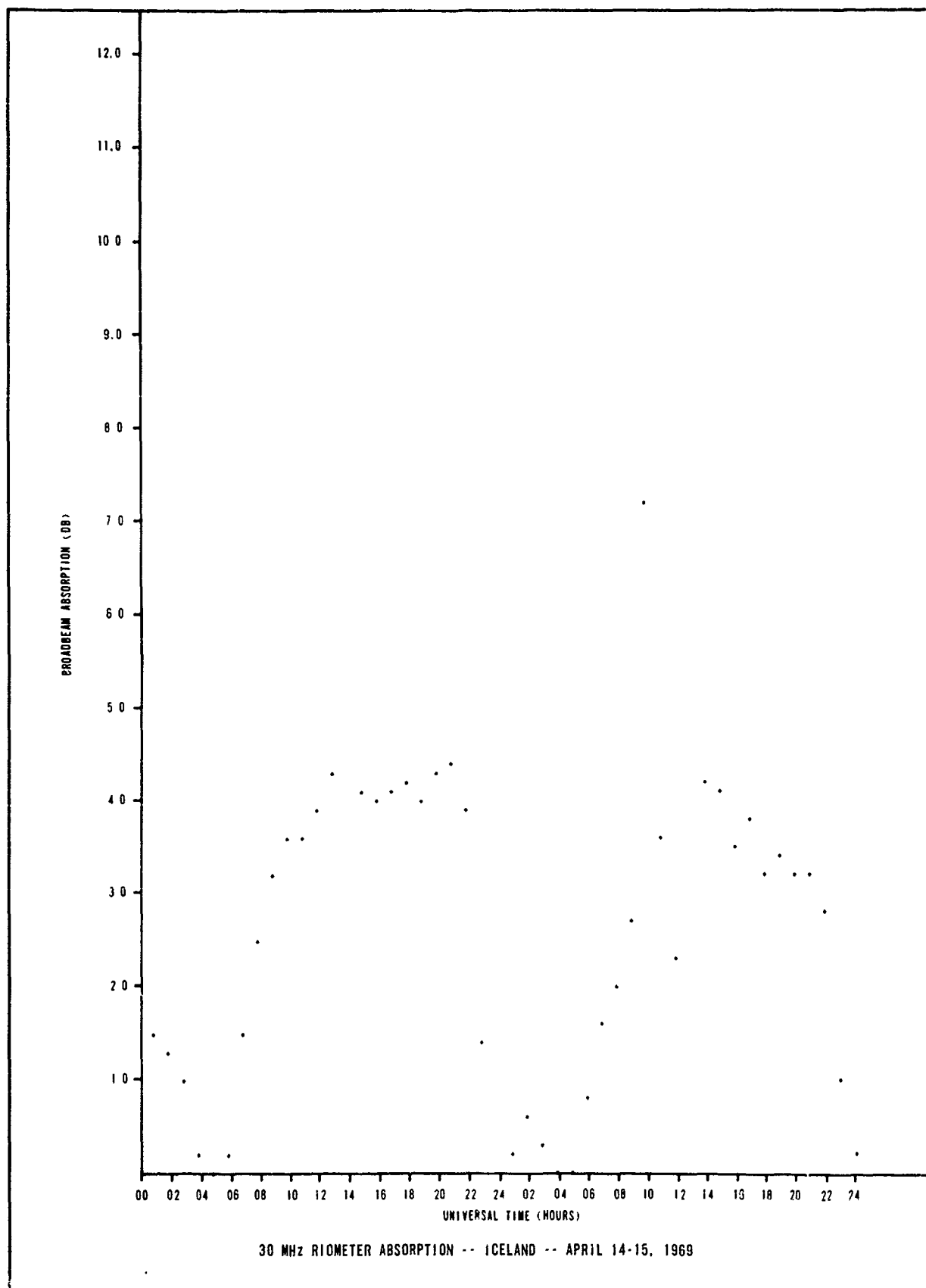


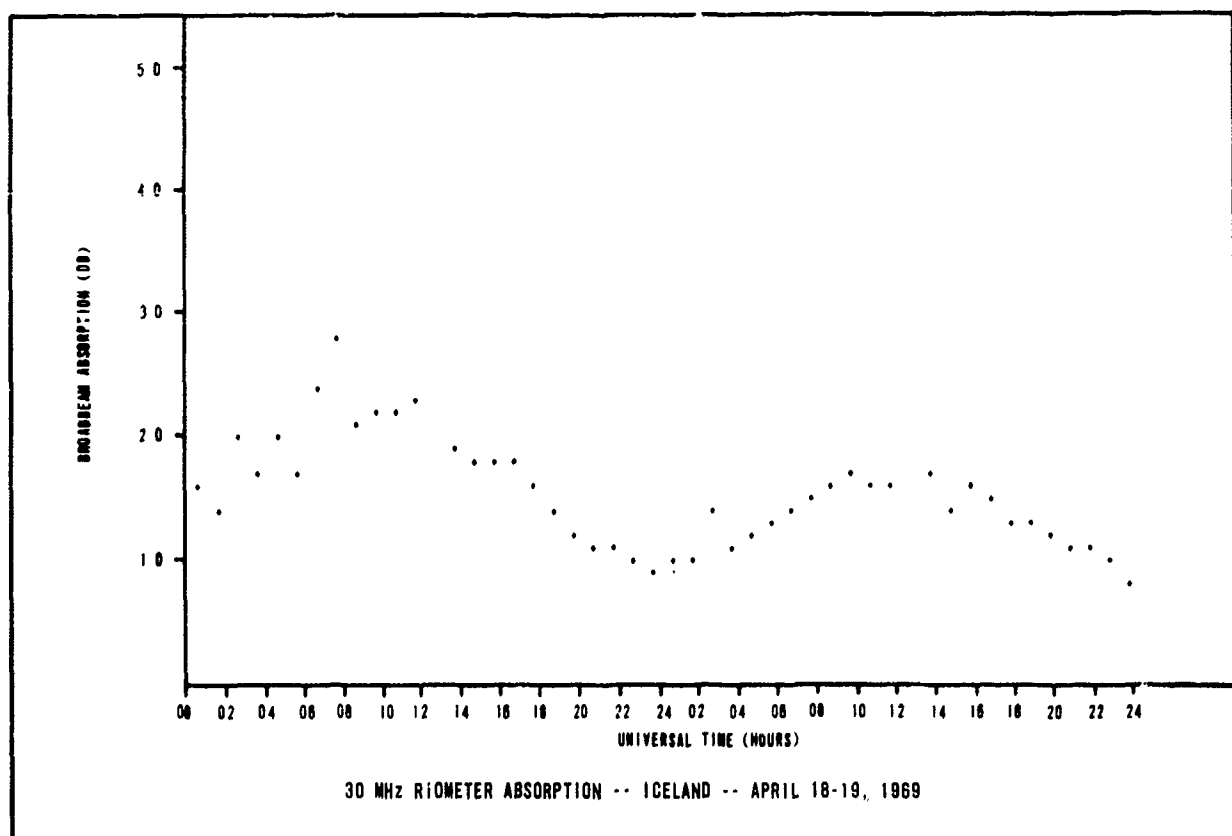
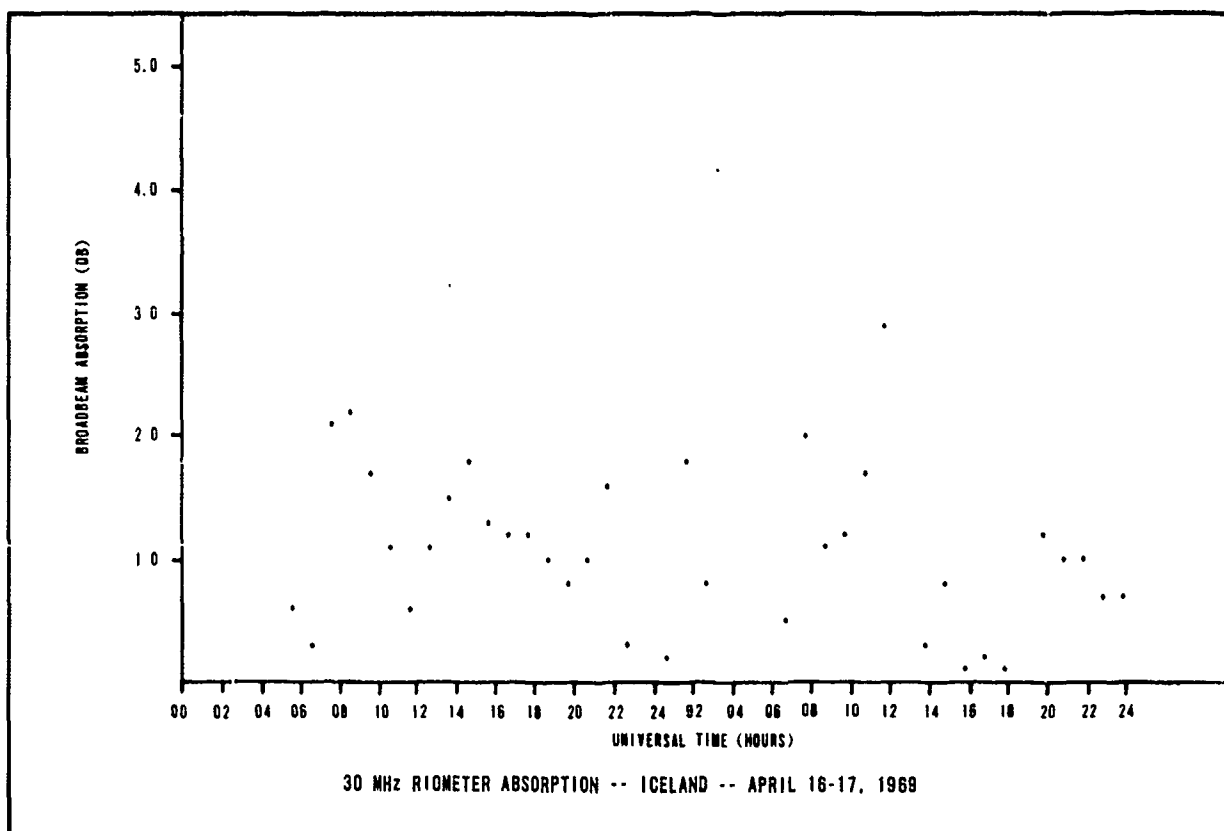


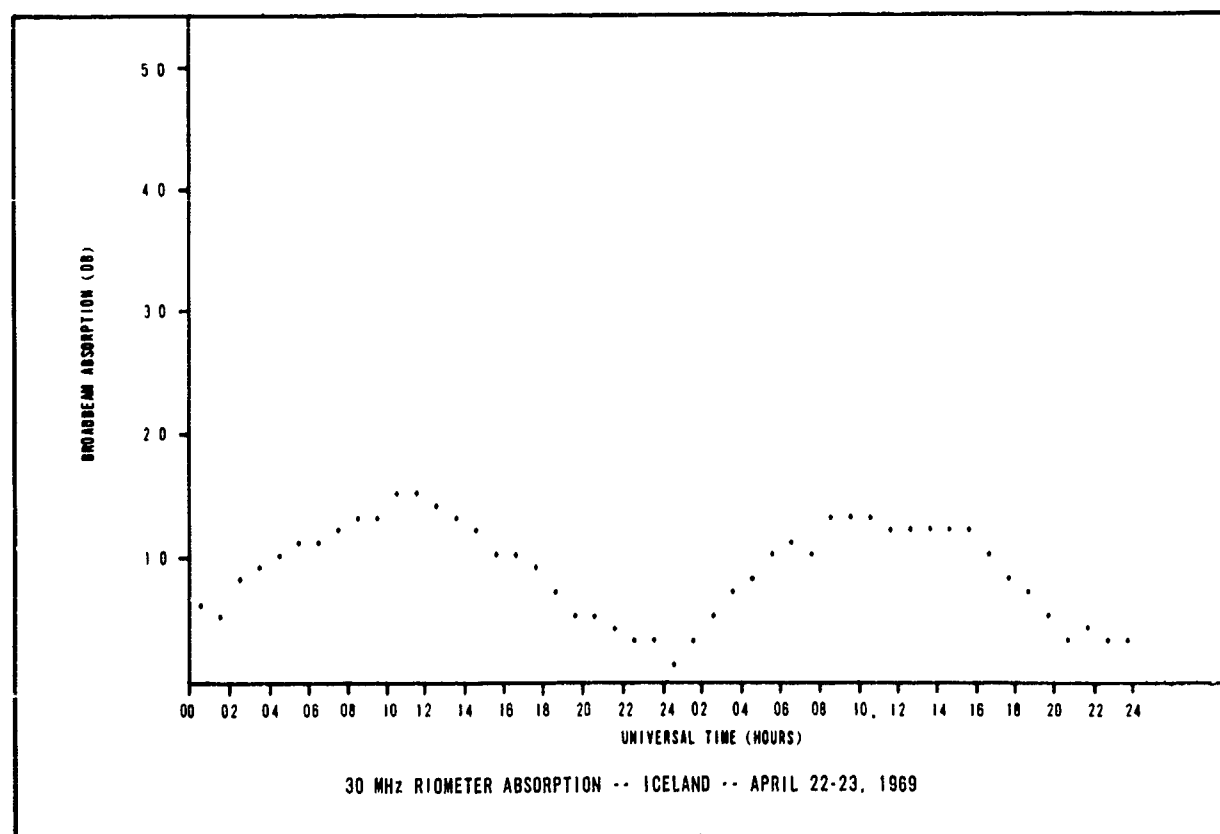
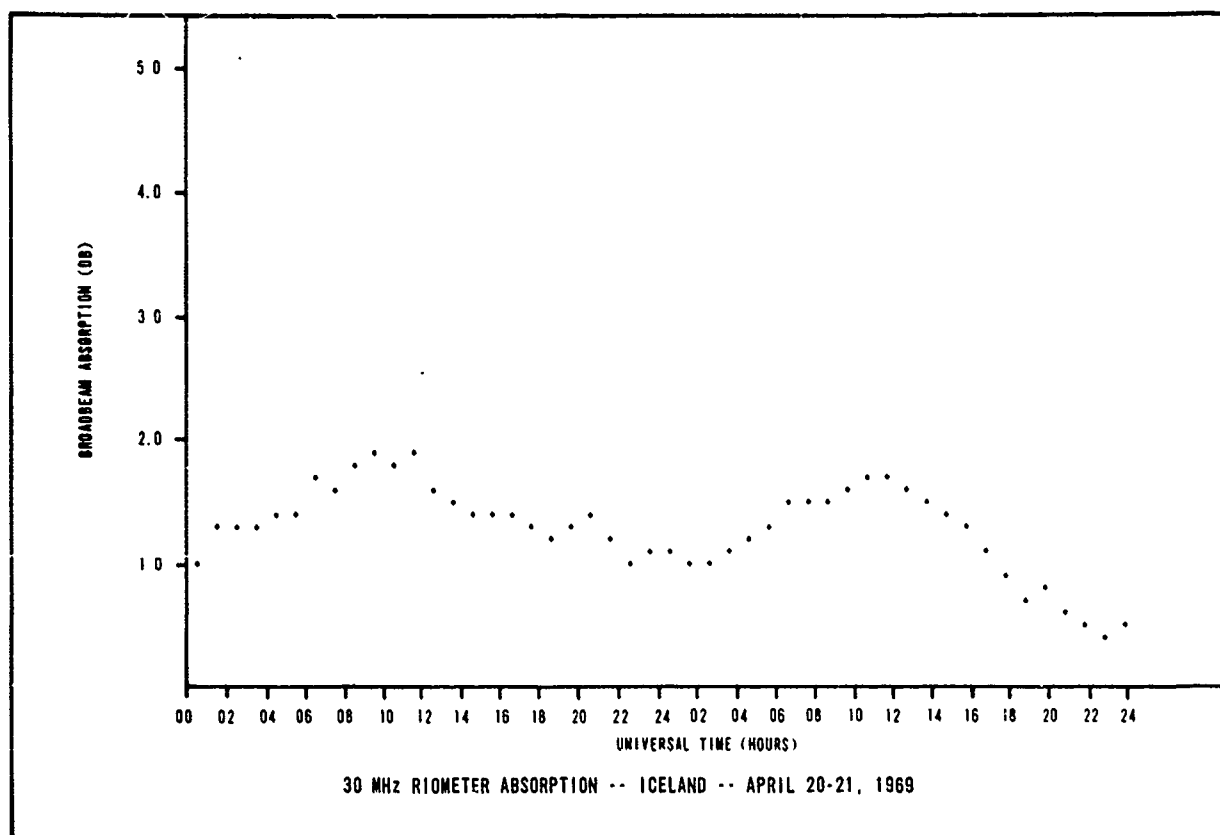


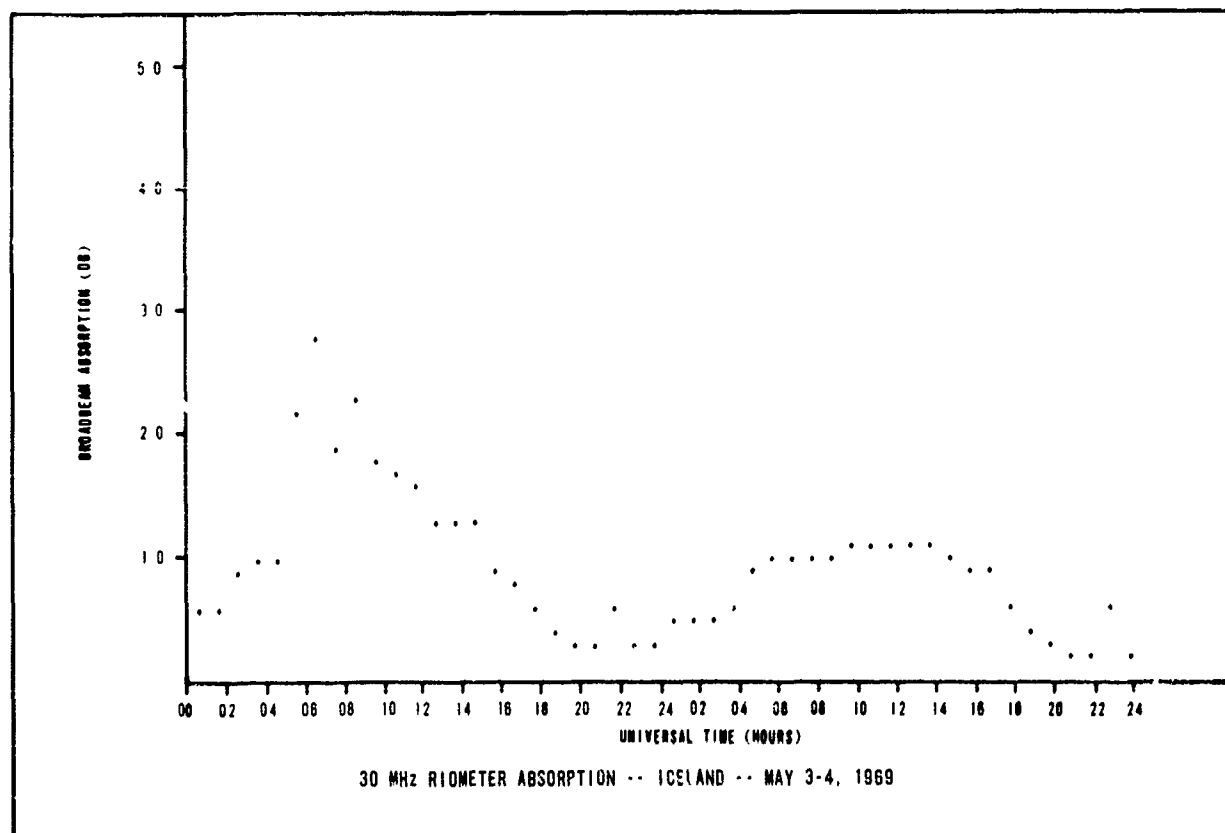
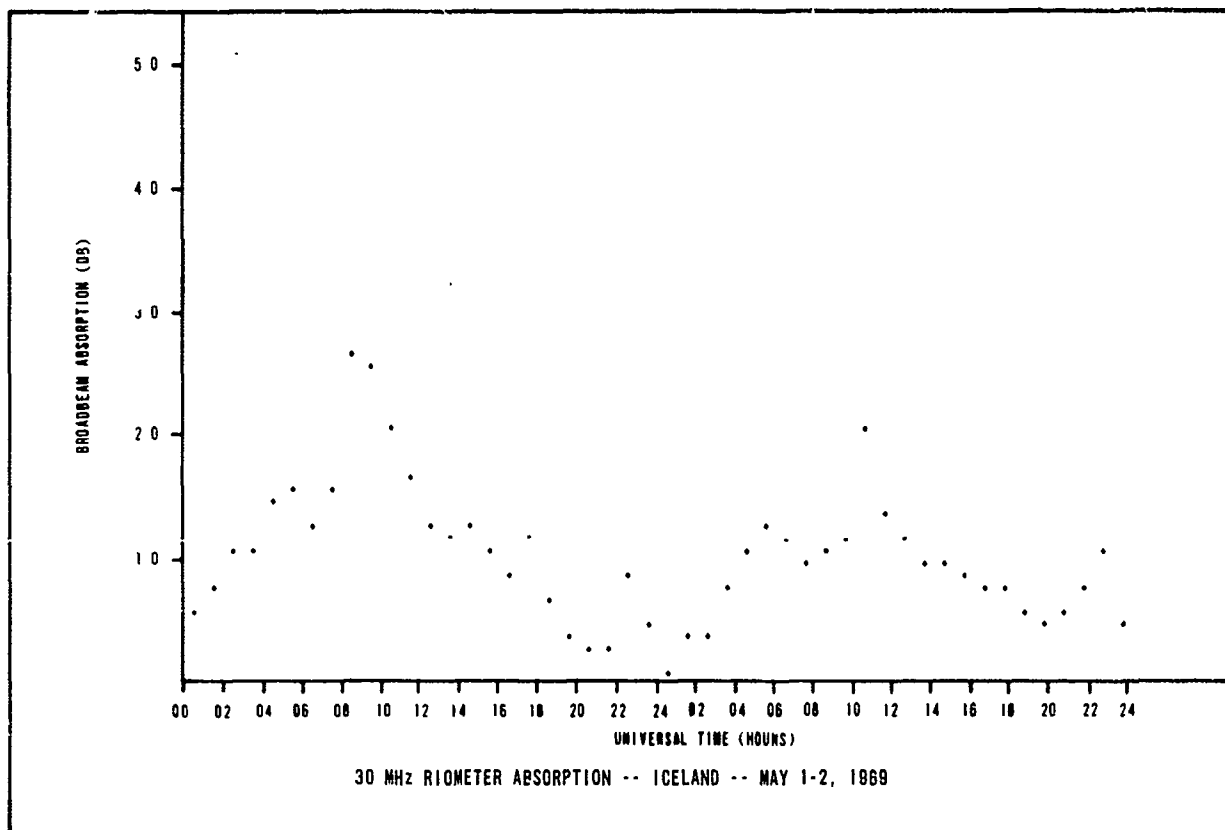


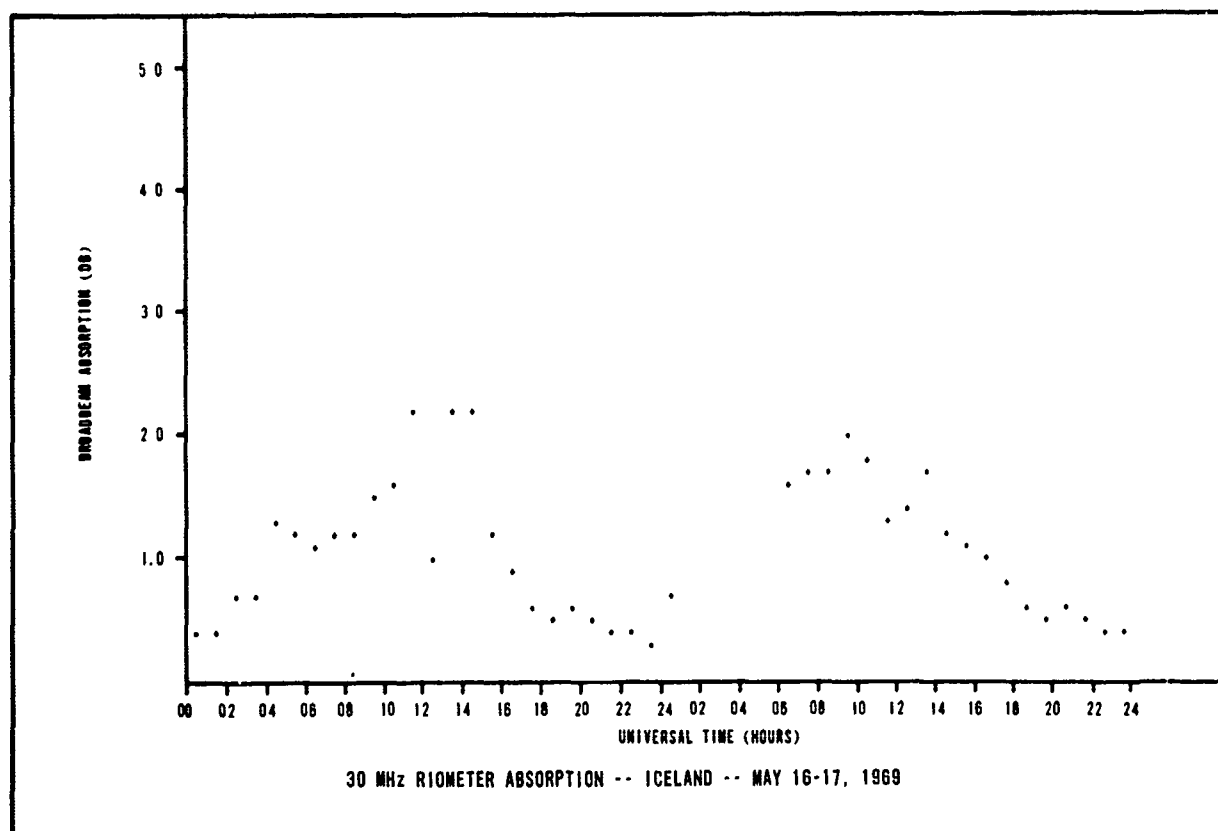
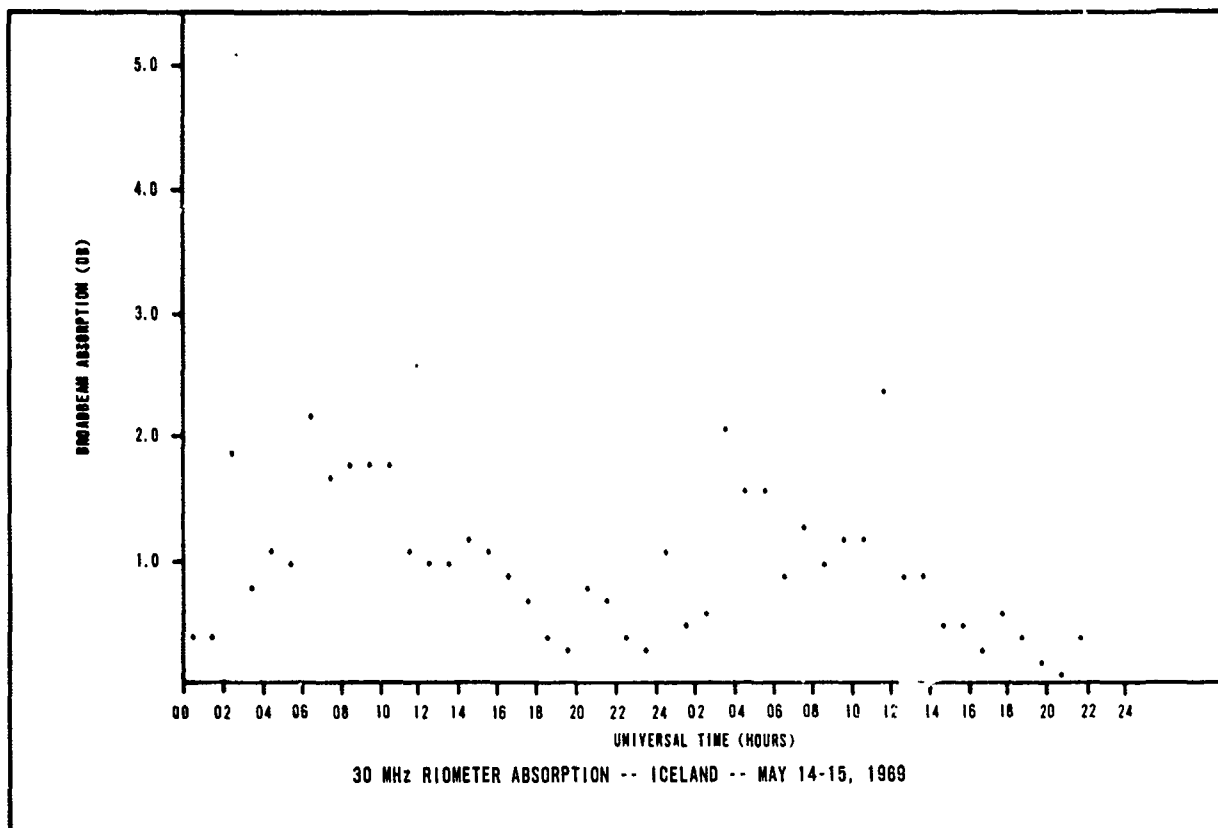




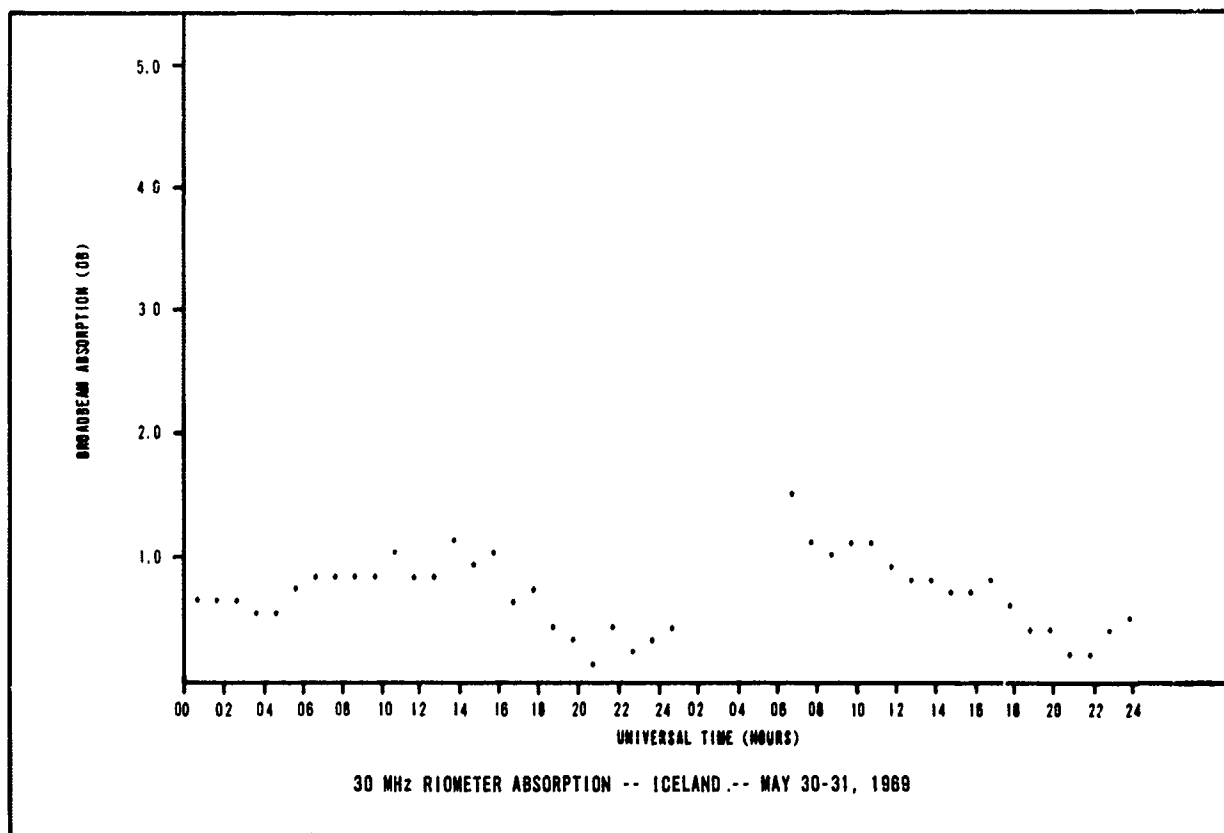
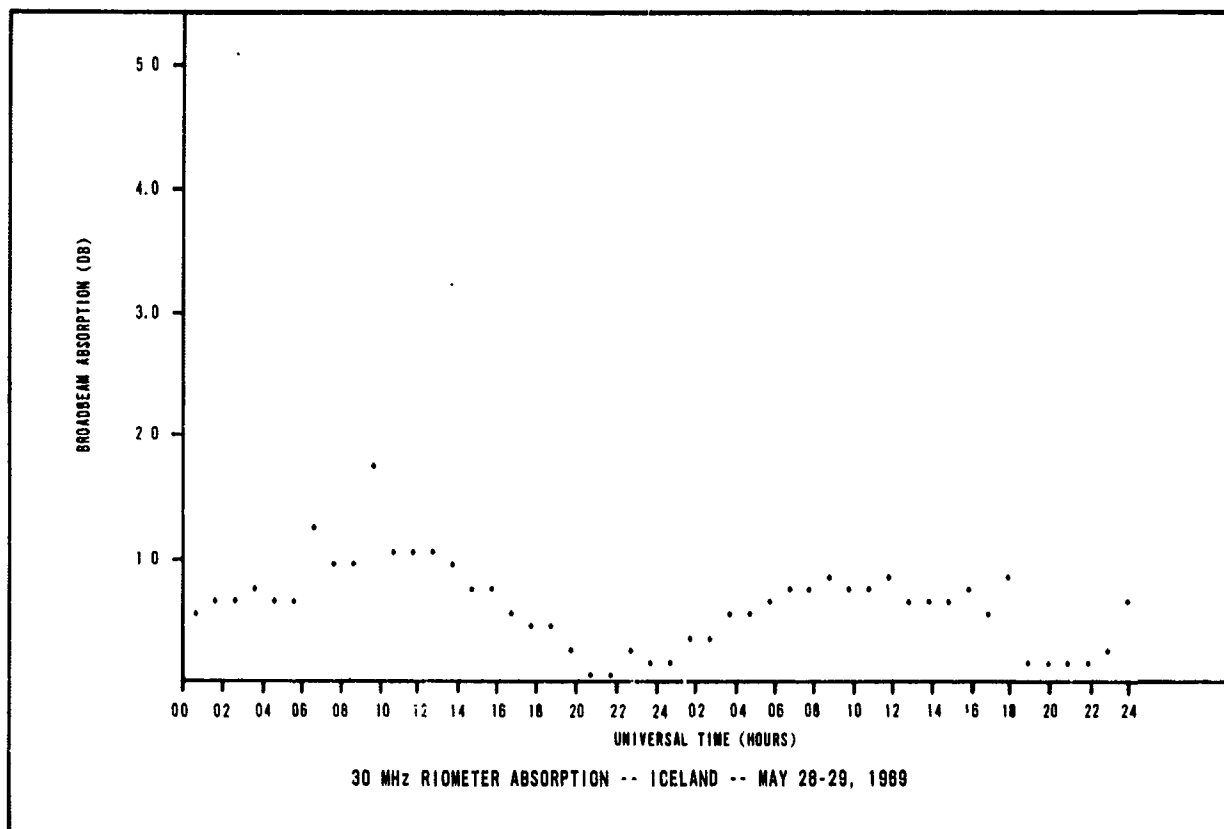


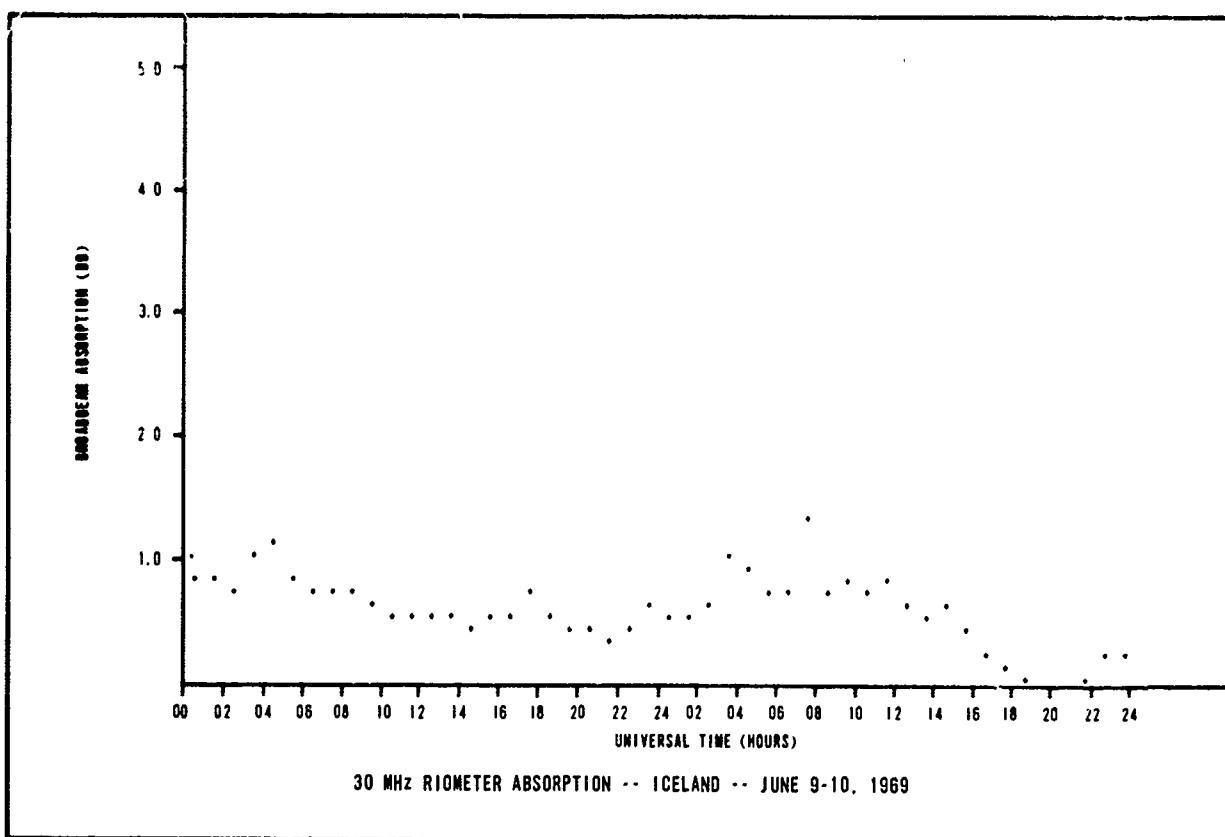
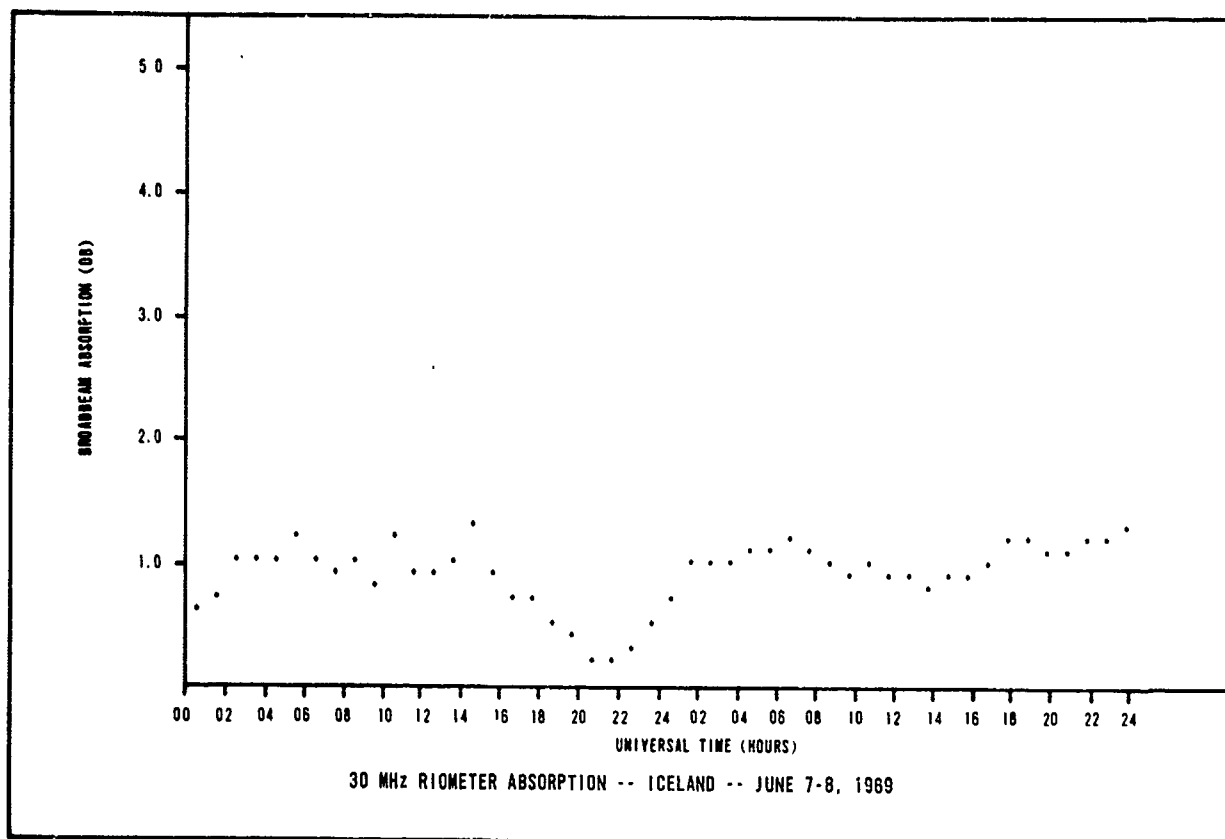




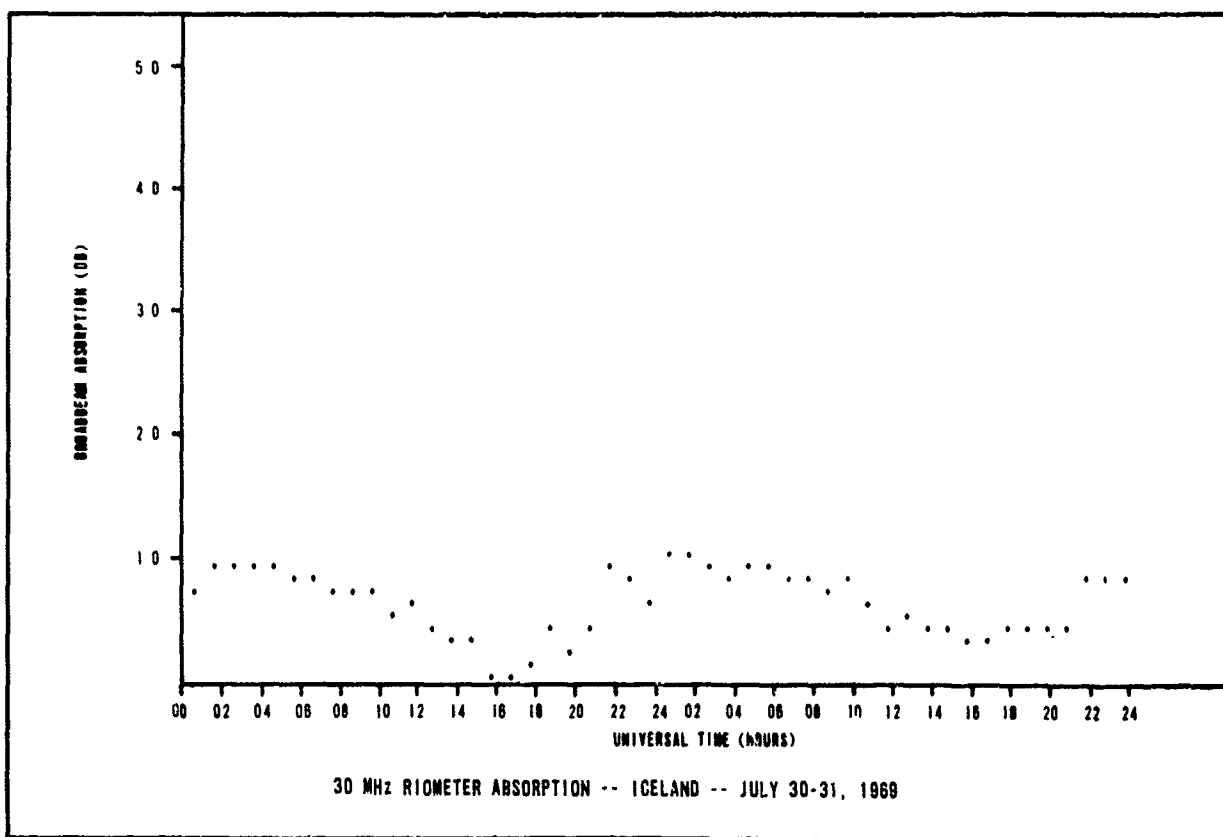
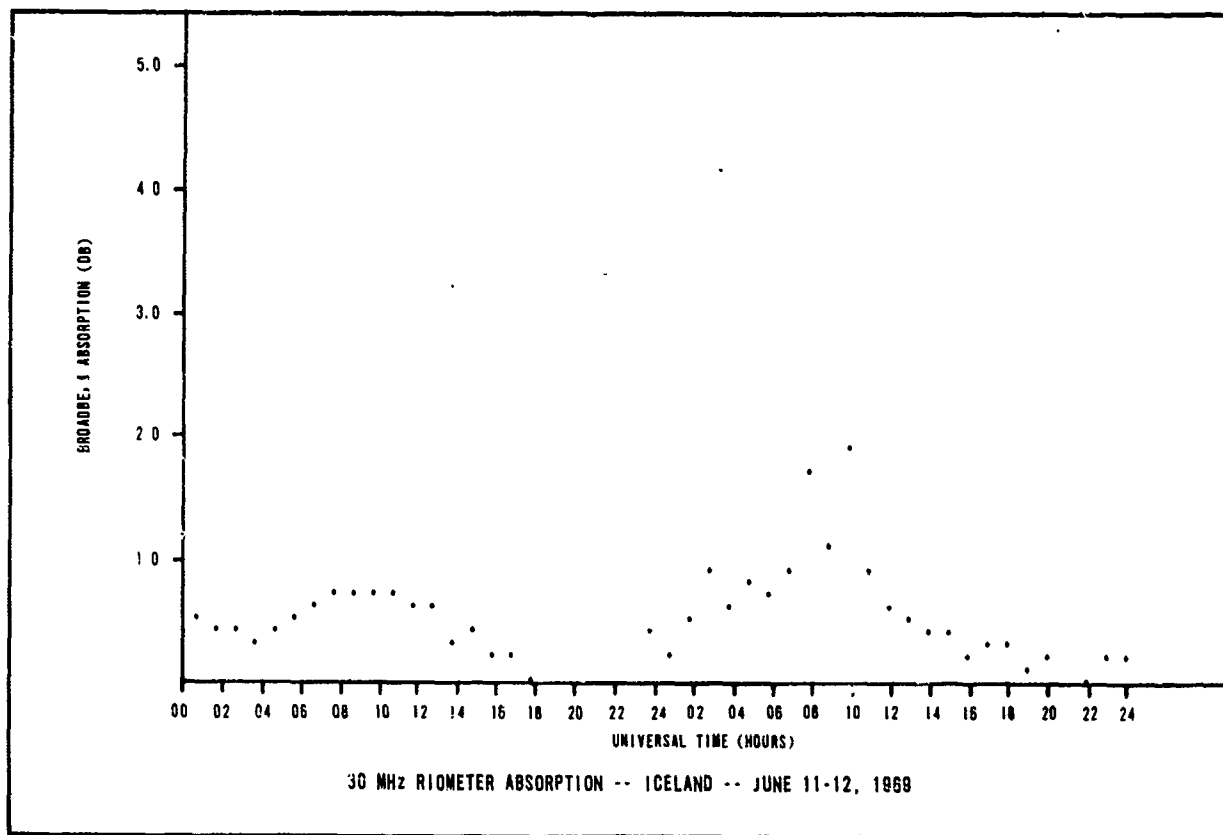


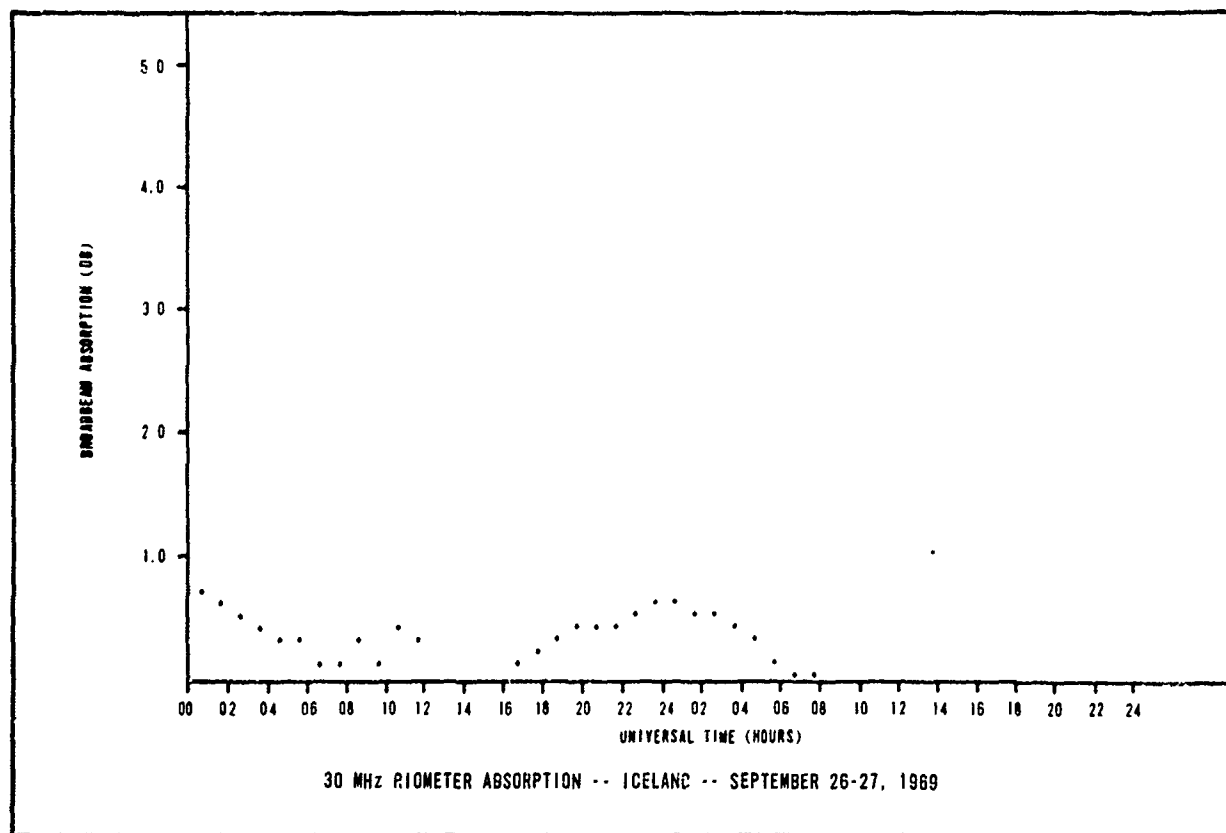
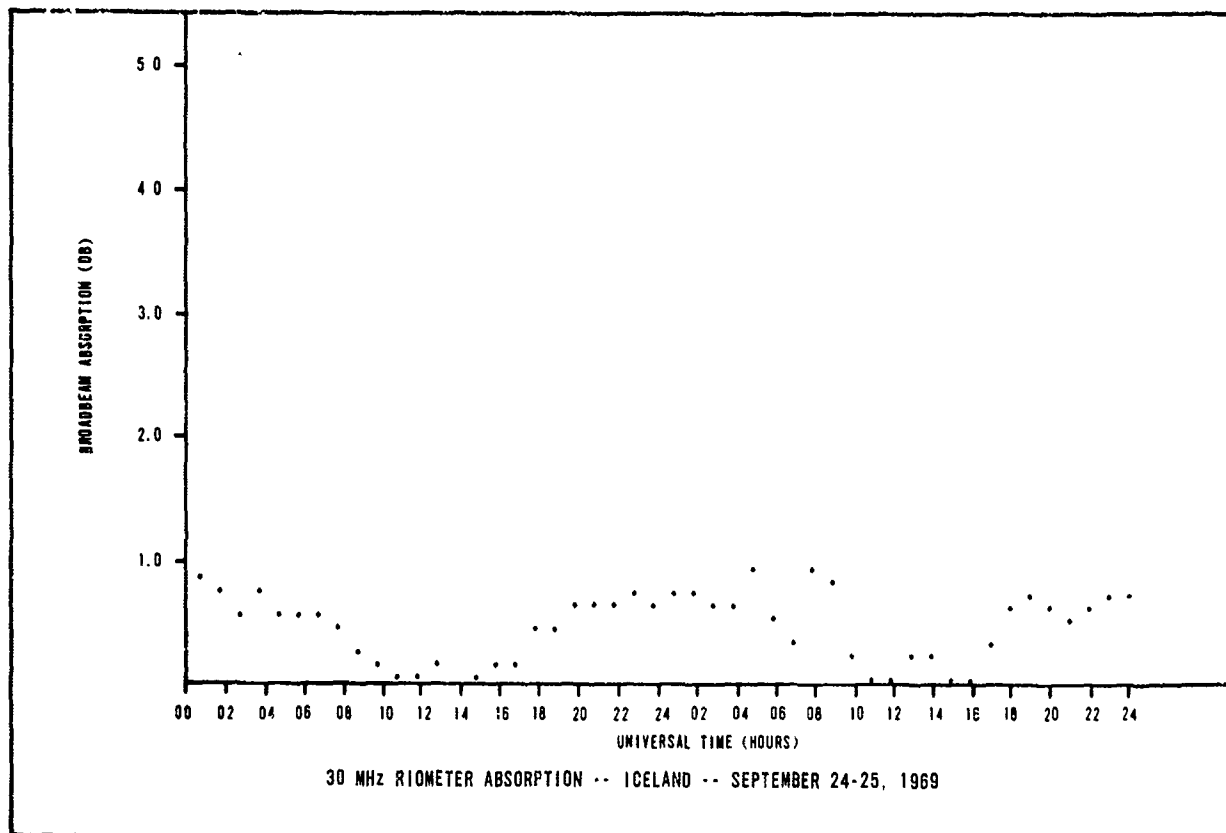
B-180

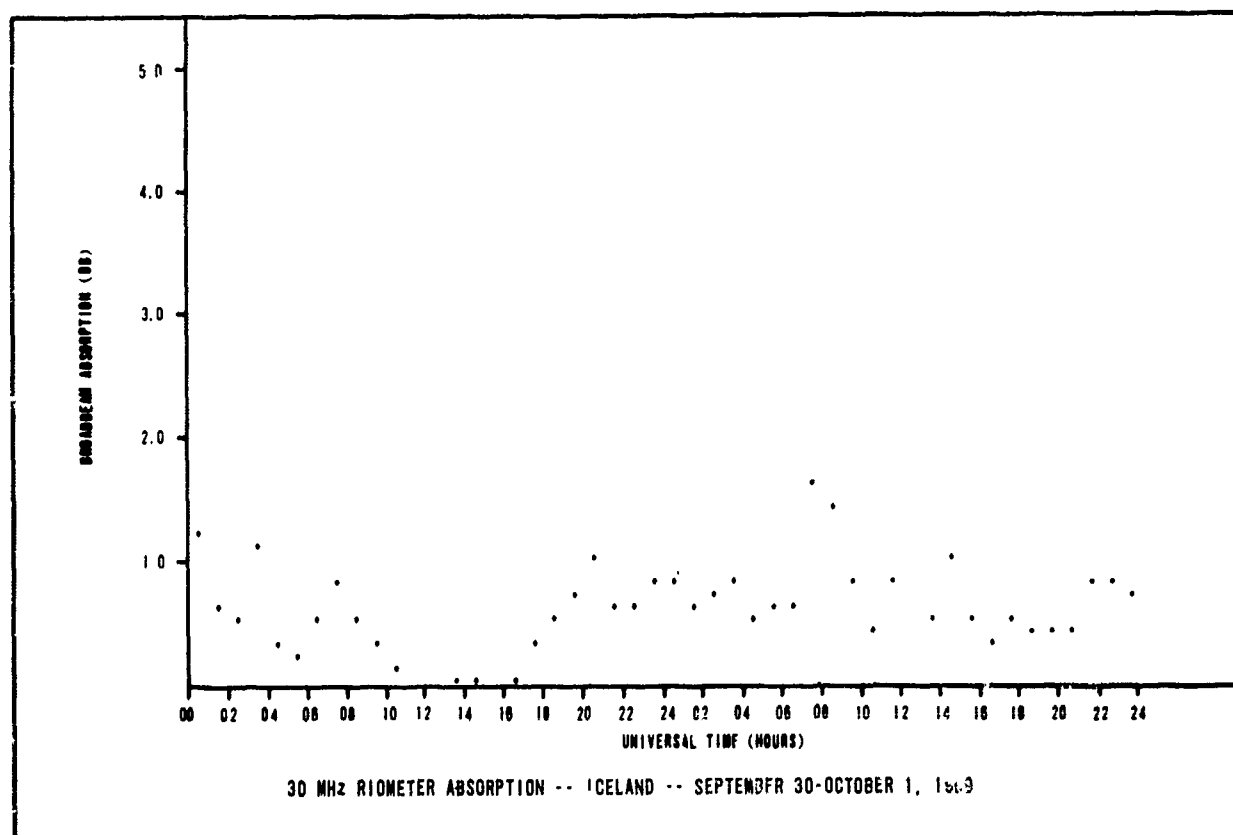
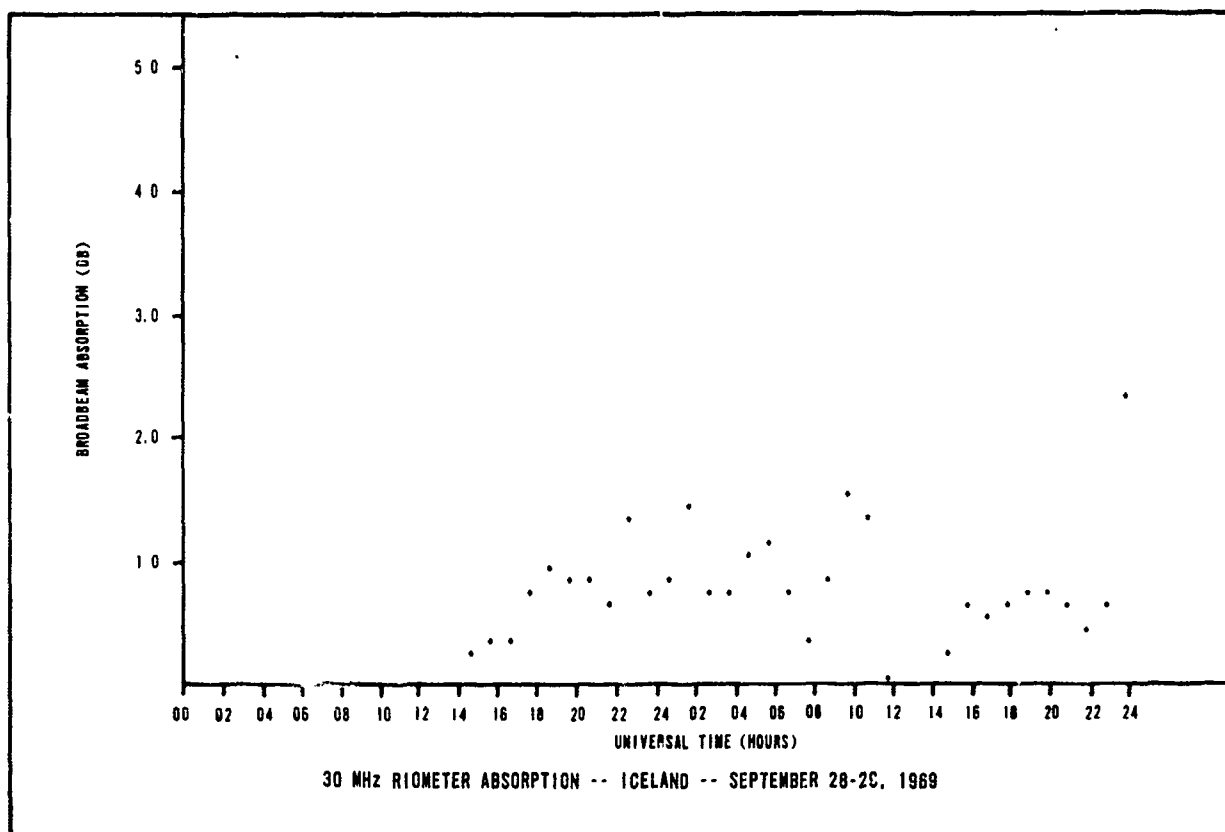


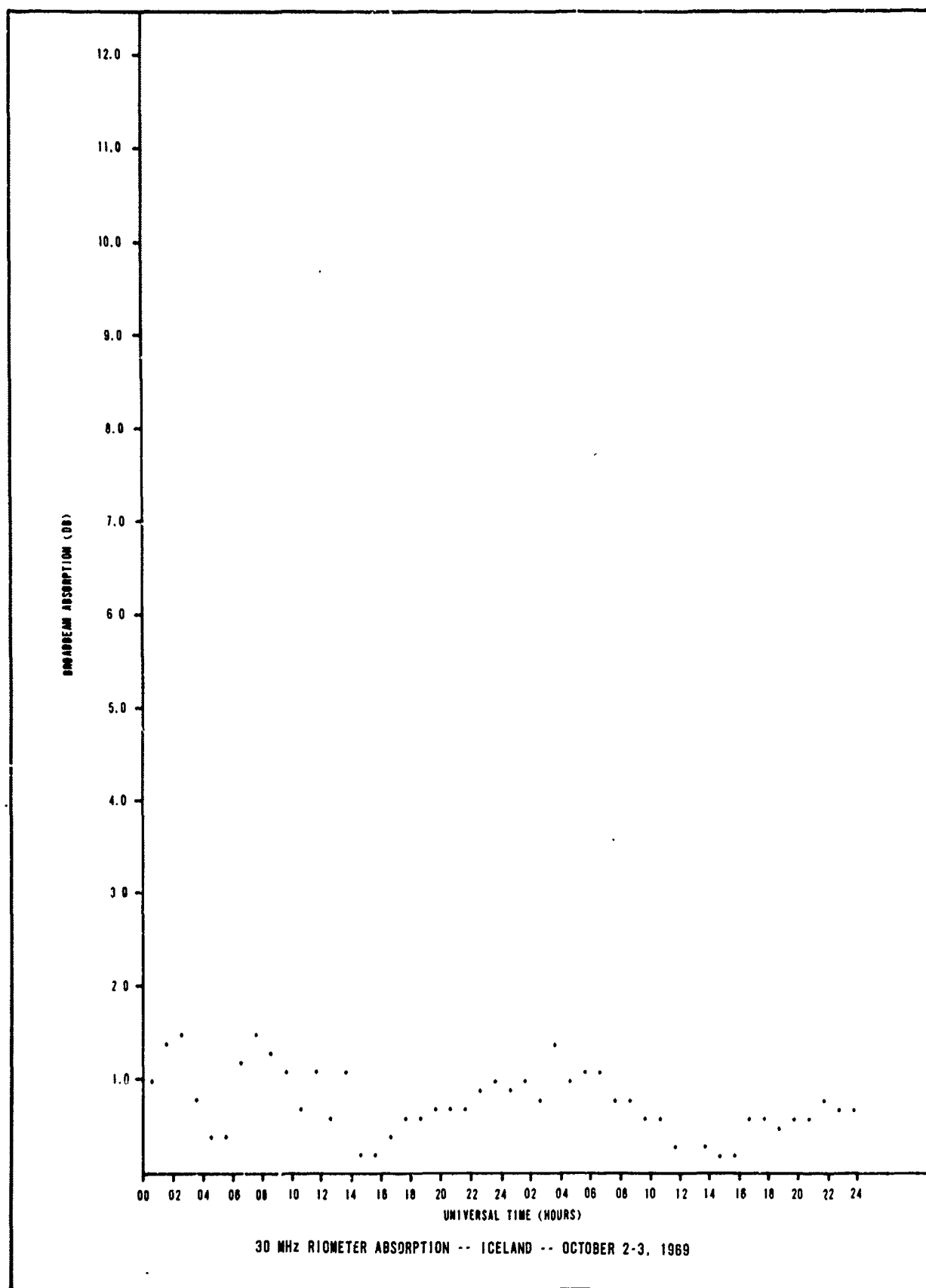


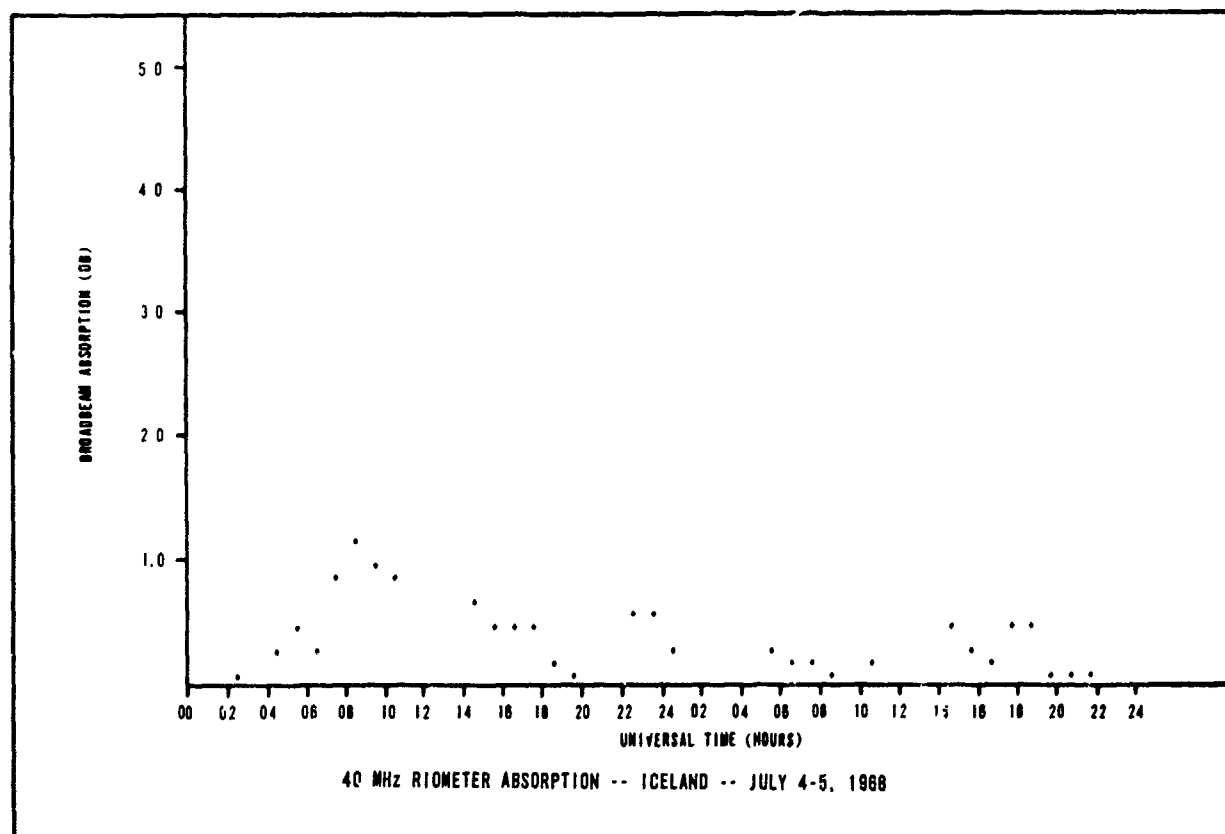
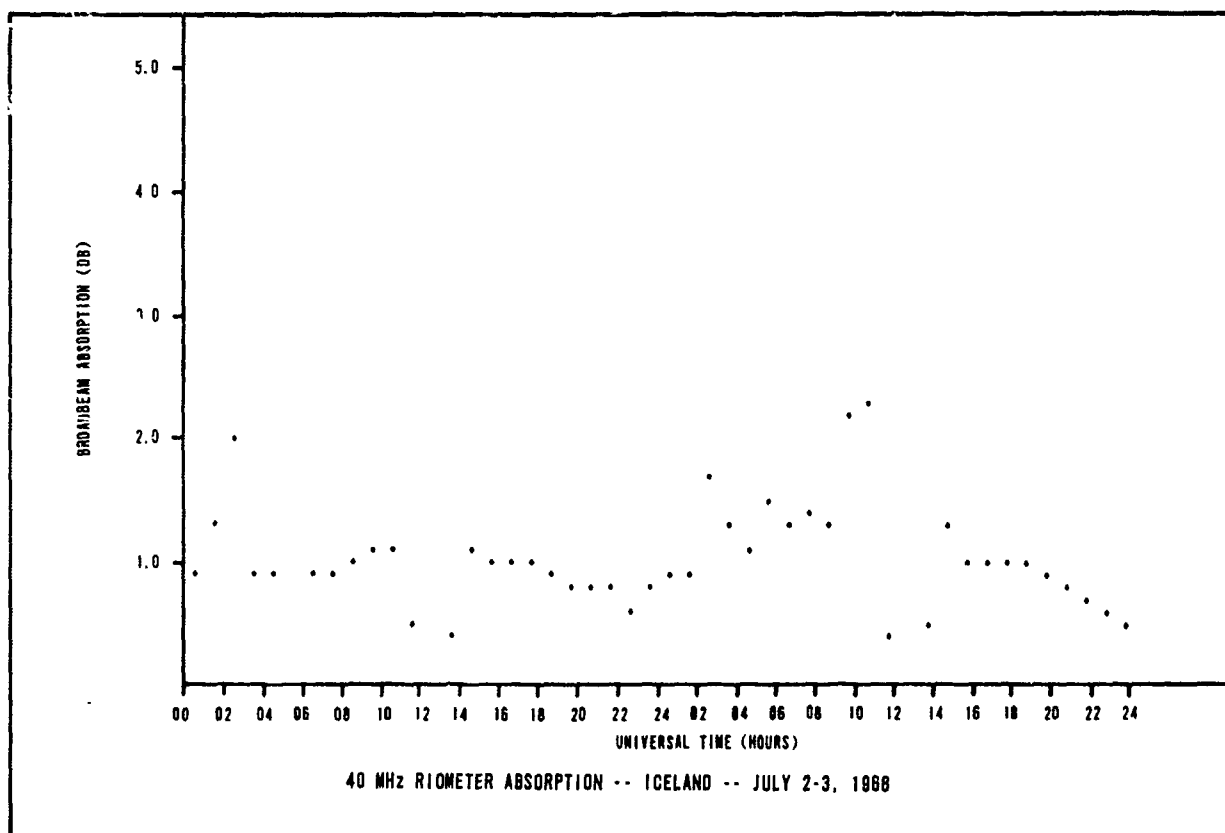


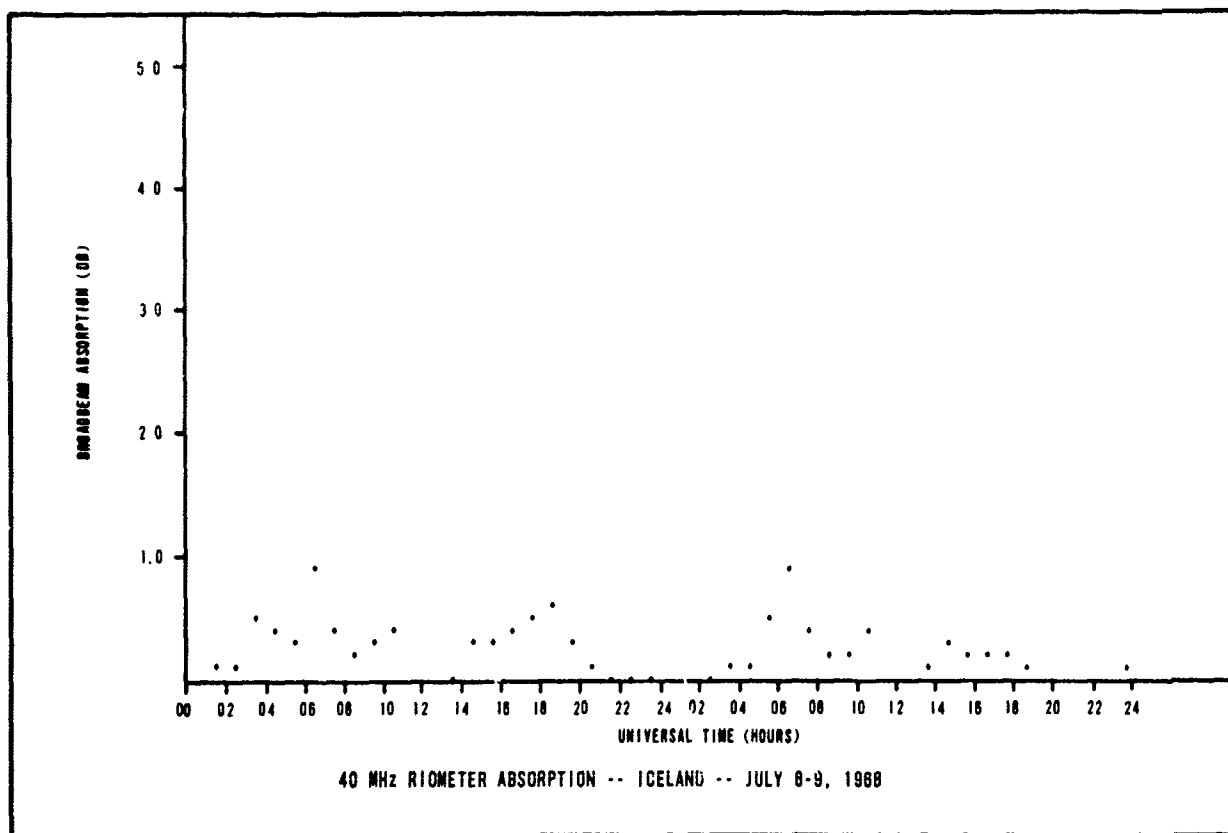
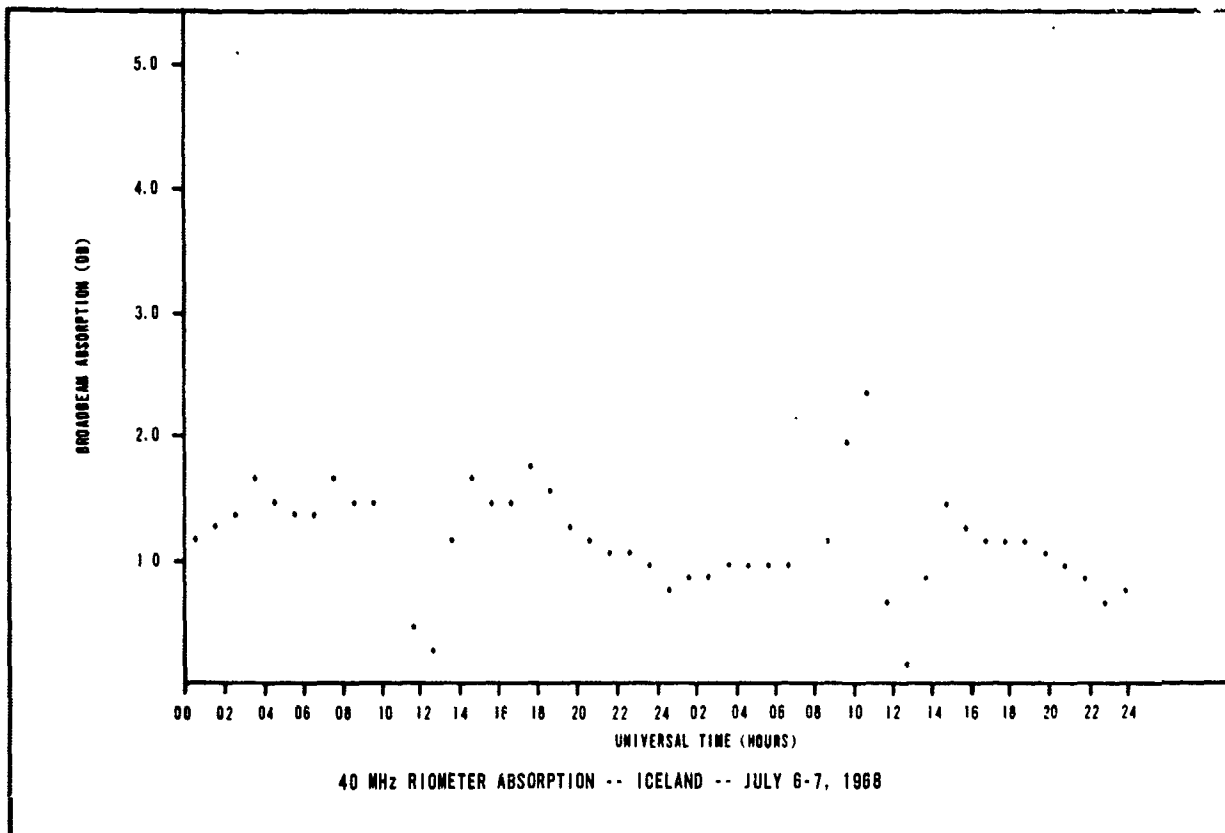


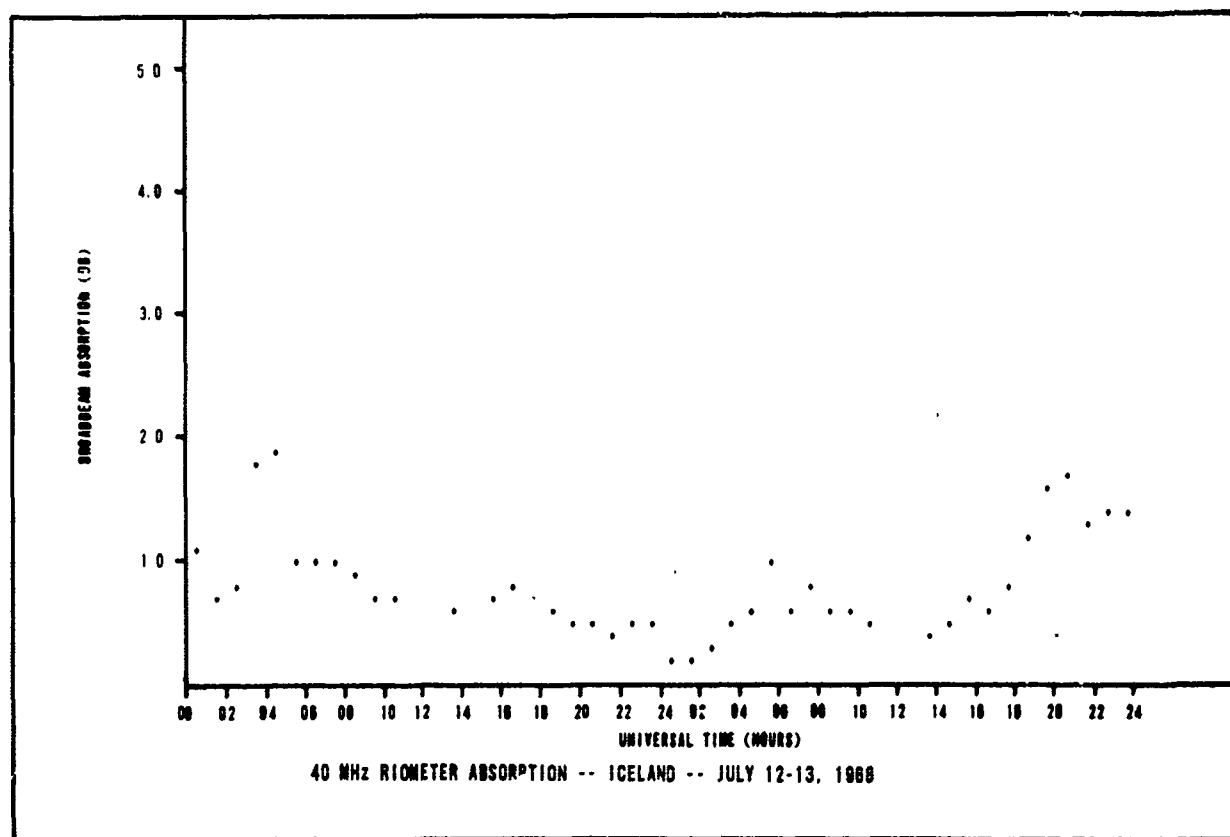
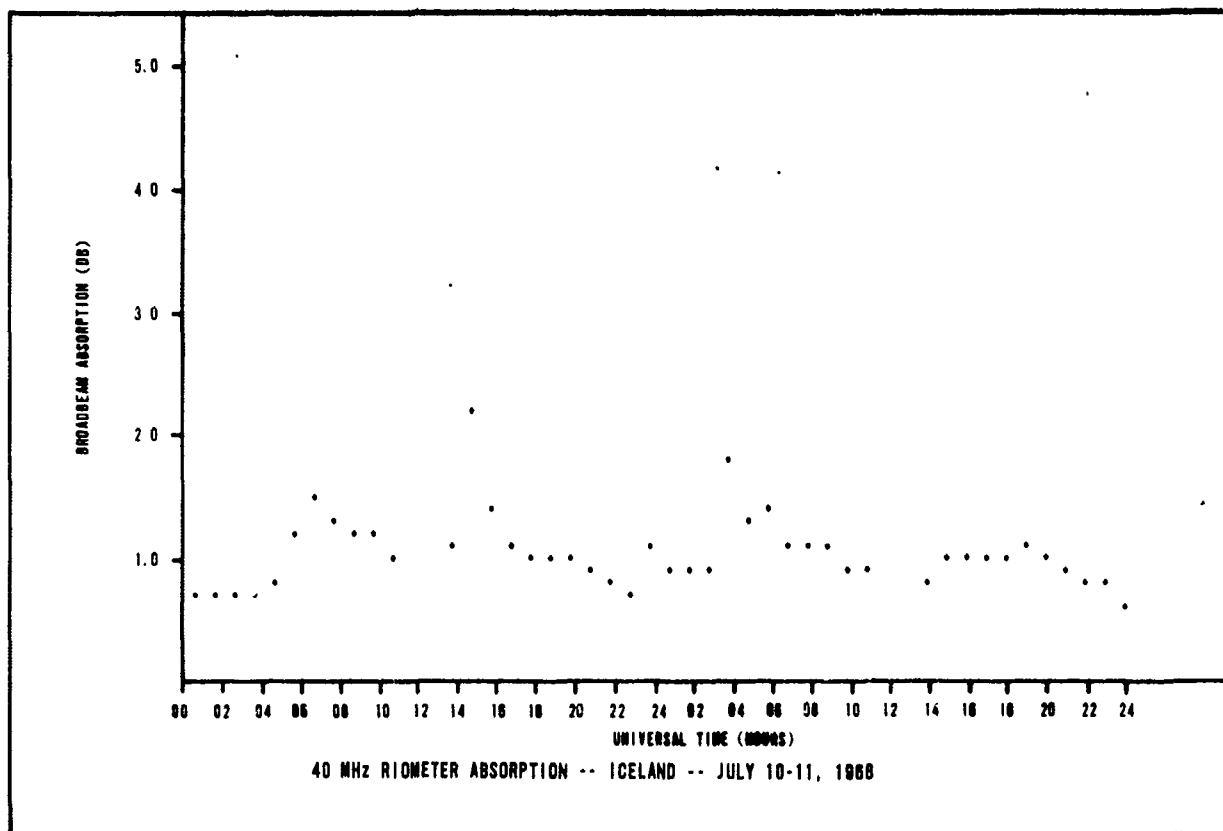


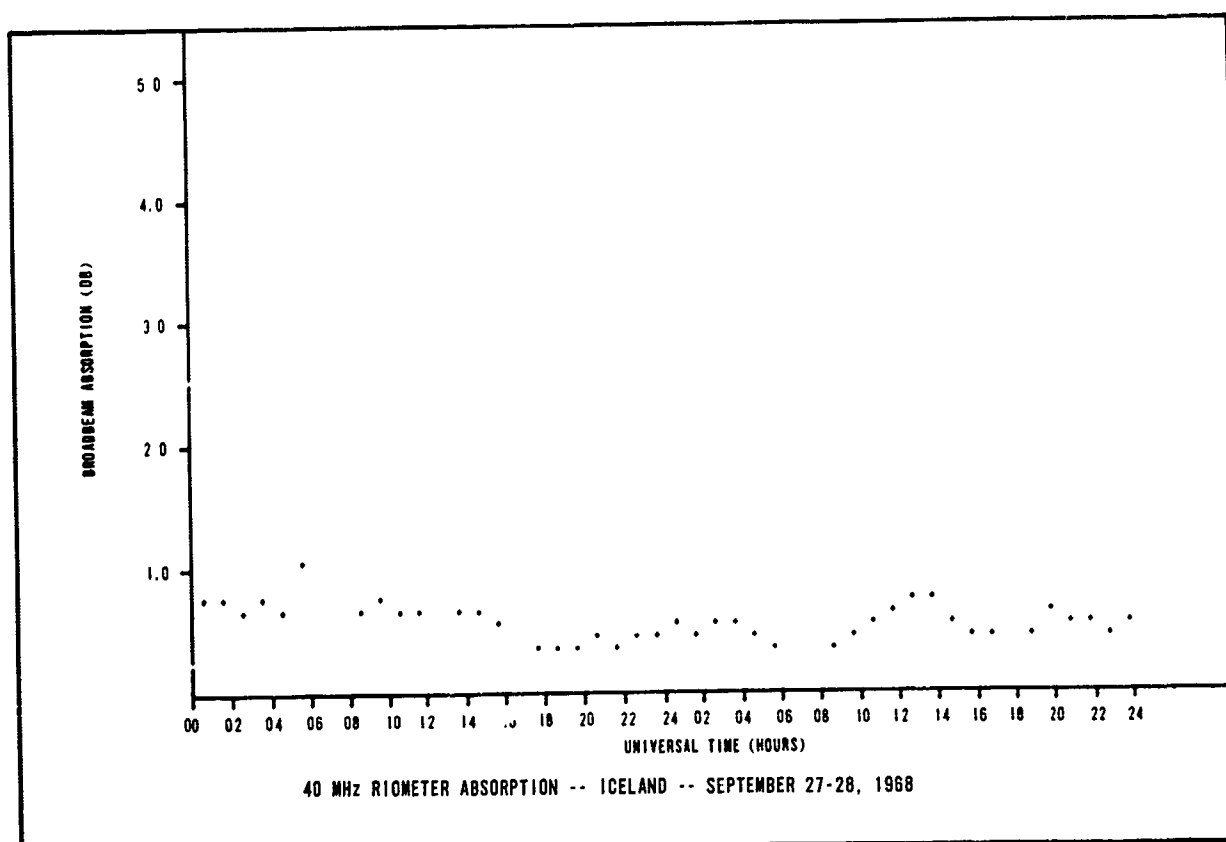
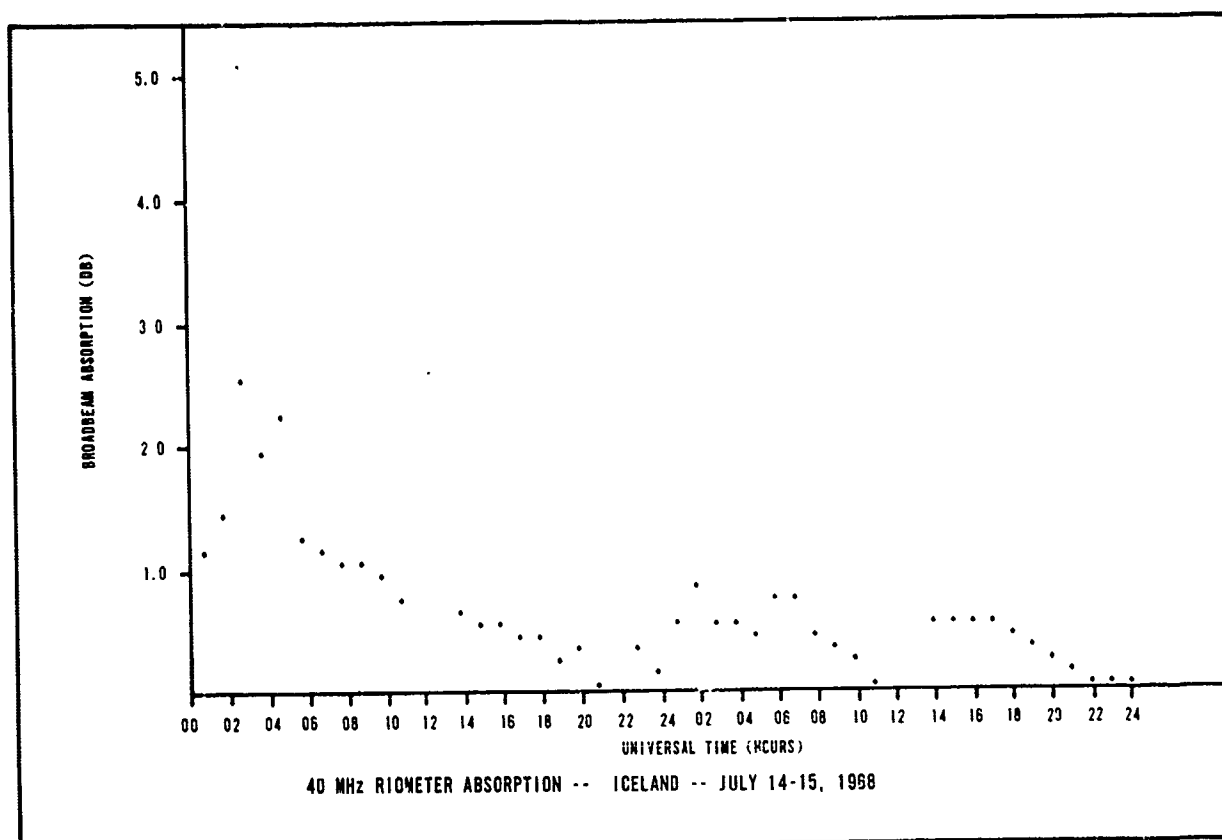




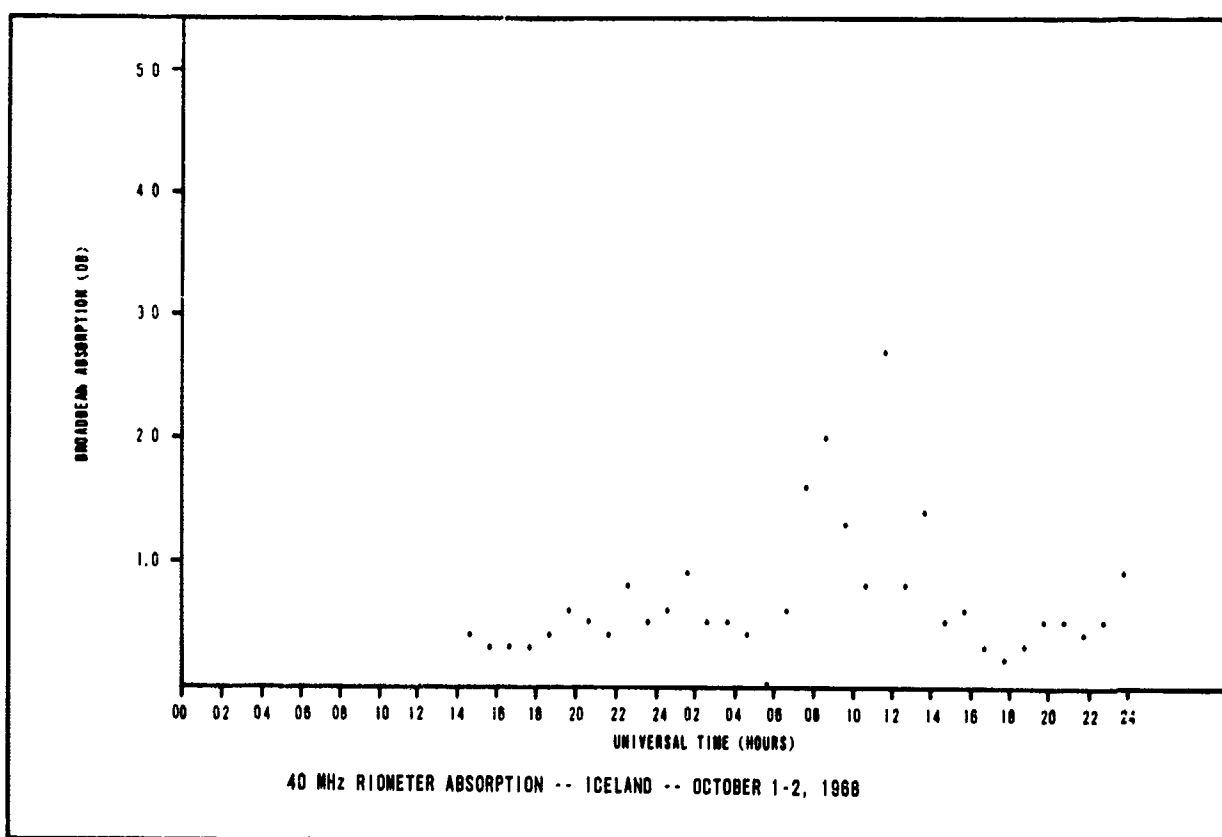
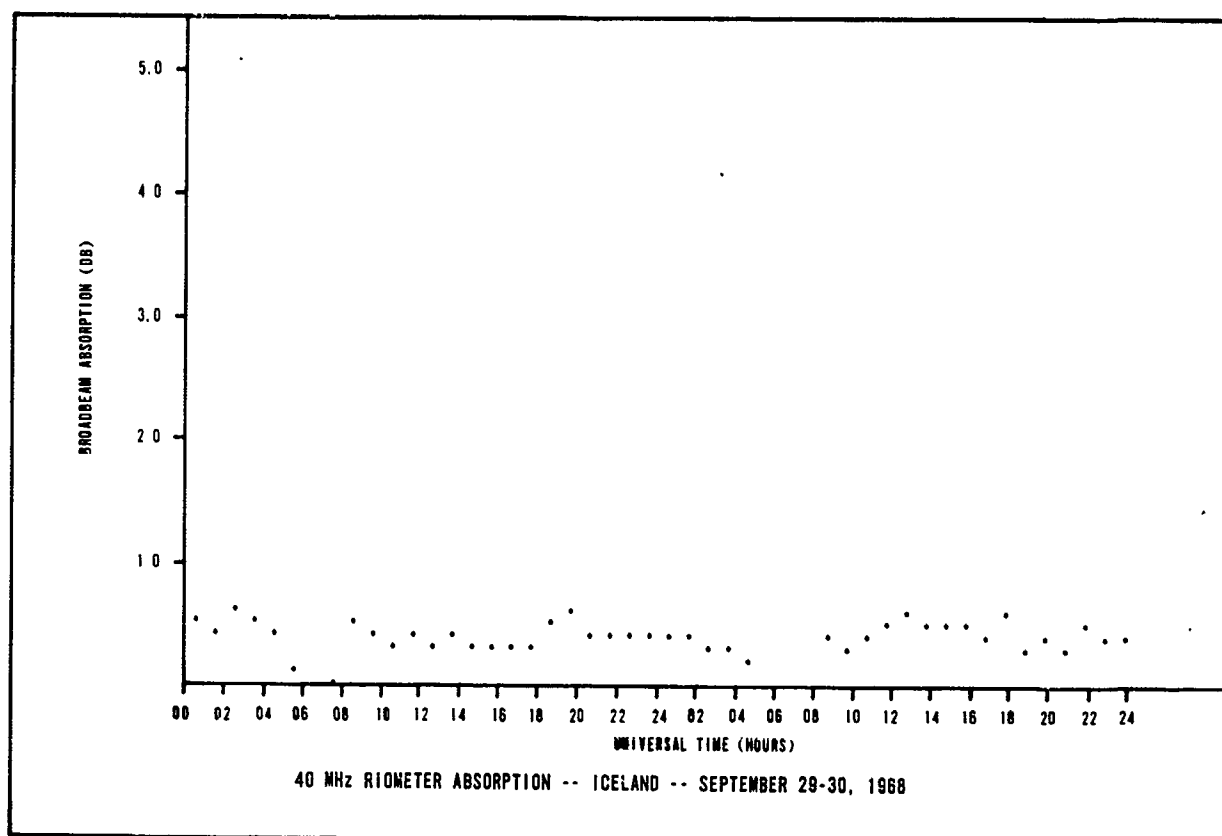


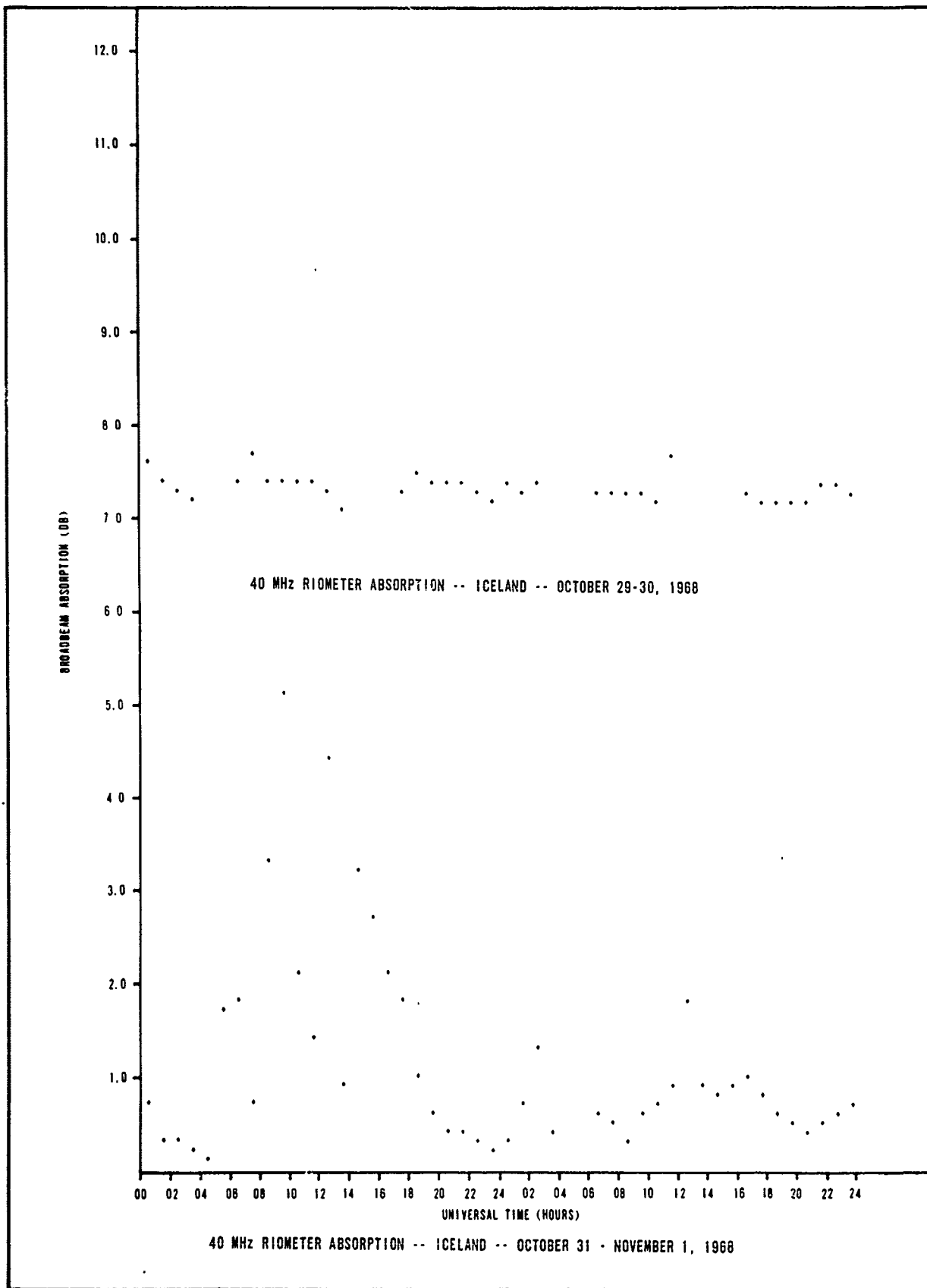


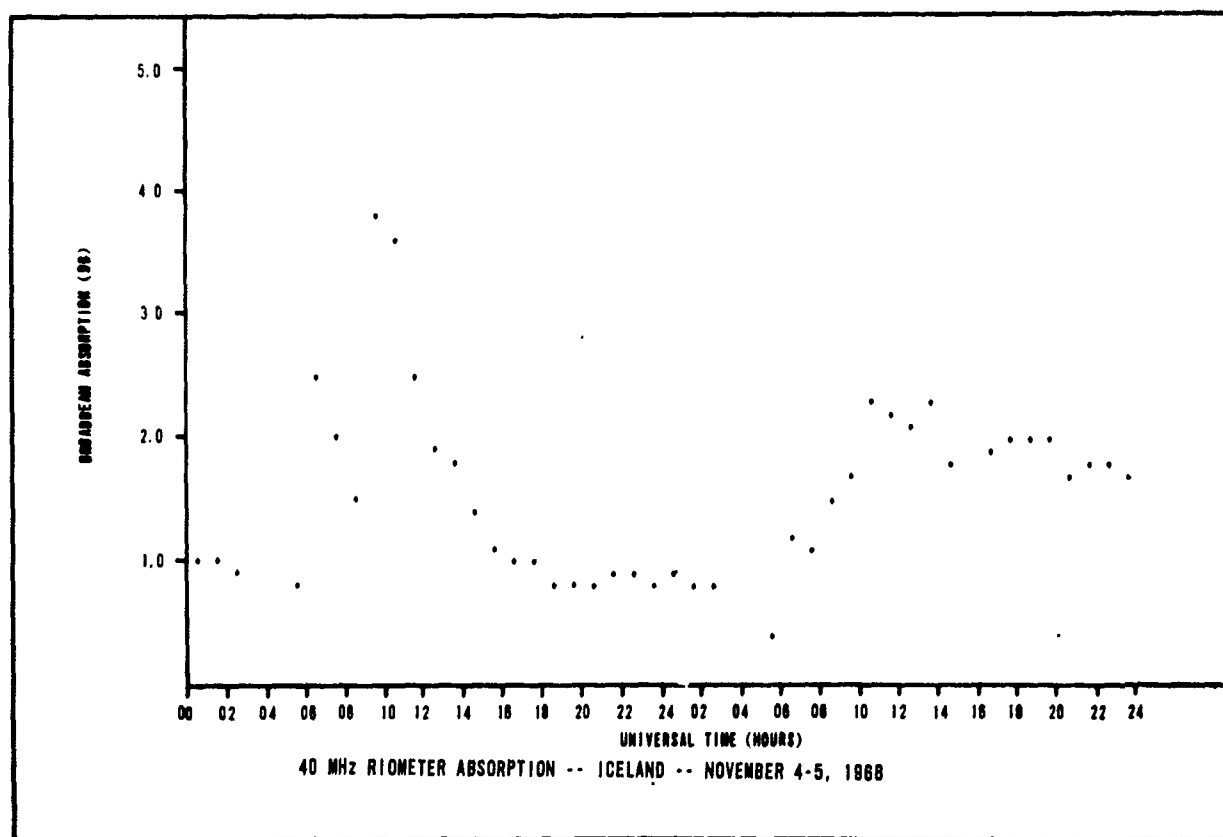
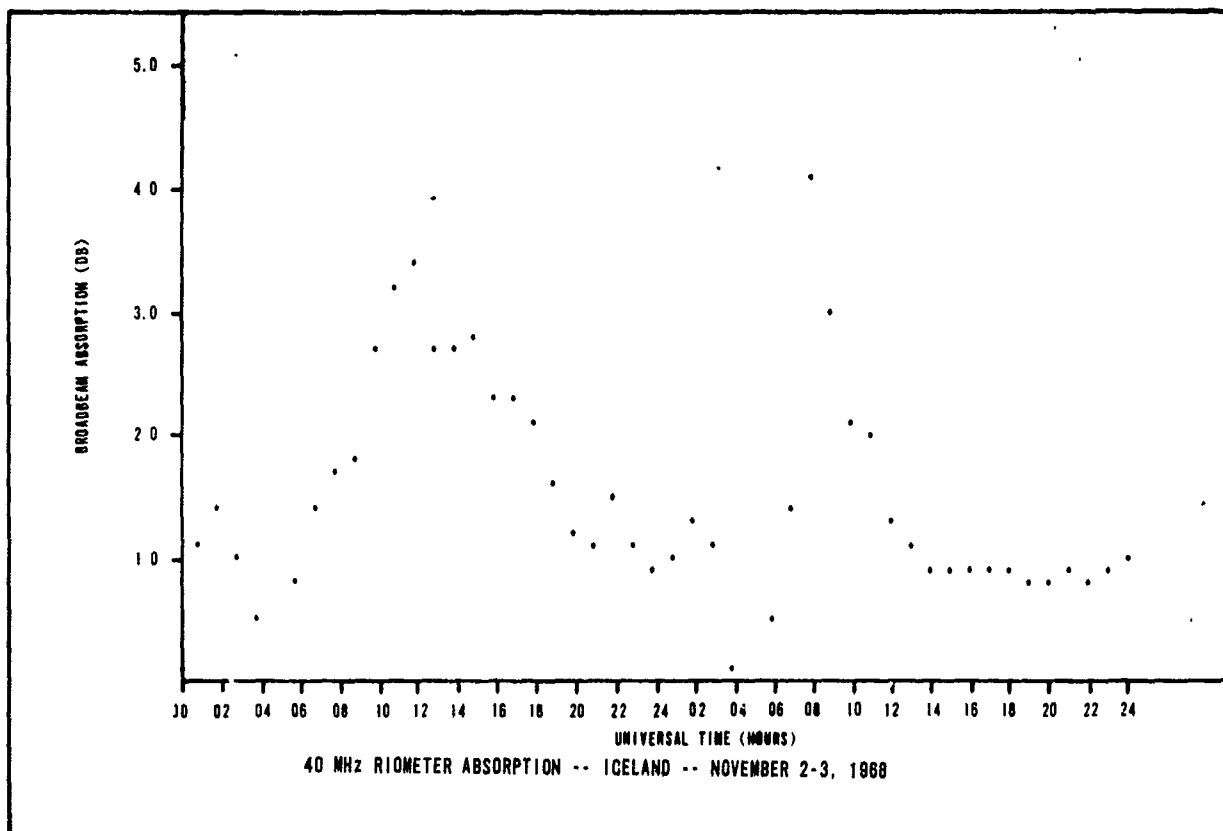


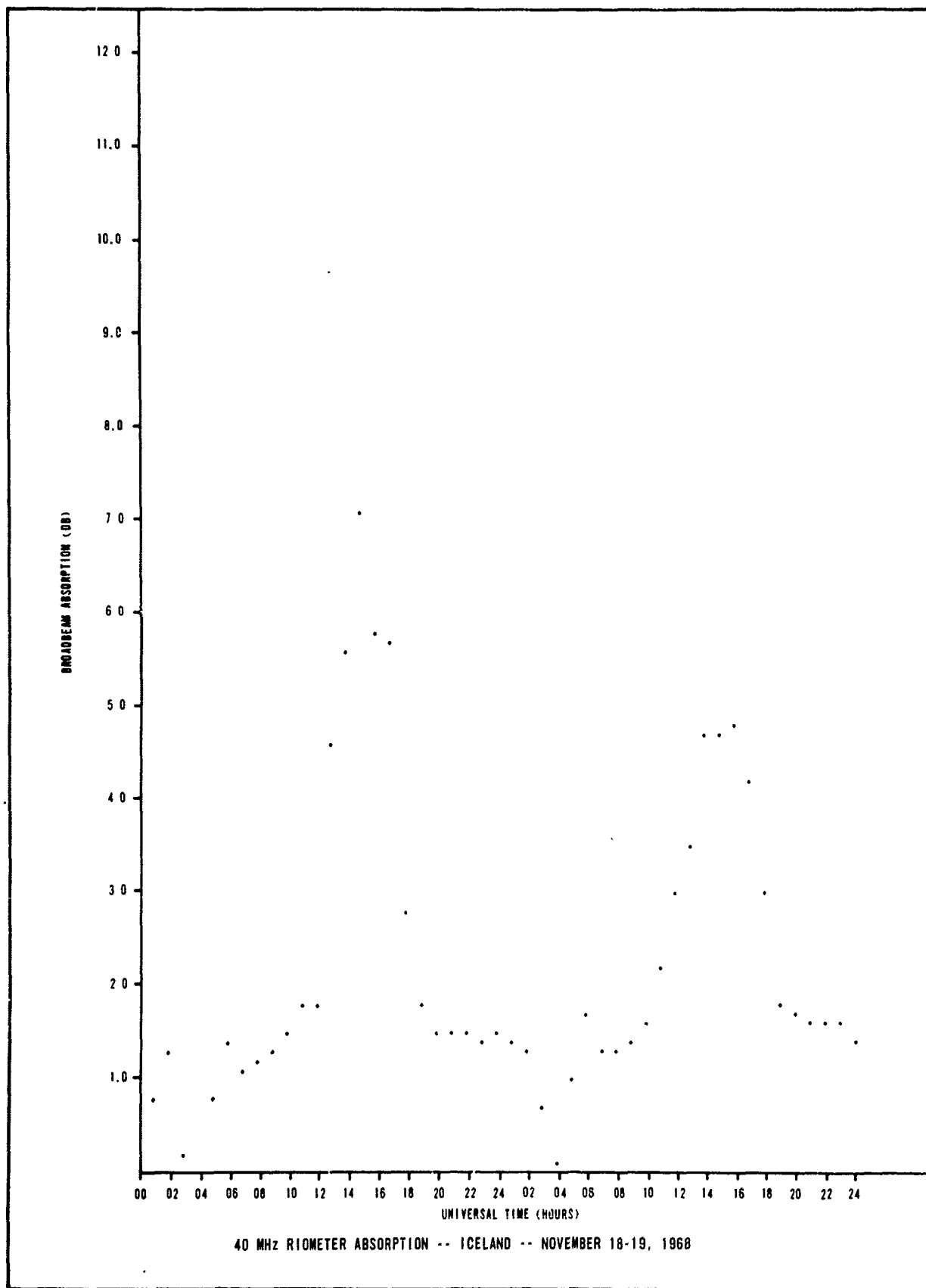




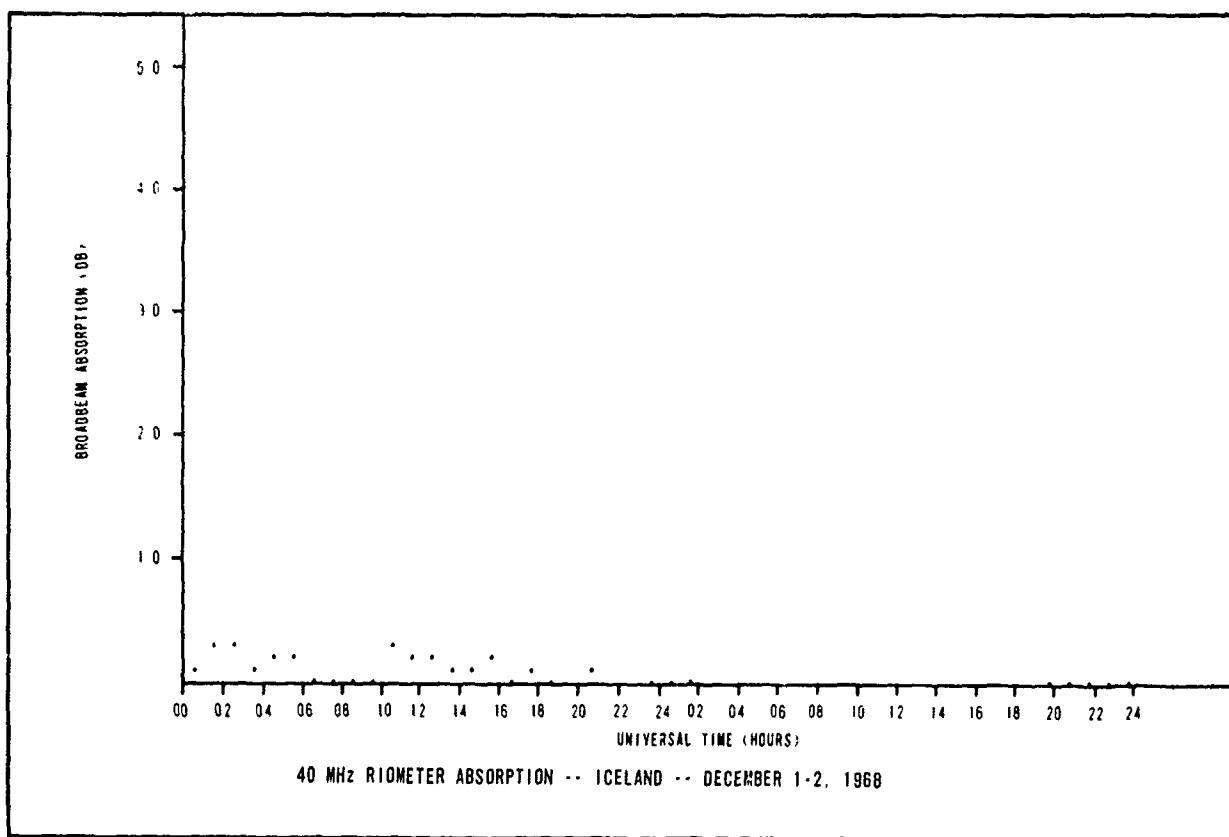
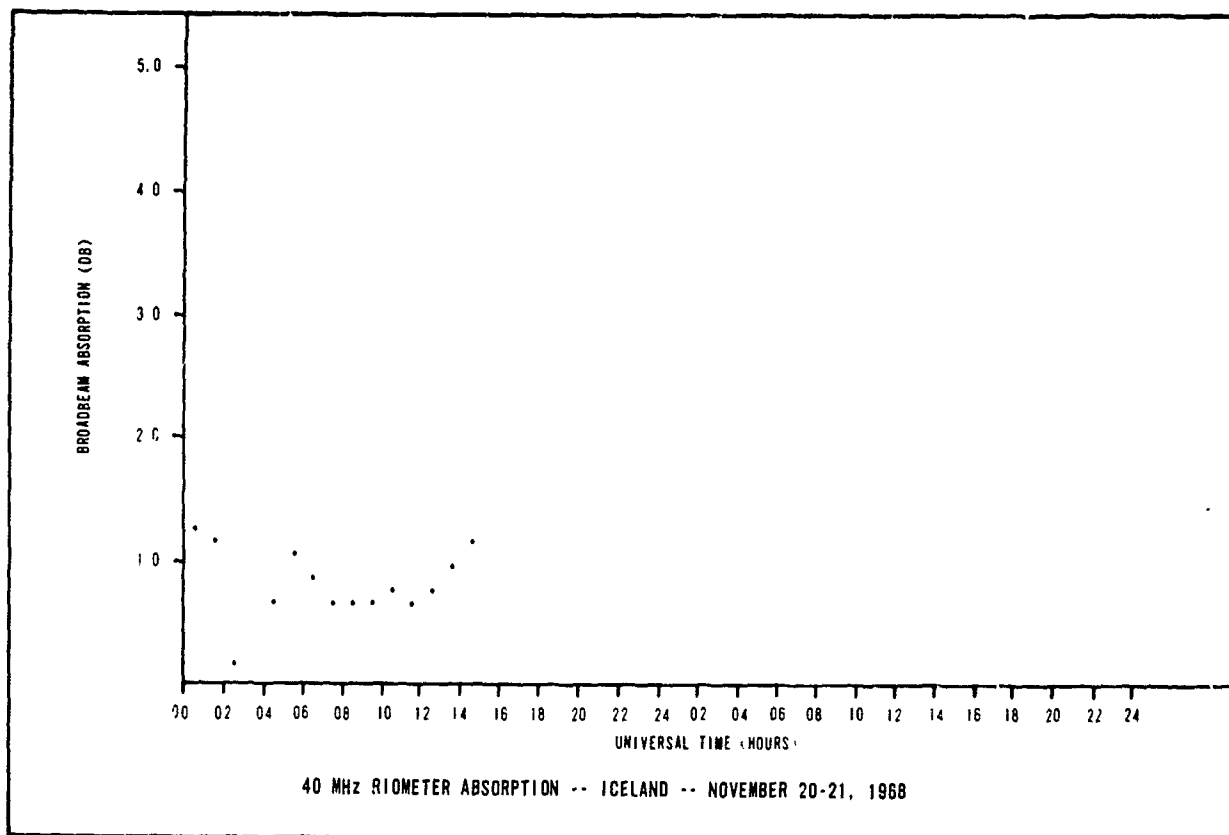


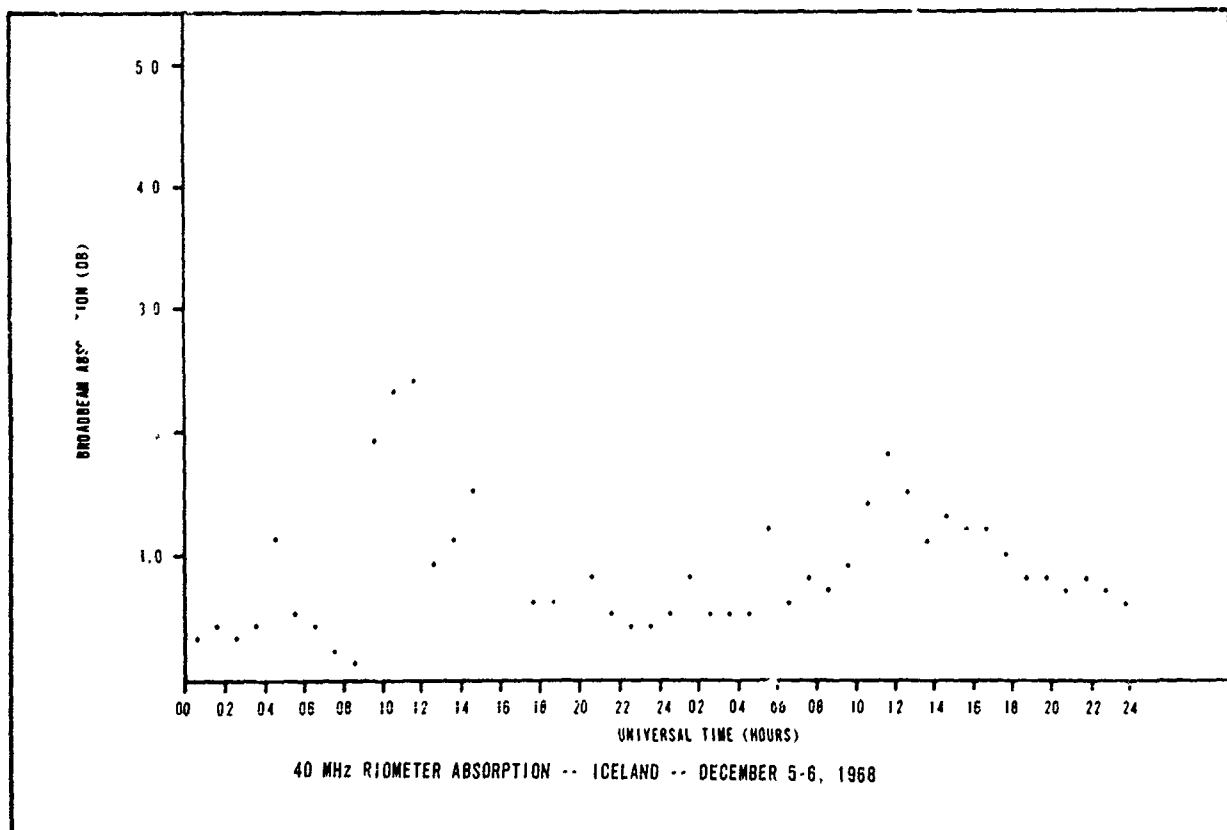
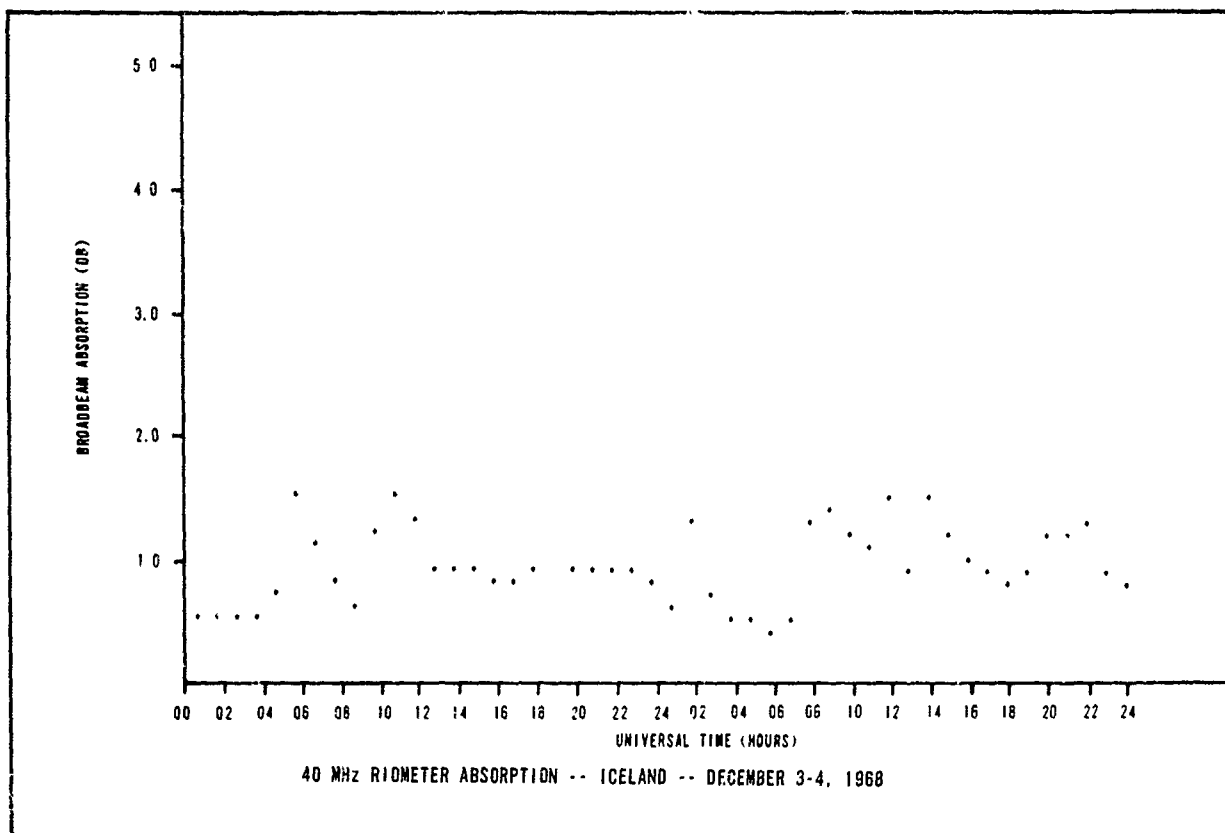


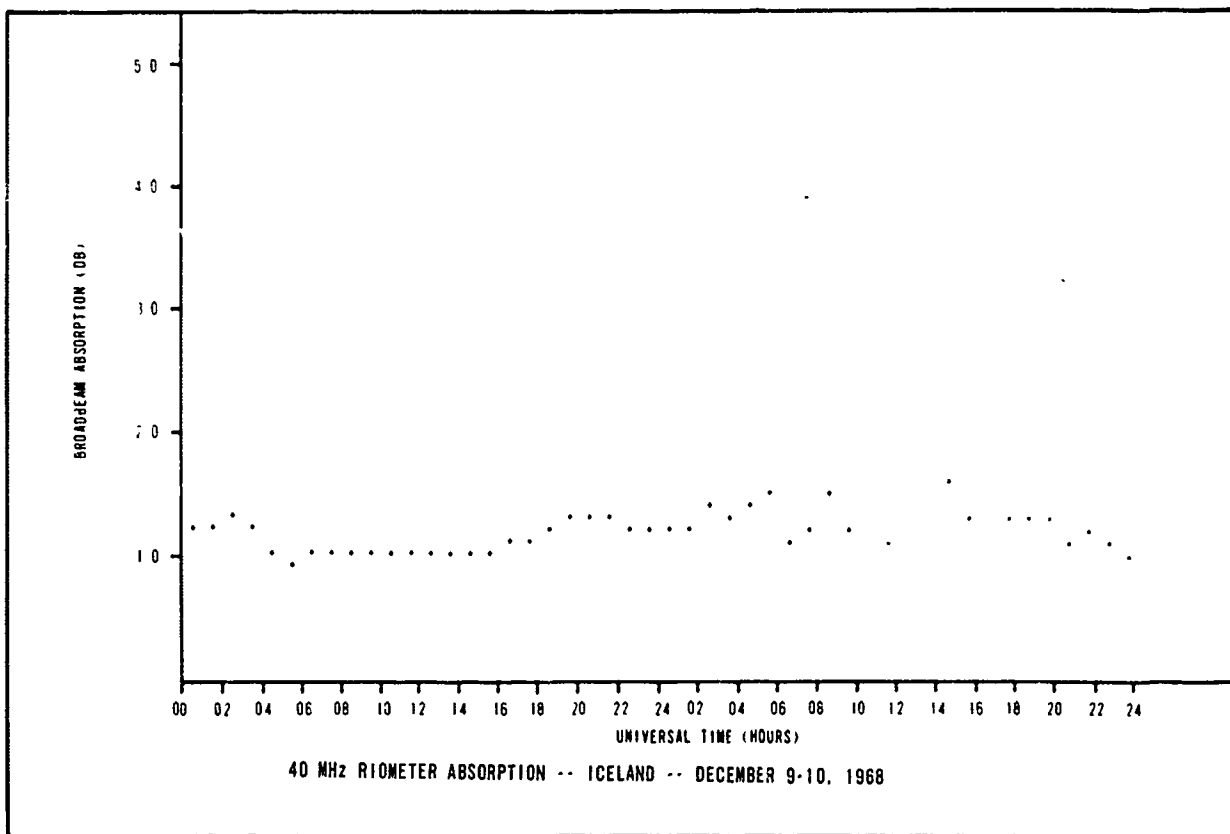
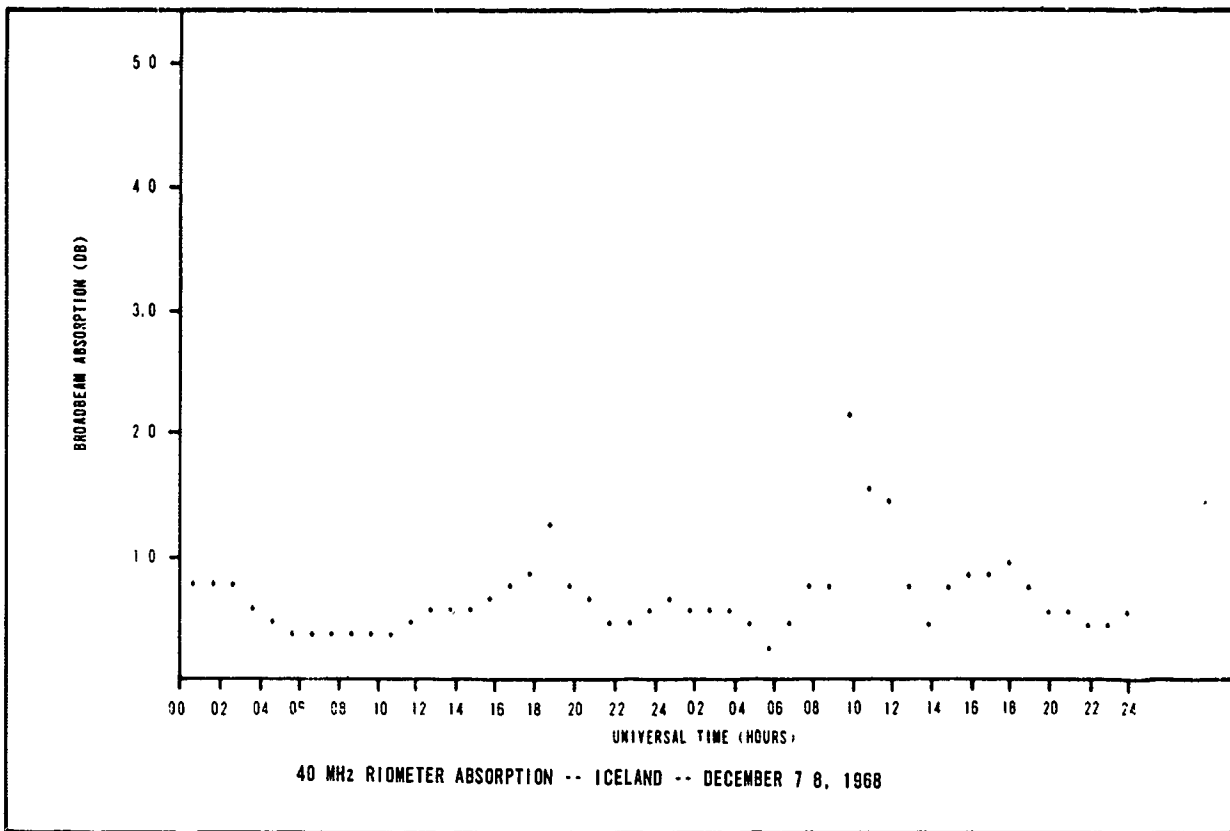


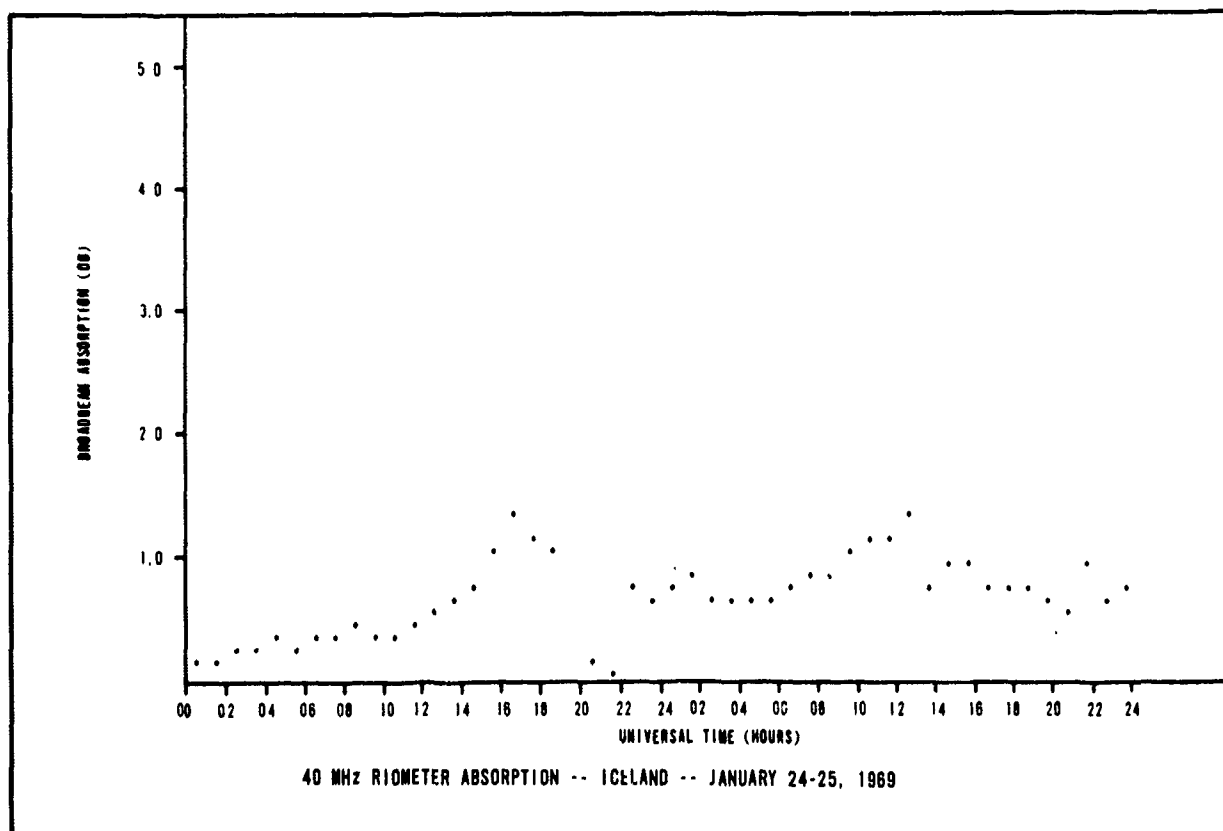
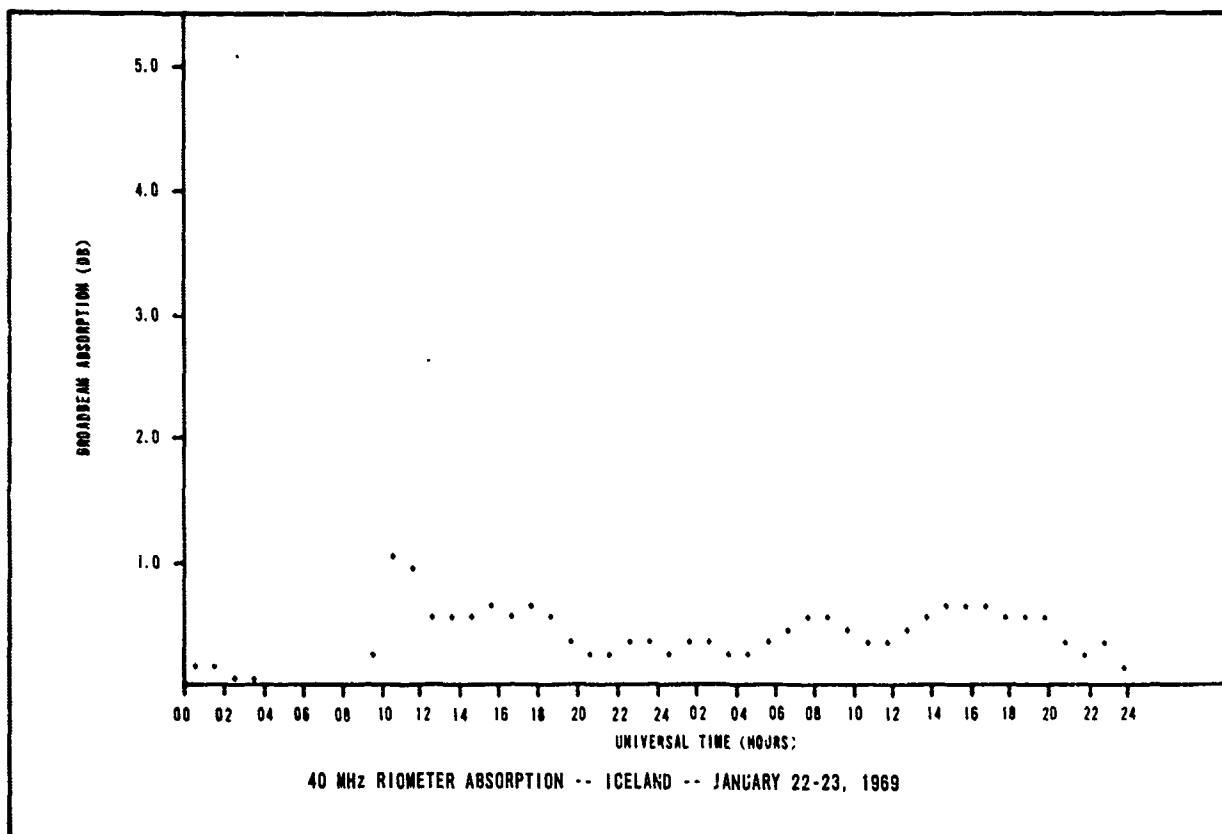


B-194

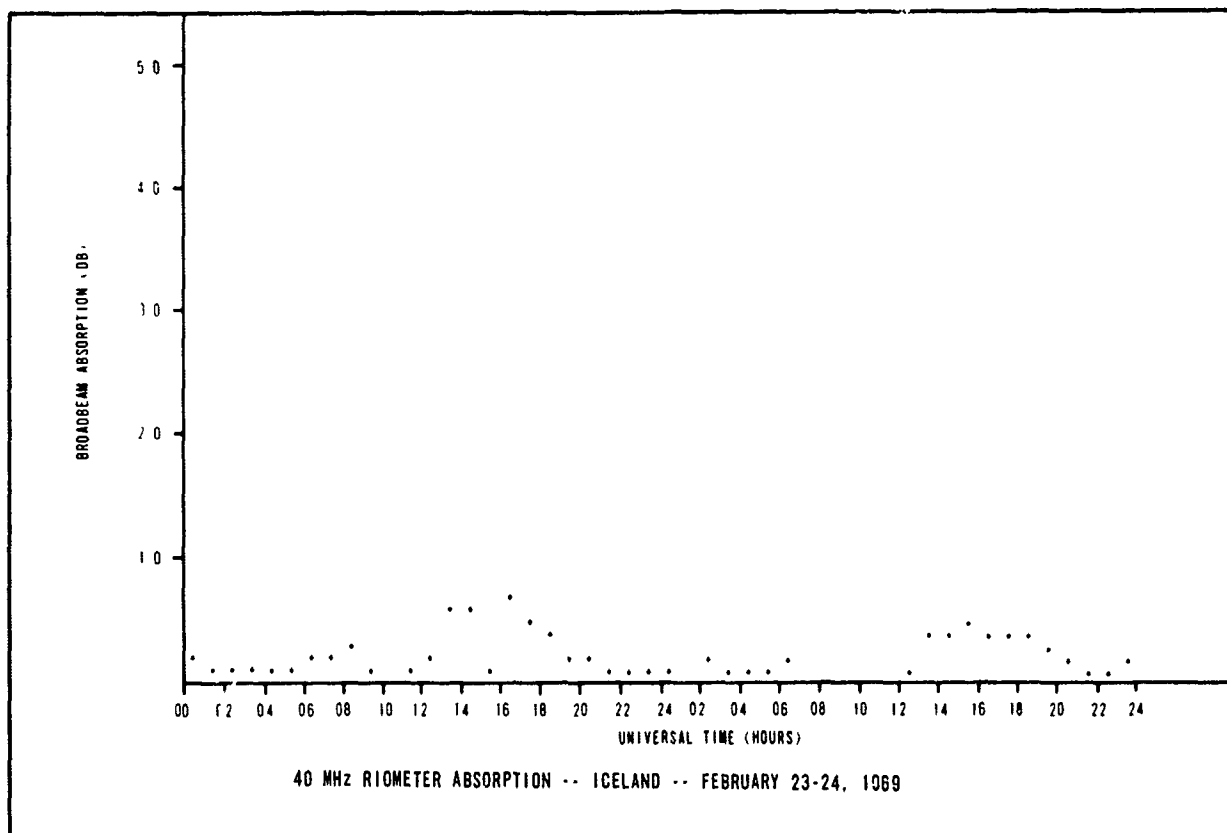
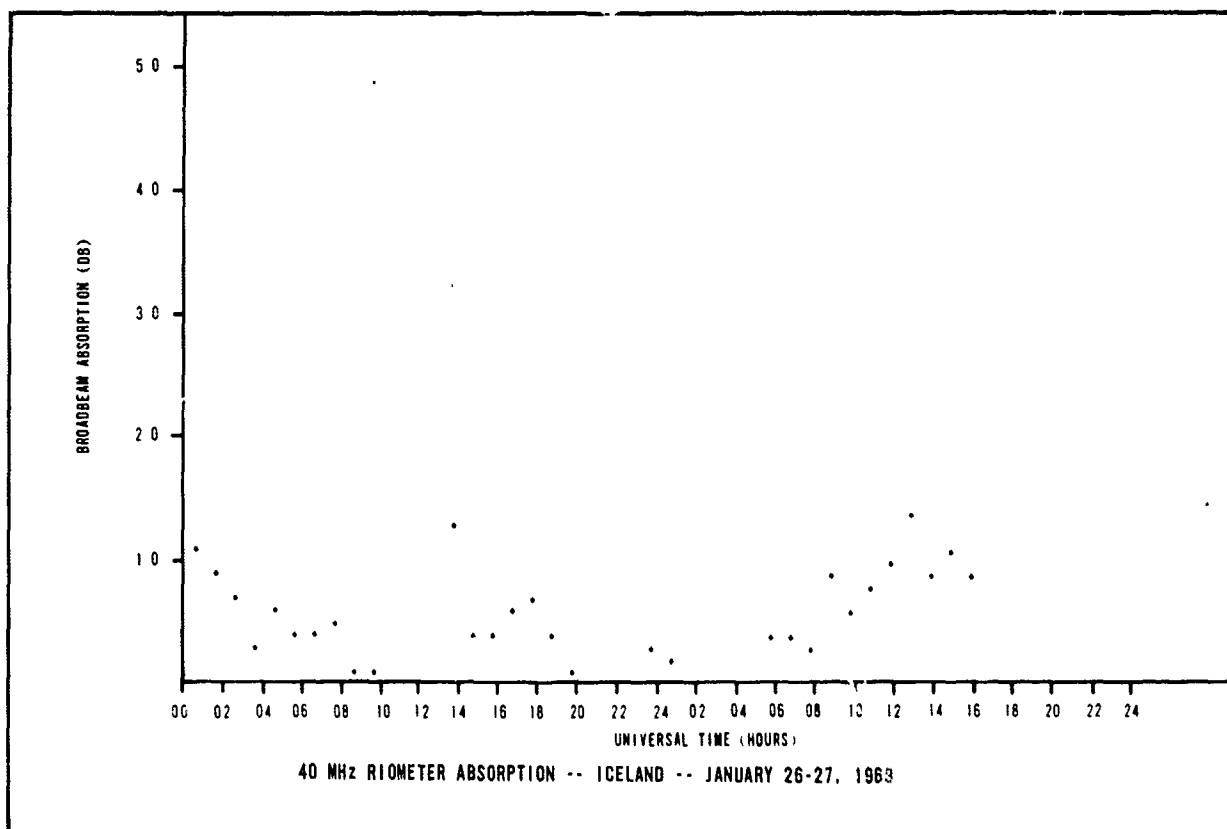


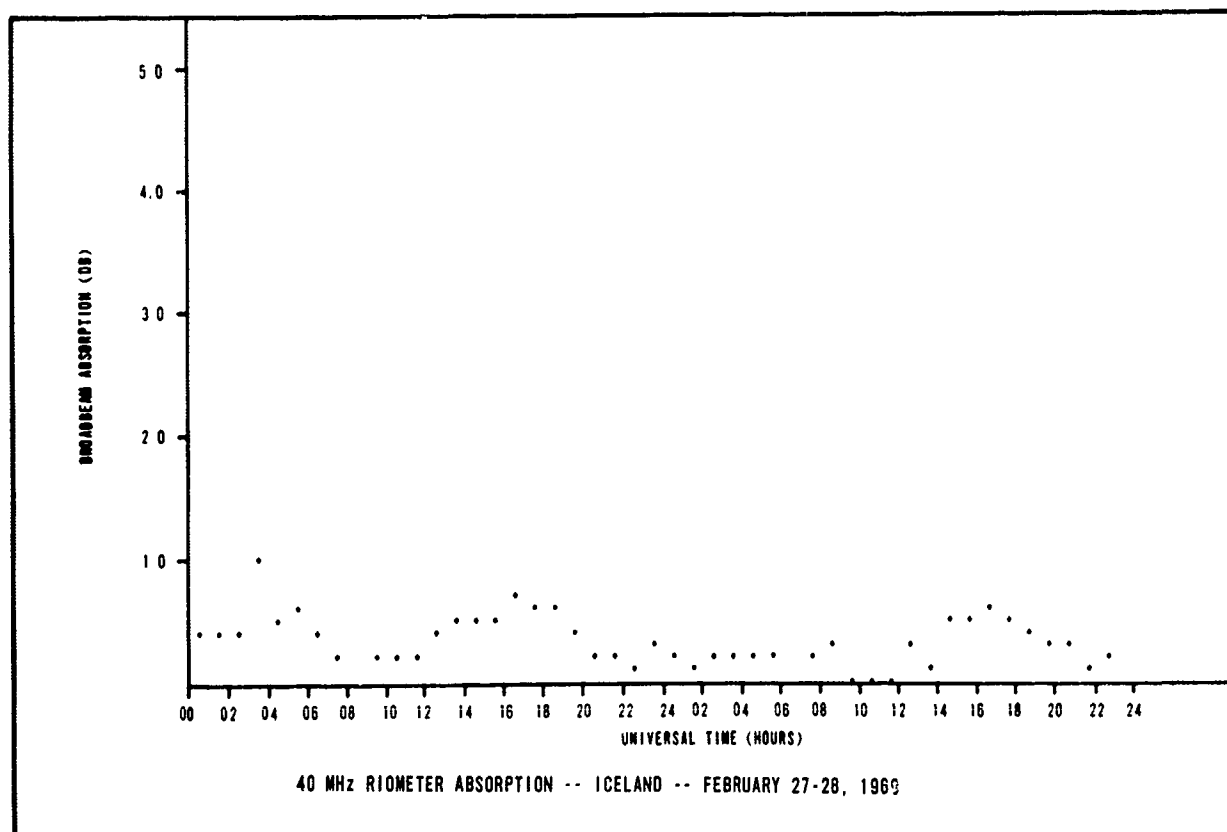
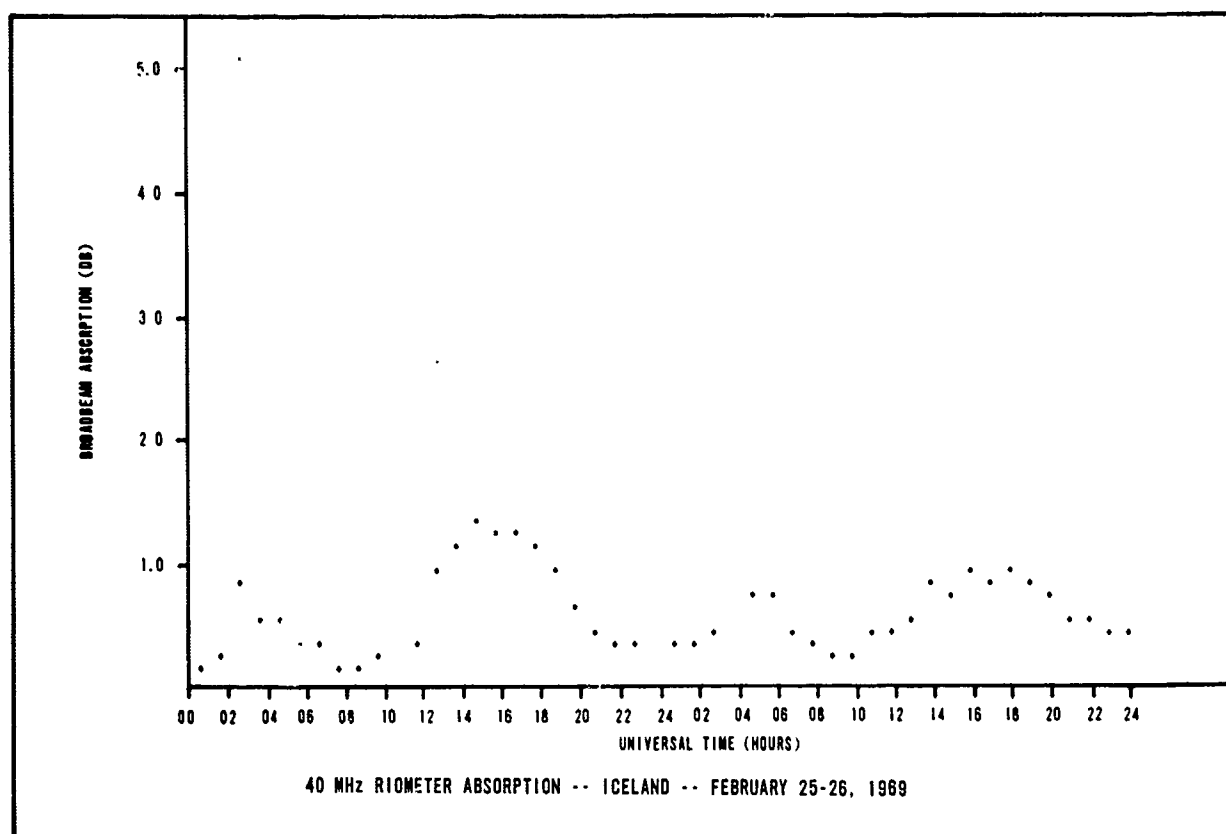


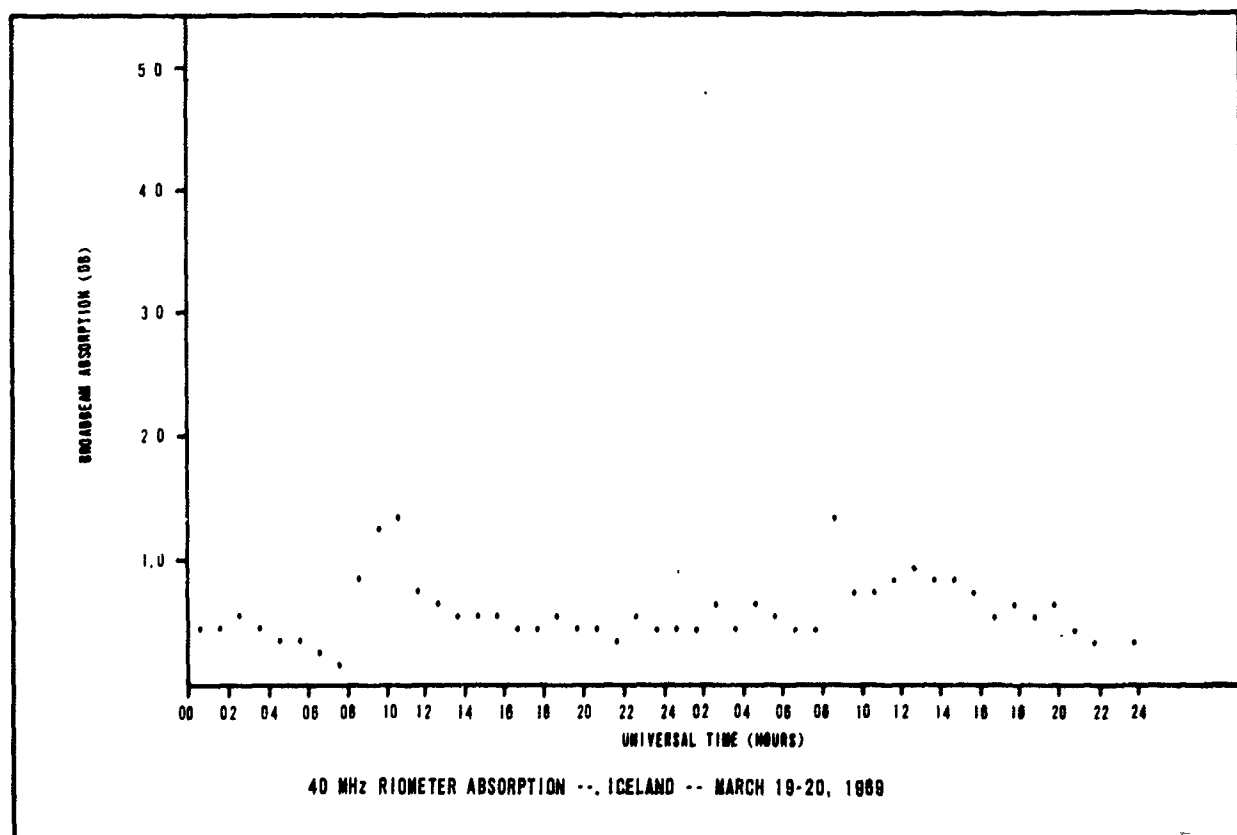
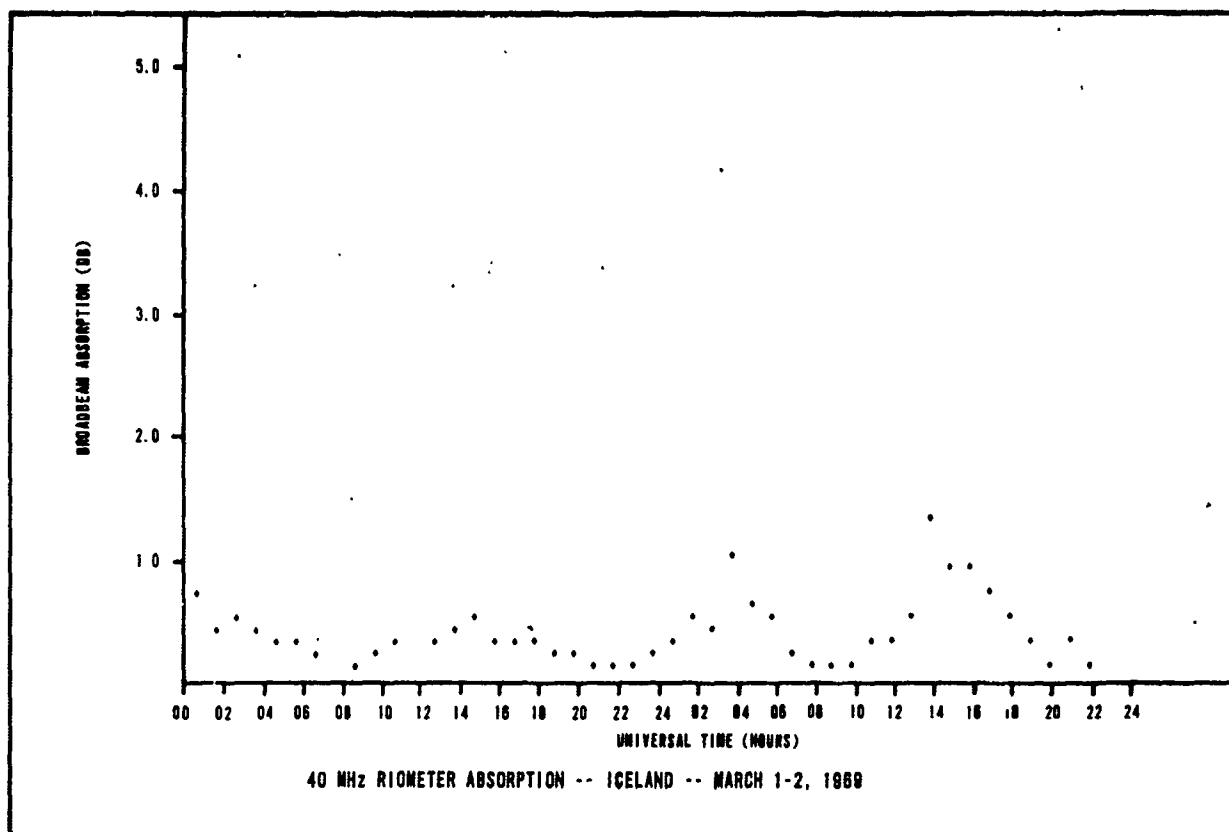


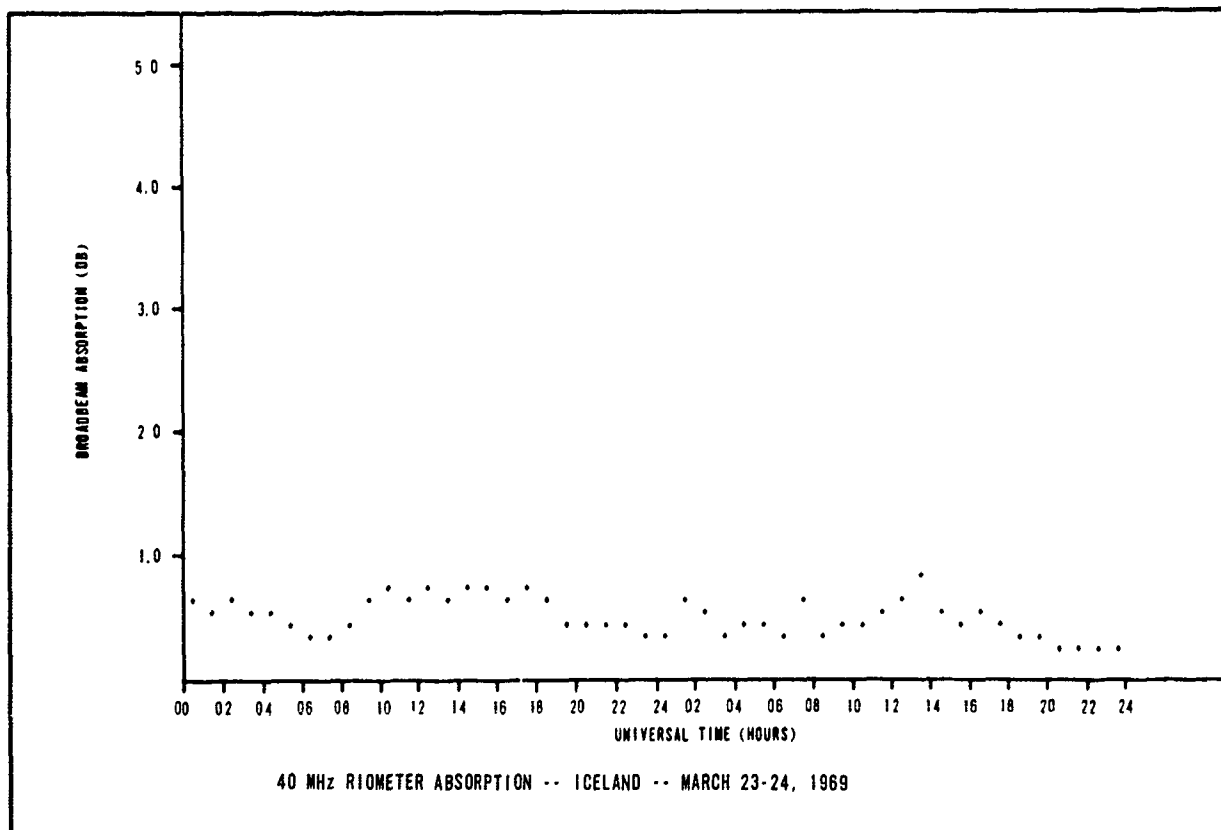
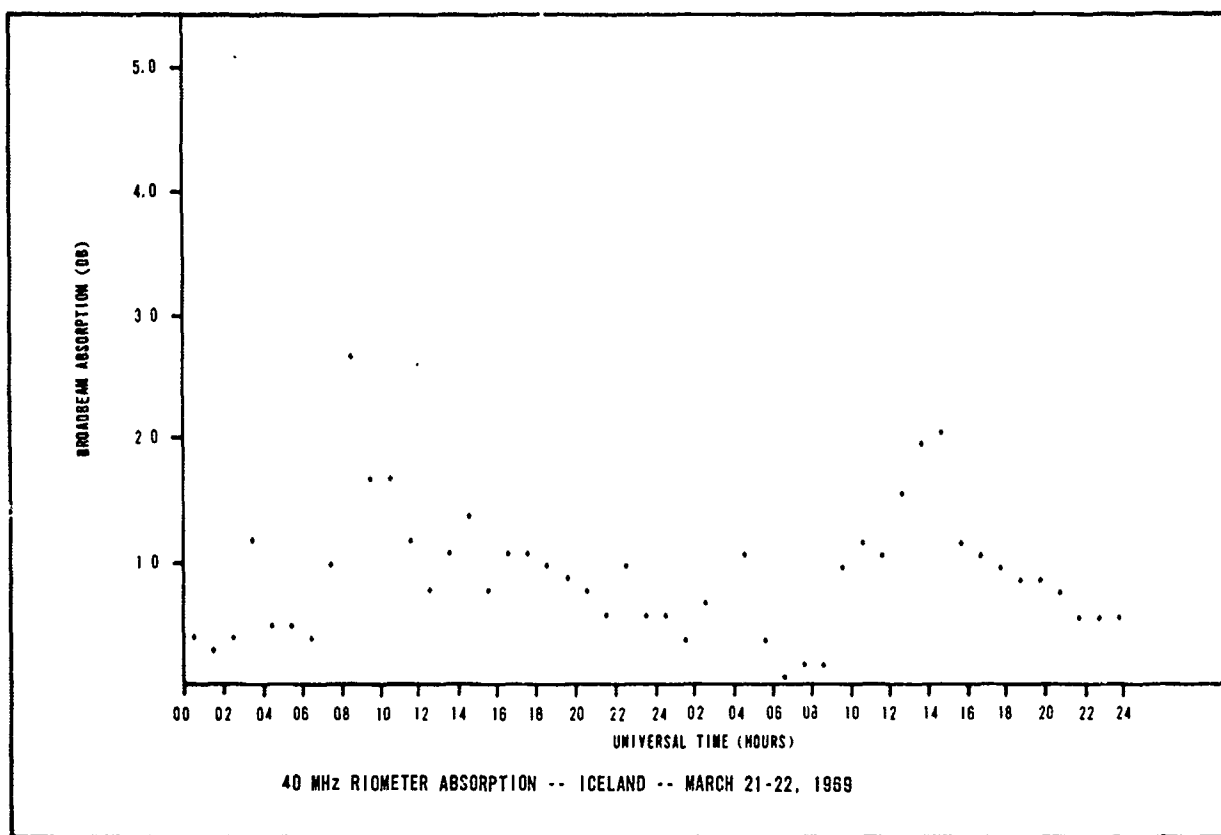


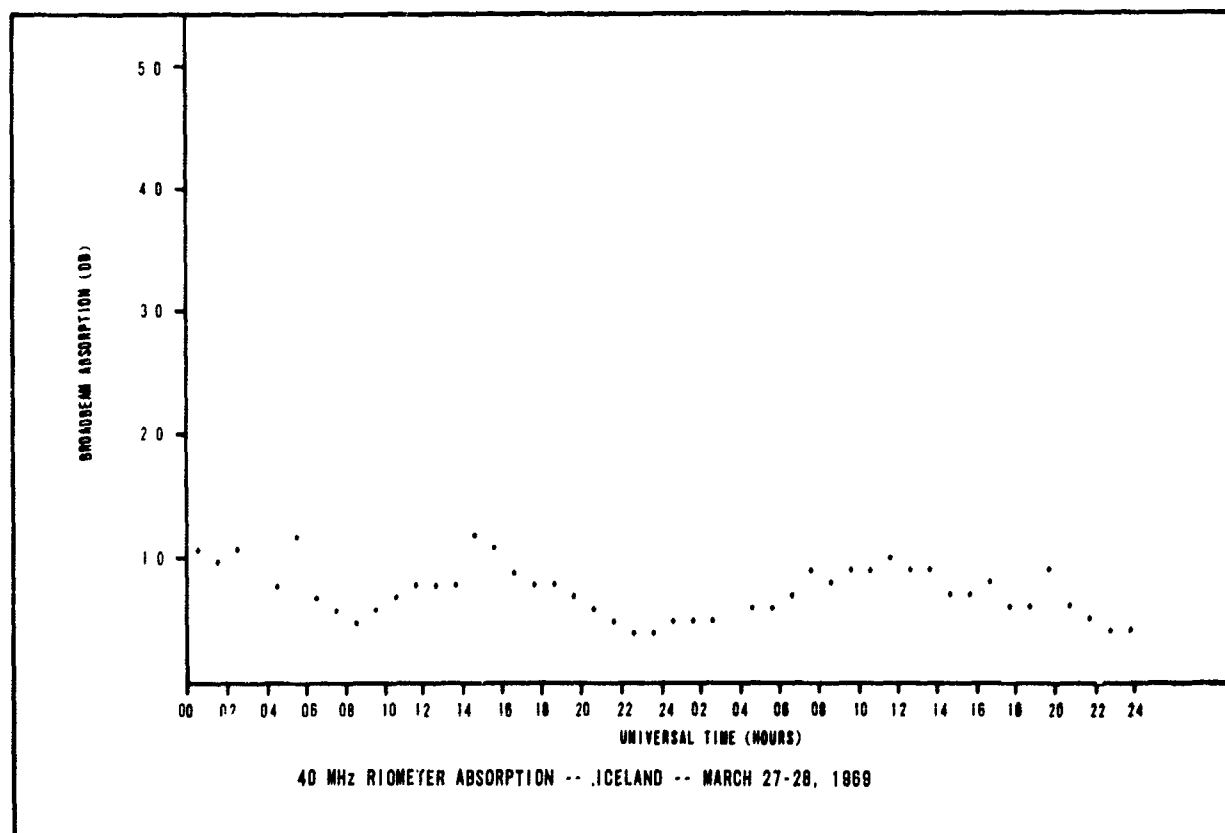
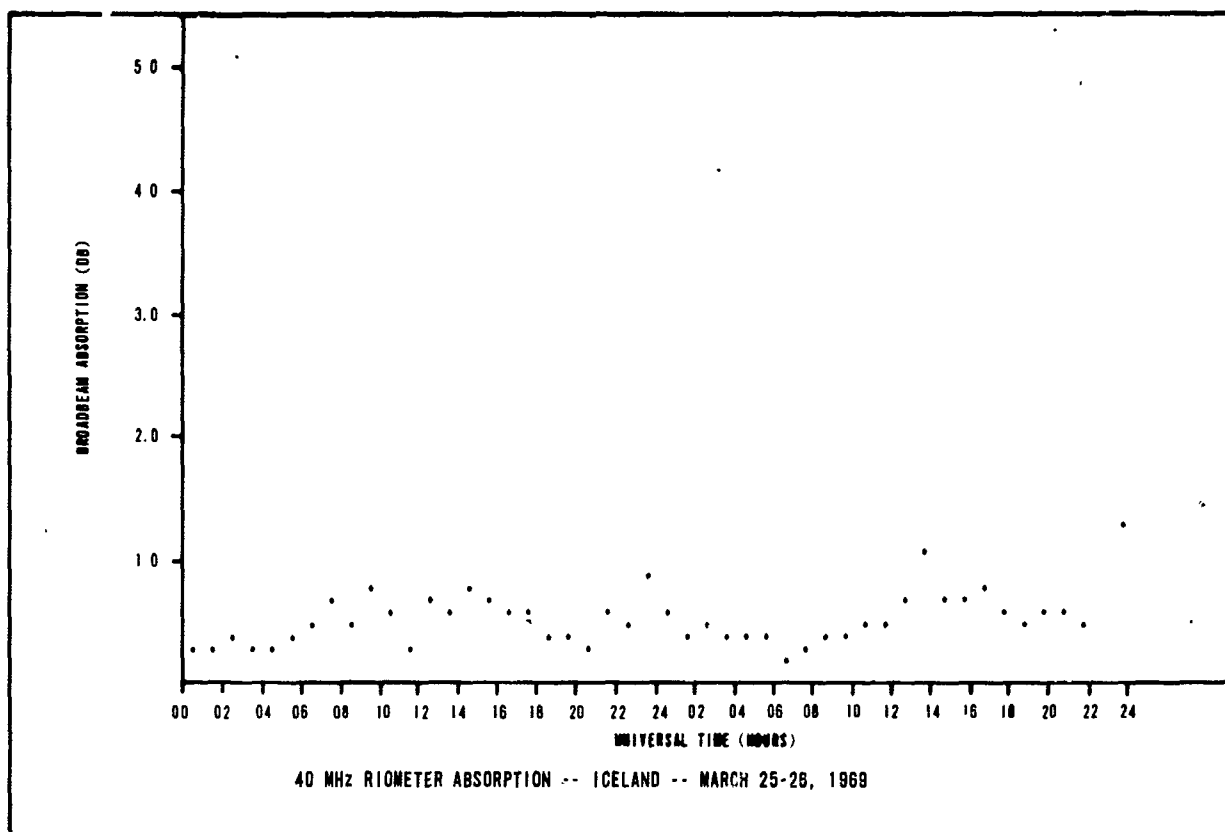


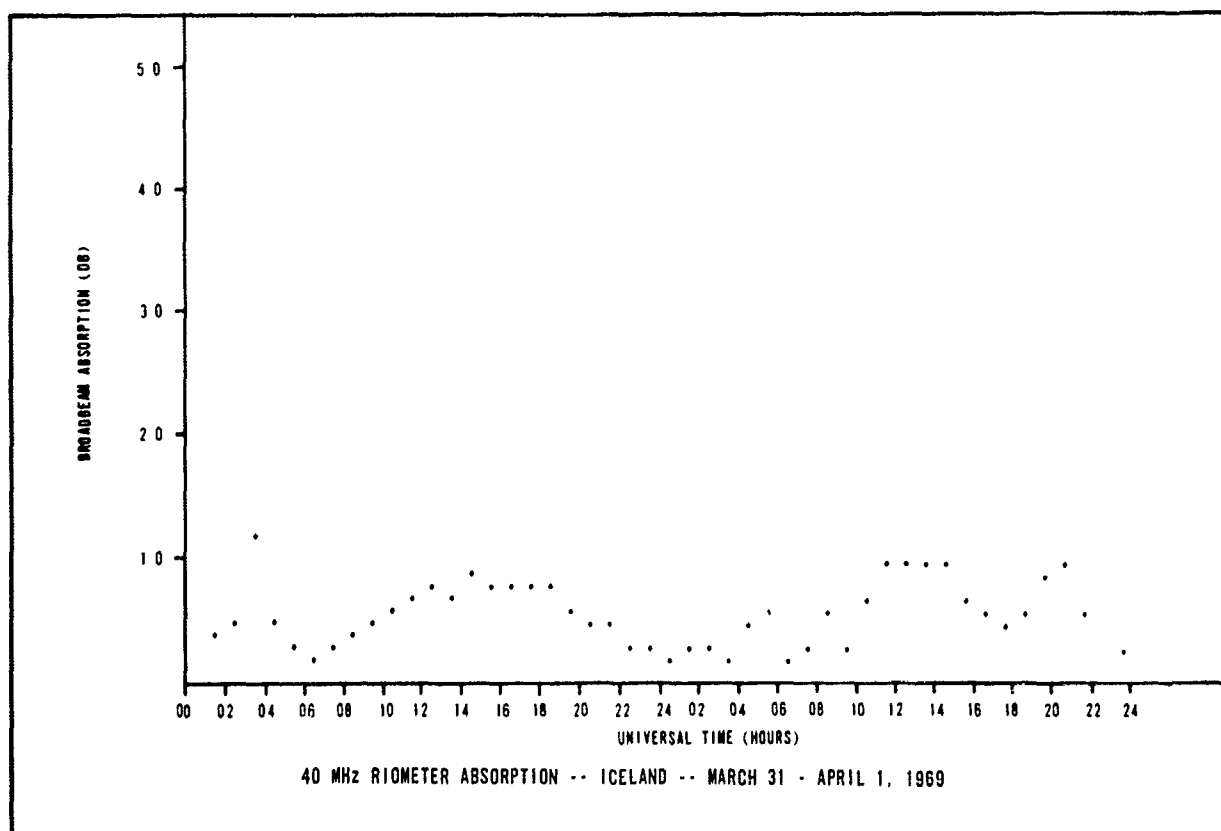
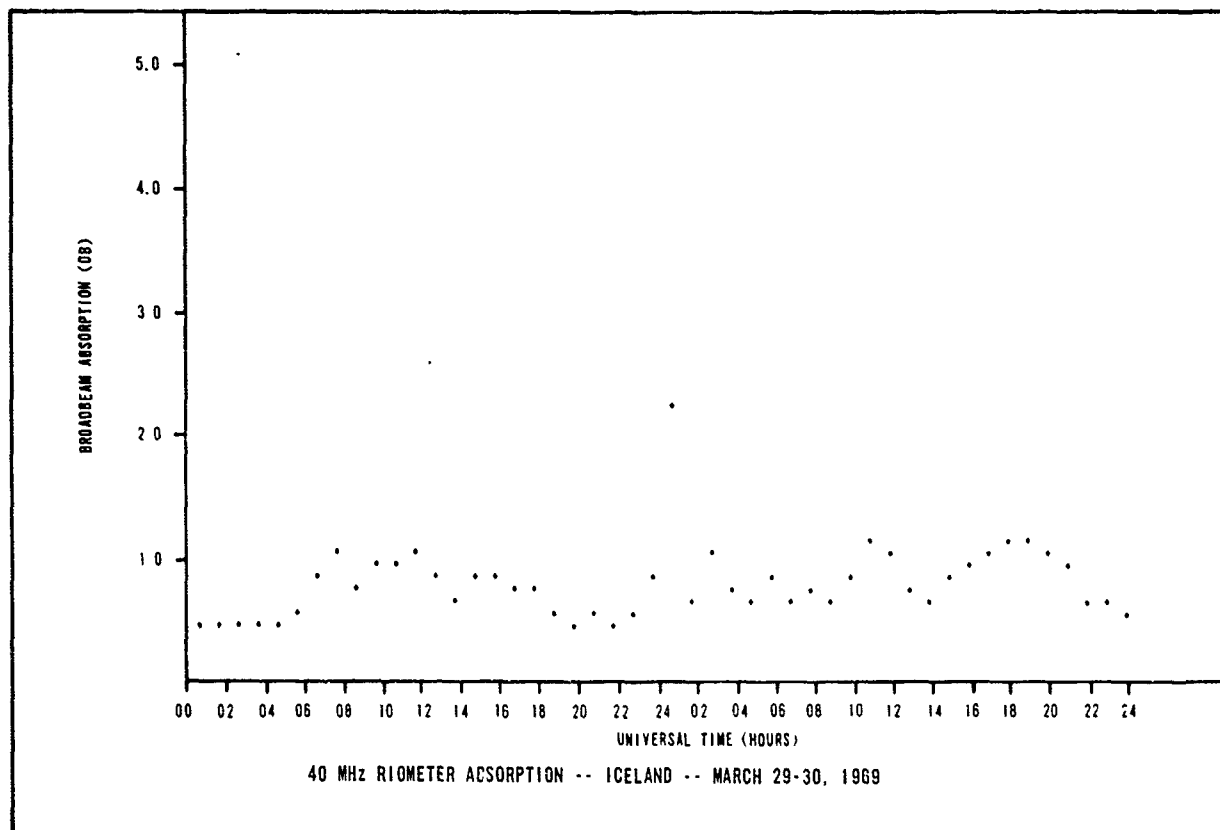


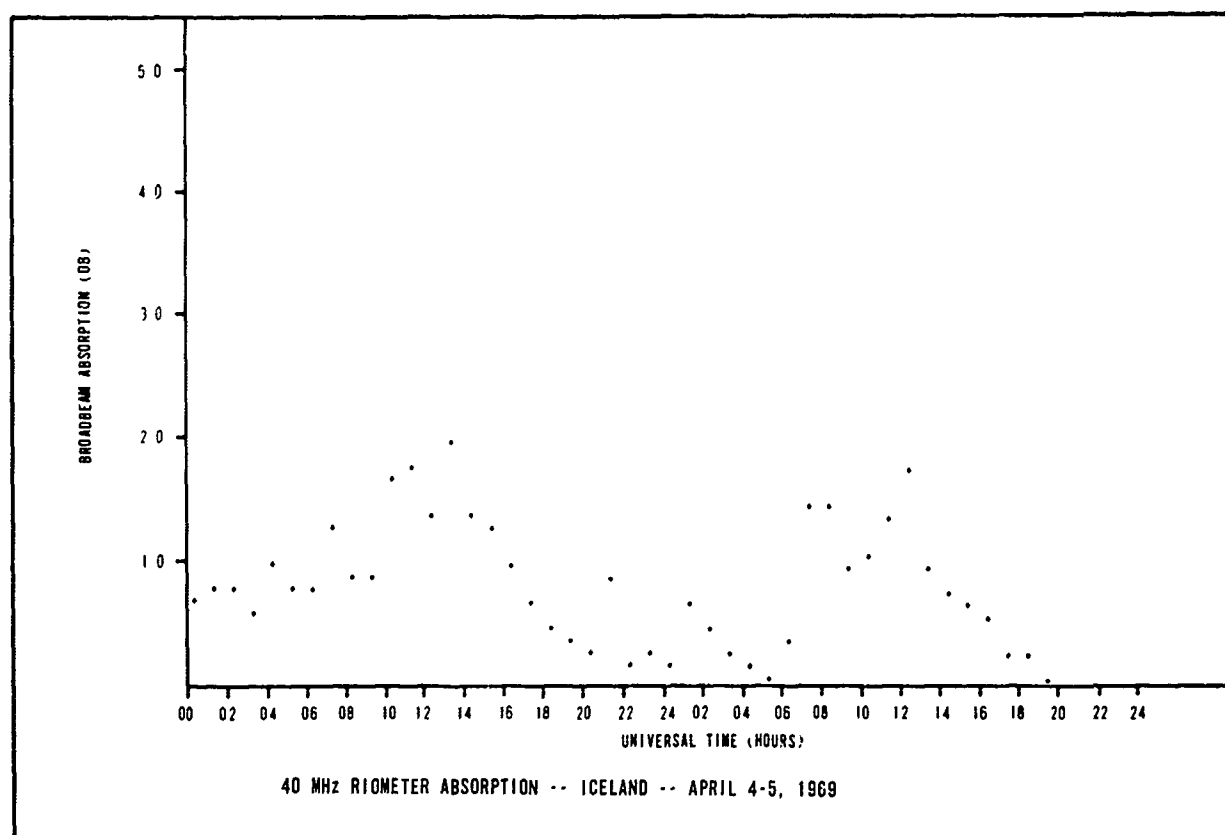
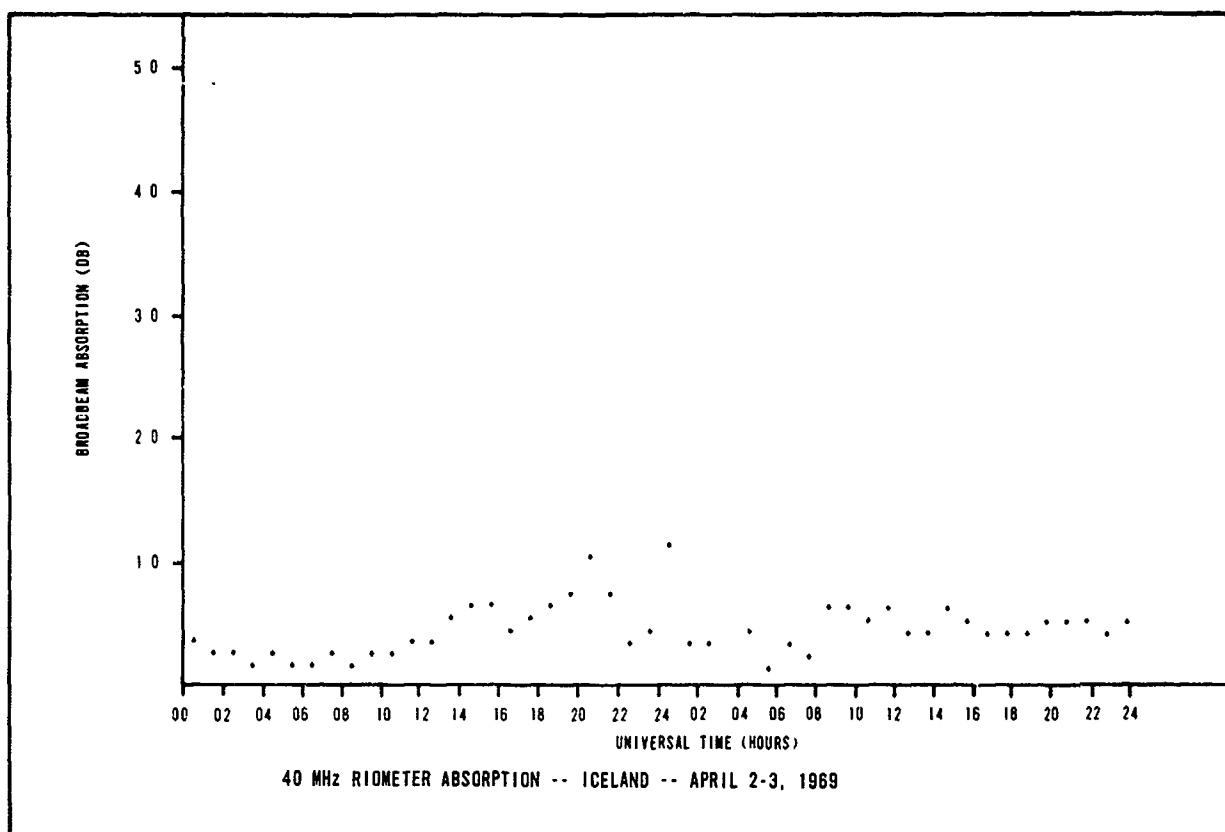


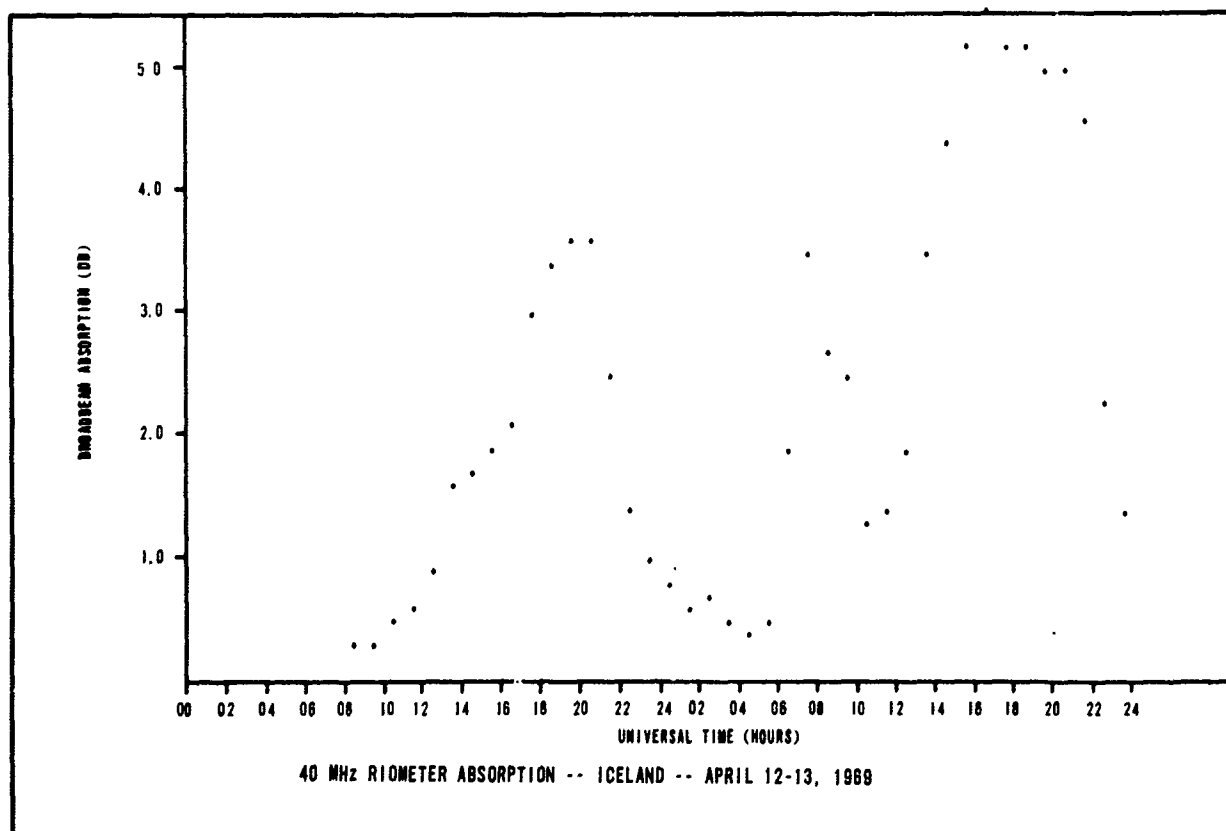
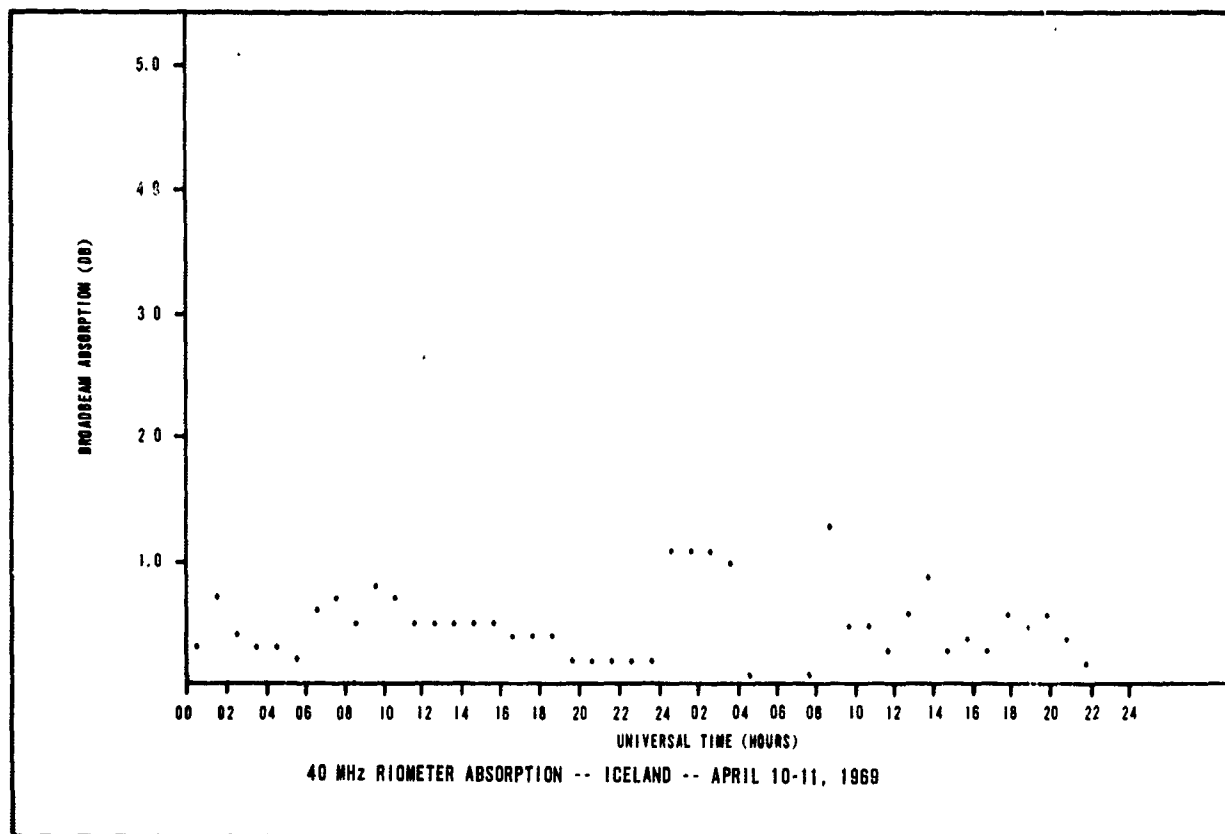




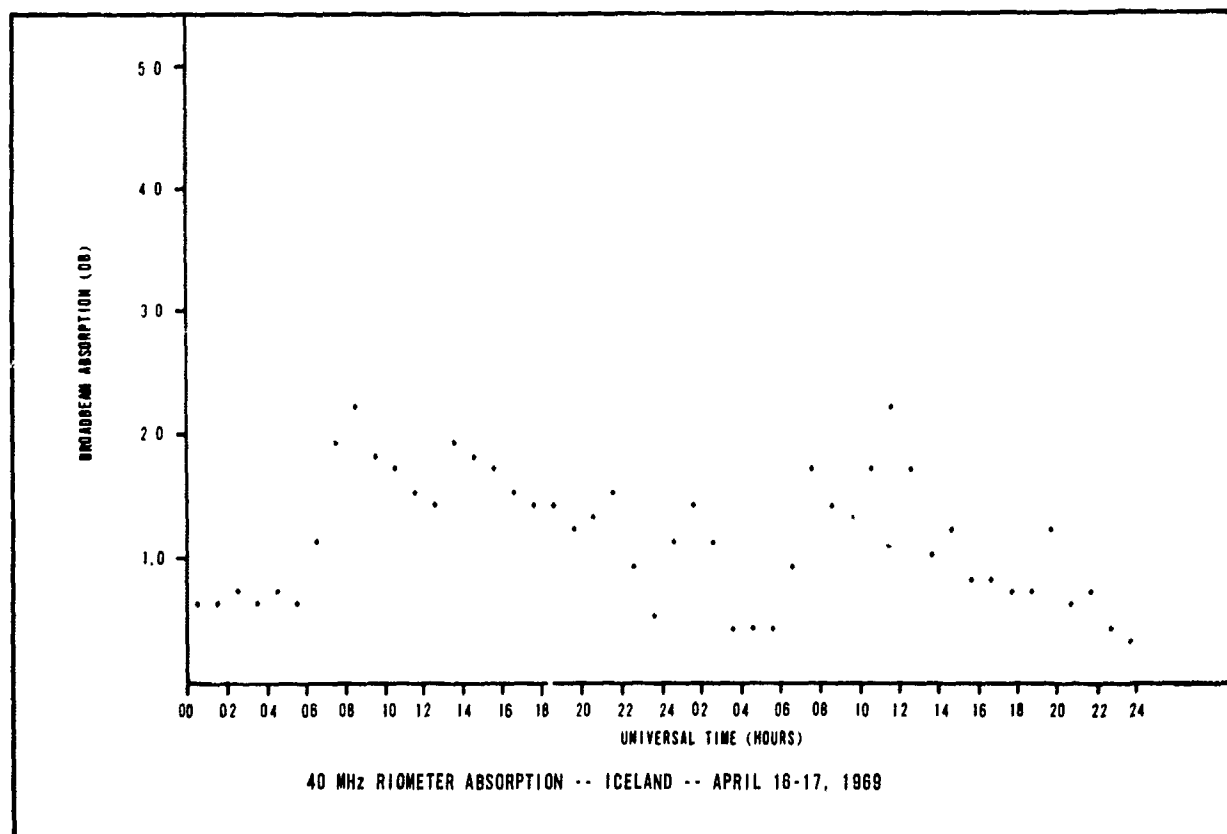
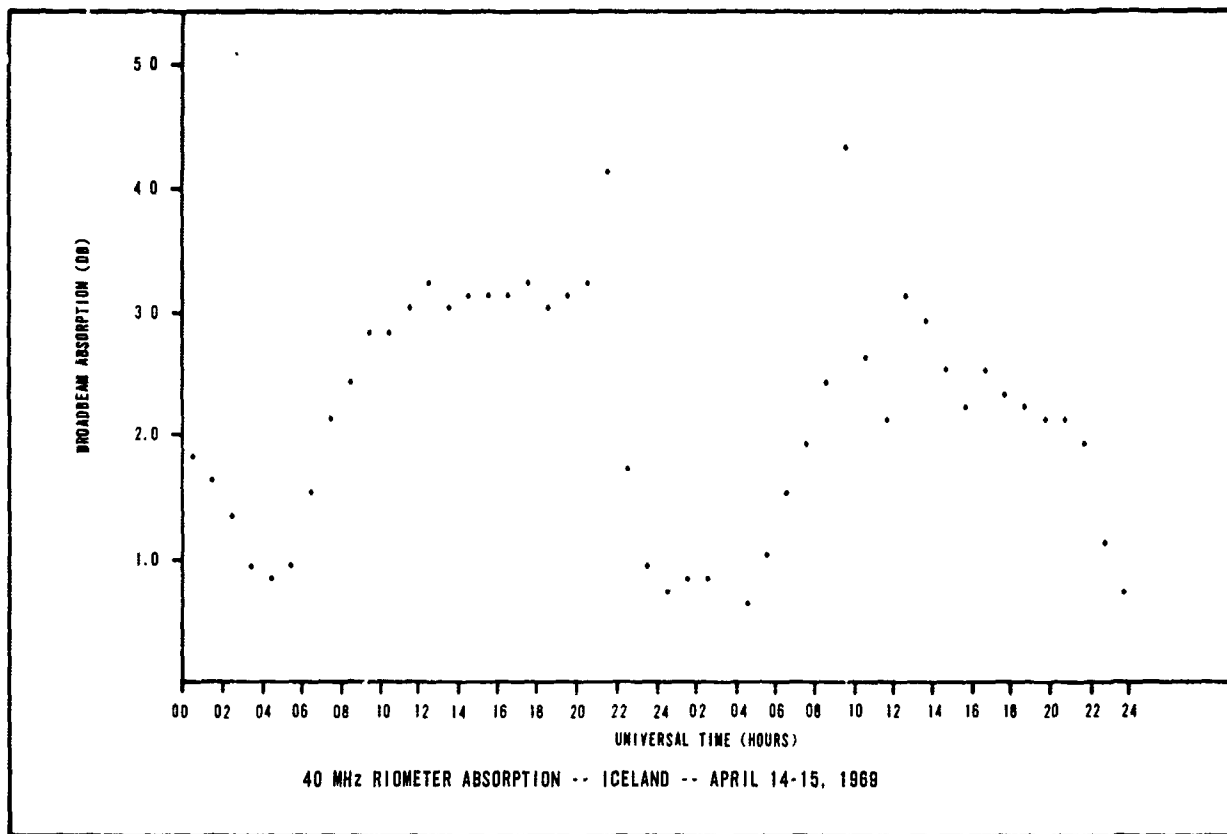


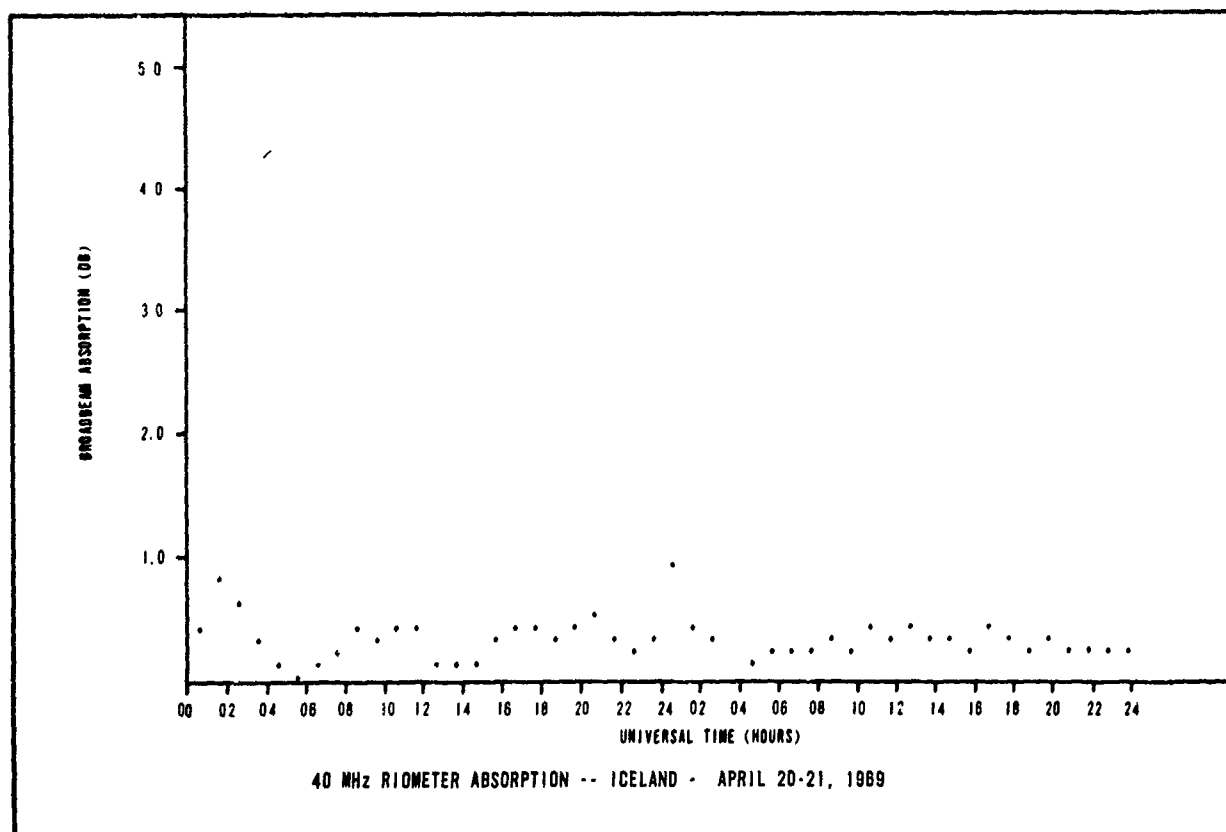
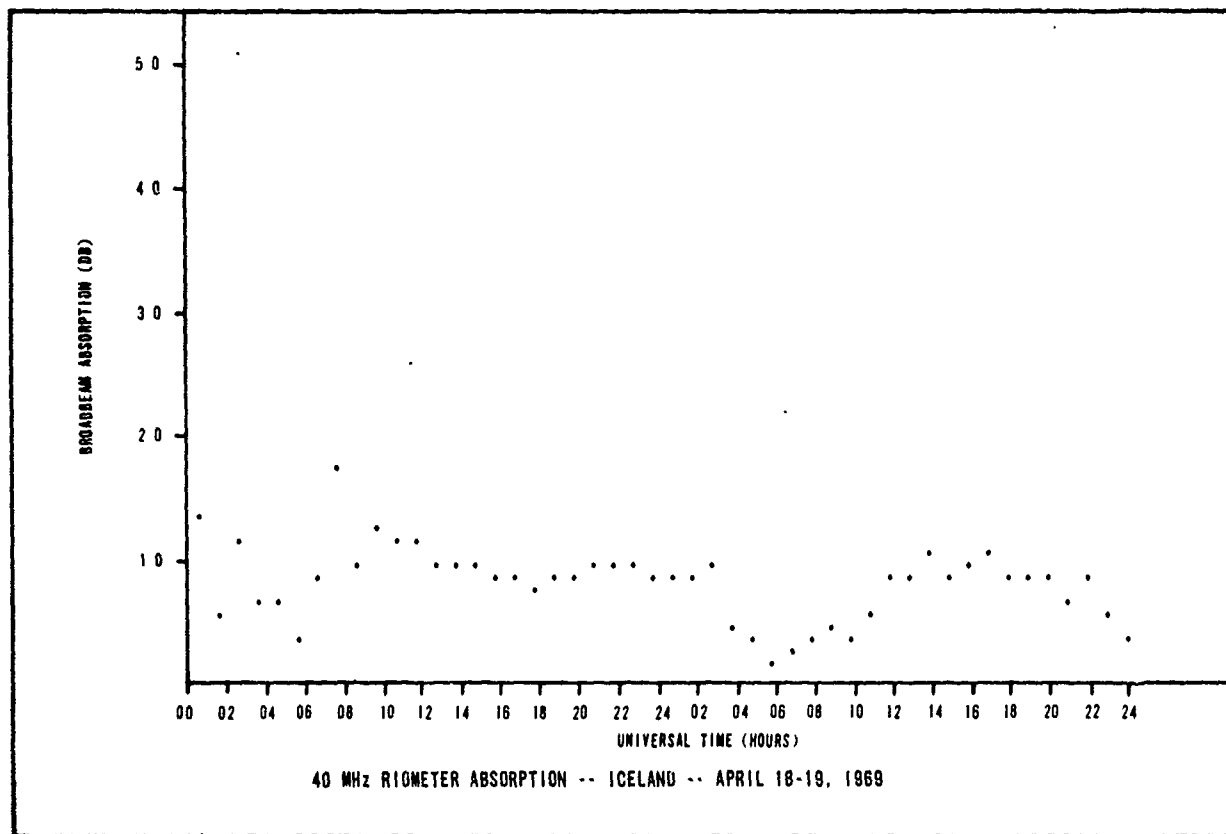


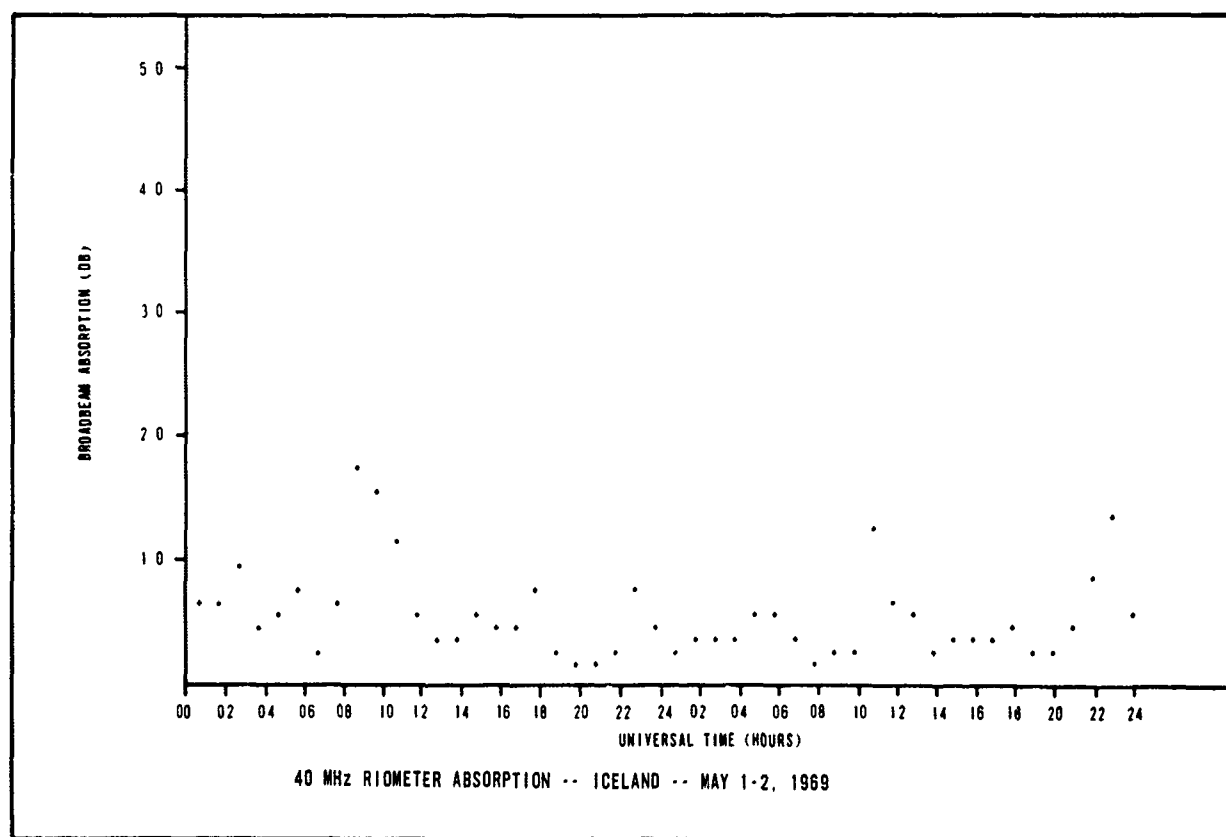
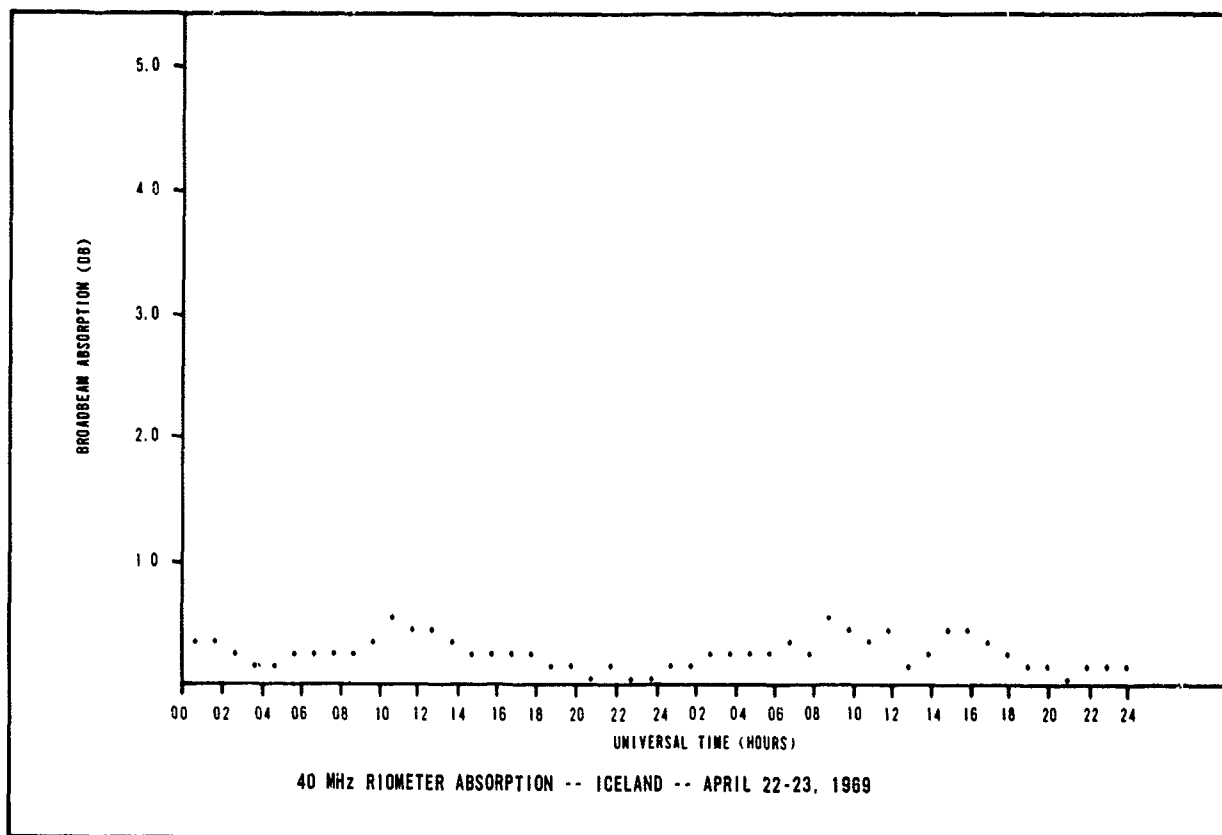


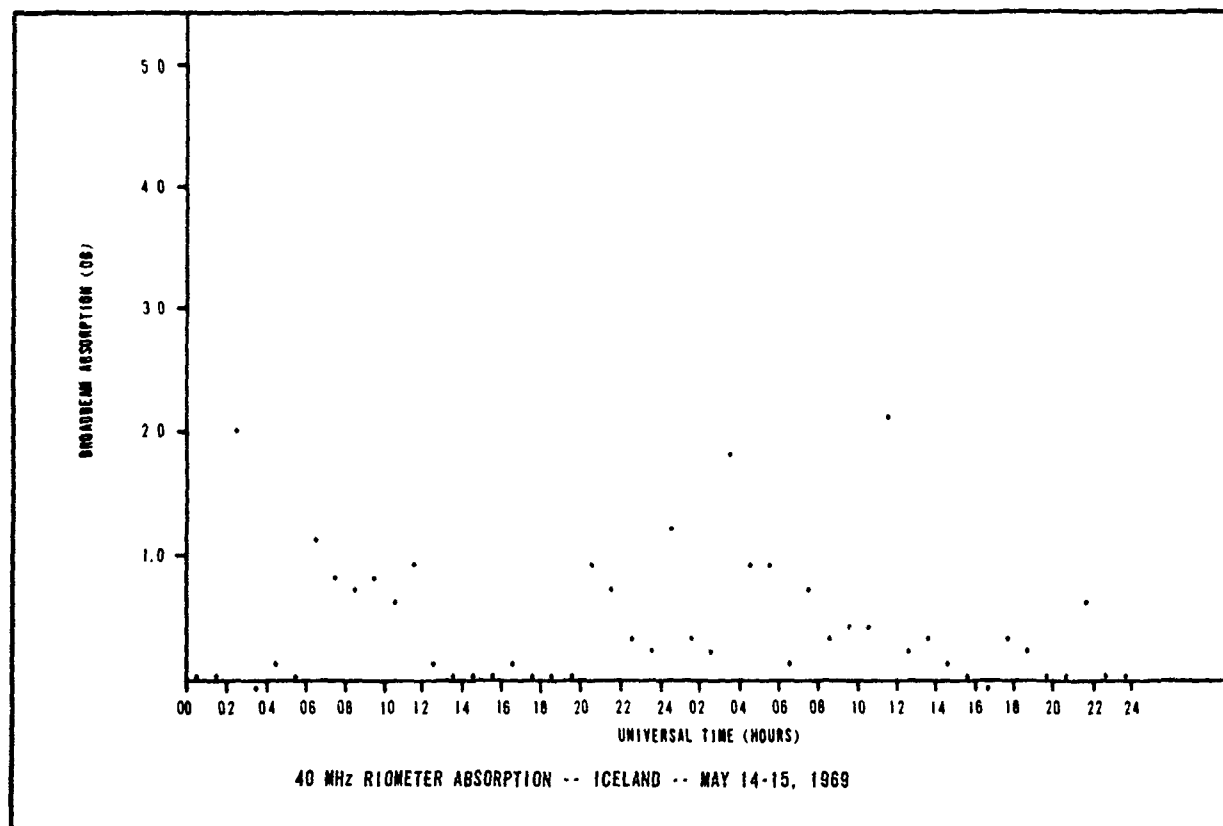
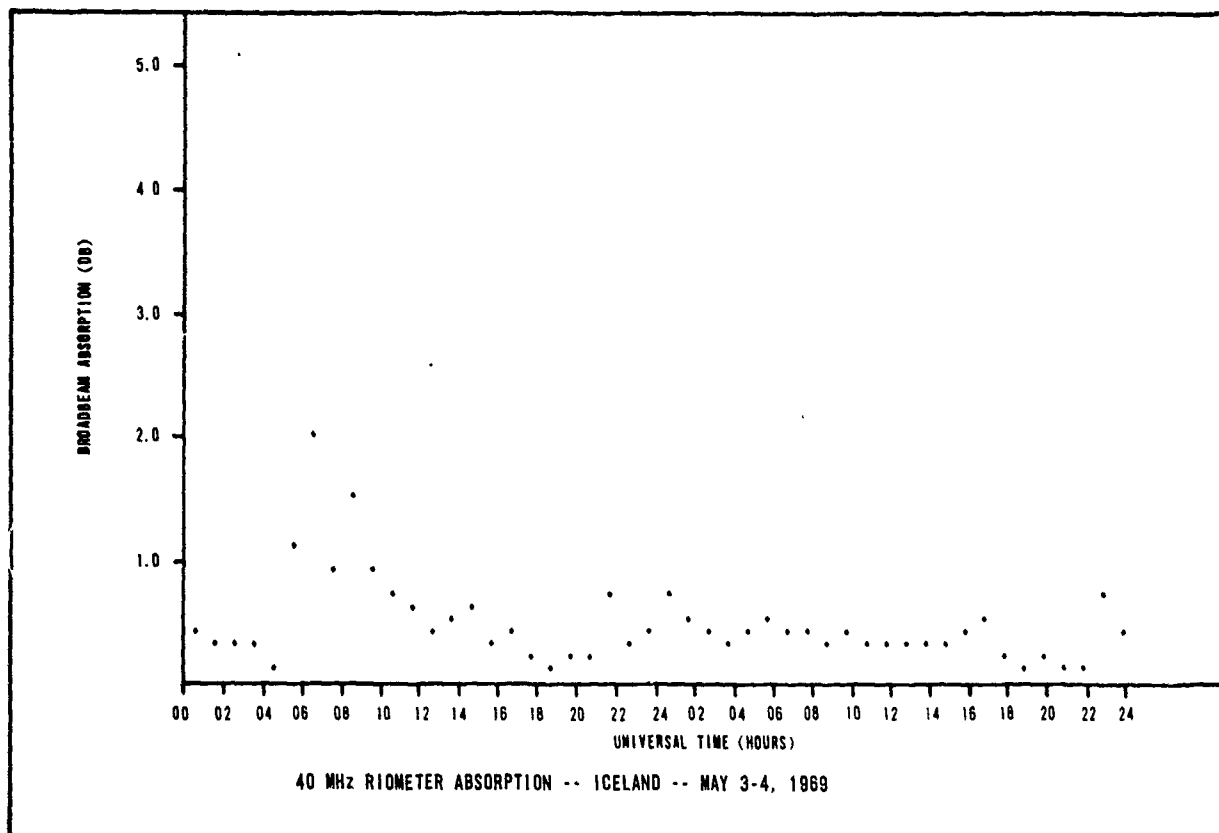


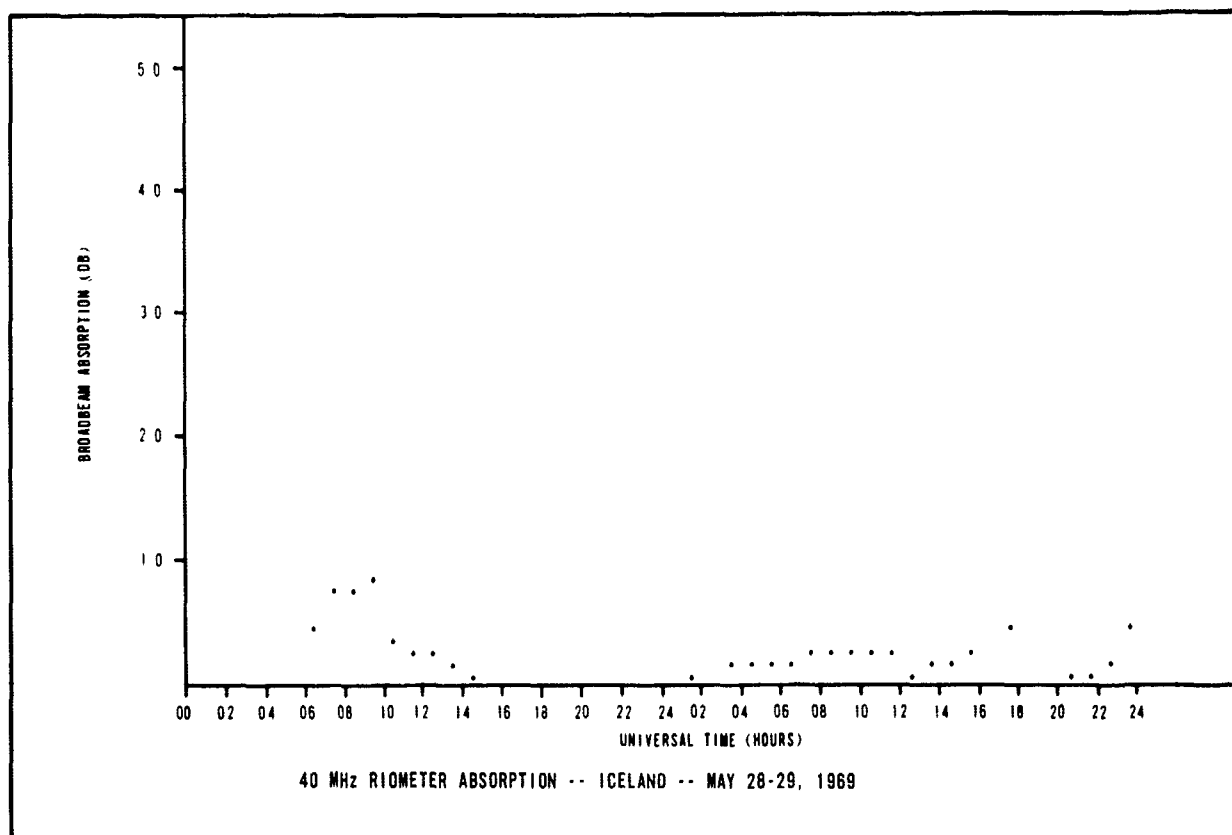
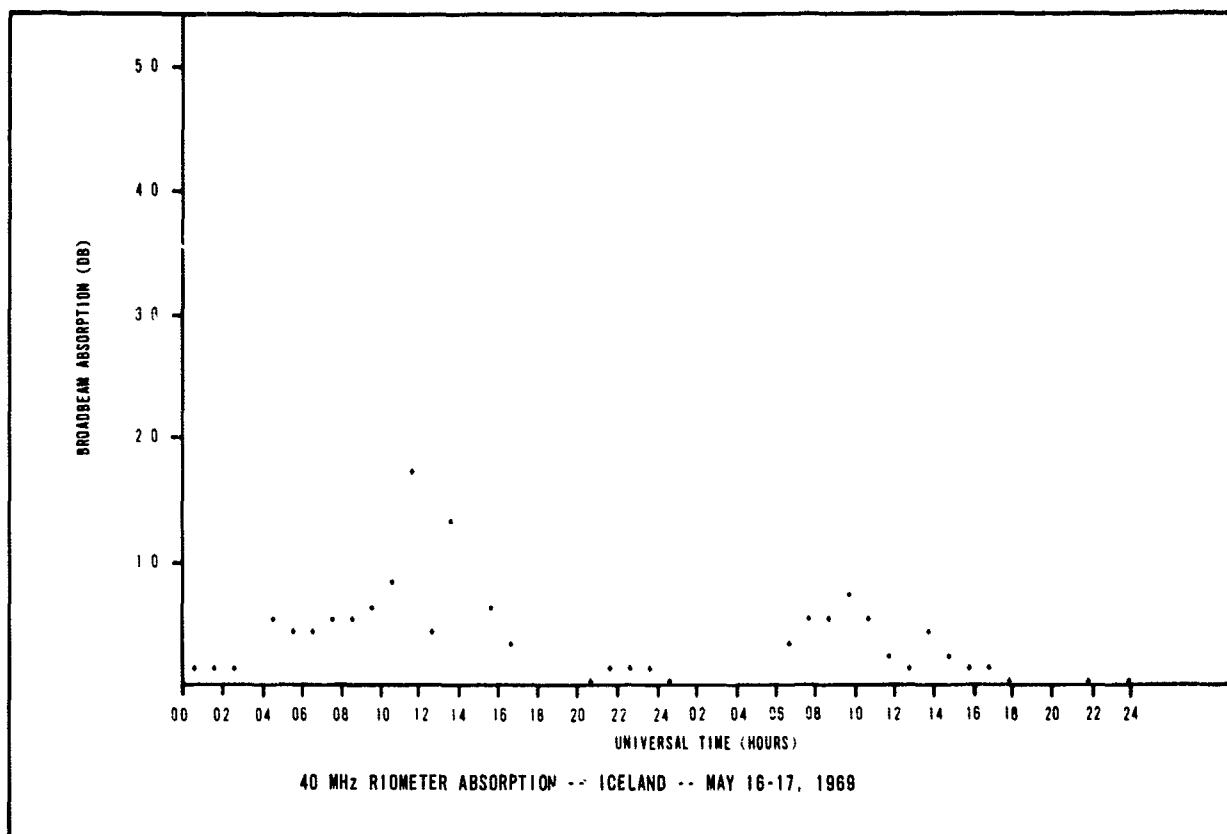


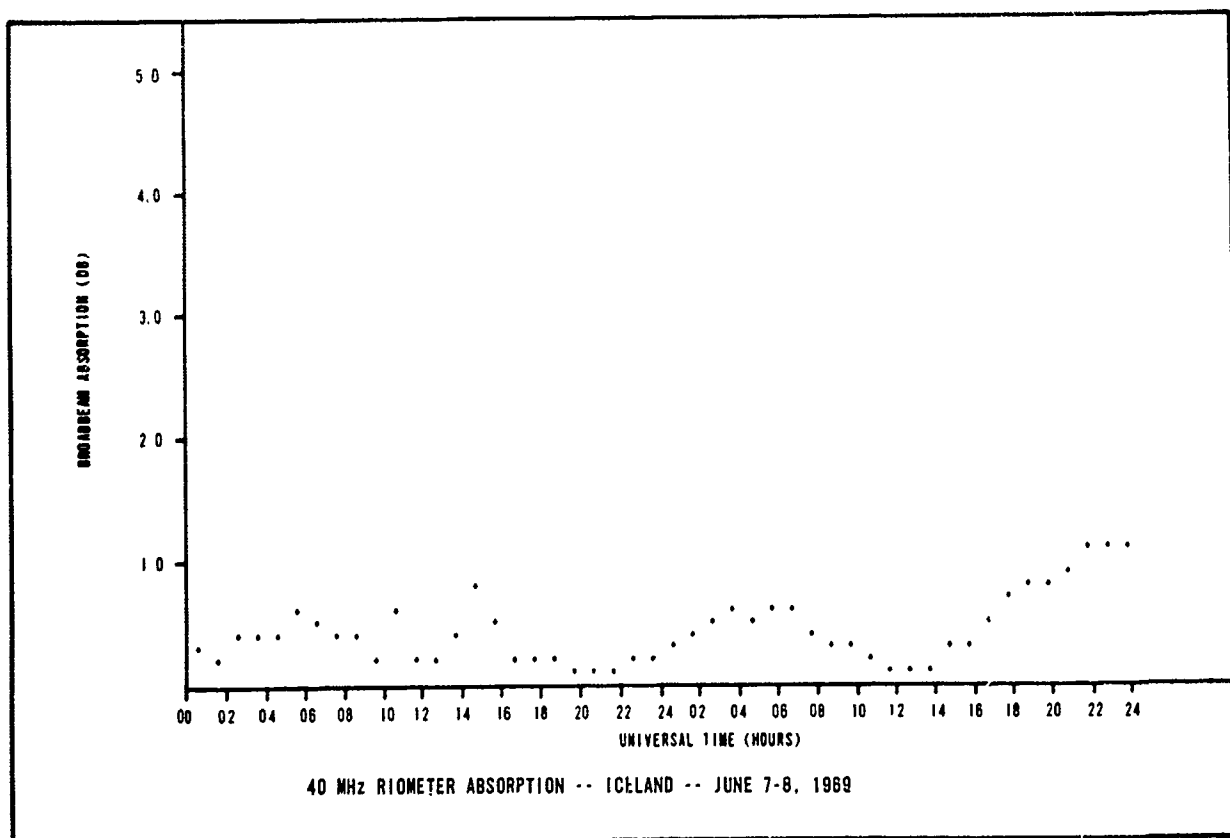
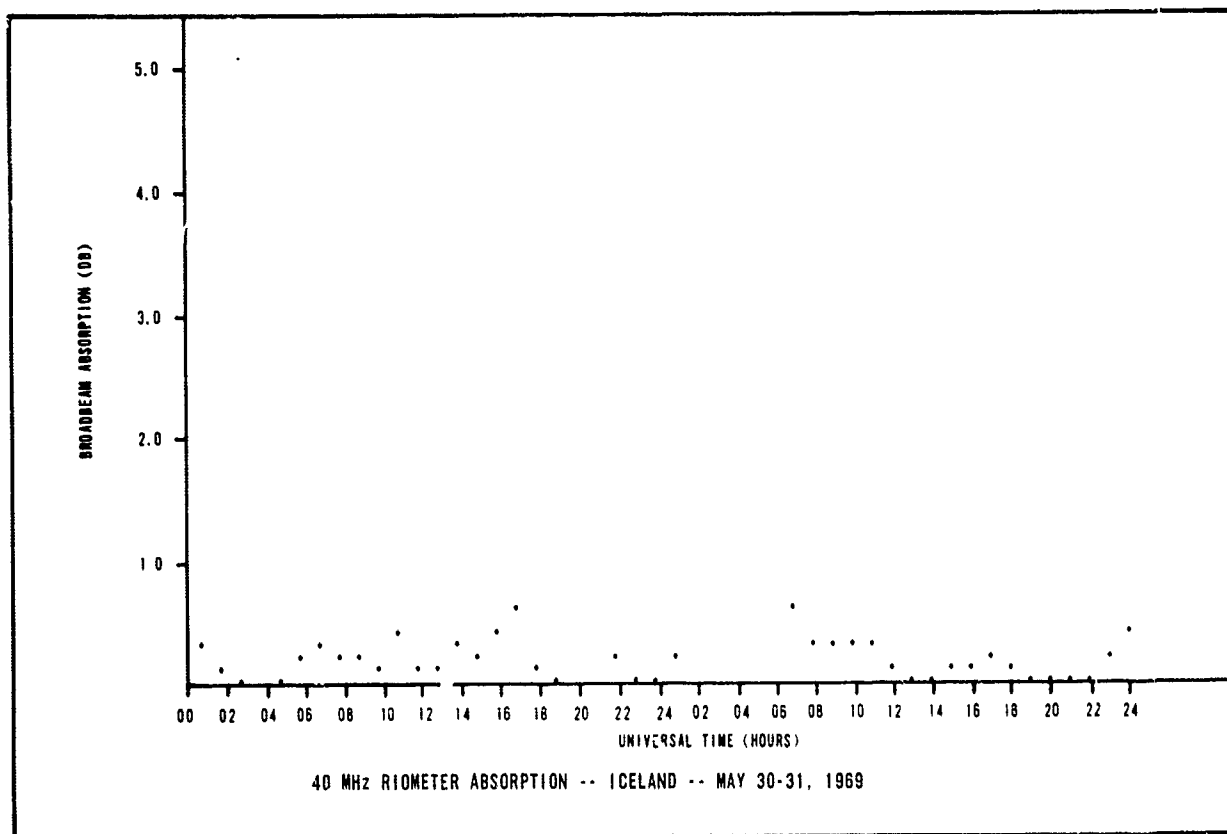


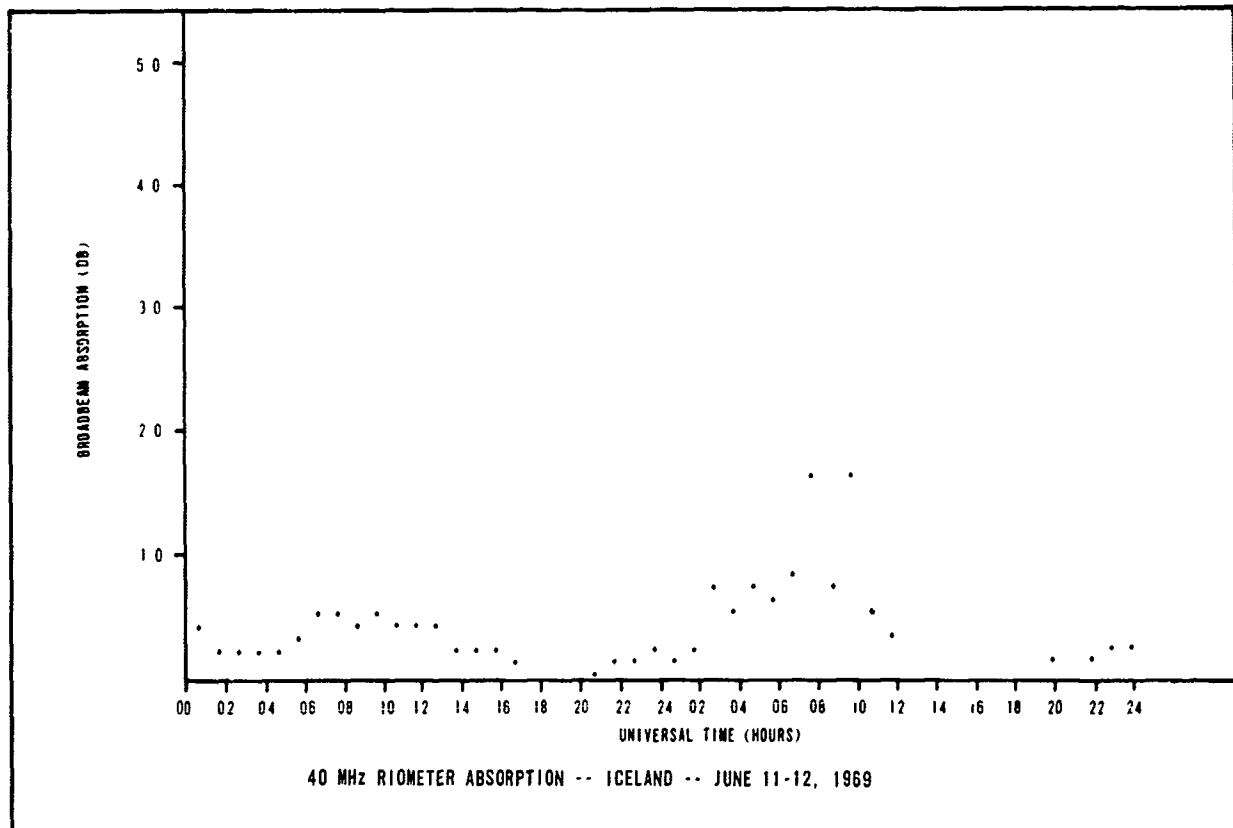
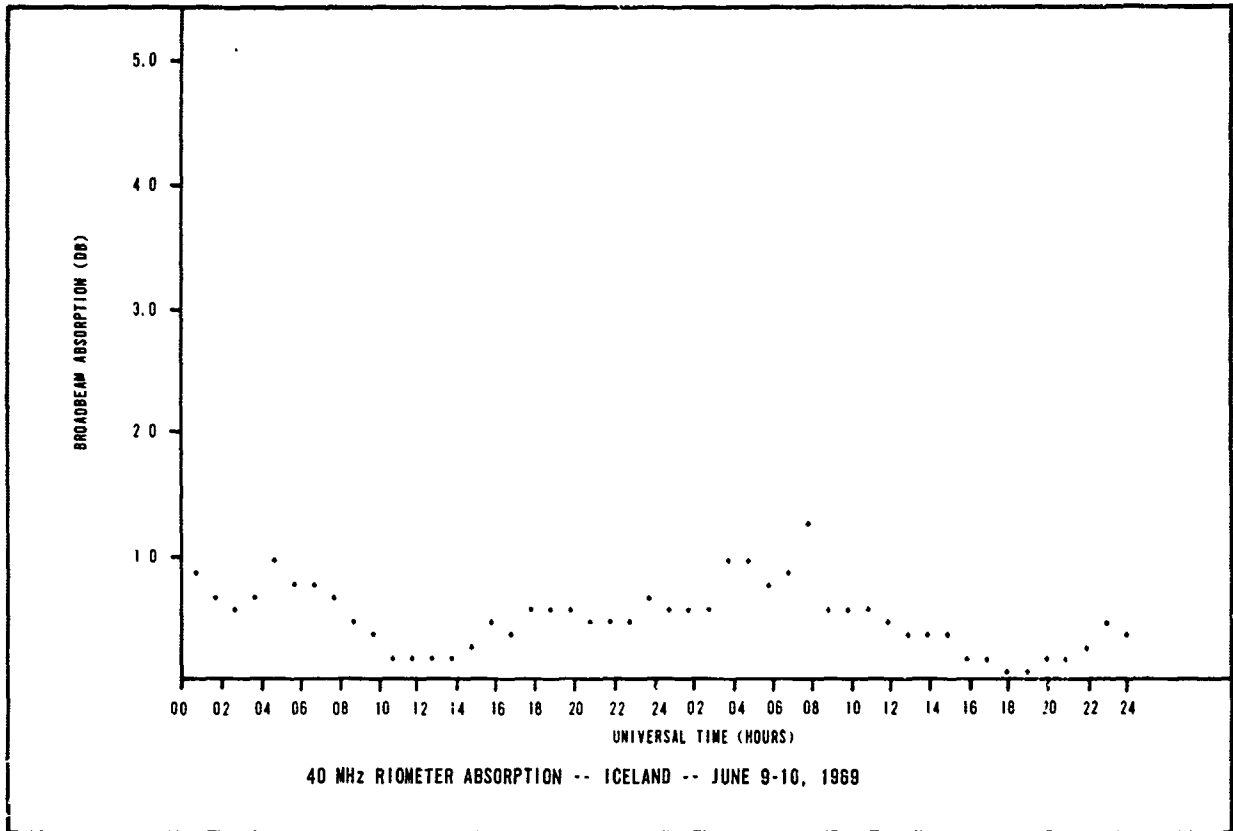


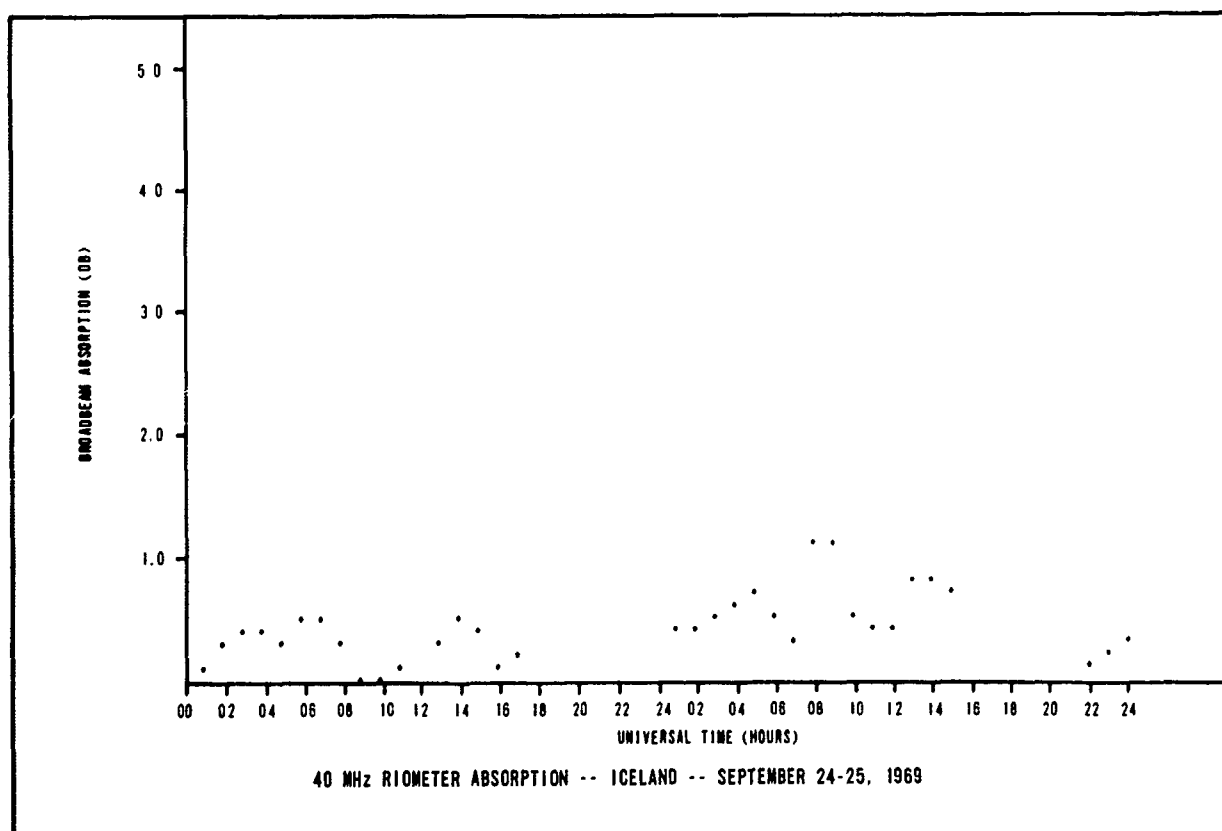
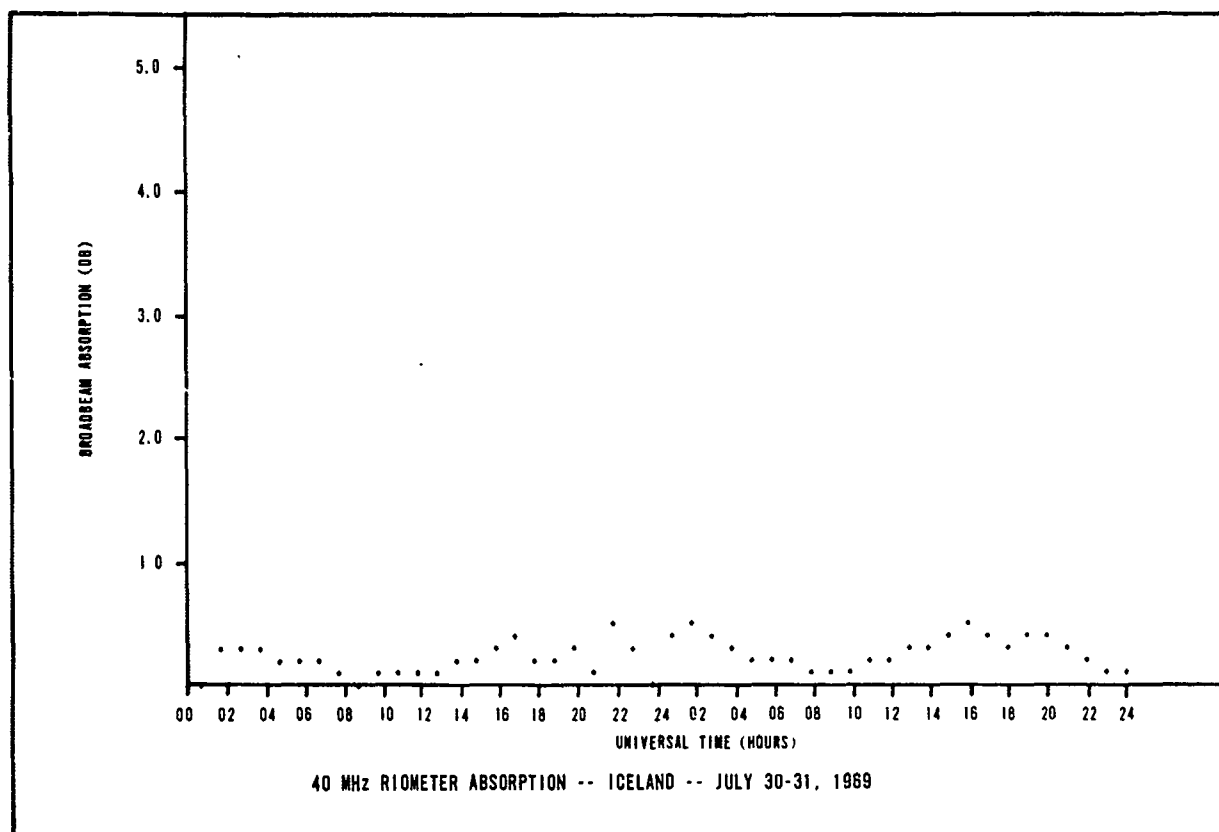




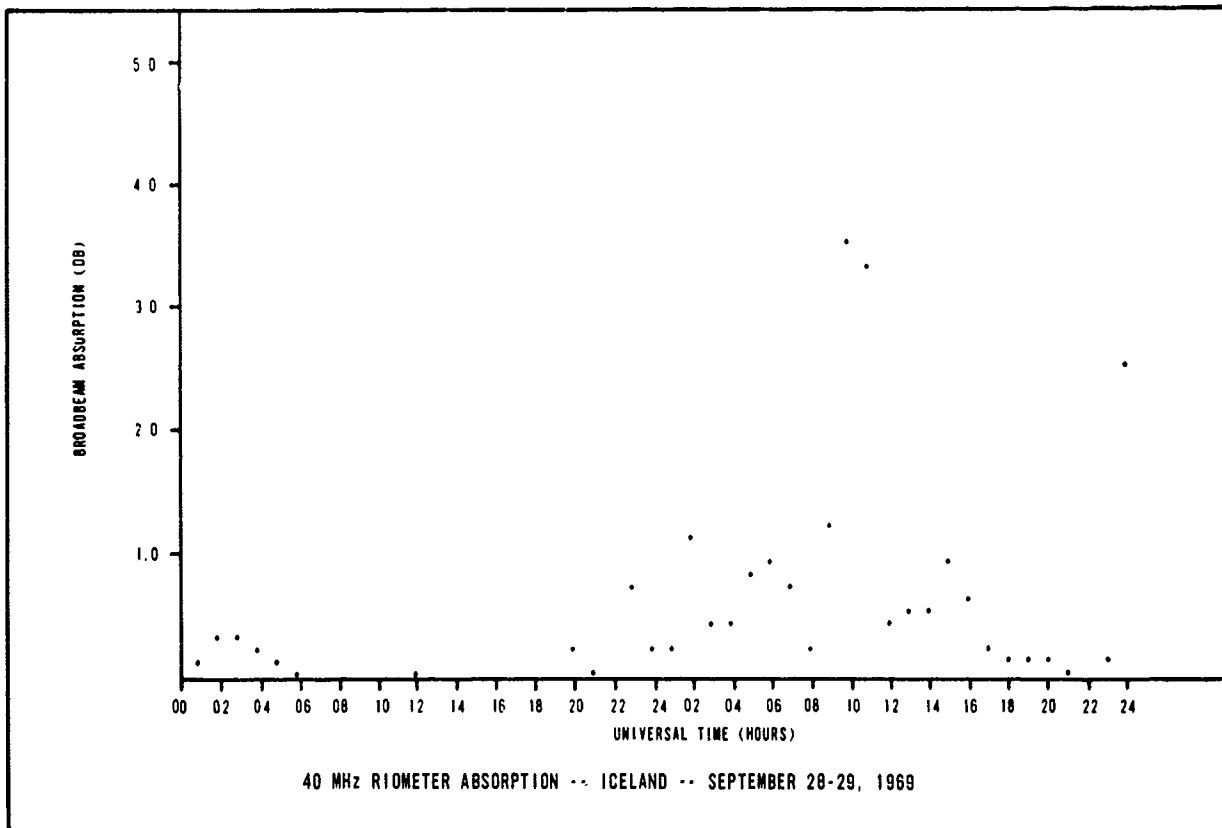
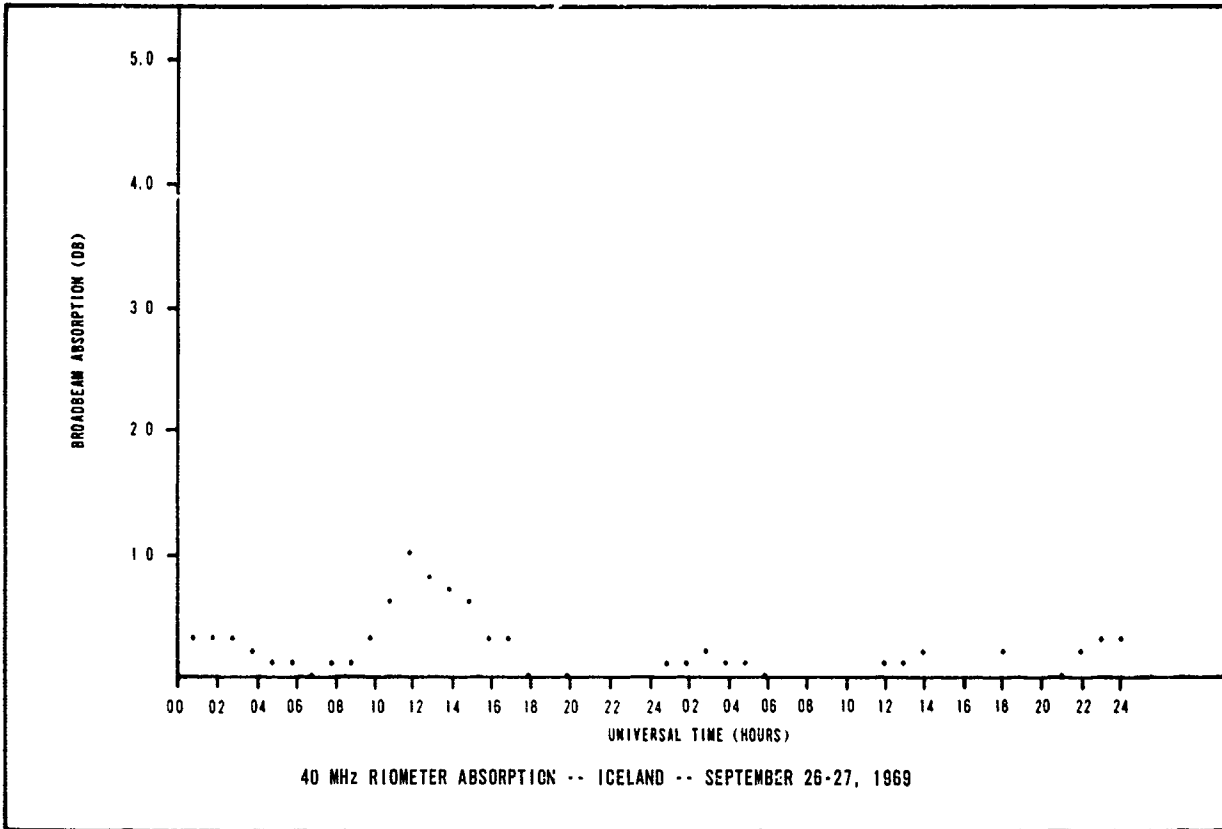


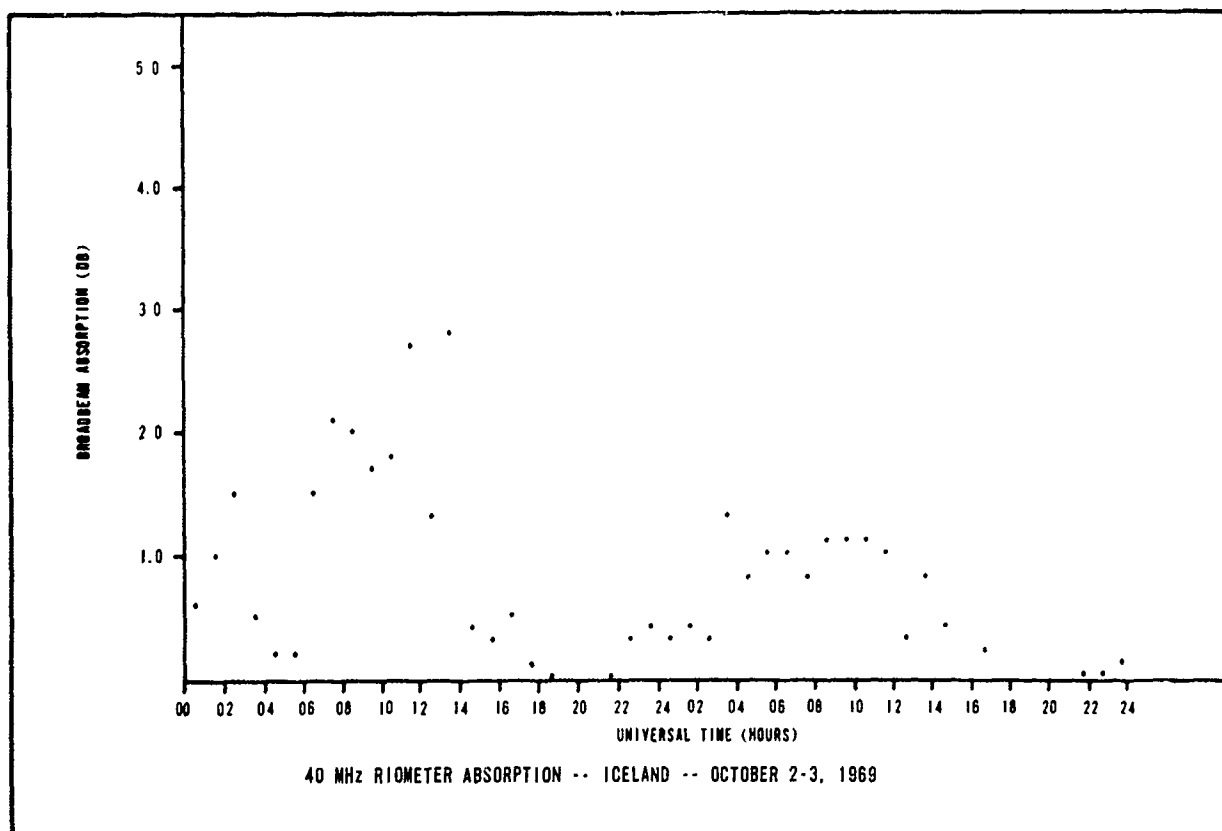
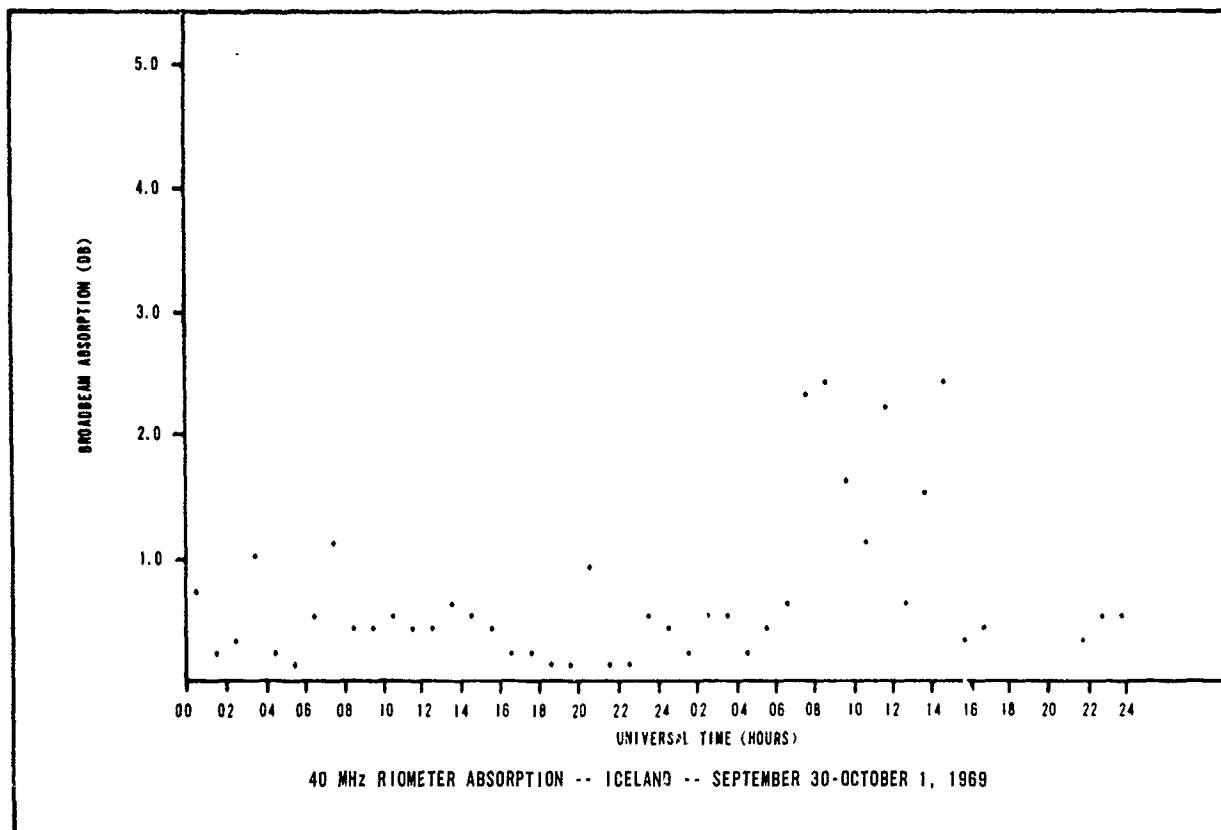












APPENDIX C  
DISTRIBUTION LIST

UNCLASSIFIED

Security Classification

DOCUMENT CONTROL DATA - R & D		
(Security classification of title, body of abstract and indexing annotation must be entered when the overall report is classified)		
1. ORIGINATING ACTIVITY (Corporate author) HRB-Singer, Inc. Science Park State College, Pennsylvania		2a. REPORT SECURITY CLASSIFICATION Unclassified
		2b. GROUP
3. REPORT TITLE Coordinated High-Latitude Experiments for the Simulation of Nuclear Burst Effects on VLF Systems		
4. DESCRIPTIVE NOTES (Type of report and inclusive dates)		
5. AUTHOR(S) (First name, middle initial, last name) Oelbermann, E.J. Imhof, G.W.		
6. REPORT DATE November 1969	7a. TOTAL NO. OF PAGES 135	7b. NO. OF REFS 11
8a. CONTRACT OR GRANT NO. Nonr 3851-(00)	9a. ORIGINATOR'S REPORT NUMBER(S) Final Technical Report Report No. 356-F	
b. PROJECT NO.		
c.	9b. OTHER REPORT NO(S) (Any other numbers that may be assigned this report)	
d.	None	
10. DISTRIBUTION STATEMENT "This document is subject to special export controls and each transmittal to foreign governments or foreign nationals may be made only with the prior approval of the Office of Naval Research, Field Projects Branch, Washington, D. C. 20360."		
11. SUPPLEMENTARY NOTES		12. SPONSORING MILITARY ACTIVITY Office of Naval Research Code 418 Washington, D. C.
13. ABSTRACT This report describes some coordinated high-altitude experiments which are being conducted by HRB-Singer, Inc., for simulating nuclear-burst effects on long-range VLF propagation. The program consists of five parts: 1. Collection and study of VLF phase and amplitude data over six long-range, high-latitude VLF propagation paths and 2-middle-latitude control paths. 2. Collection and study of ionospheric data (cosmic noise absorption data) near Reykjavik, Iceland, and Thule, Greenland. 3. Collection and study of other VLF data and ionospheric data from external sources (including satellite data). 4. Study and comparison of items 1 through 3 with nuclear test VLF data. 5. Collection and study of rapid phase VLF data at Thule, Greenland.		

DD FORM 1473  
1 NOV 65

UNCLASSIFIED

Security Classification